Version 1.0
June 1996

Space Telescope Imaging Spectrograph Instrument Handbook

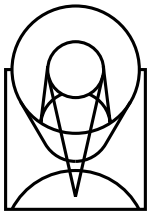

SPACE
TELESCOPE
SCIENCE
INSTITUTE

STScI
3700 San Martin Drive
Baltimore, Maryland 21218

Operated by the Association of Universities for Research in Astronomy, Inc., for the National Aeronautics and Space Administration

User Support

For prompt answers to any question, please contact the STscI Help Desk.

- **E-mail:** `help@stsci.edu`
- **Phone:** (410) 338-1082

World Wide Web

Information and other resources are available on the STIS World Wide Web page:

- **URL:** `http://www.stsci.edu/ftp/instrument_news/STIS/topstis.html`

STIS Instrument Team

Name	Title	Phone	e-mail
Stefi Baum	Instrument Scientist	(410) 338-4797	sbaum@stsci.edu
Mark Clampin	Instrument Scientist	(410) 338-4711	clampin@stsci.edu
George Hartig	Instrument Scientist	(410) 338-4966	hartig@stsci.edu
Phil Hodge	Scientific Programmer	(410) 338-4465	hodge@stsci.edu
Steve Hulbert	Instrument Scientist	(410) 338-4911	hulbert@stsci.edu
Susan Keener	Data Analyst	(410) 338-4939	keener@stsci.edu
Ellyne Kinney	Data Analyst	(410) 338-4516	ekinney@stsci.edu
Claus Leitherer	Instrument Scientist	(410) 338-4425	leitherer@stsci.edu
Kailash Sahu	Instrument Scientist	(410) 338-4930	ksahu@stsci.edu

Revision History

Version	Date	Editor
1.0	June 1996	S. Baum

Acknowledgements

M. Clampin, G. Hartig, E Kinney, and K. Sahu contributed greatly to the content of this handbook. C. Ritchie helped with the plots and M. Stevens helped with presentation and the format of the handbook in Frame. Guidance with content and organization came from C. Blades and R. Gilliland. Careful readings by C. Biagetti, R. Bohlin, K. Carpenter, R. Dempsey, J. Dolan, R. Kutina, C. Leitherer, K. Long, R. Pitts, M. Rosa, Sid Parsons, J. Walsh and the STIS IDT were much appreciated. O. Lupie helped with a last minute acquisition simulation. Finally, we thank the STIS IDT, in particular C. Bowers, M. Kaiser, R. Kimble, S.Kraemer, D. Lindler, and B. Woodgate, for sharing of data and figures and for numerous technical discussions on STIS and its scientific operation.

Citation

In publications, refer to this document as:
Baum, S. et al., 1996, “STIS Instrument Handbook”, Version 1.0
(Baltimore: STScI).

Table of Contents

PART 1

Introduction

The chapters in this part explain how to use this handbook, where to go for help, and describe special considerations for using STIS in Cycle 7.

CHAPTER 1
Introduction

In This Chapter...

The Space Telescope Imaging Spectrograph, STIS, is a second-generation instrument to be installed on the Hubble Space Telescope (HST) during the Second Servicing Mission in February 1997. STIS was designed to replace the major capabilities of the Faint Object Spectrograph (FOS) and Goddard High Resolution Spectrograph (GHRS) and to provide a major improvement in HST's spectroscopic capability through the use of two-dimensional detectors. This Handbook provides instrument specific information you need to propose for HST observations (Phase I), design accepted proposals (Phase II), and understand STIS in detail.

This chapter explains the layout of the handbook and describes how to use the Help Desk at STScI (`help@stsci.edu`) and the STScI STIS World Wide Web site to get help and further information. Instrument and operating updates will be posted on the STIS web page.

Purpose

The *STIS Instrument Handbook* is the basic reference manual for the Space Telescope Imaging Spectrograph, and describes the instrument's properties, expected performance, operations, and calibration. The Handbook is maintained by scientists at STScI. Dr. B.E. Woodgate, the Principal Investigator for the STIS, and scientific staff at GSFC and Ball Aerospace kindly provided information and test data in support of this handbook.

We have designed the document to serve three purposes:

- To provide instrument-specific information for preparing Cycle 7 Phase I STIS observing proposals.
- To provide instrument-specific information to support the design of Phase II proposals for accepted STIS proposals in Cycle 7.
- To provide technical information about the operation and performance of the instrument which can help in the understanding of problems and in the interpretation of data acquired with STIS.

This Handbook is not meant to serve as a manual for the reduction and analysis of data taken with STIS. Near the start of the STIS GO observing era, we will publish an addition to the *HST Data Handbook* describing how to work with STIS data.

Document Conventions

This document follows the usual STScI convention in which terms, words, and phrases which are to be entered by the user in a literal way on an HST proposal are shown in a typewriter font (e.g., `STIS/CCD,SHADOW`). Names of software packages or commands (e.g., **calstis**) are given in bold type.

Wavelength units in this handbook are in Angstroms (Å).

Examples Used in this Handbook

The Handbook uses five observational examples as illustration throughout the text. These same examples form the basis of the Phase I and Phase II templates and will eventually form the basis of tutorial information in the *HST Data Handbook.* The examples are:

- Long slit optical spectroscopy of the nearby galaxy, NGC 4406 (M86).
- Long slit optical and ultraviolet spectroscopy and optical imaging of NGC 6543, the Cat's Eye planetary nebulae.
- First order low resolution spectroscopy covering STIS's full wavelength range from 1150 Å in the UV to 11000 Å in the near-IR of the continuous viewing zone (CVZ) solar analog star P041-C.
- Echelle spectroscopy of the O-type star, Sk 69-215, in the Large Magellanic Cloud (LMC), a target in the CVZ.
- Deep optical imaging of a random field.
- Time resolved ultraviolet spectroscopy of the flare star, AU-MIC.

In addition, we use stellar spectra throughout the handbook to illustrate signal-to-noise ratio calculations and derive limiting magnitudes. Figure 1.1 below shows the normalized spectra of O, A, G, and M stars that we use.

Figure 1.1: Normalized spectra of O5V, A0V, G0V, and M0V stars used throughout the handbook. Note the dramatic differences in the UV properties.

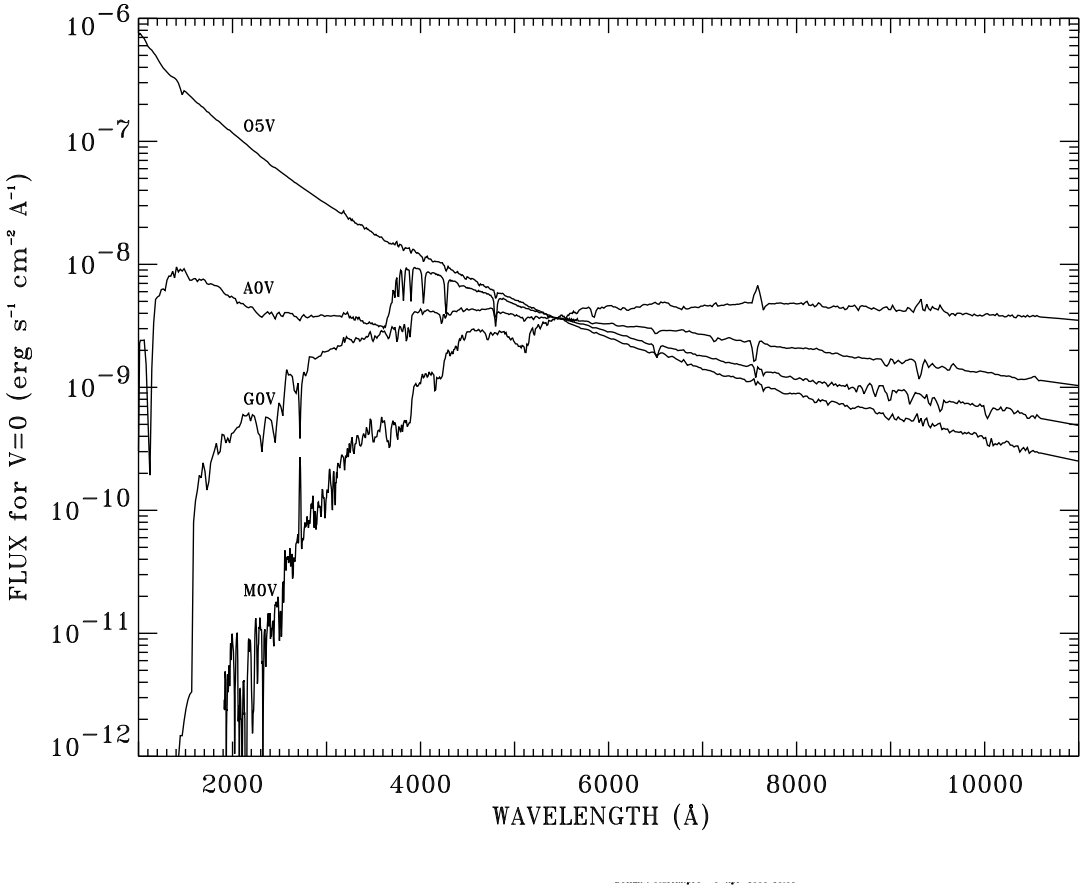

Handbook Layout

STIS is a versatile imaging spectrograph. The instrument provides spatially-resolved spectroscopy from 1150 to 11,000 Å at low to medium spectral resolution, echelle spectroscopy in the ultraviolet, solar-blind imaging in the ultraviolet, time tagging of photons in the ultraviolet for high time resolution, and direct and coronographic imaging in the optical. To guide you through STIS's capabilities and help optimize your scientific use of the instrument we have divided this handbook into four parts:

- Part I - Introduction.
- Part II - User's Guide.
- Part III - Supporting Material.
- Part IV - Calibration.

Figure 1.2 provides a roadmap to the use of this handbook.

Figure 1.2: Handbook Roadmap

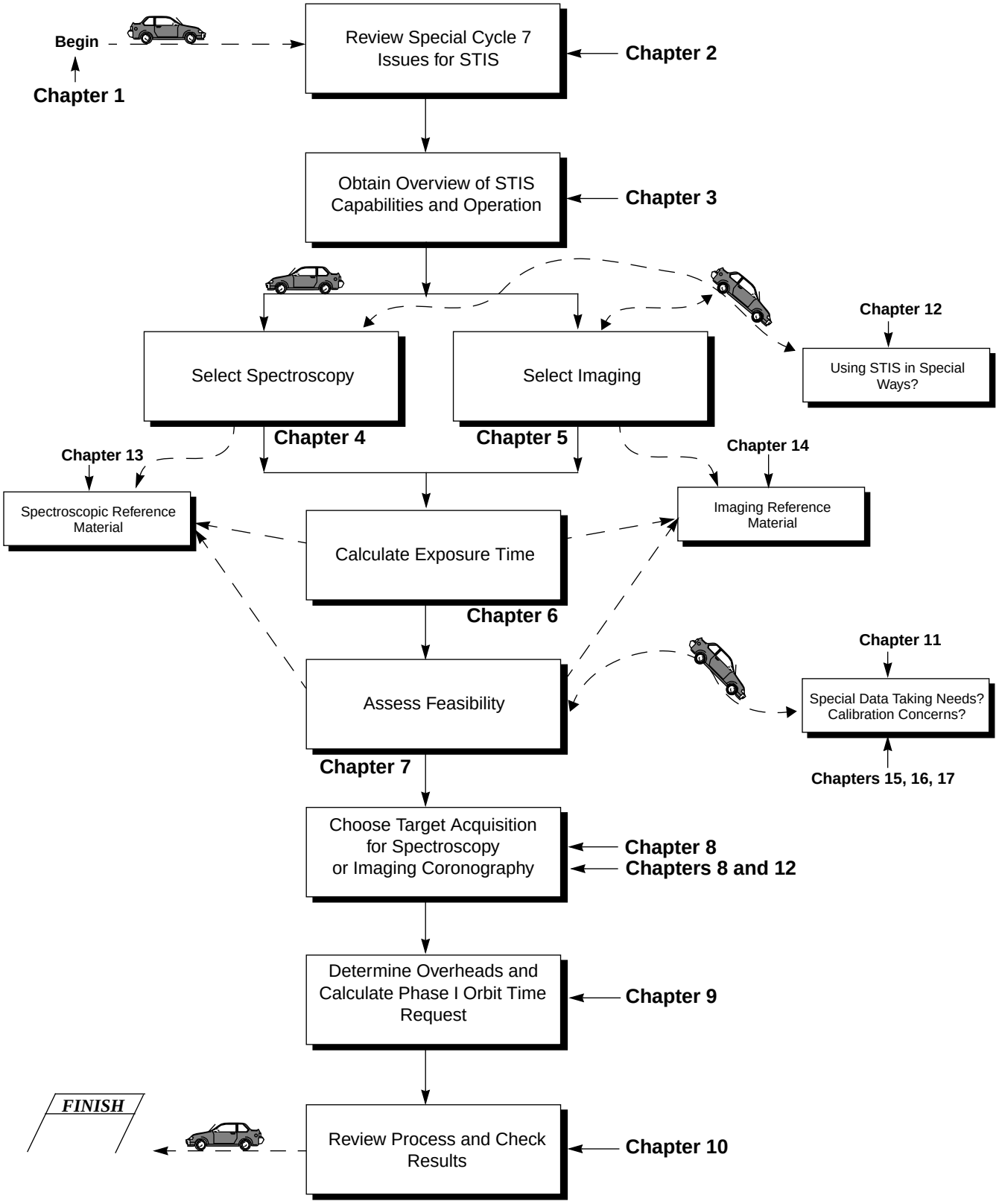

The Supporting Material and Calibration sections contain technical information which supports the material found in the User's Guide; readers are referred to the information at appropriate points in the User's Guide.

The chapters of this handbook are as follows:

- Part I - Introduction
  - Chapter 1, *Introduction* on page 3. Includes information about getting help and additional information about STIS.
  - Chapter 2, *Special Considerations for Cycle 7* on page 11 describes special considerations for using STIS during Cycle 7.
- Part II - Users Guide
  - Chapter 3, *Introduction to STIS* on page 19 provides an overview of STIS's full capabilities. A discussion is provided to help guide you through the technical details you need to consider in choosing the optimum STIS configuration and in determining the number of orbits to request.
  - Chapter 4, *Spectroscopy* on page 33 provides a detailed, grating-by-grating description of STIS's spectroscopic capabilities, including spectral resolutions, throughputs, and descriptions of the slits and apertures.
  - Chapter 5, *Imaging* on page 47, provides a detailed, filter-by-filter description of STIS's imaging capabilities.
  - Chapter 6, *Exposure Time Calculations* on page 65, describes how to perform signal-to-noise calculations, either by using pencil and paper, or by using software tools that are provided on the World Wide Web.
  - Chapter 7, *Feasibility and Detector Performance* on page 87, provides a description of the three detectors, their physical characteristics, capabilities, and limitations, including saturation, linearity, and bright object limits.
  - Chapter 8, *Target Acquisition* on page 103, helps you select the optimum target acquisition sequence needed to place the target in the desired science aperture.
  - Chapter 9, *Overheads and Orbit Time Determination* on page 123, provides information to convert from a series of planned science exposures to an estimate of the number of orbits, including spacecraft and STIS overheads. This chapter applies principally to the planning of Phase I proposals.
  - Chapter 10, *Summary and Checklist* on page 137, presents a summary and a checklist that you should use to assure there are no major omissions in your Phase I and Phase II proposals.
- Part III - Supporting Material
  - Chapter 11, *Data Taking* on page 141, describes data taking with STIS, including the instrument operating modes (`ACCUM`, `TIMETAG`) the various "associated" types of observations (`CRSPLIT`, `REPEATOBS`, `PATTERNS`, and `WAVECALS`), and the use of subarrays and binning. This chapter also discusses how to orient the long slits.

- Chapter 12, *Special Uses of STIS* on page 161, provides information on special science uses of STIS, covering slitless spectroscopy and long slit echelle spectroscopy, time resolved spectroscopy and imaging, observations of very bright targets, coronographic spectroscopy and imaging, possible techniques for obtaining higher signal-to-noise and spectral sampling, observations of planetary objects, and parallel observing.
- Chapter 13, *Spectroscopic Reference Material* on page 175, contains the detailed plots of sensitivity, signal-to-noise and saturation times, predicted line spread functions, and tables of bright object limits referred to in Chapter 4.
- Chapter 14, *Imaging Reference Material* on page 257, contains the detailed plots of sensitivities, signal-to-noise and saturation times, and tables of bright object limits referred to in Chapter 5.

• Part IV - Calibration

- Chapter 15, *Overview of Pipeline Products* on page 311, briefly describes the processing of STIS data by the STScI pipeline and the data that are sent to observers.
- Chapter 16, *Expected Accuracies* on page 319, summarizes the accuracies expected for STIS data calibrated by the STScI pipeline in Cycle 7.
- Chapter 17, *Calibration Plans* on page 323, provides an overview of the planned thermal vacuum (ground), SMOV (commissioning phase) and Cycle 7 calibration and verification plans.

Preparing and Observing with STIS

Use the *STIS Instrument Handbook* and the *Cycle 7 Call for Proposals and Phase I Proposal Instructions* (CP) when assembling your STIS Phase I Proposal. The CP provides policy and instructions for proposing; the *STIS Instrument Handbook* contains technical information about STIS, describing its expected performance, and presenting suggestions for use. The next chapter in the handbook describes special considerations for Cycle 7.

If your Phase I proposal is accepted, you will be asked to submit a Phase II proposal in which you specify the exact configurations, exposures times and sequences of observations that STIS and the telescope should perform. To assemble your Phase II proposal, you should use the *STIS Instrument Handbook* in conjunction with the *Phase II Proposal Instructions*. These instructions describe the exact rules and syntax that apply to the planning and scheduling of STIS observations and provide relevant observatory information.

Our current understanding of STIS as an instrument is in its formative stages as the flight detectors have yet to be fully calibrated. We are in the midst of developing the ground system to support STIS operations.

At this time, predictions of the performance of STIS should be treated as provisional, and users should adopt conservative expectations for the performance of the instrument in Cycle 7.

The Help Desk at STScI

STScI maintains a Help Desk. The Help Desk staff at STScI quickly provide answers to any HST-related topic, including questions regarding STIS and the Cycle 7 proposal process. The Help Desk staff has access to all of the resources available at the Institute, and they maintain a database of answers so that frequently asked questions can be immediately answered. The Help Desk staff also provide STScI documentation, in either hardcopy or electronic form, including *Instrument Science Reports*, *Instrument Handbooks*, etc. Questions sent to the Help Desk during normal business hours are answered within one hour. Questions received outside normal business hours will be answered within the first two hours of the next business day. Usually, the Help Desk staff will reply with the answer to a question, but occasionally they will need more time to investigate the answer. In these cases, they will reply with an estimate of the time needed to reply with the full answer.

We ask that you please send *all* initial inquiries to the Help Desk. If your question requires a STIS Instrument Scientist to answer it, the Help Desk staff will put a STIS Instrument Scientist in contact with you. By sending your request to the Help Desk, you are guaranteed that someone will provide you a timely response.

To contact the Help Desk at STScI:

- **Send e-mail**: `help@stsci.edu`
- **Phone**: 1-410-338-1082
  Toll-free in the U.S.: 1-800-544-8125

The Space Telescope European Coordinating Facility (ST-ECF) also maintains a help desk. European users should generally contact the (ST-ECF) for help: all other users should contact STScI. To contact the ST-ECF Help Desk:

- **Send e-mail**: `stdesk@eso.org`

The STIS Instrument Team at STScI

STScI maintains a team of Instrument Scientists, Scientific Programmers and Data Analysts who support the development, operation and calibration of STIS. The team is also responsible for supporting STIS users.

Supporting Information and the STIS Web Site

The STIS Instrument Team at STScI maintains a World Wide Web (WWW) page, as part of the STScI's home page. The URL (uniform resource locator) for the STScI STIS web page is:

`http://www.stsci.edu/ftp/instrument_news/STIS/topstis.html`

The STScI STIS web site includes:

- **Documentation**: An electronic version of this handbook will be maintained on the WWW site. In addition, more detailed technical information (not needed to propose for Cycle 7) concerning the development, performance, ground testing, operation and calibration of STIS itself are contained in a series of *STIS Instrument Science Reports* and other related reports. They can be downloaded from the WWW or requested from the Help Desk.
- **Software**: Some software can be retrieved or run directly over the web, including an exposure time calculator.
- **Advisories**: This is where we will post updates to instrument performance as information is learned from ground testing and on-orbit investigations.
- **Calibration related information**: A description of the Servicing Mission Orbital Verification (SMOV) plan and the Cycle 7 STIS calibration plan will be posted here, as they become available.
- **Frequently Asked Questions**: A list of frequently asked questions and answers about STIS, ranging from proposal preparation to data analysis.

CHAPTER 2
Special Considerations for Cycle 7

In This Chapter...

HST's second servicing mission will put in place two second-generation scientific instruments, NICMOS (the Near Infrared Camera and Multi-Object Spectrometer) and STIS, while removing the FOS (Faint Object Spectrograph) and GHRS (Goddard High Resolution Spectrograph). In addition, a Fine Guidance Sensor will be replaced and a solid state data recorder will be installed. The increased data capacity of the new recorder, exploited through a series of changes to the ground system, considerably increases the capacity of HST to take simultaneous data from multiple instruments running in parallel. Cycle 7 should mark an exciting new phase in HST science. On the other hand, observers must understand that it will take time for us to understand, calibrate, and optimize the uses of these new instruments.

STIS is a New Instrument

While planning your Cycle 7 observations, keep in mind that STIS will be a *new* instrument. As of the writing of this handbook, two of the three STIS flight detectors have not yet been selected and the instrument has not yet been fully integrated. Sensitivities, brightness limits, optical performance, software and hardware execution times, and other characteristics contained in this handbook represent our best estimates at this time. In many cases they are based on component testing of either flight or flight-candidate optics and detectors. Integrated testing of STIS in a thermal vacuum chamber is currently scheduled for

August 1996, integrated operations with the ground system is scheduled for November 1996, and on-orbit verification of STIS (SMOV) for March through June 1997.

We note that the present design of the Multi Anode Microchannel Array (MAMA) detector which STIS uses in the ultraviolet has not been flown before on an astronomical satellite; nor are MAMAs commonly used at ground-based observatories. As our current knowledge of the STIS MAMA detector performance is limited, predictions of the ultraviolet performance of STIS should be treated as provisional, and users should adopt conservative expectations in planning their Cycle 7 science.

We note also that the final CCD detector properties, including the read noise, dark current, and full well depth, are also uncertain at this time, and could deviate from the values quoted in this handbook by as much as a factor of two (in the sense of poorer performance).

Updates to Instrument Performance for Cycle 7

We are planning for two major updates to the instrument performances presented in this Handbook, as needed. The first update, to be available by mid-August, will contain new information about instrument performance obtained during ground testing which may affect your Phase I Proposal. This update will be distributed to all who requested a STIS Instrument Handbook from STScI, and will also be available upon request from the Help Desk and for direct downloading from the STScI STIS WWW site (see “The Help Desk at STScI” on page 9 and “Supporting Information and the STIS Web Site” on page 10). Your STIS HST proposal for Cycle 7 must be based on the sensitivities, performance, and capabilities published *at that time*.

A second major update is planned for late 1996. This update will be applicable to Phase II planning, and will be distributed in association with the Cycle 7 proposal acceptance letters.

Support of STIS Capabilities for Cycle 7

We have established a set of core scientific capabilities of STIS which will be supported for Cycle 7 science and which are described in this handbook. These capabilities cover an enormous range of science applications and bring dramatic new capabilities to HST. In practice, the supported capabilities will be phased in during Cycle 7, as our understanding of the instrument and on-orbit performance grows. This gradual phasing-in will increase the likelihood that observations are successfully executed and assure that necessary calibration observations are obtained.

STIS has additional capabilities that are not described in this handbook, and which are not supported for Cycle 7. These capabilities include additional slits, additional *redirected* (backup redundant) grating modes, additional data taking formats and increased flexibility in specification of target acquisitions. These capabilities are “available”, upon consultation with a STIS Instrument Scientist. If you find that your science *cannot* be performed with the capabilities described in this handbook, you may wish to consider use of an unsupported capability. The most relevant of these available capabilities are described or referenced within this handbook (e.g., see “Observing Too-Bright Objects with STIS” on page 165, or “High Signal-to-Noise Ratio Observations” on page 167, or “Improving the Sampling of the Line Spread Function” on page 168 or “Considerations for Observing Planetary Targets” on page 168). A full list of STIS’s available and Engineering-only capabilities is being compiled in the form of an appendix to this handbook and will be available from STScI upon request from the Help Desk.

Use of unsupported modes comes at a price, and they should be used only if the need and scientific justification are particularly compelling. Proposers should be aware of the following caveats in the use of unsupported modes:

- Calibrations for unsupported capabilities will not be provided by STScI. Users must either determine that they can create calibration files from data in the HST Archive or they must obtain calibrations as part of their observations. The STScI pipeline will not calibrate data taken in unsupported modes but will deliver uncalibrated FITS files (or in some cases partially calibrated FITS files) to the observer and the HST Archive.
- STScI adopts a policy of shared risk with the observer for the use of unsupported capabilities. Requests to repeat failed observations taken using unsupported capabilities will not be honored if the failure is related to the use of the unsupported capability.
- User support from STScI for the reduction and analysis of data taken using unsupported capabilities will be limited and provided at a low priority. Users taking data with unsupported capabilities should be prepared to shoulder the increased burden of calibration, reduction and analysis of these data.

Cycle 7 Proposals which include use of unsupported STIS capabilities must include a justification of why the science cannot be done with a supported configuration, must include a request for any observing time needed to perform calibrations, must justify the added risk of using an unsupported mode in terms of the science payback, and must include a demonstration that the observers are able to shoulder the increased burden of calibration reduction and analysis of their data.

Constraints on STIS Observing in Cycle 7

Time Critical Observations

Commissioning of the prime capabilities of STIS (and NICMOS) will be the first priority for these instruments in Cycle 7. Therefore, time critical observations using STIS (and NICMOS), for example Target of Opportunity programs or programs with very tight orientation constraints, will not be allowed until January 1, 1998, the midpoint of Cycle 7, except on a shared risk basis. If approved, they will be executed on a no-interference basis with ongoing efforts to bring full capabilities on-line for the new instruments as first priority. Should an early STIS target of opportunity observation fail, it will not be a candidate for repeat or later scheduling. Common sense should apply. See the CP/Phase I Proposal Instructions for more details.

Policy for Prime and Parallel Observing with the STIS MAMA Detectors

As explained in greater detail in “MAMA Bright Object Limits” on page 97, the MAMA detectors STIS utilizes in the ultraviolet are subject to damage at high illumination rates. To protect the health and safety of the instrument, we have established limits on the maximum count rate at which the detectors may be illuminated. These count rate limits translate into a set of configuration dependent bright object limits. The bright object limits are summarized in Table 13.24, “MAMA Spectroscopic Bright Object Limits - V Mags and cgs units.,” on page 255 and Table 14.16, “MAMA Imaging Bright Object Limits, V Magnitudes and CGS as indicated.,” on page 308.

STScI will perform screening of all MAMA exposures prior to scheduling. Targets which cannot be established to be safe in the configuration in which they are being observed will not be scheduled. Observations which pass screening but are lost on orbit due to a bright object violation will not be rescheduled. The observer is responsible for assuring that their observations do not violate the MAMA count rate limits. A detailed description of the MAMA bright object limits, and the observer’s responsibility are presented in “MAMA Bright Object Limits” on page 97; we refer MAMA observers there.

In addition, to assure STScI can adequately screen observations, special constraints are imposed on parallel observing with the MAMAs:

- No pure parallels are allowed using the MAMA detectors.
- Coordinated parallels are allowed with the MAMA detectors only if an exact spacecraft orientation (ORIENT) is requested and the RA and Dec of the parallel field determined. Note that the specification of an exact orient limits the scheduability of observations to a ~4-8 week period each year.

The observer is responsible for assuring that their observations do not violate the MAMA count rate limits both for coordinated parallel MAMA observations and for primes.

Table 2.1 below summarizes the policy with respect to MAMA observing in Cycle 7.

Table 2.1: Bright Object Protection Policy for MAMA Observations

Type of Observing	Spectroscopy[a]	Imaging[b]
Prime	Allowed if target passes screening	Allowed if target passes screening
Coordinated parallel	Allowed only if ORIENT is exactly specified and field passes screening	Allowed only if ORIENT is exactly specified and field passes screening
Pure parallel	Not allowed	Not allowed

a. Targets which are 1 magnitude or more fainter than the limits in the screening tables will automatically pass screening. For targets which are within one magnitude of the screening limits after correction for extinction and slit losses, observers must provide a spectrum of the source at the intended observing wavelength. If such a spectrum is not available, the GO must request an orbit for a pre-qualification exposure, during which the target spectrum must be determined by observing in an allowed configuration (see "MAMA Bright Object Limits" on page 97 for more details).

b. For imaging observations, screening cannot be automatically performed due to the faintness of the safe limits and the observer must provide either a pre-existing UV image of the intended field of view or an optical image with a list of the magnitudes of all sources in that field. If those magnitudes exceed the O star safe limits, the observer must provide B-V colors or spectral types for all sources (see "MAMA Bright Object Limits" on page 97 for more details).

Policy for CCD Clear Pure Parallels

No pure parallels will be allowed in Cycle 7 using the `50CCD` clear aperture. This restriction is imposed to guard against accidental illumination of the CCD by a strong source of ultraviolet photons, which can cause a residual elevation in dark current which would impact subsequent observations (see "UV Light and the STIS CCD" on page 91).

Planetary Acquisitions in the First Part of Cycle 7

As described in "Acquisitions of Bright (V>5.4 arcsec^{-2}) Extended Objects" on page 116, targets which are extended on scales of 0.5 arcseconds or more and have surface brightness exceeding V=5.4 per square arcsecond will not be able to be acquired autonomously using on-board acquisitions during the first 6 months of Cycle 7. The only targets affected are some planetary targets, such as the Jovian moons or very bright comets. As needed, if the ~1 arcsecond of point and shoot accuracy is insufficient, they can be acquired using interactive acquisitions or the re-use offset capability during the early part of Cycle 7. Requests for interactive acquisitions should be justified in your Phase I proposal and an extra 30 minutes

in addition to the time for the science exposure should be added to your orbit time request. See the CP/Phase I Proposal Instructions for more details.

PART 2

User's Guide

The chapters in this part describe the basics of observing with STIS. Included are: a description of the instrumental layout and basic operation; the spectroscopic and imaging capabilities of STIS; the performance and limitations of its detectors; exposure time calculations; target acquisitions, and overhead and orbit request determination.

This part of the handbook is all you need to read to plan your Phase I STIS Proposal.

CHAPTER 3
Introduction to STIS

In This Chapter...

In this chapter we provide an overview of the capabilities and science applications of STIS. We describe the opto-mechanical layout and basic operation of the instrument and provide a flow chart and discussion to help you design a technically-feasible and scientifically-optimized STIS observing proposal.

Instrument Capabilities

STIS, the Space Telescope Imaging Spectrograph, uses two-dimensional detectors operating from the ultraviolet to the near-infrared (1150–11,000 Å). STIS has first order gratings covering this spectral range, which are designed for spatially resolved spectroscopy using a long slit, and echelle gratings, available only in the ultraviolet, and designed to maximize the free spectral range covered in a single spectrum for observations of point sources. The STIS Flight Software supports on-board target acquisitions and peakups to place science targets on slits and coronagraphic bars. The optics and detectors have been designed to exploit HST's high spatial resolution.

STIS can be used to obtain:

- Spatially resolved, long slit (or slitless) spectroscopy from the ultraviolet to the near infrared (1150–11,000 Å) at low to medium spectral resolution (R ~ 400–14000) in first order.
- Echelle spectroscopy at medium to high spectral resolution (R ~ 23,500–100,000), covering a broad instantaneous spectral range ($\Delta\lambda$ ~ 800 or 250 Å, respectively) in the ultraviolet (1150–3100 Å).

In addition to the these two prime capabilities, STIS also provides:

- A modest imaging capability using the solar-blind far ultraviolet MAMA detector (1150–1700 Å); using the solar-insensitive near ultraviolet MAMA detector (1700–3100 Å), and the optical CCD (2000–11,000 Å) through a small complement of narrow band and broad band filters.
- Objective prism spectroscopy (R ~1000–26) in the vacuum ultraviolet (1200–3100 Å).
- High time resolution ($\Delta\tau$ = 125 microseconds) imaging and spectroscopy in the ultraviolet (1150–3100 Å) and moderate time resolution ($\Delta\tau$ ~10 seconds) CCD imaging and spectroscopy in the optical and near IR (2000–11,000 Å).
- Coronagraphic imaging in the optical and near IR (2000–11,000 Å) and bar-occulted spectroscopy over the entire spectral range (1150–11,000 Å).

See Table 4.1, “STIS Spectroscopic Capabilities,” on page 34 and Table 5.1, “STIS Imaging Capabilities,” on page 48 for a full list of grating and filters, respectively.

STIS is a versatile instrument which will be able to address a broad range of scientific programs. For instance, the combination of high spectral resolution covering a large instantaneous wavelength range and low per pixel background will dramatically improve the efficiency of programs such as QSO (quasi-stellar object) and interstellar absorption line studies, where STIS’s wavelength coverage in a single exposure is 15 to 35 times that of GHRS. Studies of the dynamics of galactic nuclei and the kinematics of the emission line regions of active galaxies and diffuse Galactic nebulae will benefit from the ability to obtain spatially resolved spectra over a 50 arcsecond slit and from the high quantum efficiency in the optical provided by the charge-coupled device (CCD). The wide wavelength coverage of STIS will facilitate line ratios studies; for instance, use of the low resolution first order gratings spans the range 1150–11,000 Å in just four exposures. Slitless spectroscopy can provide emission line images of astronomical objects, and coronagraphic imaging and spectroscopy can reveal the nature of extended gaseous regions surrounding bright continuum sources.

Instrument Design

In this section we provide a high-level summary of the basic design and operation of STIS, concentrating on the information most relevant to the design of your HST observing proposal. Subsequent chapters provide more detailed information.

Detectors

STIS uses three large format (1024 x 1024 pixel) detectors (see Chapter 7 for more detail). STIS’s three detectors are:

- A Scientific Image Technologies (SITe) CCD, called the `STIS/CCD`, with 0.05 arcsecond square pixels, covering a nominal 51 x 51 arcsecond square field of view (FOV), operating from ~2000 to 11,000 Å.
- A Cs_2Te Multi-Anode Microchannel Array (MAMA) detector, called the `STIS/NUV-MAMA`, with 0.024 arcsecond square pixels, and a nominal 25 x 25 arcsecond square field of view (FOV), operating in the near ultraviolet from 1650 to 3100 Å.
- A solar blind CsI MAMA, the `STIS/FUV-MAMA`, with 0.024 arcsec pixels, and a nominal 25 x 25 arcsecond square FOV, operating in the ultraviolet from 1150–1700 Å.

The CCD

The CCD provides high quantum efficiency and good dynamic range in the near-ultraviolet through near-infrared. The CCD produces a time integrated image in the so-called `ACCUM` data taking mode. As with all CCDs, there is noise (*read noise*) and time (*read time*) associated with reading out the detector. Time resolved work with this detector is done by taking a series of multiple short exposures. The minimum exposure time is 0.1 sec, and the minimum time between successive identical exposures is 37 seconds for full frame and 11 seconds for subarray readouts. CCD detectors are capable of high dynamic range observations. The dynamic range, for a single exposure, ultimately is limited by the depth of the CCD full well (which in this case is ~120,000 to 170,000 e^-), which limits the total amount of charge (or counts) that can accumulate in any one pixel during any one exposure, without saturation. Cosmic rays will affect all CCD exposures; CCD observations should be broken into multiple exposures whenever possible, to allow removal of cosmic rays in post-observation data processing.

The MAMAs

The two MAMA detectors are *photon counting* detectors which provide a two-dimensional ultraviolet capability. They can be operated either in `ACCUM` mode, to produce a time integrated image, or in `TIMETAG` mode to produce an event stream with fast (125 μsec) time resolution. Doppler correction for the spacecraft motion is applied automatically on-board for data taken in `ACCUM` high spectral resolution modes. The shortest time between identical MAMA `ACCUM` mode exposures for Cycle 7 will be ~1.0 minute.

The STIS MAMA detectors are subject to both *scientific* and *absolute* brightness limits. At high local (>50 count sec^{-1} $pixel^{-1}$) and global (>300,000 counts sec^{-1}) illumination rates counting becomes nonlinear in a way that is not correctable. At only slightly higher illumination rates, the MAMA detectors are subject to damage. We have therefore defined local and global count rate limits, which translate to a set of configuration-dependent bright object limits. Sources brighter than these limits *cannot be observed in those configurations*.

The STIS IDT is working to enable better than 100:1 per resolution element (2 x 2 pixel) signal-to-noise ratio science with the MAMA detectors, and indeed MAMA detectors have achieved such signal-to-noise ratios in ground based studies. Ultimately, the signal-to-noise ratios possible in flight with the MAMAs

will be dependent on the time and wavelength dependence of their flat field performance and our ability to track that evolution with on-orbit calibrations. At the start of Cycle 7, signal-to-noise ratios much greater than ~30:1 per resolution element may not be routinely achieved with the MAMAs and observers requiring high signal-to-noise ratio MAMA observations may wish to consider employing special observing techniques (see also “High Signal-to-Noise Ratio Observations” on page 167). As we gain familiarity with the MAMA detectors and their in flight performance, we will work to devise techniques to provide the highest possible signal-to-noise ratios, within the constraints of the calibration program (see also “Summary of Expected Accuracies” on page 319).

STIS Physical Configuration

The STIS optical design includes corrective optics to compensate for HST’s spherical aberration, a focal plane slit wheel assembly, collimating optics, a grating selection mechanism, fixed optics and focal plane detectors. An independent calibration lamp assembly can illuminate the focal plane with a range of continuum and emission line lamps. A simplified schematic showing major detectors and mechanisms, and a medium echelle mode light path, is shown in Figure 3.1.

Figure 3.1: Simplified STIS Optical Design

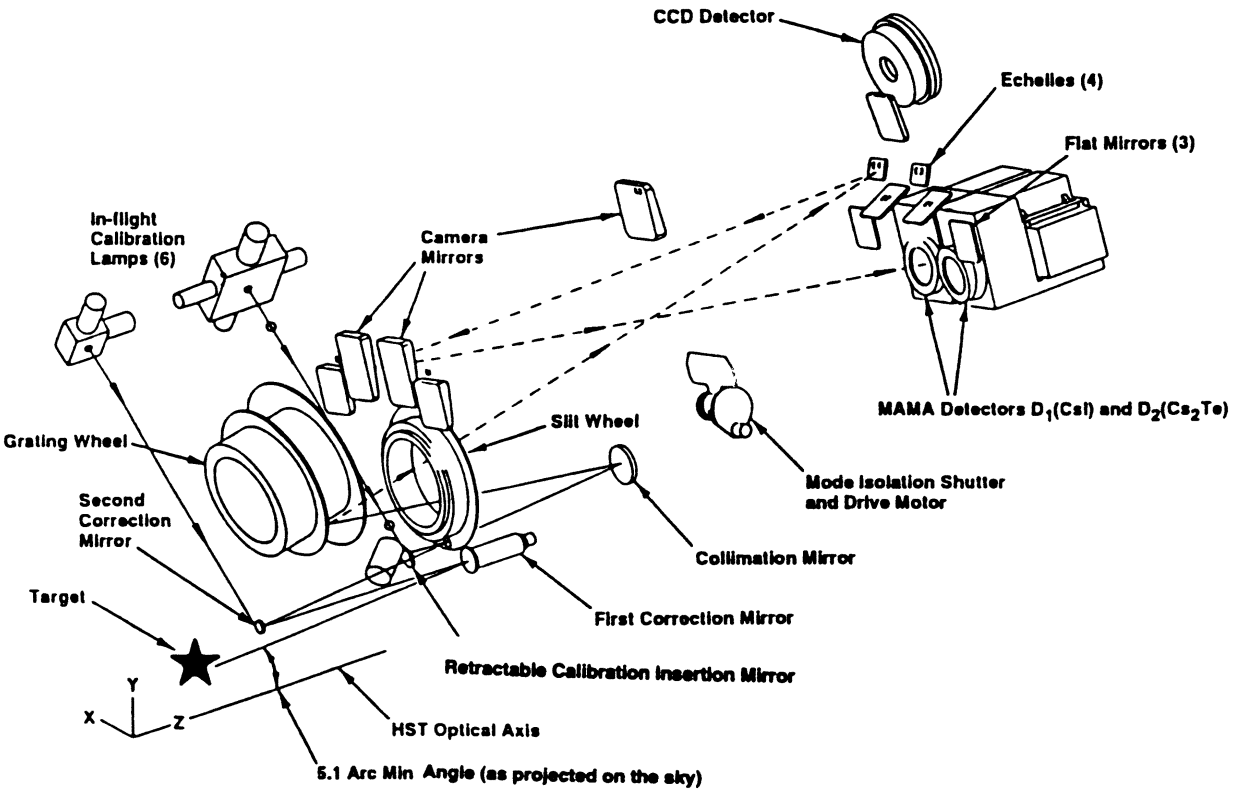

STIS Instrument Axes

Slit and Grating Wheels

The *slit wheel* contains apertures and slits for spectroscopic use and the clear, filtered, and coronagraphic apertures for imaging. The slit wheel positioning is repeatable to very high precision; +/- 7.5 and 2.5 milli-arcseconds in the spatial and spectral directions, respectively.

The *grating wheel*, or so called Mode Selection Mechanism (MSM), contains the first order gratings, the cross disperser gratings used with the echelles, the prism, and the mirrors used for imaging. The MSM is a nutating wheel which can orient optical elements in three dimensions. It permits the selection of one of its 21 optics as well as adjustment of the tip and tilt angles of the selected grating or mirror. As described in “Routine Wavecals” on page 24, the grating wheel exhibits non-repeatability which is corrected for in post-observation data processing using contemporaneously obtained comparison lamp exposures.

For some gratings, only a portion of the spectral range of the grating falls on the detector in any one exposure. These gratings can be scanned (tilted by the MSM) so that different segments of the spectral format are moved onto the detector for different exposures. For these gratings a set of pre-specified central wavelengths, corresponding to specific MSM positions, i.e., grating tilts, have been defined.

Calibration Lamp Systems

STIS has two independent calibration subsystems, the so-called HITM (Hole in the Mirror) system and the IM (Insert Mechanism) system. The HITM system contains two Pt-Cr/Ne line lamps, used to obtain wavelength comparison exposures and to illuminate the slit during target acquisitions. Light from the HITM lamps is projected through a hole in the second correction mirror (CM2), thus when the HITM lamps are used light from the external sky still falls on the detector. The IM system contains flat fielding lamps and a single Pt-Cr/Ne line comparison lamp. When the IM lamps are used, the Calibration Insert Mechanism (CIM) is inserted into the light path and all external light is blocked. Observers will be relieved to know that the ground system will *automatically* choose the right subsystem (see next section) and provide the necessary calibration exposures.

Basic Instrument Operations

Target Acquisitions and Peakups

Once the telescope acquires its guide stars, your target will be within ~1–2 arcseconds of the aperture center. For science observations taken through slits which are less than 3 arcseconds in either dimension, and for science observation taken using the coronagraphic bars, you will need to specify a target acquisition exposure to center the target in your chosen science aperture followed by one or more peakup exposures to refine the target centering of point or point-like sources. Acquisition exposures always use the CCD, one of the filtered or unfiltered apertures for CCD imaging, and a mirror as the optical element in the grating wheel. Peakup exposures use a science slit or coronagraphic aperture and can be taken with either the CCD or one of the MAMAs, and with either a mirror or a spectroscopic element in the grating wheel. Target acquisitions and acquisition peakups are described in detail in Chapter 8.

Routine Wavecals

Each time the MSM is moved to select a new optical element or to tilt a grating, the resulting spectrum is projected onto the detector with an error (lack of repeatability) of roughly plus or minus ~4-6 pixels. An internal calibration lamp observation (WAVECAL) will automatically be taken following each use of a new grating element or new scan position (grating tilt) in order to allow calibration of the zero point of the wavelength (dispersion) and spatial (cross dispersion) axes in the spectroscopic science data during post observation data processing. These routine, automatically-occurring, wavecal observations are expected to provide sufficient wavelength zeropoint accuracy for the vast majority of GO science; only if your science requires particularly accurate tracking of the wavelength zeropoints do you need to insert additional wavecal observations in your exposure sequence (see also “Wavecals” on page 151).

Data Storage and Transfer

At the conclusion of each exposure, the science data is read out from the detector in use and placed in STIS's internal buffer memory, where it is stored until it can be transferred to the HST data recorder (and thereafter to the ground). This design makes for more efficient use of the instrument, as up to 7 CCD or 4 MAMA full frame images can be stored in the internal buffer at any time. The frames can be transferred out of the internal buffer to the data recorder during subsequent exposures, so long as those exposures are longer than 3 minutes in duration.

STIS's internal buffer stores the data in a 16 bit per pixel format. This imposes a maximum of 65,536 data numbers per pixel. For the MAMA detectors this is equivalent to a limit on the total number of *photons* per pixel which can be accumulated in a single exposure. For the CCD, operating at a default gain of 4 e^-/data number, the CCD full well (and not the 16 bit buffer format) limits the photons per pixel which can be accumulated without saturating in a single exposure. See Chapter 11 for a detailed description of data taking with STIS.

Parallel Operations

STIS's three detectors do *not* operate in parallel to one another—only one detector can be used at any one time. Exposures with different STIS detectors can, however, be freely interleaved in an observing sequence, and there is no extra setup time or overhead in moving from one detector to another. The three detectors, sharing the bulk of their optical paths, also share a common field of view of the sky.

STIS *can* be used in parallel with any of the other three science instruments on HST. The figure below shows the HST field of view following the second servicing mission, with STIS and NICMOS installed. Policy for applying for parallel observing is described in the CP. We provide suggestions for designing parallel observations with STIS in "Parallel Observing with STIS" on page 169. While the STIS CCD can be used in parallel with another instrument, there are restrictions on the use of the MAMA detectors in parallel, as described in "Constraints on STIS Observing in Cycle 7" on page 14.

Figure 3.2: HST Field of View Following the Second Servicing Mission

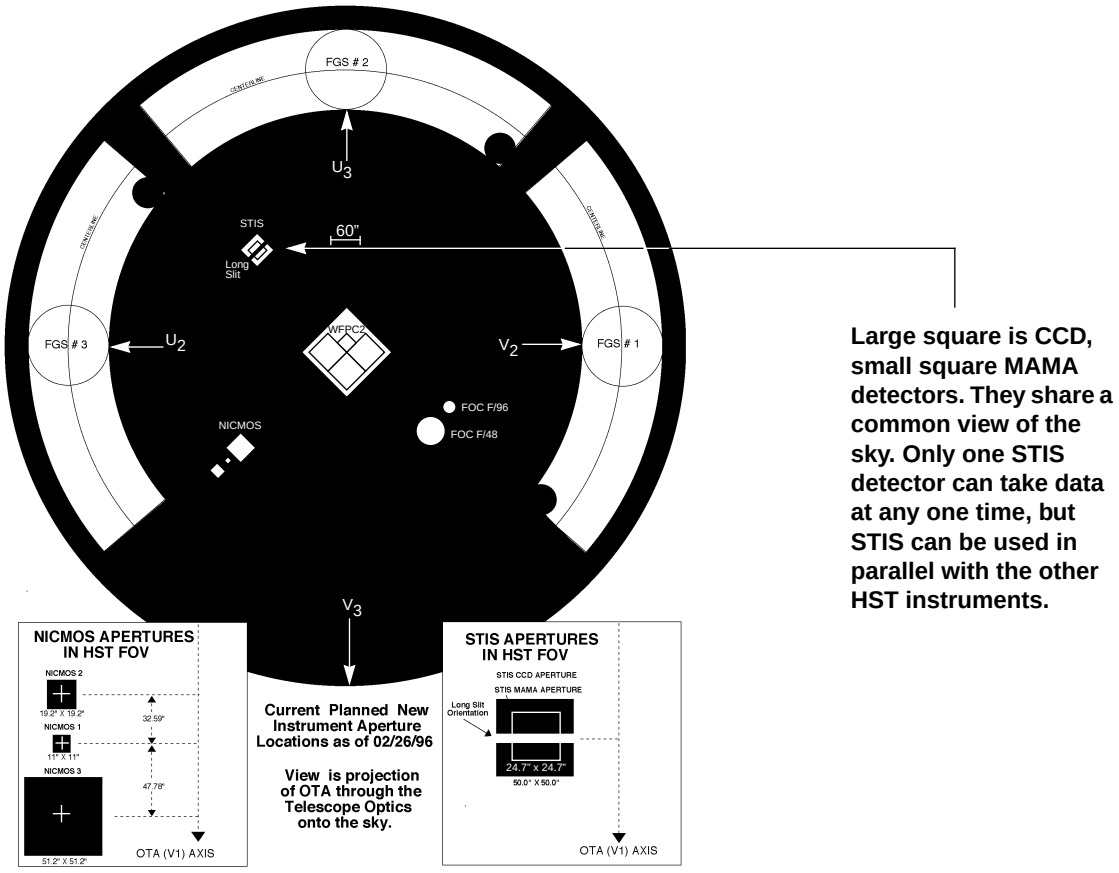

Typical STIS Observing Sequence

In the optical, STIS is expected to be used principally to observe extended objects, so long observations are expected to be the norm. The combination of high spatial resolution, spectral resolution, and low read noise from the CCD will encourage the taking of multiple (~20 minute) exposures; multiple to allow cosmic ray rejection. Observations with the MAMA detectors do not suffer from cosmic rays or read noise, but long integration times will often be needed to obtain sufficient signal-to-noise in the photon starved ultraviolet.

A typical STIS observing sequence is expected to consist of an initial target acquisition and acquisition peakup to center the target in a long or echelle slit, followed by a series of long (~10-40 minute) exposures with a single optical element at a given wavelength setting; it may also include a series of multiple long exposures taken with different gratings or with a single grating at a number of tilts. Observers will generally not take their own wavecal exposures; routine automatic wavecals will allow wavelength and spatial zero-points to be determined in post-observation data processing, requiring no input from the user.

Designing STIS Observations

In this section, we describe the sequence of steps you will need to take when designing your STIS observing proposal. The process is an iterative one, as you trade off between maximum spatial and spectral resolution, signal-to-noise, and the limitations of the instrument itself. The basic sequence of steps in defining a STIS observation (see Figure 3.3, below) are:

- Identify science requirements and select base STIS configuration to support those requirements.
- Estimate exposure time to achieve required signal-to-noise ratio and check feasibility, including saturation and bright object limits.
- Identify any additional non-science (target acquisition, peakup, and calibration) exposures needed.
- Calculate total number of orbits required, taking into account the overhead.

Identify Science Requirements and Define STIS Configuration

First and foremost, of course, you must identify the science you wish to achieve with STIS. Basic decisions you will need to make are:

- Spectroscopy or Imaging?
- Wavelength region(s) of interest?
- Spectral resolution and spectral coverage required?
- Nature of target—extended source (long slit or full aperture) or point source?

In addition you will need to establish whether you require:

- High signal-to-noise ratio.
- Time resolution.
- Coronagraphy.
- High photometric accuracy.

As you choose your science requirements and work to match them to the instrument's capabilities, it is important to keep in mind that those capabilities differ greatly depending on whether you are observing in the optical with the CCD, or in the ultraviolet, using the MAMA detectors. Tradeoffs are described in Table 3.1.

Spectroscopy

For spectroscopic observations, the base configuration you need is: grating (`SP_ELEMENT`), detector (`CONFIG`), central wavelength (`WAVELENGTH`), operating mode (`MODE=ACCUM` or `TIMETAG`), and slit (`APERTURE`). In Chapter

Figure 3.3: Defining a STIS Observation

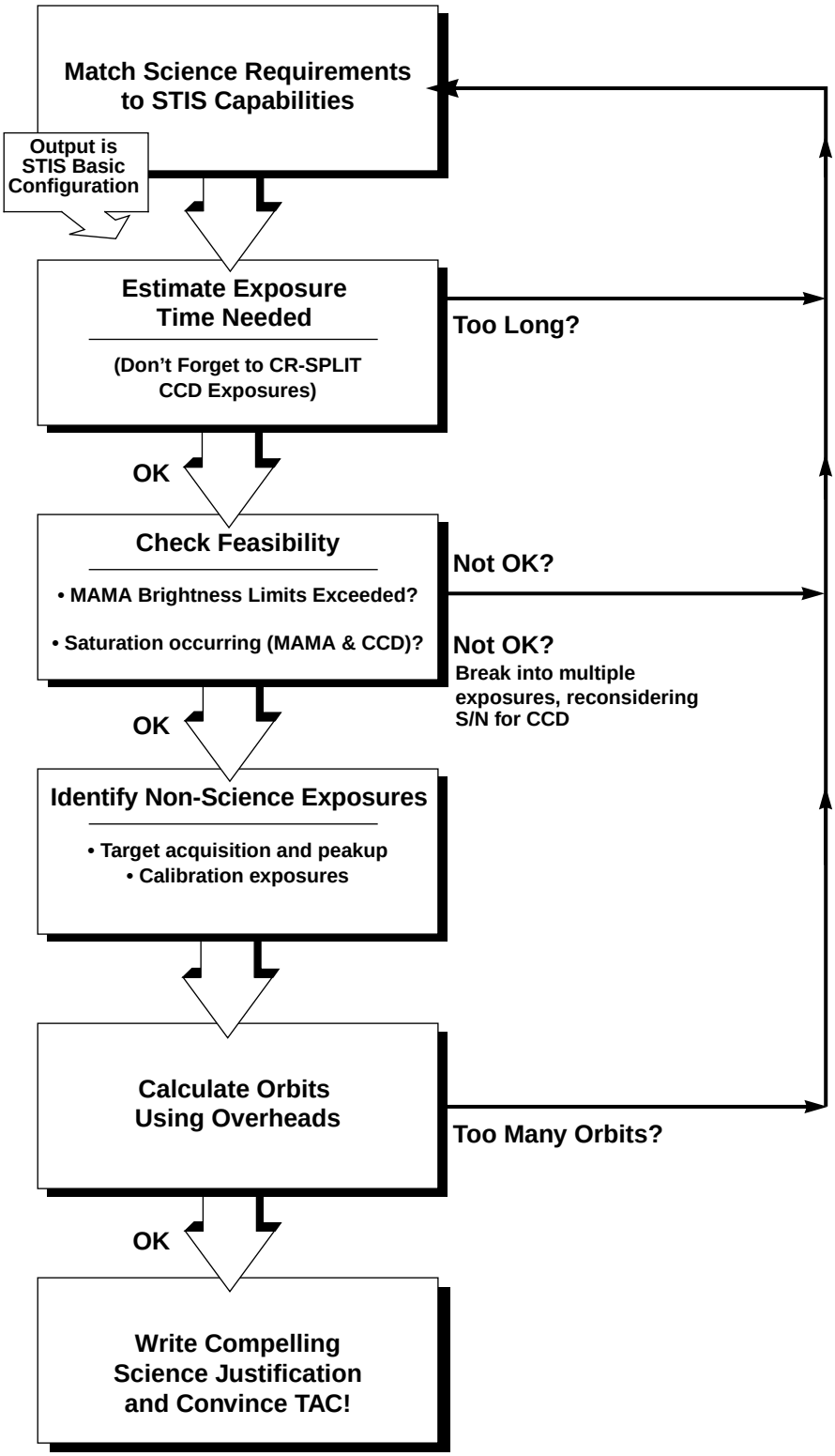

Table 3.1: Science Decision Guide

Decision	Affects	Tradeoffs
Wavelength regime	detector	2500-11000 Å — CCD 1650-3100 Å — NUV-MAMA 1150-1700 Å — FUV-MAMA
Spectral resolution	gratings and detector	R < 10,000 (first order) with CCD, NUV or FUV-MAMA, or R > 10,000 (echelle) with NUV or FUV-MAMA only
Free spectral range	gratings	Spectral range covered in a single exposure differs radically for different gratings.
Extended or point source	gratings	First order gratings designed for spatially resolved and point source observations. Echelle gratings designed for point source observations (long slit echelle spectroscopy will suffer order overlap).
Time resolution	detector	If time resolution <10 seconds required must use NUV or FUV-MAMA.
High signal-to-noise	detector	If high signal-to-noise required (S/N>30), use CCD or consider employing special techniques for MAMA observations (see page 167).
Coronagraphy	detector	*Bright object*[a] coronagraphy available with CCD only. Coronagraphic imaging available with CCD only. Barred coronagraphic spectroscopy available with all detectors.

a. The bright object limits for MAMA observations apply to coronagraphic observations as well, i.e., coronagraphic observations of targets which are too bright for the MAMA detectors are not allowed.

4, we provide detailed information about each of the spectroscopic grating modes of STIS.

Imaging

For imaging observations, the base configuration is detector (CONFIG), filter (APERTURE), and operating mode (MODE=ACCUM or TIMETAG). Chapter 5, presents detailed information about each of STIS's imaging modes.

Special Uses

We refer you to Chapter 12 if you are interested in any of the following special uses of STIS: time resolved work, planetary studies, coronagraphy, high signal-to-noise ratio or bright object observations, parallel observations, and slitless spectroscopy or extended source echelle observations.

Determine Exposure Time and Check Feasibility

Once you have selected your base STIS configuration, the next steps are to:

- Estimate the exposure time needed to achieve your required signal-to-noise ratio, given your source brightness.
- For observations using the MAMA detectors, assure that your observations do not exceed brightness (count rate) limits.
- For observations using the MAMA detectors, assure that for pixels of interest, your observations do not exceed the 65,536 accumulated counts per pixel per exposure limit imposed by the STIS 16 bit buffer.

- For observations using the CCD detector, assure that for pixels of interest, you do not exceed the per pixel saturation count limit of the CCD full well (for CCD observations with gain =4e^-/ADU, the full well limit supersedes the STIS buffer limit on counts per pixel).

To determine your exposure time requirements consult Chapter 6 where an explanation of how to calculate signal-to-noise and a description of the sky backgrounds are provided. To assess whether you are close to the brightness, signal-to-noise and dynamic range limitations of the detectors, refer to Chapter 7.

If you find that the exposure time needed to meet your signal-to-noise requirements is too great, or that you are constrained by the detector's brightness or dynamic range limitations, you will need to adjust your base STIS configuration. Table 3.2 below, summarizes the options available to you and steps you may wish to take as you iterate to select a STIS configuration which is both suited to your science and technically feasible.

Table 3.2: Feasibility Guide

Action	Outcome	Recourse
Estimate exposure time	If too long -> re-evaluate instrument configuration.	Reduce resolving power, or use wider slit, or change detectors and wavelength regime.
Check full well limit for CCD observations	If full well exceeded and you wish to avoid saturation-> reduce time per exposure.	Divide total exposure time into multiple, short, exposures.[a,b]
Check bright object limits for MAMA observations	If source is too bright -> re-evaluate instrument configuration.	Increase spectral resolution, or choose narrower slit, or use neutral density filter, or change detectors and wavelength regime.
Check 65536 counts per pixel limit for MAMA observations	If limit exceeded -> reduce time per exposure.	Divide total exposure time into multiple, short exposures.[a,b]

a. Splitting CCD exposures affects the exposure time needed to achieve a given signal-to-noise ratio because of the read noise. Splitting MAMA exposures has no effect since there is no read noise with the MAMAs.
b. Splitting an exposure into multiple exposures increases the overheads, slightly reducing on-source time.

Identify Need for Non-Science Exposures

Having identified your desired sequence of *science* exposures, you need to determine what *non-science* exposures you may require to achieve your scientific goals. Specifically, you need to:

- Determine which (if any) target acquisition and acquisition peakup exposures will be needed to center your target in your aperture to the accuracy required for your scientific aims (e.g., you may wish to center the nucleus of a galaxy in the 52 x 0.1 arcsecond slit and orient the long axis of the slit along the major axis of the galaxy to some accuracy).
- If you require more accurate wavelength zeropoints than the routine calibrations expect to provide, you can insert additional comparison lamp exposures (`TARGET=WAVE`) at shorter intervals or of longer duration than the routine, automatic `WAVECAL` observations.

To assess your acquisition needs, refer to Chapter 8. To determine how to specify a specific orientation for the STIS long slit, refer to “Fixing Orientation on the Sky” on page 157. To determine your internal calibration exposure needs, refer to “GO Wavecals” on page 152.

Determine Total Orbit Request

In this, the final step, you lay all your exposures (science and non-science, alike) into orbits, using tabulated overheads, and determine the total number of orbits you require. Refer to “Orbit Use Determination Examples” on page 127 when performing this step. If you are observing a point source and find your total time request is significantly affected by data transfer overheads (which will be the case *only* if you are taking many separate exposures under 3 minutes), you should consider the use of subarrays to lessen the data volume impacts. Subarrays are described on page 148.

At this point, if you are happy with the total number of orbits required, you’re done! If you are unhappy with the total number of orbits required, you can, of course, re-iterate, adjusting your instrument configuration, lessening your acquisition requirements, changing your signal-to-noise or wavelength requirements, until you find a scenario which allows you to achieve (and convince the Telescope Allocation Committee (TAC) of the merits of) your science goals with STIS.

CHAPTER 4
Spectroscopy

In This Chapter...

In this chapter, we provide information to help you choose the most appropriate spectroscopic configuration for your science application. We briefly describe the properties of each grating mode and their counterpart slits, and provide an overview of their scientific uses. Curves of sensitivity, exposure time as a function of source brightness to achieve a given signal-to-noise ratio and avoid saturation are referenced in this chapter, but presented in Chapter 13, as are the central wavelengths and wavelength ranges for the scanned gratings and the detailed aperture throughputs and line spread functions.

For MAMA spectroscopy there are bright object limits. We describe these limits here, and again in detail in Chapter 7. Tables of the MAMA spectroscopic bright object limits are presented in Chapter 13.

Overview

There are 15 spectroscopic modes, summarized in Table 4.1. These include low and intermediate resolution first order modes designed to be used with a complement of long slits covering the entire wavelength range, and intermediate and high resolution echelle modes which have been optimized for point source observations through short echelle slits and are available only in the ultraviolet (see Figure 4.1).

Table 4.1: STIS Spectroscopic Capabilities

Grating	Spectral Range (Å)		Spectral Resolution		# Prime Tilts[a]	Detector	reference material page	Slits (apertures)[b, c, d, e]
	Complete	Per Tilt	Scale Δλ (Å per pixel)	Resolving Power (λ/2Δλ)				
CCD First Order Spectroscopy								
G750L	5240-11490	5030	4.92	535-1170	2	CCD	179	52X0.1 52X0.2 52X0.5 52X2 52X0.2F1
G750M	5450-11150	570	0.56	4870-9950	11	CCD	184	
G430L	2900-5700	2900	2.73	530-1040	1	CCD	188	
G430M	3025-5615	286	0.28	5330-10270	10	CCD	192	
G230LB	1685-3065	1380	1.35	615-1135	1	CCD	196	
G230MB	1635-3190	155	0.15	5550-10335	11	CCD	201	
MAMA First Order Spectroscopy								
G230L	1570-3180	1610	1.58	600-1--5	1	NUV-MAMA	206	
G230M	1640-3175	90	0.09	9110-17500	19	NUV-MAMA	210	
G140L	1150-1736	610	0.60	935-1440	1	FUV-MAMA	214	
G140M	1145-1740	55	0.05	11500-17400	12	FUV-MAMA	218	
MAMA Echelle Spectroscopy								
E230M	1575-3110	800	λ/60,000	30000	2	NUV-MAMA	222	0.2X0.2, 0.2X0.06
E230H	1625-3150	267	λ/228,000	114000	6	NUV-MAMA	226	0.1X0.2, 0.1X0.09
E140M	1150-1735	620	λ/91,700	45800	1	FUV-MAMA	230	0.2X0.2, 0.2X0.06
E140H	1150-1700	210	λ/228,000	114000	3	FUV-MAMA	234	0.2X0.2, 0.2X0.09
MAMA Prism Spectroscopy								
PRISM	1150-3100	1950	1.2-120	1000-26	2	NUV-MAMA	238	25MAMA (clear)

a. Number of exposures at distinct tilts needed to cover spectral range of grating, with 10% overlap between spectra.
b. Naming convention gives dimensions in arcseconds of slit. For example `52X0.1` indicates the slit is 52 arcsec long in the cross-dispersion direction and 0.1 arcsec wide in dispersion. The `F` (e.g., in `52X0.2F1`) indicates that it is the fiducial on the bar which is specified for coronographic spectroscopy.
c. For the MAMA first order modes, only ~ 25 arcseconds of the long slit projects on the detector.
d. Full aperture clear (`50CCD` or `25MAMA`), longpass filtered (`F25QTZ` or `F25SRF2` in UV), and neutral density filtered slitless spectroscopy is also supported with the first order and echelle gratings.
e. A 6 arcsec long slit (`6X0.2`) is also supported for use with the echelle gratings, but with order overlap.

Figure 4.1: Sample Uncalibrated Spectra (distortion is exaggerated)

a.) Uncalibrated Long Slit Spectrum of Point Source

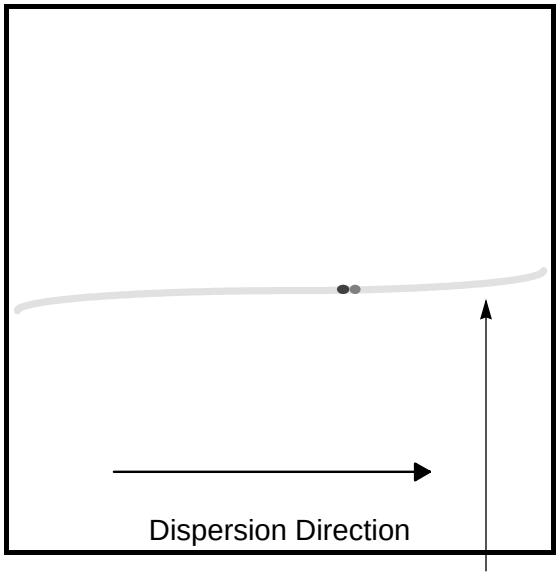

Point source showing continuum and two strong emission lines

b.) Uncalibrated Long Slit Spectrum of Diffuse Source

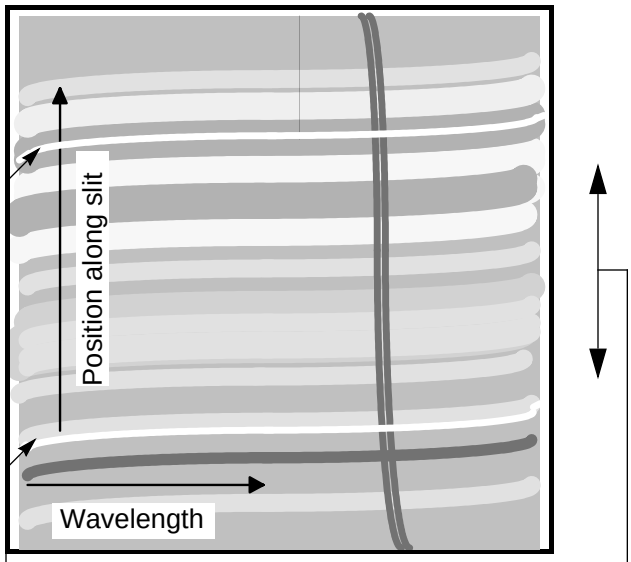

Strong doublet emission line

Bars on long slit

Spatially varying continuum

c.) Echelle Spectrum of Point Source Showing Multiple Orders on One Image

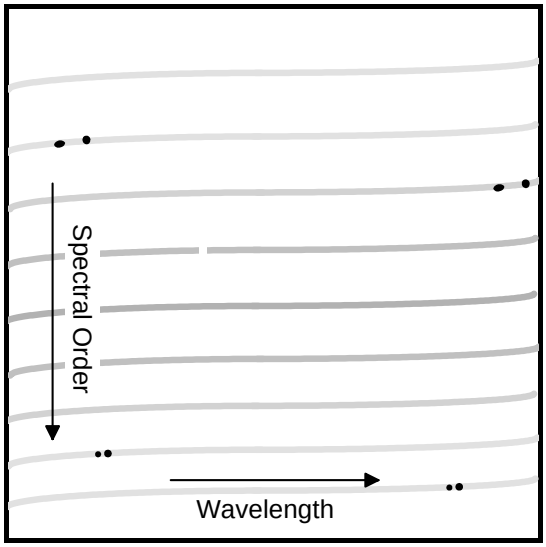

Two strong emission lines. Adjacent orders have ~10% overlap in wavelength so lines appearing at the start of one order will also appear at the end of the next.

d.) Echelle Spectrum of Diffuse Source

Absorption lines at wavelength near center of order. Continuum from extended object fills short slit.

Throughputs

To illustrate the broad wavelength coverage provided by STIS, and the relative throughputs achievable across STIS's wavelength regime, we show, in Figure 4.2, the system throughput of the four low resolution first order modes on a single plot (where the throughput is defined as the end to end effective area divided by the geometric area of a filled, unobstructed, 2.4 meter aperture). To allow you to judge the relative throughputs of different spectroscopic configurations, we plot, in Figure 4.3, the efficiency of all grating modes for the four primary wavelength regimes on a common plot. These plots allow you to gauge the relative efficiencies of STIS in different configurations.

Figure 4.2: System Throughput of STIS's First Order Low Resolution Grating Modes

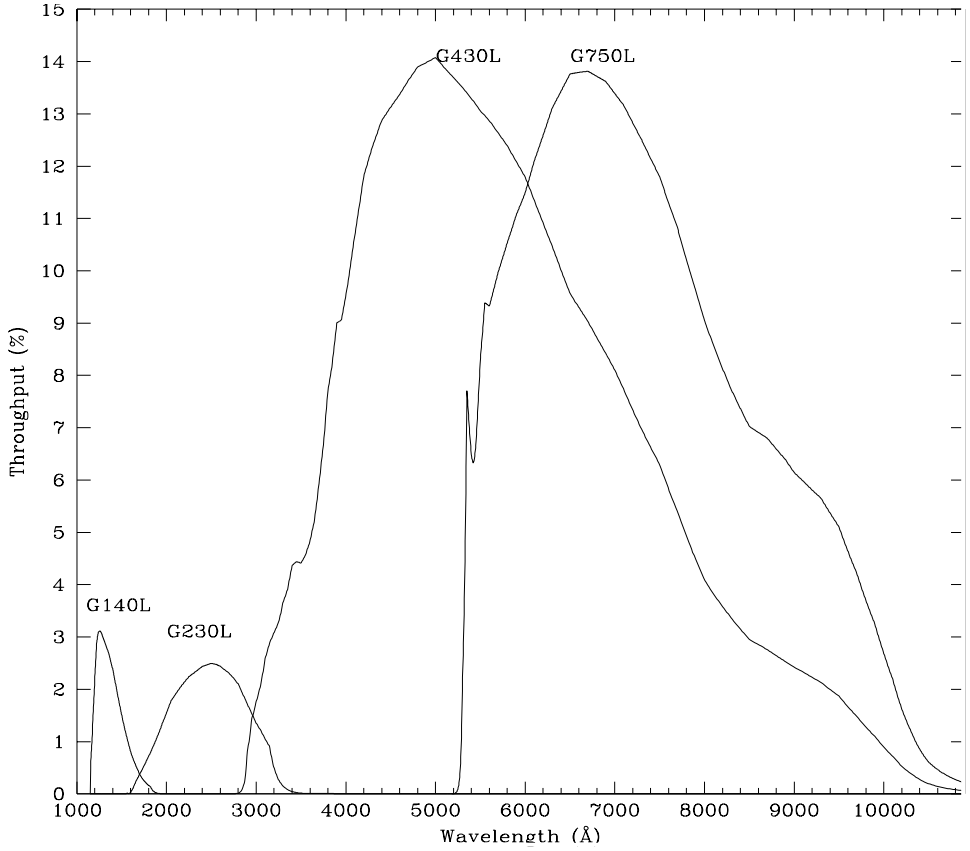

Figure 4.3: System Throughput of STIS's Grating Modes

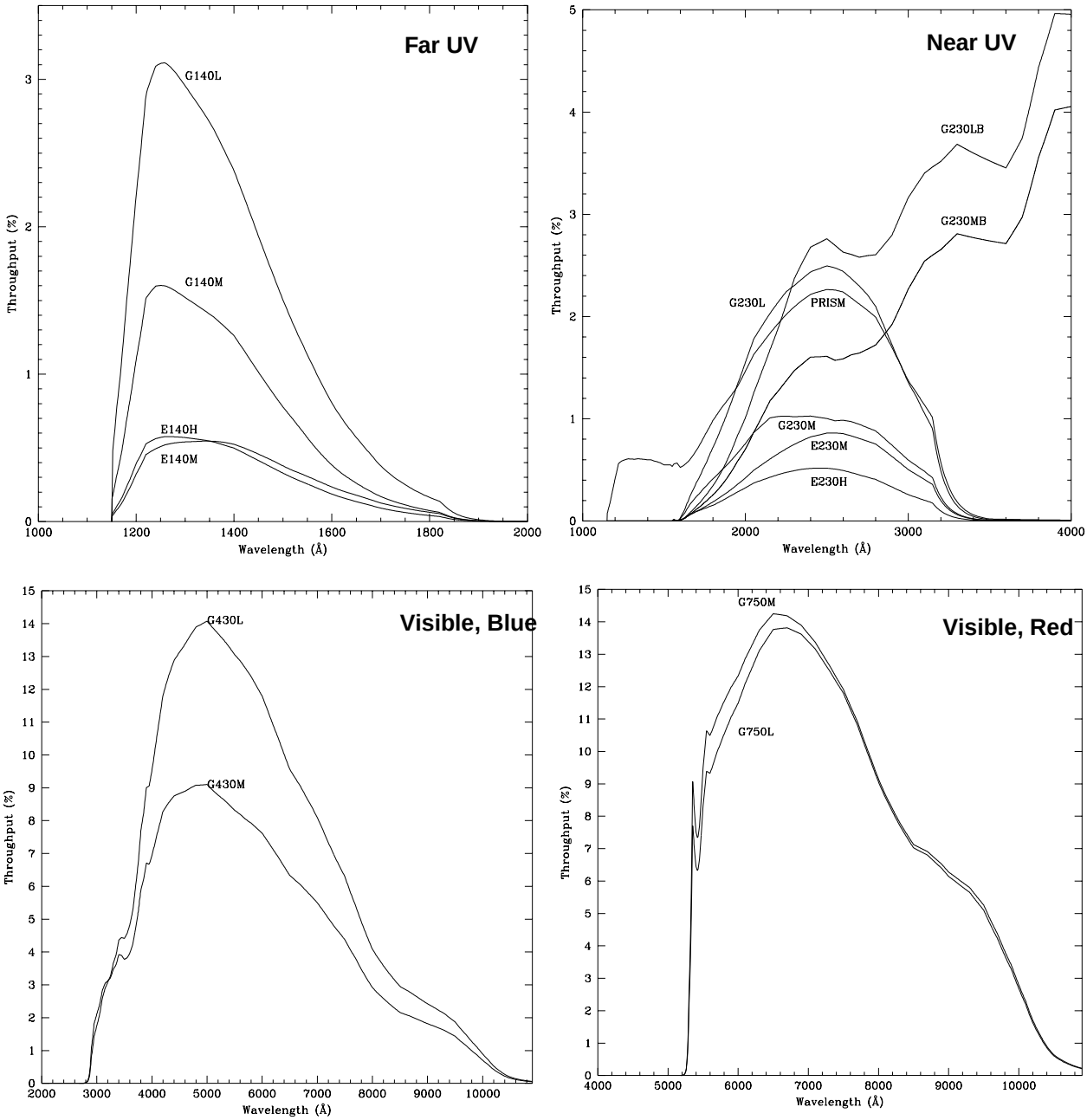

Limiting Magnitudes

In Table 4.2 below, we give the (anticipated) A type star V magnitude reached during a 1 hour integration which produces a signal-to-noise ratio of 10 in the continuum per spectral resolution element at the peak of the grating response, where we have integrated over the PSF in the cross dispersion direction, and assumed a wide slit which transmits 80% of the light from the source.

Table 4.2: Limiting A Star V Magnitude Achieved in a One Hour, signal-to-noise ratio =10 integration

Grating	Magnitude	Grating	Magnitude
G750L	21.0	G140L	17.9
G750M	18.6	G140M	14.5
G430L	21.6	E230M	13.7
G430M	18.8	E230H	11.8
G230LB	17.7	E140M	12.3
G230MB	14.8	E140H	11.2
G230L	18.9	PRISM	21.2 @ λ = 2300
G230M	14.9		

Signal-to-Noise Ratios

In Chapter 13 on page 175, we present, for each grating mode, plots of exposure time versus flux (and magnitude) to achieve a signal-to-noise ratio of 10 at several wavelengths. These plots are very useful for getting an idea of the exposure time you need to perform your science.

Saturation

Both CCD and MAMA imaging observations are subject to saturation at high total accumulated counts per pixel, the CCD due to the depth of the full well, and the MAMA, due to the 16-bit format of the MAMA buffer memory. The nature of the saturation for CCD and MAMA spectroscopic observations is described in “CCD Saturation: the CCD Full Well” on page 90 and “MAMA Saturation—Overflowing the 16 Bit Buffer” on page 95, respectively. Chapter 13 contains plots of the time to saturation as a function of source brightness for each grating mode. For the CCD, these plots also show where the signal plus background exceeds twice the read noise squared (i.e., where the observations are no longer read noise limited).

MAMA Bright Object Limits

The MAMA detectors are subject to:

- Absolute bright object limits, above which targets cannot be observed.
- Science limits, above which the MAMA response becomes non-linear and photometric information is lost.

We direct MAMA observers to the discussion presented in “MAMA Bright Object Limits” on page 97. For summary tables of absolute bright object limits for all spectroscopic modes, see “MAMA Spectroscopic Bright Object Limits” on page 254. It is the observer’s responsibility to be sure they do not exceed the MAMA bright object limits.

Scanned Gratings: Prime and Secondary Positions

For the intermediate resolution gratings only a portion of the full spectral range of the grating falls on the detector in any one exposure and the gratings must be scanned (tilted), with a separate exposure taken at each tilt, in order to cover the full spectral range (see Figures 4.4 and 4.5 below). Accordingly, for these scanned gratings, a single exposure at a given wavelength or a series of exposures at different wavelengths to cover a larger wavelength range, can be selected by the user. You must choose either prime or secondary settings. The prime settings cover the full spectral range with 10% overlap between spectra taken at adjacent settings. The secondary settings cover selected absorption or emission lines and may be more convenient to use in some applications. We expect the photometric and spectral calibration accuracy to be higher for the prime settings than the intermediate settings, as calibrations for intermediate settings will be inferred from those taken at prime settings. The central wavelengths, and corresponding minimum and maximum wavelengths, are presented in the individual grating sections in Chapter 13.

Figure 4.4: Scanned First Order Gratings

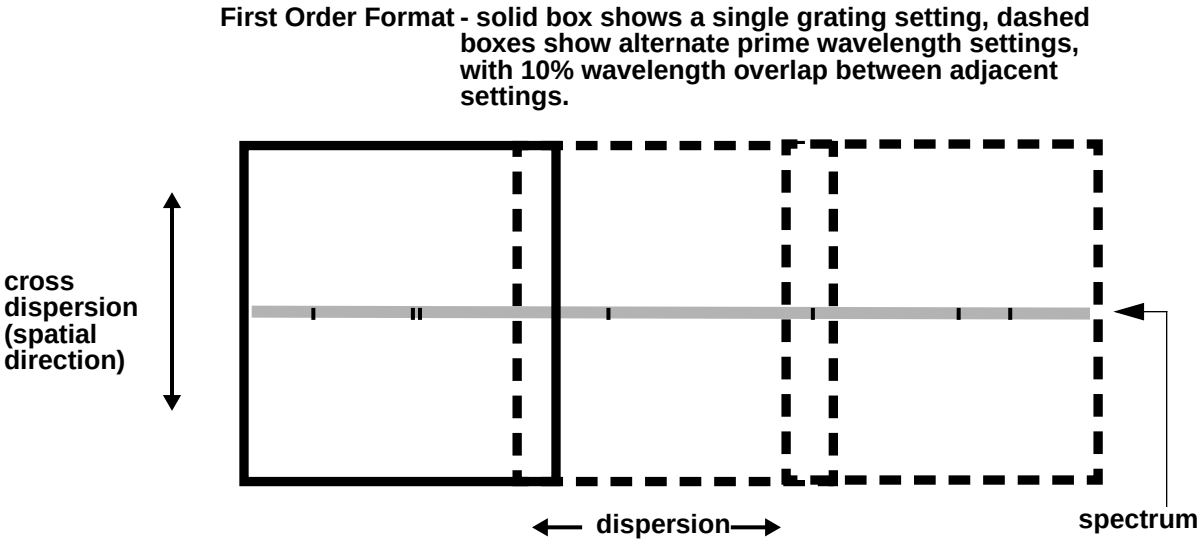

Figure 4.5: Scanned Echelle Gratings

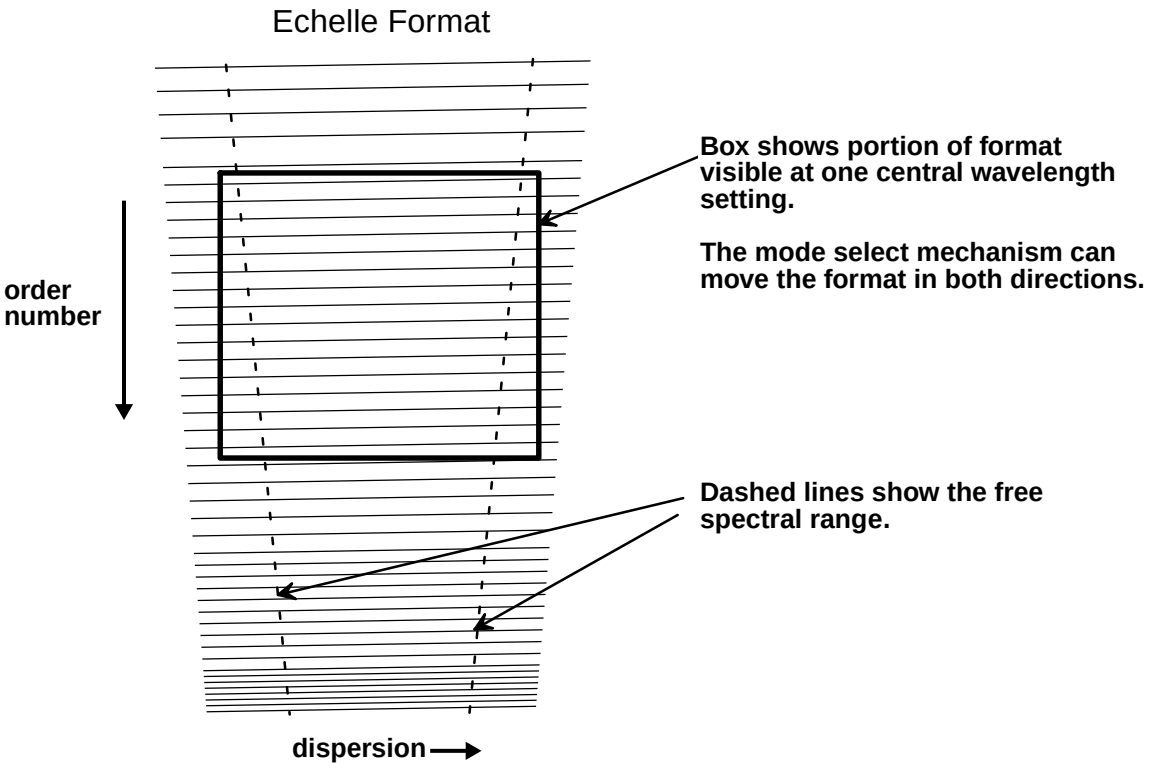

Cross-Over Regions

In the near UV, where the CCD has comparable sensitivity to the NUV-MAMA, you may want to consider using the G230LB or G230MB gratings with the CCD instead of the more standard G230L and G230M gratings. You will get improved throughput out to ~2,500 Å, a large slit length, and use of the CCD rather than the MAMA (see pages 197 and 202).

First Order Long Slit Spectroscopy

Gratings for First Order Spectroscopy

There are 10 first order gratings available for long slit spectroscopy, covering resolving powers from ~500–14000 from the UV at 1150 Å through the near-IR at ~ 11,000 Å. The wavelength coverage and kinematic resolution of the first order gratings are summarized in Figure 4.6. Briefly:

- For resolutions of ~500 km sec^{-1} use:
  - G140L from ~1150–1700Å.
  - G230L (MAMA) or G230LB (CCD) from ~1650–3100 Å.
  - G430L from ~3050–5550Å.
  - G750L from ~5500–11000Å.
- For resolutions of ~50 km sec^{-1} use:
  - G140M from ~1150–1700Å.
  - G230M (MAMA) or G230MB (CCD) from ~1650–3100Å.
  - G430M from ~3050–5550 Å.
  - G750M from ~5500–11000Å.

Figure 4.6: Wavelength Coverage Versus Kinematic Resolution of First Order Modes. The hatches indicate the wavelength coverage at a single scan setting.

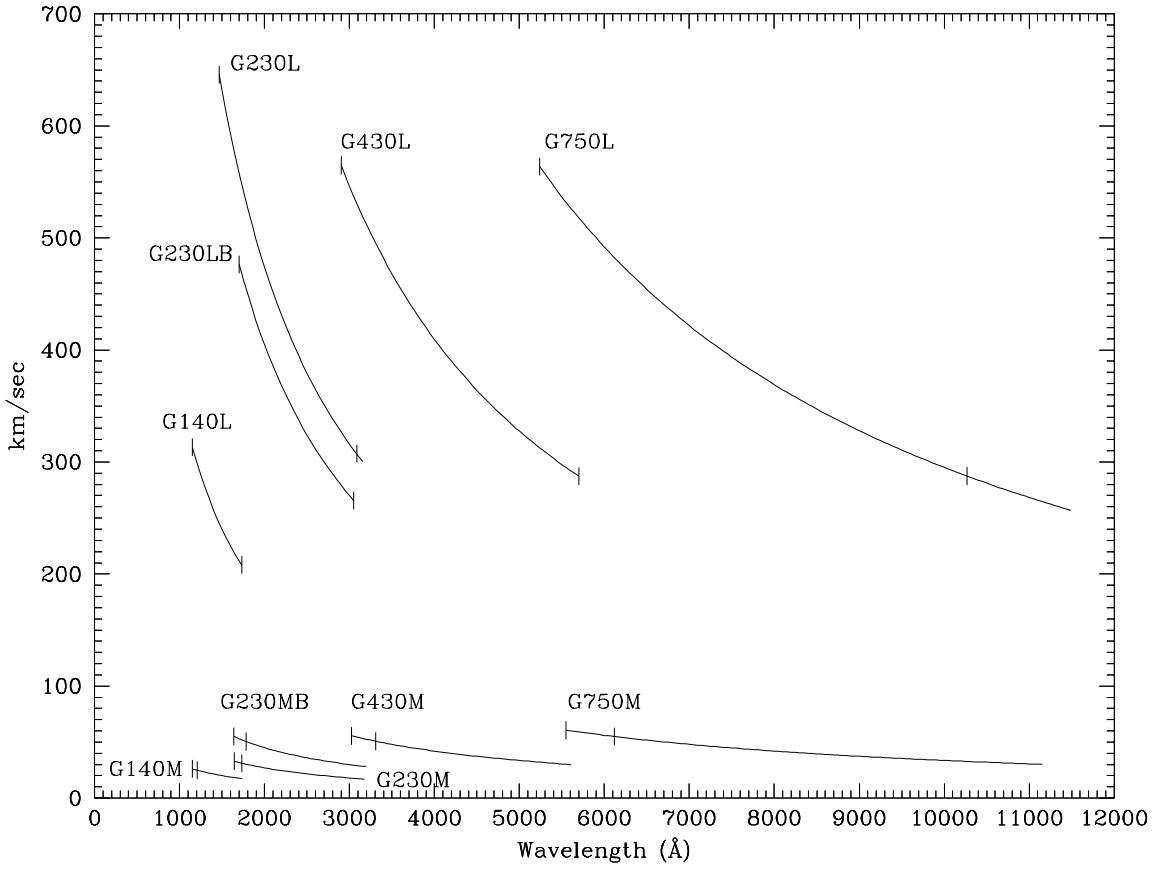

Slits for First Order Spectroscopy

Supported for use with the first order gratings are long slits of width 0.1, 0.2, 0.5, and 2.0 arcseconds (in dispersion) and 51 arcsecond length (as projected on the CCD detector) or 25 arcsecond length (projected on the MAMA detectors) for the MAMA low resolution first order gratings (G230L and G140L) and 28 arcseconds for the MAMA intermediate resolution first order gratings (G230M and G140M)[1]. The narrow 0.1 arcsecond wide slit provides the maximum spectral and spatial resolution. The 0.2 arcsecond wide slit is the general utility slit we expect to be used most often; it provides a good compromise between resolution and throughput. Finally, we expect the wider 0.5 and 2.0 arcsecond wide slits to be used predominantly in photon-starved ultraviolet observations of extended sources, but provide them for use in the optical as well to assure that line ratios studies with coverage from the ultraviolet to the optical can sample the same physical region on the sky.

1. The MAMA first order modes have varying spatial plate scales; see page 248.

The first order gratings can also be used “slitless” to obtain two-dimensional emission line images. Slitless spectroscopic data will not be fully calibrated by the STScI pipeline, and will require extensive post-observation data processing by the user as ambiguous overlap of wavelengths from different parts of sources can occur in the image (see “Slitless First Order Spectroscopy” on page 161).

Detailed First Order Spectroscopic Information

The properties of each of the first order gratings are described in detail, grating by grating, in Chapter 13; see the second to last column of Table 4.1 on page 34 for easy reference to the appropriate page for each grating.

The detailed properties of the long slits (e.g., throughputs as a function of wavelengths, line spread functions as a function of wavelength), plate scales and encircled energies for the first order gratings are presented in “First Order Slits, LSFs, Scales and Encircled Energies” on page 242.

Echelle Spectroscopy in the Ultraviolet

Echelle Gratings

There are four echelle grating modes, providing spectroscopic coverage from 1150 Å to 3100 Å at resolutions from R~25,000 to R~110,000. Through simultaneous observation of multiple orders, they are designed to maximize the spectral coverage achieved in a single exposure of a point source. Figure 4.7 summarizes the wavelength coverage and kinematic resolutions of the echelle gratings. In short:

- For ~10 km sec^{-1} resolution use:
  - E140M from 1150–1700Å.
  - E230M from 1650–3100Å.
- For ~2.5 km sec^{-1} resolution use:
  - E140H from 1150–1700Å.
  - E230H from 1650–3100Å.

Figure 4.7: Echelle Wavelength Coverage Versus Kinematic Resolution. Hatches indicate wavelength coverage at a single scan setting.

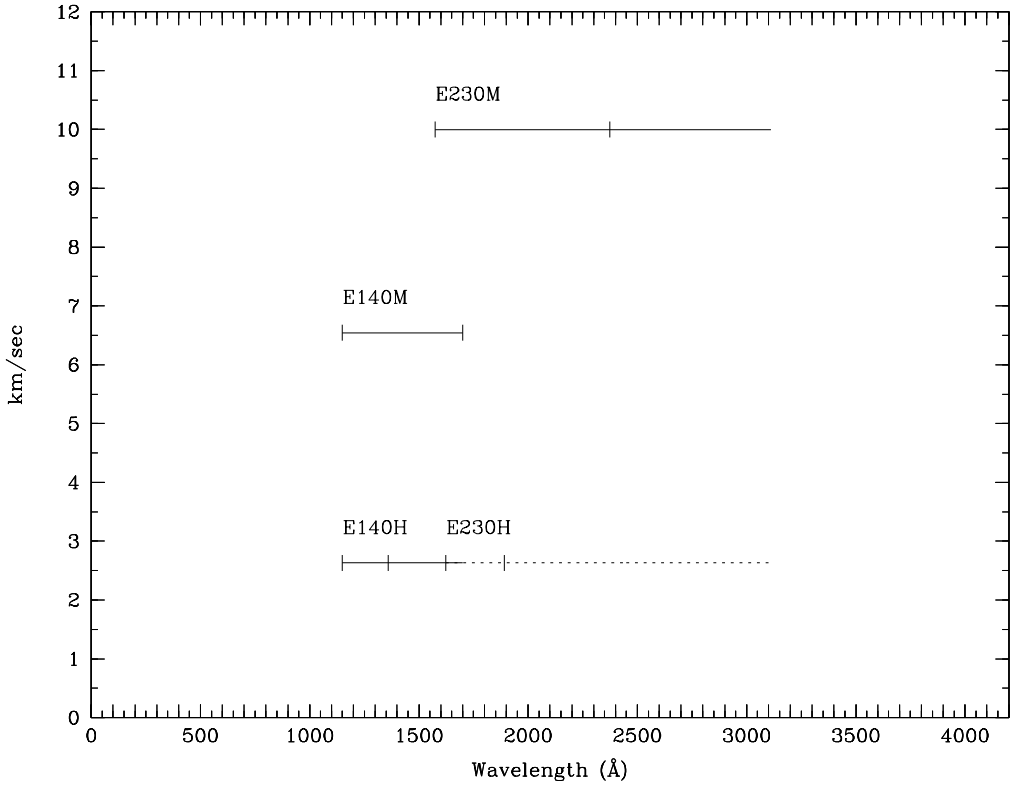

Slits for Echelle Spectroscopy

Short echelle slits, which ensure order separation, are available for use with the echelle gratings. Since the magnification and order separation varies across the echelle gratings, the echelle slits are matched explicitly to the grating mode. For each echelle grating mode a short slit of width 0.2 arcseconds is provided, along with a slit whose width matches two pixels in the dispersion direction, either 0.09 or 0.06 arcseconds, depending on the echelle grating.

Although we don’t recommend routine use, the echelle gratings can be used with a long slit (6 x 0.2 arcseconds) to obtain echelle spectroscopy of extended objects. Long slit echelle spectroscopy is more complicated, as order overlap will occur. Long slit echelle data will not be calibrated by the STScI pipeline, and will require more extensive post-observation data processing by the user since ambiguous overlap of wavelengths from different parts of sources will occur in the image (see “Long Slit Echelle Spectroscopy” on page 163 if you are considering such observations).

Detailed Echelle Information

The properties of each of the echelle gratings are described in detail, grating by grating, in Chapter 13; see the second to last column of Table 4.1 on page 34 for easy reference to the appropriate page for each grating.

The detailed properties of the echelle slits (e.g., throughputs as a function of wavelengths and line spread functions as a function of wavelength), the plate scales and the encircled energies for the echelle modes are presented in “Echelle Slits, LSFs, Scales, and Encircled Energies” on page 248.

Objective Prism Spectroscopy

The STIS PRISM is used with the STIS/NUV-MAMA and provides spectra from 1150-3100 Å at resolving powers of ~1000 in the ultraviolet declining to ~25 in the optical. A highly idealized schematic of a STIS objective prism observation of a star cluster is shown in Figure 4.8. This illustrates the power of the prism mode to simultaneously provide spectra covering a wide wavelength range of many objects in single field of view.

Figure 4.8: Schematic Example of a PRISM Image of a Star Cluster

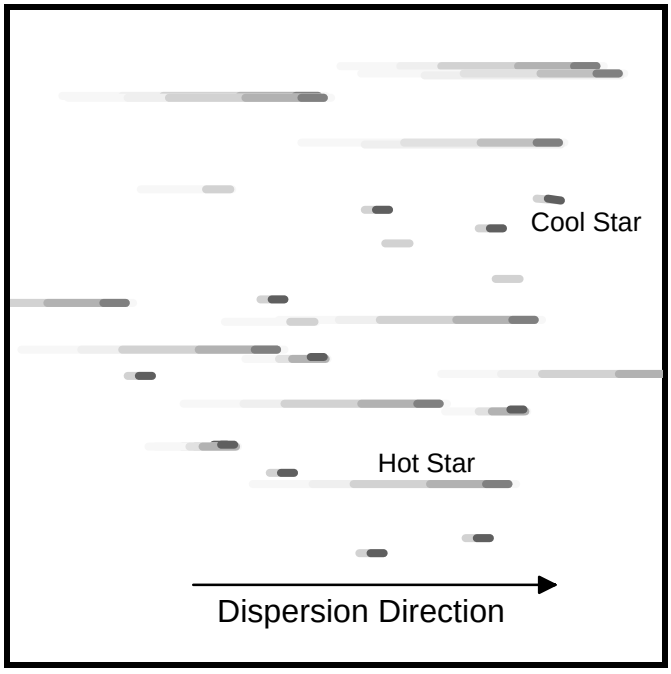

The PRISM can be used with the clear MAMA aperture (25MAMA) or with either of the two longpass ultraviolet filtered apertures (F25SRF2 or F25QTZ) to provide a 25 x 25 arcsecond field of view (see also “F25SRF2 - NUV-MAMA - longpass” on page 278 and “F25QTZ - NUV-MAMA - longpass” on page 275). The longpass filter F25SRF2 blocks Geocoronal Lyman α 1216 Å and the

F25QTA longpass filter blocks both geocoronal Lyman α and geocoronal OI 1301 Å, thereby significantly reducing the background from these lines (which is otherwise spread throughout the image), at the price of losing the short wavelength range of the spectrum.

Observers will generally want to obtain an *image* of the field they are taking a prism spectrum of, to allow them to post-facto determine the centering of the objects in their prism data. Because the prism and the mirrors used for imaging are both in the Mode Select Mechanism, zero point shifts will occur between the prism and image data (see “Slit and Grating Wheels” on page 23). These can be taken out by taking a wavecal image of a short slit with the mirror in place. For Phase I planning purposes, GOs should allot the additional time for the image plus an additional 5 minutes overhead for this extra zero-point wavecal image. The Phase II proposal instructions will contain information about how to assure the proper calibration is taken in these cases.

Note that PRISM spectroscopy produces images in which, a priori, the wavelength at a given pixel is not known, and in which source-dependent overlap of spectra can occur. For these reasons, PRISM spectroscopic data will not be calibrated automatically by the STScI pipeline. Instead, users will have to reduce and analyze their data off-line.

CHAPTER 5
Imaging

In This Chapter...

In this chapter we describe the imaging capabilities of STIS. Each imaging mode is described, and plots of throughput and comparisons to the capabilities of WFPC2 and FOC are provided. Curves of sensitivity, exposure time as a function of source brightness to achieve a given signal-to-noise ratio and time to saturate are referenced in this chapter, but presented in Chapter 14. We note the existence of bright object observing limits for MAMA imaging modes; these are described in detail in Chapter 7 and tables of the MAMA imaging bright object limits are presented in Chapter 14.

Imaging Overview

STIS can be used to obtain images in undispersed light in the optical and ultraviolet. When STIS is used in imaging mode, the appropriate clear or filtered aperture is rotated into position on the slit wheel, and a mirror is moved into position on the Mode Select Mechanism (see Figure 3.1 on page 23).

Table 5.1, below, provides a complete summary of the clear and filtered apertures available for imaging with each detector. In Figures 5.1 through 5.5 we show the integrated system throughputs.

Table 5.1: STIS Imaging Capabilities

Aperture Name	Filter	Central Wavelength ($\lambda_{c\ in}$ Å)	FWHM ($\Delta\lambda$ in Å)	Field of View (arcsec)	Detector	reference material page
		Visible - plate scale ~0.05 arcseconds per pixel				
50CCD	clear	---	---	51x51	STIS/CCD	260
F28X50LP	optical longpass	λ>5500 Å		28x51	STIS/CCD	263
F28X50OIII	[OIII]	5007	5	28x51	STIS/CCD	266
F28X50OII	[OII]	3740	80	28x51	STIS/CCD	269
50CORON	clear + coronagraphic fingers	---	---	51x51	CCD	271
		Ultraviolet - plate scale ~0.024 arcseconds per pixel				
25MAMA	clear	~1750-3100 Å ~1150-1700 Å		25x25	STIS/NUV-MAMA STIS/FUV-MAMA	272 293
F25QTZ	UV near longpass	λ > 1450 Å		25x25	STIS/NUV-MAMA STIS/FUV-MAMA	275 296
F25SRF2	UV far longpass	λ > 1280 Å		25x25	STIS/NUV-MAMA STIS/FUV-MAMA	278 299
F25MGII	MgII	2800	70	25x25	STIS/NUV-MAMA	281
F25CN270	continuum near 2700Å	2700	350	25x25	STIS/NUV-MAMA	284
F25CIII	CIII]	1909	70	25x25	STIS/NUV-MAMA	287
F25CN182	continuum near 1800Å	1820	350	25x25	STIS/NUV-MAMA	290
F25LYA	Lyman alpha	1216	85	25x25	STIS/FUV-MAMA	302
		Neutral Density Filtered Imaging				
F25NDQ1	neutral density filter, ND=10^{-1}	1150-11000 Å		12x12	CCD, NUV-MAMA, FUV-MAMA	63
F25NDQ2	neutral density filter, ND=10^{-2}			12x12		
F25NDQ3	neutral density filter, ND=10^{-3}			12x12		
F25NDQ4	neutral density filter, ND=10^{-4}			12x12		
F25ND5	neutral density filter, ND=10^{-5}	1150-11000 Å		25x25		
F25ND6	neutral density filter, ND=10^{-6}	1150-11000 Å		25x25		

Why Image With STIS?

Despite its very limited complement of filters, STIS brings three new imaging capabilities to HST:

- The STIS CCD detector, although it covers a much smaller field of view (51 x 51 arcsec) than the WFPC2, has higher throughput over a much wider range of the spectrum (2000–11000 Å) than does WFPC2. The STIS CCD also has a low read noise and dark current, thus STIS CCD observations using the clear aperture have significantly higher sensitivity to faint sources than WFPC2 (see Figure 5.6 on page 55). The STIS CCD clear imaging mode is scientifically useful when no color information is needed, for example, for finding faint variable sources, or imaging the faintest possible sources in a given integration time.
- The STIS MAMA detectors enable true solar blind imaging from 1150–1700 Å using the FUV-MAMA with a considerably higher throughput than WFPC2 or FOC. The NUV-MAMA is also relatively insensitive to red light. Both provide near critical sampling of the PSF (0.024 arcsecond per pixel). See “Unfiltered (Clear) MAMA Imaging” on page 58.
- The STIS MAMA detectors enable very high time resolution (τ ~125 microsecond) imaging in the ultraviolet, using `TIME-TAG` mode.

Caveats For STIS Imaging

There are several important points about imaging with STIS which should be kept in mind:

- The filters are housed in the slit wheel, and while they are displaced from the focal plane, they are not far out of focus. This means that imperfections (e.g., scratches, pin holes, etc.) in the filters may cause artifacts in the images. These features will not directly flat field out because the projection of the focal plane on the detector shifts from image to image due to the non-repeatability of the Mode Select Mechanism’s placement of the mirror (careful post processing may be able to account for registration errors).
- Accurate across-the-detector photometric calibration of the imaging modes requires mapping of the two-dimensional illumination pattern of the sky; for the MAMAs this is likely to be a time-intensive process, and may limit the photometric accuracy obtained in Cycle 7 (see “Summary of Expected Accuracies” on page 319).
- The focus varies across the field of view for imaging modes, with the optical performance degrading by ~30% at the edges of the field of view.

Throughputs and Limiting Magnitudes

In Figure 5.1, below, we show the throughput (where the throughput is defined as the end to end effective area divided by the geometric area of a filled (unobstructed) 2.4 meter aperture) of the three STIS clear imaging modes (with

the CCD, the NUV-MAMA, and the FUV-MAMA). Superposed on this plot, we show the broad band WFPC2 throughputs. In Figure 5.3, 5.4 and 5.5, below, we show the throughputs of the full set of available filters, for the CCD, the NUV-MAMA and the FUV-MAMA, respectively. In the near-UV, FOC has comparable throughput to STIS, as can be see in Figure 5.2.[1]

Figure 5.1: STIS's Clear Imaging Throughputs Versus WFPC2

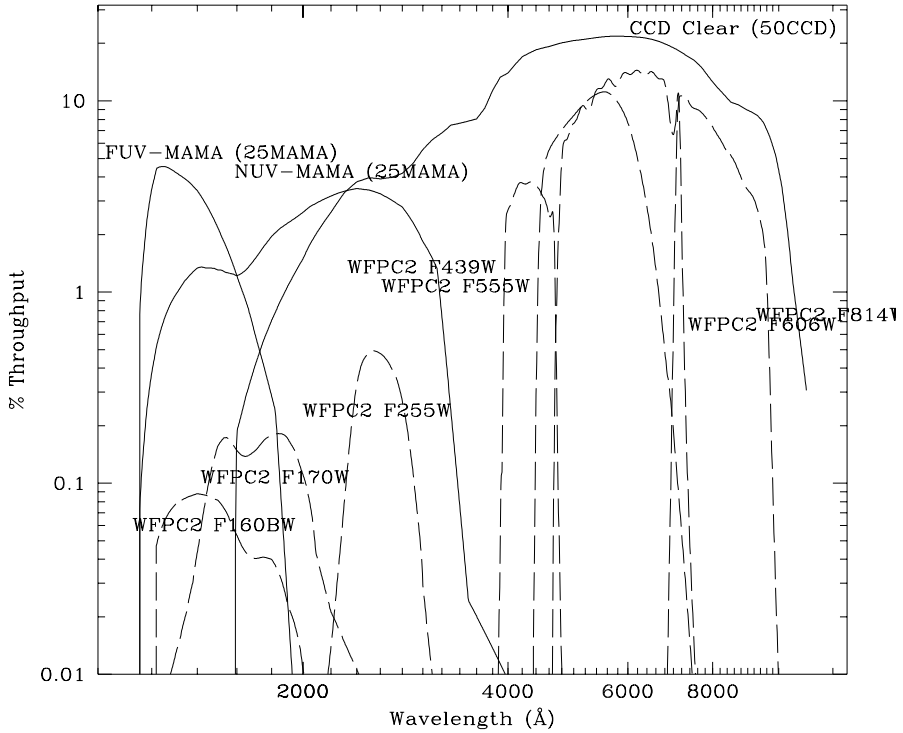

1. Although the FOC ultraviolet imaging capability is not solar blind, FOC does provide the best sampling of the UV or optical PSF of any HST instrument, over a limited field of view and with limited dynamic range. The FOC *near*-UV medium and narrow band imaging throughput and red rejection is similar to STIS's and the FOC has a good choice of filters for NUV imaging (see the FOC Instrument Handbook for more details).

Figure 5.2: STIS's NUV Filtered Imaging Modes Versus FOC

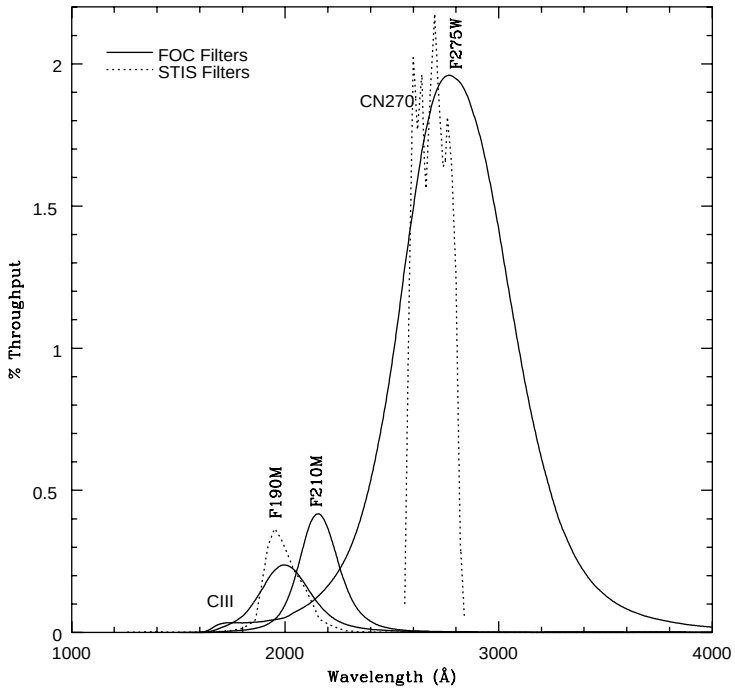

Figure 5.3: STIS's Clear and CCD Filtered Imaging Mode Throughputs

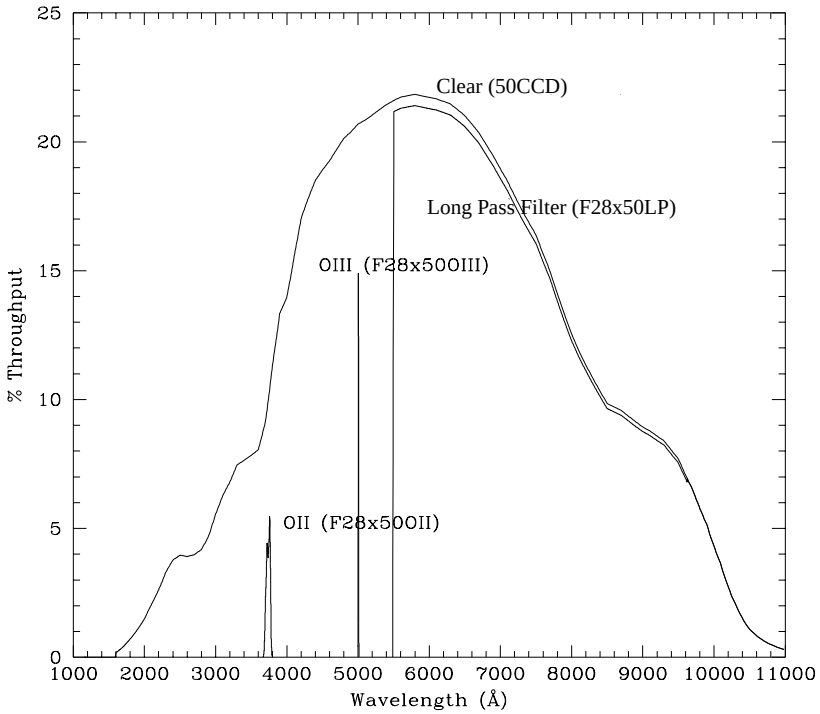

Figure 5.4: STIS's NUV-MAMA Filtered Imaging Mode Throughputs

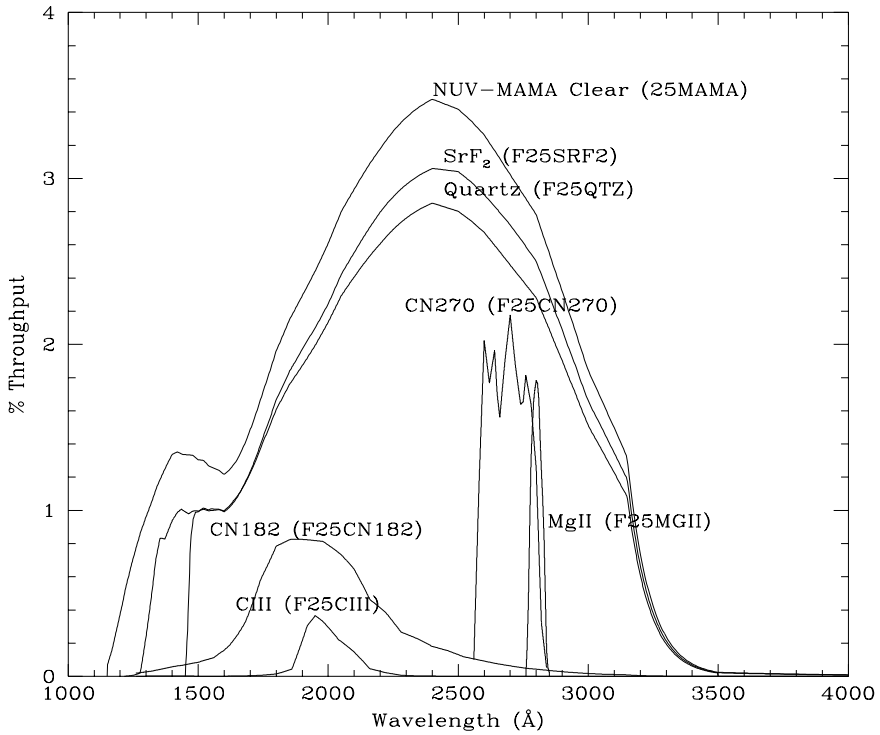

Figure 5.5: STIS's FUV-MAMA Clear and Filtered Imaging Mode Throughputs

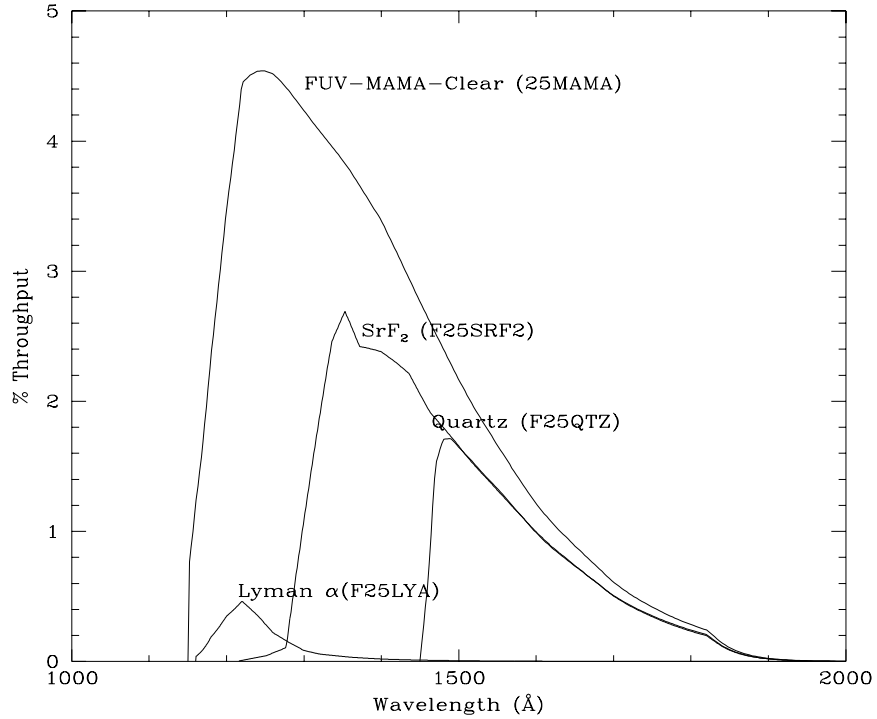

Limiting Magnitudes

In Table 5.2, below, we give the (anticipated) A star V magnitude reached during a one hour integration which produces a signal-to-noise ratio of 10 in the continuum, integrated over the bandpass and the PSF.

Table 5.2: Anticipated Limiting A0V star V Magnitude and Flux Achieved in a One Hour Signal-to-Noise Ratio = 10 Integration.

Detector	Filter	Magnitude	Filter	Magnitude
CCD	Clear	28.0	OII	23.0
CCD	LongPass	27.3	OIII	20.8
NUV-MAMA	Clear	25.8		
NUV-MAMA	LongPass QTZ	25.9	Longpass SrF_2	25.8
NUV-MAMA	CIII	21.8	CN182	23.9
NUV-MAMA	MgII	21.9	CN270	23.6
FUV-MAMA	Clear	23.1	Lyman α (F25LYA)	19.1
FUV-MAMA	Longpass QTZ	23.5	Longpass SrF_2	23.8

Signal-To-Noise Ratios

In Chapter 14 we present, for each imaging mode, plots of exposure time versus flux (and magnitude) to achieve a signal-to-noise ratio of 10. These plots, which are referenced in the individual imaging mode sections below, are very useful for getting an idea of the exposure time you need to perform your science.

Saturation

Both CCD and MAMA imaging observations are subject to saturation at high total accumulated counts per pixel; the CCD due to the depth of the full well, and the MAMA, due to the 16-bit format of the buffer memory (see “CCD Saturation: the CCD Full Well” on page 90 and“MAMA Saturation—Overflowing the 16 Bit Buffer” on page 95). In Chapter 14, plots of time to saturate as a function of source brightness are presented for each imaging mode. For the CCD, these plots also show when the source and background exceeds twice the read noise (i.e., when the observations are no longer read noise limited).

MAMA Bright Object Limits

See “Bright Object Limits” on page 57.

Optical CCD Imaging

The CCD imaging capability of STIS was designed primarily for target acquisitions, and, therefore, only a small number of filters are available. Nevertheless, STIS CCD imaging has scientific utility of its own, due to the high throughput and relatively low read noise of the CCD detector. STIS CCD imaging can be obtained as prime science or in parallel with other instruments. In each filter section below, we include comparisons to the existing WFPC2 imaging capabilities (you should keep in mind, of course, that the WFPC2 field of view covers roughly eight times more sky area than the STIS CCD).

The optical performance of the CCD in image mode is expected to be good and the plate scale of the CCD is ~0.05 arcsecond per pixel, providing a good compromise between sampling of the PSF and field of view. There will be some degradation of the image quality towards the edge of the field. Observers can assume that ~30 percent of the light from a point source falls in a single STIS CCD pixel and that ~80 percent of the light from a point source is contained within a 2 x 2 pixel region. See Figure 14.61 on page 306 for plots of encircled energies as a function of observing wavelength.

Unfiltered (Clear) CCD Imaging - 50CCD

The `50CCD` aperture is a clear, unvignetted aperture which provides maximum sensitivity over the full 50 x 50 arcsecond field of view. The shape of the bandpass is governed by the detector, which has sensitivity from ~2000–11000 Å. Figure 5.1 on page 50 shows the throughput as a function of wavelength for this imaging mode (see also page 260 for sensitivities, signal-to-noise and saturation plots).

Figure 5.6 shows a plot of time to achieve signal-to-noise ratio of 5 for this aperture, with results for the WFPC2 broad band filter modes superposed, assuming a A star spectrum for the source. If color information and a wide field of view are not required, then there is an advantage in using this imaging mode over the WFPC2.

No pure parallel observing is permitted with the clear (50CCD) aperture. In addition 50CCD exposures cannot be shorter than 15 minutes in duration, and if they include UV bright sources will have to be dithered (i.e., positional offsets applied between read outs) to assure that the target flux is moved on the detector. These rules are imposed to ensure that the UV tail from bright objects does not cause a residual elevation in dark current which could negatively impact subsequent science observations (see “UV Light and the STIS CCD” on page 91). The single exposure time limit has no practical scientific implications, since the sky background plus detector background equals twice the read noise in a ~13 minute clear CCD image even under low sky background conditions.

Figure 5.6: Signal-to-Noise Ratio Comparison of STIS 50CCD Imaging Versus WFPC. Plot shows the limiting V magnitude at a signal-to-noise ratio of 5 versus exposure time.

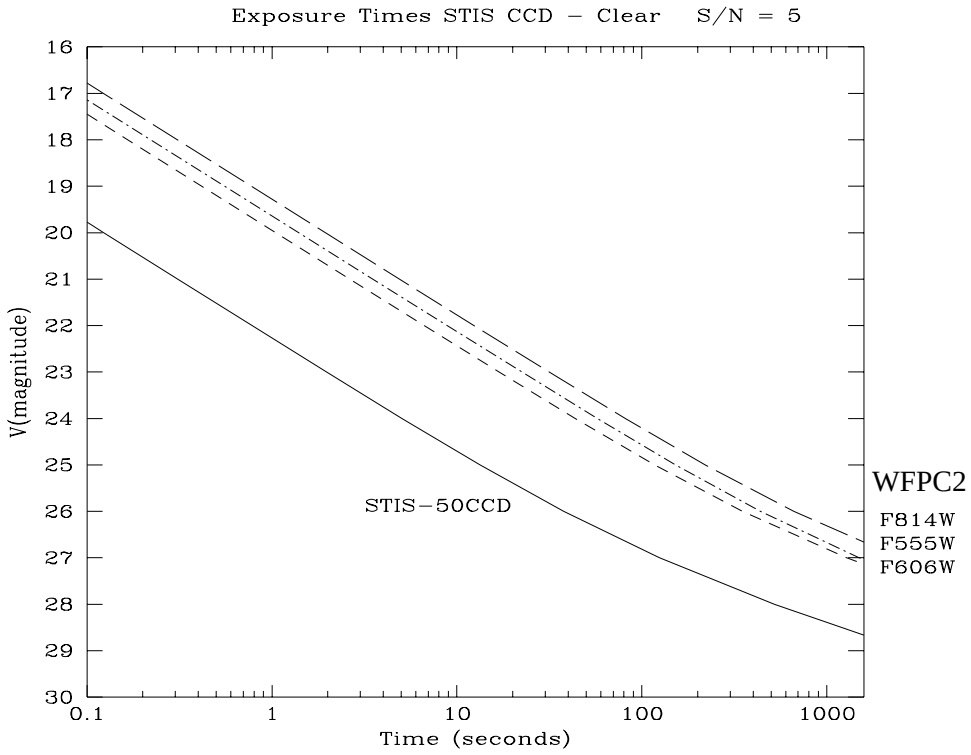

Optical Longpass-F28X50LP

STIS's longpass filter cuts off at $\lambda < 5500$ Å. It images a 28 x 50 arcsecond field of view. The `F28X50LP` filter is the principal target acquisition aperture, (see "Imaging Apertures for Use in Target Acquisitions" on page 111). The integrated system throughput for this filter is given in Figure 5.3 on page 51 (see also page 263 for sensitivities, signal-to-noise, and saturation plots).

[OIII] - F28X50OIII

This filter images a 28 x 50 arcsecond field of view and can be used in target acquisitions or for direct science, to obtain images of Galactic objects in the light of [OIII]. The [OIII] filter integrated system throughput and a signal-to-noise comparison with the WFPC2 [OIII] filter is shown in Figure 5.7 (see also page 266 for sensitivities, signal-to-noise, and saturation plots). The STIS [OIII] filter is very narrow; only 5 Å wide, compared to the WFPC2 [OIII] filter which is roughly 30 Å wide.

Figure 5.7: F28X50OIII (a) Integrated System Throughput and (b) Flux vs. exposure time to achieve a signal-to-noise=5 versus WFPC2 for a FWHM=1 Å line,.

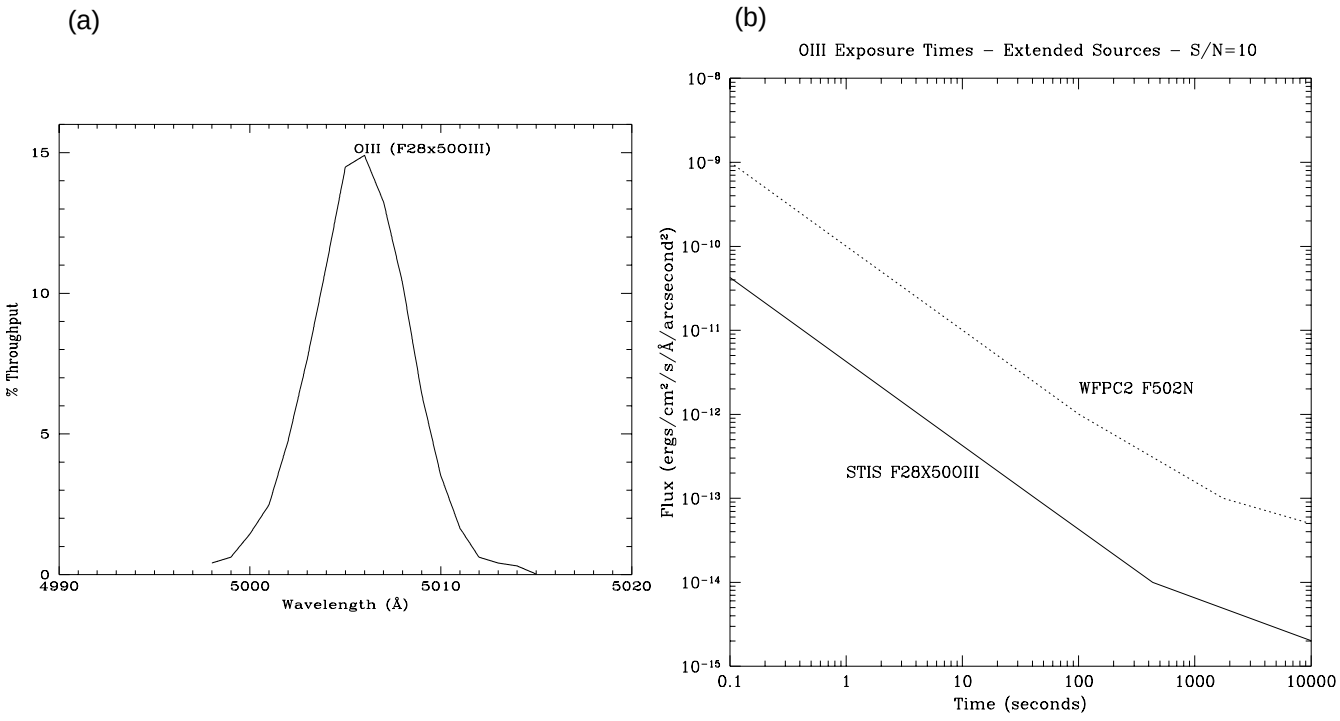

Figure 5.8: F28X50OII (a) Integrated System Throughput and (b) Flux vs. exposure time to achieve a signal-to-noise=5 versus WFPC2 for a FWHM=1 Å line.

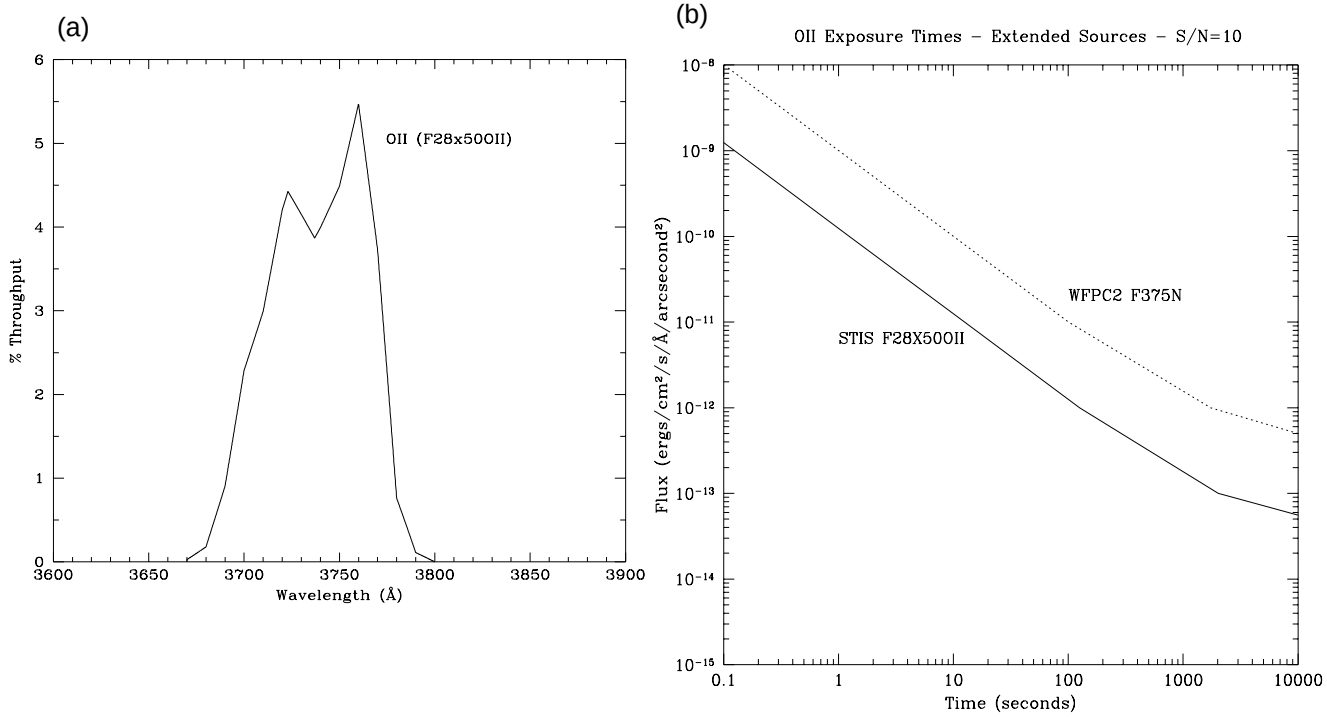

[OII] - F28X50OII

The [OII] filter images a 28 x 50 arcsecond field of view and can be used in target acquisitions or for direct science, to obtain images in the light of [OII]. The [OII] filter integrated system throughput and a signal-to-noise ratio comparison with WFPC2's [OII] filter are shown in Figure 5.8 (see also page 269 for sensitivities, signal-to-noise and saturation plots).

Coronagraphic Imaging - 50CORON

The coronagraphic mask (see Figure 12.3 on page 172) comprises a pair of crossed wedges and one finger at the edge of the field of view. The mask resides in the slit wheel and provides a clear (unfiltered) coronagraphic imaging capability. See "Unfiltered (Clear) CCD Imaging - 50CCD" on page 54 for the spectral properties of the images obtained. A number of locations on the occulting masks have been specified, to correspond to widths of 2.75, 2.5, 2.0, 1.75 and 1.5 arseconds on each wedge. See "Coronagraphic Imaging and Spectroscopy" on page 170 for more information about the use of the coronagraphic aperture.

Ultraviolet Imaging with the MAMA Detectors

The filtered and clear apertures available for ultraviolet imaging are summarized in Table 5.1 on page 48. Although there are only a small number of filters available, the solar blind and solar insensitive properties of the FUV-MAMA and NUV-MAMA detector, respectively, coupled with their 25 x 25 arcsecond field of view, good spatial sampling, and their ability to detect rapid variability, makes the STIS ultraviolet imaging capability unique to HST.

Bright Object Limits

The MAMA detectors are subject to absolute bright object limits, above which targets cannot be observed. These are particularly stringent for the MAMA imaging modes (being V=20.5 for the clear modes), and apply to all sources illuminating the field of view.

We direct MAMA observers to "MAMA Bright Object Limits" on page 97. For summary tables of absolute bright object limits for the imaging modes, see "MAMA Imaging Bright Object Limits" on page 307.

It is the observer's responsibility to ensure that their observations do not exceed the MAMA bright object limits.

Optical Performance

The MAMA plate scale is ~0.024 arcsecond pixel^{-1} in image mode, providing a good compromise between sampling of the PSF in the ultraviolet and field of view. Figure 14.61 on page 306 shows encircled energies as a function of wavelength for MAMA imaging. The MAMA detector PSF's exhibit broad wings, with the wings being substantially higher in the NUV-MAMA than the FUV-MAMA. Figure 7.3 on page 95 shows sample detector PSFs for the MAMAs.

Unfiltered (Clear) MAMA Imaging

Each MAMA can be used with the 25MAMA clear aperture to image a 25 x 25 arcsecond field of view of the sky, providing the maximum throughput and wavelength coverage in the NUV and FUV as shown in Figure 5.1 on page 50. The FUV-MAMA quantum efficiency drops dramatically longward of ~3000 Å making it effectively solar blind, while the NUV-MAMA also has a reduced response in the red, longward of ~3500Å (see Figure 5.9 on page 59 below). Tables 5.3 and 5.4 give the percent of detected photons arising in the UV versus optical for observations of different stellar types with the clear MAMA imaging modes. The red rejection of the MAMA detectors make them well suited to UV imaging of red objects.

Table 5.3: Visible Light Rejection of the FUV-MAMA Clear Imaging Mode

Stellar Type	% of all Detected Photons which have λ<1800 Å	% of all Detected Photons which have λ<3000 Å
O5	99.4	100
B1V	99.3	100
A0V	98.5	100
G0V	76.0	100
K0V	70.8	99.8

Table 5.4: Visible Light Rejection of the NUV-MAMA Clear Imaging Mode

Stellar Type	% of all Detected Photons which have λ<3000 Å	% of Detected Photons which have λ<5000 Å
O5	96.7	100
BIV	96.4	100
A0V	90.6	99.9
G0V	70.8	99.2
K0V	60.3	98.6

Figure 5.9: Out of Band Spectral Response of FUV and NUV MAMA Clear Imaging modes.

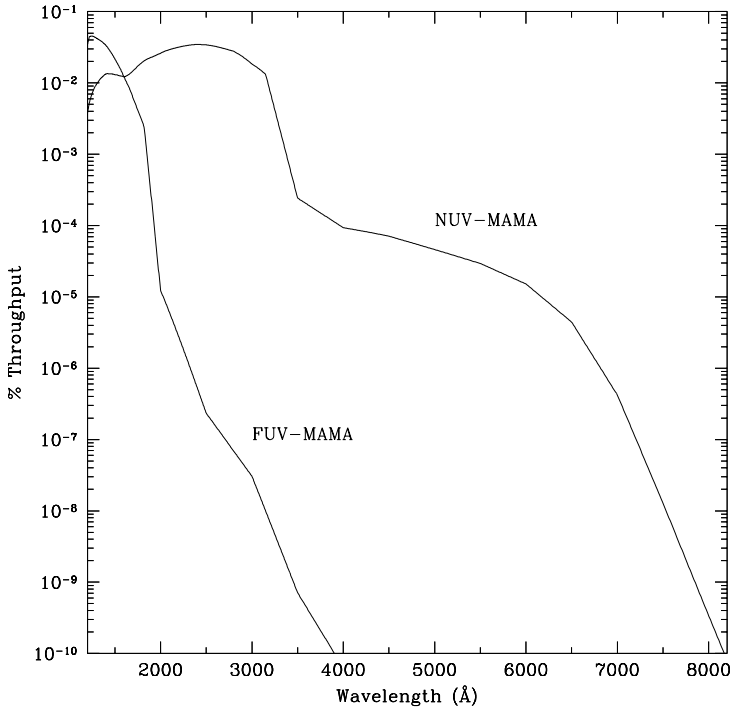

Longpass Filtered MAMA Imaging - F25SRF2 and F25QTZ

The integrated system throughputs of the two UV longpass filters when used with the NUV-MAMA and FUV-MAMAs are shown in Figure 5.5 on page 52 (see also Chapter 14 for sensitivities, signal-to-noise and saturation plots). The filter (only) throughputs of these two filters are shown in Figure 5.10. These filters image a 25 x 25 arcsecond field of view. Their cutoff wavelengths were chosen to exclude Geocoronal Lyman α 1216 Å and OI 1302 + 1356 Å, respectively; use of these filters significantly reduces the total sky background in the ultraviolet. These filters can be used individually in imaging mode, or with the prism or any first-order UV grating in slitless spectroscopic observations, to reduce the background due to Geocoronal emission (see “Objective Prism Spectroscopy” on page 45 and “Slitless First Order Spectroscopy” on page 161). The F25SRF2 filter, with images taken in series with the 25MAMA FUV-MAMA clear, can also be used to obtain Lyman α images (see “Lyman Alpha - F25LYA and Clear-minus-SRF2” on page 62).

Figure 5.10: F25SRF2 and F25QTZ Filter Only Transmissions

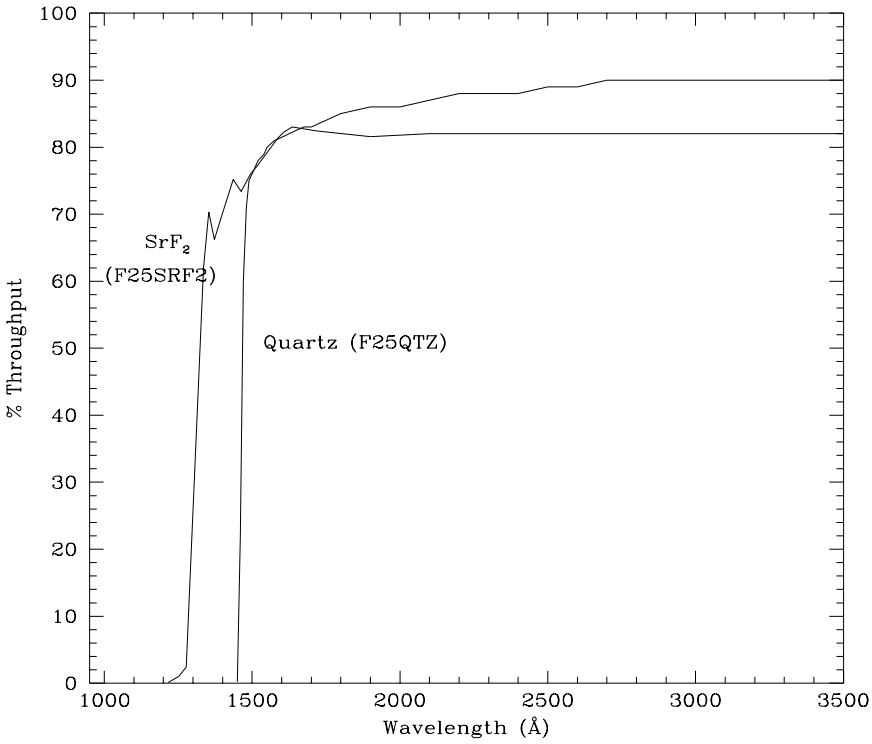

MAMA Filtered Imaging

The filters for MAMA imaging include:

- A narrow band filter (F25MGII) which images the magnesium doublet at 2798/2802 Å, and a matched medium band continuum filter (F25CN270) centered at 2700 Å.
- A narrow band filter (F25CIII) which images the semi-forbidden CIII] lines at 1906/1909 Å, the strongest nebular (low-density) lines in the UV, and a matched medium band continuum filter (F25CN182) centered at 1800 Å.
- A narrow band filter which images Lyman α; this filter has an unusually poor throughput, and we recommend that you consider, instead, obtaining two FUV-MAMA images, one through the 25MAMA unfiltered aperture and a second with the SRF2 longpass filter. The difference of these two images will isolate Lyman α with much higher throughput than the F25LYA filter.

MgII- F25MGII

The F25MGII filter images a 25 x 25 arcsecond field of view in the light of the doublet lines of MgII (2798 and 2802 Å). Figure 5.11 shows the integrated system throughput (see also page 281 for sensitivities, signal-to-noise and saturation plots).

Figure 5.11: F25MGII and F25CN270 Integrated System Throughputs

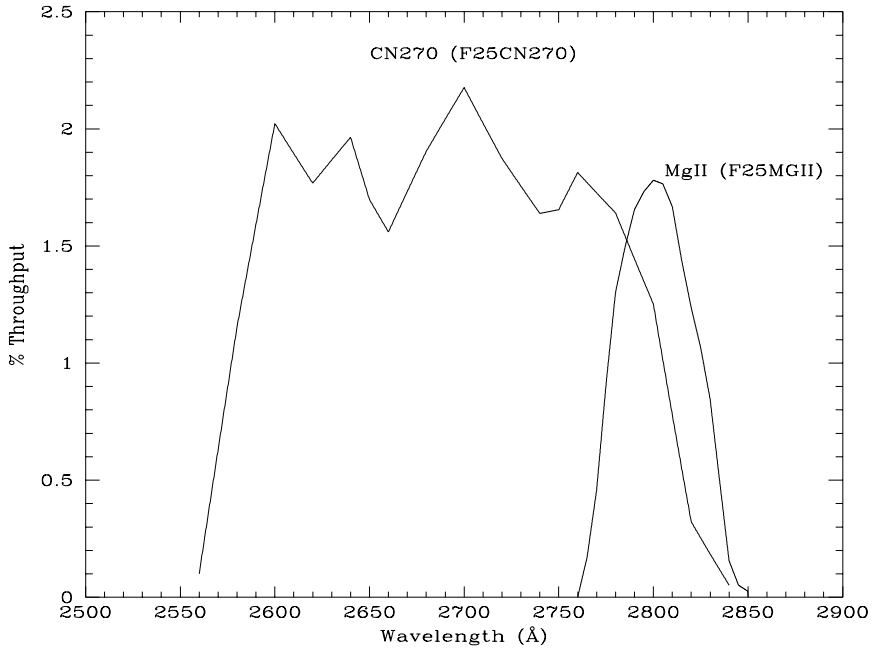

2700Å continuum - F25CN270

The 2700 Å continuum filter images a 25 x 25 arcsecond field of view and can be used to measure the continuum for MgII emission line images. The `F25CN270` filter integrated system throughput is shown in Figure 5.11, above (see also page 284 for sensitivities, signal-to-noise and saturation plots).

CIII] - F25CIII

The `F25CIII` filter images a 25 x 25 arcsecond field of view in the light of CIII]. The `F25CIII` integrated system throughput is shown in Figure 5.12 (see also page 287 for sensitivities, signal-to-noise, and saturation plots).

Figure 5.12: F25CIII and F25CN182 Integrated System Throughputs

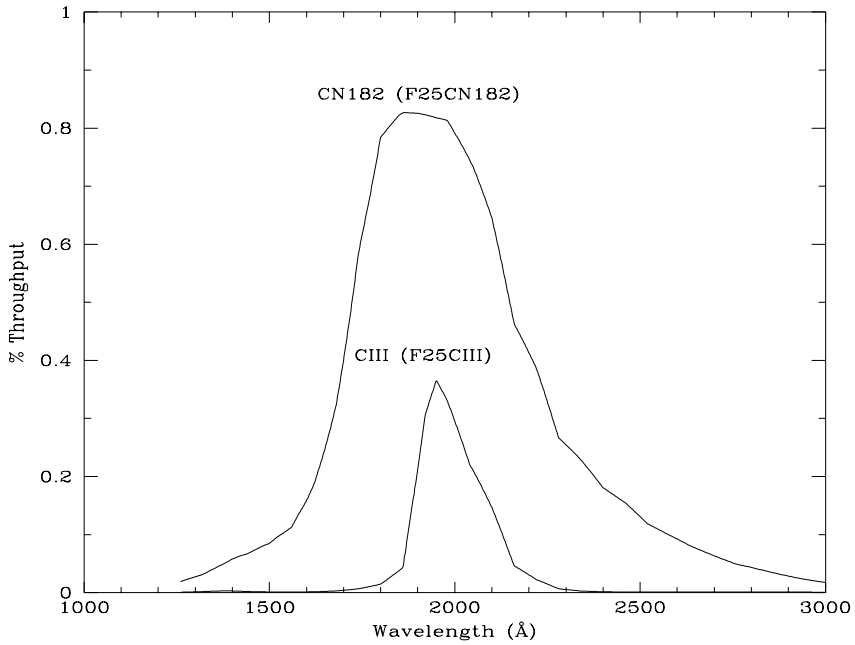

1800Å continuum - F25CN182

The 1800 Å continuum filter images a 25 x 25 arcsecond field of view, and can be used to measure the continuum for CIII] emission line images. The F25CN182 filter integrated system throughput is shown in Figure 5.12, above (see also page 290 for sensitivities, signal-to-noise and saturation plots).

Lyman Alpha - F25LYA and Clear-minus-SRF2

The F25LYA filter images a 25 x 25 arcsecond field of view and can be used to obtain emission line images in the light of the Lyman α. The F25LYA filter integrated system throughput is shown in Figure 5.13 (see also page 302 for sensitivities, signal-to-noise and saturation plots).

At the price of a slightly wider bandpass, and the need to take two exposures, Lyman α can isolated by taking one image using the clear (25MAMA) aperture and a second using the longpass (F25SRF2) filter and differencing the two. The integrated system throughput for this imaging sequence is appreciably higher than for the narrow band F25LYA filter, as shown Figure 5.13

Figure 5.13: Lyman α Imaging Integrated System Throughputs

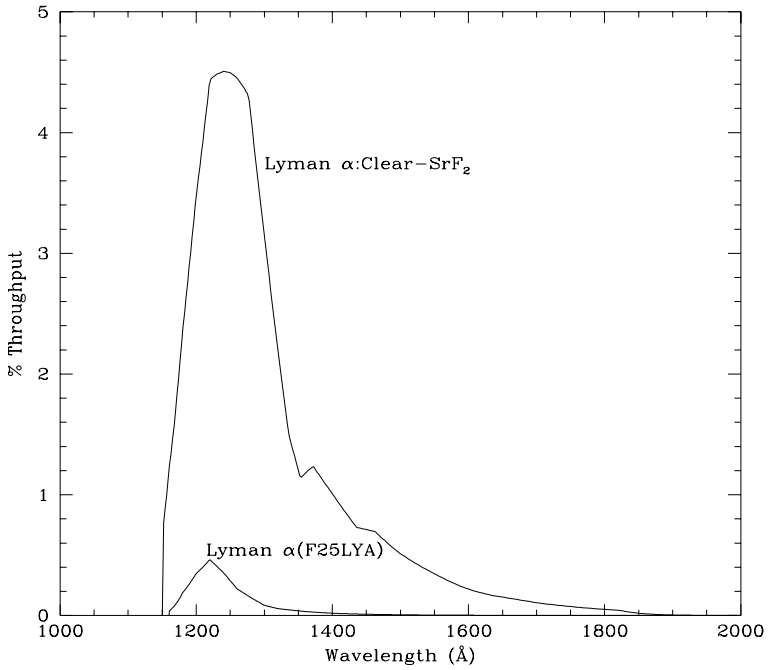

Neutral Density Filters

STIS has a complement of neutral density (ND) filters. spanning from ND1 (attenuation of 10^{-1}) to ND6 (attenuation of 10^{-6}, or 15 magnitudes) which can be used with the CCD, the NUV-MAMA and the FUV-MAMA.

`F25ND1`, `F25ND2`, `F25ND3`, and `F25ND4` are physically four separate quadrants of a single 25 x 25 arcsecond filter occupying a single slot on the slit wheel. The target is centered in the appropriate quadrant when one of these apertures is requested. However, it should be noted that all four quadrants project onto the detector, and the full detector domain must be considered for bright object limits.

`F25ND5` and `F25ND6` are each individual 25 x 25 arcsecond filtered apertures, occupying unique locations on the slit wheel.

As of the writing of this handbook, the wavelength dependence of the transmissions for the ND filters have not yet been measured; proposers should assume attenuations of 10^{-1} for ND1, 10^{-2} for ND2, 10^{-3}, for ND3, 10^{-4} for ND4, 10^{-5} for ND5 and 10^{-6} for ND6 at all wavelengths.

CHAPTER 6
Exposure Time Calculations

In This Chapter...

Overview

In this chapter we explain how to use sensitivities to determine the expected count rate from your source and how to calculate exposure times to achieve a given signal-to-noise ratio for your STIS observations. At the end of the chapter, in “Exposure Time Examples” on page 77, you will find examples to guide you through specific cases.

The WWW STIS Exposure Time Calculator

A World Wide Web STIS exposure time calculator will be available to aid you in planning your STIS observations. The STIS exposure calculator provides count rates for given source parameters (spectral type and magnitude or flux at a given wavelength) and will calculate signal-to-noise ratios for a given exposure time, or count-rates and exposure time for a given signal-to-noise ratio. If you have a calibrated UV spectrum of your source, you can pass that spectrum as input directly to the exposure time calculator. The task will also determine peak per-pixel count rates and total (integrated over the detector) count rates to aid you in your feasibility assessment and will warn you if your observations exceed the local or global brightness limits for MAMA observations (see Chapter 7). Lastly, the task will be able to produce one-dimensional spectra for a given STIS configuration and source. A graphical interface will allow WWW browsers to plot

the output spectra or write the spectrum out as an ASCII text file to the user's local disk. The tool can be found via the STScI STIS home page.

We suggest that you utilize the STIS World Wide Web exposure time calculator when designing your Phase I proposals.

Determining Count Rates from Sensitivities

In the most simple terms, the instrumental sensitivity (*Sens*) times the flux from your object of interest gives the counts sec^{-1} (C_s) expected from your source:

$$C_s = Sens \times Flux$$

Sensitivities are presented in graphical and tabular form as a function of wavelength for the spectroscopic modes in Chapter 13 "Spectroscopic Reference Material" on page 175 and for the imaging modes in Chapter 14 "Imaging Reference Material" on page 257. Given your source characteristics and the sensitivity of your STIS configuration, calculating the expected count rate over a given number of pixels is straight forward. The additional information you will need for spectroscopic observations is the aperture transmission (T_A), the encircled energy fraction (ε_f) in the direction perpendicular to dispersion, the number of pixels per spectral resolution element (or line spread function FWHMs) and the plate scale. For imaging observations you need only the encircled energies. The location of this information is summarized in Table 6.1, below.

Table 6.1: Location of Information Needed to Compute Expected Counts

Spectroscopic Mode	Sensitivities	Slit Transmission	Line Spread Function FWHM	Plate Scales	Encircled Energies
CCD first order	page 179	page 243	page 243	page 247	page 247
MAMA first order	page 206	page 243	page 243	page 248	page 248
MAMA echelle	page 222	page 250	page 250	page 253	page 253
PRISM	page 238	N/A	N/A	page 238	page 242[a]
CCD imaging	page 260	N/A	N/A	page 305	page 305
MAMA imaging	page 272	N/A	N/A	page 305	page 305

a. Numbers for G230M and G140M can be used for PRISM.

Below, we describe how to determine two quantities:

1. The counts sec^{-1} (C_s) from your source over some selected area of N_{pix} pixels.

2. The peak counts sec^{-1} $pixel^{-1}$ (P_{cr}) from your source—useful for avoiding saturated exposures and for assuring that MAMA observations do not exceed the bright object limits.

We consider the cases of point sources and diffuse sources separately.

Spectroscopy

Sensitivity Units and Conversions

The *spectroscopic point source sensitivity,* $Sens^P_\lambda$, has the unit:

counts sec^{-1} pix_λ^{-1} per incident erg cm^{-2} sec^{-1} $Å^{-1}$, where:

- pix_λ = a pixel in the dispersion direction.
- counts refer to the total counts from the point source integrated over the PSF in the direction perpendicular to the dispersion (along the slit).

The *spectroscopic diffuse source sensitivity,* $Sens^d_\lambda$, has the unit:

counts sec^{-1} pix_λ^{-1} pix_s^{-1} per incident dimensional erg cm^{-2} sec^{-1} $Å^{-1}$ $arcsec^{-2}$

Where:

- pix_λ= a pixel in the dispersion direction.
- pix_s= a pixel in the spatial direction.

$Sens^P_\lambda$ and $Sens^d_\lambda$ are related through the relation:

$$Sens^d_\lambda \cong (Sens^P_\lambda \times m_s \times W)$$

Where:

- m_s is the plate-scale in arcsec per pixel in the direction perpendicular to the dispersion.
- W is the slit width in arcseconds.

Here, we have assumed that the diffuse source has a uniform brightness over the area of interest.

Point Source

For a point source, the count rate, C_s, from the source integrated over an area of $N_{pix} = N_{\lambda pix}$ x N_{spix} pixels can be expressed as:

$$C_s = F_\lambda \times Sens^P_\lambda \times T_A \times \varepsilon_f \times N_{\lambda pix}$$

Where:

- F_λ = the flux from the astronomical source, in ergs sec^{-1} cm^{-2} $Å^{-1}$.
- T_A = the aperture transmission (a fractional number less than 1).
- ε_f = the fraction of the point source energy contained within N_{spix} pixels in the spatial direction.
- $N_{\lambda pix}$ = the number of wavelength pixels integrated over. For an unresolved emission line, $N_{\lambda pix}$ is just the number of pixels per spectral resolution element and I_λ is simply the total flux in the line in ergs sec^{-1} cm^{-2} divided by the dispersion in Å per pixel times $N_{\lambda pix}$.

The peak counts sec^{-1} $pixel^{-1}$ from the point source, is given by:

$$P_{cr} = \varepsilon_f(1) \times F_\lambda \times Sens_\lambda^P \times T_A$$

where,

- $\varepsilon_f(1)$ is the fraction of energy contained within the peak pixel, and
- F_λ, $Sens_\lambda^P$,and T_A are as above.

Diffuse Source

For a diffuse source, the count rate, C_s due to the astronomical source integrated over $N_{pix} = N_{\lambda pix}$ x N_{spix} can be expressed as:

$$C_s = I_\lambda \times Sens_\lambda^d \times N_{\lambda pix} \times N_{spix}$$

Where:

- I_λ = the surface brightness of the astronomical source, in ergs sec^{-1} cm^{-2} $Å^{-1}$ $arcsec^{-2}$.
- $N_{\lambda pix}$ = the number of wavelength pixels integrated over in dispersion. For an unresolved emission line, $N_{\lambda pix}$ is just the number of pixels per spectral resolution element and I_λ is simply the total flux in the line in ergs sec^{-1} cm^{-2} $arcsec^{-2}$ divided by the dispersion in Å per pixel times $N_{\lambda pix}$.
- N_{spix} = the number of pixels integrated over in the spatial direction.

For a diffuse continuum source the peak counts sec^{-1} $pixel^{-1}$ P_{cr} is given by:

$$P_{cr} = I_\lambda \times Sens_\lambda^d$$

For a diffuse, *spectrally unresolved emission line* source the peak count sec^{-1} $pixel^{-1}$ P_{cr} is essentially independent of slit size and is given by:

$$P_{cr} = I_{line} \times Sens_\lambda^d \times m_\lambda \div (W \times d)$$

Where:

- $\boldsymbol{I}_{line}$ is the intensity in ergs sec^{-1} cm^{-2} $arcsec^{-2}$ in the line.
- d is the dispersion, in Å per pixel.

- m_λ is the plate scale in the dispersion direction.
- W is the slit width in arcseconds.

Imaging

Sensitivity Units and Conversions

The *imaging point source sensitivity,* $Sens^P_\lambda$, has the units:

counts sec^{-1} $Å^{-1}$ per incident erg cm^{-2} sec^{-1} $Å^{-1}$

Where:

- counts refer to the total counts from the point source integrated over the PSF.

The *imaging diffuse source sensitivity,* $Sens^d_\lambda$, has the unit:

counts sec^{-1} $Å^{-1}$ $pixel^{-1}$ per incident dimensional erg cm^{-2} sec^{-1} $Å^{-1}$ $arcsec^{-2}$.

Thus $Sens^P_\lambda$ and $Sens^d_\lambda$ are related through the relation:

$$Sens^d_\lambda \cong (Sens^P_\lambda \times {m_s}^2)$$

where m_s is the plate-scale in arcsec per pixel.

Point Source

For a point source, the count rate, C_s, over an area of N_{pix} pixels due to the astronomical source can be expressed as:

$$C_s = \int F_\lambda \times Sens^P_\lambda \times \varepsilon_f d\lambda$$

Where:

- F_λ = the flux from the astronomical source, in ergs sec^{-1} cm^{-2} $Å^{-1}$.
- ε_f = the fraction of the point source energy encircled within N_{pix} pixels.
- the integral is over the bandpass.

The peak counts sec^{-1} $pixel^{-1}$ from the point source, is given by:

$$P = \int F_\lambda \times Sens^P_\lambda \times \varepsilon_f(1) d\lambda$$

Where:

- $\varepsilon_f(1)$ is the fraction of energy encircled within the peak pixel.
- $F_{\lambda,}$ and $Sens^P_\lambda$ are as above.
- the integral is over the bandpass.

Diffuse Source

For a diffuse source, the count rate, C_s due to the astronomical source can be expressed as:

$$C_s = \int I_\lambda \times Sens_\lambda^d \times N_{pix} d\lambda$$

Where:

- I_λ = the surface brightness of the astronomical source, in ergs sec^{-1} cm^{-2} $Å^{-1}$ $arcsec^{-2}$.
- N_{pix} = the number of pixels integrated over.
- the integral is over the bandpass.

For a diffuse source the peak counts sec^{-1} $pixel^{-1}$, P_{cr}, is given trivially by:

$$P_{cr} = \int I_\lambda \times Sens_\lambda^d d\lambda$$

Computing Exposure Times

To derive the exposure time to achieve a given signal-to-noise ratios, or to derive the signal-to-noise ratio you will achieve in a given exposure time for your source, there are four principal ingredients:

- Expected counts from your source over some area (C_s).
- The area (in pixels) over which those counts are received (N_{pix}).
- Sky background (B_{sky}) in counts $pixel^{-1}$ sec^{-1}.
- The detector background, or dark, (B_{det}) in counts $pixel^{-1}$ sec^{-1} and the read noise (RN) in counts for the CCD.

"Detector and Sky Backgrounds" on page 72 provides the information you need to determine the sky plus detector background for your observation.

Calculating Exposure Times for a Given Signal-to-Noise

The signal-to-noise ratio, *StoN* is given by

:

$$StoN = \frac{C_s \times t}{\sqrt{C_s \times t + N_{pix} \times (B_{sky} + B_{det})t + ((N_{pix} / N_{bin}) \times N_{read} \times RN^2)}}$$

Where:

- C_s = the signal from the astronomical source in counts sec^{-1}.
- N_{pix} = the total number of detector pixels integrated over to achieve C_s.
- B_{sky} = the sky background in counts sec^{-1} $pixel^{-1}$.
- B_{det} = the detector dark current in counts sec^{-1} $pixel^{-1}$.
- N_{bin} = the total number of on-chip binned pixels for the CCD (N_{bin} = `BINAXIS1` x `BINAXIS2` (see “Binning” on page 143).
- *RN* = the read noise in counts; = 0 for MAMA observations.
- N_{read} = the number of CCD readouts.
- *t* = the integration time in seconds.

Observers using the CCD normally take sufficiently long integrations that the CCD read noise is not important. This condition is met when:

$$C_s \times t + N_{pix}(B_{sky} + B_{det}) \times t \; > \; 2(N_{pix}/N_{bin}) \times N_{read} \times RN^2$$

If you are observing with the CCD and are in the regime where read noise is not important, and for all MAMA observations, the integration time to reach a signal-to-noise ratio *StoN*, is given by:

$$t \; = \; \frac{(StoN)^2(C_s + N_{pix} \times [B_{sky} + B_{det}])}{{C_s}^2}$$

If your source count rate is much brighter than the sky plus detector backgrounds, then this expression reduces further to:

$$t \; = \; \frac{(StoN)^2}{C_s}$$

More generally, the required integration time to reach a signal to noise ratio *StoN*, is given by:

$$t \; = \; \frac{(StoN)^2(C_s + N_{pix}[B_{sky} + B_{det}]) + \sqrt{(StoN)^4(C_s + N_{pix}[B_{sky} + B_{det}])^2 + 4(StoN)^2 {C_s}^2((N_{pix}/N_{bin}) \times N_{read} \times RN^2)}}{2{C_s}^2}$$

Special Case—Spectroscopic CCD Observations at λ<2500 Å

In the optical, each photon generates a single electron (i.e., a count is equivalent to an electron). However, in the near-UV, shortward of ~3200 Å there is

a finite probability of creating more than one electron per UV photon (see Christensen, O, 1976, J. App. Phys. 47, 689). Theoretically, the quantum yield (*Q*, or the mean number of electrons generated per photon) is given by the energy of the photon divided by 3.65 eV, and ranges from *Q*=1.06 electrons for every UV photon at 3200 Å, to *Q*=1.89 electrons for every photon at 1800 Å. The actual electron yield of the STIS CCD has not been measured in the near-UV.

The sensitivity plots correctly predict the number of counts (electrons) generated per UV photon. However, since multiple electrons are generated from a single photon, the signal-to-noise achieved in a given integration time is affected. The explicit expression is given by:

$$StoN = \frac{Q^{-1} \times C_s \times t}{\sqrt{Q^{-1} \times (C_s + N_{pix} \times B_{sky}) \times t + N_{pix} \times B_{det} \times t + ((N_{pix} / N_{bin}) \times N_{read} \times RN^2)}}$$

For observations which are not in the read noise or dark current limited regime, the effective signal-to-noise you should expect to achieve is then ~1/sqrt(*Q*) times the signal-to-noise ratio calculated directly from the sensitivities given in Chapter 13 if you ignore this effect. This is negligible at 3000 Å but is a 40% effect at 1800 Å.

Detector and Sky Backgrounds

When calculating expected signal-to-noise ratios or exposure times, the background from the sky and the background from the detector must be taken into account.

Detector Backgrounds

Table 6.2 shows the read noise and dark current characteristics of the detectors.

Table 6.2: Detector Backgrounds

	CCD	NUV-MAMA	FUV-MAMA
Read noise	4 electrons/pixel	0	0
Dark current (counts sec^{-1} pix^{-1})	0.007	~1.25×10^{-4}	~6.25×10^{-5}

Sky Background

The sources of sky background which will affect STIS observations include:

- Earth-shine (ES).
- Zodiacal light (ZL).
- Geocoronal emission (GC).

The continuum background in counts pixel^{-1} sec^{-1} for spectroscopic observations can be computed as:

$$B_{sky} = I_{\lambda} \times Sens_{\lambda}^{d}$$

Where:

- I_{λ} is the surface brightness of the sky background, in ergs sec^{-1} cm^{-2}Å^{-1} arcsec^{-2}.
- $Sens^{d}_{\lambda}$ is the diffuse source sensitivity for the grating mode.

The background in counts pixel^{-1} sec^{-1} for imaging observations can be computed as:

$$B_{sky} = \int I_{\lambda} \times Sens_{\lambda}^{d} d\lambda$$

Where:

- I_{λ} is the surface brightness of the sky background, in ergs sec^{-1} cm^{-2} Å^{-1} arcsec^{-2}.
- $Sens^{d}_{\lambda}$ is the diffuse source sensitivity for the imaging mode.
- The integral is over the bandpass.

In Figure 6.1 we plot the total and the individual contributions to the sky background. These are typical *high values* of the background computed for a helio-ecliptic latitude and longitude of 30 and 180 degrees, respectively, and for a target which is roughly 25 degrees from the sunlit earth. The information in this figure is presented in tabular form in Table 6.5 on page 84. These are the values for the background you should use for your calculations if you do not request special observing conditions, such as `LOW-SKY` or `SHADOW` (see below).

Figure 6.1: Typical High Sky Background Intensity as a Function of Wavelength

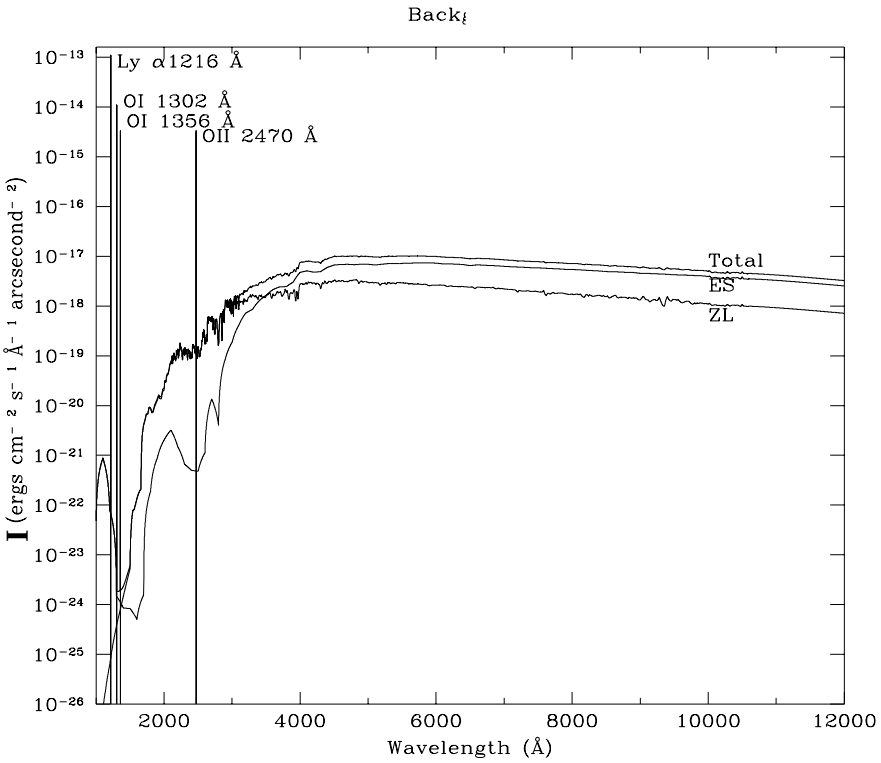

Background Variations and Low-Sky

In the ultra-violet, at wavelengths shortward of ~3500 Å, the background is dominated by the zodiacal light. The contribution of zodiacal light, does not vary dramatically with time, and is constant within a factor of about three throughout most of the sky. Table 6.3 gives the variation of the background as a function of helio-ecliptic latitude and longitude.

Earth-shine, on the other hand, varies strongly depending on the earth-target angle and the fraction of the sun-lit earth. For observations taken longward of 3500 Å the earth-shine dominates the background when observing at small earth-target angles. However, at earth-target angles of 40 degrees or more, earth-shine drops by roughly 80%, and the zodiacal light dominates.

If your observations are background limited, you may wish to consider requesting that the special requirement `LOW-SKY` be applied to your observation. `LOW-SKY` observations are obtained when the total background light is no more than 30% greater than the yearly minimum value of the zodiacal background for the target. The exposures are also taken when the target is at least 40 degrees from the bright earth to reduce earth-shine. This limits visibility time to about 48 minutes per orbit. The values of the background when `LOW-SKY` is requested can be assumed to be ~15% of the typical high values in Figure 6.1 on page 74 and Table 6.5 on page 84. See “Imaging a Faint Stellar Source” on page 83 for an

example of a background limited observation which is greatly helped by requesting LOW-SKY.

Table 6.3: Approximate Sky Background at V as a Function of Helio-ecliptic Latitude and Helio-ecliptic Longitude, in V magnitudes per square arcsecond.

	Helio-ecliptic Latitude			
Helio-ecliptic Longitude	**0**	**30**	**60**	**90**
180	22.1	22.7	23.2	23.3
145	22.4	22.9	23.3	23.3
110	22.3	22.9	23.3	23.3
50	20.9	22.2	22.9	23.3

Geocoronal Emission and Shadow

Background due to geocoronal emission originates mainly from hydrogen and oxygen atoms in the exosphere of the earth. The emission is concentrated in a very few lines. The brightest line is Lyman α at 1216Å. The only other detectable line is the OI line at 1302 Å, which rarely exceeds 10% of Lyman α. OI 1356 Å and OII 2470 Å lines may appear while observing on the daylight side of the orbit, but these lines are much weaker still. We have assumed the strength of geocoronal Lyman α to be 1.1 x 10^{-13} erg cm^{-2} sec^{-1} $arcsec^{-2}$ (=50 kiloRayleighs, where 1 Rayleigh = 10^6 photons sec^{-1} per cm^2 per 4 π steradians).

The geocoronal emission lines are essentially unresolved at the resolution of STIS but the emission covers the sky in the spatial dimension. Using a wider slit or observing slitless does not increase the background counts per pixel from geocoronal emission, but does increase the area (range of wavelengths or pixels in the dispersion direction) over which that background is received. Observations using a slit which is N pixels wide in dispersion will be affected by geocoronal emission in a roughly N pixel region centered on the relevant geocoronal emission line wavelength. For slitless spectroscopy in the UV, the effects of geocoronal emission must be taken into account at all pixels, unless a long pass filter is employed to block off the short wavelength emission (see also “Longpass Filtered MAMA Imaging - F25SRF2 and F25QTZ” on page 59 and “Slitless First Order Spectroscopy” on page 161).

It is possible to request that exposures be taken when HST is in the umbral shadow of the earth to minimize geocoronal emission (e.g., if you are observing weak lines at 1216 or 1304 Å) using the special requirement SHADOW. Exposures using this special requirement are limited to roughly 32 minutes per orbit, exclusive of the guide star acquisition (or reacquisition) and can be scheduled only during a small percentage of the year. SHADOW reduces the contribution from the geocoronal emission lines by roughly a factor of ten. If you require SHADOW, you should request it in your Phase I proposal (see the Cycle 7 CP).

Extinction Correction

Extinction can dramatically alter the counts expected from your source, particularly in the ultraviolet. Figure 6.2 on page 76 shows A/E(B-V) values applicable to our galaxy, taken from Seaton (*MNRAS*, **187**, 73p, 1979).

Extinction curves, however, have strong metallicity dependence, particularly in the UV wavelengths. Sample extinction curves can be seen from Koorneef and Code, 1981, ApJ, 247, 860 (LMC), Bouchet et al. 1985, *A&A*, 149, 330 (SMC), and Calzetti, Kinney and Storchi-Bergmann, 1994, *ApJ*, 429, 582, and references therein. At lower metallicities, the 2200 Å bump which is so prominent in the galactic extinction curve disappears, and A/E(B-V) increases at UV wavelengths.

The easiest way to understand how to determine the extinction correction for your source is to work through an example; see “Echelle Spectroscopy of a Bright Star with Large Extinction (Sk 69 -215)” on page 81.

Figure 6.2: Extinction versus Wavelength

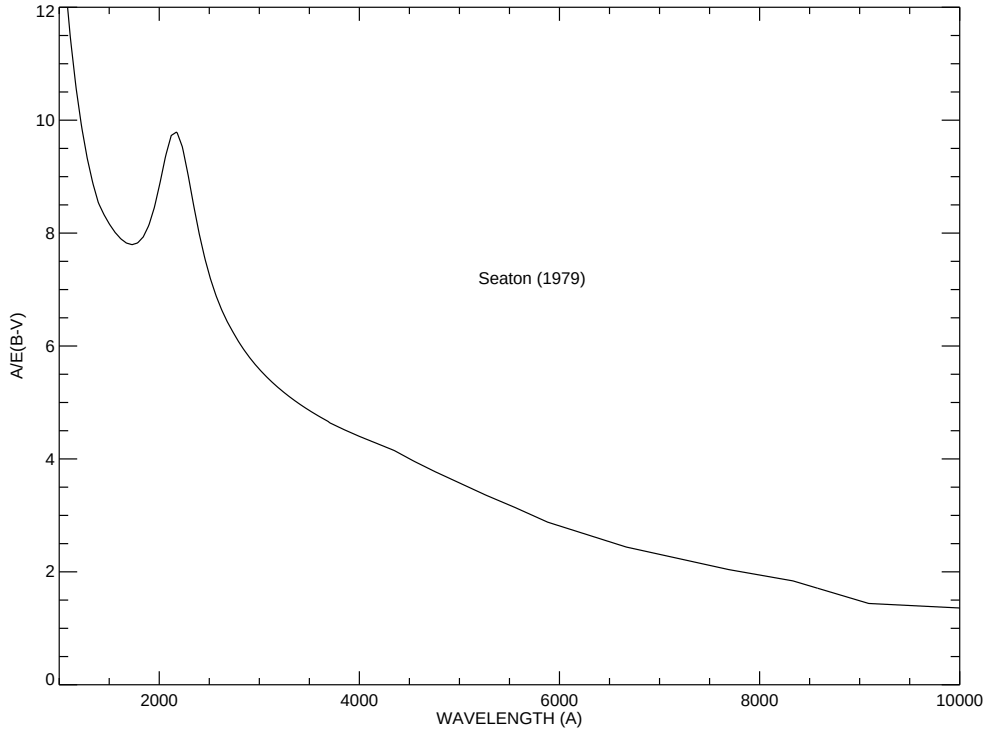

Exposure Time Examples

Here are a few simple examples to illustrate how an integration time may be computed for point sources and diffuse sources. The flux values given here are for illustrative purposes only, you would need to check the flux values if you are planning your own observations of one of these targets.

Spectroscopy of Diffuse Source (M86)

We want to observe M86, an elliptical galaxy in Virgo, using the `G750M` grating at central wavelength setting of λ_c=6768, the CCD detector and the 52 x 0.2 arcsec slit. Our aim is to calculate the count rate in the central region of M86 and the expected signal to noise ratio per resolution element in an exposure time of 1 hour. M86 has an inhomogeneous surface brightness distribution in Hα and the line is well resolved with this grating. Let us consider a region with a Hα surface brightness of $I_\lambda = 10^{-15}$ erg cm^{-2} sec^{-1} Å^{-1} arcsec^{-2} (note the unit - it is not the entire Hα flux but the flux per unit wavelength interval). To derive the count rate from the source we use:

- $Sens^d_\lambda$ = 1.2 x 10^{13} counts sec^{-1} pix_λ^{-1} pix_s^{-1} per incident erg cm^{-2} sec^{-1}Å^{-1}, taken from Table 13.2 on page 185.
- $N_{\lambda pix} = N_{spix} = 2$ (1 resolution element, see page 242).

Using the equation given on the bottom of page 70, we get the count rate C_s= 0.048 counts sec^{-1} at Hα.

The sky background is negligible in comparison, but the dark current (0.007 count sec^{-1} pixel^{-1} * 4 pixels = 0.028 count sec^{-1}) and the read noise squared (16 electrons * 4 pixels * 3 reads = 192 counts, for `CRSPLIT=3`) are important here. Substituting the numbers into the equation for signal-to-noise on page 70, we get:

$$StoN = 8 = \frac{0.048 \times 3600}{\sqrt{0.048 \times 3600 + 4 \times 0.007 \times 3600 + 4 \times 3 \times 16}}$$

To increase our signal-to-noise or decrease our exposure time, we can consider using on-chip binning. We bin 2 pixels in the spatial direction so that N_{bin}=2. To allow adequate sampling of our new binned pixels, we leave $N_{\lambda pix}$ = 2, but set N_{spix} = 4, so N_{pix}=8 and C_s=0.096. To compute the time to achieve a signal-to-noise of 8 using this configuration, we use the full expression for exposure time given on page 71 and determine that roughly 30 minutes are needed in this configuration:

$$t = 1800 = \frac{64 \times (0.096 + 8 \times 0.007) + \sqrt{4096 \times (0.096 + 8 \times 0.007)^2 + 4 \times 64 \times 0.096^2 \times (8/2) \times 3 \times 16}}{2 \times 0.096^2}$$

Spectroscopy of Solar Analog Star P041-C

We wish to study the shape of the continuum spectrum of the solar analog star, P041-C, from the near-IR to the near-UV. P041-C is a solar analog having V = 12.0. We wish to obtain spectroscopy with the CCD detector covering the entire useful spectral range from 2000 A to 11000 Å with gratings `G230LB`, `G430L`, and `G750L`. Since we require accurate photometry, we utilize the wide `52X0.5` slit. The goal is to reach a signal-to-noise ratio of 25 in the near-UV (at 2300 Å) and 100 from the visible through the near-IR.

The fluxes of P041-C at the desired wavelengths are obtained from a spectrum of the Sun (available via html://www.stsci.edu/ftp/cdbs/cdbs2/calspec filename Sun_REFERENCE), scaled from V=-26.75 to V=12.0.

G230LB

We illustrate the calculation of the exposure time calculation for the `G230LB` grating. P041-C is found to have a flux of 1.7e-15 erg sec^{-1} cm^{-2} $Å^{-1}$ at 2300 Å.

We take for `G230LB`:

- $S^{p}_{2300\ Å}$ = 1.6 x 10^{14} counts sec^{-1} pix_{λ}^{-1}per incident erg cm^{-2} sec^{-1} $Å^{-1}$ taken from Table 13.5 on page 198, and
- T_A = 0.8 for the aperture throughput, taken from Table 13.17 on page 243.
- ε_f = 0.8.
- N_{spix}=2, since 80% of the point source light is encircled with 2 pixels (see Table 13.19 on page 247).
- $N_{\lambda pix}$= 2, since two pixels resolves the LSF (see Table 13.17 on page 243).

Using the equation on page 67, we calculate a point source count rate of C_s=0.34 counts sec^{-1} over N_{pix}=4 pixels.

The source count rates can be compared with the background and detector rates. Both background and detector rates are negligibly small for all four wavelength positions. Therefore we can neglect their contributions. Since we are aiming for a signal-to-noise ratio of 25, we can estimate that we must obtain 625 counts minimum, and setting CRSPLIT=3 each exposure will have ~200 counts and the read noise squared (~64 over 4 pixels) will not be important and we can use the simplified expression for exposure time on page 71. Finally, since we are observing with the CCD in the near-UV, we must correct for the affect on the signal-to-noise calculation of the multiple-electron process (see page 71). We therefore scale the derived required exposure time by *Q*, where *Q* is ~1.5 at 2300 Å. Therefore we have:

$$t = 2757 = \frac{25^2 \times 1.5}{0.34}$$

G750L and G430L

Exposure times for the three remaining wavelength settings can be calculated directly as time = signal-to-noise^2/C_s. The results are summarized in the table below.

Table 6.4: Low Resolution Spectroscopy of Solar Analog Star

Grating	G230LB	G430L	G750L λ_c=7751	G750L λ_c=8975
Wavelength (Angstroms)	2300	5000	7800	11000
Flux (ergs sec^{-1} cm^{-2} Å^{-1})	1.7x10^{-15}	6.0x10^{-14}	3.8x10^{-14}	2.0 x10^{-14}
Point Source Sensitivity (counts sec^{-1} pix$_\lambda^{-1}$ per ergs sec^{-1} cm^{-2} Å^{-1})	1.6x10^{14}	4.3x10^{15}	8.9x10^{15}	~2x10^{14}
aperture throughput (TA)	80%	85%	85%	85%
$N_{\lambda pix}$	2	2	2	2
N_{spix} to encircle 80% of PSF	2	2	2	2
C_s (counts sec^{-1} from source over N_{pix}=4)	0.34	350	459	5.4
signal-to-noise ratio desired	25	100	100	100
total exposure time	2757 seconds	29 seconds	23 seconds	1852 seconds[a]

[a]We perform a quick rough check to assure we are not filling the CCD full well during these exposures at ~7000 Å at the peak of the G750L sensitivity where it is ~50 times more sensitive than at 11000 Å. The solar spectrum is roughly a factor 2.0 stronger as well there. The predicted peak per pixel count rate at 7000 Å is then ~135 counts sec^{-1} pixel^{-1}, assuming 25% of the point source flux falls in the peak pixel (see Table 13.19 on page 247). In each 1852/3 = 617 second exposure (recall CRSPLIT=3), the peak pixel has accumulated ~84,000 electrons, and we are safely below the full well limit.

Extended Source, with Flux in cgs units (NGC 6543): Imaging and Spectroscopy

Let us consider NGC 6543, the ‘cats eye’ planetary nebula, where the aim is to use the CCD to image using the [OIII] filter, and to obtain spectra both in the visible and in the UV.

Imaging

The aim is to get a signal-to-noise ratio of 100 using the [OIII] filter. We know that NGC 6543 is about 6.5 times stronger in [OIII] than in Hβ, and its total flux at [OIII] 5007 Å is ~1.7 x 10^{-9} erg cm^{-2} sec^{-1} contained within 1 Å. Since the radius of the object is about 10 arcsec, the average [OIII] surface brightness is about 5.4 x 10^{-12} erg cm^{-2} sec^{-1} arcsec^{-2} Å^{-1}.

We take:

- $Sens^d_\lambda$ = 3.8x10^{12} counts sec^{-1} pix^{-1} Å^{-1}per incident erg cm^{-2} sec^{-1} Å^{-1} arc-sec^{-2} as given in Table 14.3 on page 266.

- We take N_{pix} = 2x2=4, since two pixels is a resolution element (see Figure 14.61 on page 306).

To calculate the count rate we use the equation on page 70 for diffuse sources and determine a per pixel count rate of 20 counts sec^{-1} $pixel^{-1}$ or a count rate C_s = 80 counts sec^{-1}over four pixels. The background and the dark current can be safely neglected. To get a signal-to-noise of 100 we need 10^4 counts, so the read noise can also be safely neglected and we can use the simplified expression to calculate exposure time (see page 71). We obtain 10^4 counts in ~125 seconds. To allow robust post-observation removal of cosmic rays we use `CRSPLIT=4`. We note that in each ~30 second exposure we predict a mean of ~600 (=80*30/4 pixels) counts $pixel^{-1}$, and thus we are safely within the limits of the CCD full well so long as there are not local [OIII] brightness peaks which exceed the mean by more than a factor of ~200.

Diffuse Source Spectroscopy in the Visible and UV Regions

In the visible, the aim is to get a signal-to-noise of about 100 at λ = 4861 Å, using the `G430M` grating at a central wavelength setting of λ_c=4961 Å. the CCD detector and the 52X0.1 arcsec slit. In the UV, the aim is to get a signal-to-noise ratio of about 10 at the CIV ~1550 Å line using the `G140M` grating at a central wavelength setting of λ_c=1550 and the FUV-MAMA detector. To increase our signal-to-noise ratio in the UV, we utilize the `52X0.2` arcsec slit for the G140M spectroscopic observations.

Visible Region

NGC 6543 has an average Hβ surface brightness of S(Hβ) ~ 8.37 x 10^{-13} erg cm^{-2} sec^{-1} $Å^{-1}$ $arcsec^{-2}$ at 4861 Å and has a radius of about 10 arcsec.

We take:

- $Sens^d_\lambda$ = 1.4 x 10^{12} counts sec^{-1} pix_λ^{-1} pix_s^{-1} per incident erg cm^{-2} $sec^{-1}Å^{-1}$ $arcsec^{-2}$ from Table 13.4 on page 193 for `G430M`,and
- $N_{\lambda pix}$ = N_{spix} =2 since 2 pixels resolves the LSF and PSF (see Table 13.17 on page 243 and Table 13.19 on page 247).

Using the equation for diffuse sources on page 68, we derive a per pixel count rate of 1.2 counts sec^{-1} $pixel^{-1}$ and a count rate integrated over the four pixels of C_s = 4.7 counts sec^{-1} at 4861 Å from the astronomical source. The sky background and the detector background are much lower. To allow cosmic ray removal in post observation data processing, we use `CRSPLIT=3`. To achieve a signal-to-noise of 100, we require a total of roughly 10,000 counts, so read noise should be negligible, even over 4 pixels and with nread=3. We calculate the time required to achieve signal-to-noise of 100, using the simplified equation on page 71, and determine that we require roughly 35 minutes.

$$t = 2127 = \frac{10000}{4.7}$$

At a count rate of ~1 count sec^{-1} $pixel^{-1}$ for 700 seconds per CR-SPLIT exposure, we are in no danger of hitting the CCD full well limit.

UV Region

The CIV flux of NGC 6543 is ~ 2.5 x 10^{-12} erg cm^{-2} sec^{-1} $arcsec^{-2}$ spread over ~1 Å. The line, with a FWHM ~ 0.4 Å, will be well resolved in the `G140M` configuration using the `52X0.2` slit.

We take:

- $Sens^{d}_{\lambda}$ = 5.8 x10^{9} counts sec^{-1} pix_{λ}^{-1} pix_{s}^{-1} per incident erg cm^{-2} $sec^{-1}Å^{-1}$ $arcsec^{-2}$ from Table 13.10 on page 219 for G140L at λ=1550Å using the 0.2 arcsecond wide slit.
- We take $N_{\lambda pix} = N_{spix} = 8$, since the line emission is spread over the ~8 pixels of the slit width in dispersion, and we are willing to integrate flux along the slit to improve the signal-to-noise ratio.

Using the equation for diffuse sources on page 68, we determine a per pixel peak count rate of ~0.015 counts sec^{-1} $pixel^{-1}$ and a count rate over the 64 pixels of C_s = 0.93 counts sec^{-1} at 1515 Å from the astronomical source. The sky and detector backgrounds are still negligible, and the read noise is zero for the MAMA detector so we can use the simplified equation for exposure time on page 71 directly. We determine that we require ~ 7 minutes.

$$t = 430 = \frac{400}{0.93}$$

We are well below the MAMA local science linearity limit of 50 counts sec^{-1} $pixel^{-1}$. Even assuming the nebula evenly illuminates the full 28 arcseconds of the long slit, we are well below the global absolute and science linearity limits, since the flux from the nebula is concentrated in the CIV emission line. Then the global count rate, if the source fully fills the slit in the spatial direction, is given roughly by 0.015 * 8 * 1024 << 200,000 counts sec^{-1}. Finally, we are well below the MAMA 16 bit buffer limit of a maximum of 65536 counts $pixel^{-1}$ integrated over the exposure duration.

Echelle Spectroscopy of a Bright Star with Large Extinction (Sk 69 -215)

The aim here is to do high-resolution Echelle spectroscopy of an O5 star in the LMC (such as Sk 69-215) at 2500 Å, using the `E230H` grating at a central wavelength of λ_c=2513 and using the 0.1X0.09 arcsec slit. The aim is to get a signal-to-noise ratio of about 50 from photon statistics. We will assume that the exact UV flux of the star is unknown and we need to estimate it from the optical data.

This calculation of the stellar flux at 2500 Å involves 2 steps: (i) calculation of the dereddened magnitude flux at 5500 Å, and (ii) calculation of predicted flux at 2500 A taking reddening and standard extinction and stellar models into account.

Dereddened Magnitude and Prediction 2500 Å Flux

We assume that it is an O5 star with V = 11.6 (Its exact spectral type is slightly uncertain). The expected B-V value from such a star is -0.35, whereas the observed B-V is -0.09; we thus get E(B-V) = 0.26 mag for the star.

We assume all the extinction to be due to LMC, and use the appropriate extinction law (Koorneef and Code, 1981, ApJ, 247, 860). The total visual extinction is then R x E(B-V) = 3.1 x 0.26 = 0.82, leading to a intrinsic magnitude of V_0=10.78. The corresponding flux at 5500 Å (using the standard zero point where V=0 corresponds to F5500 = 3.55 x 10^{-9} erg sec^{-1} cm^{-2} $Å^{-1}$) is F5500 = 1.73 x 10^{-13} erg sec^{-1} cm^{-2} $Å^{-1}$.

The model atmosphere of Kurucz predicts F2500Å/F5500Å = 17.2 for a O5 star. This leads to a flux of F2500 Å = 2.98 x 10^{-12} erg sec^{-1} cm^{-2} $Å^{-1}$ at 2500 Å for the unreddened star. Reddening will diminish this by a factor 0f $10^{-0.4xA(2500)}$, where the absorption at 2500 Å can be determined from the extinction curve; the result in this case is A(2500 Å) = 1.3. Thus the predicted flux of this star at 2500 A is 9.0 x 10^{-13} erg sec^{-1} cm^{-2} $Å^{-1}$.

Exposure Time Calculation

We take:

- $S^{p}_{2500\ Å}$ = 3.2 x 10^{11} counts sec^{-1} pix_{λ}^{-1}per incident erg cm^{-2} sec^{-1} $Å^{-1}$ from Table 13.12 on page 227 for `E230H`, and
- T_A = 0.6 for the aperture throughput, taken from Table 13.22 on page 250.
- ε_f = 0.8 for the encircled energy, taken from Table 13.23 on page 253.
- $N_{\lambda pix}$= 2, since two pixels resolves the LSF (see Table 13.22 on page 250).
- N_{spix}=4, since 80% of the point source light is encircled with 4 pixels (see Table 13.23 on page 253).

Using the equation for point sources on page 67, we determine a total count rate from the star of C_s = 0.3 counts sec^{-1} over 8 pixels. From Table 13.23 on page 253 we see that ~22 percent of the point source flux will be contained within the peak pixel. Thus the peak per pixel count rate will be ~0.3x0.22/(0.8x2)=0.045 counts sec^{-1} $pixel^{-1}$ and well within the local linear counting regime. We can use the information that we register ~0.3 counts sec^{-1} for every two pixels in the dispersion direction to estimate the global count rate (over the entire detector) as follows. Each order contains ~1024 pixels, and the E230H grating at the central wavelength setting of 2513 covers 33 orders (see Figure 13.55 on page 226). A rough estimate of the global count rate is thus ~33 x 512 x 0.3/ 0.8 ~6400 count sec^{-1} and we are well within the linear range.

To calculate the integration time, we can ignore both the sky background and the detector dark current which are several orders of magnitude fainter than the source. To achieve a signal-to-noise ratio of 50 we then require ~2500 counts which would take a total of ~3 hours. Fortunately, this is a CVZ target!

Imaging a Faint Stellar Source

Consider a case where the aim is to image a faint (V=29), A-type star, using the clear filter and the CCD detector. We want to calculate the integration time required to achieve a signal-to-noise ratio of 5. The count rate from the source is 0.07 counts sec^{-1} distributed over about 4 pixels. If we assume the background to be “typical high” (Table 6.5 on page 84), the count rate due to the background integrated over the bandpass is ~ 0.3 counts sec^{-1} $pixel^{-1}$ or 1.2 counts sec^{-1} in 4 pixels (and the detector dark rate is 50 times lower). We will need to be able to robustly distinguish cosmic rays if we are looking for faint sources, so we will use `CRSPLIT=4`. We use the full equation for exposure time given on page 71, and plugging in the numbers determine exposure time = 6530 seconds, or 108 minutes.:

$$t = 6530 = \frac{5^2 \times (0.07 + 4 \times 0.3) + \sqrt{5^4 \times (0.07 + 4 \times 0.3)^2 + 4 \times 5^2 \times 0.07^2 \times 4 \times 4 \times 16}}{2 \times 0.07^2}$$

Alternately, we could have requested `LOW-SKY` (see “Sky Background” on page 72), since these observations are sky background limited. In that case the sky background integrated over the bandpass produces ~0.04 counts sec^{-1} $pixel^{-1}$ to which we add the detector dark current to get a total background of 0.047 counts sec^{-1} $pixel^{-1}$. Using the full equation for exposure time again, we then determine that we require only ~30 minutes. This is the preferable way to perform this experiment.

$$t = 1976 = \frac{5^2 \times (0.07 + 4 \times 0.047) + \sqrt{5^4 \times (0.07 + 4 \times 0.047)^2 + 4 \times 5^2 \times 0.07^2 \times 4 \times 4 \times 16}}{2 \times 0.07^2}$$

Time-Tag Observations of a Flare Star (AU Mic)

Suppose the aim is to do `TIME-TAG` observations of a flare star such as AU Mic, in the Hydrogen Ly α 1216 Å line (see “MAMA TIMETAG Mode” on page 146. We wish to observe it with the G140M grating, the MAMA detector and a 0.2 arcsec slit. AU Mic has V = 8.75, the intensity of its the Ly α line is about 6 (+/- 3) x 10^{-12} erg cm^{-2} sec^{-1} $Å^{-1}$, and the width (FWHM) of the line is about 0.7 (+/- 0.2) Å. We will assume that during bursts, the flux might vary by a factor of 10, so that the line flux may be up to 60 x 10^{-12} erg cm^{-2} sec^{-1} $Å^{-1}$. AU Mic is an M star and its ultraviolet continuum is small and can be neglected.

We use:

- $Sens^P_\lambda$ = 1.97 x 10^{12} counts sec^{-1} $pix_\lambda{}^{-1}$per incident erg cm^{-2} sec^{-1} $Å^{-1}$ (see page 218).
- Aperture throughput T_A = 0.6 (from Table 13.18 on page 243).

- "Ensquared energy" $\varepsilon_f = 0.8$ (see page 242).
- $N_{spix} = 8$ (see Table 13.20 on page 248).
- Derive $N_{\lambda pix}$= 14 since the line FWHM is ~ 0.7 Å and the dispersive plate scale for G140M is 0.05 Å pixel^{-1}

Plugging these values into the point source equation on page 67, we get C_s = 795 counts sec^{-1} over 8 x 14 pixels, or ~1000 count sec^{-1} from the source (taking ε_f = 1.0). This is well below the MAMA `TIME-TAG` global linearity limit of 30,000 count sec^{-1} and the continuous observing limit of 26,000 count sec^{-1}. The line is spread over 14 pixels in dispersion and only roughly 10% of the flux in the dispersion direction falls in the peak pixel, thus the peak per pixel count rate, P_{cr}, is roughly 795/(14x8)=8 counts sec^{-1} pixel^{-1} and we are not near the MAMA local linearity limit.

For a `TIME-TAG` exposure, we need to determine our maximum allowed total observation time, which is given by 6.0 x 10^7/ C_s seconds or roughly 1258 minutes or 21 hours. For Phase II only, we will also need to compute the value of the `BUFFER-TIME` parameter, which is the time in seconds to count 2 x 10^6 counts, or in this case is 2515 seconds (=2x10^6/795).

Tabular Sky Backgrounds

We provide a table of the typical sky background numbers, for easy reference.

Table 6.5: Typical High Sky Backgrounds

Wavelength	Earthshine	Geo-Coronal Emission	Zodiacal Light	Total Background
Å	ergs cm^{-2} s^{-1} Å^{-1} arcsec^{-2}	ergs cm^{-2} s^{-1} arcsec^{-2}	ergs cm^{-2} s^{-1} Å^{-1} arcsec^{-2}	ergs cm^{-2} s^{-1} Å^{-1} arcsec^{-2}
1000.	4.8E-23		7.3E-29	4.8E-23
1100.	8.8E-22		6.0E-27	8.8E-22
1200.	8.0E-23		6.1E-26	8.0E-23
1215		1.1E-13		
1400.	8.6E-25		1.5E-24	2.3E-24
1302		1.1E-14		
1356		3.3E-15		
1500.	8.3E-25		5.3E-24	6.1E-24
1600.	5.1E-25		1.3E-22	1.3E-22
1700.	1.6E-24		4.1E-21	4.1E-21
1800.	1.9E-22		8.8E-21	8.9E-21
1900.	8.8E-22		1.3E-20	1.4E-20
2000.	2.0E-21		2.0E-20	2.2E-20
2100.	3.2E-21		7.0E-20	7.4E-20
2200.	1.5E-21		1.3E-19	1.3E-19
2300.	6.6E-22		1.0E-19	1.0E-19

Table 6.5: Typical High Sky Backgrounds (Continued)

Wavelength	Earthshine	Geo-Coronal Emission	Zodiacal Light	Total Background
Å	ergs cm^{-2} s^{-1} $Å^{-1}$ $arcsec^{-2}$	ergs cm^{-2} s^{-1} $arcsec^{-2}$	ergs cm^{-2} s^{-1} $Å^{-1}$ $arcsec^{-2}$	ergs cm^{-2} s^{-1} $Å^{-1}$ $arcsec^{-2}$
2400.	5.0E-22		1.0E-19	1.0E-19
2470		3.3E-15		
2500.	4.8E-22		1.4E-19	1.4E-19
2600.	1.1E-21		1.7E-19	1.7E-19
2700.	1.4E-20		5.8E-19	5.9E-19
2800.	4.1E-21		1.6E-19	1.7E-19
2900.	8.6E-20		1.2E-18	1.3E-18
3000.	1.9E-19		7.0E-19	8.8E-19
3100.	4.1E-19		8.5E-19	1.3E-18
3200.	7.2E-19		1.3E-18	2.0E-18
3400.	1.3E-18		1.6E-18	2.9E-18
3500.	1.6E-18		1.6E-18	3.2E-18
3600.	2.1E-18		1.8E-18	3.9E-18
3700.	2.4E-18		1.9E-18	4.3E-18
3800.	2.5E-18		1.9E-18	4.3E-18
3900.	3.0E-18		1.9E-18	5.0E-18
4000.	4.8E-18		2.8E-18	7.5E-18
4200.	4.8E-18		2.9E-18	7.7E-18
4400.	6.0E-18		2.9E-18	8.9E-18
4600.	6.8E-18		3.1E-18	1.0E-17
4800.	6.7E-18		3.4E-18	1.0E-17
5000.	6.9E-18		3.0E-18	9.9E-18
5200.	6.9E-18		2.8E-18	9.7E-18
5400.	7.1E-18		2.8E-18	9.9E-18
5600.	7.4E-18		2.7E-18	1.0E-17
5800	7.4E--18		2.7E-18	1.0E-17
6000.	7.3E-18		2.6E-18	9.9E-18
6200.	7.0E-18		2.5E-18	9.5E-18
6400.	6.8E-18		2.5E-18	9.3E-18
6600.	6.7E-18		2.4E-18	9.1E-18
6800.	6.5E-18		2.3E-18	8.8E-18
7000.	6.3E-18		2.2E-18	8.5E-18
7200.	6.2E-18		2.2E-18	8.3E-18
7400.	5.9E-18		2.0E-18	7.9E-18
7600.	5.8E-18		1.7E-18	7.5E-18
7800.	5.6E-18		1.8E-18	7.4E-18
8000.	5.4E-18		1.7E-18	7.2E-18
8200.	5.2E-18		1.7E-18	6.9E-18
8400.	5.1E-18		1.6E-18	6.7E-18
8600.	4.9E-18		1.6E-18	6.4E-18

Table 6.5: Typical High Sky Backgrounds (Continued)

Wavelength	Earthshine	Geo-Coronal Emission	Zodiacal Light	Total Background
Å	ergs cm^{-2} s^{-1} $Å^{-1}$ $arcsec^{-2}$	ergs cm^{-2} s^{-1} $arcsec^{-2}$	ergs cm^{-2} s^{-1} $Å^{-1}$ $arcsec^{-2}$	ergs cm^{-2} s^{-1} $Å^{-1}$ $arcsec^{-2}$
8800.	4.7E-18		1.5E-18	6.2E-18
9000.	4.5E-18		1.3E-18	5.9E-18
9200.	4.4E-18		1.3E-18	5.8E-18
9400.	4.3E-18		1.6E-18	5.9E-18
9600.	4.2E-18		1.3E-18	5.6E-18
9800.	4.1E-18		1.2E-18	5.3E-18
10000.	3.9E-18		1.1E-18	5.0E-18
10200.	3.8E-18		1.1E-18	4.8E-18
10400.	3.6E-18		1.0E-18	4.7E-18
10700.	3.5E-18		9.8E-19	4.4E-18
10800.	3.4E-18		9.6E-19	4.4E-18
11000.	3.3E-18		9.3E-19	4.2E-18

CHAPTER 7
Feasibility and Detector Performance

In This Chapter...

STIS employs two fundamentally different types of detector; a UV-optimized CCD for use from the near-UV to the near-IR and Multi-Anode Microchannel Array detectors, known as MAMAs, for use in the ultraviolet. The CCD and the MAMA detectors are used in different ways and impose their own unique limitations on the feasibility of science performed using them. In this chapter we present the properties of the STIS detectors, describe how to use them to optimize science and list the steps you should take to assure your observations are feasible.

The CCD

Detector Properties

The `STIS/CCD` is a low noise device capable of high sensitivity in the visible and the near-UV. It is a thinned, backside illuminated device manufactured by Scientific Imaging Technologies (SITe). In order to provide a near-UV imaging performance, the CCD has been backside treated and coated with a wide band AR coating. The process produces acceptable near-UV quantum efficiency (QE) without compromising the high QE of the visible bandpass. The CCD camera design incorporates a warm dewar window, designed to prevent build up of contaminants on the window which we have found to cause a loss of UV

throughput for the WFPC2 CCDs. A summary of the CCD's expected performance is given in Table 7.1. We note, that the actual properties (read noise, dark current, and full well depth) of the STIS flight CCD detector are not known at the time of the writing of this handbook. We expect to have more information by August, and updates will be made at that time (see"Updates to Instrument Performance for Cycle 7" on page 12).

Table 7.1: Provisional CCD Detector Performance Characteristics

Detector	CCD
Architecture	Thinned, backside illuminated
Wavelength range	2000 - 11000 Å
Pixel format	1024x1024
Pixel field of view	51x51 arcseconds
Pixel size	21 μm
Pixel plate scale	0.05 arcseconds
Quantum efficiency	≥20% @ 3000 Å ≥60% @ 5000 Å ≥20% @ 9000 Å
Dark count @-80^{o}c	0.007 counts sec^{-1} pix^{-1}
Read Noise	4 e^{-} RMS
Full well	170,000 e^{-} over the inner portion of the detector 120,000 e^{-} over the outer portion of the detector

CCD Spectral Response

The spectral response of the unfiltered CCD is shown in Figure 5.1 on page 50 (labelled as 50CCD). This figure illustrates the extremely wide bandpass over which this CCD can operate. The wide wavelength coverage can be used to advantage for deep optical imaging. The near-UV sensitivity of the CCD makes it a good alternative to the NUV-MAMA for low and intermediate resolution spectroscopy from ~2500–3100 Å using the G230LB and G230MB grating modes (see Table 4.1, "STIS Spectroscopic Capabilities," on page 34).

Based on test data to date, the STIS CCD does not suffer from Quantum Efficiency Hysteresis (QEH)—that is the CCD responds in the same way to light levels in the same way over its whole dynamic range, irrespective of the previous illumination level.

Preliminary testing of the STIS CCD indicates that it exhibits some fringing in the red, longward of ~7000 Å. This fringing may limit the signal-to-noise routinely achievable in the red and near-IR. Depending on the stability and wavelength dependence of the effect, it may be possible to employ special techniques when observing to minimize the effect.

Optical Performance

The CCD plate scale is 0.05 arcseconds per pixel, for both imaging and spectroscopic observations. Predicted encircled energies as a function of observing wavelength are described for the CCD spectroscopic modes and the CCD Imaging modes in Chapters 13 and 14 respectively.

Read Out

A full detector readout is 1064 x 1044 pixels with physical and virtual overscans. Science data are obtained on 1024 x 1024 pixels, each projecting to ~0.05 x 0.05 arcseconds on the sky. For spectroscopic observations, the dispersion axis runs along `AXIS1` (image x or along a row of the CCD), and the spatial axis of the slits runs along `AXIS2` (image y or along a column of the CCD). The CCD supports the use of subarrays to read out only a portion of the detector, and on-chip binning. For more details see “CCD ACCUM Mode” on page 141.

Analog-To-Digital Conversion

Electrons which accumulate in the CCD wells are read out and converted to data numbers (DN, the format of the output image) by the analog-to-digital converter at a default `GAIN` of 4 e^-/DN (i.e., every 4 electrons register 1 DN). The analog-to-digital converter operates at 16-bits, producing a maximum of 65536 data numbers $pixel^{-1}$. At 4 e-/DN, the maximum 170,000 e- of the CCD full well (see “CCD Saturation: the CCD Full Well” on page 90 below) can be used without saturating during the conversion.

The CCD is also capable of operating at gains of 1, 2, or 8 e^-/DN. In principal, use of a lower gain can increase the dynamic range of faint source observations by reducing the quantization noise, however in practice this improvement may be insignificant. At this time the read noise and analog-to-digital conversion noise of the STIS CCD has not been categorized. If, following ground science calibration, and prior to Phase II, we determine that there is significant benefit to using a lower GAIN in faint source applications, the default GAIN will be changed, and GAIN made a fully selectable user parameter. Note that at a gain of 1 or 2, the 16-bit format of the A-D converter, which limits its output to 65535 DN, will saturate prior to the CCD full well.

Hot Pixels

It is expected that hot pixels, caused by radiation damage, will occur in the STIS CCD. Dark frames will be obtained about once per week in order to maintain a master list of hot pixels. We expect that, on a monthly time scale, the `CCD` will be raised to ambient temperature, from its normal operating temperature of ~-80^o C, in order to permit annealing of hot pixels. These measures are similar to those used currently for WFPC2 to deal with hot pixels.

CCD Operation and Feasibility Considerations

CCD Saturation: the CCD Full Well

There are no hard bright object limits to worry about for CCD observations, since the CCD cannot be damaged by observations of bright sources. However, the CCD pixels do saturate at high accumulated count levels, due to the finite depth of the CCD full well. The full well properties of the CCD have yet to be fully characterized. It appears that there will be a region near the center of the chip where the CCD saturates at ~170,000 electrons pixel^{-1}, however over the outer (serial) portion the CCD saturates at 120,000 electrons pixel^{-1}. The variation of the CCD full well over the chip occurs because of non-uniformity in the process of boron implantation, which creates the potential wells in this type of CCD.

Saturation imposes a limit on the product of the count rate and the integration time. Keep the total counts *in the pixels of interest* below the saturation level, either by keeping the exposure time short enough that the limit is not violated in any single integration or by choosing a more appropriate configuration. You can allow saturation to occur in regions of the image over which you do not wish to extract information (e.g., you can allow a star or single emission line to saturate if you are interested in other features). Remember, however, that once the CCD full well is over full, charge will bleed along the columns of the CCD so that neighboring pixels (along the slit for spectroscopic observations) will also be affected. Saturation *cannot* be corrected for in post observation data processing.

In “Determining Count Rates from Sensitivities” on page 66 we explained how to determine the peak counts sec^{-1} pixel^{-1} expected for your observation. In Chapter 13 (page 175) for each grating mode and in Chapter 14 (page 257), for each imaging mode, we provide, for spectroscopy and imaging respectively, plots of exposure time to fill the CCD full well versus source flux for each STIS configuration. Lastly, an exposure time calculator is available on the STScI STIS World Wide Web site. Use one of these to assure your observations will not saturate sources of interest.

The minimum CCD exposure time is 0.1 seconds, providing a true limit to the brightest source that can be observed *without saturating*.

Keep the accumulated electrons pixel^{-1} per exposure below 120,000.

Cosmic Rays

All CCD exposures are expected to be affected by cosmic rays. To allow removal of cosmic rays in post-observation data processing we recommend that wherever possible, given signal-to-noise constraints, you take two or more exposures in any given CCD configuration (see also “CRSPLIT” on page 153).

The greater the number of independent exposures, the more robust is the removal of cosmic rays. However, observers must balance the decrease in signal-to-noise which results from the splitting of exposures when in the read noise limited regime with the desire to remove cosmic rays.

In observations of faint sources, particularly for dispersed light exposures, the intrinsic count rates can be very low. With a dark current of 0.007 e^-/sec it takes ~35 minutes of integration for the Poisson statistics on the minimal background to equal the read noise. Therefore, repeated exposures when observing faint sources, can significantly increase the total noise from added readouts. Selecting the correct number, and length of repeated integrations requires a consideration of the trade-off between increased read noise and more robust cosmic-ray elimination. The saturation curves in the grating sections in Chapter 13 (page 175) and the filter sections in Chapter 14 (page 257) show, for a given source flux, the integration time where source plus background counts exceed 2 times the read noise (i.e., when you are no longer in the read noise limited regime). You can use these plots to guide your CR-SPLIT observation strategy.

Be sure to take at least two identical CCD exposures in each configuration to allow removal of cosmic rays in post observation data processing.

UV Light and the STIS CCD

In the optical, each photon generates a single electron. However, in the near-UV, shortward of ~3200 Å there is a finite probability of creating more than one electron per UV photon (see Christensen, O, 1976, *J. App. Phys*. 47, 689). Users will need to take this into account when calculating signal-to-noise ratios and exposure times for the `G230LB` and `G230MB` gratings, as described in “Special Case—Spectroscopic CCD Observations at λ<2500 Å” on page 71.

Excessive illumination by UV light can cause an elevation in residual dark current, due to a surface chemistry effect. This is a concern only for clear (`50CCD`) imaging observations. To guard against the impact of such a dark current elevation on science observations:

- Use the LongPass filtered aperture, `F28X50LP`, rather than the `50CCD` clear aperture, for CCD imaging observations of bright fields, including during target acquisitions (see also “Imaging Apertures for Use in Target Acquisitions” on page 111) as possible.
- All clear CCD imaging observations are limited to at most 15 minutes per exposure (see “Unfiltered (Clear) CCD Imaging - 50CCD” on page 54) and observations of fields with ultraviolet bright sources may require dithering.
- Pure parallel observations with the `50CCD` clear aperture are not allowed.
- Following coronographic observations of bright (V<10) targets, the CCD will not be used for science for roughly 1 hour, to allow the dark current to equilibrate to near its normal value before other CCD science is begun.

Observers taking such bright coronagraphic exposures will need to allocate an orbit per visit in their proposal for this clean up (see “Coronagraphic Imaging and Spectroscopy” on page 170).

The MAMA Detectors

MAMA Properties

There are two MAMA detectors; the `STIS/FUV-MAMA` provides coverage from 1150–1700 Å and the `STIS/NUV-MAMA` provides coverage from 1650–3100 Å (with lower response to below 1200 Å). The STIS MAMA detectors are photon counting detectors which process events serially. They can be used to take data in either an accumulate (`ACCUM`) mode in which a time integrated image is produced, or in a time series (`TIME-TAG` mode) in which the detector location and time of arrival of each photon is recorded as an event stream (see “MAMA ACCUM” on page 143 and “MAMA TIMETAG Mode” on page 146, respectively). The primary benefits afforded by the STIS MAMAs, in comparison with existing HST UV spectroscopic detectors such as the GHRS and FOS, are high spatial resolution, two-dimensional imaging over a relatively large field of view, and low background for point sources. The MAMA detector was developed by J. Timothy and R. Bybee (Timothy and Bybee 1975) for X-ray and UV imaging applications. The provisional properties of the MAMA detectors are summarized below in Table 7.2.

Table 7.2: Provisional MAMA Detector Performance Specification

Detector	Far-UV MAMA	Near-UV MAMA
Photocathode	CsI	Cs_2Te
Wavelength range	1150–1700 Å	1650–3100 Å
Pixel format	1024 x 1024	1024 x 1024
Pixel size	25 x 25 μm	25 x 25 μm
Image mode pixel size	0.024 x 0.024 arcseconds	0.024 x 0.024 arcseconds
Field of view	24.9 x 24.9 arcseconds	24.9 x 24.9 arcseconds
Quantum efficiency	25% @ 1216 Å	10% @ 2537 Å
Dark count	$6.25x10^{-5}$ cnts pix^{-1} sec^{-1}	$1.25x10^{-4}$ cnts pix^{-1} sec^{-1}
Global count rate linearity limit[a]	300,000 cnts sec^{-1}	300,000 cnts sec^{-1}
Local count rate linearity limit[a]	~50 cnts pix^{-1} sec^{-1}	~50 cnts pix^{-1} sec^{-1}

[a]Rate where counting shows 10% deviation from linearity.

Figure 7.1 and 7.2 illustrate the design of the NUV and FUV MAMAs. A photocathode material is deposited on the front surface. The FUV-MAMA has an opaque CsI photocathode deposited directly on the face of the curved micro-channel plate (MCP); the NUV-MAMA has a semi-transparent Cs_2Te photocathode deposited on the back side of the detector's entrance window.

Target photons strike the photocathode, liberating single photo-electrons which pass into the microchannel plate (MCP). There they are multiplied to a pulse of ~$4x10^5$ electrons. The pulse is recorded by an anode array behind the photocathode and detected by the MAMA electronics which process it, rejecting false pulses and determining the origin of the photon event on the detector.

Figure 7.1: Design of the FUV MAMA

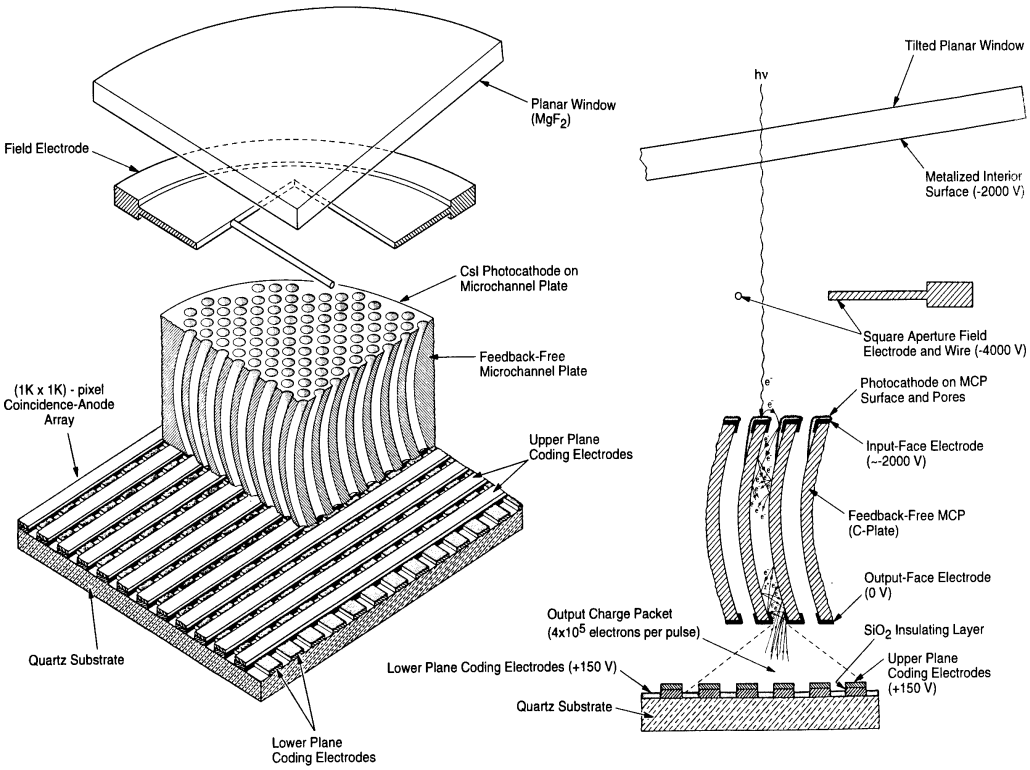

Figure 7.2: Design of the NUV MAMA

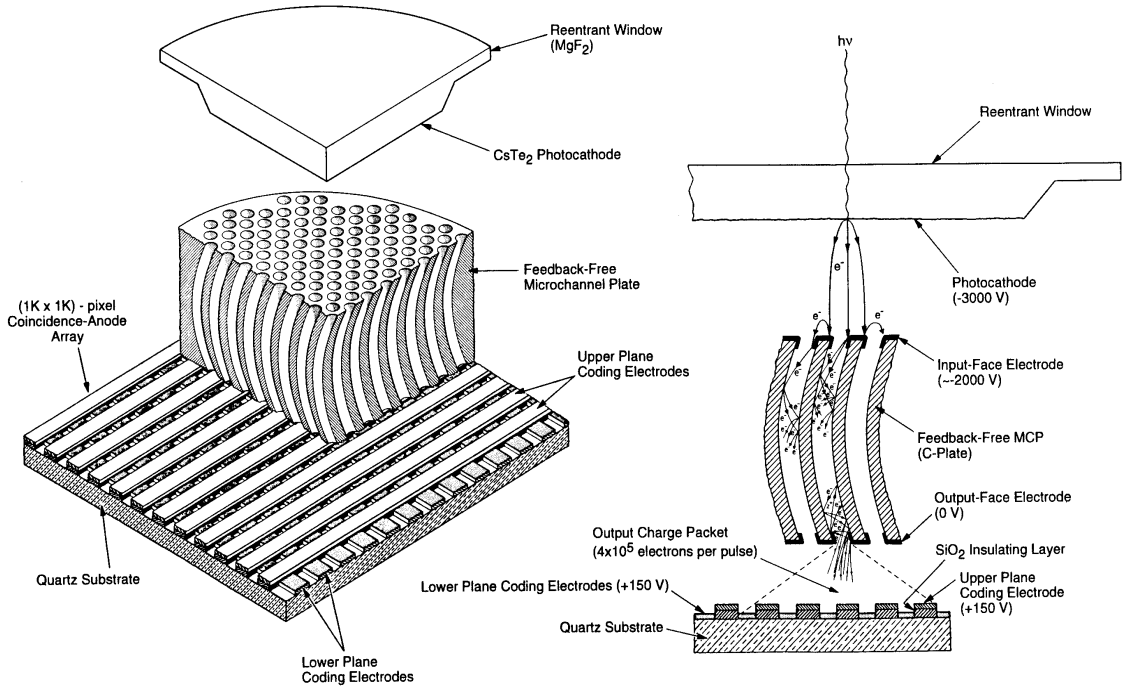

MAMA Spectral Response

The spectral responses of the unfiltered NUV and FUV MAMAs are illustrated in Figure 5.9 on page 59. The peak photocathode response of the FUV-MAMA occurs at Lyman α. Its spectral response is defined by the cutoff of the MgF window at 1150 Å at short wavelengths, and by the relatively steep decline of the CsI photocathode at long wavelengths. Out of band QE at longer wavelengths (>2000 Å) is $<10^{-6}$ yielding excellent solar blind performance. The NUV-MAMA spectral response has a relatively flat maximum (~10%) which encompasses 1800-2600 Å. The photocathode QE declines to ~4% at 3150 Å, while at longer wavelengths the out of band QE is $\sim10^{-4}$. (See also “Unfiltered (Clear) MAMA Imaging” on page 58.)

Optical Performance

Both the MAMAs exhibit low level extended wings in their detector point spread functions (PSF), with the NUV-MAMA PSF being considerably worse. Sample MAMA detector PSFs are shown in Figure 7.3. For those wishing to model their affect on absorption or emission line equivalent width measurements or coronographic observations, the LSFs and detector PSFs are maintained on the STScI STIS World Wide Web page.

Figure 7.3: MAMA Detector PSFs

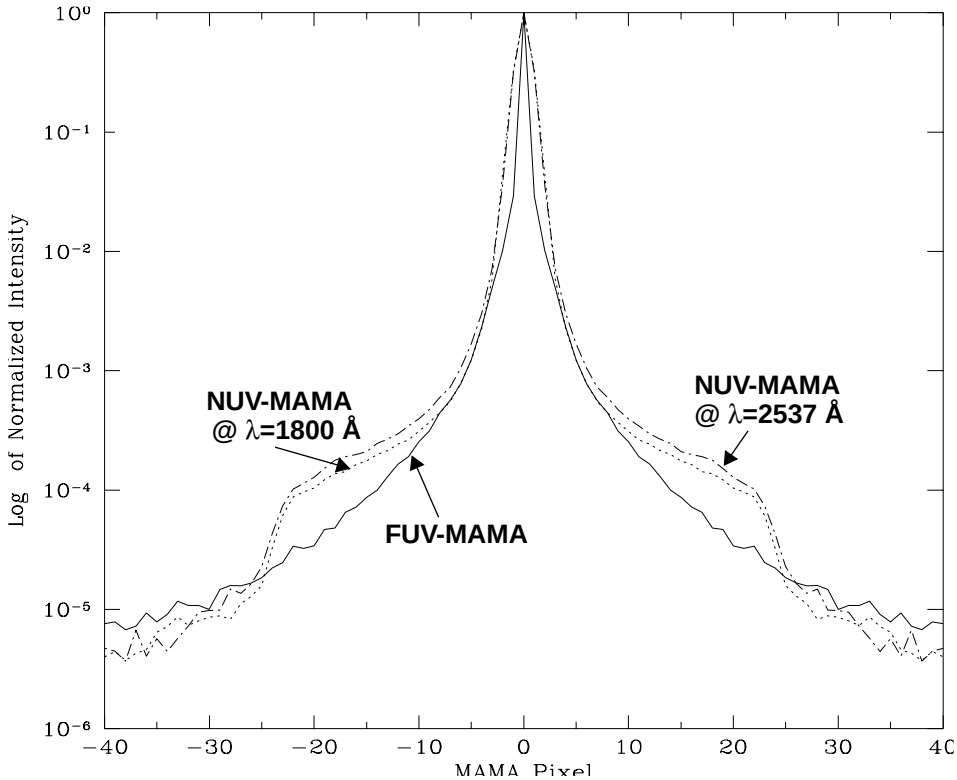

MAMA Operation and Feasibility Considerations

MAMA Saturation—Overflowing the 16 Bit Buffer

The MAMA's are photon counting detectors; as each photon is recorded it is placed into buffer memory. The STIS buffer memory stores values as 16-bit integers, hence the maximum number it can accommodate is 65536 counts per pixel in a given ACCUM mode observation. At accumulated counts per pixel which exceed this number, the values will wrap. As an example, if you are counting at the limit of 25 count sec^{-1} $pixel^{-1}$, you will reach the MAMA saturation limit in ~24 minutes.

Keep accumulated counts $pixel^{-1}$ below this value, by breaking individual exposures into multiple identical exposures (see also "REPEATOBS" on page 153) each of which is short enough that less than 65536 counts are accumulated per pixel. There is no read noise for MAMA observations, so no penalty is paid in lost signal-to-noise ratio when breaking exposures. There is a small overhead (~1 minute) for each MAMA exposure, however (see Chapter 9 on page 123).

▽ Keep the accumulated counts per pixel below 65536, by breaking single exposures into multiple exposures, as needed.

MAMA Signal-to-Noise Ratio Limitations

MAMA detectors may be capable of delivering signal-to-noise ratios of the order of 100:1 per resolution element (2x2 pixels) or even higher. However, inherent structure in the MAMA flat fields and our ability to track the temporal behavior of those flats are likely to limit routine observations to maximum signal-to-noise values in the range ~30:1 during Cycle 7. Achieving higher high signal-to-noise ratios will require very high quality flat fields or the use of an observation procedure that allows the observer to remove the photocathode component and the fixed pattern component of the MAMA flat field. The fixed pattern noise is a combination of several effects including beating between the MCP channel array and the anode pixel array, variations in charge cloud structure at the anode, and low-level capacitive cross-coupling between the fine-fine anode elements. A special project during Cycle 7 is to investigate the optimum techniques for removing fixed pattern noise from the MAMA flat fields. See also “High Signal-to-Noise Ratio Observations” on page 167.

MAMA Non-Linearity

Global

The MAMA detectors begin to experience non-linearity (photon impact rate not equal to photon count rate) at global (across the entire detector) count rates of 200,000 count sec^{-1}. The non-linearity reaches 10% at 300,000 count sec^{-1} and can be corrected for in post-observation data processing at the price of a loss of photometric reliability. The MAMA detectors are not able to count at rates exceeding 300,000 count sec^{-1}, and at rates above this observations are disallowed as damage to the detectors can ensue (see “MAMA Bright Object Limits” on page 97, below).

Local

The MAMA detectors remain linear in their counting up to ~50 counts sec^{-1} $pixel^{-1}$. At rates exceeding this, they experience local (at a given pixel) non-linearity. The non-linearity effect is image dependent—that is, the non-linearity observed at a given pixel depends on the photon rate affecting neighboring pixels. This makes it impossible to reliably correct for the local non-linearity in post-observation data processing. In addition, the MAMA detectors are subject to damage at high local count rates, and observations at per pixel count rates exceeding 25 counts sec^{-1} $pixel^{-1}$ for the FUV-MAMA and 50 counts sec^{-1} $pixel^{-1}$ are for the NUV-MAMA are disallowed (see “MAMA Bright Object Limits” on page 97, immediately below).

MAMA Bright Object Limits

STScI has responsibility to ensure that the MAMA detectors are not damaged through over-illumination. Consequently, we have had to develop procedures and rules in order to protect the MAMAs. We ask all potential users to share in this responsibility by reading and taking note of the information in this section and designing observing programs which operate in the safe regime for these detectors.

Overview

The MAMA detectors are subject to catastrophic damage at high global and local incident count rates and cannot be used to observe sources which exceed the defined safety limits. The potential detector damage mechanisms include over-extraction of charge from the micro channel plates causing permanent diminution of response, and ion-feedback from the micro channel plates causing damage to the photo-cathode and release of gas which can overpressure the tube.

To safeguard the detectors, checks of the global (over the whole detector) and local (per pixel) illumination rates are automatically performed in flight for all MAMA exposures. The *global illumination rate* is monitored continuously; if the global rate approaches the level where the detector can be damaged, the high voltage on the detector is automatically turned off. This will result in the loss of all observations scheduled to be taken with that detector for the remainder of the calendar (~1 week). The *peak local illumination rate* is measured over the MAMA field at the start of each new exposure; if the local rate approaches the damage level, STIS will shutter, and the exposure will be lost.

Sources that would over-illuminate the MAMA detectors cannot be observed. It is the responsibility of the observer to avoid specifying observations that exceed the limits described below.

Observational Limits

To ensure the safety of the MAMA detectors and the robustness of the observing timeline, we have established observational limits on the incident count rates. The three observational limits apply in both spectroscopic and imaging applications. The restrictions are (see also Table 7.3):

1. The maximum *global* count rate at which you will be allowed to observe is 300,000 counts sec^{-1} integrated over the detector.
2. The peak per pixel count rate from your source cannot exceed 50 counts sec^{-1} $pixel^{-1}$ for observations utilizing the NUV-MAMA.

3. The peak per pixel count rate from your source cannot exceed 25 counts sec^{-1} $pixel^{-1}$ for observations utilizing the FUV-MAMA.

Note that these limits are at or below the maximum rate at which the MAMA detectors remain linear in their counting (see “MAMA Non-Linearity” on page 96).

Table 7.3: Absolute MAMA Count Rate Limits

Limit Type	Count Rate Limit	Applies to?
Absolute global	300,000 counts sec^{-1}	Over detector
Absolute peak count rate	50 count sec^{-1} $pixel^{-1}$	All NUV-MAMA observations
Absolute peak count rate	25 count sec^{-1} $pixel^{-1}$	All FUV-MAMA observations

How Do You Determine if You Violate a Bright Object Limit?

As a first step, you can check your source V magnitude and peak flux against the Bright Object Limits in Table 13.24, “MAMA Spectroscopic Bright Object Limits - V Mags and cgs units.,” on page 255 or Table 14.16, “MAMA Imaging Bright Object Limits, V Magnitudes and CGS as indicated.,” on page 308 for your chosen observing configuration. In many cases, your source properties will be much fainter than these limits, and you need not worry further.

However, if you are near these limits (within 1 magnitude or a factor of 2.5 of the flux limits), then you need to carefully consider whether your source will be observable in that configuration. Remember the limits in these tables assume zero extinction and for spectroscopic observations do not include slit losses. Thus you will want to correct the limits appropriately for your source’s reddening and the aperture throughput.

You can use the information presented in “Determining Count Rates from Sensitivities” on page 66 to calculate your peak and global count rates. Perhaps, better, you can use the STIS exposure time calculator available through the STScI STIS World Wide Web page to calculate the expected count rate from your source. It has available to it a host of template stellar spectra. If you have a spectrum of your source (e.g., from IUE, GHRS or FOS) you can also input that spectrum directly to the calculator. The calculator will evaluate the global and per pixel count rates and will warn you if your exposure exceeds the absolute and bright object limits. We recommend you utilize the STIS exposure time calculator if you are in *any doubt* that your exposure may exceed the bright object MAMA limits.

Policy and Observer's Responsibility in Phase I and Phase II

It is the observer's responsibility to ensure that their observations do not exceed the Bright Object count limits of 50 counts sec^{-1} $pixel^{-1}$ for the NUV-MAMA, 25 counts sec^{-1} $pixel^{-1}$ for the FUV-MAMA and 300,000 counts sec^{-1} over the detector for both MAMA detectors.

It is your responsibility to assure that you have checked your planned observations against the brightness limits prior to proposing for Phase I. If your proposal is accepted and we, or you, subsequently determine (in Phase II), that your source violates the absolute limits, then you will either have to change target, if allowed, or lose the granted observing time. We encourage to include a justification in your Phase I proposal if your target is within 1 magnitude of the Bright Object Limits for your observing configuration

STScI will screen all STIS observations that utilize the MAMA detectors to ensure that they do net exceed the Bright Object Limits. In Phase II, you will be required to provide sufficient information to allow screening to be performed.

Here we describe the required information you must provide.

Spectroscopy

To allow screening of your target in Phase II for spectroscopic MAMA observations you must provide the following for your target (i.e., for all sources which will illuminate the detector during your observations):

- V magnitude
- Expected source flux at observing wavelength.
- Spectral type (one of the types in the screening tables).
- E_{B-V}.
- B-V color.

If you wish to observe a target which comes within one magnitude (or a factor of 2.5 in flux) of the limits in the Spectroscopic Bright Object Screening table (page 255) for your configuration, after correction for aperture throughput and reddening, but which you believe will not exceed the absolute limits in Table 7.3, "Absolute MAMA Count Rate Limits," on page 98 and so should be observable, you must provide auxiliary information to justify your request. Specifically:

- You must provide an existing UV spectrum (e.g., obtained with IUE, FOS, or GHRS) of the star which proves that neither the global nor the local absolute limits will be exceeded.

- If you do not have such a spectrum, then you must obtain one, by taking a 'pre-exposure' in a MAMA-safe configuration (e.g., with a ND filter in place or in a higher resolution mode) before we will schedule your observations. *Be sure to include the time (1 orbit in its own visit) for such an observation in your Phase I Orbit Time Request, as needed.*

Imaging

The MAMA imaging Bright Object Limits (see Table 14.16 on page 308) are very stringent, ranging from V=15 to V=20.5 for the different imaging apertures, and apply to all sources imaged onto the MAMA detector (i.e., not just the intended target of interest). Automatic screening by STScI can only be performed down to a limiting magnitude of V~12.5. For this reason, if you wish to perform MAMA imaging you must prove that your field will not violate the limits with your chosen filter. Specifically, you must provide:

- V magnitudes and B-V colors for all the targets in the field of view along with an optical image of that field, ***or***
- an existing UV image (e.g., from FOC, WFPC2, or UIT) which proves that your field will not exceed the absolute limits.

Neither prime nor coordinated parallel imaging observations with the STIS MAMAs will be allowed unless this information is provided. Phase I Proposals for MAMA imaging should demonstrate that they have considered the MAMA Bright Object Limits.

MAMA imaging exposures will only be allowed if the observer provides V magnitudes and B-V colors for all sources which will be imaged onto the MAMA field of view. Alternately, the observer can provide a UV image (e.g., from FOC or WFPC2) which demonstrates that the field is safe.

Policy on Observations Which Fail Because they Exceed Bright Object Limits

If your source passes screening, but causes the automatic flight checking to shutter your exposures or shut down the detector voltage causing the loss of your observing time, *then that lost time will not be returned to you*; it is the responsibility of the observer to ensure that their observations do not exceed the bright object limits.

What To Do If Your Source is Too Bright for Your Chosen Configuration?

If your source is too bright for one configuration, it is likely that it will be observable in another configuration (e.g., in a higher dispersion configuration). The options open to you if your source count rate is too high in a given configuration include:

1. Select a narrower slit which passes only a fraction of the source flux, for spectroscopic observations.
2. Select a higher dispersion grating.
3. For near-UV low resolution and medium resolution spectroscopy, consider using the CCD G230LB and G230MB modes (see “Cross-Over Regions” on page 41).
4. Employ a neutral density filter.
5. Change configurations totally to observe a different portion of the spectrum of your target (e.g., switching to the CCD).

For further advice, see “Observing Too-Bright Objects with STIS” on page 165.

CHAPTER 8
Target Acquisition

In This Chapter...

All STIS spectroscopy using slits and all coronographic observations will require an on-board STIS target acquisition and possibly an acquisition/peakup exposure to center the target in the science aperture. In this Chapter we provide the basic information you need to choose an acquisition strategy for your science.

Overview

Following the initial guide star acquisition for your visit, the target location in the aperture plane will be known to an accuracy of ~1-2 arcseconds. For science observations taken through spectroscopic slits which are less than 3 arcseconds in either dimension and for imaging observations taken using one of the coronagraphic apertures, you will need to use an on-board STIS target acquisition and possibly an acquisition peakup exposure to center your target.

On-board target acquisitions with STIS differ considerably from previous HST instruments such as FOS and GHRS, which required raster scans to locate the target. STIS target acquisitions employ the CCD camera to image the target's field directly and onboard flight software processes the image to locate the position of the target. This should make STIS target acquisitions more robust than with the earlier generation HST spectrographs. Below we describe acquisition and peakup exposures for spectroscopy. Acquisitions and centering of targets behind coronographic bars and wedges is described in "Coronagraphic Imaging and Spectroscopy" on page 170.

Figure 8.1 shows a decision flow for selecting whether you require an acquisition, an acquisition/peakup, or both, to center your target.

Figure 8.1: Determining Acquisition Needs

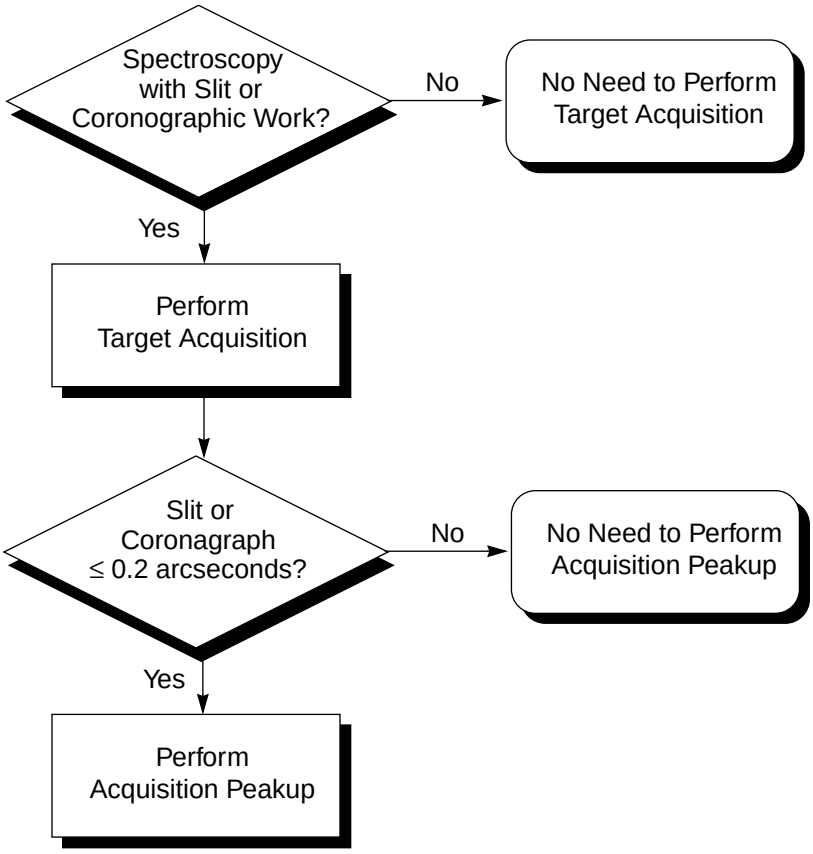

Acquisitions

STIS target acquisition exposures (`MODE=ACQ`) always use the `CCD`, one of the filtered or unfiltered apertures for `CCD` imaging and a mirror as the optical element in the grating wheel. Acquisition exposures center your target in the slit or behind a coronographic bar to an accuracy of ~0.1 arcseconds. A typical STIS target acquisition exposure takes ~8 minutes (see “On-board Target Acquisition and Peakup Overheads” on page 135).

Peakups

Additionally, an acquisition peakup exposure (`MODE=ACQ/PEAKUP`) must be taken following the target acquisition exposure to refine the target centering of point or point-like sources in slits less than or equal to 0.2 arcseconds wide (or tall). Peakup exposures use a science slit or coronographic aperture and can be taken with either the CCD or one of the MAMAs as the detector and with either a mirror or a spectroscopic element in the grating wheel. Typical centering

accuracies following a peakup sequence are 0.3 and 0.2 times the dimension of the slit or bar for CCD and MAMA acq/peaks, respectively. Typical STIS imaging point source peakups take ~ 5-10 minutes, though a peakup with the very small 0.1x0.09 echelle aperture will take ~20 minutes (see “On-board Target Acquisition and Peakup Overheads” on page 135).

STIS On-board Target Acquisitions

How STIS On-Board Acquisitions Work

Acquisition exposures are controlled by the Flight Software (FSW). Figure 8.2 highlights the basic steps in the acquisition process.

Figure 8.2: Target Acquisition Schematic

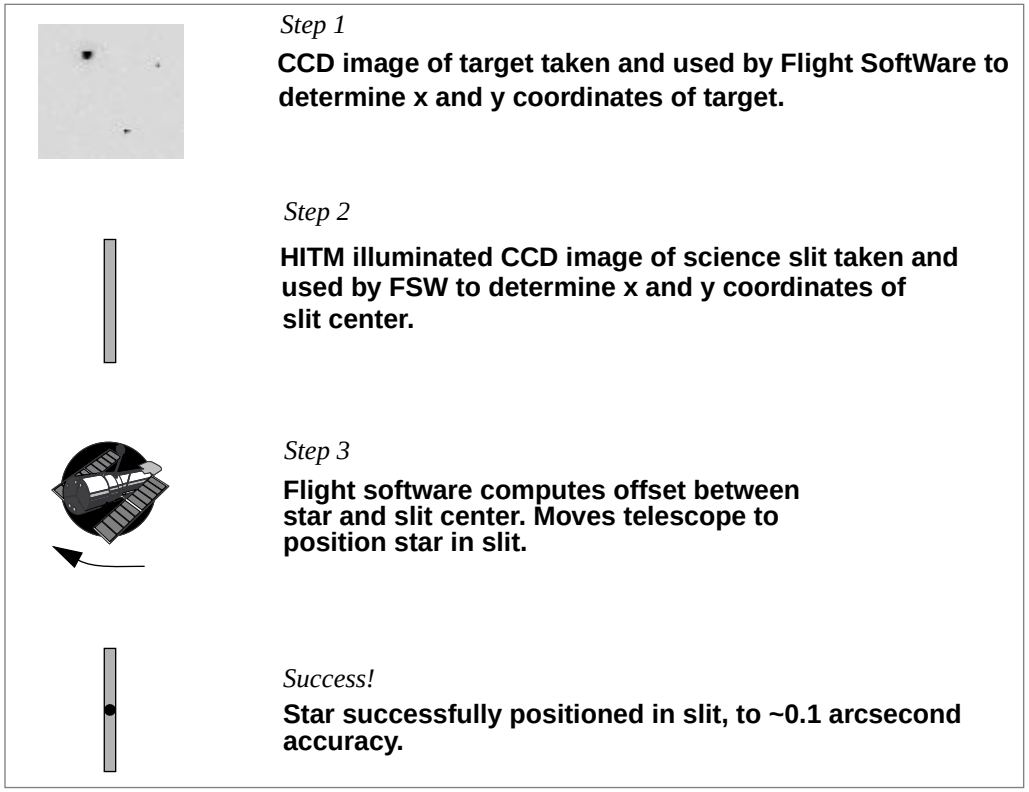

In step 1, the target is located. A 100 x 100 pixel `CR-SPLIT` CCD image is taken of the sky using a user selected filtered or unfiltered imaging aperture. The flight software processes the image as needed (to remove the bias level, flag bad pixels and remove cosmic rays)[1] and applies a user-selected finding algorithm to determine the pixel coordinates of the target. The spacecraft is then moved to place the target at the nominal aperture center, the target is re-imaged and the target detector coordinates are re-determined. This second target location is

performed to minimize the final slew in step 3, to reduce the error associated with that slew.

In step 2, the location of the science slit (i.e., the slit you are trying to center the target in) is determined relative to the target. The science slit is rotated into the slit wheel and an image of the slit is obtained by illuminating the slit with the HITM line lamps. The slit image is processed and a finding algorithm is then used to determine the pixel coordinates of the center of the slit.

In step 3, the final phase, the flight software calculates the offset between the target location and the slit center, and performs a small angle maneuver of HST to place the target in the aperture.

An acquisition exposure produces science data, which includes the image of the target and the image of the science slit. These data will be returned to you with your science data as part of the pipeline products.

Target Location Algorithms

STIS supports two basic types of acquisitions; point source acquisitions (`ACQTYPE=POINT`) and diffuse source acquisitions (`ACQTYPE=DIFFUSE`). Diffuse source acquisitions are appropriate for sources that exhibit smooth or systematically peaking surface brightnesses *on some size scale*, such as centers of galaxies, planets, or nebulae.

To locate the target the flight software first passes a square *checkbox* over the image and determines the flux contained within the checkbox at each pixel in the subarray. The flight software then selects the checkbox with the maximum flux and determines the target center within that checkbox according to the type of acquisition specified.

Point Source Acquisition

For point source acquisitions (`ACQTYPE=POINT`), the checkbox size is fixed at 3 x 3 pixels and the flight software determines the target location by finding the flux weighted centroid of the pixels in the brightest checkbox (see Figure 8.3).

1. The processing done by the FSW is rudimentary; a single bias number is subtracted, bad pixels are set to the average of the adjacent pixels, and negative valued pixels are set to zero, and each pixel is assigned the minimum from the two (CR-SPLIT) images.

Figure 8.3: How the Checkbox Works for Point Source Acquisitions

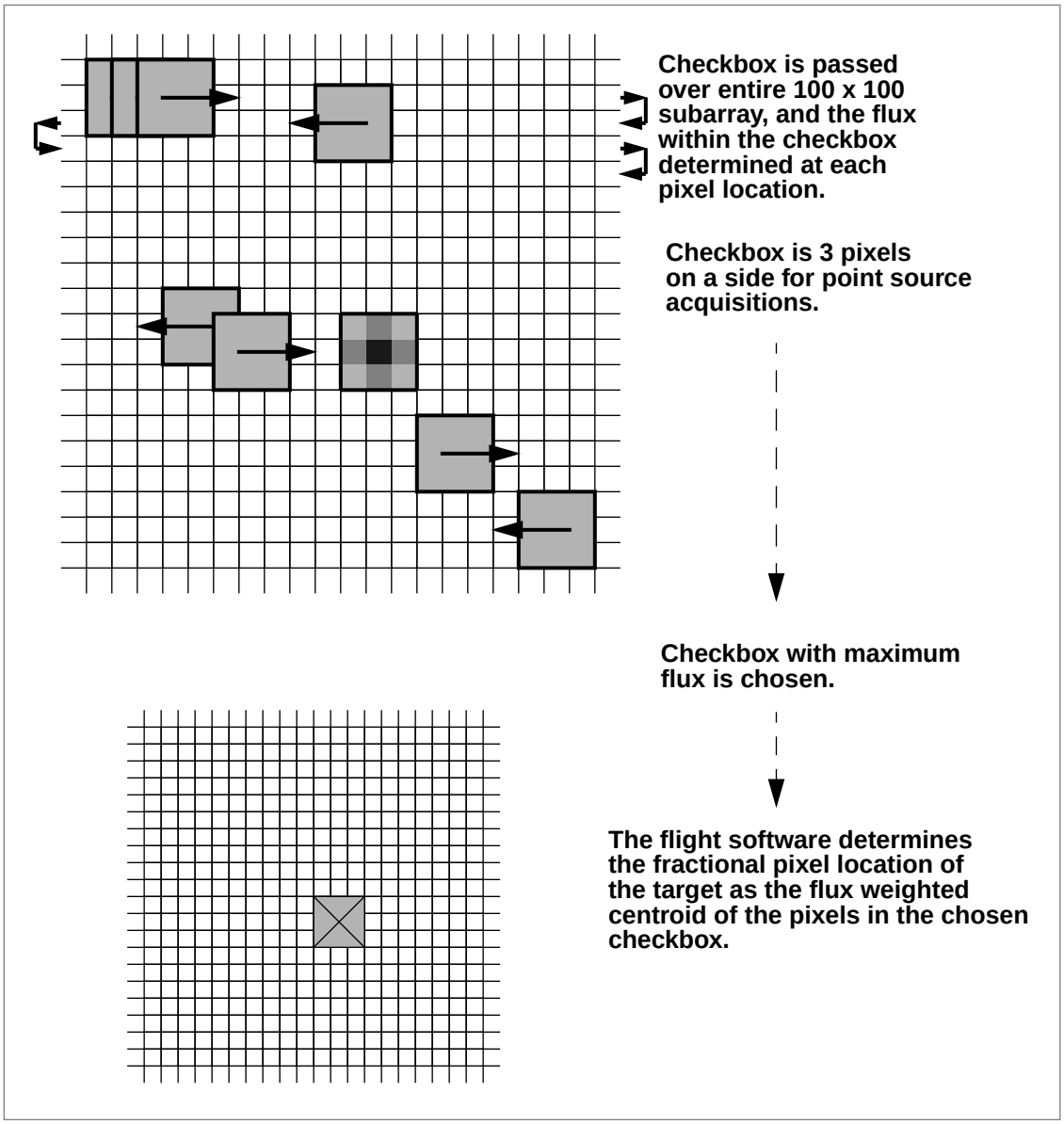

Diffuse Acquisition

For diffuse acquisitions (ACQTYPE=DIFFUSE), the flight software determines the target location either by finding the flux weighted centroid of the pixels in the brightest checkbox or by determining the geometric center of the brightest checkbox. For DIFFUSE acquisitions, the user must specify both the centering method (DIFFUSE-CENTER=GEOMETRIC or CENTROID) and the checkbox size. The user sets CHECKBOX=*n*, where *n* must be an odd number less than 105: the checkbox will then have dimension *n* x *n* pixels. CHECKBOX should be set to the minimum size which assures that the brightest checkbox will be the one centered on the region of interest (i.e., if your object is peaked within a region of 1 arcsecond, set CHECKBOX=21 (= 1 + 1 arcsecond/0.05 arcsecond/pixel). The maximum checkbox is 105 pixels on a side, or ~5 x 5

arcseconds. The subarray used for a diffuse source acquisition target image is CHECKBOX+101 pixels on a side.

Figure 8.4: How the Checkbox Works for Diffuse Acquisitions

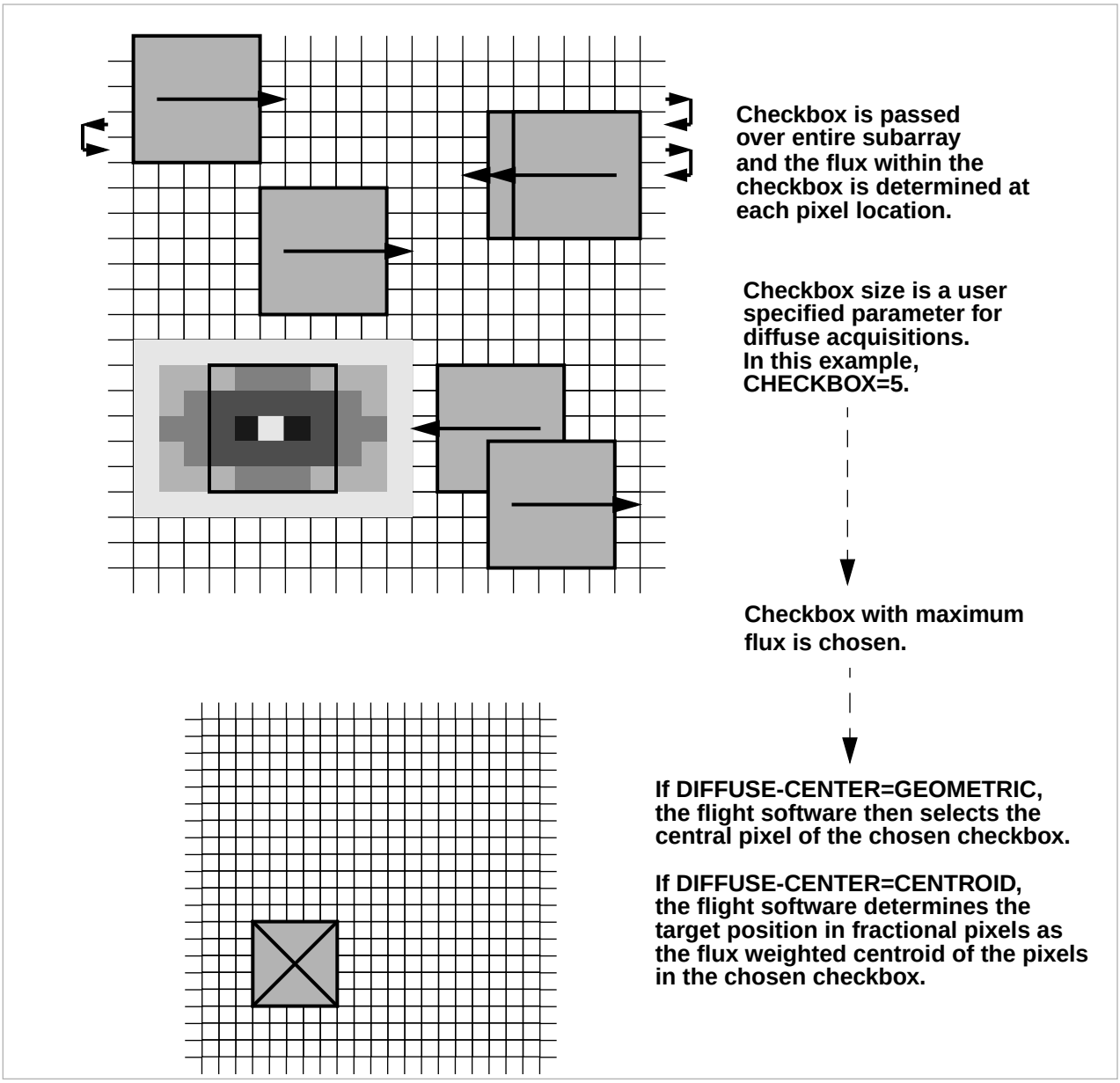

Figure 8.5 shows a simulated example of a diffuse source, the nucleus of the galaxy M86, acquired using a diffuse source acquisitions.

Figure 8.5: Simulated Diffuse Acquisition of Elliptical Galaxy M86, creating by running the flight software algorithm on a WFPC2 image. CHECKBOX=25 produced good centering. Smaller values caused checkbox to center on local brightness enhancements offset from galaxy center.

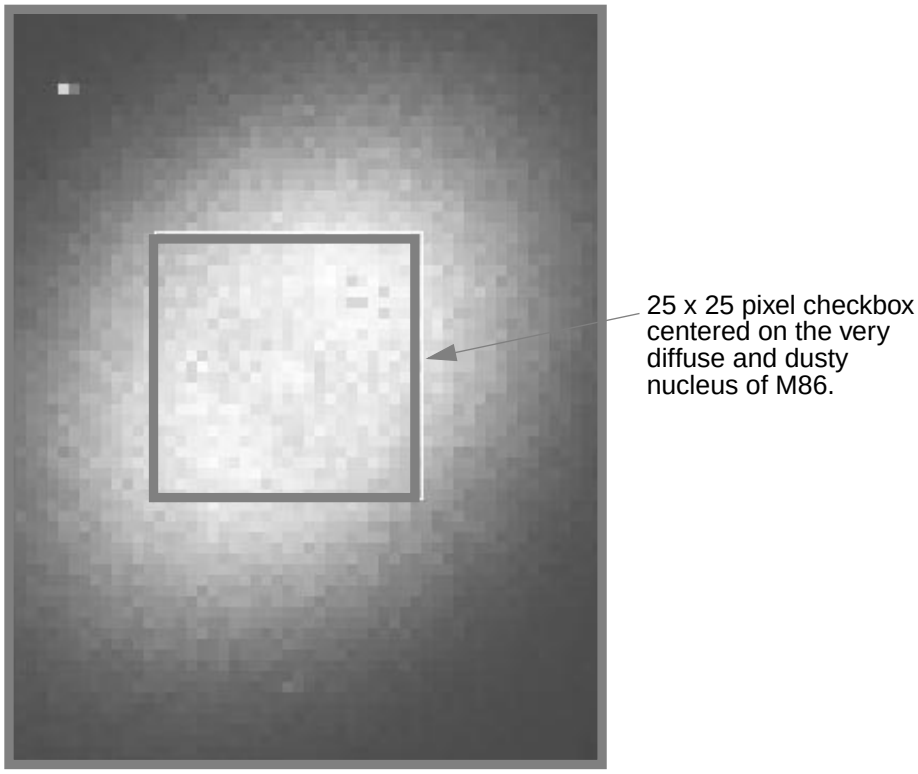

Selecting Target Acquisition Parameters

To plan your acquisition, you must select:

- The type of acquisition, point or diffuse, and if you are performing a diffuse acquisition, the centering algorithm and checkbox size (see “Diffuse Acquisition” on page 107).
- The filtered APERTURE to be used for target imaging during the acquisition.
- The exposure time for the image used to determine the location of the target.
- The science or acquisition peakup exposure the acquisition is performed for; the slit specified in that exposure is used during the slit illumination phase of the acquisition.

Figure 8.6 shows the flow of specifying a target acquisition exposure.

Figure 8.6: Process of Choosing Target Acquisition Exposure

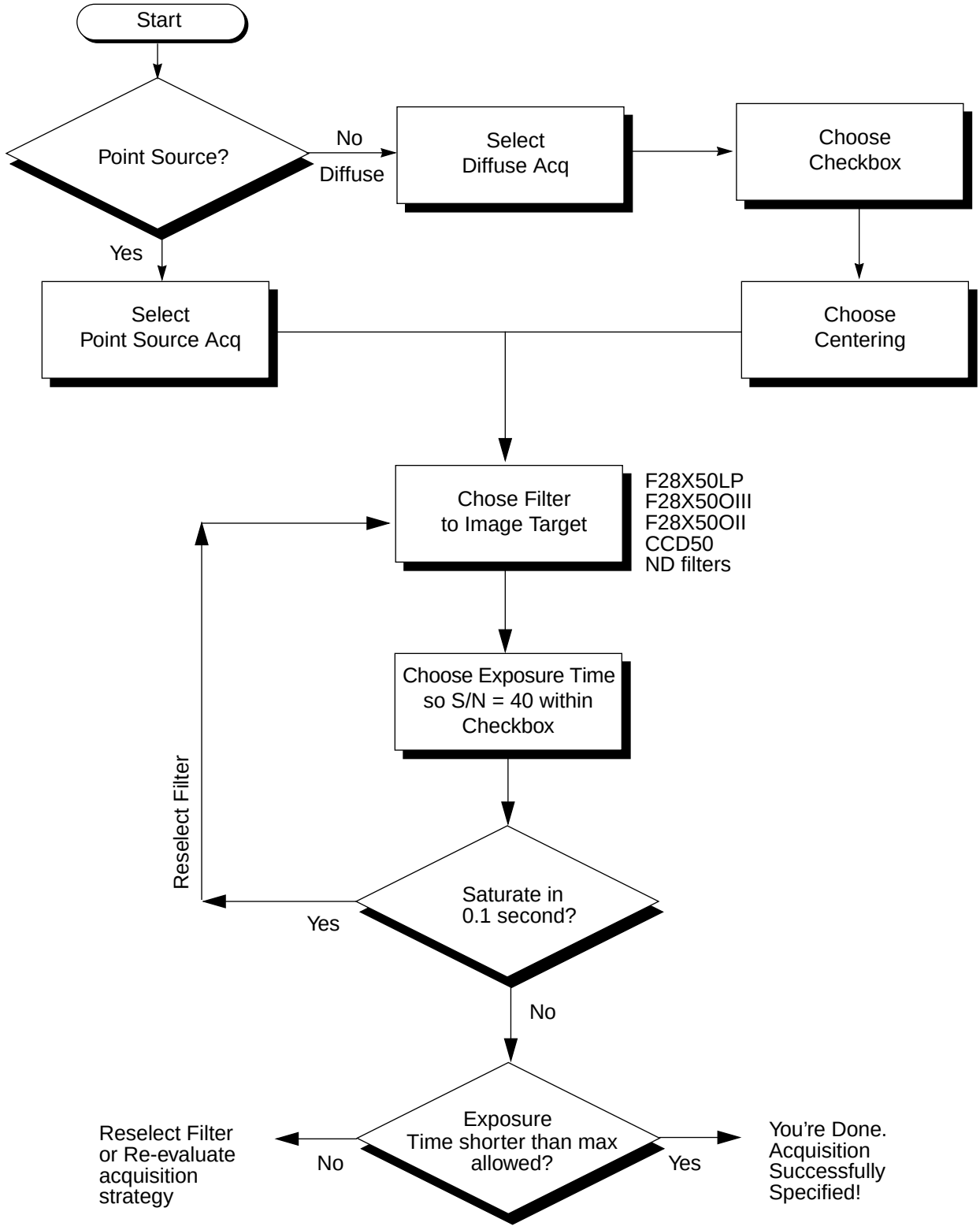

Imaging Apertures for Use in Target Acquisitions

The apertures available for target acquisitions are the same set that can be used for CCD imaging and are listed in Table 8.1 below. They include the visible long pass filter, the clear unfiltered aperture, the [OIII] narrowband filter, the [OII] narrowband filter, and the full set of neutral density filters which provide attenuations for bright sources between 10^{-1} and 10^{-6}.

Table 8.1: Apertures for Target Acquisitions. Note that F28X50LP is the preferred target acquisition aperture. See “Optical CCD Imaging” on page 54 for more information on the properties of the apertures.

APERTURE Name	Filter	Comment
F28X50LP	optical longpass	preferred target acquisition aperture
F28X50OII	[OII]	use for bright sources or to center on emission line structure
F28X50OIII	[OIII]	use for bright sources or to center on emission line structure
F25NDQ1	neutral density filter, ND=10^{-1}	use only for targets too bright for other filters
F25NDQ2	neutral density filter, ND=10^{-2}	use only for targets too bright for other filters
F25NDQ3	neutral density filter, ND=10^{-3}	use only for targets too bright for other filters
F25NDQ4	neutral density filter, ND=10^{-4}	use only for targets too bright for other filters
F25ND5	neutral density filter, ND=10^{-5}	use only for targets too bright for other filters
F25ND6	neutral density filter, ND=10^{-6}	use only for targets too bright for other filters
50CCD	clear	use for acquisitions of faintest sources only

We recommend that you use the longpass filtered aperture F28X50LP for all target acquisitions of sources with V magnitudes between 5 and 23. The longpass filter is the preferred target acquisition aperture (compared to say the clear 50CCD aperture) because it blocks the ultraviolet photons, which can otherwise elevate the detector dark count in the subsequent science exposures. For bright sources which saturate the CCD in 0.1 second with the longpass filter (see Table 8.2 on page 113), you can use either the narrow band OIII (F28X50OIII) or OII filters (F28X50OII) as the acquisition aperture, or one of the neutral density filters. The [OII] and [OIII] filters can also be used to locate the target in the light of an emission line.

Use the F28X50LP longpass filter for the target acquisition whenever possible.

Determining the Exposure Time for the ACQ Exposure

To achieve robust target location:

- A signal-to-noise ratio of 40 (over the checkbox) must be obtained on each target image obtained during the `ACQ` exposure.
- The target image cannot be allowed to saturate the CCD full well.
- The exposure time must be less than 5 minutes for point source acquisitions and less than the maximum allowed (see below) for diffuse acquisitions.

You can use the information presented in earlier chapters (see “Calculating Exposure Times for a Given Signal-to-Noise” on page 70) to determine the required exposure time and assure you are not saturating the CCD full well. To assist you in determining your exposure times, in Figure 8.7 on page 114, we plot exposure time versus V magnitude to achieve a signal-to-noise ratio of 40, for stars having a range of spectral types, for the clear, longpass, OIII, and OII filters.

The maximum possible exposure time for a point source (`ACQTYPE=POINT`) acquisition exposure is 5 minutes; this limits acquisitions to sources brighter than 24.5 magnitudes in V. This limit is imposed because for exposure times longer than this, the target acquisitions become compromised by coincident cosmic ray impacts, which will lead to acquisition failures.

The maximum possible exposure time for a diffuse acquisition (`ACQTYPE=DIFFUSE`) depends on the checkbox and is given by:

$$t_{max} = 5 \times 100/(101 + \mathrm{CHECKBOX}) \qquad \mathrm{minutes}$$

Table 8.2 gives the limiting magnitudes at which the CCD will saturate in a 0.1 second exposure; sources brighter than these limits cannot be acquired with the CCD using these filters. However, remember that the ND filters can be used to acquire targets; they provide attenuations from 10^{-1} (2.5 Magnitudes) to 10^{-6} (15 Magnitudes) relative to `50CCD` (note that the ND filters are in the single slit wheel, and so cannot be used in conjunction with other filters).

Table 8.2: V Magnitude Limits for 0.1 Second CCD Exposure Time as a Function of Aperture. The neutral density filters, providing attenuations up to 15 magnitudes are also available, though not listed in this table.

Spectral type	Limiting Magnitude			
	50CCD	F28X50LP	F28X50OIII	F28X50OII
O5	10.1	8.8	3.2	5.1
B1V	10	8.8	3.4	4.9
B6V	9.8	8.9	3.3	4.2
B9V	9.8	8.9	3.2	4.2
A1V	9.8	8.9	3.3	4.4
A2V	9.7	8.9	3.2	3.5
A7V	9.7	9	3.2	3.4
F4V	9.7	9.1	3.1	3.3
F8V	9.8	9.3	3.1	3.2
G0V	9.8	9.3	3.1	3.2
G5V	9.8	9.3	3.1	3.1
K0V	9.8	9.3	3	3.2
M0V	10.2	10	2.7	1.2
K0III	10	9.7	2.9	1.6
K4III	10	9.8	2.7	0.8
M0III	10.6	10.5	2.6	0.7
50000°	10.1	9.7	5	5.1

Figure 8.7: Time to Achieve a Signal-to-Noise ratio of 40 for CCD Acquisitions

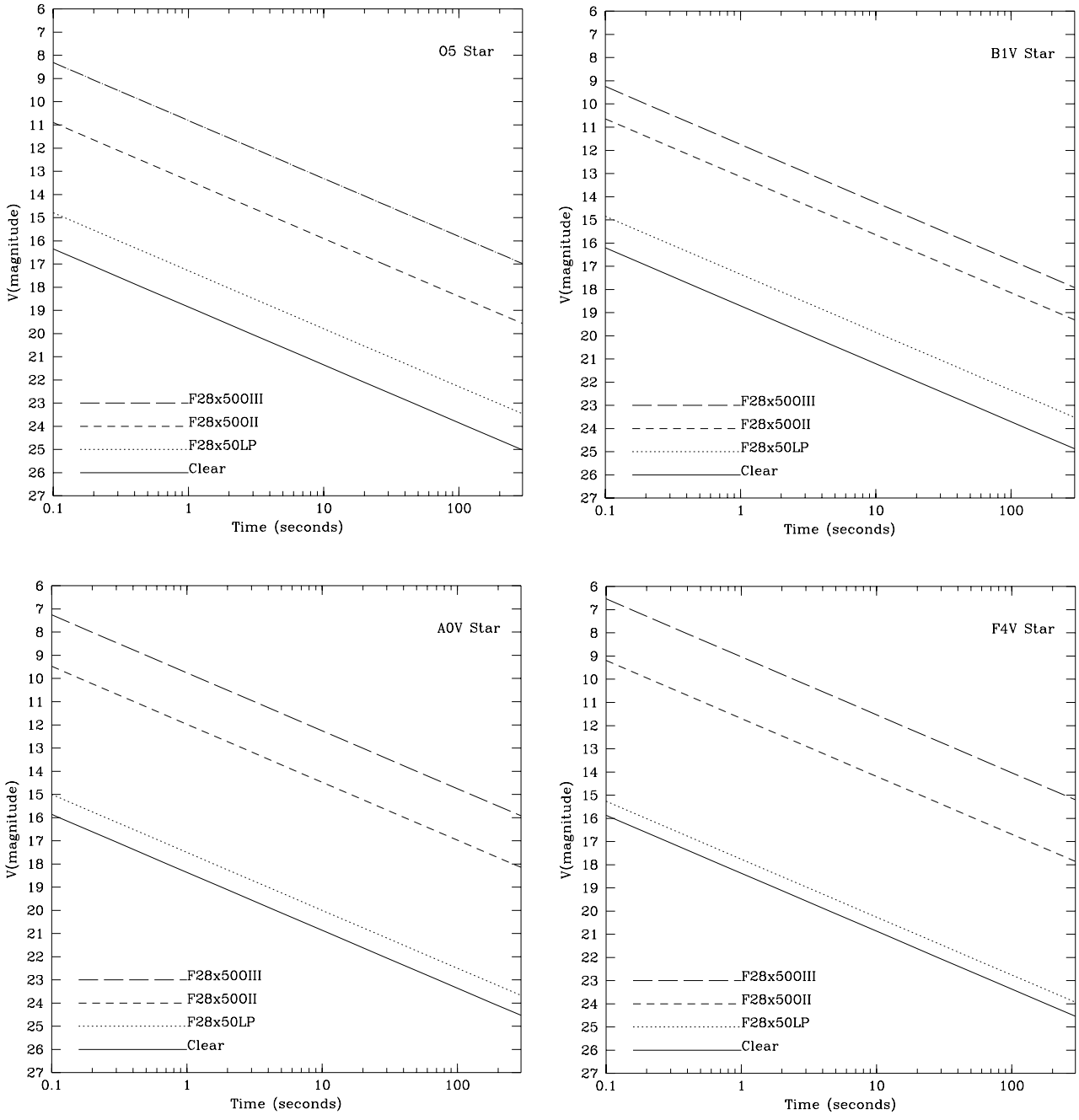

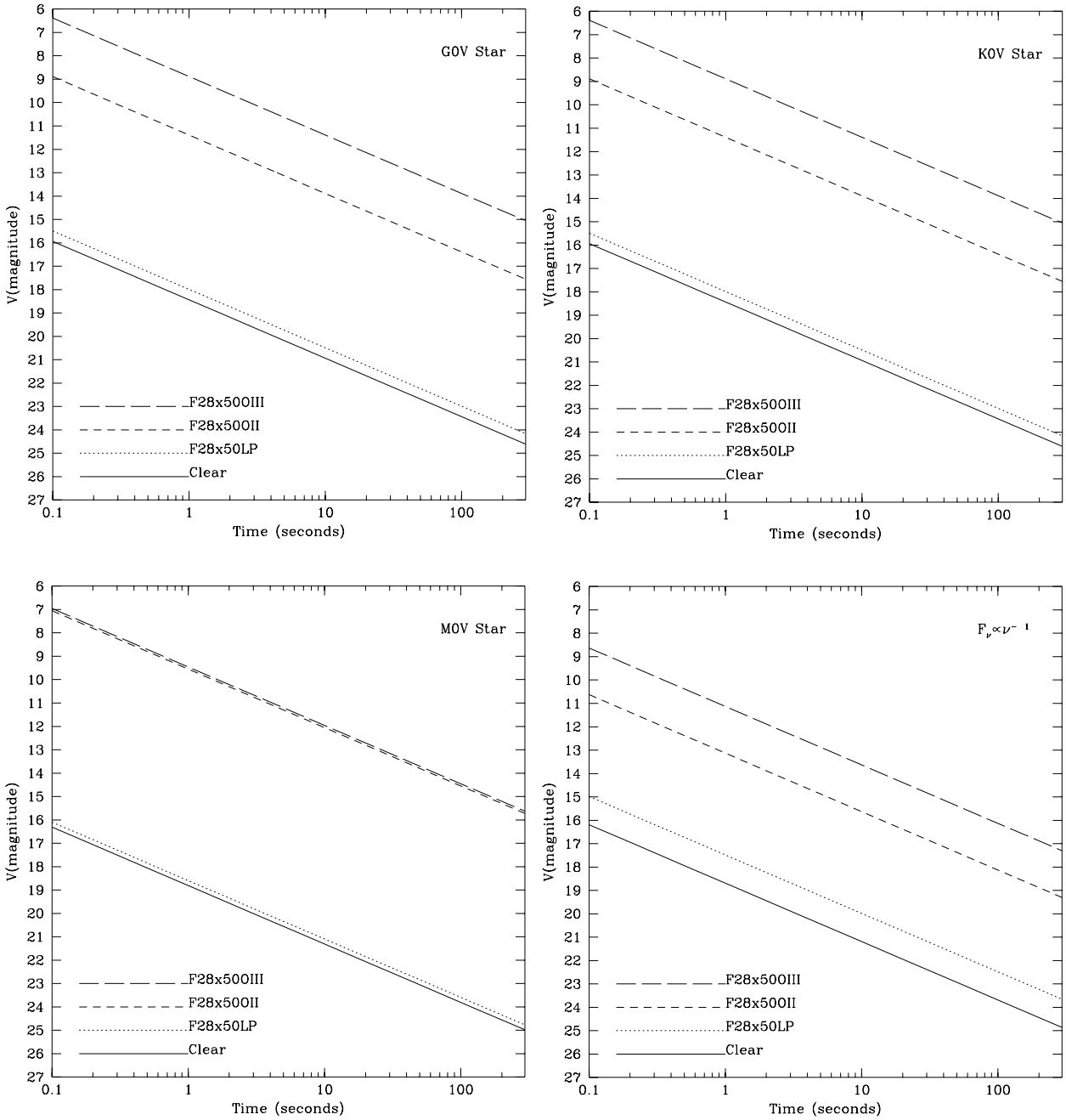

Tips for Planning Your Acquisitions

We expect most acquisitions to be of point sources, using point source acquisitions. If you are observing a diffuse source, you should first check to see if there is a suitable star which you can use as an acquisition target. You can acquire the star and center it in your slit, and then perform an offset to your science target. The maximum allowed distance between the acquisition star and your target is 2

arcminutes (this assures a single set of guide stars can be used for the acquisition sequence and your science target). The error on an offset is ~0.02 arcseconds, so the offset should not significantly affect target centering accuracy even in the 0.1 arcsecond wide slits, and your centering uncertainty will generally be dominated by your knowledge of the absolute offset between the acquisition star and your target.

If you are observing a crowded field, remember that the flight software will find the *brightest* checkbox in the subarray. If you wish to observe a star that is not the brightest in a crowded field, use the brightest star as your acquisition target, and then perform an offset to move to your desired science target. The acquisition target should be the brightest source within a ~3 arcsecond radius for point source acquisitions (the subarray is 5 arcseconds on a side, and the initial centering accuracy is ~1 arcsecond).

If you are observing a diffuse object, for which there is no suitable offset acquisition star, then you will need to use a diffuse acquisition. For diffuse acquisitions, it is important to know your source structure as seen at ~0.1 arcsecond resolution, to properly plan your acquisition strategy, if you need accurate (a few tenths of an arcsecond) centering. We recommend that you first check the HST archive to determine if your target has been observed with HST by WF/PC, WFPC2, or FOC. If it has, that exposure can be used to determine the optimal acquisition strategy. If it has not yet been observed with HST, we suggest you take an early acquisition image, either with the STIS or with WFPC2, which you can use to determine your optimal acquisition strategy (software to emulate the target acquisition flight should be available prior to Phase II). This is particularly important if your science requires placement of a narrow slit accurately on a diffuse object. An offset can then be used to move to the desired position, as needed. Be sure you include the time request for your early acquisition exposure in your orbit time request in Phase I.

Acquisitions of Bright (V>5.4 arcsec^{-2}) Extended Objects

Targets which are extended on scales of 0.5 arcseconds or more and have surface brightness exceeding V=5.4 per square arcsecond will not be able to be acquired autonomously during the first 6 months of Cycle 7 using CCD acquisitions.[2] The only targets affected are some planetary targets. As needed, if the ~1 arcsecond of point and shoot accuracy is insufficient, they can be acquired using interactive acquisitions or the re-use offset capability during the early part of Cycle 7. Requests for interactive acquisitions should be justified in your Phase I proposal and an extra 30 minutes in addition to the time for the science exposure should be added to your orbit time request. See the CP/Phase I Proposal Instructions for more details.

---

2. In the current implementation of CCD acquisitions, bright objects which would otherwise saturate the CCD during the slit illumination phase of acquisitions are moved off the slit by 1 arcsecond to ensure they do not illuminate the slit and cause saturation which will affect the slit location. However, extended bright sources will still spill over into the slit. Future changes to the implementation of CCD acquisitions will solve this problem, but we do not anticipate those changes being in place until the latter half of Cycle 7.

Specifying Acquisitions in Phase II

Acquisition exposures must be specified during Phase II as individual exposure logsheet lines which precede the science exposures for which they are intended. The user requests a target acquisition exposure by specifying `MODE=ACQ` on the proposal logsheet, and setting the optional parameter `ACQTYPE=POINT` or `ACQTYPE=DIFFUSE`. If `ACQTYPE=DIFFUSE` is selected, the observer must also specify `DIFFUSE-CENTER` and `CHECKBOX`. The special requirement "onboard acq for <exp IDs>'' must be supplied for acquisition exposures, where the exp IDs given identify the subsequent science exposures the acquisition is being taken for. This information is used to determine the science slit to center the target in during the acquisition.

In addition, in Phase II, you will also be required to provide the V magnitude and spectral type of the acquisition target. It is vital that you include your source's V magnitude during Phase II as special processing is given to acquisition exposures of sources brighter than 10th magnitude, to ensure the target doesn't saturate the detector during the slit illumination phase of the acquisition.

Logsheet examples will be made available prior to Phase II.

On-board Target Acquisition Peakups

When using slits which are 2 arcseconds wide or less or the coronographic bar, an acquisition peakup exposure should be performed following the acquisition exposure to center the target in a slit or coronographic bar. Peakups can also be performed intermittently during long observing sequences, to recenter targets in the small slits.

Figure 8.8 illustrates the basic peakup sequence. When a peakup exposure is performed, the telescope is moved to step the target across the slit or bar. At each step (or dwell point), an image[3] of the sky is taken and the total flux in a specified subarray is determined. The flight software then selects the position of maximum flux, using either a flux weighted centroiding technique to determine the optimum position to a fraction of a dwell step (`CENTROID=YES`) or by simply returning to the brightest dwell point (`CENTROID=NO`) At the conclusion of the `ACQ/PEAK` exposure, the FSW moves the telescope to position the target at the derived optimal position within the aperture.

3. For CCD Acq/Peaks the image is a CR-SPLIT image and the same type of processing applied in acquisitions by the FSW to remove the bias and cosmic rays is applied (see also footnote on page 106).

Figure 8.8: Schematic of Peakup Sequence

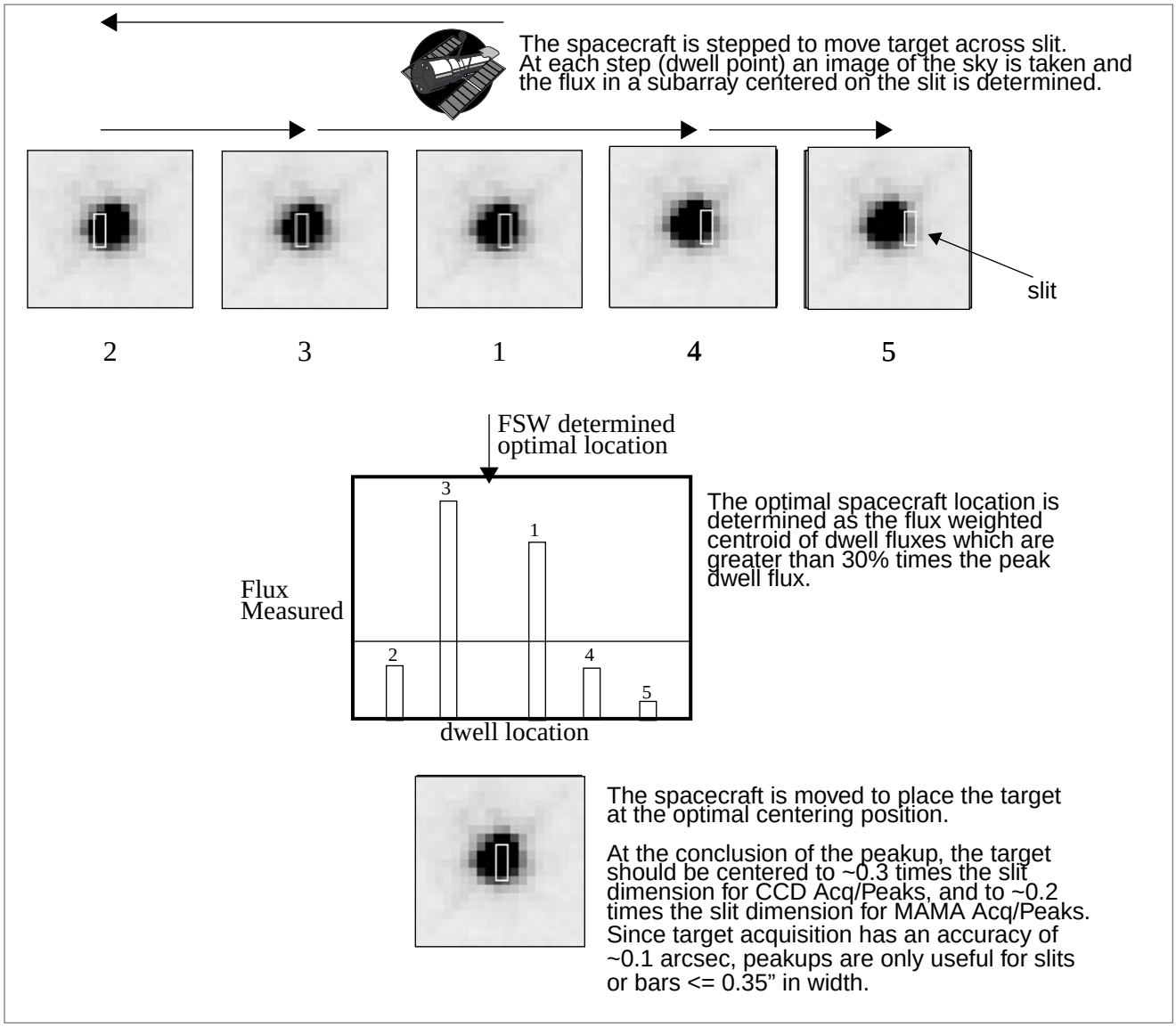

Peakup exposures can be taken using either a mirror (to peak up in undispersed white light) or a grating (to peak up in dispersed light) and using either the CCD or the MAMA detectors. Subarrays can be specified to limit the region of the detector (sky) over which the flux is determined at each dwell point. The default subarray sizes, 32 by 32 for white light (mirror) peakups and 32 in cross dispersion by 1024 in dispersion for dispersed light peakups, are appropriate for peakups on point sources. They should be changed only upon consultation and if you are performing diffuse source peakups or if you wish to isolate a single line in dispersed light peakups.

You do not specify the parameters of the stepping sequence employed during the peakup; it is predetermined, based on the aperture you have chosen. Table 8.3

below shows the scan sequence employed for all of the long and echelle slits. The scan sequence for a peakup may include a linear scan in the dispersion direction (SEARCH=LINEARAXIS1), a linear scan in the cross-dispersion direction (SEARCH=LINEARAXIS2), or a spiral search pattern (SEARCH=SPIRAL) and includes a number of steps (NUMSTEPS) and step intervals between each dwell point (STEPSIZE).

Table 8.3: . Scan Sequences and Parameters for Spectroscopic Slits

Slit (APERTURE)	AXIS2 spatial (arcsec)	AXIS1 dispersion (arcsec)	AXIS2 step size (arcsec)	AXIS1 step size (arcsec)	Scan Type	NSTEPS AXIS2	NSTEPS AXIS1	Total NSTEPS (numsteps)
52X0.1	52	0.1		0.075	LINEARAXIS1		5	5
52X0.2	52	0.2		0.150	LINEARAXIS1		3	3
0.2X0.2	0.2	0.2	0.150	0.150	1) LINEARAXIS2 2) LINEARAXIS1	3	3	6
0.2X0.09	0.2	0.09	0.069	0.069	1) LINEARAXIS2 2) LINEARAXIS1	3	5	8
0.2X0.06	0.2	0.063	0.048	0.048	1) LINEARAXIS1 2) LINEARAXIS2	3	5	8
0.1X0.2	0.1	0.,2	0.075	0.150	1) LINEARAXIS1 2) LINEARAXIS2	5	3	8
0.1X0.09	0.1	0.09	0.075	0.069	SPIRAL			25
6.0X0.2	6	0.2		0.150	LINEARAXIS1		3	3

Selecting Peakup Parameters

To plan your acquisition peakup, you must specify:

- The detector and optical element.
- The APERTURE (science slit) upon which to peak up.
- The exposure time for the peakup image.

Peakup Configuration: Detector, Optical Element, Aperture

Peakups can be performed using either the CCD, the NUV-MAMA, or the FUV-MAMA. They can be performed either with a dispersive element in a spectroscopic configuration using any of the allowed gratings detector combinations (see Table 4.1 on page 34) or in undispersed white light in an imaging configuration (see Table 5.1 on page 48). “Tips on Acquisition Peakups” on page 121 provides advice on when to use a white light (mirror) and when to use a dispersive element (grating) for your peakup.

A peakup can be done using any of the long or echelle slits in Table 8.3 on page 119 as the APERTURE. You will (almost always) want to specify the peakup aperture as the aperture used for the subsequent science observations.

Determining Peakup Exposure Time

The required exposure time is the time to achieve a signal-to-noise ratio of 40 in a single exposure of the peakup target in the peakup subarray. For imaging (mirror) peakups of point sources, this is just the time to achieve a signal-to-noise ratio of 40 on the source; for dispersive peakups, it is the time to achieve a signal-to-noise ratio of 40, summed over the 32 pixels containing source in the spatial (AXIS2) direction and summed over the full 1024 pixels in the spectral (AXIS1) direction.

Use the information presented in the earlier chapters (Section 4, “Spectroscopy,” on page 33, Section 5, “Imaging,” on page 47, and “Calculating Exposure Times for a Given Signal-to-Noise” on page 70) to determine the appropriate exposure times for your white light (imaging) or dispersed light (spectroscopic) peakups. Be sure to include the effect of your chosen slit throughput in your calculation. For CCD peakups you must be sure not to saturate the CCD during your peakup exposure.

Figure 8.7 on page 114 provides exposure times as a function of source magnitude for stars of different spectral types for CCD white light peakups and Table 8.2 on page 113 lists the brightest magnitude star for a range of spectral types on which a CCD peakup exposure can be performed in white light, assuming zero slit losses. There is a limit on the maximum exposure time allowed for CCD peakups, which is imposed to ensure that multiple coincident cosmic rays do not affect the centering accuracy. Table 8.4, below, lists the maximum CCD exposure time for point source white light and dispersed light peakups for each aperture.[4]

Table 8.4: Maximum Allowed Exposure Times for CCD Peakups

Slit (APERTURE)	Maximum Exposure Time for Dwell (minutes)
52x0.1	7.5
52x0.2	9.5
0.2x0.2	6.5
0.2x0.09	6.0
0.2x0.06	6.0
0.1x0.2	6.0
0.11x0.09	3.5
6.0x0.2	9.5

4. More generally, the maximum allowed exposure time for CCD ACQ/PEAKs is: $t_{max} = 17 \times 1/(\sqrt{\text{numsteps} \times (\text{SIZE} - \text{AXIS2}) \times (\text{SIZE} - \text{AXIS2})/32 \times 32})$ minutes.

Tips on Acquisition Peakups

When do you Need to do a Peakup?

For Cycle 7, we recommend that peakups be employed for all slits which are less than or equal to 0.2 arcseconds wide or tall. For the larger slits 52x2, 52x0.5, there is no benefit in performing a peakup and peakups are therefore not permitted with these slits.

White Light or Dispersed Light, CCD or MAMA Peakups?

Most peakup exposures will be performed using the CCD in imaging mode (white light). Peakups for ultraviolet science observations can be done using the MAMAs in imaging mode.

Only when a target is too bright to perform a peakup with a camera mirror in place, or when you wish to peakup in a particular line for which there is no imaging filter, should peakups be performed in dispersed light using a grating. Targets which are too bright fall into two categories:

- CCD observations which cannot be imaged through the science aperture (which is unfiltered) without saturating the CCD, even for the minimum exposure time of 0.1 second (see the CLEAR column in Table 8.2 on page 113 and apply a correction for the aperture throughput).
- MAMA observations which cannot be imaged through the science aperture (which is unfiltered) without exceeding the bright object limitations.

Observers should generally perform dispersed light peakups with the same grating and aperture they intend to use for their science observations.

Observers using the small echelles slits in the ultraviolet should consider performing a MAMA (instead of a CCD) peakup, to get the higher centering accuracy (~20% of the slit width accuracy versus ~30% for the CCD), of MAMA peakups (a result of the finer MAMA plate scale).

Specifying Acquisitions in Phase II

The user requests a peakup acquisition exposure during Phase II by specifying `MODE=ACQ/PEAK` on the proposal logsheet. The default setting for the scan (`SEARCH`, `NUMSTEPS`, `STEPSIZE`) for your chosen `APERTURE` is then automatically selected from the lookup table. You specify a link to the science exposures following the target acquisition, using the logsheet special requirement `ONBOARD ACQ FOR` *<exp IDs>*. You specify the target level parameters and optional parameters for `ACQ/PEAK` exposures including:

- `CONFIG` (detector).
- `OPTICAL ELEMENT` (grating or mirror).
- `APERTURE` (science slit).
- Exposure time.

Examples will be made available prior to Phase II.

CHAPTER 9
Overheads and Orbit Time Determination

In This Chapter...

In this chapter we describe the overheads associated with observing with STIS and give examples of how to determine the number of orbits that your program will require.

Overview

Once you have determined the set of science exposures and any additional target acquisition or calibration exposures you require for your science program, you are ready to determine the total number of orbits to request. Generally, this is a straightforward exercise involving tallying the overheads on the individual exposures, packing the exposure plus overhead time into individual orbits, and tallying up the results to determine your total orbit request. In some cases, it may be an iterative process as you refine your exposure requests to more fully exploit the orbits.

We refer you to the CP/Phase I Proposal Instructions for information on the observatory policies and practices with respect to orbit time requests and for the orbit determination work sheets. Below, we provide a summary of the STIS specific overheads, and give several examples to illustrate how to calculate your orbit requirements for Phase I Proposals.

STIS Exposure Overheads

Our current estimates of the overheads on exposures are summarized in Table 9.1. All numbers given are preliminary, approximate, rounded where appropriate to the nearest half minute, and do not differentiate in detail the overheads for different STIS modes and configurations. They are subject to change prior to the actual scheduling of Cycle 7 proposals (i.e., prior to Phase II). They represent our current best, conservative, but still very uncertain predictions. These overhead times are to be used (in conjunction with the actual exposure time and the Cycle 7 Phase I Proposal Instructions) to estimate the total time in orbits for your Cycle 7 proposal time request. After your HST proposal is accepted, you will be asked to submit a Phase II proposal to allow scheduling of your approved observations. At that time you will be presented with actual, up-to-date overheads by the scheduling software. Allowing sufficient time for overhead in your Phase I proposal is important; additional time to cover unplanned overhead will not be granted later.

We note the following important points:

- Generic (Observatory Level) overheads:
  - The first time you acquire an object you must include the overhead for the guide star acquisition (9 minutes).
  - In subsequent contiguous orbits you must include the overhead for the guide star reacquisition (6 minutes); if you are observing in the continuous viewing zone (see the CP/Phase I Proposal Instructions), no guide star *reacquisitions* are required.
  - Time must be allowed for each deliberate movement of the telescope; e.g., if you are performing a target acquisition exposure on a nearby star and then offsetting to your target, or if you are taking a series of exposures in which you move the target relative to the slit, you must allow time for the moves (10 seconds to 60 seconds depending on length of slew, see table).
- On-board STIS target acquisition overheads:
  - All STIS spectroscopic exposures which use a slit (long slit or echelle slit) will need to include a target acquisition exposure to place the target in the slit (see “STIS On-board Target Acquisitions” on page 105). As discussed in “On-board Target Acquisition Peakups” on page 117, for the narrower slits you will also wish to perform a peakup exposure to center the target in the slit.
  - An on-board target acquisition need only be done once in a series of continuous orbits. If you are expecting to perform a series of exposures separated in time by up to 2–4 weeks so that you will be on the same set of guide stars, then you can use the re-use offset command (during Phase II) and you need not re-perform the target acquisition the second time you acquire the object.
  - The drift rate induced by the observatory is less than 10 milli-arcseconds per hour. Thermal drifts internal to STIS are expected to be of the same

magnitude. We recommend that for long series of exposures taken through slits which are less than 0.1 arcseconds in either dimension, a peakup be performed every 4 orbits. This will assure that drifts (caused either by thermal changes in the observatory or within STIS itself) do not cause the target to move out of the slit.

- Science exposures:
  - The large overhead times are dominated by the time to move the grating wheel (MSM), which is currently estimated to be ~3.0 minutes per move.
  - For CCD exposures, you must be sure to include the readout time for each exposures, e.g., if you take a series of identical one minute exposure, there is overhead between the exposures, predominantly the read-time, which you must include for each exposure in your overhead estimation.
- CCD and MAMA spectroscopic exposures and wavecals.
  - The quoted overheads on first spectroscopic exposure in a visit, or spectroscopic exposure within a visit with change of grating or grating tilt, allow for the taking of a single automatic wavecal exposure to allow post-observation determination of the zeropoint of the wavelength (and spatial) scales. As indicated in the table, if you plan a series of exposures at a given grating setting which extend over 60 minutes in exposure time, then you need to include time for an additional automatic wavecal for each 60 minute period. We note that the wavecal times are extremely uncertain at this time; in general the times will be shorter than those quoted, but for some configurations the times may be longer.

Table 9.1: STIS Overheads

Action	Overhead
Generic (Observatory Level)	
Guide star acquisition	initial acquisition overhead = 9.0 minutes reacquisitions on subsequent orbits = 6 minutes per orbit
Spacecraft pos-targ moves	for offsets less than 1 arcminute and more than 10 arcseconds = 1 min. for offsets between 10 arcseconds and 1 arcsecond = 0.5 minute for offsets less than 1 arcsecond in size = 106seconds
Acquisitions and Peakups	
Target acquisition (to place target in STIS aperture); see also "On-board Target Acquisition and Peakup Overheads" on page 135	point source acquisitions for sources with V<22 = 8.0 minutes, diffuse source acquisitions = $(425 + 4 * t_{exp} + 0.2 * \text{checkbox}^2)$ sec
Acquisition peakups; (see also "On-board Target Acquisition and Peakup Overheads" on page 135)	white light long slit peakups for sources with V<21 = 5 minutes, white light echelle slit peakups for sources with V<21 = 10 minutes white light coronographic bar peakups for sources with V<21 = 7 mins.
CCD Spectroscopic Science Exposures	
First spectroscopic science exposure in visit	5.0 minutes

Table 9.1: STIS Overheads (Continued)

Action	Overhead
Exposure readout For crsplit full frame exposures, overhead = crsplit * 0.5 (e.g., if crsplit=3, overhead is 3* 0.5 = 1.5 minutes). More generally for crsplit subarrayed exposures add read time + 7 seconds for each.	0.5 minutes = overhead for each single full frame CCD exposure read time +7 seconds = overhead for subarrayed CCD exposures [see page 149 for CCD read times if using subarrays] note - the 0.5 minutes is an approximation, real time is ~37 seconds.
Identical exposure in the series (within an orbit)	zero
Exposure in series with only move of grating wheel (i.e., change in tilt of element or selection of new element)	5.0 minutes
Move of aperture wheel—change of slit or aperture	1.0 minutes
Additional automatic wavecal for series of identical spectroscopic exposures extending for more than 60 minutes	1.5 minutes per 60 minutes
Overhead for data management, for a series of full frame exposures, each longer than 3 minutes in duration	zero
Overhead for data management, for a series of full frame exposures, each SHORTER than 3 minutes in duration (see “Use of Subarrays to Reduce Data Volume” on page 149 for subarray rules)	3 minutes every 7 exposures
CCD Imaging Exposures	
First imaging science exposure in orbit	4.5 minutes
Exposure readout For crsplit full frame exposures, overhead = crsplit * 0.5 (e.g., if crsplit=3, overhead is 3* 0.5 = 1.5 minutes). More generally for crsplit subarrayed exposures add read time + 7 seconds for each.	0.5 minutes = overhead for each single full frame CCD exposure read time +7 seconds = overhead for subarrayed CCD exposures [see page 149 for CCD read times if using subarrays] note - the 0.5 minutes is an approximation, real time is ~37 seconds.
Identical exposure in the series (within an orbit)	zero
Change of filter	1.0 minutes
Overhead for data management, for a series of full frame exposures, each longer than 3 minutes in duration	zero
Overhead for data management, for a series of full frame exposures, each SHORTER than 3 minutes in duration (see “Use of Subarrays to Reduce Data Volume” on page 149 for subarray rules)	3 minutes every 7 exposures
MAMA Spectroscopy Science Exposures	
First spectroscopic science exposure of visit	8.0 minutes
Identical exposure in the series (within the visit)	1.0 minutes
Exposure in series with only move of grating wheel (i.e., change in tilt of element or selection of new element)	8.0 minutes
Additional automatic wavecal for series of identical spectroscopic exposures extending for more than 60 minutes	4.0 minutes per 60 minutes
Move of aperture wheel—change of slit or aperture	1.0 minute
Overhead for data management, for a series of 1024 x 1024 exposures, each longer than 3 minutes in duration	zero
Overhead for data management, for a series of 1024 x 1024 exposures, each shorter than 3 minutes in duration (see “Use of Subarrays for MAMA ACCUM mode Observations” on page 150 for subarray rules)	3 minutes every 4 exposures

Table 9.1: STIS Overheads (Continued)

Action	Overhead
MAMA Imaging Science Exposures	
First imaging science exposure in visit	5.0 minutes
Identical exposure in the series (within an orbit)	1.0 minutes
Exposure in series with change of filter, but using same detector	1.5 minutes
Exposure in series with change of filter and detector	5.0 minutes
Overhead for data management, for a series of 1024 x 1024 exposures, each longer than 3 minutes in duration	zero
Overhead for data management, for a series of 1024 x 1024 exposures, each shorter than 3 minutes in duration (see "Use of Subarrays for MAMA ACCUM mode Observations" on page 150 for subarray rules)	3 minutes every 4 exposures
Additional Calibration Exposures - EXTRA GO Wavecals[a]	
MAMA wavecal exposure	4.0 minutes
CCD wavecal exposure	1.5 minutes

a. Use these only to add additional wavecal exposures beyond those taken automatically.

Orbit Use Determination Examples

The easiest way to learn how to compute total orbit time requests is to work through a few examples. Below we provide five different examples:

- Example 1 is a pattern stepped series of long slit CCD spectroscopic exposures mapping out the H α nebula in the center of the galaxy M86.
- Example 2 is a series of spectroscopic observation of the solar analog CVZ star P041-C, using all of the first order low resolution CCD gratings.
- Example 3 is an imaging and spectroscopic program observing NGC6543, the Cats Eye Nebula,
- Example 4 is a set of long MAMA spectroscopic exposures of Sk 69-215 using the E230H grating through a narrow echelle slit taken in the CVZ.
- Example 5 is a faint CCD imaging program.

These represent fairly typical expected uses of STIS. The target acquisitions used in each example different slightly as well:

- Example 1 uses a diffuse source acquisition and no peakup.
- Example 2 uses a point source acquisition and peakup on the target.
- Example 3 uses a point source acquisition.

- Example 4 uses a point source acquisition and peakup on the target and includes re-peakups during the course of the long observations.
- Example 5 uses no acquisition.

Sample Orbit Calculation 1: Long Slit Spectroscopy of the Galaxy M86

In this example, the proposed science is to observe the Hα nebula in the center of the Virgo elliptical M86, using the `52X0.2` slit and the `G750M` grating, taking a series of exposures, each stepped relative to the next by 0.2 arcsecond, in the direction perpendicular to the slit, in order to cover the inner 0.6 arcseconds of the galaxy completely. Based on the signal-to-noise ratio calculation presented in "Spectroscopy of Diffuse Source (M86)" on page 77, we require an integration time of ~30 minutes per position to obtain a signal-to-noise ratio of 8. The science exposures for this proposal, therefore, comprise *all* of the following:

- A `CRSPLIT=2` ~30 minute spectroscopic exposure using `G750M` at a central wavelength of λ=6768 at location 1.
- A `CRSPLIT=2` ~30 minute spectroscopic exposure using `G750M` at a central wavelength of λ= 6768, at location 2.
- A `CRSPLIT=2` ~30 minute spectroscopic exposure using `G750M` at a central wavelength of λ=6768 at location 3.

We need to include time for the guide star acquisition at the start of the first orbit, followed by an acquisition exposure. No peakup will be done, since we are covering the nebulae by stepping the slit. In this example, we assume that the acquisition is done using the diffuse acquisition, with a checkbox size of 25 pixels (roughly 1.25 arcseconds). The checkbox needs to be large as this galaxy has a very flat and dusty profile; see Figure 8.5: on page 109.

The mean surface brightness of the galaxy within this region is ~2 x 10^{-15} ergs sec^{-1} cm^{-2} $arcsec^{-2}$ $Å^{-1}$, based on WFPC2 V band images in the HST archive. Using the information in "Computing Exposure Times" on page 70 or the STIS exposure time calculator we determine that, using the CCD LongPass filter, `F28X50LP`, for t_{exp}= 1 second, we more than achieve the required signal-to-noise ratio of 40 over the checkbox for the target acquisition.[1] We use the formula in

1. A rough sample calculation, adequate for Phase I planning, follows. We assume the source has a roughly flat (in F_λ) spectrum over the longpass filter, which covers ~4500 Å, with a mean sensitivity ~6x10^{12} counts sec^{-1} $pixel^{-1}$ per erg sec^{-1} cm^{-2} $arcsec^{-2}$ (see Table 14.2 on page 263). We take a mean F_λ=1.5x10^{-15} ergs sec^{-1} cm^{-2} $Å^{-1}$ $arcsec^{-2}$. The counts from the source over a 25 x 25 pixel area are then 1.5x10^{-15} x 6x10^{12} x 625 x 4500 = 2.5 x 10^4 counts sec^{-1}. The read noise squared over this regions is 1x10^4, and the detector and sky backgrounds are also substantially less. Thus, with ~0.1 second integration time, a signal-to-noise ratio of ~50 over the checkbox is achieved. We choose t_{exp}=1 second to assure success. (Note the mean counts accumulated in a singe pixel is only ~45 in 1 second, so we are in no danger of saturating the CCD full well).

Equation 9.1, plug in CHECKBOX=25 and exptime=1.0, and determine that the acquisition will take roughly 10 minutes.

This is not a CVZ observation, so because more than 1 orbit is required we need to include time for the guide star reacquisition at the beginning of each orbit. The individual exposures in this example are long enough that we do not need to include extra overhead for data management. We are satisfied with the automatic wavecal exposures which are taken for each spectroscopic observation at a new MSM position.

We assume a visibility period of 52 minutes per orbit, appropriate for a target at M86's declination (see the CP). Based on the reasoning presented in Table 9.2, below, we conclude that the observations can be squashed into ~ 2 orbits with some loss of sensitivity. Alternately, one could choose to increase the signal-to-noise, and ask for 3 orbits.

Table 9.2: Orbit Calculation for Example 1

Action	Time (minutes)	Explanation
	Orbit 1	
Initial guide star acquisition	9.0	Needed at start of observation of new target
Target acquisition	10.0	Diffuse acquisition with checkbox=25, t_{exp}=1.01 sec
Offset target 0.2" to initial position	10 seconds	Position target to position 1 in pattern
Science exposure, `G750M`, λ_c = 6768, position 1	33.0	27.0 minutes exposure time 5.0 minutes for first CCD spect. exposure in orbit 1.0 minutes for readout (crsplit=2)
	Orbit 2	
Guide Star Reacq	6.0	Start of new orbit
Offset target 0.2" to position 2	10 seconds	Position target to position 2 in pattern
Science exposure, `G750M`, λ_c = 6768, position 2	23.0	22.0 minutes exposure time 1.0 minutes for readout (crsplit=2)
Step target 0.2" perp to slit	10 seconds	Move to position 3 in pattern
Science exposure, `G750M`, λ_c = 6768, position 3	23.0	22.0 minutes exposure time 1.0 minutes for readout (crsplit=2)

Sample Orbit Calculation 2; Low Dispersion Spectra of Solar Analog Star P041-C

In this example the science is to observe the solar analog CVZ star P041-C from the near-IR to the near-UV using STIS's low resolution first order gratings and the `52X0.5` arcsecond slit. The series includes:

- `CRSPLIT`=2, ~10 minute spectroscopic exposure using `G750L` at a central wavelength of λ=7751.

- `CRSPLIT=3,` ~20 minute spectroscopic exposure using `G750L` at a central wavelength of λ=8975.
- `CRSPLIT=4,` ~1 minute spectroscopic exposure using `G750L` at a central wavelength of λ=7751.
- `CRSPLIT=4`, ~1 minute spectroscopic exposure using `G430L` at the central wavelength of λ=4300.
- `CRSPLIT=2`, ~35 minute spectroscopic exposure using `G230LB` at the central wavelength of λ=2375.

We need to include time for the guide star acquisition at the start of the first orbit, followed by an acquisition exposure. This is a bright point source; we will use the LongPass filter `F28X50LP` for the target acquisition and use the default overhead of 8.0 minutes from Table 9.1 on page 125. No peakup is needed as we are using the 0.5 arcsecond wide slit. This is a CVZ observation so each orbit is ~96 minutes. As shown in Table 9.3, we can perform this observation in a single orbit.

Table 9.3: Orbit Calculation for Example 2

Action	Time (minutes)	Explanation
	Orbit 1	
Initial guide star acquisition	9.0	Needed at start of observation of new target
Target acquisition	8.0	Point source acquisition on target
Science exposure, `G750L`, λ = 8975	24.0	17.5 minutes exposure time 5.0 minutes - first CCD spect. exposure in visit 1.5 minutes for `CRSPLIT=3`
Science exposure, `G750L`, λ = 7751	8.0	1.0 minutes exposure time 5.0 minutes - CCD spect. exp with grating wheel move 2.0 minutes for `CRSPLIT=4`
Science exposure, `G430L`, λ = 4300	8.0	1.0 minutes exposure time 5.0 minutes - CCD spect. exp with grating wheel move 2.0 minutes for `CRSPLIT=4`
Science exposure, `G230LB`, λ = 2375	39.0	33.0 minutes exposure time 5.0 minutes - CCD spect. exp with grating wheel move 1.0 minutes for `CRSPLIT=2`

Sample Orbit Calculation 3: Imaging and Spectroscopy of the Cat's Eye Planetary Nebula, NGC6543

In this example the science is to obtain an [OIII] image of planetary nebula NGC6543, as well as an optical spectrum at H β and an ultra-violet spectrum at

CIV. The exposure time calculations for these observations are presented on page 79. The specific exposures in this series include:

- A `CRSPLIT=4` ~1 minute exposure using the `F28X50OIII` filter.
- A `CRSPLIT=4`, ~1 minute exposure using the `F28X50OII` filter.
- A `CRSPLIT=3`, ~45 minute exposure using `G430M` at a central wavelength of λ_c = 4961, using the `52X0.1` long slit and
- A ~10 minute exposure using `G140L` of CIV using the `52X0.2` long slit.

We need to include time for the guide star acquisition at the start of the first orbit, followed by an acquisition exposure. The central star of the Cat's Eye nebula is used as the acquisition target. It has a V magnitude ~11. 5. Checking Table 8.2 on page 113, we conclude that the star is not so bright that it will saturate the CCD in imaging mode with the LongPass aperture `F28X50LP` and we therefore use it for the target acquisition. We use the overhead information in Table 9.1 on page 125 directly and conclude that the target acquisition will take ~8 minutes. We wish to perform a peakup exposure as well, to center the star in the 0.1 arcsecond wide slit. We consult Table 8.2 on page 113 and conclude that the source is not bright enough to saturate the CCD if we perform a CCD undispersed (white light) peakup using the mirror. Again using the information in Table 9.1, we conclude the peakup will take ~5 minutes.

This is not a CVZ observation, so because more than 1 orbit is required we need to include time for the guide star reacquisition at the beginning of each orbit. The individual exposures in this example are long enough that we do not need to include extra overhead for data management. We are satisfied with the automatic wavecal exposures which are taken for each spectroscopic observation at a new MSM position.

We assume a visibility period of 57 minutes per orbit, appropriate for a target at our sources declination of 66 degrees (see the CP). Based on the reasoning presented in Table 9.4, below, we conclude that a total of 2 orbits is required to perform these science observations

Table 9.4: Orbit Calculation for Example 3

Action	Time (minutes)	Explanation
	Orbit 1	
Initial guide star acquisition	9.0	Needed at start of observation of new target
Target acquisition	8.0	Performed on central star
Peakup acquisition	5.0	White light peakup performed on nearby star
CRSPLIT=3 science exposure using G430M at λ_c=4961.	35.0	29 minutes exposure time, exposure 1 and 2 of `CRSPLIT=3` 5.0 minutes - first CCD spect. exposure in visit 1.0 minutes for read outs
	Orbit 2	
Guide star reacquisition	6.0	Start of new orbit
Last of the 3 `CRSPLIT=3` science exposures, using G430M at λ_c=`4961`.	18.0	17.5 minutes exposure time 0.5 minutes overhead on CCD exposure
Science exposure `G140L`	19.5	11.5 minutes exposure time 8.0 minutes - first spectroscopic MAMA exp in visit
`CRSPLIT=4` CCD Imaging Science exposure, through F28X50OIII	8.5	1.0 minute exposure time 4.5 minutes - first imaging exposure in orbit. 2.0 read time
`CRSPLIT=4` CCD Imaging Science exposure, through F28X50OII	5.0	1.0 minute exposure time 1.0 minute - filter wheel move. 2.0 read time

Sample Orbit Calculation 4: MAMA Echelle Spectroscopic Exposures in the CVZ

In this example we wish to obtain a long total integration (360 minutes) CVZ observation using `E230H` and the `0.1X0.09` slit. The exposure time calculations for this examples are presented in “Echelle Spectroscopy of a Bright Star with Large Extinction (Sk 69 -215)” on page 81.

We choose to break the observation up into 6 roughly identical 60 minute exposures. We acquire the target using a CCD point source acquisition and then peakup in dispersed light using the MAMA detector in the same mode as we intend for the science. The star is Sk 69-215, an O5 star with a V magnitude of 11.6. Checking Table 8.2 on page 113, we conclude the source is not so bright that it will saturate the CCD if observed for 0.1 seconds in the LongPass filter `F28X50LP` and we choose to perform the acquisition then on Sk 69-215 with this filter as the aperture. We take the acquisition time as 8 minutes, from the overheads in Table 9.1 on page 125.

We then perform a dispersed light echelle peakup using `E230H` with the MAMA (the target is too bright to be observed unfiltered with the MAMAs so an undispersed MAMA peakup is out of the question and by peaking up using the MAMA instead of the CCD we assure a higher accuracy of centering which can be important for such a small slit). To determine the exposure time per dwell point, we must calculate the time to achieve a signal-to-noise ratio of 40 over the 1024 (AXIS1 or dispersion) x 32 (AXIS2 or cross dispersion) pixels of the subarray used for the peakup. From the example exposure time calculation in “Echelle Spectroscopy of a Bright Star with Large Extinction (Sk 69 -215)” on page 81, we perform a rough calculation sufficient for Phase I planning and conclude that we will receive ~0.15 count sec^{-1} $pixel^{-1}$ * 1024 pixels = 153 count sec^{-1} over the central order, so it will take roughly 10 seconds integration time to achieve the desired signal-to-noise ratio. To determine the peakup overhead for this slit, we look at Table 9.7 on page 136. We thus conclude that the peakup will require 780 + 27x10 = 1050 seconds or ~ 18 minutes.

Since this is a CVZ observation, we do not need to include time for reacquisitions, however since it is along observation we decide we will re-perform a peakup midway through the observation.

Additionally, since this is a long observation taken at a given grating position, we need to include time for the automatic wavecals which will be taken every 60 minutes of elapsed pointed time.

Since this is CVZ time, an “orbit” maps into 96 minutes of time. We conclude we require a total of 5 orbits to perform this science, as summarized in Table 9.5.

Table 9.5: Orbit Calculation for Example 4

Action	Time (minutes)	Explanation
CVZ Observations - Total Time = 480 minutes or 480/96=5 orbits		
Initial guide star acquisition	9.0	Needed at start of observation of new target
Target acquisition	8.0	point source acquisition on target
Peakup exposure in `0.1X0.09` slit	18.0	Echelle slit peakup
First science exposure `E230H`	57.0	49.0 minutes exposure time 8.0 minutes for first MAMA spect. exposure in visit
Automatic wavecal after 60 minutes	4.0	4.0 minutes
Second science exposure `E230H`	60.0	59.0 minutes exposure time ~1 minutes overhead on identical exposure
Automatic wavecal after 60 minutes	4.0	4.0 minutes
Third science exposure	60.0	59.0 minutes exposure time ~1 minute overhead on identical exposure
Automatic wavecal after 60 minutes	4.0	4.0 minutes
Peakup to recenter target	18.0	Echelle slit peakup
Fourth science exposure	56.0	55.0 minutes exposure time ~1 minutes overhead on identical exposures
Automatic wavecal after 60 minutes	4.0	4.0 minutes
Fifth science exposure	60.0	59.0 minutes exposure time ~1 minutes overhead on identical exposure
Automatic wavecal after 60 minutes	4.0	4.0 minutes
Sixth science exposure	60.0	59.0 minutes exposure time ~1 minutes overhead on identical exposure
Automatic wavecal after 60 minutes	4.0	4.0 minutes
Seventh science exposure	50.0	49.0 minutes exposure time ~1 minutes overhead on identical exposure

Sample Orbit Calculation 5: Faint CCD Imaging

In this program we wish to take deep images of a field to look for faint point sources, as described in “Imaging a Faint Stellar Source” on page 83. We request `LOW-SKY` as this observation is background limited. At our declination, we find from the CP/Phase I Proposal Instructions, that there are 45 minutes of visibility per orbit. The observations consist of:

- A single `CRSPLIT=4` ~20 minute exposure using the `50CCD` clear aperture with the CCD.

We determine that we can execute this program in 1 orbit, as summarized in Table 9.6.

Table 9.6: Orbit Calculation for Example 5

Action	Time (minutes)	Explanation
	Orbit 1	
Initial guide star acquisition	9.0	Needed at start of observation of new target
`CRSPLIT=4` exposure, using `50CCD` in imaging mode.	36.0	29.0 minutes exposure time 5.0 minutes for first imaging exposure in orbit 2.0 minute overhead for reads

On-board Target Acquisition and Peakup Overheads

In Table 9.1, we provided standard acquisition and peakup exposure durations using the CCD in white light to observe stars brighter than V=22. Here, we provide more detailed information, and procedures for determining acquisition and peakup exposure times in the more general case, including faint point source and diffuse acquisitions and peakups using the CCD and the MAMA detectors.

Acquisitions

The acquisition overhead time is given by:

$$acqtime = 425 + 4 \times t_{\mathrm{exp}} + 0.2 \times CHECKBOX^2 \quad \text{seconds} \qquad \text{(Eq. 9.1)}$$

where t_{exp} is the time per exposure (the time to achieve a signal-to-noise of 40 observing the target you are acquiring) and `CHECKBOX` is the size (length) in pixels of the checkbox over which the flux is summed (page 107). For point source acquisitions, `CHECKBOX=3`. For diffuse acquisitions, you choose the checkbox size (see Chapter 8).

Peakups

In Table 9.7 below, we provide formula for determining the peakup durations for the CCD and MAMA detectors. Here, t_{exp} is the exposure time per dwell point, and should be calculated as the time to achieve a signal-to-noise of 40 over the target. Note that the dwell point exposure time has a dramatic effect on the

peakup duration. These formula are still approximate; during Phase II the scheduling software will use and report the actual durations.

Table 9.7: Acquisition Peakup Times, White Light or Dispersive

Aperture	Peakup	CCD Duration (seconds)	MAMA Duration (seconds)
	All Long Slits		
52X0.1	5 steps AXIS1	$180+12*t_{exp}$	$180+6*t_{exp}$
52X0.2	3 steps AXIS1	$120+8*t_{exp}$	$120+4*t_{exp}$
52X0.5	3 steps AXIS1	$120+8*t_{exp}$	$120+4*t_{exp}$
52X2.0	3 steps AXIS1	$120+8*t_{exp}$	$120+4*t_{exp}$
52X0.5F1	3 steps AXIS1 3 steps AXIS2	$240+16*t_{exp}$	$240+8*t_{exp}$
	Echelle Slits for E230M and E140M		
0.2X0.06	7 steps AXIS1 3 steps AXIS2	$360+24*t_{exp}$	$360+12*t_{exp}$
0.2X0.2	3 steps AXIS1 3 steps AXIS2	$240+16*t_{exp}$	$240+8*t_{exp}$
	Echelle Slits for E230H		
0.1X0.09	25 step SPIRAL	$780+52*t_{exp}$	$780+27*t_{exp}$
0.1X0.2	5 steps AXIS1 3 steps AXIS2	$300+20*t_{exp}$	$300+10*t_{exp}$
	Echelle Slits for E140H		
0.2X0.09	5 steps AXIS1 3 steps AXIS2	$300+20*t_{exp}$	$300+10*t_{exp}$
0.2X0.2	3 steps AXIS1 3 steps AXIS2	$240+16*t_{exp}$	$240+8*t_{exp}$

CHAPTER 10
Summary and Checklist

In This Chapter...

In this chapter we provide a summary and a checklist to help ensure that you have correctly planned your Phase I (proposing for HST time) and Phase II (scheduling your approved observations) submissions.

Phase I Proposing

At this point you should have assembled all the information you need to submit your Phase I HST observing time proposal. During the course of this process you should have done the following:

- Checked that your source does not exceed the absolute bright object count rate limits for MAMA exposures.
- Checked your exposure times and configuration to assure they are sufficient to provide the desired signal-to-noise ratios and accuracies.
- Assured that you have appropriately crsplit your CCD exposures to allow cosmic ray removal.
- Checked that you are not exceeding the CCD full well counts $pixel^{-1}$ limit for pixels (lines or objects) of interest.
- Checked that you are not exceeding the MAMA 65536 counts $pixel^{-1}$ buffer imposed limit over pixels (lines or objects) of interest.

- Selected a target acquisition with appropriate centering accuracy; if a pre-acquisition image is needed, included the necessary extra orbit in the total orbit time request.
- Considered whether your science requires particularly accurate wavelength determination requiring additional (non-automatic) wavecal exposures.
- Justified any special requirements (e.g., SHADOW)
- Considered the need for and benefit of obtaining coordinated parallel exposures with NICMOS, WFPC2, or FOC.
- Included all applicable overheads so that in Phase II you will have enough orbits available to successfully implement your observation.

Phase I Templates

Sample Phase I templates for the STIS examples worked through in this Handbook (see “Examples Used in this Handbook” on page 4, “Exposure Time Examples” on page 77, and “Orbit Use Determination Examples” on page 127) are presented in the Phase I Proposal Instructions.

Phase II—Scheduling Approved Observations

Below, we provide a checklist for observers filling out their Phase II proposal. Have you:

- Properly specified exposures?
- CR-SPLIT CCD exposures, as appropriate?
- Included target acquisition and peakups as needed?
- Specified accurate V magnitude, fluxes, spectral type and colors for your target?
- Included any additional wavecal exposures if needed?
- Specified orientation requirements?
- Specified any coordinated parallel exposures?

Phase II Templates

Phase II templates for the examples worked out in this Handbook will be made available in the Phase II Proposal Instructions and on the World Wide Web, when the Phase II Proposal Instructions are released, towards the end of 1997.

PART 3

Supporting Material

The chapters in this part present more detailed material in support of the Users Guide. Included are a description of the data taking modes of STIS; special uses of the instrument; and spectroscopic and imaging reference material.

"Space is big, really big."
A. Douglas, HHG.

CHAPTER 11
Data Taking

In This Chapter...

In this chapter we describe the basic ways in which data can be taken with STIS. Included are descriptions of the operating modes of the STIS CCD and MAMAs, the use of subarrays, the taking of associated exposures in a series, the taking of automatic and extra wavecals, and the fixing of the slit orientation on the sky.

Basic Operating Modes

STIS currently supports four basic operating modes:

- `ACCUM` operating modes for the CCD and MAMA, which produce a time integrated accumulated image and are expected to be the most commonly used modes.
- `TIMETAG` operating mode for the MAMA detectors, used for high time resolution observations in the UV, which outputs an event stream.
- `ACQ` (acquisition) and `ACQ/PEAKUP` operating modes for the CCD and MAMA used to acquire targets in the spectroscopic slits and behind coronographic bars and masks. Target acquisitions are described further in Chapter 8, “Target Acquisition” on page 103.

CCD ACCUM Mode

The STIS CCD has only the single operating mode, `ACCUM` mode for images and spectra. The CCD pixels accumulate charge during the exposure in response

to photons. The charge is read out at the end of the exposure and converted to 16 bit data numbers (DN) at a selectable gain (number of electrons per DN) by the A-to-D converter. The DN are stored as 16 bit words (with a range 0to 65535) in the STIS data buffer memory array. At a default `GAIN=4`, the `CCD` full well (170,000 e^- over the inner portion of the chip, 120,000 e^- at the edge), and not the 16-bit format limits the total counts that can be sustained in a single exposure without saturating (see also “Analog-To-Digital Conversion” on page 89 and “CCD Saturation: the CCD Full Well” on page 90).

A full detector readout is actually 1064 x 1044 pixels with physical and virtual overscans. Science data are obtained on 1024 x 1024 pixels, each projecting to ~0.05 x 0.05 arcseconds on the sky. The dispersion axis runs along `AXIS1` (image x or along a row of the CCD), and the spatial axis of the slits runs along `AXIS2` (image y or along a column of the CCD). Figure 11.1 illustrates the full CCD format and its orientation with respect to the spacecraft (U2 and U3 or V1 and V3) axes. The readout includes 20 columns of leading and 20 columns of trailing physical overscan in `AXIS1`, and 20 trailing rows of virtual overscan in `AXIS2`. The leading and trailing serial overscan pixels are used to determine the bias level in post observation data processing, the parallel overscan can be used in the diagnosis of charge transfer problems.

Figure 11.1: CCD ACCUM Mode Format for a Long Slit Spectrum

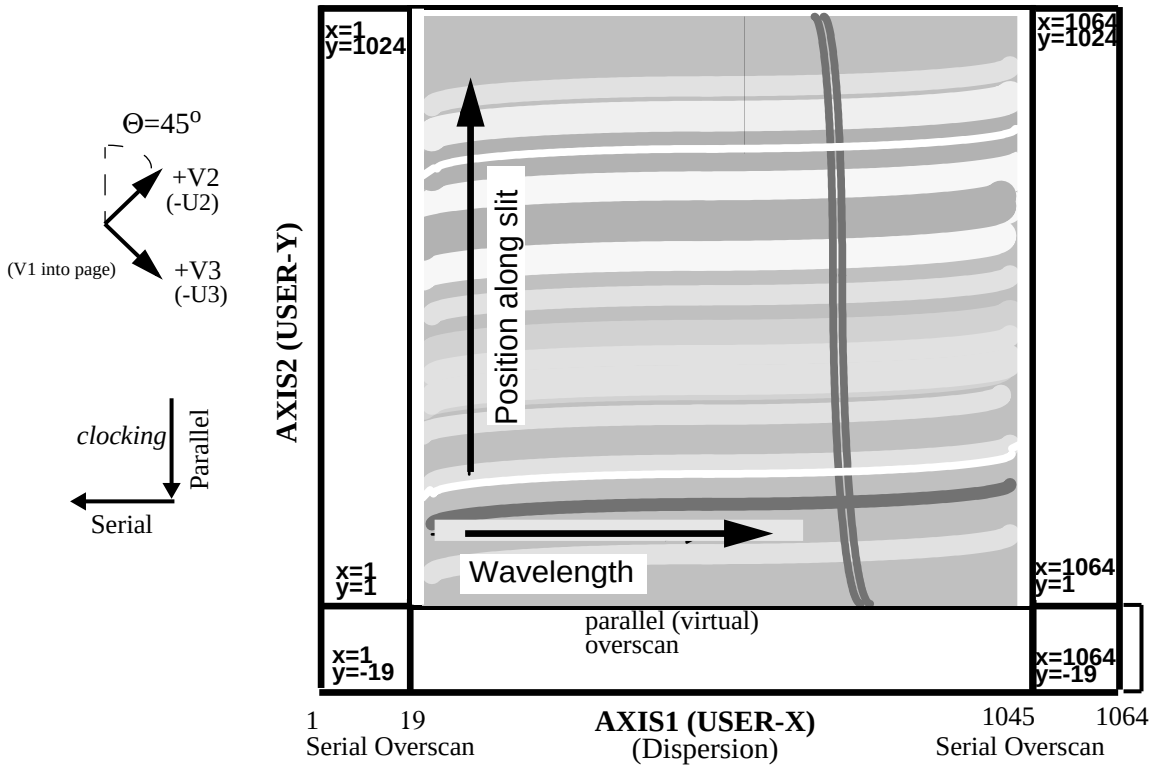

The minimum `CCD` exposure time is 0.1 second and the maximum possible exposure time is 4.7 hours (though we cannot imagine wanting a single exposure

longer than 60 minutes). The minimum time between *identical* exposures for CCD full frame (1064 x 1044) images is 37 seconds. This time is dominated by the time it takes to read out the CCD (28 seconds for the full frame) and can be reduced to ~11 seconds if you use a subarray (see “Subarrays” on page 148).

Binning

The CCD supports on-chip binning. When on-chip binning is used, the specified number of pixels in the serial and parallel directions are read out as a single pixel. The advantage of CCD binning is that the read noise per binned pixel is the same as the read noise per unbinned pixel; thus if your signal to noise per pixel is dominated by read noise when no binning is used, you can increase the signal to noise by binning (see also “Computing Exposure Times” on page 70). The disadvantage of using on chip binning is that it reduces the resolution of your spectrum/image. On-chip binning of 1, 2, or 4 pixels in both the AXIS1 and/or AXIS2 directions are supported. Note that on chip binning is not allowed when subarrays are used.

During Phase II, you specify the binning for your CCD observations using the BINAXIS1 and BINAXIS2 optional parameters. The default values are 1.

MAMA ACCUM

In MAMA ACCUM mode exposures, photons are accumulated into a 2048 x 2048, 16 bit per element array in the STIS data buffer memory as they are received. At the end of the exposure, the data are binned by two along AXIS1 and two in AXIS2 to produce a 1024 x 1024 pixel image of integrated counts which is transmitted to the ground. ACCUM is the mode of choice for all observations that do not require time resolution on minute or less scales. Dispersion runs along AXIS1 and the spatial dimension of the slit (and the orders for echelle observations) run along AXIS2. Figures 11.2 and 11.3 illustrates the format and coordinate system for MAMA images, showing how a first order and echelle ACCUM mode spectra would appear. PRISM images would have dispersion along AXIS1.

Figure 11.2: Example MAMA ACCUM Mode Spectrum for First Order Long Slit Spectroscopy

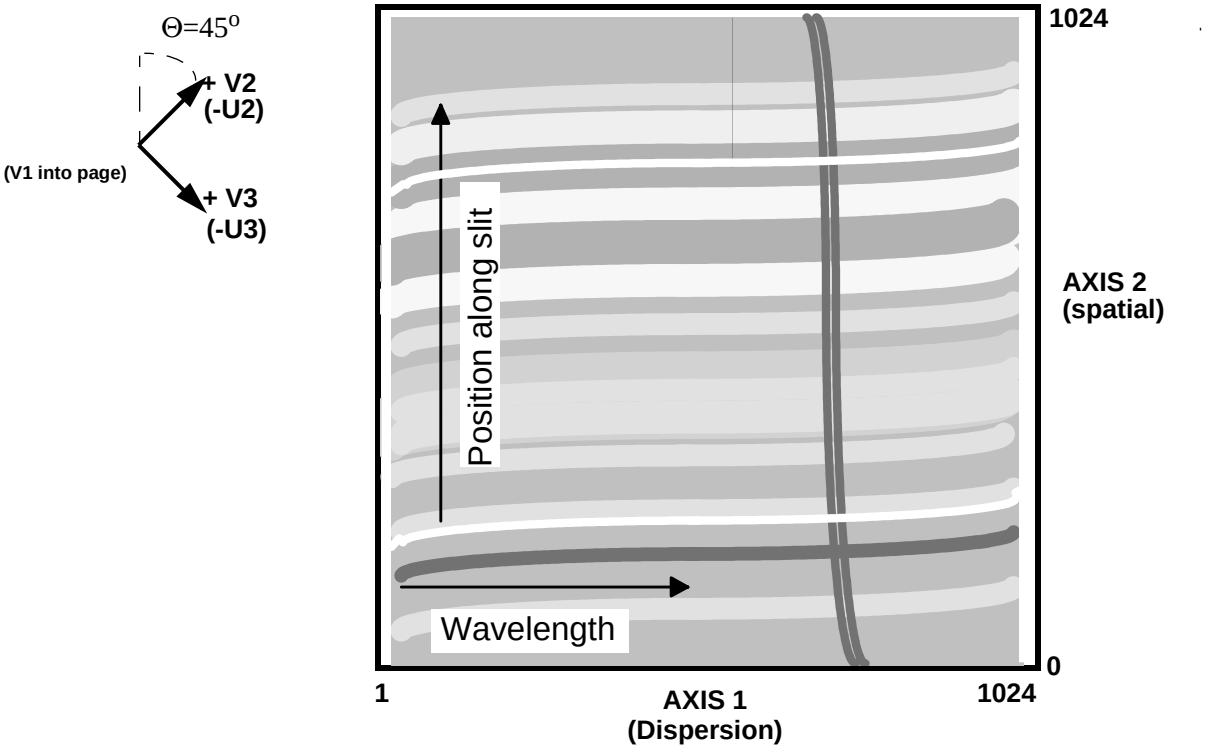

Figure 11.3: Example MAMA ACCUM Mode Spectrum for Echelle Modes

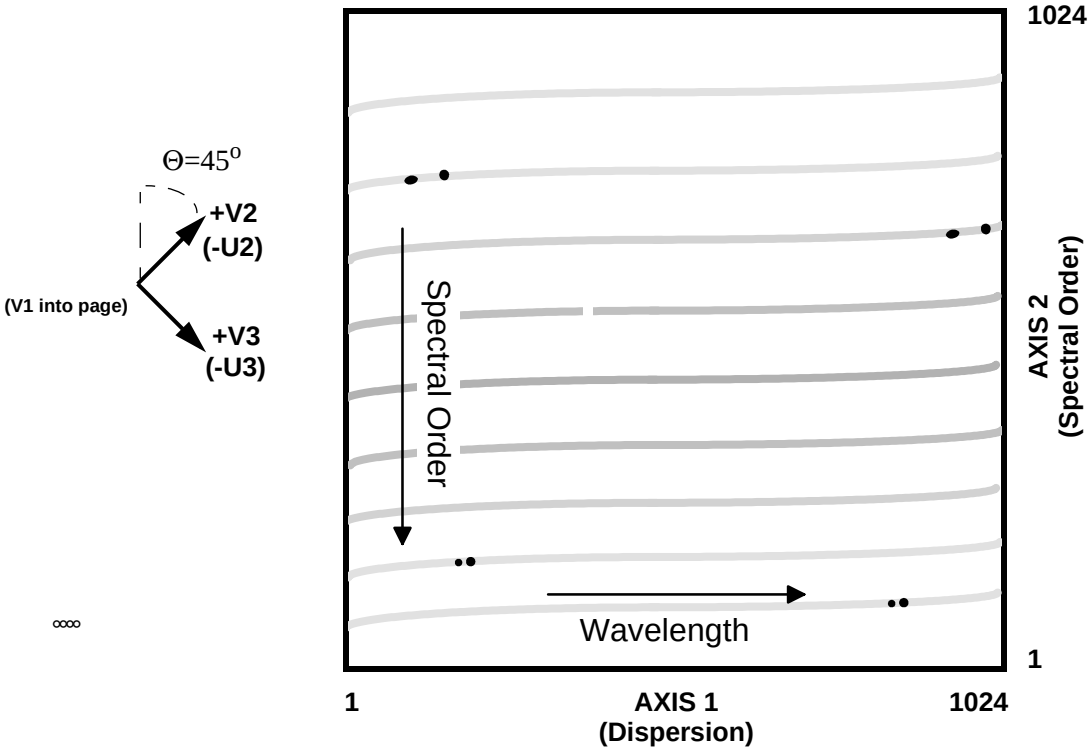

The minimum MAMA ACCUM mode exposure time is 0.1 second and the maximum exposure time is 1.8 hours. The minimum time between *identical* MAMA ACCUM exposures is 1 minute, and is influenced by the need to shutter the MAMAs and perform a bright object check each exposure in order to be protect the detectors from accidental exposure to bright light.

For the MAMA medium resolution first order modes and medium and high resolution echelle modes (i.e., gratings G140M, G230M, E230M, E230H, E140M, and E140H) correction for Doppler shifting of the photon energies due to HST spacecraft motion is applied as the photons are counted, prior to their addressing in STIS data buffer memory. The leading and trailing pixels in the dispersion direction (AXIS1) for Doppler corrected exposures therefore receive less effective integration time, since source photons at the corresponding wavelengths have been Doppler shifted off the edge of the detector for some fraction of the total exposure time. This effect is strongest in the high resolution echelle modes, where for a maximum HST spacecraft velocity of 8 km sec^{-1}, the leading and trailing ~20 AXIS1 pixels will have reduced effective exposure times. When subarrays are used (see “Subarrays” on page 148), the under-exposed region is double in size, i.e., for the example above the leading and trailing 40 pixels along AXIS1 would receive less effective integration time. [1]

Highres

The MAMA detectors are capable of recording data in the so-called *highres* mode, producing 2048 x 2048 images of super resolution (one half the 1024 format scale) pixels.

While the MAMA detectors have 1024 x 1024 pixels., each pixel is defined by 3 electrodes, so the ratio of charge distribution between the 3 electrodes can be used to centroid the incident charge cloud to sub-pixel resolutions. The gain of the *highres* 2048 x 2048 mode is expected to be a ~10-30% increase in resolution at the price of decreased signal-to-noise ratio per pixel arising from the increased fixed pattern noise of the statistics of charge partition between the electrodes. The lack of flat field reproducibility (adjacent columns and rows typically differ by ~5% and can differ by as much as ~10-20% in an off/on pattern whose time variability is not yet established, and the flat field response in *highres* mode may be rate dependent), and the inherently lower signal to noise ratio in the full resolution flat field images (nominally ~20 to 1 per *highres* pixel) suggest that it may be difficult to routinely realize the benefit in resolution. Highres is most likely to have application at low to intermediate signal-to-noise ratios (below 20:1) and low to intermediate incident count rates (exact range to be determined - expected to be applicable only at rates less than 5-10 counts sec^{-1} $pixel^{-1}$). However, we note that data taken in *highres* mode can always be binned to 1024 x 1024 on the ground in post observation data processing, and observers wishing to achieve the highest possible spectral resolution may wish to consider utilizing it. The overheads for *highres* mode are not yet established; they may ultimately differ slightly from those for normal MAMA ACCUM exposures.

1. This occurs due to the sequencing of discarding events which fall outside the sub-array and application of the Doppler shift correction in the flight software.

Highres sampling is currently an available-but-unsupported mode (see “Support of STIS Capabilities for Cycle 7” on page 12), however if we can establish that it is a robust method of data taking, it may become a supported mode for Cycle 7. Advice on the use of *highres* should be available by Phase II.

MAMA TIMETAG Mode

TIMETAG mode is used for high time resolution spectroscopy and imaging in the ultraviolet. When used in TIMETAG mode, the MAMA produces an event stream of AXIS1, AXIS2, and TIME data points, with a time resolution of 125 microseconds. The volume of data produced in TIMETAG mode can be very large and the data therefore must be continuously transferred from the STIS internal buffer to the tape recorders to sustain TIMETAG exposures of any significant duration.

The axis orientation in TIMETAG is the same as in ACCUM mode (see page 143). The spacecraft time (absolute zero point of the time) is routinely known to ~1 second accuracy (although higher precision can be achieved later). No Doppler correction is applied by the flight software for TIMETAG mode, but the correction is applied in the STScI pipeline. TIMETAG mode is illustrated in Figure 11.4 (processing of TIMETAG data by the STScI pipeline is described in “Pipeline Processing Overview” on page 311).

Figure 11.4: TIMETAG Mode

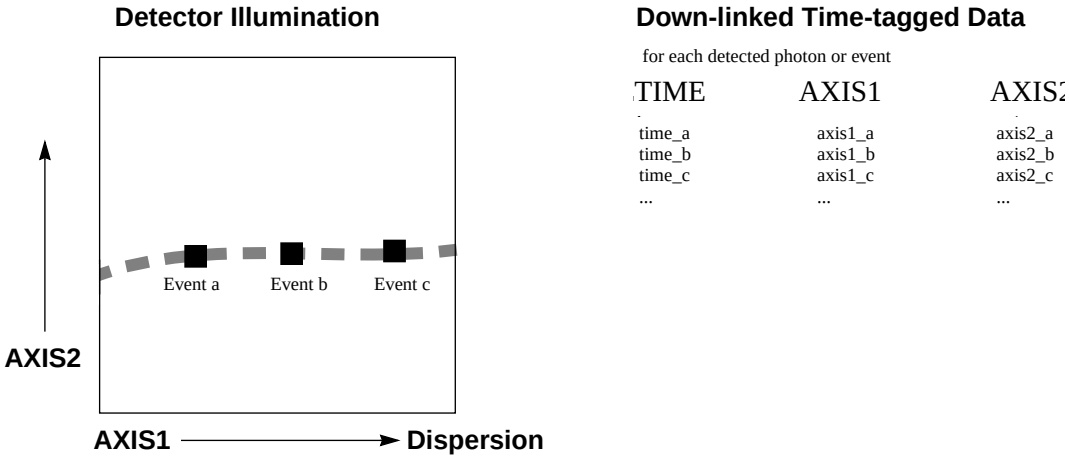

Time-Tag Constraints

There are several limitations in TIMETAG mode of which users should be aware:

- The maximum count rate from your source (within the full format or a specified subarray) must be less than 21,000 count sec^{-1} to sustain TIME-TAG exposures of any substantial duration (>2 minutes).

- At count rates between 21,000 and 30,000 count sec^{-1}, the maximum TIMETAG exposure is $4x10^6/R$ seconds, where *R* is the count rate from the source, or between 80 and 190 seconds. The MAMA detectors are not able to count at rates greater than 30,000 count sec^{-1} in TIMETAG mode (i.e., uncorrectable non-linearity and time-tagging sets in).
- The maximum total *exposure duration* that can be sustained during any one visit (where a visit is a set of exposures at a single pointing which must be scheduled together) within TIMETAG mode is $6.0 \times 10^7/R$ seconds. For example, at count rate of R=21,000 count sec^{-1} the maximum exposure time in any one visit is ~48 minutes. In special cases, for special science needs, the HST data recorder can be devoted exclusively to a single observing program for a predetermined period of time, allowing longer total exposure durations. Requests for such special handling should be included in your Phase I proposal justification

The count rate *R* from the source refers to the counts received within the subarray of the detector which is being recorded (see subarrays below). Subarrays can be usefully employed in TIMETAG mode observations of bright fields, to limit either the region being recorded (in imaging mode) or the portion of the spectrum being recorded (e.g., for echelle observations).[2]

Specifying Time-Tag Observations: BUFFER-TIME

The ground system must know the data rate to expect in order to schedule data transfers. Transfers are done in blocks of 8 megabytes (half the buffer capacity). The frequency of scheduled dumps depends on observer-specified information about the expected count rate. Specifically, during Phase II, TIMETAG observers must specify a BUFFER-TIME parameter, where BUFFER-TIME is the time to fill one half the STIS buffer, i.e., the time to accumulate $2x10^6$ TIMETAG events. Thus:

$$BUFFER-TIME = 2 \times 10^6/R \qquad \text{seconds}$$

where, the parameter *R* is the maximum expected event rate in counts sec^{-1} from your source.

Explicitly, for calculation of BUFFER-TIME (Phase II), R should be determined -as the maximum total counts accumulated in any 95 second interval, divided by 95 seconds. This *R*, the maximum mean count rate sustained over any ~1.5 minute interval during your exposure, is equivalent to the maximum instantaneous count rate, so long as your source does not vary dramatically.

If you underestimate your count rate, you will overestimate the time it will take to fill the STIS buffer, and you will be filling up the STIS internal memory faster than it is being emptied to tape recorder. Once the STIS internal memory fills up, events are not recorded until the buffer is emptied, at which point events are once more recorded, resulting in an exposure with periodic 95 second time gaps in it.

2. Note, however, that the absolute bright object limits (see “MAMA Bright Object Limits” on page 97) apply to all light falling on the detector and are not affected by the use of subarrays.

Conversely, if you overestimate your count rate and underestimate the time to fill the STIS buffer, your total exposure time will be restricted unnecessarily.

Subarrays

Overview

When a subarray is used, only the portion of the detector which is within the specified subarray is read out and transmitted to the ground (see Figure 11.5). Generally, there is no need to use a subarray when taking STIS data and the full array (which is the default) will be read out and transmitted to the ground. This maximizes the science return.

Figure 11.5: Using Subarrays (curvature of the spectrum is exaggerated)

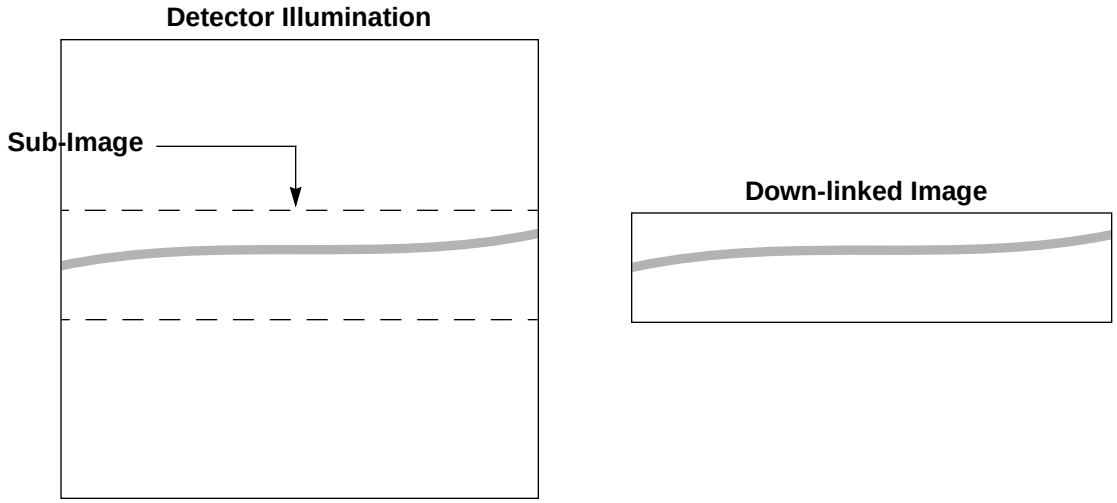

There are a few special instances in which subarrays can be gainfully used:

- If you are using the CCD to obtain many short, t_{exp}< 3 minutes, closely spaced exposures (e.g., to obtain time resolved information in the optical) subarrays can be used to reduce the CCD read time and keep the data volume at a manageable level.
- If you are using the MAMA detectors in ACCUM mode (see “MAMA ACCUM” on page 143) to observe a bright source and are therefore taking a series of short (t_{exp}< 3 minutes) exposures to avoid the buffer saturation limits, subarrays can be used to reduce the overall data volume, thereby avoiding large overheads for data transfer.

- If you are using the MAMA detectors in TIMETAG mode (see “MAMA TIMETAG Mode” on page 146) subarrays can be used to limit the count rate, thereby reducing the data transfer problems and extending the total exposure time.

Subarray sizes and centers, as specified in Phase II, are given by four parameters:

- SIZEAXIS1 – size in pixels of the subarray in the axis1 direction.
- SIZEAXIS2 – size in pixels of the subarray in the axis2 direction.
- CENTERAXIS1 – central pixel of the subarray in the axis1 direction.
- CENTERAXIS2 – central pixel of the subarray in the axis2 direction.

Rules for specifying subarrays differ for CCD and MAMA spectroscopic and imaging observations, as described below.

CCD Subarrays

As described in “CCD ACCUM Mode” on page 141, full frame CCD read outs are composed of 1064 x 1044 pixels; 1024 x 1024 science pixels, 20 leading and 20 trailing serial overscan pixels, and 20 trailing parallel overscan pixels. Dispersion runs along AXIS1 and the long axis of the slit runs along AXIS2. Subarrays are required to span the full width of the CCD detector in the serial (dispersion) direction in order to assure they contain the serial overscan needed to determine the bias level, however you can control the height of the subarray in the parallel direction (i.e., along the slit for longslit spectroscopic observations). The minimum allowed value of SIZEAXIS2 is 16 pixels (corresponding to 0.9”) and SIZEAXIS2 must be an even number of pixels. The subarray is centered on the target position.

Use of Subarrays to Reduce the CCD Read Time

The minimum time between identical CCD exposures is the readtime + 9 seconds. The time to read out a CCD subarray is:

$$readtime = 1.0 + SIZEAXIS2 \times 0.027 \qquad \text{seconds}$$

Thus, using the smallest available subarray which is 16 pixels high, you can reduce the minimum time between identical exposures to ~ 11seconds (9 seconds overhead plus 2 seconds read time). The minimum time between full frame CCD exposures is ~9 + 28 = 37 seconds.

Use of Subarrays to Reduce Data Volume

The format of the data you receive when you use a CCD subarray will have dimensions 1062 x SIZEAXIS2, will cover the full range in the dispersion direction, and will include the full overscan. The STIS buffer can hold 7 full frame CCD exposures at one time, or 8 × (1024 / SIZEAXIS2) exposures at any one time. Data acquired in one exposure can be transferred to the HST data recorder during the subsequent exposure(s) so long as the integration time of the subsequent exposure is longer than 3.0 minutes in duration. If you are taking a

series of exposures which are shorter than this, the buffer cannot be emptied during exposures, and once the STIS buffer fills up, there will be a pause in the exposures sequence of roughly 3 minutes as the buffer is emptied. This problem can sometimes be avoided with the judicious use of subarrays to allow all desired sequential exposures to fit within the STIS buffer.

MAMA Subarrays

As described in "MAMA ACCUM" on page 143 above, full frame MAMA images are 1024 x 1024 pixels; dispersion runs along `AXIS1` and the long axis of the slit and echelle orders run along `AXIS2`. When subarrays are used with the MAMA detectors, the gating electronics into the MAMA Interface Electronics discards photon events that fall outside of the subarray boundaries, and photons are accumulated from within the subarray only. Note however, that the full field of view still exposes the MAMA detector, so that the absolute bright object limits (see "MAMA Bright Object Limits" on page 97) are the same, whether or not subarrays are used.

All MAMA subarrays must have dimensions that are powers of 2 and be equal to or larger than 16, i.e., only the specific values of 16, 32, 64, 128, 256, 512, or 1024 are possible for `SIZEAXIS1` and `SIZEAXIS2`. The observer can fully specify all of the subarray parameters (`SIZEAXIS1`, `SIZEAXIS2`, `CENTERAXIS1`, and `CENTERAXIS2`) for MAMA observations, however for spectroscopic observation `SIZEAXIS1` should generally be left at the default value of 1024, to assure that the full spectrum from the source is retained. By default, the center of the subarray is located on the target position.

Use of Subarrays for MAMA ACCUM mode Observations

The STIS buffer can hold 4 full frame MAMA exposures or:

$$4 \times (1024 \times 1024) / (SIZEAXIS1 \times SIZEAXIS2)$$

exposures at any one time. Data acquired in one exposure can be transferred to the HST data recorder in the subsequent exposure(s) so long as the integration times of the subsequent exposures are longer than 3.0 minutes in duration. If you are taking a series of exposures that are shorter than this, the buffer cannot be emptied during exposures, and once the STIS buffer fills up there will be a pause in the exposure sequence of roughly 1.5 minutes as the buffer is emptied. That interruption can be avoided through the judicious use of subarrays to limit the data volume (note however that if your exposure times are greater than 3 minutes, there is *no* benefit and a *loss* of information when you use subarrays in `ACCUM` mode).

Caveat on MAMA Subarray Use

There is a caveat on the use of subarrays if you require high photometric accuracy and are operating near the global science linearity limit, i.e., at global (over the detector) count rates > 200,000 counts second^{-1}. The global science non-linearity limit is affected by subarrays in a poorly understood way and it is likely that the correction for global non-linearity will be poorer for data taken using subarrays than for data taken using the full frame. The local linearities are not affected by the use of subarrays.

Use of Subarrays for TIMETAG Mode Observations

For TIMETAG mode observations, the two relevant science limits, the 30,000 count sec^{-1} global science non-linearity limit and the 21,000 count sec^{-1} maximum rate for continuous TIMETAG exposures both apply only to the photons received within the subarray ("MAMA TIMETAG Mode" on page 146). Subarrays which isolate a target or wavelength of interest can be used to maintain the processed count rate within the limiting levels.

Exposure Sequences: auto-wavecal, crsplits, repeats, and patterns

There are several instances where a series of associated STIS exposures (rather than a single exposure) will be taken. The data from these exposure sequences are processed as a single unit through the STScI calibration pipeline, with the science data from the multiple *associated* exposures appearing in a single file (for a discussion of the planned STIS calibration pipeline and the data product format see Chapter 15, "Overview of Pipeline Products" on page 311). While you do not have to specify that you plan a series of associated exposures in your Phase I proposal, it is helpful to know about these sequences when planning your proposal. In Phase II, once your proposal has been accepted and you are working on scheduling your observations, you will be able to use these sequences. All are generated from a single exposure logsheet line in your Phase II proposal.

We discuss several types of associated exposures below:

- *Automatic and GO* wavecal exposures taken with science data to allow calibration of the spectroscopic and spatial zeropoints.
- CCD CRSPLIT exposures taken to allow removal of cosmic rays in the science data during post-observation data processing.
- Multiple identical *repeat* exposures (REPEATOBS), which can be taken to provide time resolutions of tens of seconds (CCD) or minutes (MAMA).
- *Pattern* sequences, in which the target is stepped, either along the slit or perpendicular to the slit (to map a two-dimensional region) for spectroscopic observations, or in a dither pattern for imaging observations.

Wavecals

Auto-wavecals

On STIS, the optical path from source to detector passes through the aperture (slit) wheel (where the filters are housed for imaging) and then through the Mode Select Mechanism (MSM) which houses the first order gratings and prism, the cross dispersers for use with the echelles and the mirrors for imaging work (see Figure 3.1 on page 23). Lack of repeatability in the MSM causes the center of the spectrum (as defined by the aperture and wavelength centers) to fall on a slightly

different location in the detector each time there is a movement of the MSM (the MSM induced offsets in dispersion and space have been measured in component testing to be roughly plus or minus ~4 pixels). In addition, for MAMA observations, the aperture location on the detector will be deliberately shifted each month, to ensure equalization of extracted charge across the detector.

To allow calibration of the zero point of the aperture location and the zero point of the wavelength scale for spectroscopic observations, a line lamp observation (so called wavecal) will be taken *automatically* each time the MSM is moved. In addition, if a series of exposures or a single long exposure is taken at a single MSM setting, then an additional wavecal will automatically be taken when there is a pause in data taking *if* 60 minutes of exposure time has passed since the last wavecal. Here, 60 minutes is the time constant expected for thermal changes which might affect the wavelength accuracy; if on-orbit experience shows a different performance, this time will be adjusted accordingly. Each set of spectroscopic science exposures taken at a given grating tilt (i.e., MSM position) will therefore be accompanied by at least one automatically taken wavecal exposure. These wavecal exposures will be processed along with the science data, and used by the pipeline to automatically correct the zero point offsets in the wavelength and spatial scales.

The automatic wavecals are designed to be of sufficient duration to produce spectra which contain at least 3 emission lines with 3 counts per pixel and 50 summed over the line. In those regions of the spectrum where 3 lines are not obtainable, there will be at least 1 emission line with 18 counts per pixel and 300 summed over the line. For the CCD where integration times are short, the automatic wavecals will typically be taken to assure roughly 8 times this signal.

It is expected that the combination of thermal changes between the wavecal and science exposures, coupled with the ability to measure the zeropoints in the wavecal exposures will ultimately limit the accuracy of the absolute zeropoints to <=0.5 pixels (see “Summary of Expected Accuracies” on page 319). In addition to the automatic wavecals, observers can also take their own wavecal exposures, using the WAVE target option (see “GO Wavecals”, below) if they desire more accurate wavelengths than will automatically be provided, or are particularly concerned about the time variation of the zeropoint.

GO Wavecals

Only if you require particularly accurate wavelengths for the science you are performing do you need to consider using the `TARGET=WAVE` option to insert additional wavecal exposures into your observing sequence.

The wavecals taken with `TARGET=WAVE` are identical to those taken automatically (i.e., the auto-wavecals) with two important exceptions. First, you can explicitly specify which aperture (slit) you wish to use for the `TARGET=WAVE` exposure (whereas for automatic wavecals the science slit or a pre-defined alternative for each grating is used). Second, observers can set the exposure time to take longer exposures, increasing the signal-to-noise of the lamp exposures they receive or possibly saturating some lines to bring out weaker lines near astronomical lines of interest.

Tables of lines and observed count rates from the line lamp for each grating mode for several different apertures will be made available prior to Phase II. TARGET=WAVE exposures *cannot be taken with all slit-grating combinations* as the line lamps can be too bright for the MAMA detectors when used with wide slits. Therefore only certain aperture-grating combinations can be used for MAMA TARGET=WAVE observations (all are available for the CCD). The list of allowed combinations will be published prior to Phase II. Although the slit wheel repeatability is very high (see "Slit and Grating Wheels" on page 23), observers wishing particularly accurate wavelength calibrations are best off using a slit for which there is an allowed slit-grating wavecal, otherwise the slit wheel will be moved each time they take a wavecal exposure, providing an additional uncertainty.

TARGET=WAVE exposures are processed through the STScI pipeline as individual (unassociated) exposures and are not used to process the science data in the pipeline itself.

CRSPLIT

In order to allow rejection of cosmic rays in post-observation data processing, observers using the STIS CCD should always try (as much as possible given signal-to-noise ratio constraints when in the read noise limited regime) to obtain at least two, preferably three or more, identical CCD exposures (see "Cosmic Rays" on page 90). In Phase II, the CRSPLIT optional parameter (default value 2) allows easy scheduling of such multiple associated exposures. You specify the total exposure time and set CRSPLIT=*n*, where *n* is the number of exposures to break the total observing time into. For example, if the total exposure time is 12 minutes, and CRSPLIT=3, then three 4-minute exposures will be taken. Those three exposures will be associated with one another, passed through the STScI calibration pipeline as a unit, and a cosmic-ray free image will be produced during pipeline processing (see Figure 15.1 on page 313). Allowed values of CRSPLIT are 1, 2, 3, 4, 5, 6, 7, or 8.

REPEATOBS

A series of multiple repeated identical exposures can be taken most efficiently with STIS by using the so-called REPEATOBS mode. This mode can be used to obtain time resolved observations at minimum time intervals of roughly 8 seconds for the CCD (if subarrays are used) and 60 seconds for the MAMA, using ACCUM operating mode. The output of this mode is a series of identical exposures. Repeats are specified during Phase II, using the NEXP=*n* (number of exposures = many) option. For example, if your exposure time is 60 seconds, and you set NEXP=50, you will obtain fifty 60 second exposures. These fifty exposures will be associated with one another and processed through the pipeline as a unit—the individual exposures will be fully calibrated and a summed image will also be produced (see Figure 15.5 on page 317).

Patterns

A pattern refers to a series of exposures of a single target taken at slightly different telescope pointings, using the same set of guide stars. For STIS, patterns will be used to:

- *Dither* to decrease the effects of small-scale detector non-uniformity and/or increase the spatial resolution (the latter requires subpixel stepping) by offsetting the target along a long slit in the spatial direction for long slit spectroscopic observations or performing a small stepping pattern for imaging observations.
- Spectroscopically map out a two-dimensional region of the sky, by stepping perpendicular to the spatial axis of the slit.
- Spectroscopically subsample the line spread function by stepping a fraction of a pixel perpendicular to the spatial axis of the slit (i.e., along dispersion - see “Improving the Sampling of the Line Spread Function” on page 168

Two standard pattern sequences will be made available in Phase II. These are:

1. `PATTERN=ALONG-SLIT`, which allows stepping of the target along the slit (see Figure 11.6 on page 155), and
2. `PATTERN=PERP-TO-SLIT`, which allows stepping of the slit in a direction perpendicular to the slit axis (see Figure 11.7 on page 156,

Figure 11.6: Stepping Target Along Long Slit to Increase Dynamic Range

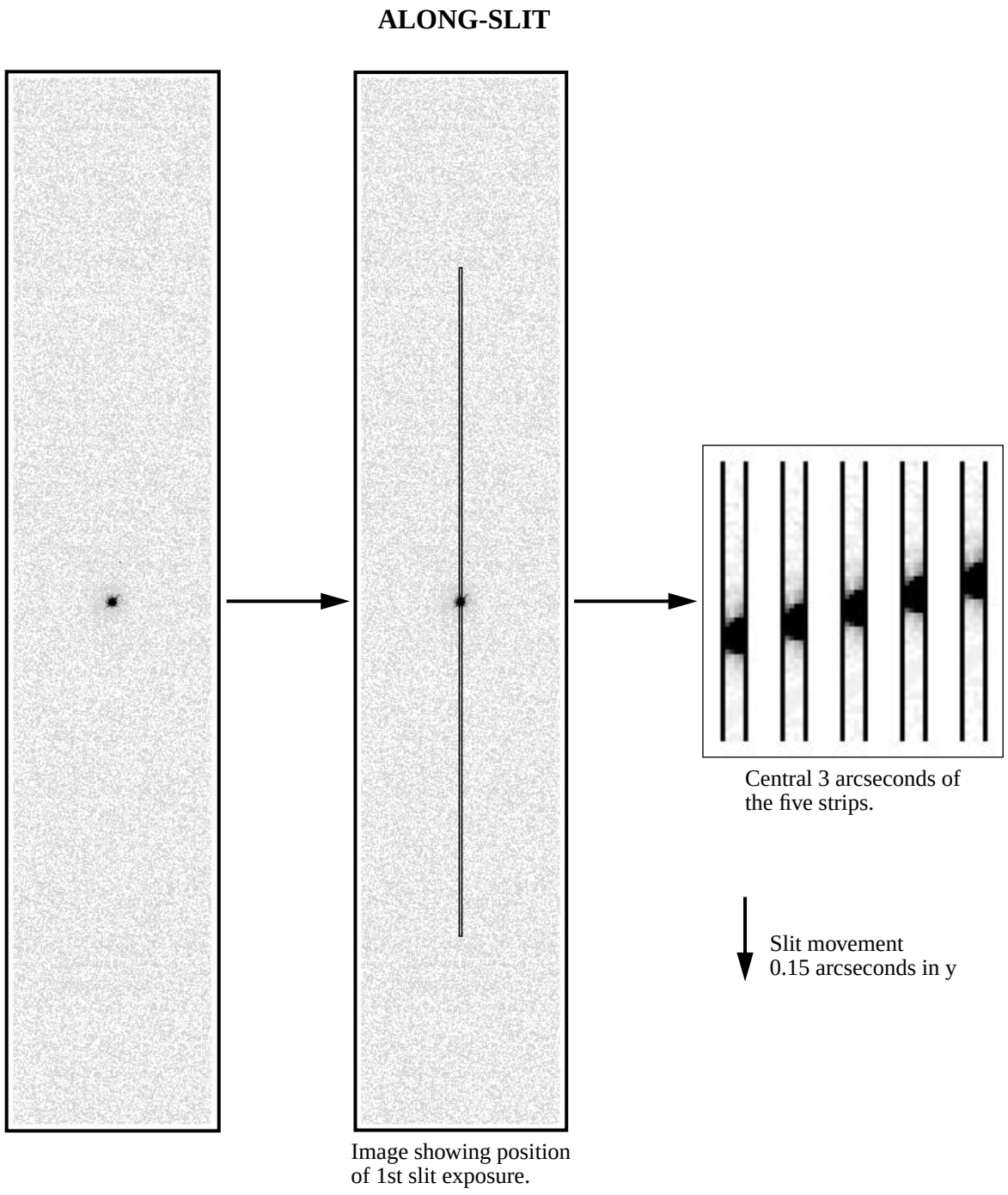

Figure 11.7: Stepping Target Perpendicular to Slit to Map 2-D Region of Sky

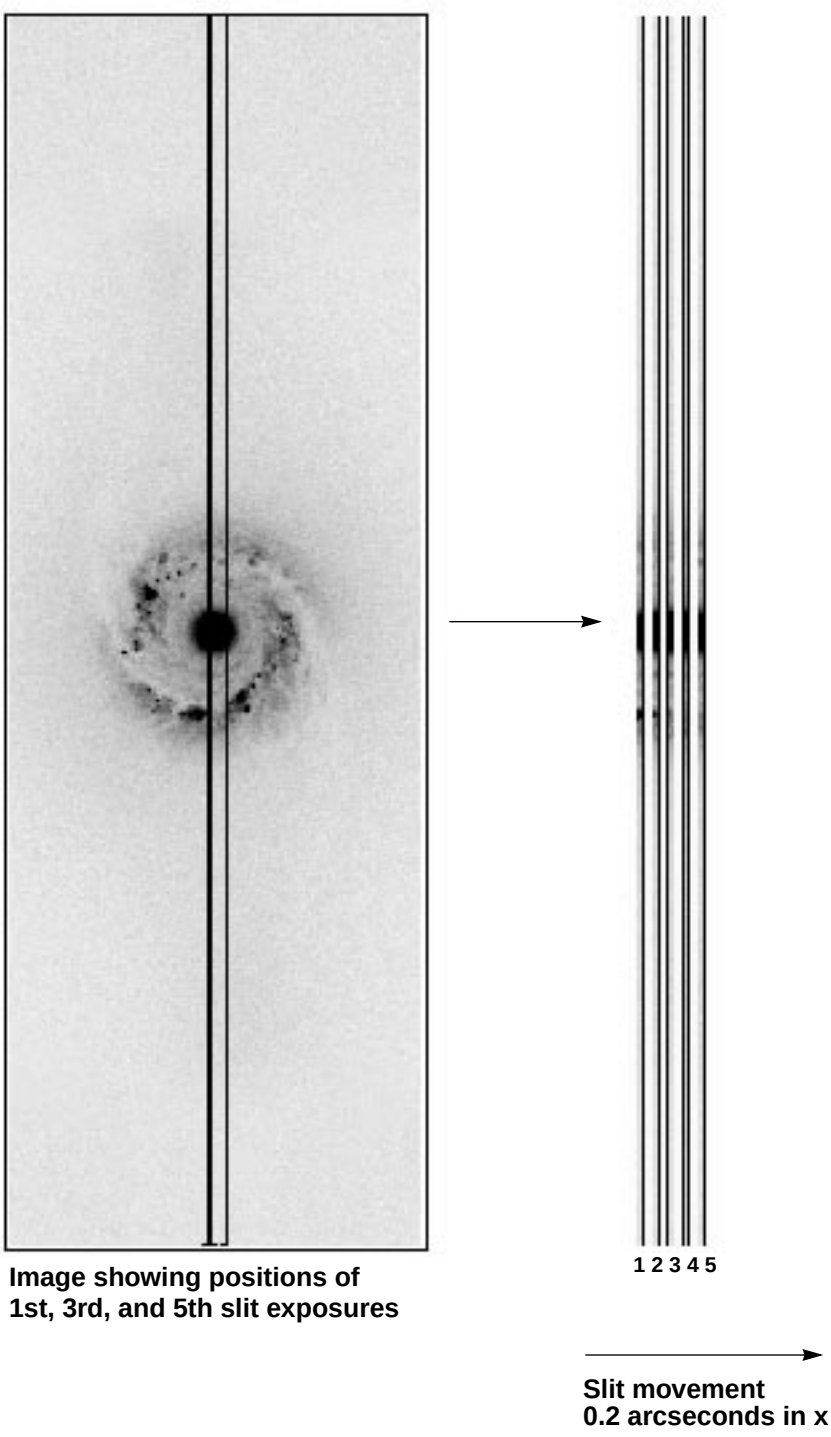

Fixing Orientation on the Sky

STIS users, particularly those using the long slit to observe extended sources, will commonly wish to specify the orientation of the slit on the sky. Observers planning coordinated parallel observations may also wish to specify the orientation of the HST focal plane, so as to place the appropriate instrument to cover a given patch of sky. When you set the orientation of the telescope, you effectively constrain the times when your observation can be scheduled, since HST must maintain a spacecraft orientation (sometimes called roll angle) which keeps its solar panels roughly perpendicular to the incoming sunlight.

The orientation of the spacecraft (and therefore of the STIS long slits which are fixed in relation to the HST focal plane) is controlled by the `ORIENT` parameter, which is entered during Phase II. The Phase II Proposal Instructions will contain a detailed description of orientations and how to specify them. A specific orientation can be set, or a range of allowed orientations (e.g., 90–110 degrees) can be given. The tighter the constraints, the more difficult it will be to schedule the observation.

The `ORIENT` parameter gives the orientation of the HST focal plane projected onto the sky and is defined by U2 and U3 axes. Figure 3.2 on page 26 shows the HST focal plane containing all the HST instruments, with the U2 and U3 axes defined and Figure 11.1 on page 142 shows the relationship between orient and the PA of the long slit on the sky. Note that to the accuracy of current knowledge the long slit is aligned with the detector's `AXIS2`, i.e., is directly perpendicular to the dispersion axis (`AXIS1`). The important point to note is that if you fix the orientation of the long slit on the sky to be PA X, where X is measured in degrees east of north, then the `ORIENT` parameter (which determines where the other HST instruments lie for parallel observations) is given as X+45 or X+225 degrees. Likewise, for `PRISM` mode observations, if you wish to fix the orientation of the cross-dispersion (i.e., spatial) axis to be X, then the `ORIENT` parameter should be set to X+45 or X+225 degrees.

We show two examples below. Figure 11.8 on page 158 illustrates how to set the `ORIENT` parameter to place the long slit along the M87 jet. Figure 11.9 on page 159 illustrates how to set the `ORIENT` parameter to fix the dispersion axis for `PRISM` observations to be perpendicular to a double star system.

Figure 11.8: Placing the STIS Long Slit Along the Jet of M8

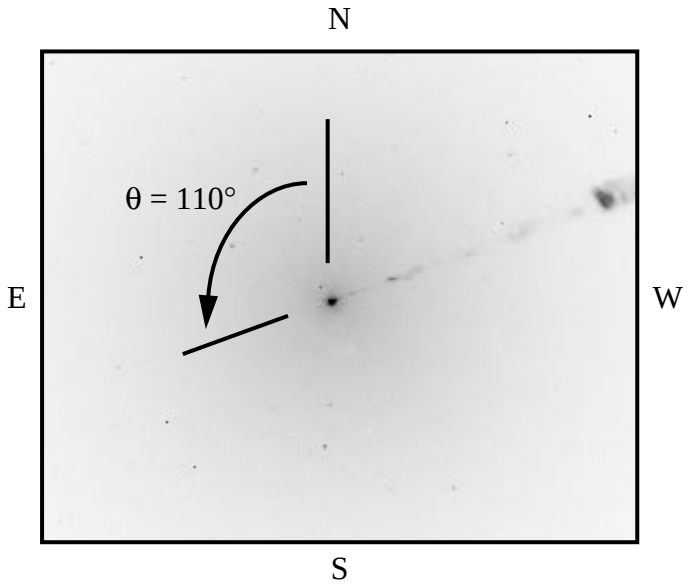

Radio galaxy with jet

θ = Angle of jet on sky = 110°

To place long slit axis on jet:

Orient = θ + 45° or θ + 225°

Orient = 110° + 45° or 110° + 225°

Orient = 155° or 335°

Figure 11.9: Placing Dispersion Direction Perpendicular to a Binary Star System

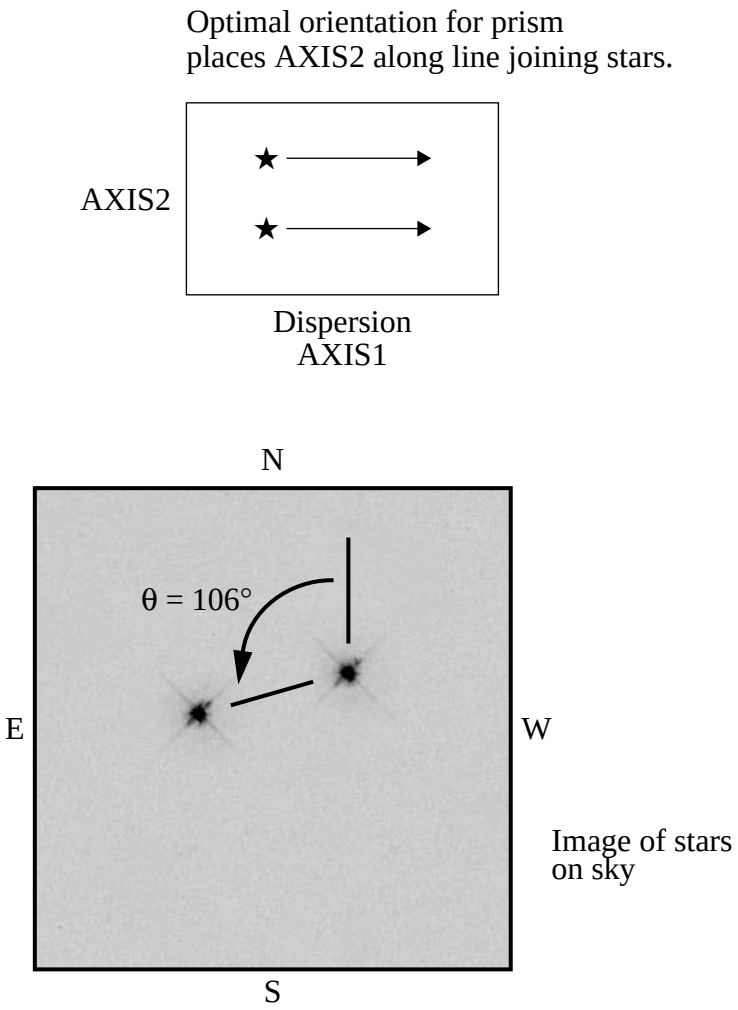

θ = Angle of line joining stars on sky = 106°

To place AXIS2 along θ:

Orient = θ + 45° or θ + 225°

Orient = 106° + 45° or 106° + 225°

Orient = 151° or 331°

CHAPTER 12
Special Uses of STIS

In This Chapter...

In this chapter we describe some of the non-standard uses of STIS and provide guidance in the use of the standard capabilities for specific scientific purposes.

Slitless First Order Spectroscopy

We expect the vast majority of STIS first order grating mode observations to use a long slit. The use of a long slit assures a clean separation of emission lines arising from different spatial features. However, all of STIS's first order gratings (see Table 4.1 on page 34) can also be used slitless to obtain emission line images. Figure 12.1 shows a simulated example of a slitless spectrum.

Figure 12.1: Schematic Slitless Spectrum of Planetary Nebula

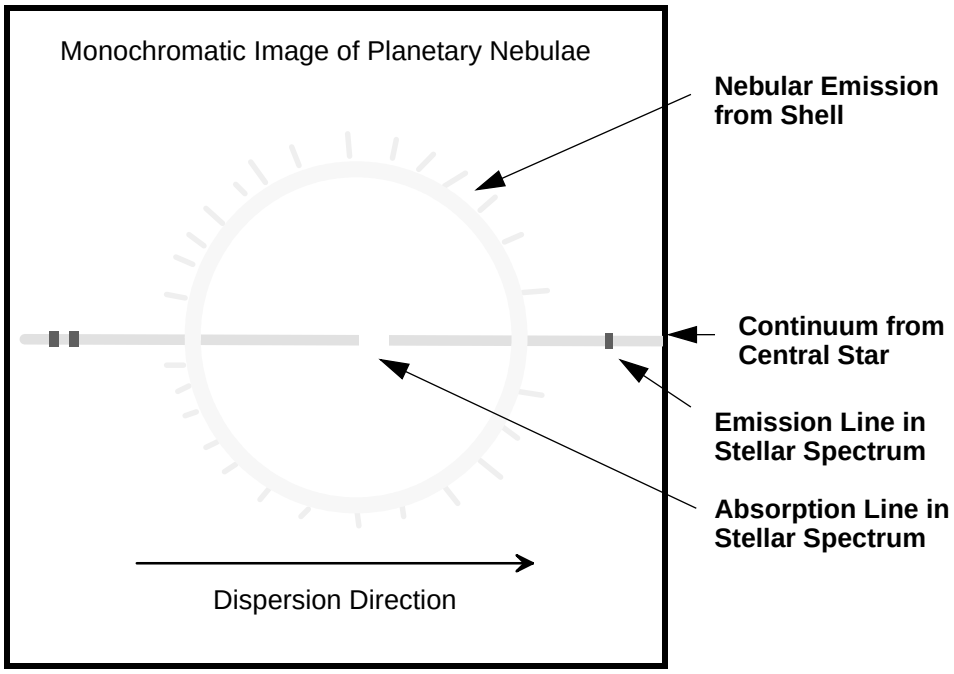

When used slitless, the image you obtain will be the sum of a series of monochromatic images of the field of view at a single wavelength where prior to summing the monochromatic images are shifted relative to one another by the resolution (Å/pixel) of the grating, and where the range of wavelengths covered in the series of monochromatic images is dictated by the spectral range of the grating.

The result is that there is *not* a one-to-one mapping of pixel location to wavelength in your image or of pixel location to spatial location on the sky. Depending on the structure of your source and the grating you use, it may be easy to deconvolve the spatial and spectral information, or it may be very difficult.

Slitless spectroscopy can be employed either for prime or parallel STIS observing. If you are designing a slitless spectroscopic observation there are a few important points to keep in mind:

- The more complex the emission line, velocity, and spatial structure of your target field the more difficult it will be to deconvolve the spatial and spectral information. It is important to match the grating you choose to the structure of your source. Gratings which produce images of multiple, kinematically resolved emission lines will be the most challenging to deconvolve. At the other extreme, a grating which covers only a single strong emission line at a resolution where the lines are kinematically unresolved will produce a clean image of the source in the single emission line (see Figure 12.1, above). You may also wish to specify the orient for slitless spectroscopic observations to assure that the most complex source structure is oriented perpendicular to the dispersion axis (see “Fixing Orientation on the Sky” on page 157).

- Since each point in the sky emits geocoronal light, the background due to the geocoronal emission lines (Lyman α λ1216, OI λ1304 and occasionally on the day side OI λ1356 and OII λ2470; see “Geocoronal Emission and Shadow” on page 75) will be observed at all pixels in the image when a slitless spectrum is obtained which covers these wavelengths. This background must be taken into account in your signal to noise calculations (note that when a slitted spectroscopic exposure is obtained, these sky emission lines are localized in the resultant image to the pixels at the corresponding wavelengths). For this reason, you may wish to consider using one of the two longpass ultraviolet blocking filters (see “Longpass Filtered MAMA Imaging - F25SRF2 and F25QTZ” on page 59) instead of a clear aperture when performing ultraviolet slitless spectroscopy.
- Slitless spectroscopic data will not be fully calibrated by the STScI STIS pipeline. Slitless spectroscopic data will be passed through the first phase of calibration and a pre-flat fielded flat fielded image will be produced, however, the pipeline will not attempt to spectroscopically calibrate the data; this must be interactively done by the observer since, as described above, ambiguous overlap of spatial and spectral information will occur.
- An automatic wavecal (see “Wavecals” on page 151) will be taken for slitless spectroscopic observations using a narrow long slit, to allow post-observation determination of the wavelength zeropoints.
- Observers may want to obtain an *image* of the field they are taking a slitless spectrum of, to allow them to post-facto determine the centering of the objects in their data. Because the gratings and the mirrors used for imaging are both in the Mode Select Mechanism, zero point shifts will occur between the slitless spectrum and image data (see “Slit and Grating Wheels” on page 23). These can be taken out by taking a wavecal image of a short slit with the mirror in place. For Phase I planning purposes, GOs wishing to take such a ‘target finding image’ should allot the additional time for the image plus an additional 5 minutes overhead for this extra zero-point wavecal image. The Phase II proposal instructions will contain information about how to assure the proper calibration is taken in these cases.

Long Slit Echelle Spectroscopy

The STIS echelle gratings (see “Echelle Gratings” on page 43) were designed to maximize the spectral range covered in a single echellogram. The orders are therefore closely spaced and to avoid overlap between orders, short echelle slits must be used. Indeed, we expect the vast majority of STIS echelle observations to be of point sources and to use these customized echelle slits (see “Slits for Echelle Spectroscopy” on page 44). Nevertheless, at the price of confusion due to order overlap, the echelle gratings can be used with a long slit to obtain high resolution spectroscopy of extended objects or can be used slitless with a full clear, filtered, or ND aperture. An example of a science application that would benefit from long

slit echelle spectroscopy might be observations designed to map the kinematics of planetary nebulae and stellar outflows around young stars.

The `6X0.2` slit (6 arcseconds in the spatial direction and 0.2 arcseconds wide in the dispersion direction) is supported for use with all four of the echelle gratings. However, because there will be ambiguous overlap of wavelengths in the resulting echellogram, the STIS STScI pipeline will not calibrate echelle data that uses the long echelle slit. The pipeline will produce an uncalibrated FITS image and the user will be responsible for calibrating the data, since due to the ambiguous mapping of wavelength to pixel, the reduction of long slit echelle data is an inherently source dependent and interactive process.

Figure 12.2: Echelle Long Slit Spectrum of Extended Emission Line Source Filling the Long Slit. Only part of the image is shown.

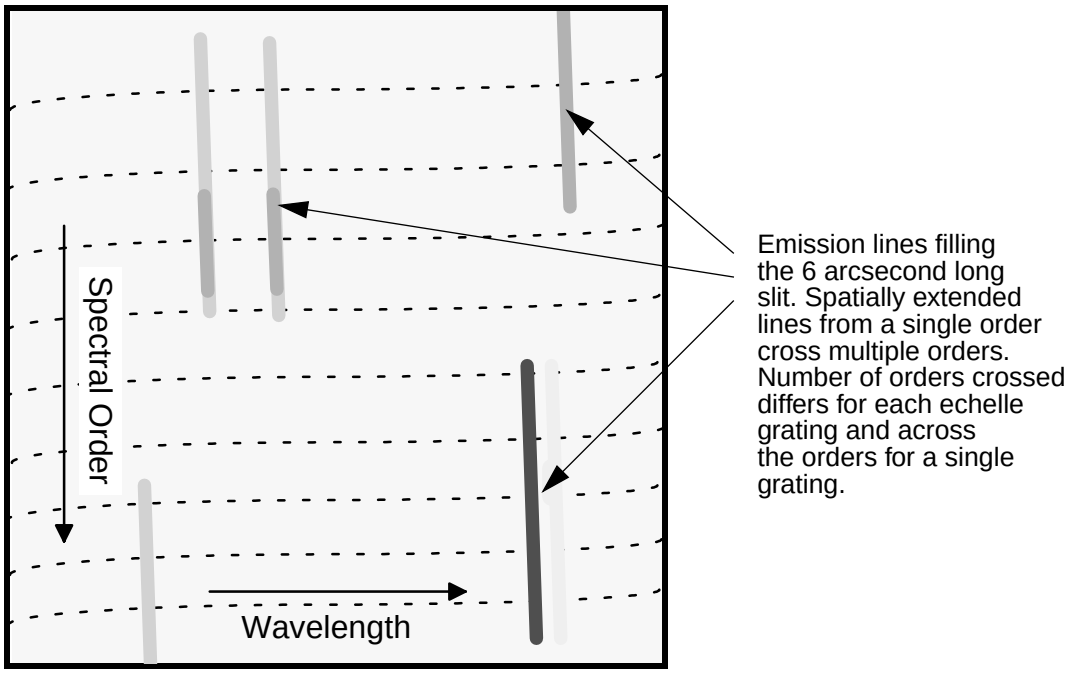

Time Resolved Observations

There are two ways to obtain time resolved spectroscopic and imaging observations with STIS:

- Use the MAMA `TIMETAG` operating mode (described in “MAMA TIME-TAG Mode” on page 146) in the ultraviolet.
- Take a series of multiple, short, identical `REPEATOBS` (described in “REPEATOBS” on page 153) observations of your target in `ACCUM` operating mode with either the CCD or the MAMAs.

Both the data products received (an event stream in the case of TIMETAG and a series of individual images from each ACCUM mode exposure in REPEATOBS) and the basic parameters of the time-resolved observations (e.g., sample time, interval between samples, total number of samples or equivalently duration) differ dramatically in these modes. In Table 12.1 below we summarize and contrast the ranges of parameter space covered by the different methods of obtaining time resolved observations.

The information presented in Table 12.1 can be qualitatively summarized into the following set of guidelines for performing time resolved observations with STIS:

- If you wish to observe variability on second or less timescales, observe in the ultraviolet using TIMETAG mode.
- In the optical, variability can be observed on tens of seconds timescales using the REPEATOBS mode with the CCD.
- In the ultraviolet variability on the several minute or more timescale can be observed using the REPEATOBS mode with the MAMAs.
- Subarrays can be used in both REPEATOBS and TIMETAG mode to limit the data volume and so extend the total duration of continuous monitoring.

Table 12.1: Summary of Time Resolving Imaging and Spectroscopy

Observation Type	Detector	Spectral Range (Å)	Minimum Sample Time (τ)	Interval Between Samples ($\Delta\tau$)	Total Duration of Uninterrupted Time Series[a]
repeat ACCUM	CCD	2500-11000	0.1 secs	37 secs - full frame 11secs - 1062 x 16 subarray	for τ>3min, no limit for τ<3 min: dur=(τ+$\Delta\tau$)∗ 7, full frame dur=(τ+$\Delta\tau$)∗ 512, 1062 x 16 subarray
repeat ACCUM	MAMA's	1150-3100	0.1 secs	60 secs	for τ>3min, no limit for τ<3 min: dur=(τ+$\Delta\tau$)∗ 4, full frame dur=(τ+$\Delta\tau$)∗ 127, 1024 x 16 subarray
TIMETAG	MAMA's	1150-3100	125 μsecs	0 secs	6.0×10^7/R seconds[a] where R is rate in counts/sec, and R<21,000 counts/sec

a. For count rates within subarray between 21,000 and 30,000 counts/sec, only short (~2 minutes) durations are possible. Beyond 30,000 count/sec TIMETAG mode becomes uncorrectably non-linear in its counting.

Observing Too-Bright Objects with STIS

As described in "MAMA Bright Object Limits" on page 97, the STIS MAMA detectors can be damaged at high local and global count rates. The MAMA detectors also suffer uncorrectable non-linearity at similar count rates (see "MAMA Non-Linearity" on page 96). There are therefore configuration specific

brightness limits for all observations that use the MAMA detectors; sources brighter than the limits *cannot be observed* in that configuration.

The STIS CCDs are not subject to the same bright object constraints, as the CCD cannot be damaged by observations of bright sources. At high *accumulated* count/pixel levels, however, the CCD saturates and counting becomes non-linear. As described previously (see “CCD Saturation: the CCD Full Well” on page 90), CCD saturation can be avoided by keeping exposure times short when observing bright targets. The minimum exposure time for CCD observations (0.1 sec) dictates the maximum source brightness which can be observed without saturating.

The only way to use STIS to observe a source that is too bright is to use a configuration which reduces the flux from these targets, bringing them into the observable regime. The options available to achieve this are:

- Use a smaller slit to reduce the transmitted light for spectroscopic observations (see “Slits for First Order Spectroscopy” on page 242, and “ Slits for Echelle Spectroscopy” on page 248—you will find there the percent flux transmitted through each slit as a function of wavelength).
- Select a more appropriate grating or filter configuration. This may be a configuration with higher resolving power if it is the local limit which is being violated, or a configuration that covers a smaller free spectral range if the global limit is being violated. In more extreme cases, you may be forced to choose a grating (filter) that covers an entirely different region of the electromagnetic spectrum. Note that if you are observing in first order in the near-UV, you can consider using the CCD near-UV first order spectroscopic modes G230LB and G230MB (see page “Cross-Over Regions” on page 41).
- Use a full neutral density filtered aperture. The neutral density filters are described in section “Neutral Density Filters” on page 63; they produce attenuations ranging from 10^{-1} to 10^{-6}. Note however, that the ND filters are located in the slit wheel. Thus, all supported ND filtered exposures will be slitless, i.e., you cannot use a slit and an ND filter together. Similarly you cannot use a ND filter and a filter in imaging mode. Also note that some ND filters come in quadrants, all of which are simultaneously imaged.
- Use one of the available-but-unsupported echelle or long calibration slits which contain neutral density filters. The relevant slits are 31X0.05NDA (with ND=2.9), 31X0.05NDB (with ND=2.5) and the 0.2X0.05ND (with ND=0.6) and 0.3X0.05ND (with ND=1.2), where if ND=x, the attenuation = 10^{-x}. (see also “Support of STIS Capabilities for Cycle 7,” on page 12 and the CP. These ND values for the slits are subject to change, but should be known by the time of the August 1996 information update (see “Updates to Instrument Performance for Cycle 7” on page 12).

High Signal-to-Noise Ratio Observations

The maximum signal-to-noise ratio of STIS observations for bright sources will ultimately be limited by the signal-to-noise ratio and fidelity of the flat fields. CCD observations of bright sources will have inherently higher signal-to-noise than those using the MAMA's, both because the signal-to-noise ratio of the MAMA flat fields will be limited by the long integration times needed to acquire them (see "Summary of Expected Accuracies" on page 319) and because the MAMA flats are expected to be structured and may also be time variant (see "MAMA Signal-to-Noise Ratio Limitations" on page 96). High signal-to-noise ratios should routinely be achievable for observations of bright sources using the CCD (though see the caveats on long wavelength spectroscopy in the red due to fringing in "CCD Spectral Response" on page 88). Routine per-pixel signal-to-noise ratios of ~30 per 2x2 pixel resolution element are expected for Cycle 7 observations of bright sources with the MAMAs.

In first order modes, improved signal-to-noise ratios can be achieved by stepping the target along the slit, taking separate exposures at each location which are subsequently shifted and added in post-observation data processing (`PATTERN=ALONG-SLIT`, see "Patterns," on page 154). This stepping, or dithering, effectively smooths the detector response over the number of steps, achieving a reduction of pixel-to-pixel non-uniformity by the square root of the number of steps, assuming the pixel-to-pixel deviations are uncorrelated on the scale of the steps. In imaging modes, the same dithering can be done in two-dimensions, i.e., the steps need not be along a straight line. For echelle modes, stepping is only possible using the long echelle slit (6x0.2 arcseconds) (though note that in the high dispersion echelle modes the doppler shifting due to the spacecraft will effectively cause the counts from any output pixel to have been sampled at many independent detector pixels).

In a slit-less or wide-slit mode, stepping along the dispersion would allow independent solution for spectrum and flat field, but at a cost of lower spectral resolution.

Among the available-but-unsupported contingent of slits are a set of 'fpsplit' slits designed to allow the wavelength projection of the spectrum on the detector to be shifted, so that the flat field fixed pattern noise and the spectral flux distribution of the target can be simultaneously computed using techniques that have been successfully applied to data taken with the GHRS. The performance of these slits, their ability to allow a shift in wavelength only [as required] and techniques for using them, have yet to be evaluated.

Techniques for maximizing signal-to-noise ratios are expected to be developed during the course of Cycle 7.

Improving the Sampling of the Line Spread Function

In many configurations the current *predicted* spectral line FWHM is less than two detector pixels (see for instance Table 13.17 on page 243, Table 13.18 on page 243 and Table 13.22 on page 250). The realized in-flight line spread functions will depend on the thermal properties of STIS, which have yet to be evaluated, and the final in-orbit alignment. If we find that the realized LSFs are undersampled, we will initiate a special project in Cycle 7 to determine the optimal observing strategy for those programs which require critical sampling. Possible solutions include:

- Stepping of the target in the dispersion direction in a wide slit or slitless aperture to subsample the line spread function by displacing the spectrum. This technique can also be used to increase the signal-to-noise (see above). Note that in employing this strategy one will have to trade off the benefits of the sampling with the negative impact of increased wings in the line spread function when using a wide slit, particularly for MAMA observations.
- For MAMA observations, use of *highres* sampling (currently an available mode) may provide ~15-30% better sampling, however, flat field variability and rate dependence may make it difficult to realize the benefit in resolution (see “Highres” on page 145).

Considerations for Observing Planetary Targets

STIS’s FUV solar blind and NUV solar insensitive MAMA detectors make it particularly well suited to slitted spectroscopic and imaging planetary observations. In addition, the 51X2 long slit (2 arcseconds wide in dispersion) is particularly well suited to the “slitless” ultra-violet spectroscopic study of small planetary bodies (using a slit limits the background continuum contribution, see “Sky Background” on page 72).

Target acquisitions for planetary observations can be done in a number of ways. If the ~1 arcsecond accuracy of the initial guide star pointing is sufficient, blind pointing (no acquisition sequence) should be used. If higher accuracy is required, point or diffuse acquisitions can be performed on the target or a nearby satellite. Offsets to the main target (planet) may then be made by following the acquisition sequence with science observations on the planetary target. The software will automatically calculate the necessary slew.

If you are acquiring an extended object, then you should be aware of the restriction on the V surface brightness (< 5.4 Mag/arcsec^2) and extent of the diffuse region (< 5 arcseconds) which can be acquired. See “STIS On-board Target Acquisitions” on page 105 for full details. Interactive acquisitions can be used if no other option is possible, but should be requested in your Phase I proposal as a special requirement.

Planetary observers may also wish to use the PERP-TO-SLIT pattern sequence (see “Patterns” on page 154) to map out the surface of a planet by taking a series of long slit observations, each one stepped by the slit width perpendicular to the slit’s long axis, relative to the last.

Planetary observers requiring specific long slit orientations will want to be aware of the tight scheduling constraints for specific orients for observations of targets in the ecliptic plane (see discussion of “Orient from Nominal” in the Phase II instructions). Among the available-but-unsupported slits are two long slits, the so called *planetary slits*, oriented at plus and minus 45 degrees to the dispersion axis (and the normal long slit orientation). These allow the acquisition of long slit data with the slit parallel or perpendicular to the object-sun direction (at nominal roll). Reduction of data taken with the planetary long slits will be quite complicated, however, due to the large incidence offset angle corrections which need to be applied during calibration, and which affect both the dispersion solutions and the flat fields. The planetary slits are not in the supported contingent, and data taken with them will not be calibrated by the STScI pipeline (see “Support of STIS Capabilities for Cycle 7” on page 12).

Parallel Observing with STIS

As described in Chapter 1, the second servicing mission will install solid state data recorders on HST. The volume capacity of these recorders is roughly ten times that of the mechanical tape recorders in use for Cycles 1 through 6. Coupled with changes to the ground system and STIS and NICMOS flight software designed to fully exploit this capability, this translates into a greatly increased capability for parallel observing in Cycle 7. In principle, STIS, NICMOS, WFPC2, and FOC can all be used to observe simultaneously. Figure 3.2 on page 26 shows the HST field of view following the second servicing mission; the three infrared cameras of NICMOS (which themselves can be operated in parallel), STIS, WFPC2, and FOC are all shown, with their fields of view drawn to scale, in their relative positions in the focal plane. The STIS MAMAs are shown (as the small square) inside the CCD (large STIS square); the three STIS cameras share a common field of view, and only one can be used at a time.

The policy for proposing for parallel observations and technical advice on parallel observing are provided in the Call for Proposals/Phase I Proposal Instructions. Here we provide some guidance for designing parallel observing programs, either for your STIS parallel science, or using STIS in parallel to other instruments. We remind you that there are two types of parallel observations:

- Coordinated parallels, in which you explicitly link the taking of exposures in parallel to your own prime science exposures.

- Pure parallels, in which you propose for parallel exposures to be taken in parallel to other observers' prime exposures. You specify the instrumental observing configuration for the parallel instrument and the set of observational constraints which need to be satisfied for your pure parallel exposures to be taken.

Both coordinated and pure parallels must be explicitly proposed in Phase I. Implementing parallels requires significant resources; only those pre-approved by the TAC process will be implemented. When a parallel is taken, the prime exposures are first laid into orbits, and then, thereafter, the parallel exposures are fit to accommodate the primes. If you are considering coordinated parallels, you may wish to consider constraining the orientation of HST, to place a view of interest in the parallel instrument's field of view. Orient constraints do affect observation scheduling, however, and should not be entered lightly.

Using STIS in Parallel with Other Instruments

Observations for which STIS is the parallel instrument are likely to be most useful when the full STIS field of view is used. If you wish to use a small slit, the STIS should be used prime, and the other imaging instruments used in parallel with it.

During Cycle 7, the MAMA detectors cannot be used for pure parallel observing and the MAMA detectors can be used in coordinated parallel observing only if an explicit `ORIENT` is specified and precise RA and Dec coordinates for the parallel field are given (see "Policy for Prime and Parallel Observing with the STIS MAMA Detectors" on page 14).

Four types of STIS exposures which have scientific utility with STIS as the parallel instrument are:

- Optical imaging (but remember that pure parallels with the `50CCD` clear aperture are not allowed, see "Policy for CCD Clear Pure Parallels" on page 15).
- Optical slitless spectroscopy.
- Ultraviolet slitless spectroscopy (available only for coordinated parallels with exact orient specification).
- Prism and ultraviolet imaging observations (available only for coordinated parallels with exact orient specification).

Coronagraphic Imaging and Spectroscopy

STIS offers the capability to perform spectroscopic observations with occulting bars located in the long slits, and imaging observations with occulting bars in the coronagraphic mask `50CORON`.

Spectroscopy

In Cycle 7, the 0.5 arcsecond bar in the `52X0.2` longslit will be available for occulted observations. This occulting bar is well suited to scientific problems conducting spectroscopy of faint extended material around a bright central source. Typical examples of such a program include QSO host galaxies, dynamics of jets in young stellar objects, and spectroscopy of resolved binaries.

Spectroscopic observations with the 0.4” occulting bar are limited to first order spectroscopic modes. Target acquisition for this special aperture requires a peakdown under the occulting bar, preceded by an optional peakup in the clear part of the slit, if the observer wishes to center the bright central source first. (See Chapter 8 for an overview of STIS target acquisition.)

To simplify the use of the occulting bar, an aperture has been assigned for the occulting bar itself, and an aperture for the reference position located just off the bar. The reference aperture is used if the observer wishes to center the source in the slit, prior to peaking down under the occulting bar. It should be noted that when the occulting bar is chosen the slit wheel places the occulting bar at the center of the field if view, so the full 52” width of the longslit is not available.

In the table below we show the complete set of aperture names and their application for the 0.5 arcsecond fiducial on the `52X0.2` slit.

Table 12.2: Aperture Names and Applications on 52x0.2 Slit

Aperture Name	Description	Destination	Application
`52X0.2`	Slit (width=0.2”, length=52”)	Target centered in slit	Long slit spectroscopy
`52X0.2F1-R`	Slit (width=0.2”, length=52”). Fiducial=0.5” Reference point off-fiducial	Target centered in slit at reference position, offset from fiducial bar.	Locates target at reference position ready for peakup in slit.
`52X0.2F1`	Slit (width=0.2”, length=52”). Fiducial=0.5”	Target centered in slit and located under fiducial bar	Locates target under bar ready for peakdown

Peakdowns with the Spectroscopic Occulting Bar

In order to facilitate acquisitions and peakdowns with the spectroscopic slit, the aperture selected on the ACQ/PEAK line dictates whether a peakup or peakdown is done using the following rules:

- The bar (or fiducial) is a unique aperture and when selected is placed in the field of view so that the bar reference position lies at the center of the field.
- The bar/fiducial has a reference position off of the bar. To perform a peakup in the dispersion direction (across the slit) prior to placing the target behind the bar, specify an ACQ/PEAK line with the reference position (52X0.2F1-R) as the slit.
- To perform a peakdown under the bar, specify the bar (52X0.2F1) as the aperture for an ACQ/PEAK exposure. A peakdown (as opposed to a peakup) will be automatically performed.
- A table of default peakdown parameters has been defined (Table 12.3).

Table 12.3: Default Peakdown Parameters for the Supported Occulting Bar

Aperture	Bar width (arcsec)	Scan type	Spacing (arcsec)	Num-steps
52X0.2F1	0.5	PEAKDOWN	0.30	5

Coronagraphic Imaging

STIS has one coronagraphic mask aperture for direct imaging. The aperture contains one occulting bar, and two intersecting wedges (see Figure 12.3 on page 172). The aperture cannot be combined with a filter and so, when used with the CCD, yields a bandpass of ~2500–11000 Å. The mask is not available for use with the MAMA detectors due to concerns about bright object protection of the MAMAs. In combination with the option of a coronagraphic mask, there is a limited amount of apodization via a lyot stop which masks the outer perimeter of the re-imaged exit pupil. Consequently, diffraction from the secondary mirror assembly and the telescope spider is not apodised. The STIS coronagraphic imaging facility is well suited to imaging problems involving faint material surrounding a relatively bright source. Typical examples include, circumstellar disks, such as β Pictoris, and the host galaxies of bright QSOs.

Figure 12.3: Design of the STIS coronagraphic Mask

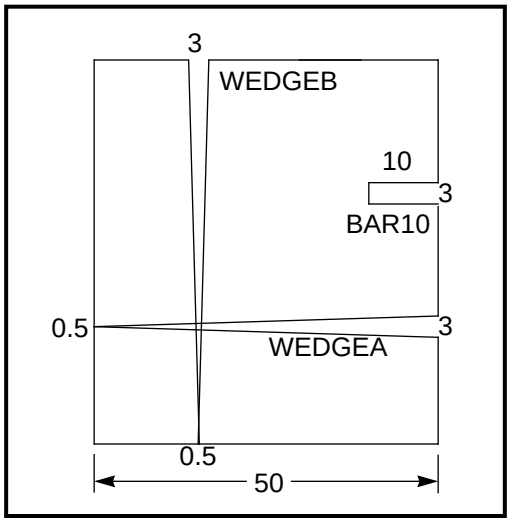

A series of apertures have been defined for the coronagraphic mask so that targets can be placed on the 0.5” wide bar, the 3” wide bar, and 4 locations on each of the two wedges. These apertures are summarized below.

Table 12.4: Apertures for Coronagraphic Mask

Proposal Instructions Aperture Name	Description
50CORON	coronagraphic mask - clear aperture in center of the field of view
BAR10	coronagraphic bar of width 1.0”
WEDGEA2.8	coronagraphic Wedge A (vertical in axis1) Posn. 1: bar width = 2.75”
WEDGEA2.5	coronagraphic Wedge A (vertical in axis1) Posn. 2: bar width = 2.5”
WEDGEA2.0	coronagraphic Wedge A (vertical in axis1) Posn. 3: bar width = - 2.0”
WEDGEA1.8	coronagraphic Wedge A (vertical in axis1) Posn. 4: bar width = 1.75”
WEDGEA1.5	coronagraphic Wedge A (vertical in axis1) Posn. 5: bar width = 1.5”
WEDGEB2.8	coronagraphic Wedge B (vertical in axis2) Posn. 1: bar width = 2.75”
WEDGEB2.5	coronagraphic Wedge B (vertical in axis2) Posn. 2: bar width = 2.5”
WEDGEB2.0	coronagraphic Wedge B (vertical in axis2) Posn. 3: bar width = 2.0”
WEDGEB1.8	coronagraphic Wedge B (vertical in axis2) Posn. 4: bar width = 1.75”
WEDGEB1.5	coronagraphic Wedge B (vertical in axis2) Posn. 4: bar width = 1.5”

In planning an observing program with the `50CORON` aperture, observers should carefully consider the required orientation of the target. The telescope’s V2 and V3 axes are at 45^{o} to the STIS `AXIS1/AXIS2` coordinate system (see Figure 11.1 on page 142) and so diffraction spikes further reduce the unocculted field of view.

If an observer wishes to image the full 360˚ region around a target, two observations, one each on the vertical and horizontal wedges are required. By combining two such images, the full 360˚ coverage is obtained, with the exception of the regions occupied by the diffraction spikes. Two options are available to address this problem, either roll the telescope by ~15^{o} on the second exposure, or schedule a second visit when the nominal telescope roll has changed by ~45^{o}.

Finally we note, that because the dark current can be elevated by exposure to a bright source of ultraviolet photons (see “UV Light and the STIS CCD” on page 91), if you are performing coronagraphic imaging with the CCD of a bright, V<10 source, you must add an extra orbit per visit to your proposed science in Phase I to allow for a ‘clean up’ period of ~ 1 hour during which the dark current of the CCD subsides, prior to its use for other science.

Coronagraphic Target Peakdowns

Peakdowns for Imaging Coronagraphy

We have defined a special coronagraphic acquisition technique for acquiring stars under the coronagraphic bars on the `50CORON` aperture. The method involves performing a bright target acquisition using a filtered aperture, then a peakup in a small, 0.2x0.2” slit., followed by a slew to a pre-defined aperture on

the coronagraphic mask. The use of the 0.2x0.2” slit is transparent to the user, who merely specifies the coronagraphic mask `50CORON` on the exposure logsheet.

CHAPTER 13
Spectroscopic Reference Material

In This Chapter...

In this Chapter, we provide spectroscopic reference material, in support of the information presented in Chapter 4.

Introduction

In this section, we provide reference material in support of the material presented in Chapter 4 to help you select your grating configuration and determine your observing plan (e.g., total required exposure time, and number of exposures). This chapter is primarily organized by *grating*. For each grating mode the following are provided:

- A brief description of the grating mode's specifications.
- The central wavelength settings and range of wavelength covered at each setting, for scanned gratings.
- Plots and tables of sensitivities as a function of wavelength.
- Plots of time as a function of source flux to achieve a signal-to-noise of 10.
- Plots of time versus source flux to saturate (and exit the read noise limited regime for CCD observations),

The optical properties of the grating modes and their accompanying slits are described in:

- "First Order Slits, LSFs, Scales and Encircled Energies" on page 242 and
- "Echelle Slits, LSFs, Scales, and Encircled Energies" on page 248.

In addition,

- "MAMA Spectroscopic Bright Object Limits" on page 254 provides a summary of the screening brightness limits for the MAMA spectroscopic modes.

The next section, "Using the Information in this Chapter" on page 176, explains the plots and tables found in the grating sections in this chapter.

Using the Information in this Chapter

Sensitivity Units and Conversions

This chapter contains plots and tables of sensitivities for each grating mode. "Determining Count Rates from Sensitivities" on page 66 in the Exposure Time Calculation chapter explains how to use these sensitivities to calculate expected counts rates from your source.

The total system[1] *spectroscopic point source sensitivity, $Sens^{p}_{\lambda}$*, has the unit:

counts sec^{-1} pix_{λ}^{-1} per incident erg cm^{-2} sec^{-1} $Å^{-1}$

1. STIS plus HST Optical Telescope Assembly (OTA).

Where:

- pix_λ = a pixel in the dispersion direction.
- counts refer to the total counts from the point source integrated over the PSF in the direction perpendicular to the dispersion (along the slit).

Note that the spectroscopic point source sensitivity does not include slit losses.

The *spectroscopic diffuse source sensitivity,* $Sens^d_\lambda$, has the unit:

counts sec^{-1} pix_λ^{-1} pix_s^{-1} per incident dimensional erg cm^{-2} sec^{-1} $Å^{-1}$ $arcsec^{-2}$

Where:

- pix_λ= a pixel in the dispersion direction.
- pix_s= a pixel in the spatial direction.

$Sens^p_\lambda$ and $Sens^d_\lambda$ are related through the relation:

$$Sens^d_\lambda \cong (Sens^P_\lambda \times m_s \times W)$$

Where:

- m_s is the plate-scale in arcsec per pixel in the direction perpendicular to the dispersion.
- W is the slit width in arcseconds.

Here, we have assumed that the diffuse source has a uniform brightness over the area of interest.

Signal-To-Noise

For each grating mode, plots of flux versus exposure time to achieve a signal-to-noise ratio of 10 are presented in the individual grating sections for both point source and diffuse sources. The plots included are:

1. *Signal-To-Noise per spectral resolution element versus Exposure Time for stars of known spectral type and V magnitude observed through the 0.2 arc-second wide slit.* The plots show V magnitude versus exposure time with a series of curves superposed showing the time to achieve a signal-to-noise of 10 per spectral resolution element at three distinct wavelengths (as indicated on the plots), for several different spectral types with unreddened main sequence stars with the flux distribution shown in Figure 1.1 on page 5. In making these plots we have assumed the appropriate 0.2 arcsecond wide slit was used, and have integrated over the PSF in the spatial direction to contain 80% of the light and the LSF in the cross dispersion direction. Plot (a) is for an O star, (b) is for a A star, (c) is for a G star, and (d) is for a M star. You can use these plots directly. If you know your source

V magnitude, simply look up (or interpolate) the exposure time to achieve a signal-to-noise = 10 per spectral resolution element at the wavelength of interest.

2. *Signal-to-Noise per spectral resolution element versus Exposure Time for Point and Diffuse Sources of known brightness, in CGS units, observed through the 0.2 arcsecond wide slit.* Plot (a) is for point sources and plot (b) is for diffuse sources. In making these plots we have integrated over the LSF in the dispersion direction for both the point and diffuse (assuming emission line fills the slit) source calculations. For the point source, we have also integrated over the PSF in the cross dispersion direction. For the diffuse sources we show the signal-to-noise *per two spatial pixels*. The series of curves on these plots show the time to achieve a signal-to-noise of 10 at three distinct wavelengths (as indicated). If you know your source flux or brightness, you can directly look up (or interpolate) the time to achieve a signal-to-noise of 10 from these plots.

At high flux levels, where the detector and sky background is negligible (and for the CCD at high count levels, where the read noise is not important) the exposure time to achieve a given signal-to-noise scales directly as signal-to-noise^2 (see also “Calculating Exposure Times for a Given Signal-to-Noise” on page 70). However, at lower flux levels, the background, dark current and read noise (the latter for the CCD only) must be taken into account when estimating the time to achieve a given signal-to-noise. The following assumptions were made in producing the signal-to-noise plots presented in the grating sections below:

- A 0.2 arcsecond wide slit was assumed for both point and diffuse sources.
- For CCD observations, in order to assure that cosmic rays could be removed from the images in post-observation data processing, all observations have been ‘taken’ using the default value of `CRSPLIT=2`, i.e., have been split into at two exposures of equal duration.
- The sky background was taken from Figure 6.1 on page 74.
- The CCD read noise and background (dark current) and the MAMA backgrounds were taken from Table 6.2 on page 72.

Saturation

Both CCD spectroscopic and MAMA spectroscopic observations are subject to saturation at high total *accumulated* counts per pixel see “CCD Saturation: the CCD Full Well” on page 90 and “MAMA Saturation—Overflowing the 16 Bit Buffer” on page 95). Plots of time to saturation as a function of source flux are presented for each grating mode in the sections below, for both point and diffuse sources, observed through the 0.2 arcsecond wide slit.

Superposed on the saturation plot, for the CCD, is a line indicating, for a given source flux, when the observation is no longer read noise dominated (taken to occur when the source plus background counts exceeds two times the square of the read noise).

Slits, Line Spread Functions, Plate Scales and Encircled Energies

See page 242 for a description of the slits, slit throughputs, line spread functions and plate scales for the First Order Grating Modes.

See page 248 for a description of the slits, slit throughputs, line spread functions and plate scales for the Echelle modes.

MAMA Bright Object Limits

See page 242 for tables of MAMA absolute and science bright object spectroscopic limits.

First Order Grating G750L

The G750L grating is used with the CCD. It has high throughput but low resolving power (~500), and is designed for efficient, full spectral coverage. The properties of the G750L grating are summarized below.

	Spectral Range		Dispersion		
Grating	Complete	Per Tilt	Å per Pixel	Tilts	Central Wavelengths
G750L	5250-11490	5030	4.92	***Prime***	7751, 8975

The grating has two prime tilt settings, one optimized for coverage of the optical, the other designed to allow measurement of the near-IR lines beyond ~10,000 Å, where the STIS CCD response, though dropping, is still significant. Figure 13.1, shows the minimum and maximum wavelengths corresponding to the two settings.

Figure 13.1: Wavelength Ranges for the G750L Grating Settings

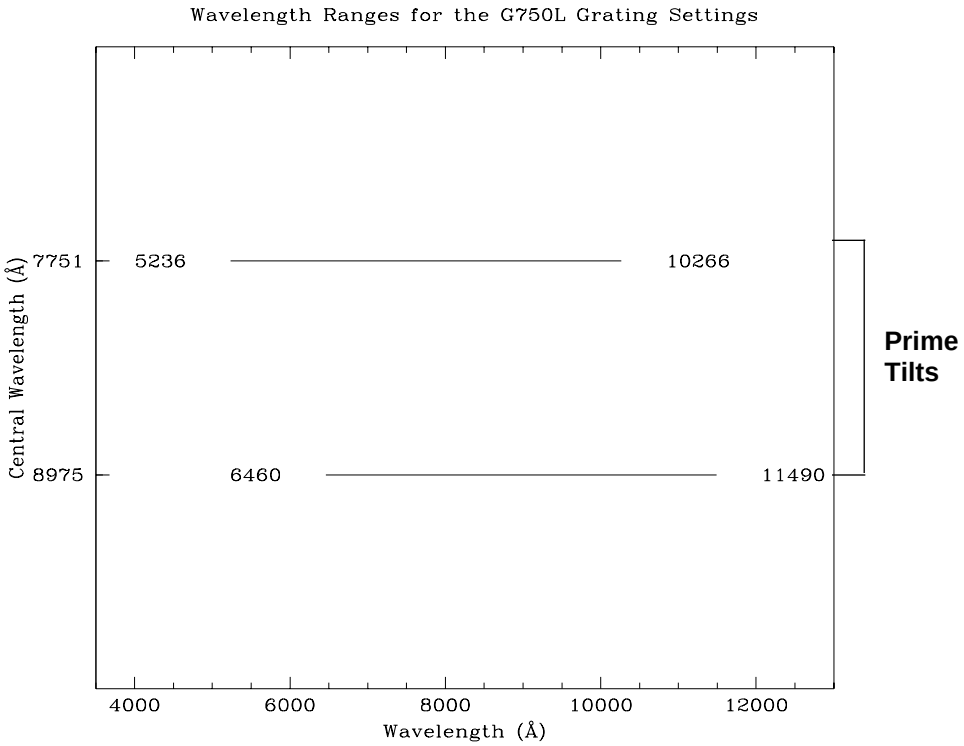

The sensitivity, signal-to-noise exposure time requirements, and saturation exposure time limits for the G750L grating are summarized below. We note that fringing in the CCD may ultimately the realizable signal-to-noise longward of 7000 Å (see also “CCD Spectral Response” on page 88)

Figure 13.2: G750L Point Source (left axis), and Diffuse Source (right axis) Sensitivities. Point source sensitivity assumes full transmission (zero slit losses). Diffuse source sensitivity assumes a 0.1” wide slit.

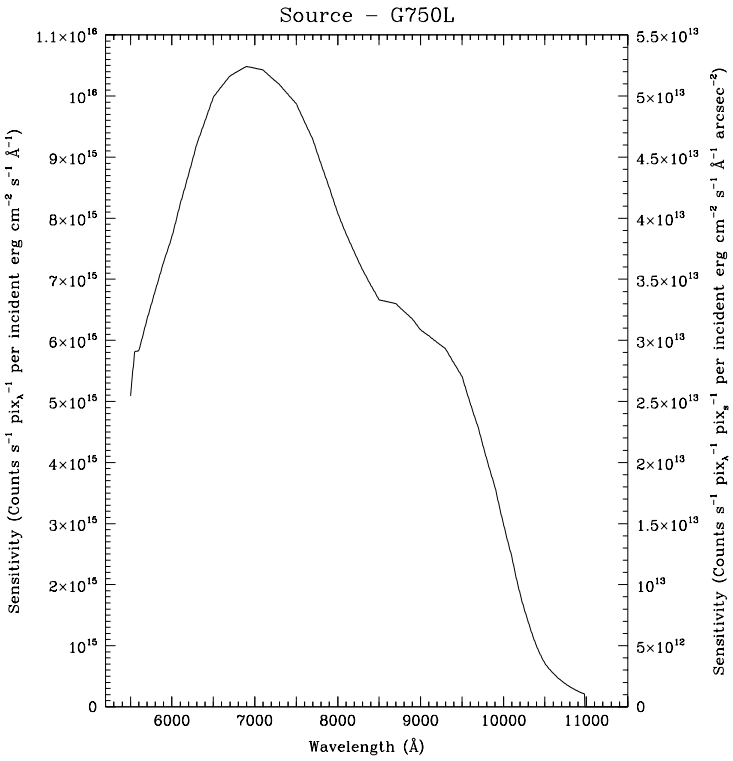

Table 13.1: G750L Point Source Sensitivities. Multiply sensitivity number by 0.05 times the slit width in arcseconds to obtain diffuse source sensitivity.

λ	**Sens.**	λ	**Sens.**	λ	**Sens.**	λ	**Sens.**
5600	5.8E15	7000	1.0E16	8400	6.9E15	9800	4.0E15
5800	6.8E15	7200	1.0E16	8600	6.6E15	10000	3.0E15
6000	7.7E15	7400	1.0E16	8800	6.5E15	10200	1.9E15
6200	8.7E15	7600	9.6E15	9000	6.2E15	10400	9.9E14
6400	9.6E15	7800	8.9E15	9200	6.0E15	10600	5.5E14
6600	1.0E16	8000	8.1E15	9400	5.6E15	10800	3.3E14
6800	1.0E16	8200	7.4E15	9600	5.0E15		

Figure 13.3: G750L Time to Achieve a Signal-to-Noise of 10 per Spectral Resolution Element for Stars of Different Spectral Types, observed through the 0.2 arcsecond wide slit.

(a) O5 star

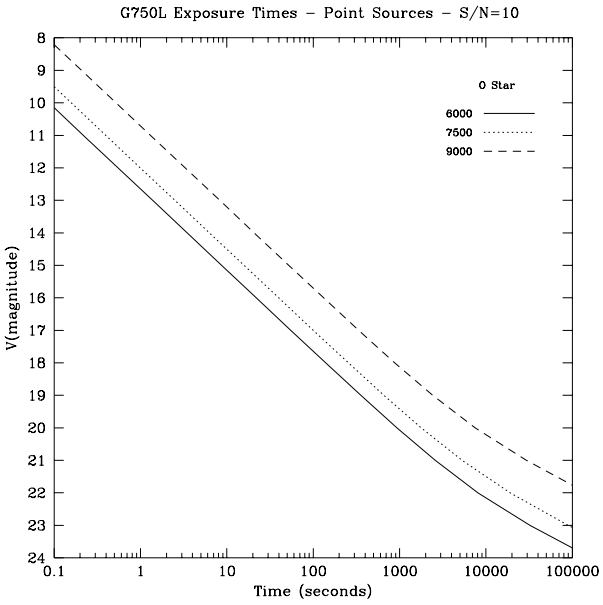

(b) AOV star

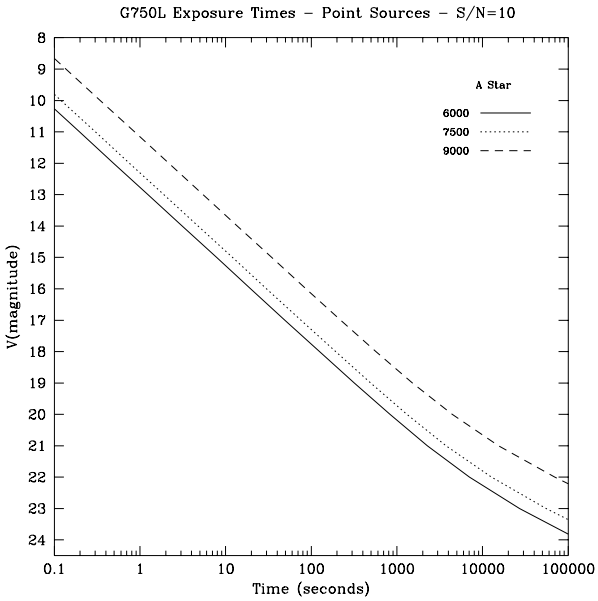

(c) G0V star

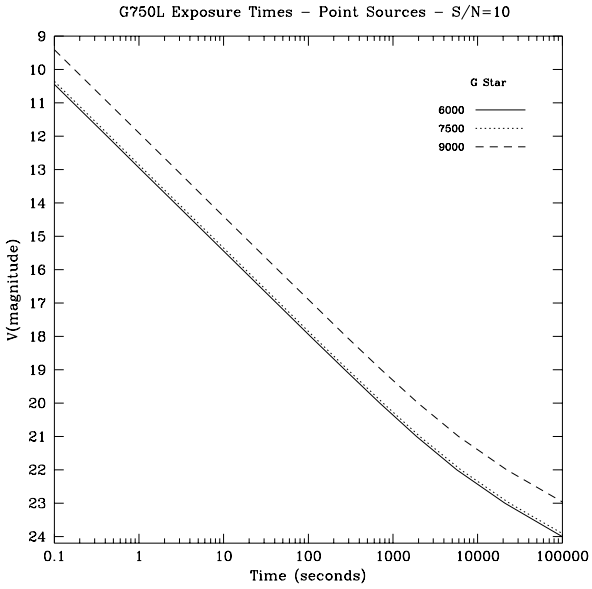

(d) M0V star

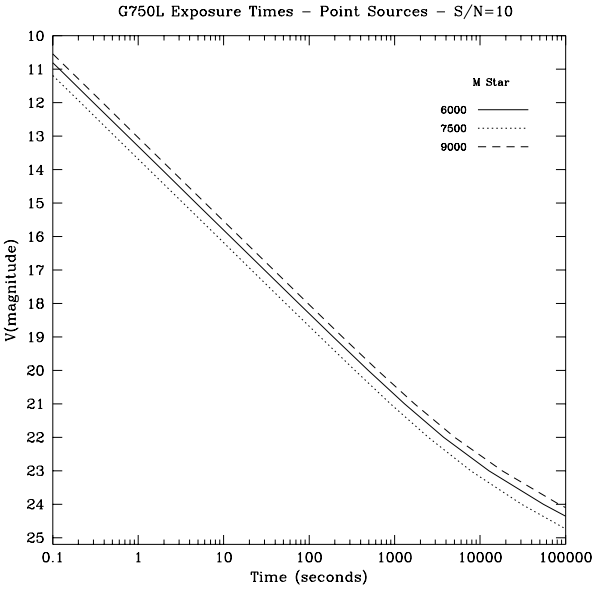

Figure 13.4: G750L Time to Achieve a Signal-to-Noise of 10 per Spectral and Spatial Resolution Element for Point and Diffuse Sources Observed with the 0.2” Wide Slit, cgs units. Point source are integrated over the PSF, Diffuse sources are per two spatial pixels.

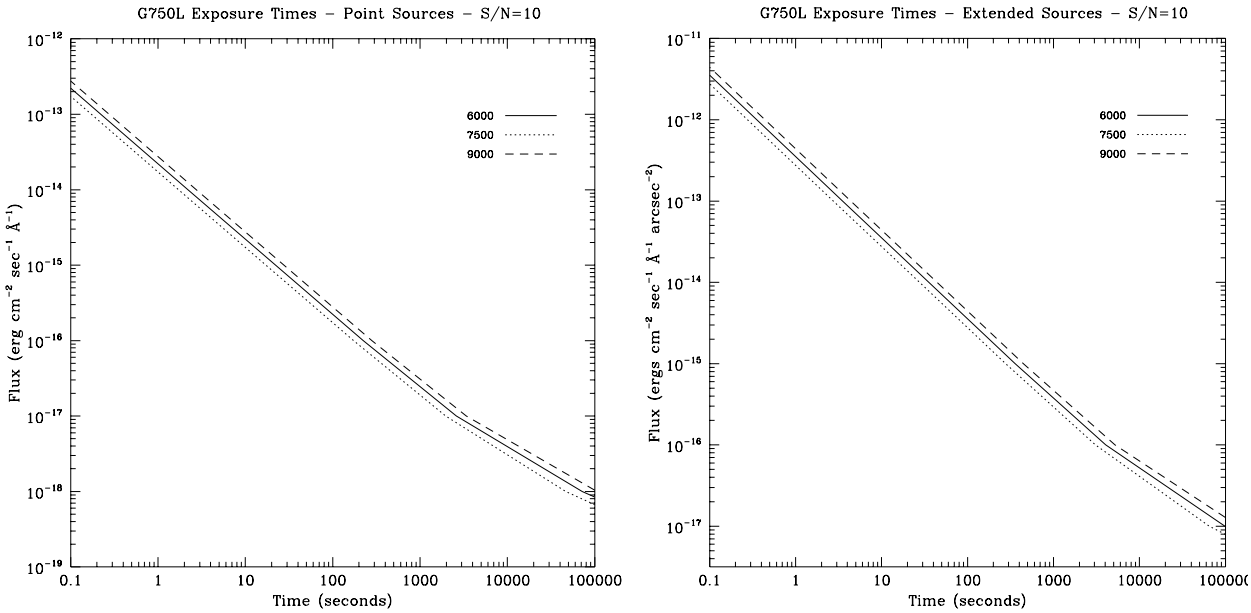

Figure 13.5: G750 Time to Saturate Peak Pixel as a Function of Source Flux, for observation taken through 0.2 arcsecond wide slit.

(a) Point Sources

(b) Diffuse Sources

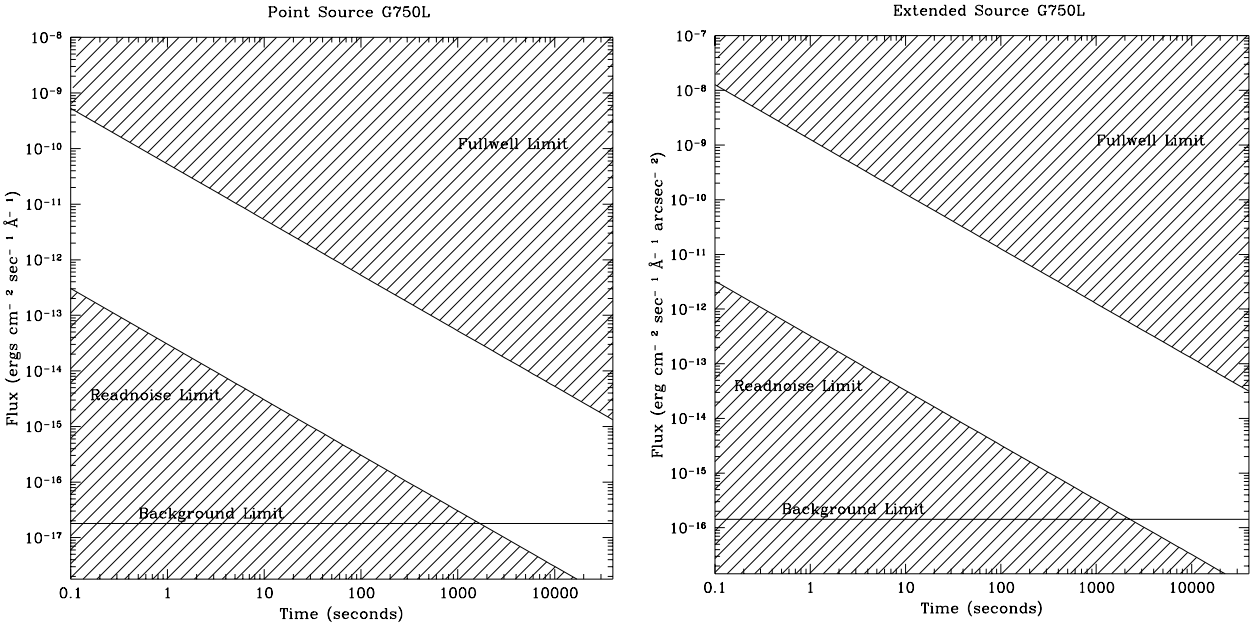

First Order Grating G750M

Like G750L, the G750M grating is used with the CCD and has a spectral range from 5500–11000 Å. However, with a resolving power R~5000 a single exposure with this grating covers only 570 Å, and the grating must be scanned, with a series of exposures taken at 11 distinct settings to cover the full range of the grating. This grating is designed for relatively high spectral resolution work centered on selected regions of the spectrum. The properties of the G750M grating are summarized below.

	Spectral Range		Dispersion		
Grating	**Complete**	**Per Tilt**	**Å per Pixel**	**Tilts**	**Central Wavelengths**
G750M	5450-11150	570	0.56	***Prime***	**5734**, **6252**, **6768**, **7283**, **7795**, **8311**, **8825**, **9336**, **9851**, **10363**, **10871**
				Secondary	6094, 6581, 8561, 9286, 9806

The minimum and maximum wavelengths covered in single exposures for each scan setting are shown graphically in Figure 13.6, below. There is a partial ghost spectrum present in the λ_c=5734 setting which is ~1.2% of, is inverted with respect to, is offset by ~ 70 pixels from, the prime spectrum, arising from back reflections between the CCD and the order sorter.

Figure 13.6: Wavelength Ranges for the G750M Grating Settings

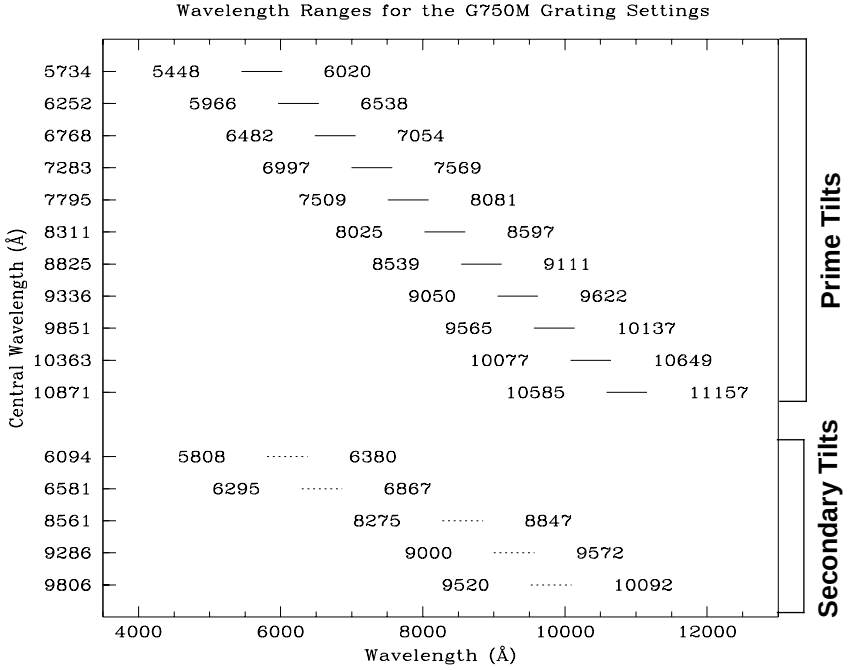

The sensitivity, signal-to-noise exposure time requirements, and saturation exposure time limits for the G750M grating are summarized below. We note that fringing in the CCD may ultimately the realizable signal-to-noise longward of 7000 Å (see also “CCD Spectral Response” on page 88).

Figure 13.7: G750M Point Source (left axis), and Diffuse Source (right axis) Sensitivities. Point source sensitivity assumes full transmission (zero slit losses). Diffuse source sensitivity assumes a 0.1” wide slit.

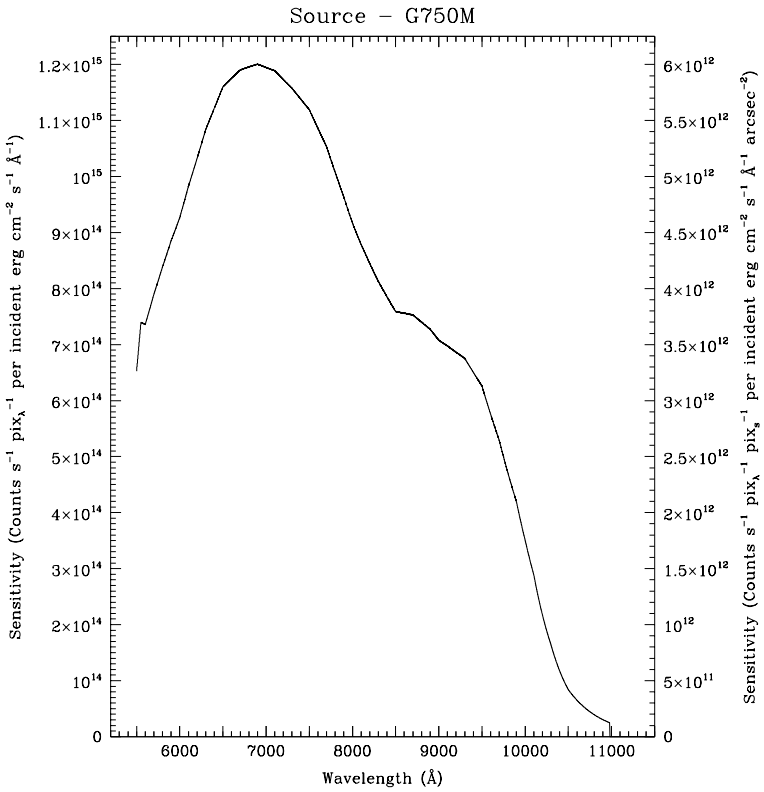

Table 13.2: G750M Point Source Sensitivities. Multiply sensitivity number by 0.05 times the slit width in arcseconds to obtain diffuse source sensitivity.

λ	Sens.	λ	Sens.	λ	Sens.	λ	Sens.
5600	7.4E14	7000	1.2E15	8400	7.9E14	9800	4.7E14
5800	8.4E14	7200	1.2E15	8600	7.6E14	10000	3.5E14
6000	9.3E14	7400	1.1E15	8800	7.4E14	10200	2.2E14
6200	1.0E15	7600	1.1E15	9000	7.1E14	10400	1.2E14
6400	1.1E15	7800	1.0E15	9200	6.9E14	10600	6.5E13
6600	1.2E15	8000	9.2E14	9400	6.5E14	10800	3.9E13
6800	1.2E15	8200	8.4E14	9600	5.8E14		

Figure 13.8: G750M Time to Achieve a Signal-to-Noise of 10 per Spectral Resolution Element for Stars of Different Spectral Types, observed through the 0.2 arcsecond wide slit.

(a) O5 star

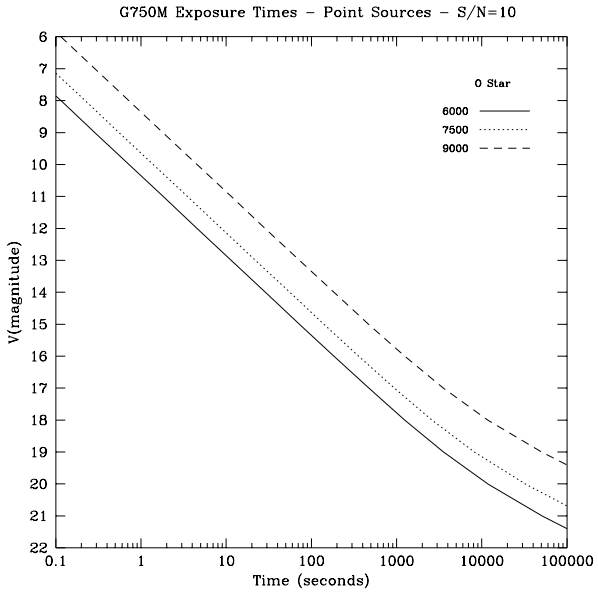

(b)AOV star

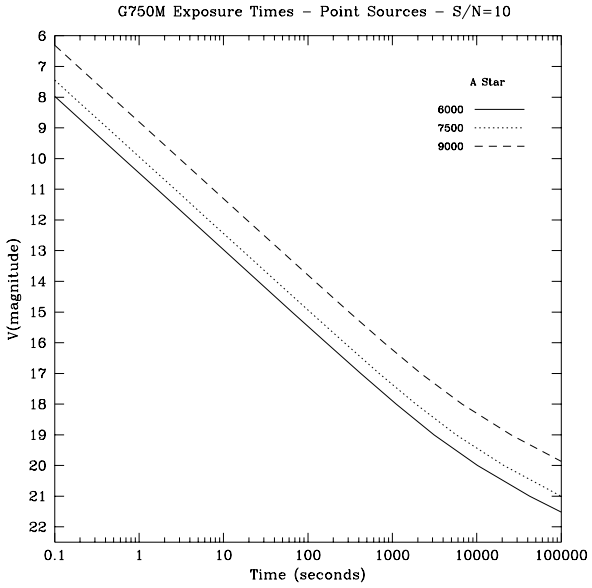

(c) GOV star

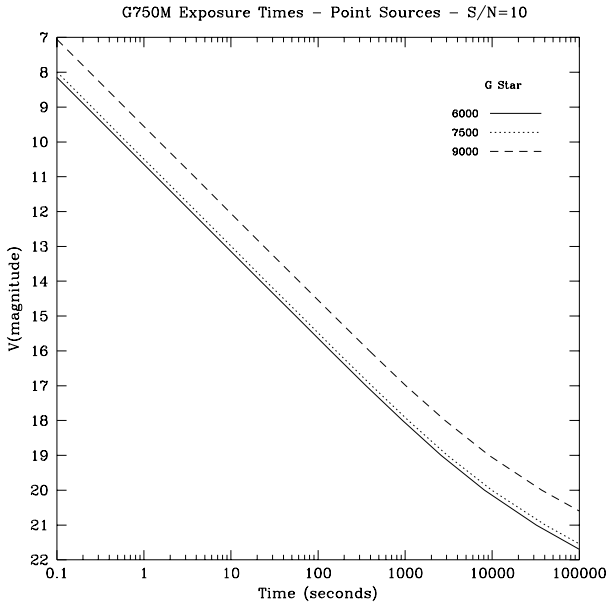

(d) MOV star

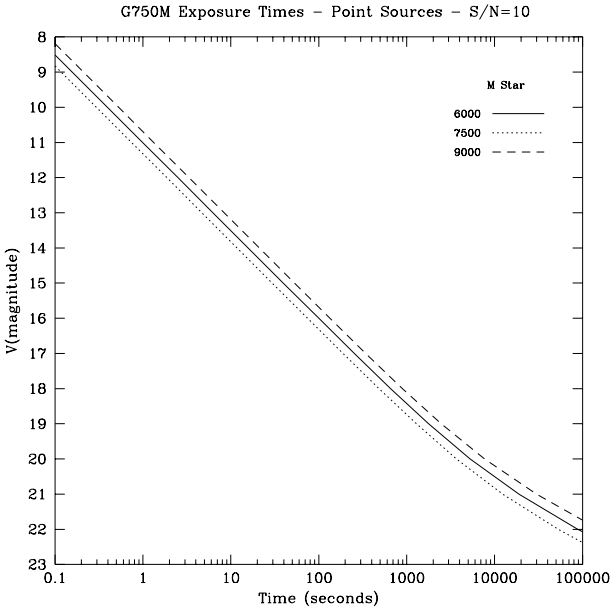

Figure 13.9: G750M Time to Achieve a Signal-to-Noise of 10 per Spectral Resolution Element for Point and Diffuse Sources Observed with the 0.2” Wide Slit, cgs units. Point sources are integrated over the PSF, diffuse sources are per two spatial pixels

.

(a) Point Sources

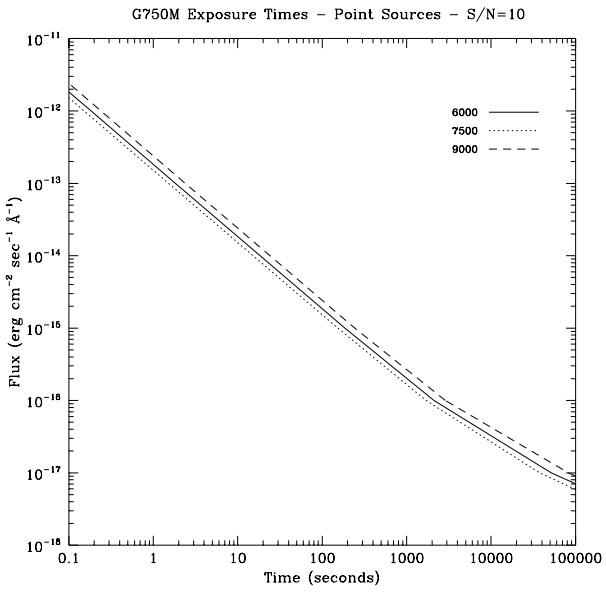

(b) Diffuse Sources

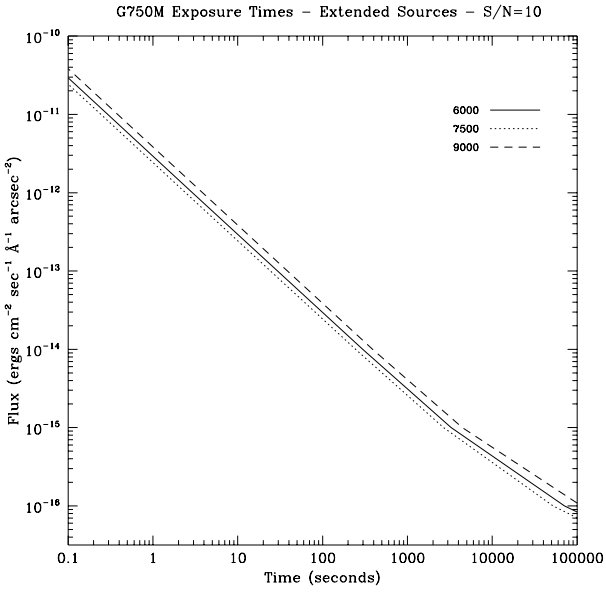

Figure 13.10: G750M Time to Saturate Peak Pixel as a Function of Source Flux, for observation taken through 0.2 arcsecond wide slit.

(a) Point Sources

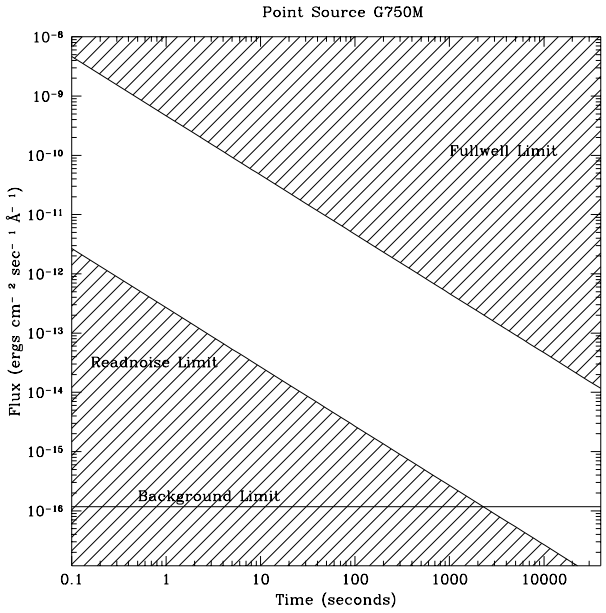

(b) Diffuse Sources

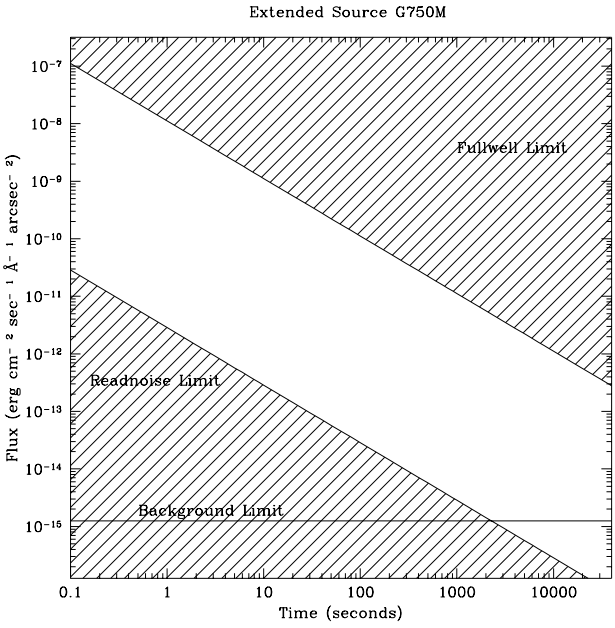

First Order Grating G430L

G430L, used with the CCD, is a low resolution grating (R~500) with a relatively high throughput. The grating has only a single setting. This grating is designed for observations where high spectral resolution is not required, but efficient spectral coverage in the blue portion of the optical is desired. Notice, that by taking two observations, one with G750L and one with G430L, the full spectral region, from the near-IR at 10000 Å through the optical at 3050 Å can be efficiently observed at an R~500. The properties of the G430L grating are summarized in the table below.

	Spectral Range		Dispersion		Central Wavelengths
Grating	**Complete**	**Per Tilt**	**Å per Pixel**	**Tilts**	
G430L	2900-5700	2900	2.73	***Prime***	**4300**

The sensitivity, signal-to-noise exposure time requirements, and saturation exposure time limits for the G430L grating are summarized below.

Figure 13.11: G430L Point Source (left axis), and Diffuse Source (right axis) Sensitivities. Point source sensitivity assumes full transmission (zero slit losses). Diffuse source sensitivity assumes a 0.1” wide slit.

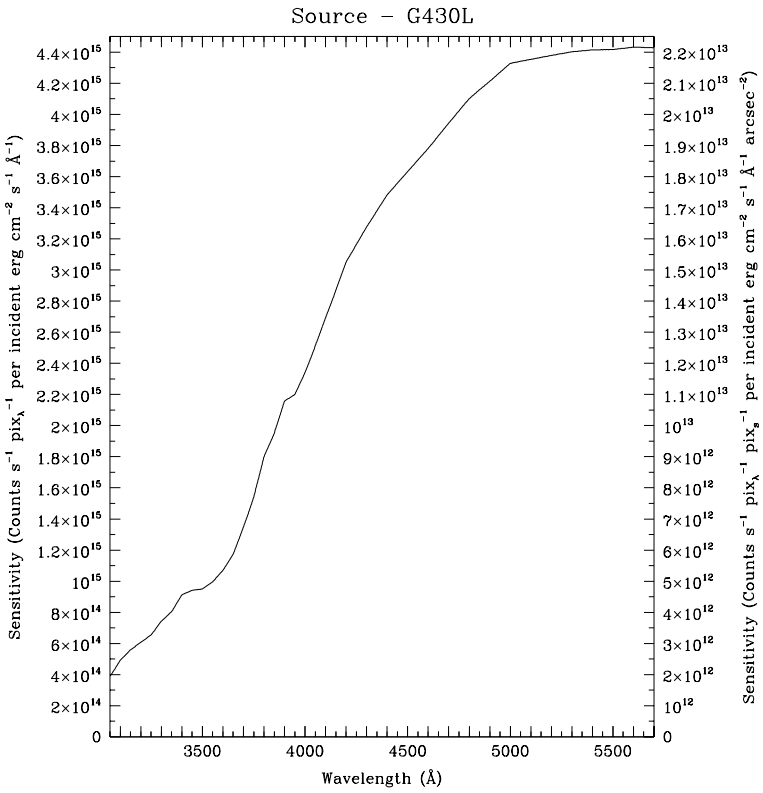

Table 13.3: G430L Point Source Sensitivities. Multiply sensitivity number by 0.05 times the slit width in arcseconds to obtain diffuse source sensitivity.

λ	**Sens.**	λ	**Sens.**	λ	**Sens.**	λ	**Sens.**
2600	1.09E9	3400	9.1E14	4200	3.0E15	5000	4.3E15
2800	2.6E12	3600	1.1E15	4400	3.5E15	5200	4.4E15
3000	3.2E14	3800	1.8E15	4600	3.8E15	5400	4.4E15
3200	6.1E14	4000	2.3E15	4800	4.1E15	5600	4.4E15

Figure 13.12: G430L Time to Achieve a Signal-to-Noise of 10 per Spectral Resolution Element for Stars of Different Spectral Types, observed through the 0.2 arcsecond wide slit.

(a) O5 star

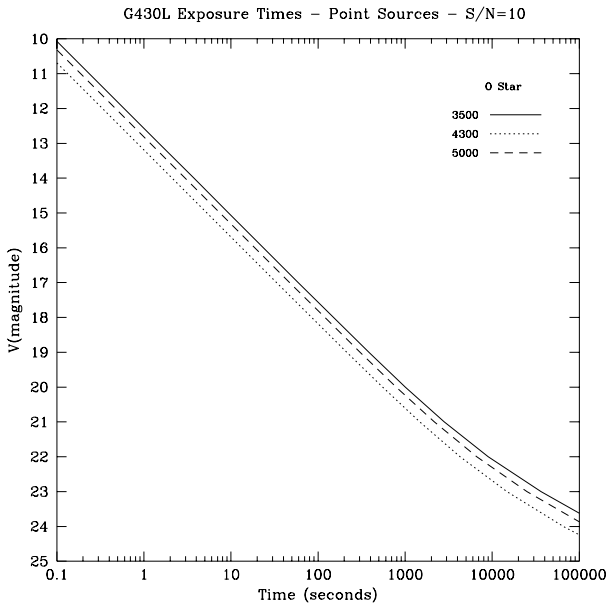

(b) AOV star

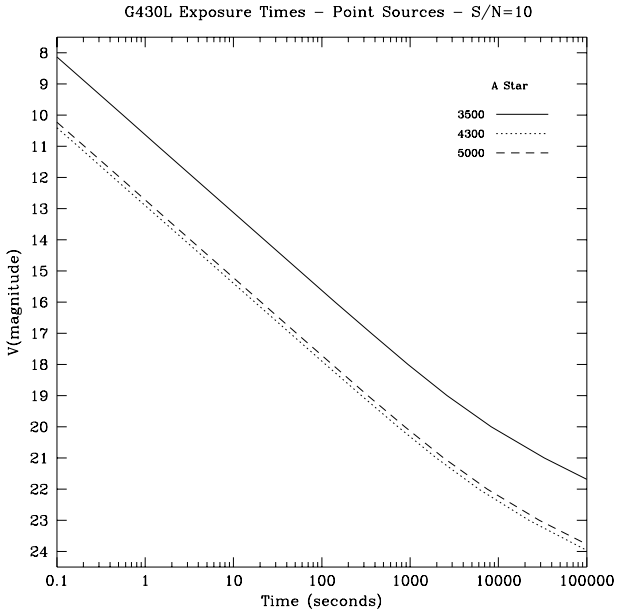

(c) GOV star

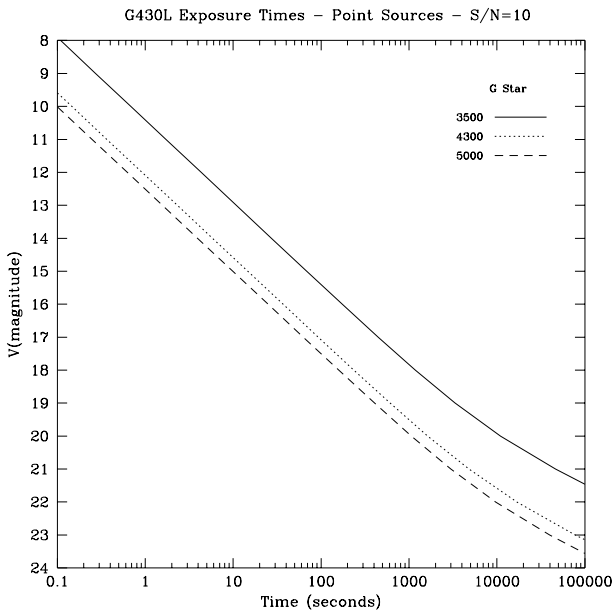

(d) M0V star

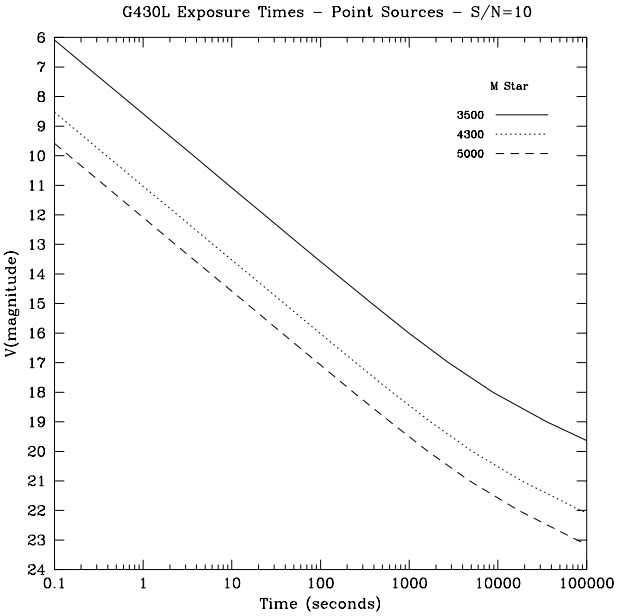

Figure 13.13: G430L Time to Achieve a Signal-to-Noise of 10 per Spectral Resolution Element for Point and Diffuse Sources Observed with the 0.2” Wide Slit, cgs units. Point sources are integrated over the PSF, diffuse sources per two spatial pixels.

.

(a) Point Sources

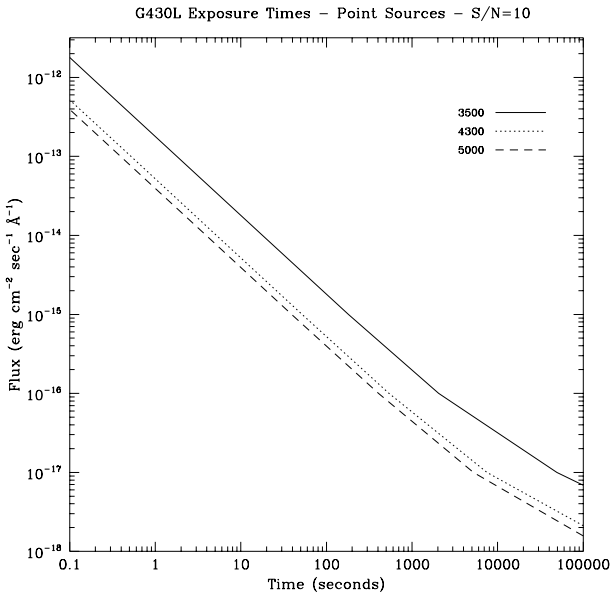

(b) Diffuse Sources

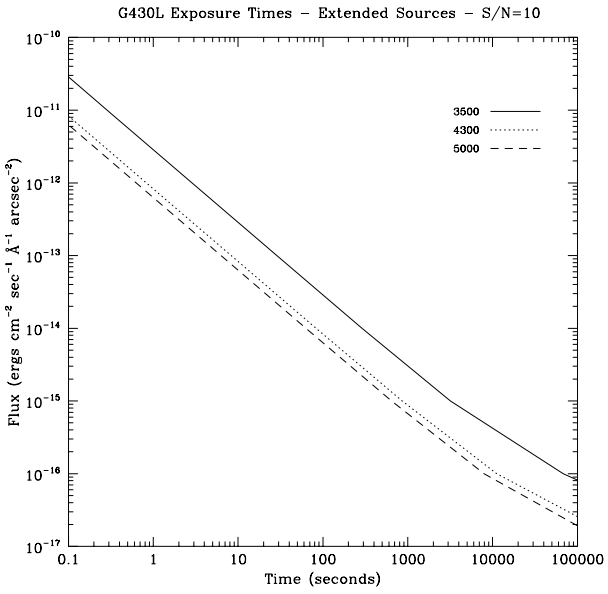

Figure 13.14: G430L Time to Saturate Peak Pixel as a Function of Source Flux, for observation taken through 0.2 arcsecond wide slit.

(a) Point Sources

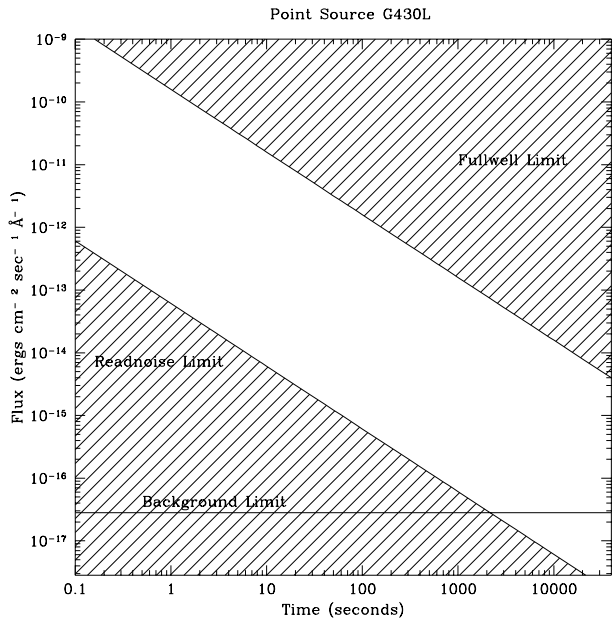

(b) Diffuse Sources

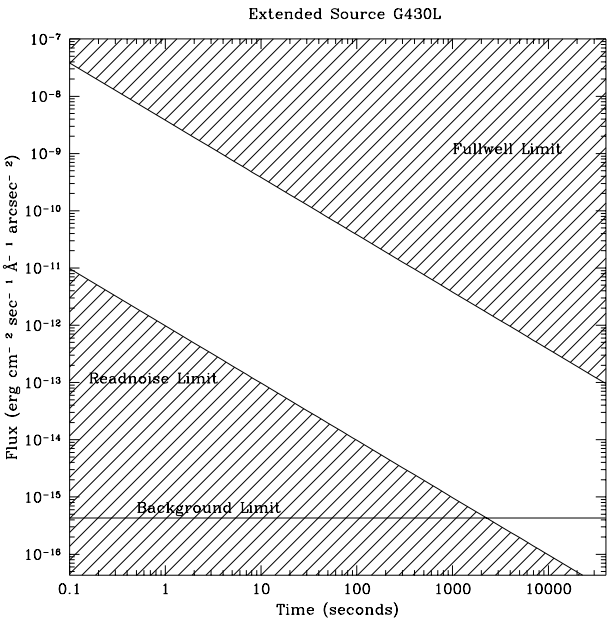

First Order Grating G430M

Like the G430L grating, the G430M grating is used with the CCD and has a spectral range from 3050–5500 Å, however a single exposure with this grating covers only 236 Å, and the grating must be scanned, with a series of exposures taken at 10 distinct settings to cover the full spectral range of the grating. The G430M grating mode is designed for observations where spatially resolved, long slit, spectroscopy is desired at relatively high spectral resolution (R~6000) over a limited region of the near-ultraviolet or optical spectrum. The properties of the G430M grating are summarized below.

Grating	Spectral Range		Dispersion		Central Wavelengths
	Complete	Per Tilt	Å per Pixel	Tilts	
G430M	3025-5610	286	0.28	***Prime***	**3165, 3423, 3680, 3936, 4194, 4451, 4706, 4961, 5216, 5471**
				Secondary	3305, 3843, 4781, 5093

The minimum and maximum wavelengths covered in single exposures for each scan setting are shown graphically in Figure 13.15, below.

Figure 13.15: Wavelength Ranges for the G430M Grating Settings

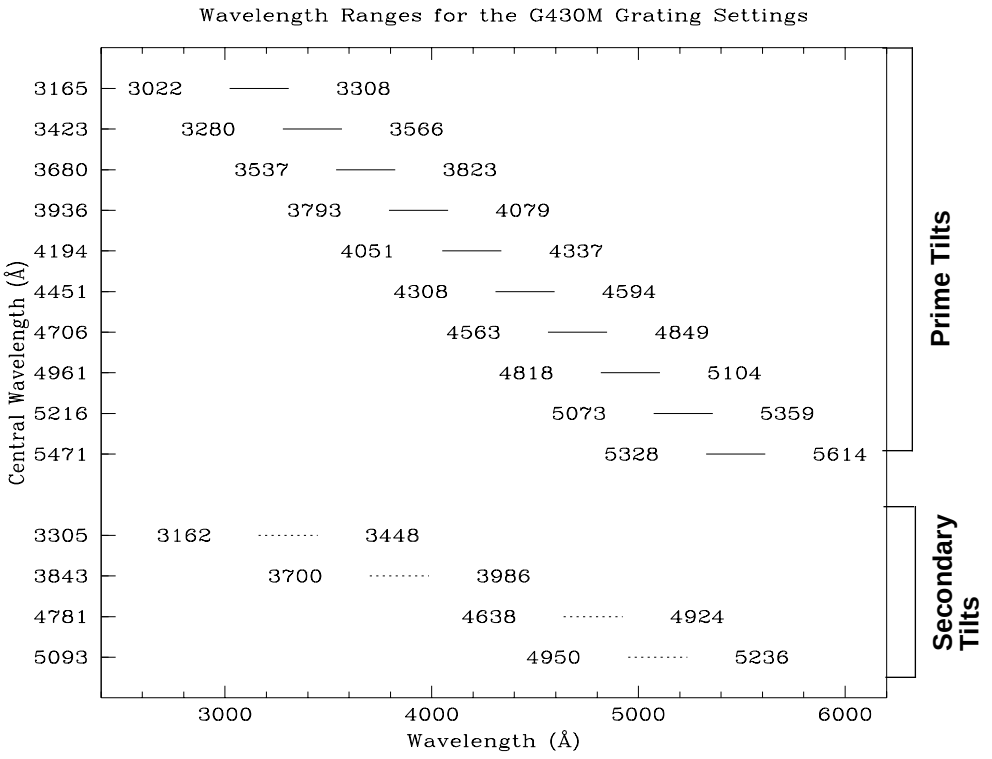

The sensitivity, signal-to-noise exposure time requirements, and saturation exposure time limits for the G430M grating are summarized below.

Figure 13.16: G430M Point Source (left axis), and Diffuse Source (right axis) Sensitivities. Point source sensitivity assumes full transmission (zero slit losses). Diffuse source sensitivity assumes a 0.1” wide slit.

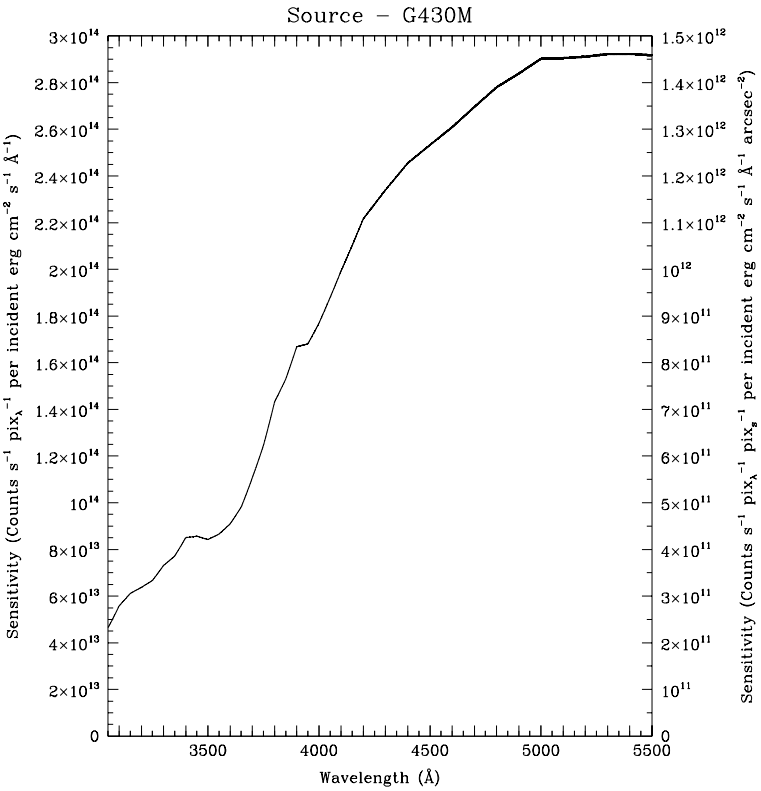

Table 13.4: G430M Point Source Sensitivities. Multiply sensitivity number by 0.05 times the slit width in arcseconds to obtain diffuse source sensitivity.

λ	**Sens.**	λ	**Sens.**	λ	**Sens.**
3000	4.0E13	4000	1.8E14	5000	2.9E14
3200	6.4E13	4200	2.2E14	5200	2.9E14
3400	8.5E13	4400	2.5E14	5400	2.9E14
3600	9.1E13	4600	2.6E14	5600	2.9E14
3800	1.4E14	4800	2.8E14	5800	2.9E14

Figure 13.17: G430M Time to Achieve a Signal-to-Noise of 10 per Spectral Resolution Element for Stars of Different Spectral Types, observed through the 0.2 arcsecond wide slit.

(a) O5 star

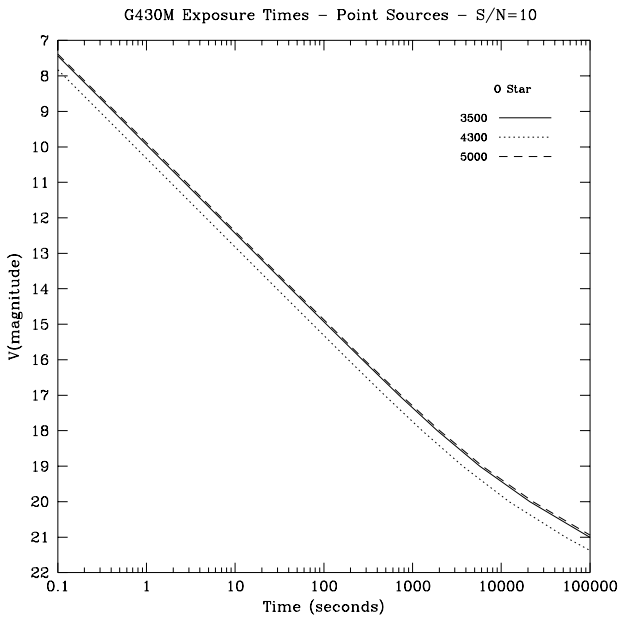

(b) AOV star

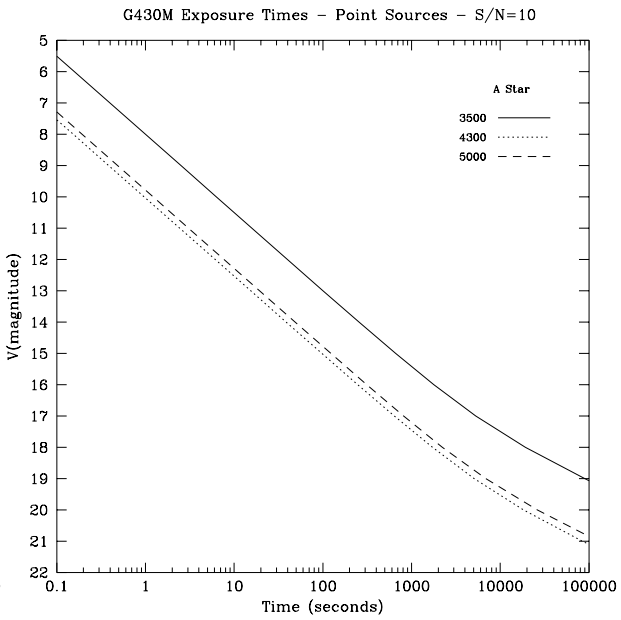

(c) G0V star

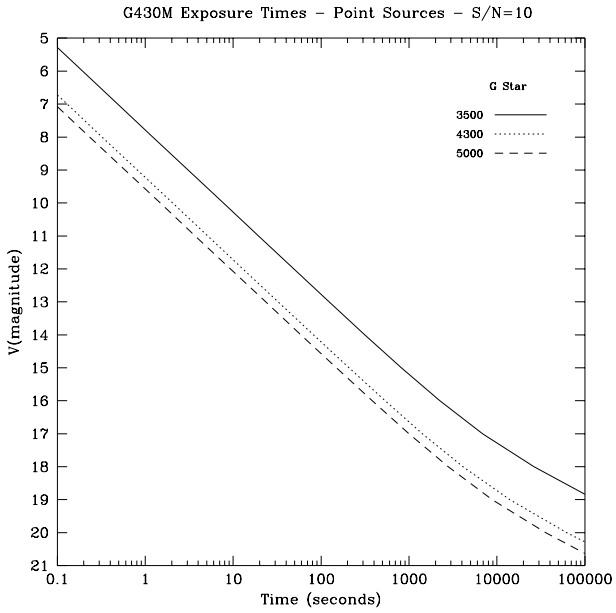

(d) M0V star

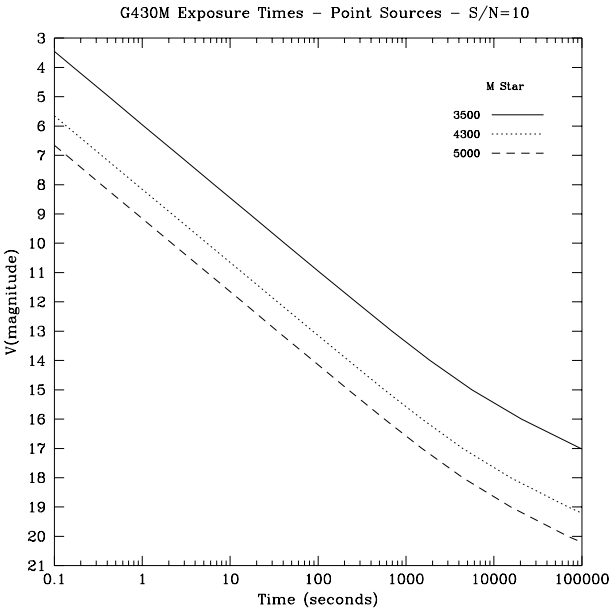

Figure 13.18: G430M Time to Achieve a Signal-to-Noise of 10 per Spectral Resolution Element for Point and Diffuse Sources Observed with the 0.2” Wide Slit, cgs units. Point sources are integrated over the PSF, diffuse sources per two spatial pixels.

(a) Point Sources

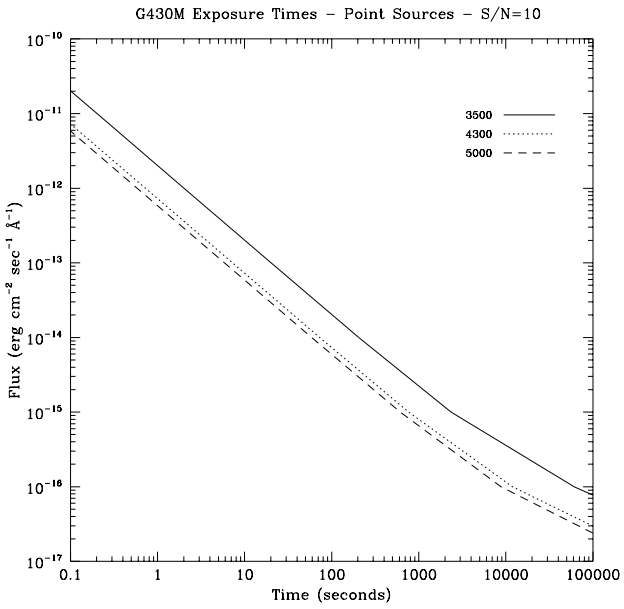

(b) Diffuse Sources

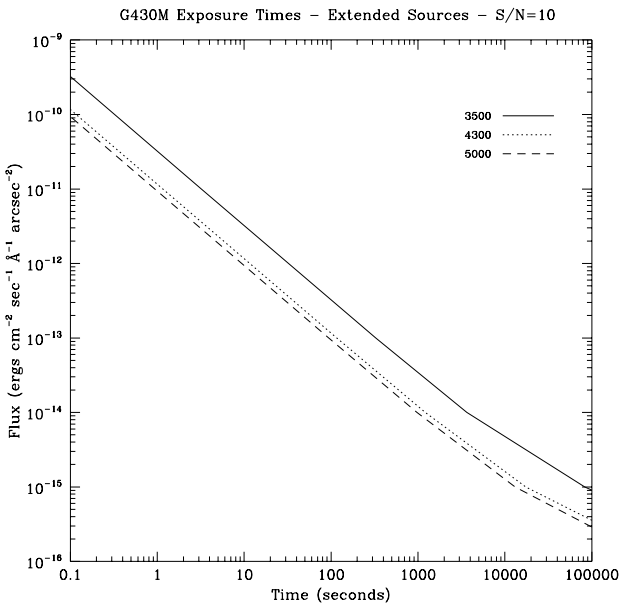

Figure 13.19: G430M Time to Saturate Peak Pixel as a Function of Source Flux, for observation taken through 0.2 arcsecond wide slit.

(a) Point Sources

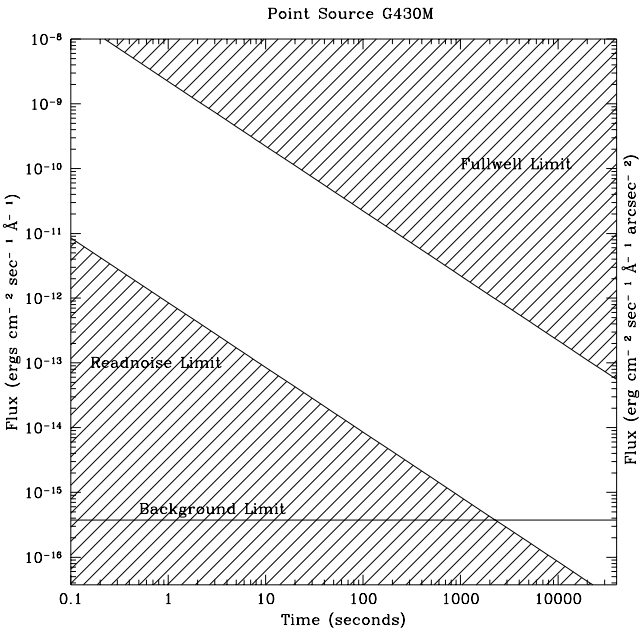

(b) Diffuse Sources

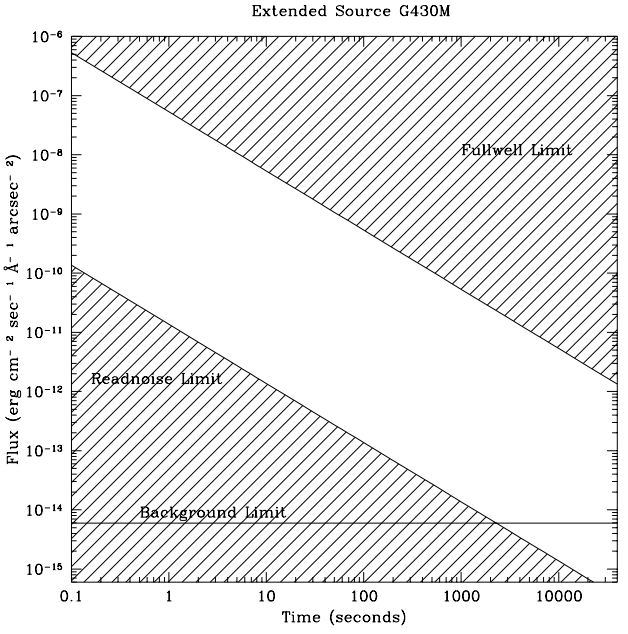

First Order Grating G230LB

The G230LB[2] grating mode is designed for science needing the highest available sensitivity in the near-UV from ~2500 to 3100 Å. The G230LB grating mode uses a low resolution grating originally designed for use with the STIS/NUV-MAMA which has been re-directed for use with the STIS/CCD to enable R~700 spectroscopy in the near-UV which takes advantage of the CCD's higher throughput and dynamic range longward of λ=2500 Å. The properties of the G230LB grating mode are summarized in the table below.

	Spectral Range		Dispersion		Central Wavelengths
Grating	Complete	Per Tilt	Å per Pixel	Tilts	
G230LB	1685-3065	1380	1.3	***Prime***	**2375**

The sensitivity, signal-to-noise exposure time requirements, and saturation exposure time limits for the G230LB grating mode are summarized below.

The trade-off between using the G230LB or the G230L (which use the NUV MAMA), depends sensitively on the science goals and your source properties, since the CCD has read noise, where the MAMA does not, the CCD does not have bright object limits, where the MAMA does, the detector PSF of the CCD is much cleaner than that of the NUV-MAMA, the spatial sampling of the MAMA is better than that of the CCD, and the CCD does not enable high time resolution ($\Delta\tau$<10 seconds), where the MAMA does. Figures 13.20 and 13.21, below, show a direct comparison of some of the properties of the G230LB and G230L modes.

2. In making the plots for the G230LB and G230MB grating modes, we assumed that the CCD is subject to a change in the effective quantum yield resulting in the creation of multiple electron-whole pairs per photon for λ<3400 Å (see "Special Case—Spectroscopic CCD Observations at λ<2500 Å" on page 71). This does not alter the curves of sensitivity as a function of wavelength, but does alter the signal-to-noise curves.

Figure 13.20: Comparison of Limiting Fluxes for G230LB and G230L. Plotted is the ratio of limiting source fluxes for G230LB relative to G230L to achieve a signal-to-noise ratio of 10 in 1 hour per 2.6 Å (the spectral resolution of G230LB).

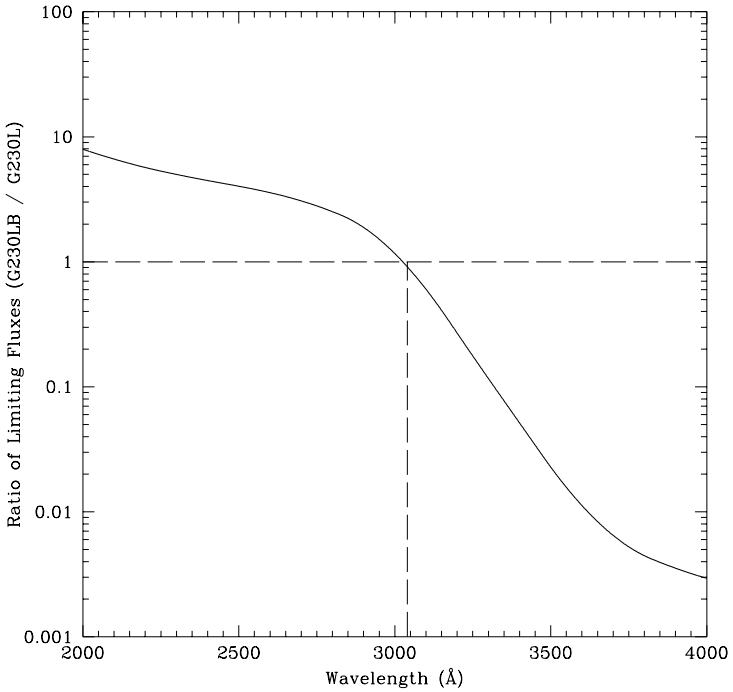

Figure 13.21: Comparison of LSFs for G230LB and G230L

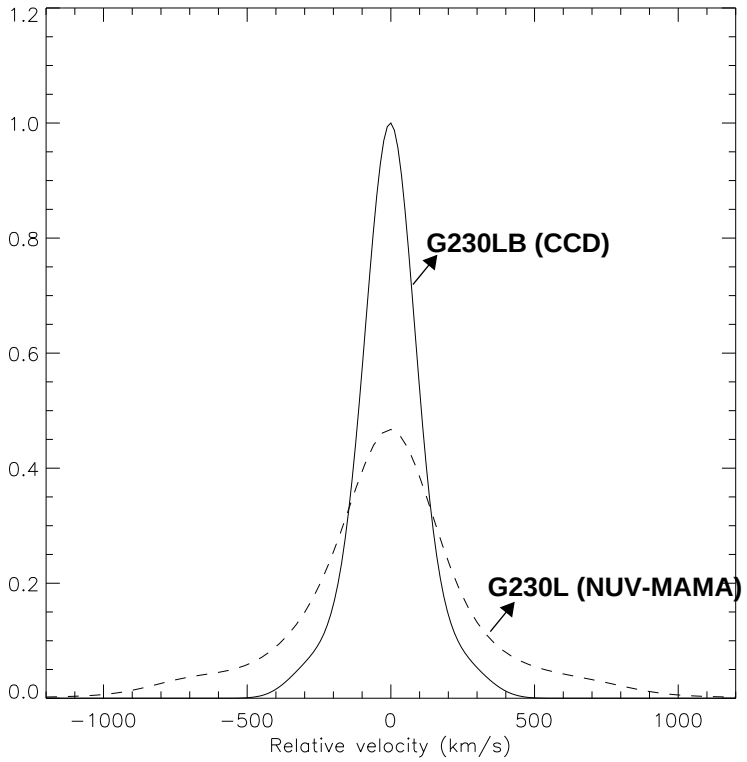

Figure 13.22: G230LB Point Source (left axis), and Diffuse Source (right axis) Sensitivities. Point source sensitivity assumes full transmission (zero slit losses). Diffuse source sensitivity assumes a 0.1” wide slit.

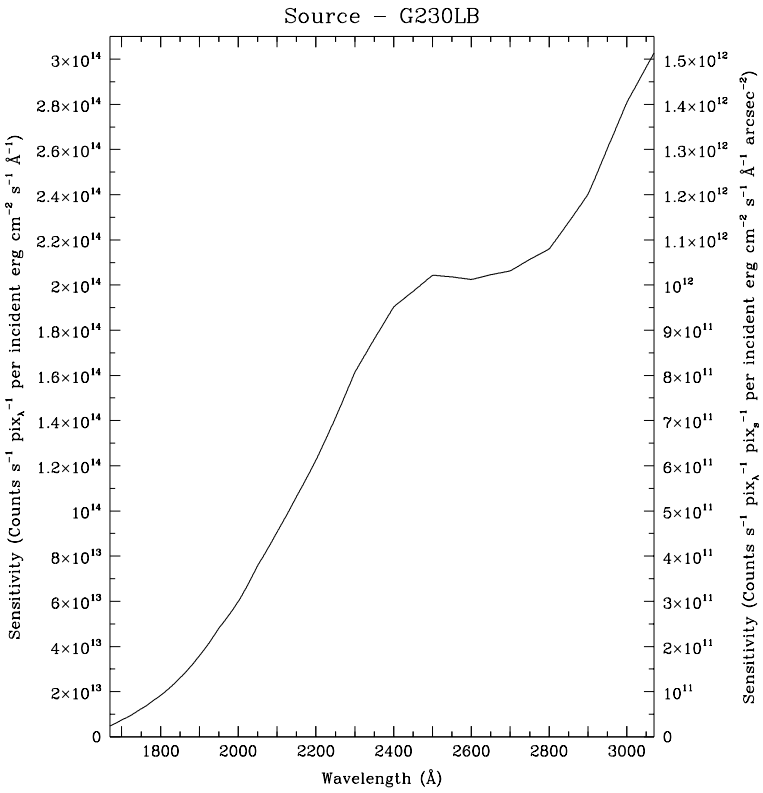

Table 13.5: G230LB Point Source Sensitivities. Multiply sensitivity number by 0.05 times the slit width in arcseconds to obtain diffuse source sensitivity.

λ	Sens.	λ	Sens.	λ	Sens.	λ	Sens.
1200	1.4E-5	2000	6.0E13	2800	2.2E14	3600	3.7E14
1300	1.7E-5	2100	9.1E13	2900	2.4E14	3700	4.1E14
1400	1.8E-5	2200	1.2E14	3000	2.8E14	3800	5.0E14
1500	1.8E-5	2300	1.6E14	3100	3.1E14	3900	5.7E14
1600	3.3E11	2400	1.9E14	3200	3.3E14	4000	5.9E14
1700	7.5E12	2500	2.0E14	3300	3.6E14		
1800	1.8E13	2600	2.0E14	3400	3.6E14		
1900	3.6E13	2700	2.1E14	3500	3.6E14		

Figure 13.23: G230LB Time to Achieve a Signal-to-Noise of 10 per Spectral Resolution Element for Stars of Different Spectral Types, observed through the 0.2 arcsecond wide slit.

(a) O5 star

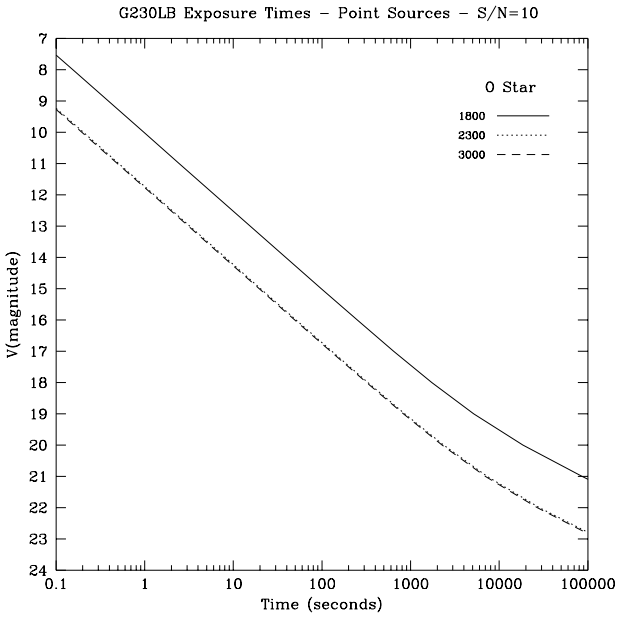

(b) AOV star

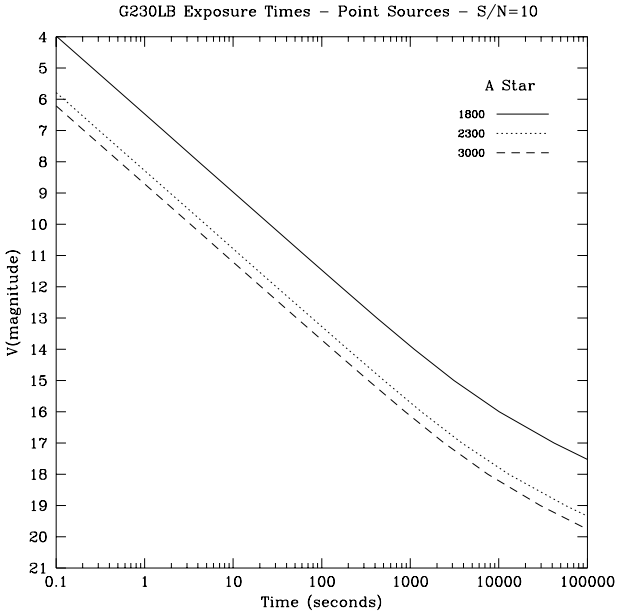

(c) G0V star

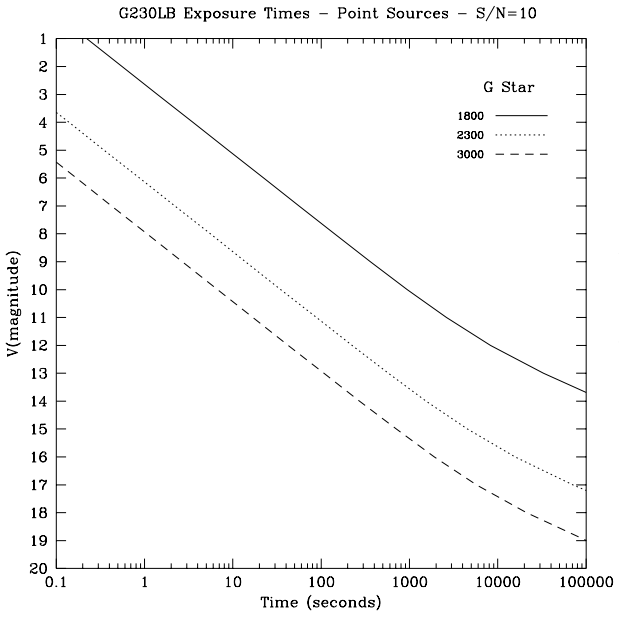

(d) M0V star

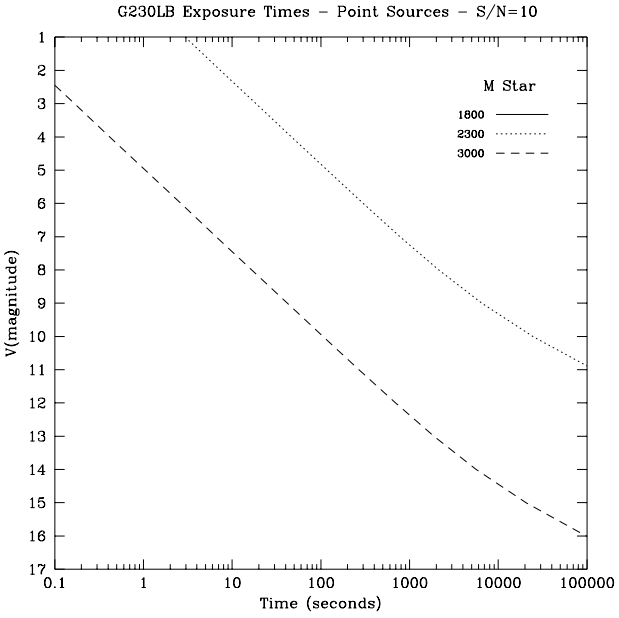

Figure 13.24: G230LB Time to Achieve a Signal-to-Noise of 10 per Spectral Resolution Element for Point and Diffuse Sources Observed with the 0.2” Wide Slit, cgs units. Point sources are integrated over the PSF, diffuse sources are per two spatial pixels.

(a) Point Source

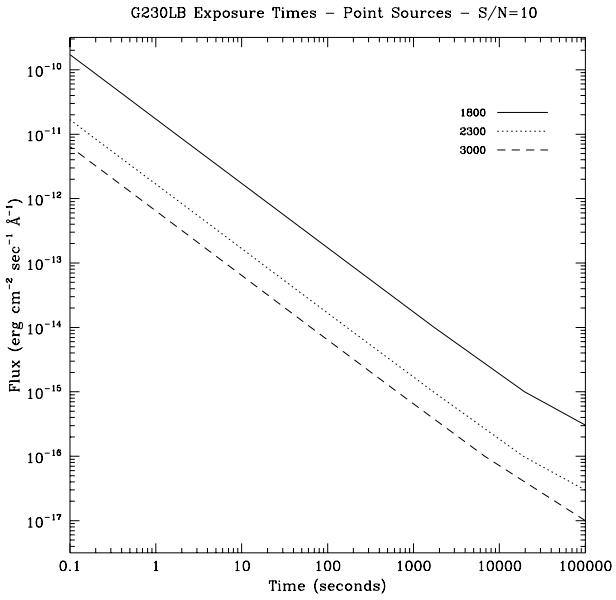

(b) Diffuse Source

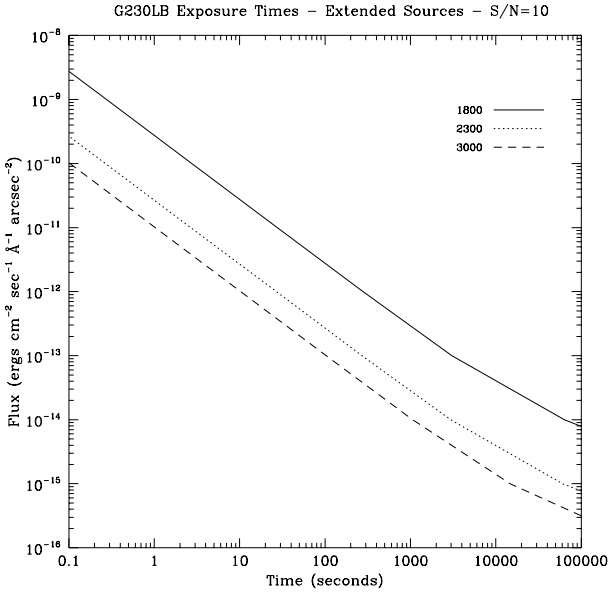

Figure 13.25: G230LB Time to Saturate Peak Pixel as a Function of Source Flux, for observation taken through 0.2 arcsecond wide slit.

(a) Point Source

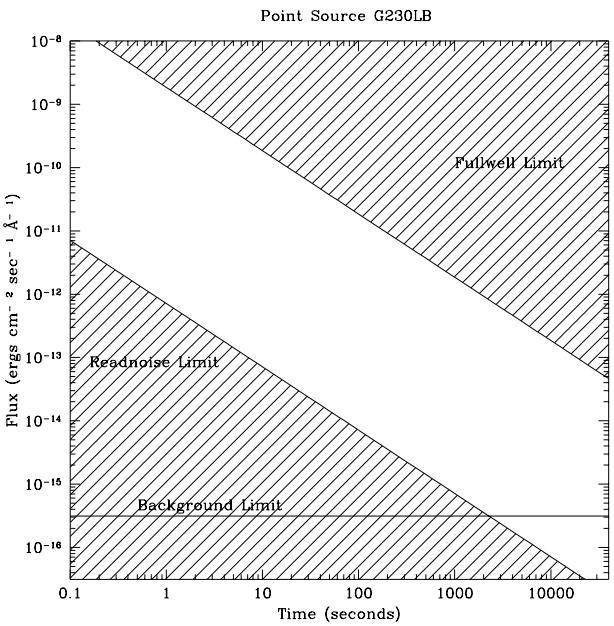

(b) Diffuse Source

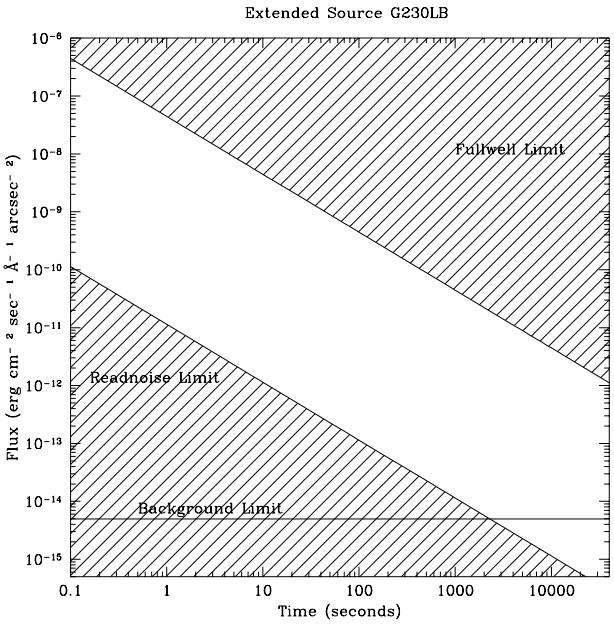

First Order Grating G230MB

The G230MB grating mode uses an intermediate resolution grating originally designed for use with the NUV-MAMA which has been redirected for use with the CCD to provide R~6000 spectroscopy in the near-UV which takes advantage of the CCD's higher throughput longward of λ=2500 Å. The properties of the G230MB grating mode are summarized in the table below.

Grating	Spectral Range		Dispersion		Central Wavelengths
	Complete	Per Tilt	Å per Pixel	Tilts	
G230MB	1635-3190	155	0.15	***Prime***	**1713, 1854,1995, 2135, 2276, 2416, 2557, 2697, 2836, 2976, 3115**
				Secondary	2794

The G230MB grating mode has a spectral range from 1640-3190 Å. However a single exposure with this grating covers only 150 Å, and the grating must be scanned, with a series of exposures taken at 12 distinct settings to cover the full spectral range of the grating. The available scan settings (central wavelength and minimum and maximum wavelengths covered in a single exposures) are shown graphically in Figure 13.26 below.

Figure 13.26: Wavelength Ranges for the G230MB Grating Settings

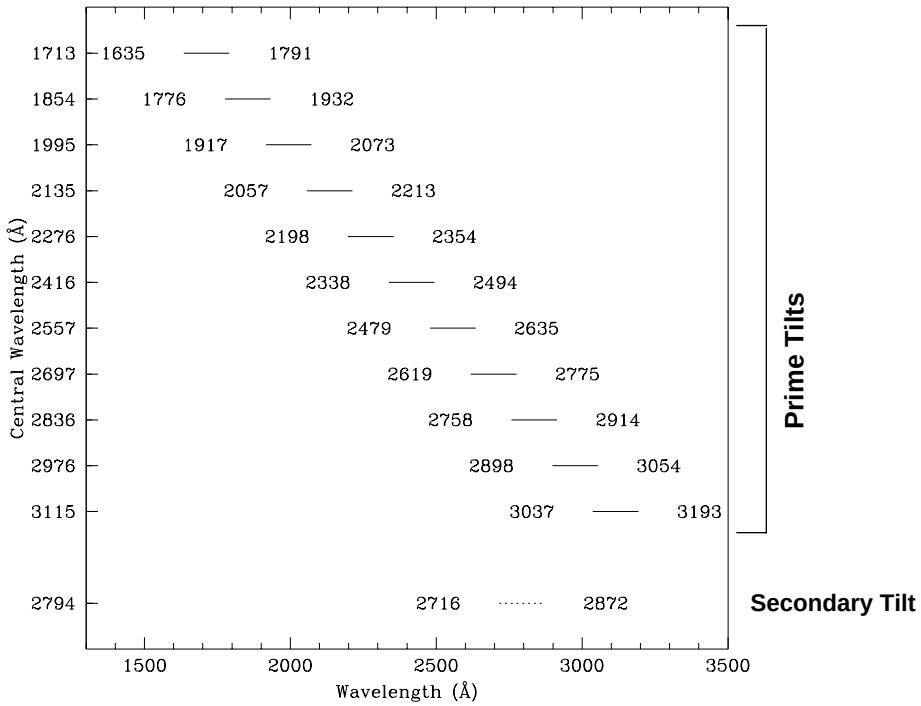

Figure 13.27: .Comparison of Limiting Fluxes for G230MB and G230M. Plotted is the ratio of limiting source fluxes for G230MB relative to G230M to achieve a signal-to-noise ratio of 10 in 1 hour per 0.3 Å (the spectral resolution of G230MB)

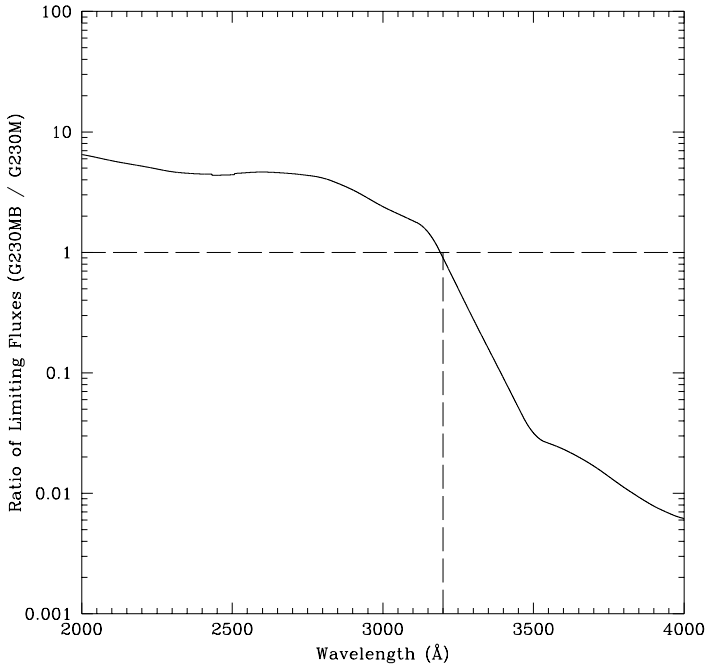

Comparison of LSFs for G230MB and G230M

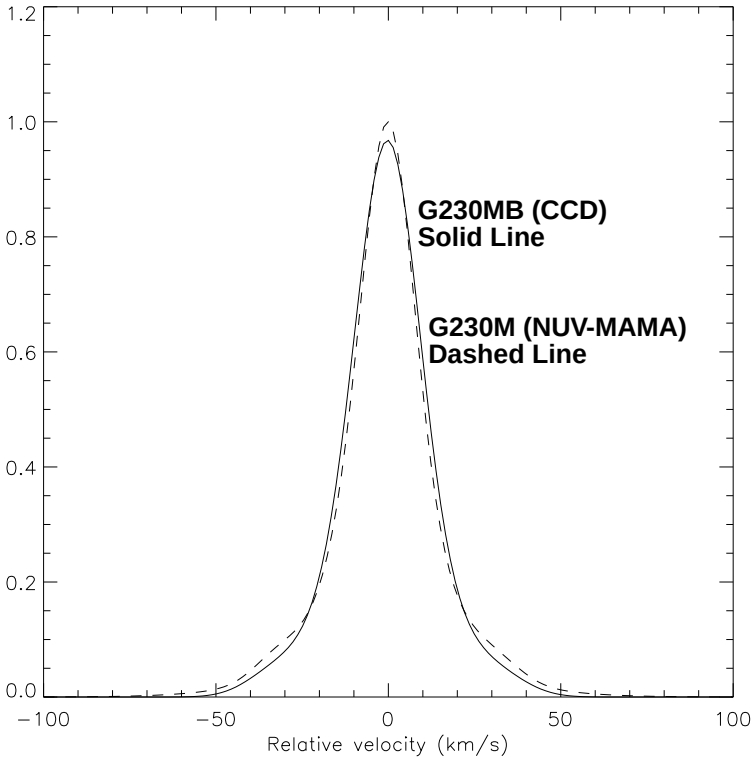

The sensitivity, signal-to-noise exposure time requirements, and saturation exposure time limits for the G230MB grating mode are summarized below. The trade-off between using the G230MB or the G230M (which use the NUV MAMA) grating modes, depends sensitively on the science goals and your source properties, as described above in “First Order Grating G230MB” on page 201. Figures below shows a direct comparison of some of the properties of the G230MB and G230M modes

Figure 13.28: G230MB Point Source (left axis), and Diffuse Source (right axis) Sensitivities. Point source sensitivity assumes full transmission (zero slit losses). Diffuse source sensitivity assumes a 0.1” wide slit.

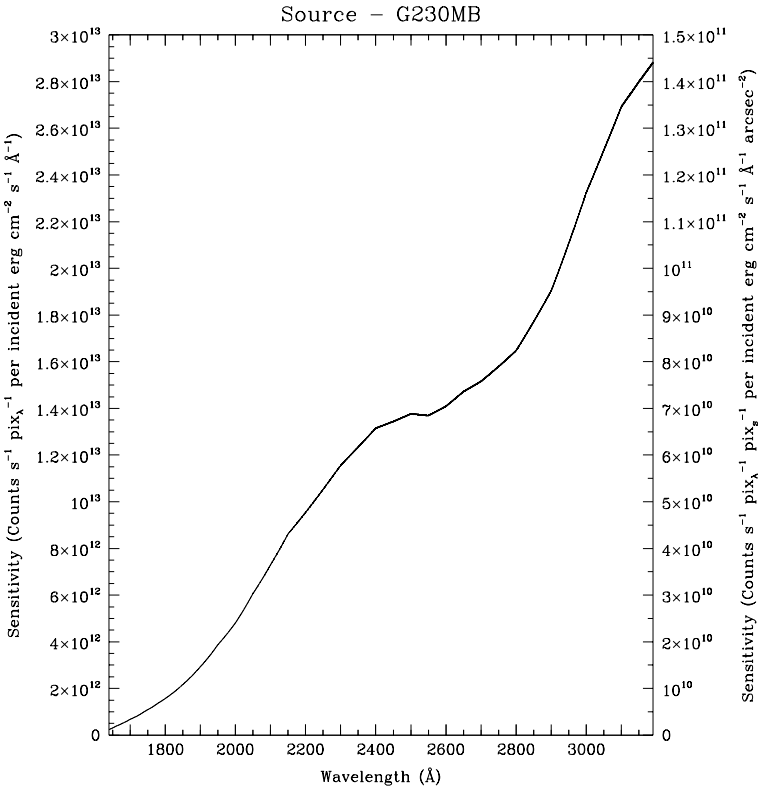

Table 13.6: G230MB Point Source Sensitivities. Multiply sensitivity number by 0.05 times the slit width in arcseconds to obtain diffuse source sensitivity.

λ	Sens.	λ	Sens.	λ	Sens.	λ	Sens.
1600	3.3E10	2100	7.3E12	2600	1.4E13	3100	2.7E13
1700	6.8E11	2200	9.5E12	2700	1.5E13	3200	2.9E13
1800	1.6E12	2100	7.3E12	2800	1.6E13		
1900	2.9E12	2200	9.5E12	2900	1.9E13		
2000	4.8E12	2500	1.4E13	3000	2.3E13		

Figure 13.29: G230MB Time to Achieve a Signal-to-Noise of 10 per Spectral Resolution Element for Stars of Different Spectral Types, observed through the 0.2 arcsecond wide slit.

(a) O5 star

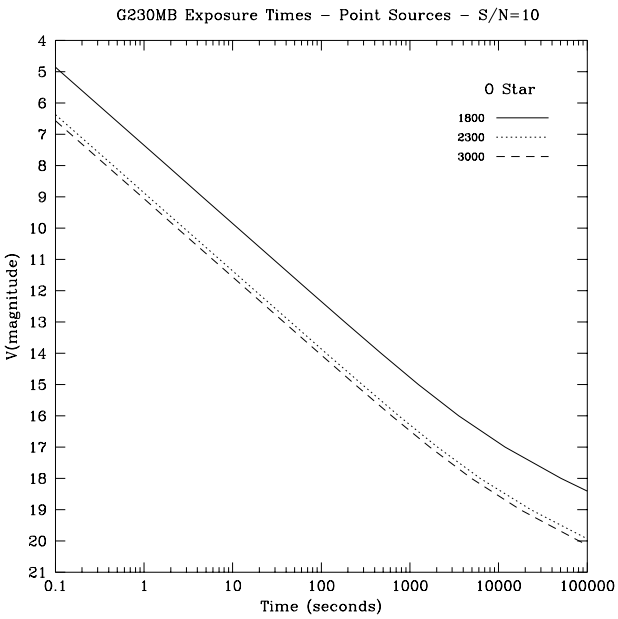

(b) AOV star

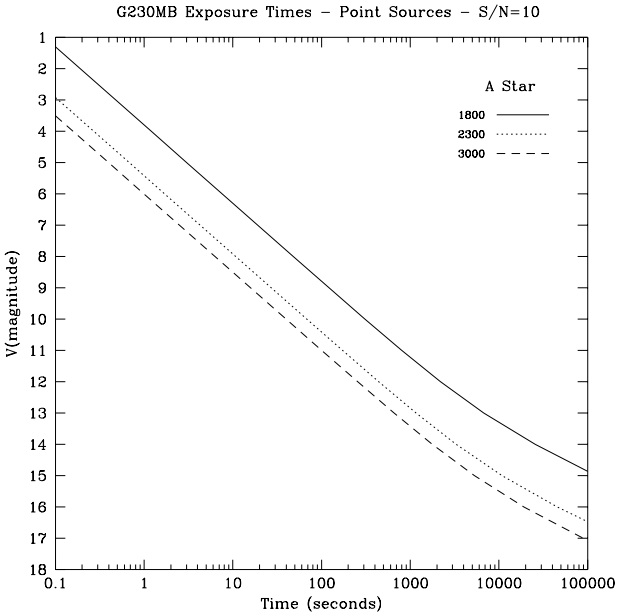

(c) G0V star

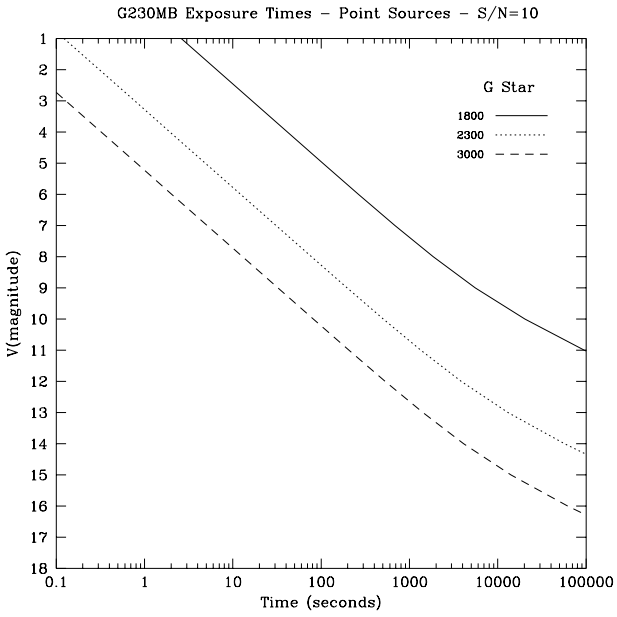

(d) M0V star

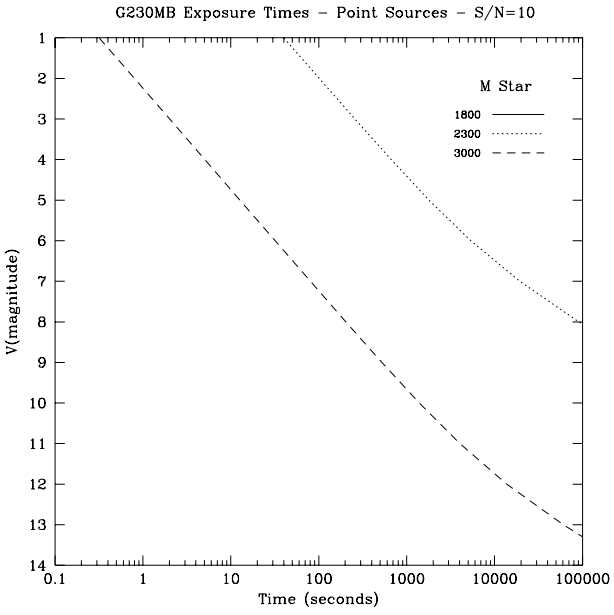

Figure 13.30: G230MB Time to Achieve a Signal-to-Noise of 10 per Spectral Resolution Element for Point and Diffuse Sources Observed with the 0.2” Wide Slit, cgs units. Point sources are integrated over the PSF, diffuse sources are per two spatial pixels.

(a) Point Source

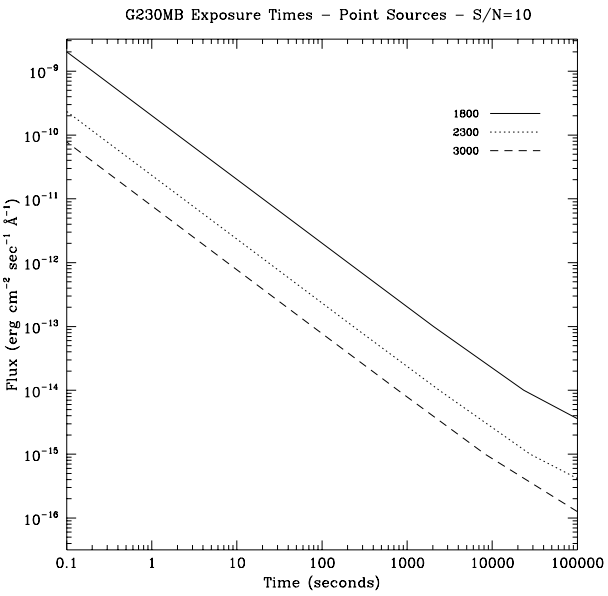

(b) Diffuse Source

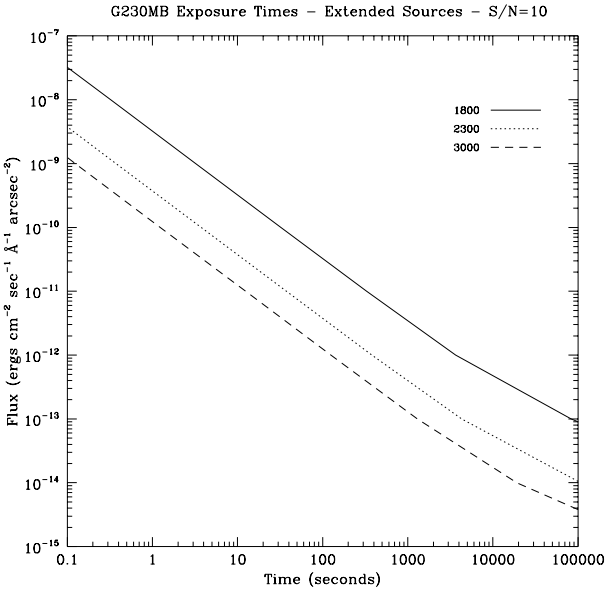

Figure 13.31: G230MB Time to Saturate Peak Pixel as a Function of Source Flux, for observation taken through 0.2 arcsecond wide slit.

(a) Point Source

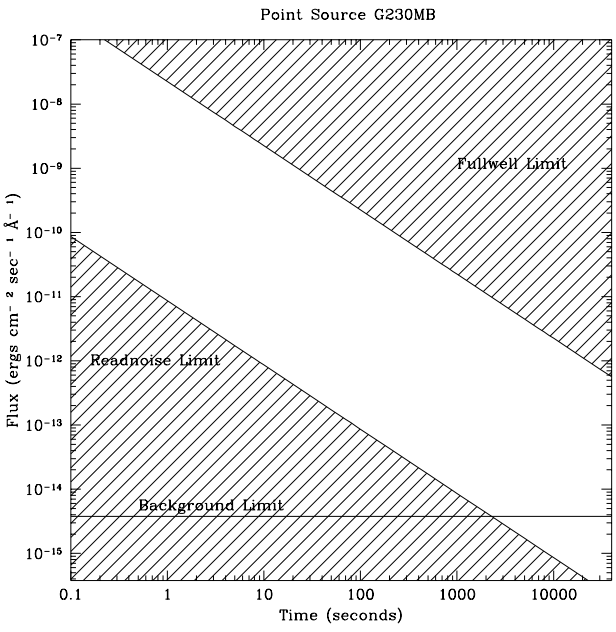

(b) Diffuse Source

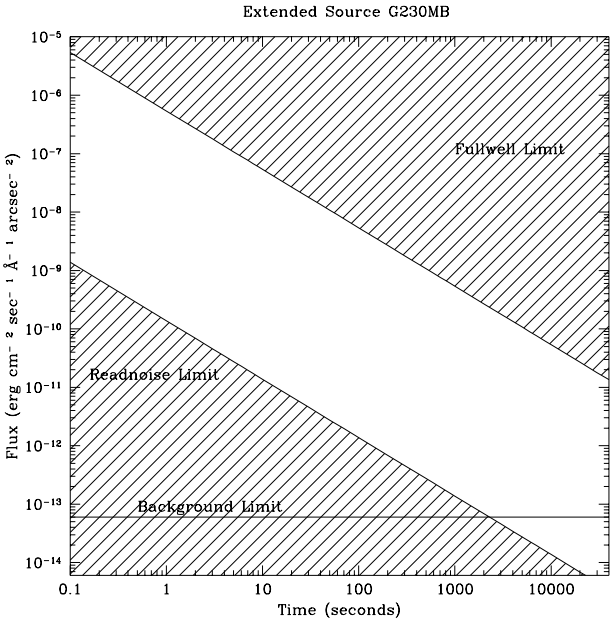

First Order Grating G230L

The G230L grating is used with the NUV-MAMA and has a relatively high throughput and a resolving power of ~500. It is designed for observations where high spectral resolution is not required, but efficient, spatially resolved spectroscopy with full spectral coverage in the near-ultraviolet is desired. Notice that the CCD `G230LB` grating mode also covers the near-ultraviolet with comparable resolution; see “First Order Grating G230LB” on page 196 for a detailed comparison of these two grating modes in that wavelength regime. The properties of the `G230L` grating are summarized below.

	Spectral Range		Dispersion		Central Wavelengths
Grating	**Complete**	**Per Tilt**	**Å per Pixel**	**Tilts**	
G230L	1570-3180	1610	1.58	***Prime***	**2376**

The sensitivity, exposure time signal-to-noise requirements, saturation exposure time limits, and bright object count limits for the `G230L` gratings are summarized below.

Figure 13.32: G230L Point Source, and Diffuse Source Sensitivities

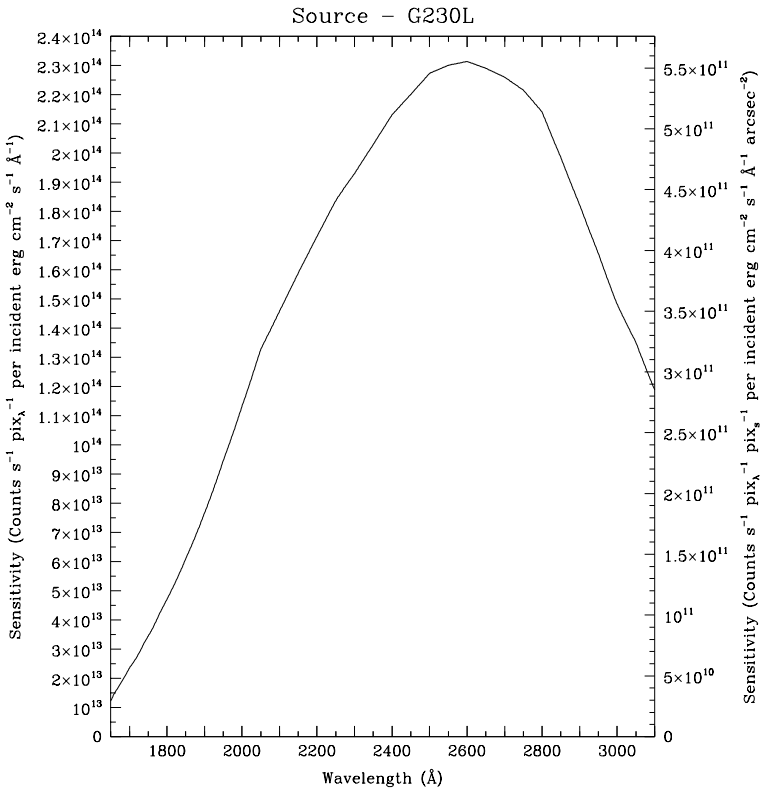

Table 13.7: G230L Point Source Sensitivities. Multiply sensitivity number by 0.0244 times the slit width in arcseconds to obtain diffuse source sensitivity.

λ	**Sens.**	λ	**Sens.**	λ	**Sens.**	λ	**Sens.**
1500	2.85E8	2000	1.1E14	2500	2.3E14	3000	1.5E14
1600	1.7E12	2100	1.5E14	2600	2.3E14	3100	1.2E14
1700	2.4E13	2200	1.7E14	2700	2.3E14		
1800	4.7E13	2300	1.9E14	2800	2.1E14		
1900	7.7E13	2400	2.1E14	2900	1.8E14		

Figure 13.33: G230L Time to Achieve a Signal-to-Noise of 10 per Spectral Resolution Element for Stars of Different Spectral Types, observed through the 0.2 arcsecond wide slit.

(a) O5 star

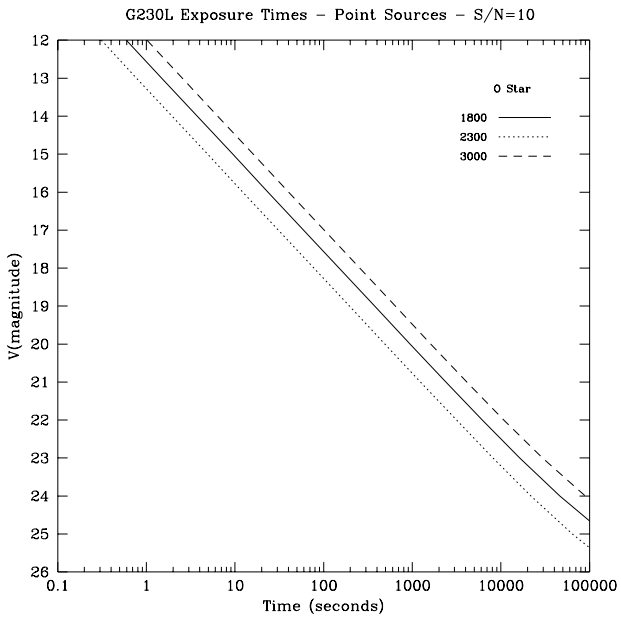

(b) AOV star

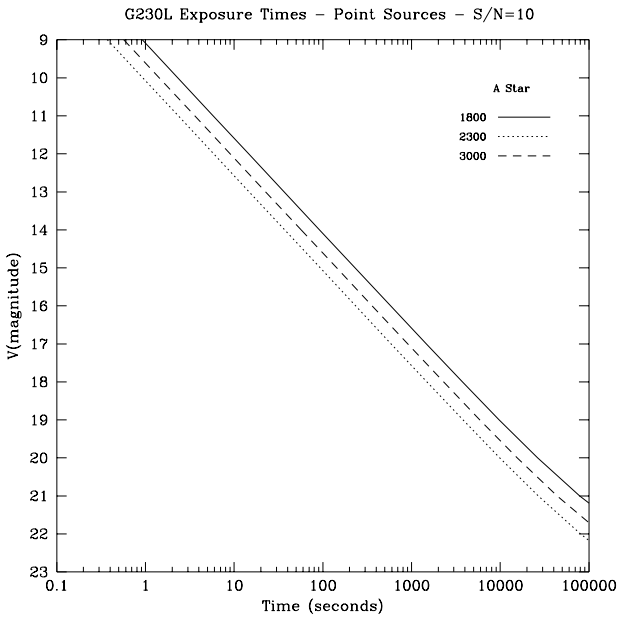

(c) G0V star

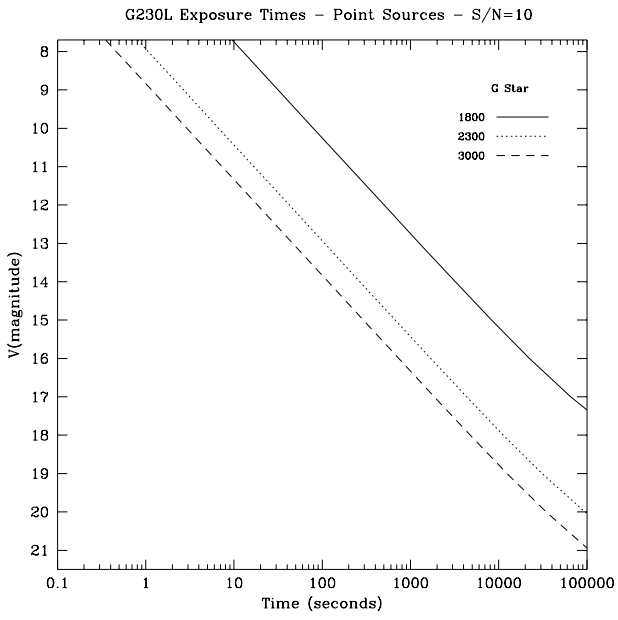

(d) M0V star

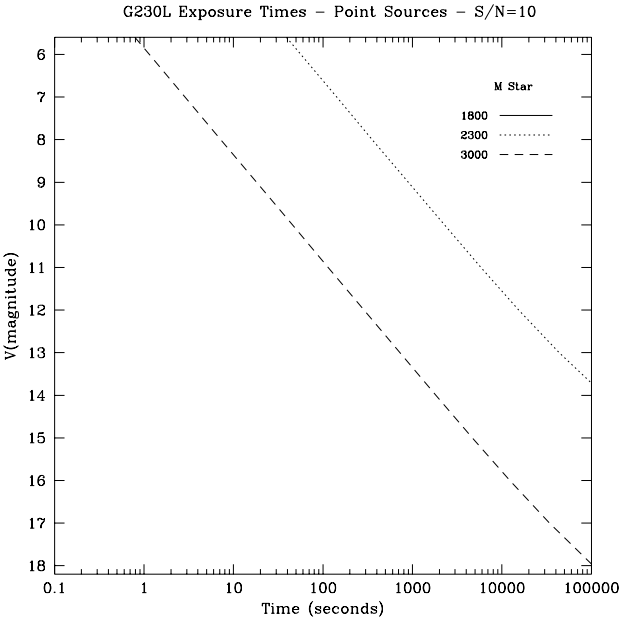

Figure 13.34: G230L Time to Achieve a Signal-to-Noise of 10 per Spectral Resolution Element for Point and Diffuse Sources Observed with the 0.2” Wide Slit, cgs units. Point sources are integrated over the PSF, diffuse sources are per two spatial pixels.

(a) Point Source

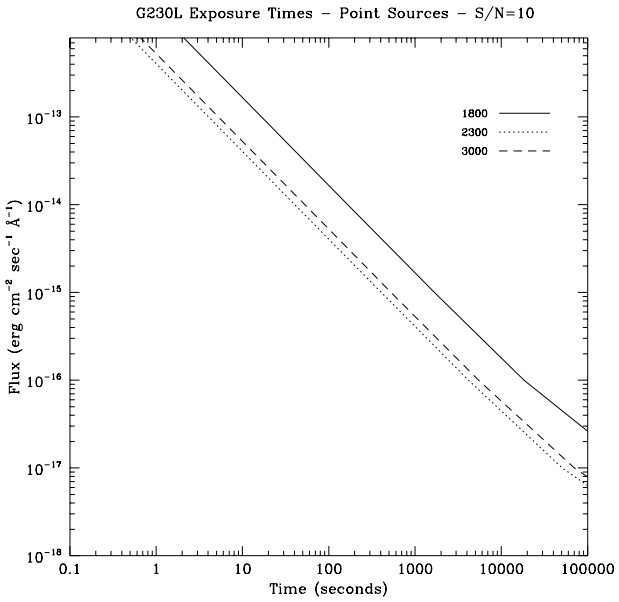

(b) Diffuse Source

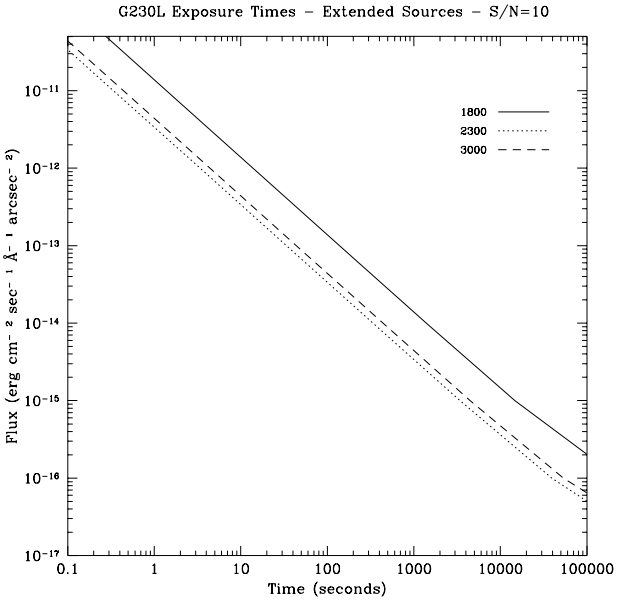

Figure 13.35: G230L Time to Saturate Peak Pixels as a Function of Source Flux, for observation taken through 0.2 arcsecond wide slit.

(a) Point Source

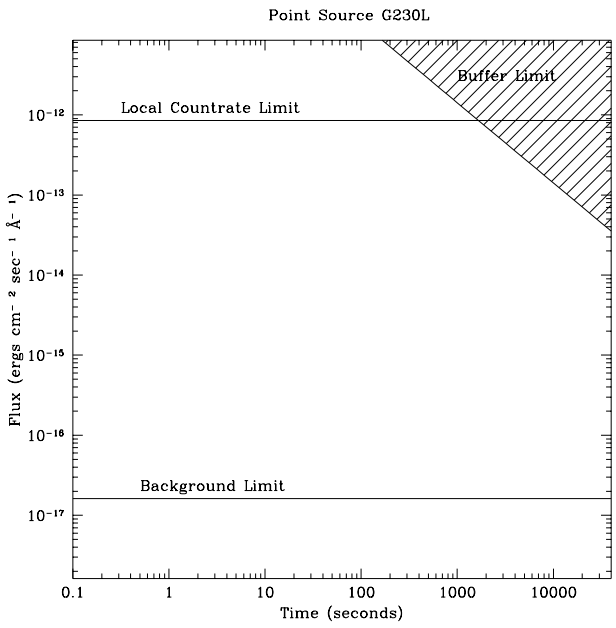

(b) Diffuse Source

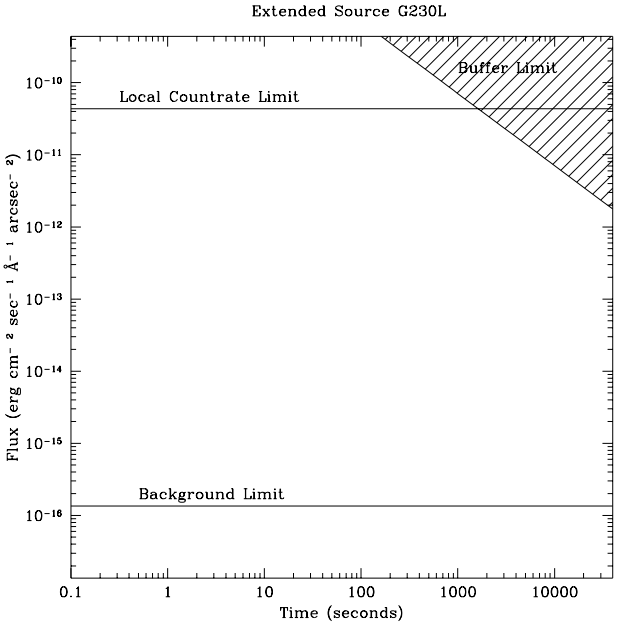

First Order Grating G230M

Like the G230L grating, the G230M grating is used with the NUV-MAMA and has a spectral range from 1650-3100 Å, however, with a resolving power R~10,000 a single exposure with the G230M grating covers only 90 Å, and the grating must be scanned, with a series of exposures taken at 19 distinct settings to cover the full spectral range. The G230M grating mode is designed for observations where spatially resolved, long slit, spectroscopy is desired at relatively high spectral resolution covering a limited region of the near-ultraviolet spectrum. The properties of the G230M grating are summarized below.

Grating	Spectral Range		Dispersion		Central Wavelengths
	Complete	Per Tilt	Å per Pixel	Tilts	
G230M	1640-3175	90	0.09	***Prime***	**1687, 1769, 1851, 1933, 2014 2095, 2176, 2257, 2338, 2419, 2499, 2579, 2659, 2739, 2818, 2898, 2977,3055, 3134**
				Secondary	1884, 2600, 2800, 2828

The available scan settings (central wavelength and minimum and maximum wavelengths covered in a single exposures) are shown graphically in Figure 13.36.

Figure 13.36: Wavelength Ranges for the G230M Grating Settings

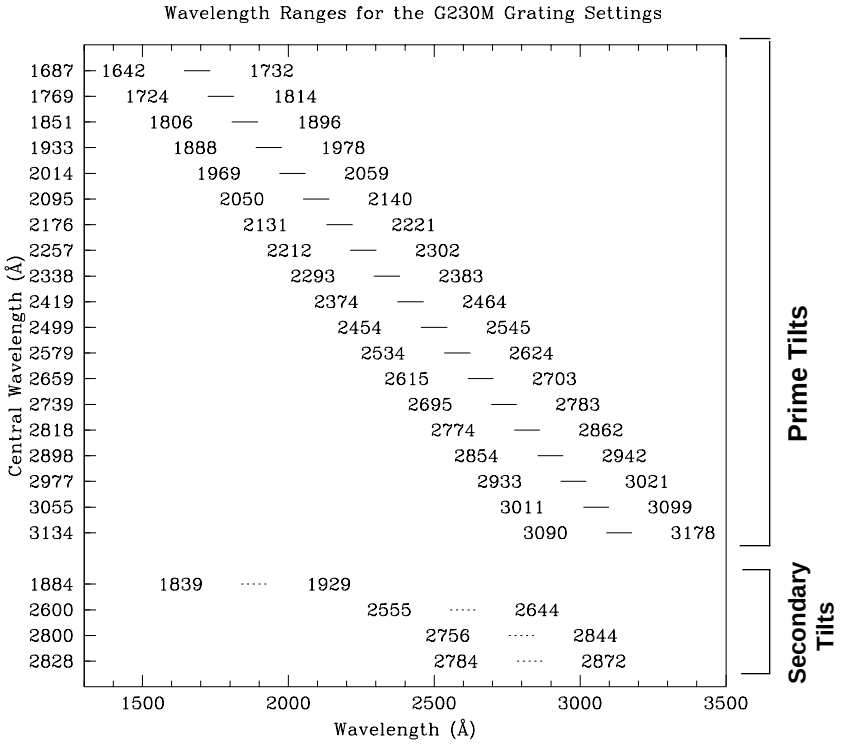

Notice that the CCD G230MB grating mode also covers the near-ultraviolet with comparable resolution. See “First Order Grating G230MB” on page 201 for a detailed comparison of these two grating modes in that wavelength regime. The sensitivity, exposure time signal-to-noise requirements, saturation exposure time limits, and bright object count limits for the G230M grating are summarized below.

Figure 13.37: G230M Point Source (left axis), and Diffuse Source (right axis) Sensitivities. Point source sensitivity assumes full transmission (zero slit losses). Diffuse source sensitivity assumes a 0.1” wide slit.

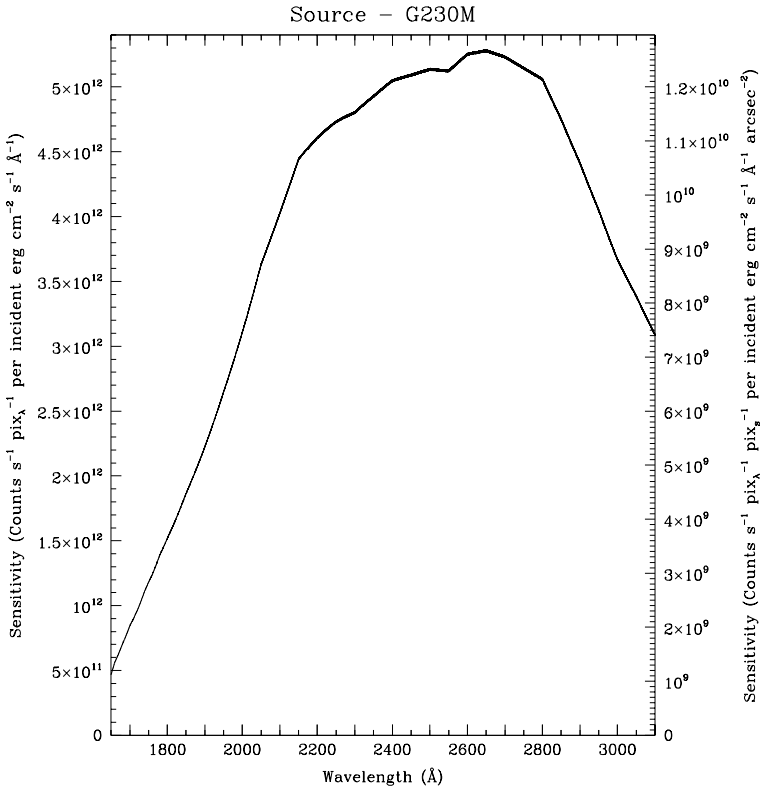

Table 13.8: G230M Point Source Sensitivities. Multiply sensitivity number by 0.029 times slit width in arcseconds to obtain diffuse source sensitivity.

λ	Sens.	λ	Sens.	λ	Sens.	λ	Sens.
1600	7.2E10	2100	4.0E12	2600	5.3E12	3100	3.1E12
1700	8.4E11	2200	4.6E12	2700	5.2E12	3200	1.5E12
1800	1.5E12	2300	4.8E12	2800	5.1E12		
1900	2.2E12	2400	5.0E12	2900	4.4E12		
2000	3.1E12	2500	5.1E12	3000	3.7E12		

Figure 13.38: G230M Time to Achieve a Signal-to-Noise of 10 per Spectral Resolution Element for Stars of Different Spectral Types, observed through the 0.2 arcsecond wide slit.

(a) O5 star

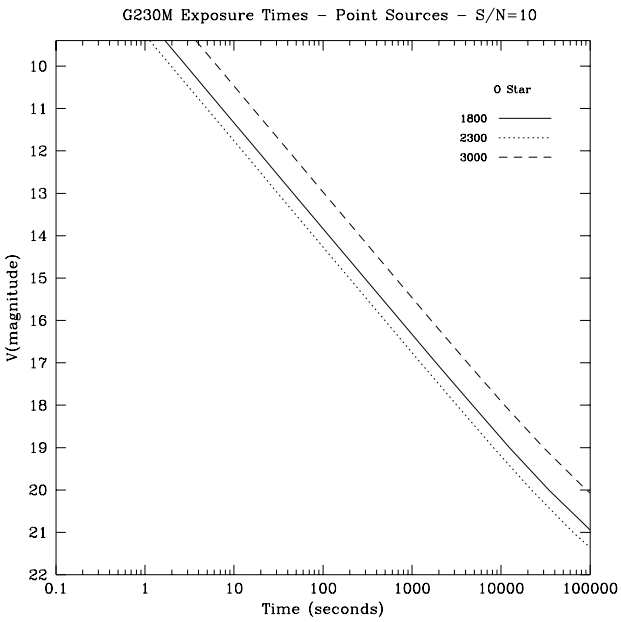

(b) AOV star

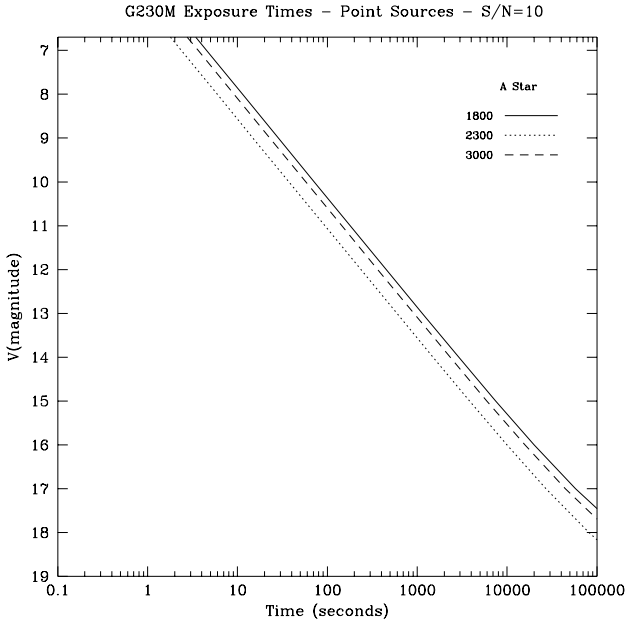

(c) G0V star

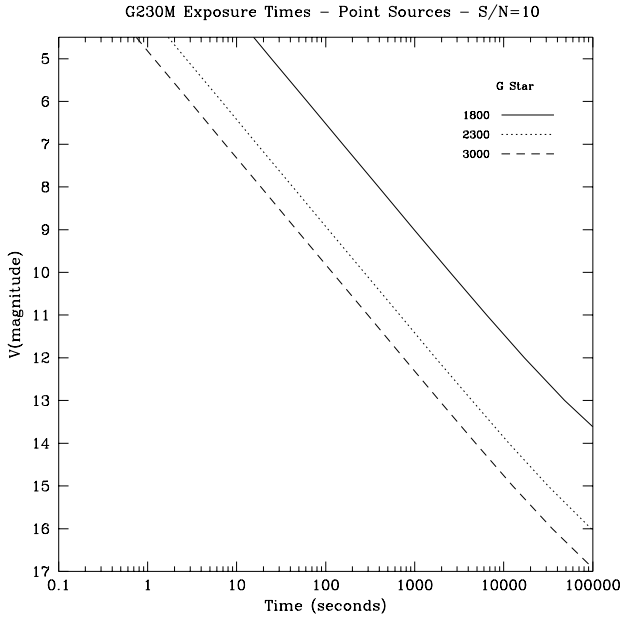

(d) M0V star

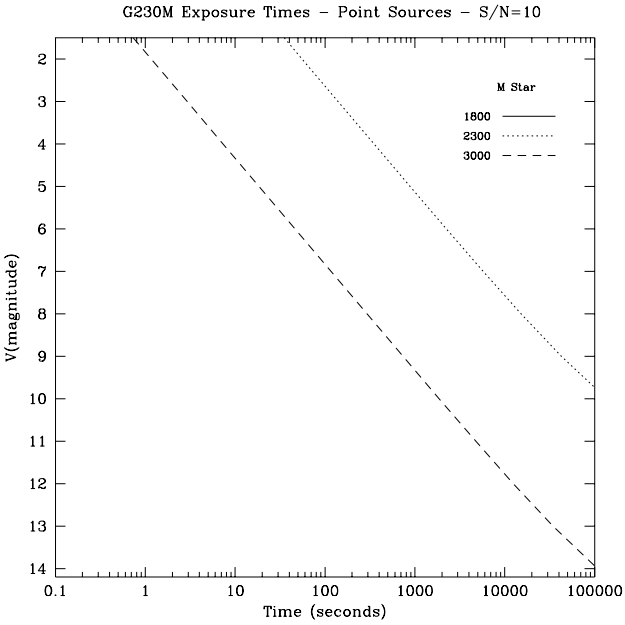

Figure 13.39: G230M Time to Achieve a Signal-to-Noise of 10 per Spectral Resolution Element for Point and Diffuse Sources Observed with the 0.2” Wide Slit, cgs units. Point sources are integrated over the PSF, diffuse sources are per two spatial pixels.

(a) Point Sources

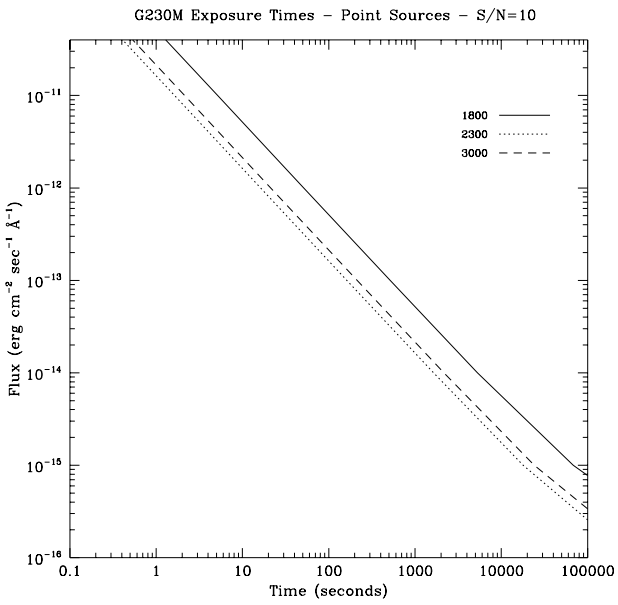

(b) Diffuse Sources

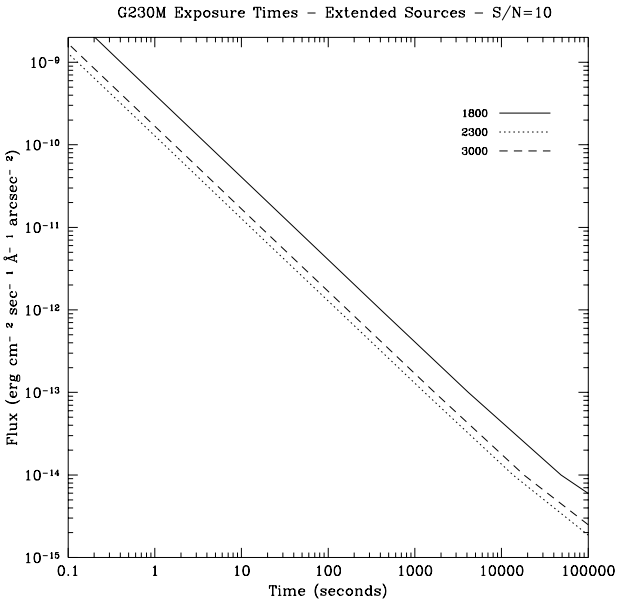

Figure 13.40: G230M Time to Saturate Peak Pixel as a Function of Source Flux, for observation taken through 0.2 arcsecond wide slit.

(a) Point Sources

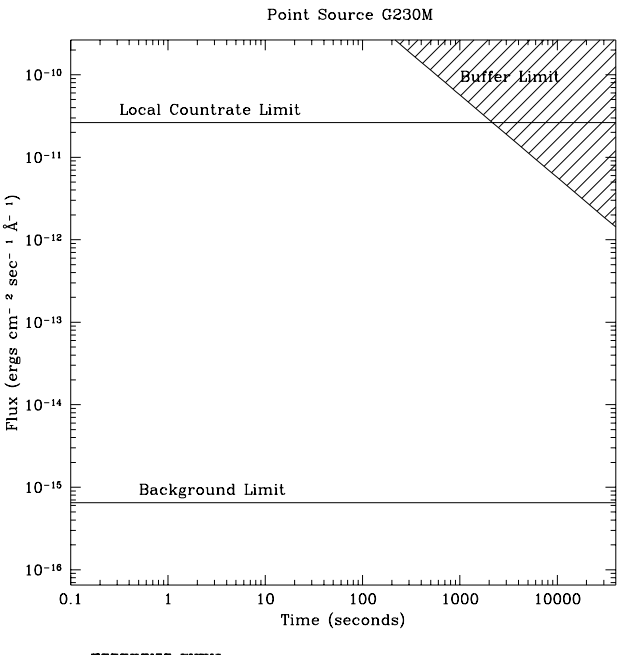

(b) Diffuse Sources

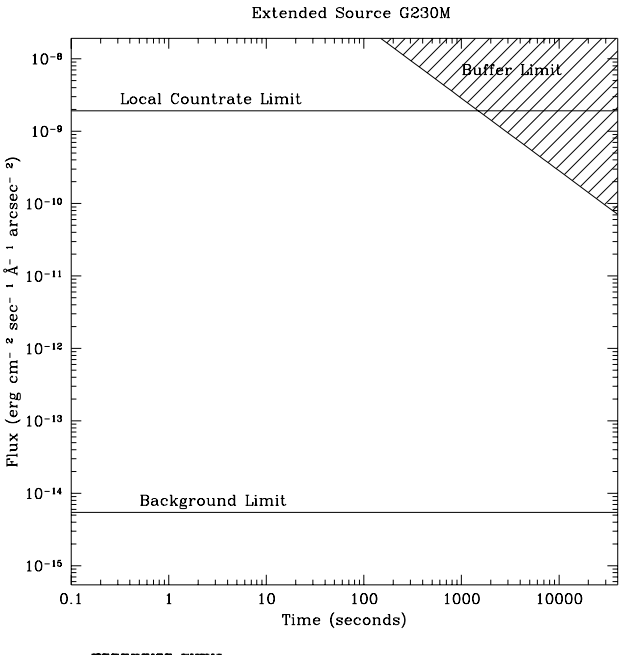

First Order Grating G140L

The G140L grating mode is used with the FUV-MAMA, has a resolving power R~1000, and covers a spectral range from 1150–1700 Å in a single exposure. The G230L grating mode is designed for observations where high spectral resolution is not required, but efficient, spatially resolved spectroscopy providing wide spectral coverage in the ultraviolet is desired. Notice, that by taking two observations, one with G230L and one with G140L, the full spectral region, from 1150 to 3100 Å can be efficiently observed at an R~1000. The properties of the G140L grating mode are summarized below.

	Spectral Range		Dispersion		Central Wavelengths
Grating	**Complete**	**Per Tilt**	**Å per Pixel**	**Tilts**	
G140L	1150-1730	610	0.6	***Prime***	**1425**

The sensitivity, exposure time signal-to-noise requirements, saturation exposure time limits, and bright object count limits for the G140L grating are summarized on page 214.

Figure 13.41: G140L Point Source (left axis), and Diffuse Source (right axis) Sensitivities. Point source sensitivity assumes full transmission (zero slit losses). Diffuse source sensitivity assumes a 0.1” wide slit.

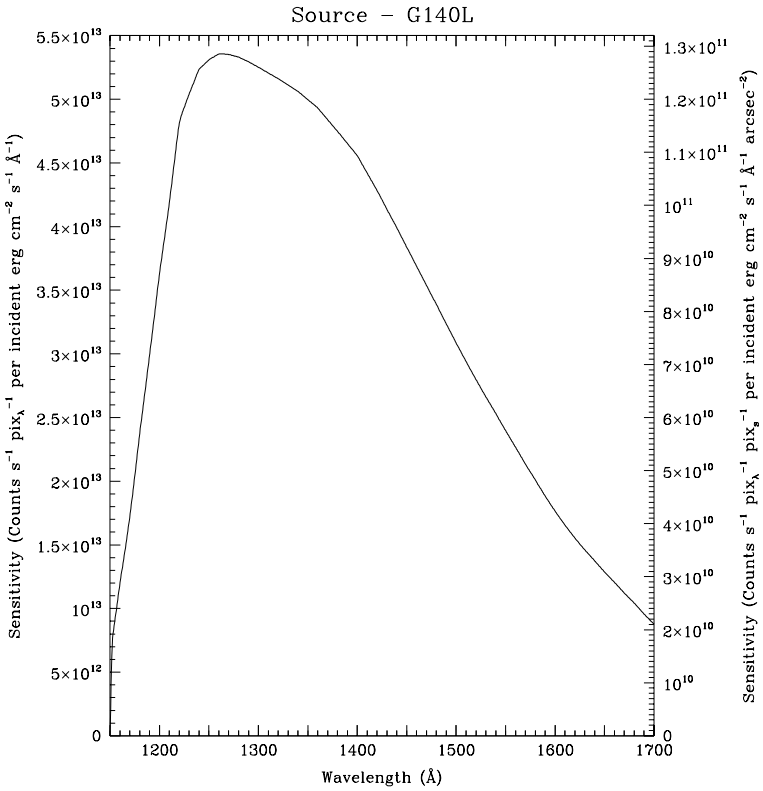

Table 13.9: G140L Point Source Sensitivities. Multiply sensitivity number by 0.0244 times the slit width in arcseconds to obtain diffuse source sensitivity.

λ	**Sens.**	λ	**Sens.**	λ	**Sens.**	λ	**Sens.**
1150	4.25E8	1350	5.0E13	1600	1.8E13	1850	1.5E12
1175	2.0E13	1400	4.5E13	1650	1.3E13	1900	3.4E11
1216	4.6E13	1450	3.8E13	1700	8.8E12	1950	7.6E10
1250	5.3E13	1500	3.1E13	1750	6.0E12	2000	1.7E10
1300	5.2E13	1550	2.4E13	1800	4.0E12		

Figure 13.42: G140L Time to Achieve a Signal-to-Noise of 10 per Spectral Resolution Element for Stars of Different Spectral Types, observed through the 0.2 arcsecond wide slit.

(a) O5 star

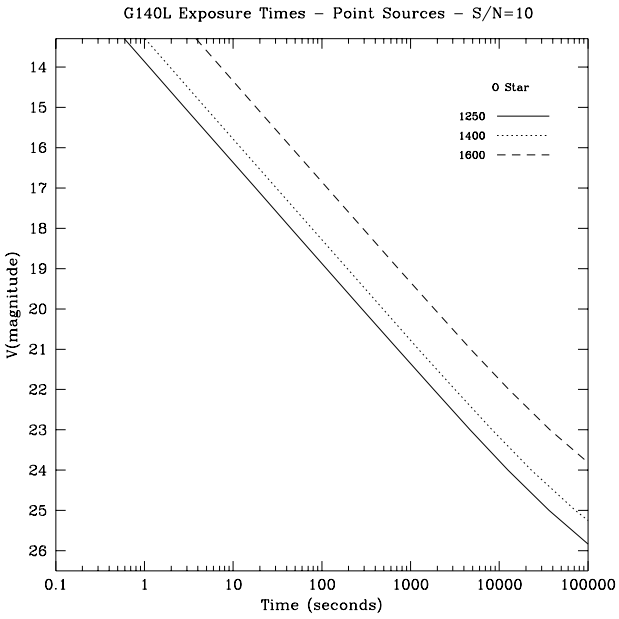

(b) AOV star

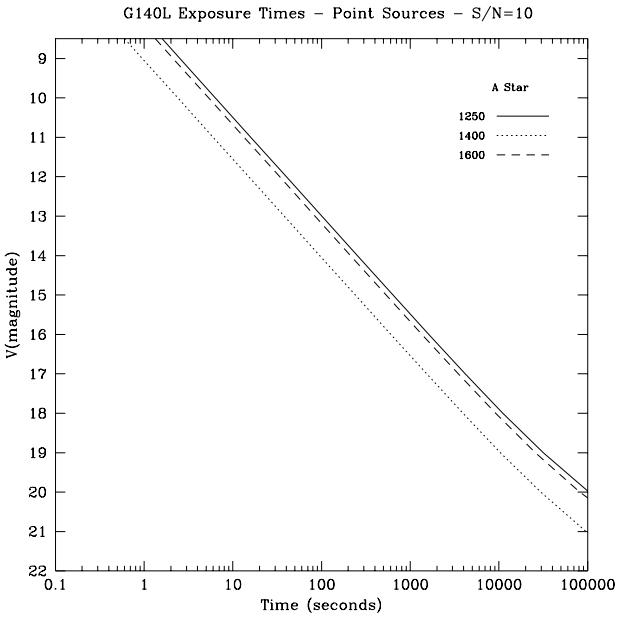

(c) G0V star

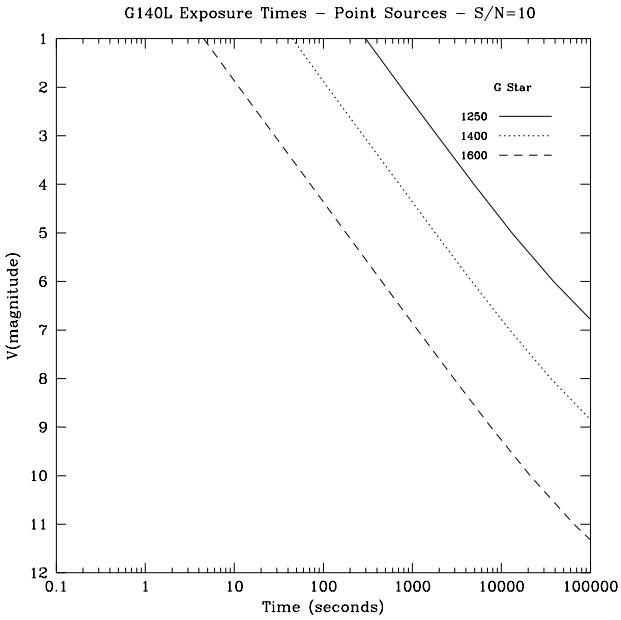

(d) M0V star

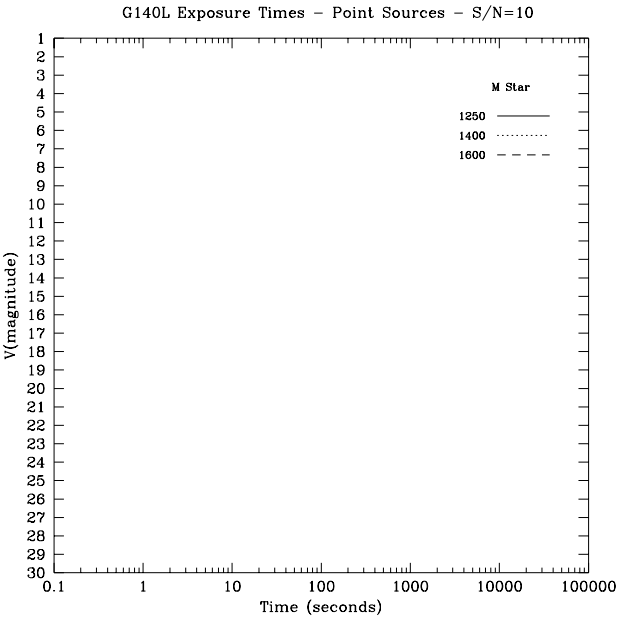

Figure 13.43: G140L Time to Achieve a Signal-to-Noise of 10 per Spectral Resolution Element for Point and Diffuse Source Observed with the 0.2” Wide Slit, cgs units. Point sources are integrated over the PSF, diffuse sources are per two spatial pixels

.

(a) Point Sources

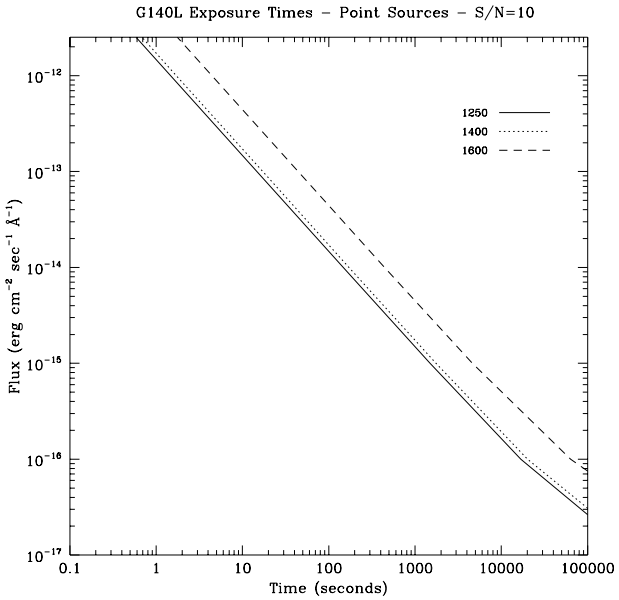

(b) Diffuse Sources

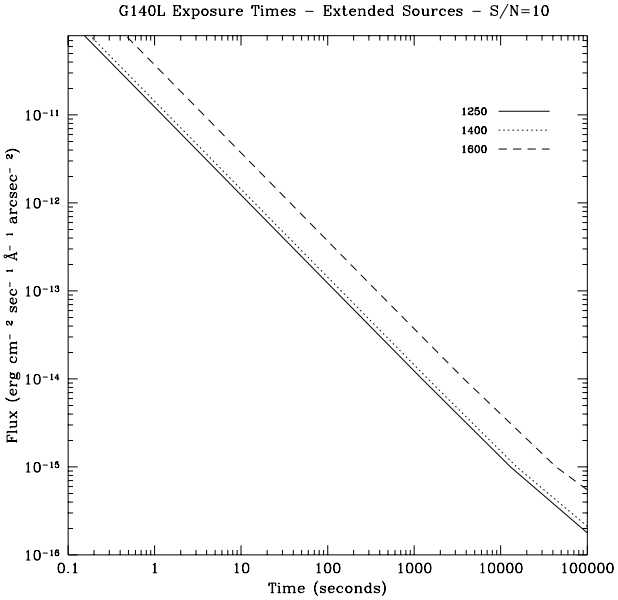

Figure 13.44: G140L Time to Saturate Peak Pixel as a Function of Source Flux, for observation taken through 0.2 arcsecond wide slit.

(a) Point Sources

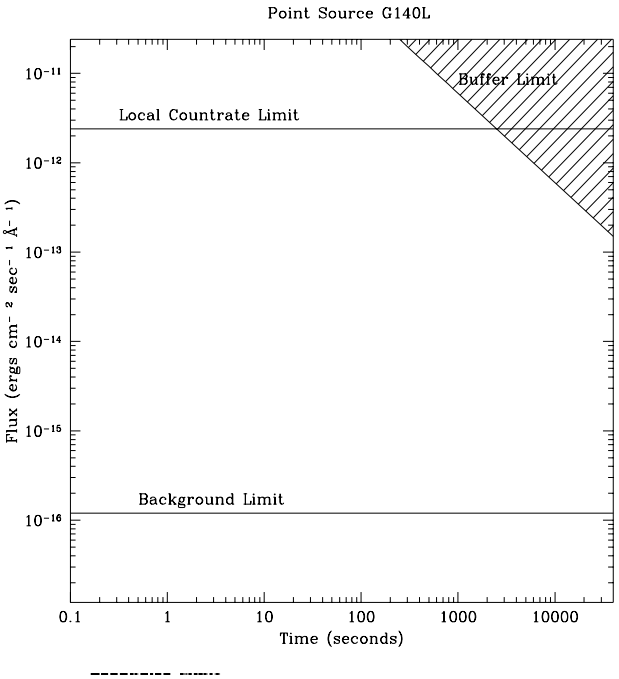

(b) Diffuse Sources

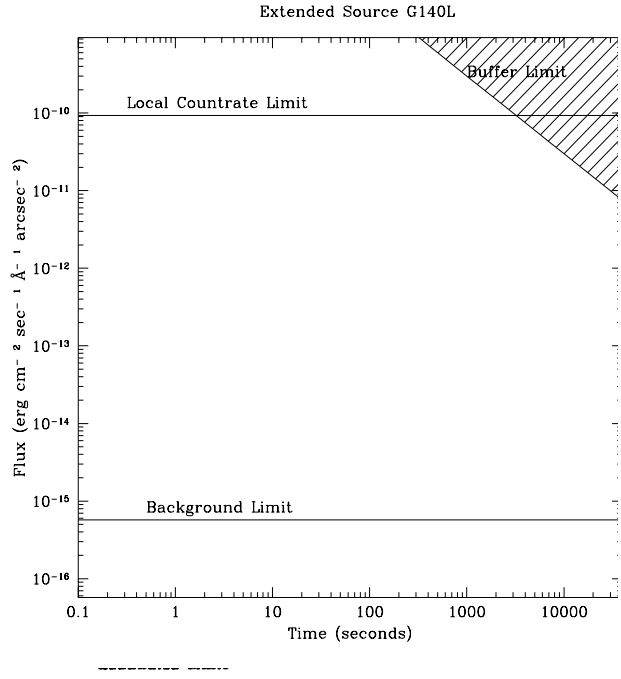

First Order Grating G140M

The G140M grating mode is used with the FUV-MAMA and has a spectral range from 1150-1700 Å, however, with a resolving power R~10,000, a single exposure with this grating covers only 55 Å. The grating must be scanned, with a series of exposures taken at 12 distinct settings to cover the full spectral range. The G140M grating mode is designed for observations where spatially resolved, long slit, spectroscopy is desired at relatively high spectral resolution over a limited region of the ultraviolet spectrum. The properties of the G140M grating are summarized in the table below.

Grating	Spectral Range		Dispersion		Central Wavelengths
	Complete	Per Tilt	Å per Pixel	Tilts	
G140M	1150-1740	55	0.05	***Prime***	**1173, 1222, 1272, 1321, 1371, 1420, 1470, 1518, 1567, 1616, 1665, 1714**
				Secondary	1218, 1387, 1400, 1540, 1550, 1640

The available scan settings (central wavelength and minimum and maximum wavelengths covered in a single exposure) are shown graphically in Figure 13.45.

The sensitivity, exposure time signal-to-noise requirements, saturation exposure time limits, and bright object count limits for the G140M grating are summarized below.

Figure 13.45: Wavelength Ranges for the G140M Grating Settings

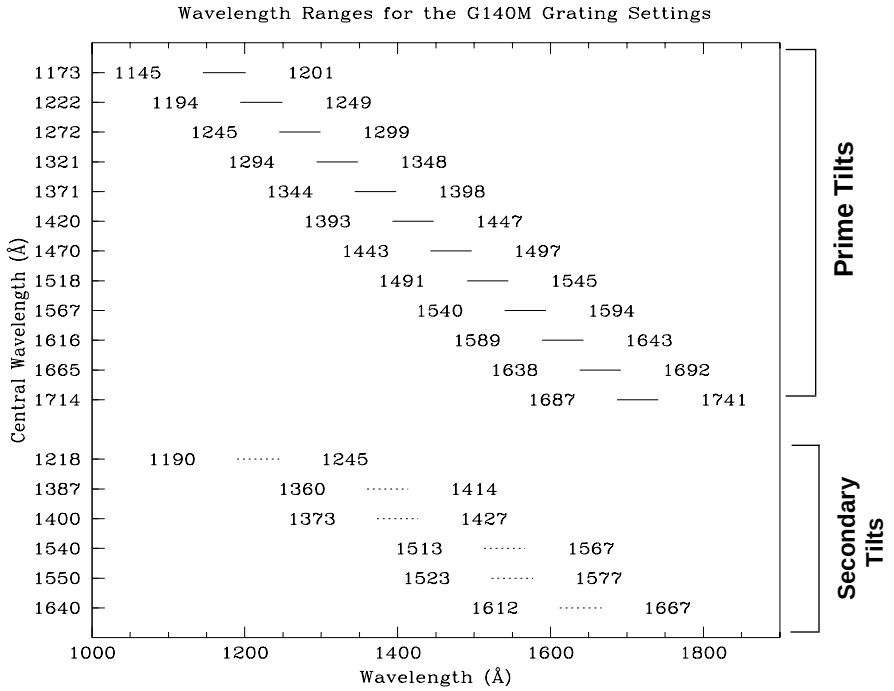

Figure 13.46: G140M Point Source (left axis), and Diffuse Source (right axis) Sensitivities. Point source sensitivity assumes full transmission (zero slit losses). Diffuse source sensitivity assumes a 0.1” wide slit.

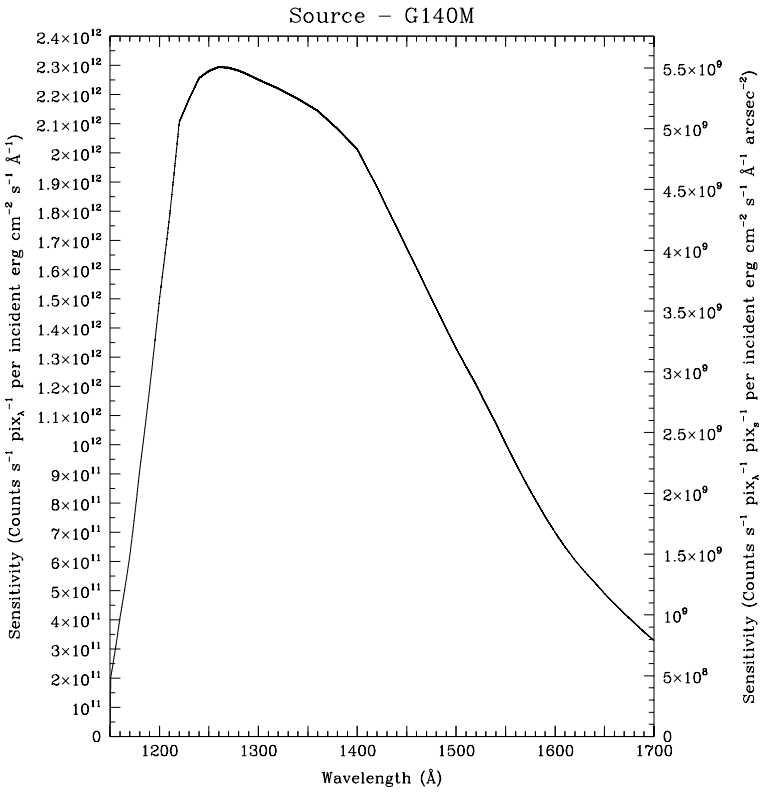

Table 13.10: G140M Point Source Sensitivities. Multiply sensitivity number by 0.029 times the slit width in arcseconds to obtain diffuse source sensitivity.

λ	**Sens.**	λ	**Sens.**	λ	**Sens.**	λ	**Sens.**
1150	3.69E7	1300	2.2E12	1500	1.3E12	1700	3.3E11
1175	7.6E11	1350	2.2E12	1550	1.0E12	1750	2.3E11
1216	2.0E12	1400	2.0E12	1600	7.0E11		
1250	2.3E12	1450	1.7E12	1650	4.9E11		

Figure 13.47: G140M Time to Achieve a Signal-to-Noise of 10 per Spectral Resolution Element for Stars of Different Spectral Types, observed through the 0.2 arcsecond wide slit.

(a) O5 star

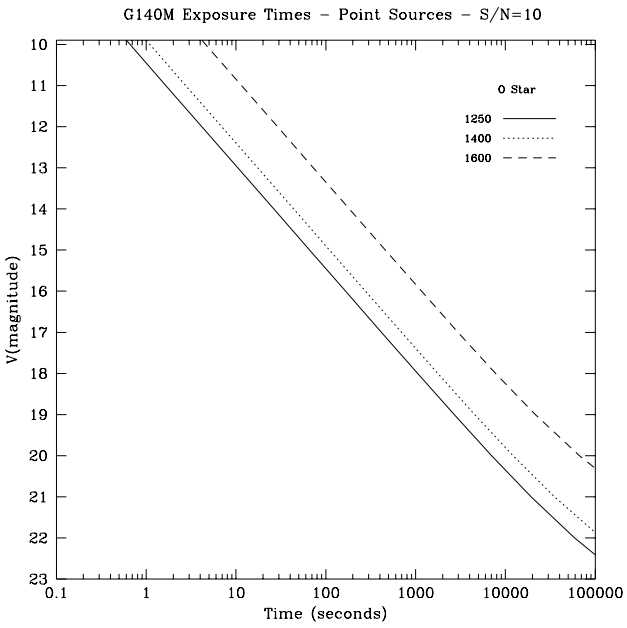

(b) AOV star

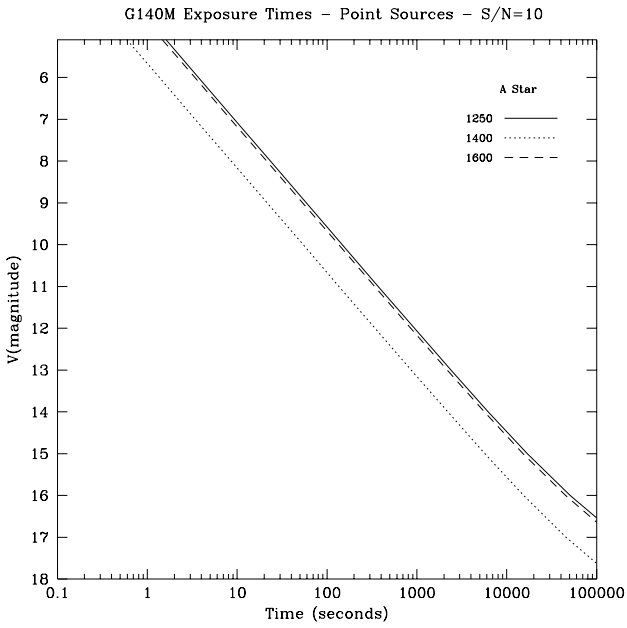

(c) G0V star

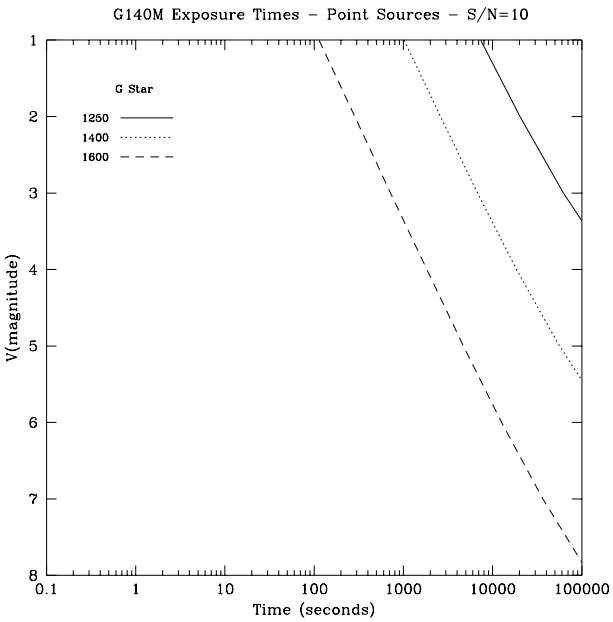

(d) M0V star

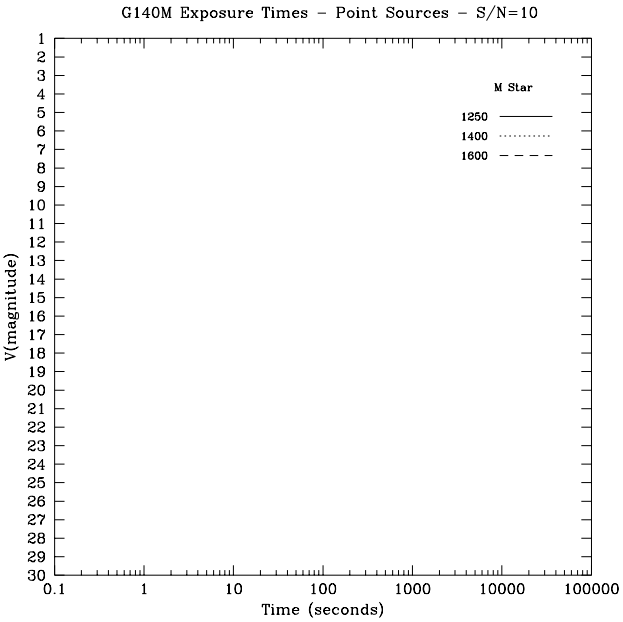

Figure 13.48: G140M Time to Achieve a Signal-to-Noise of 10 per Spectral Resolution Element for Point and Diffuse Source Observed with the 0.2” Wide Slit, cgs units. Point sources are integrated over the PSF, diffuse sources are per two spatial pixels.

.

(a) Point Source

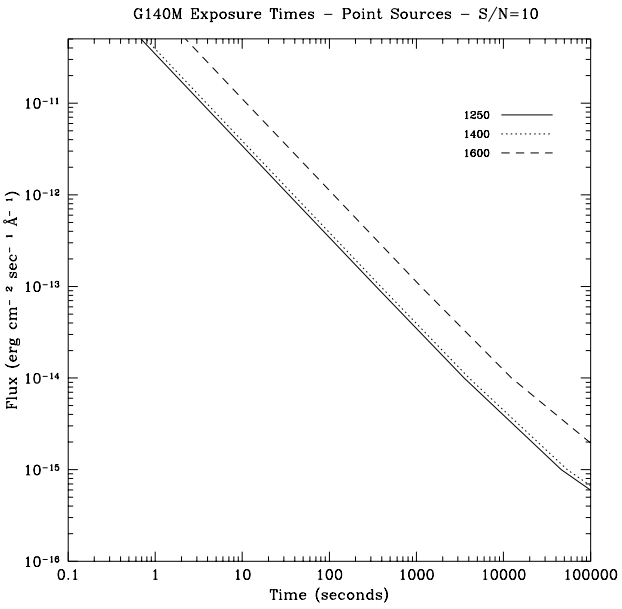

(b) Diffuse Source

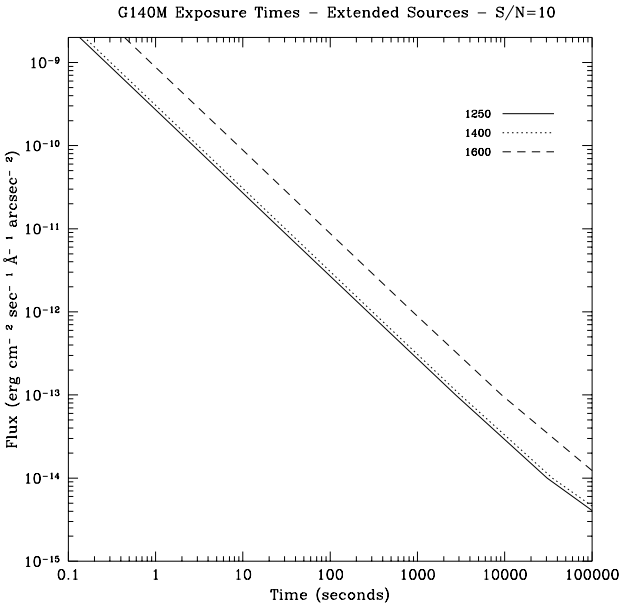

Figure 13.49: G140M Time to Saturate Peak Pixel as a Function of Source Flux, for observation taken through 0.2 arcsecond wide slit.

(a) Point Source

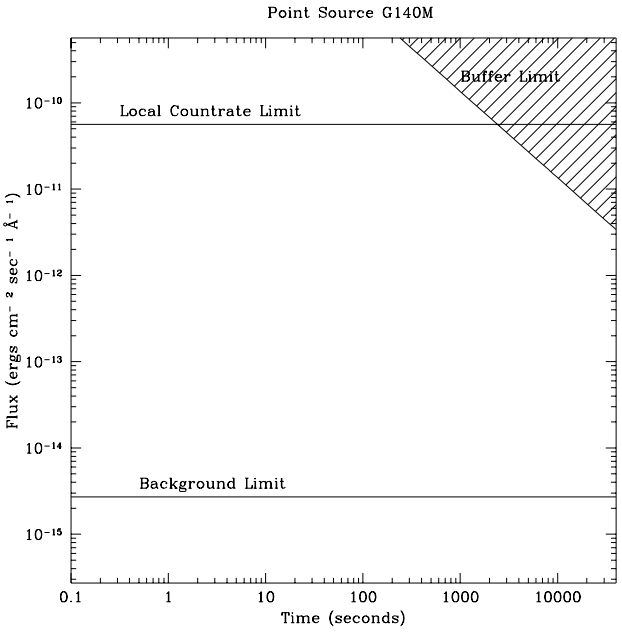

(b) Diffuse Source

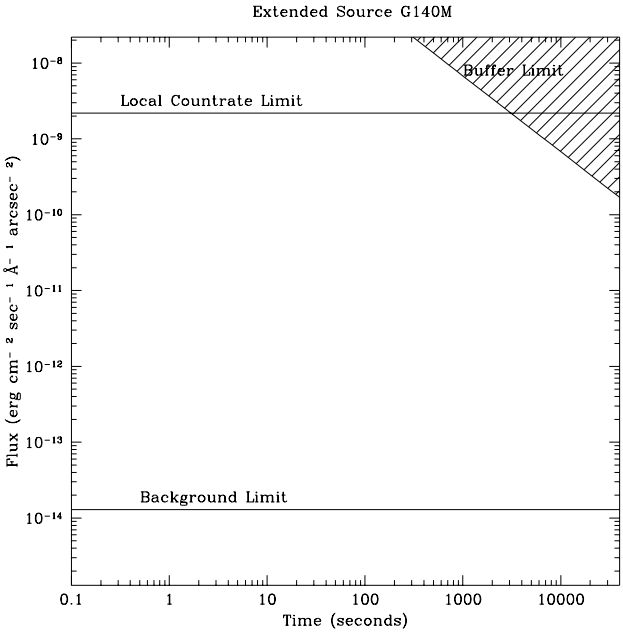

Echelle Grating E230M

The E230M grating is used with the NUV-MAMA and provides echelle spectra at a resolving power of 23500 from 1650–3100 Å. The table below summarizes this mode's properties.

Grating	Spectral Range		Dispersion		Central Wavelengths
	Complete	Per Tilt	Å per Pixel	Tilts	
E230M	1575-3110	~800	λ/60,000	***Prime***	**1978, 2707**
				Secondary	2124, 2269, 2415, 2561

A single exposure with this grating covers 800 Å over ~20-40 orders. The inter-order separation is ~18 pixels (0.52 arcseconds) at 1650 Å and 62.5 pixels (~1.8 arcseconds) at 3100 Å. The grating must be scanned, with exposures taken at two distinct settings to cover the full spectral range of the grating. The full set of available scan settings (central wavelength and minimum and maximum wavelengths covered in a single exposures) are shown graphically in Figure 13.50.

Figure 13.50: Wavelength Ranges for the E230M Grating Settings

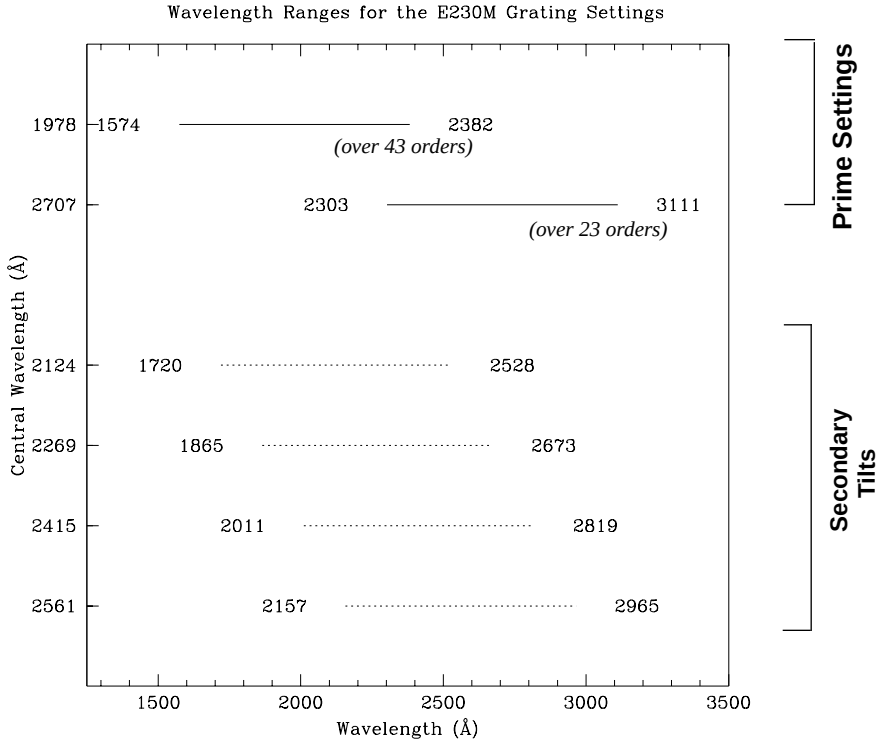

The sensitivity, exposure time signal-to-noise requirements, saturation exposure time limits, and bright object count limits for the E230M echelle grating mode are summarized below.

Figure 13.51: E230M Point Source (left axis), and Diffuse Source (right axis) Sensitivities. Point source sensitivity assumes full transmission (zero slit losses). Diffuse source sensitivity assumes a 0.1” wide slit.

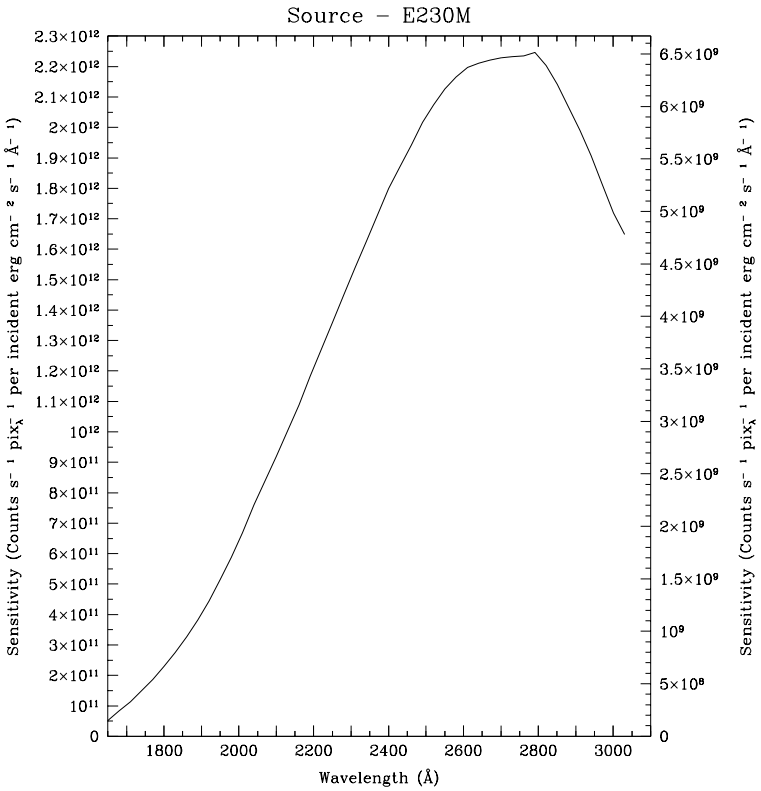

Table 13.11: E230M Point Source Sensitivities. Multiply sensitivity number by 0.029 times the slit width in arcseconds to obtain diffuse source sensitivity.

λ	**Sens.**	λ	**Sens.**	λ	**Sens.**	λ	**Sens.**
1700	1.0E11	2100	9.2E11	2500	2.0E12	2900	2.0E12
1800	2.3E11	2200	1.2E12	2600	2.2E12	3000	1.7E12
1900	4.0E11	2300	1.5E12	2700	2.2E12		
2000	6.4E11	2400	1.8E12	2800	2.2E12		

Figure 13.52: E230M Time to Achieve a Signal-to-Noise of 10 per Spectral Resolution Element for Stars of Different Spectral Types, observed through the 0.2 arcsecond wide slit.

(a) O5 star

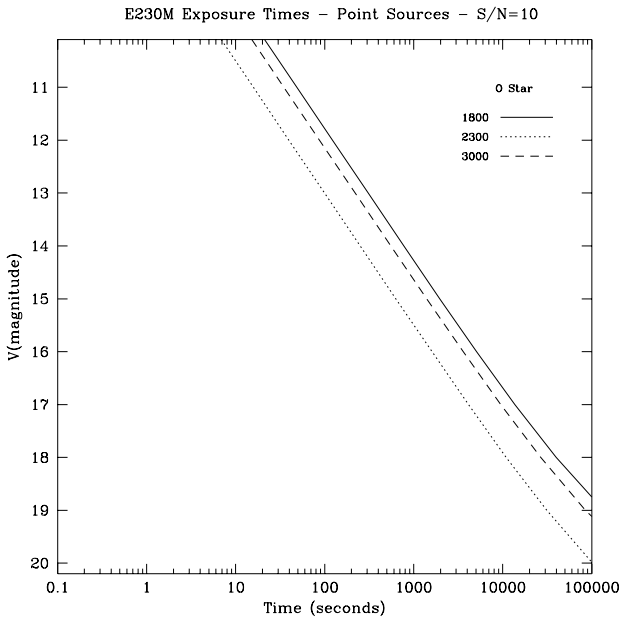

(b) AOV star

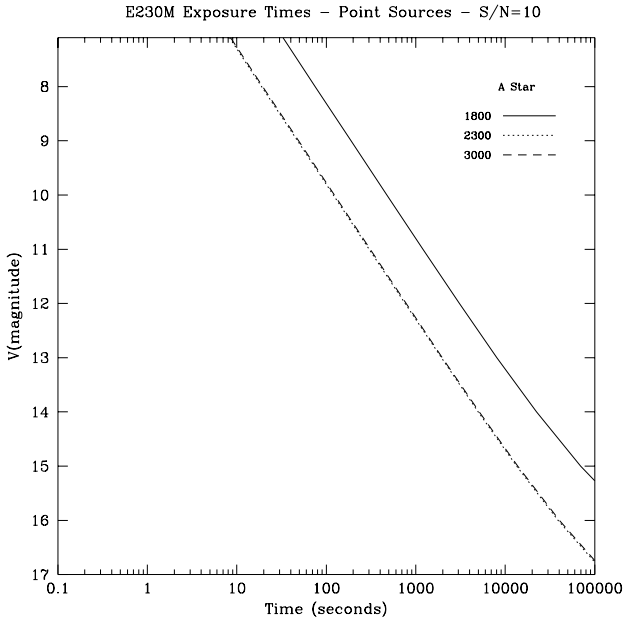

(c) G0V star

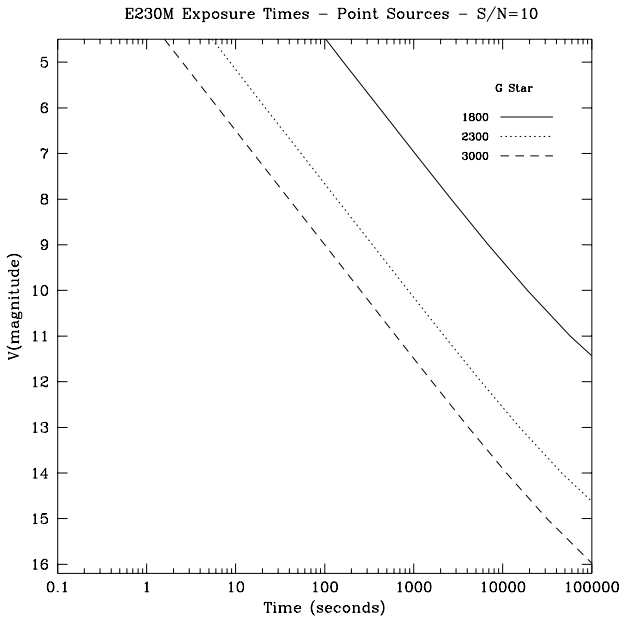

(d) M0V star

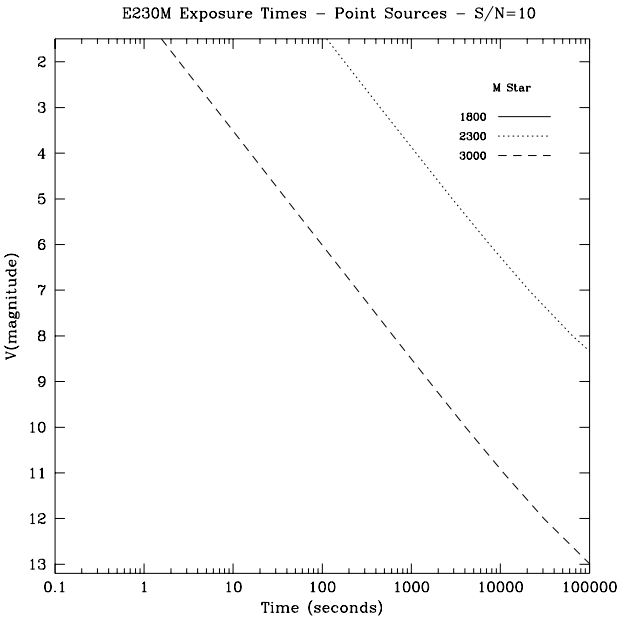

Figure 13.53: E230M Time to Achieve a Signal-to-Noise of 10 per spectral resolution element for Point and Diffuse Source Observed with the 0.2” Wide Slit, cgs units. Point sources are integrated over the PSF, diffuse sources are per two spatial pixels

(a) Point Sources

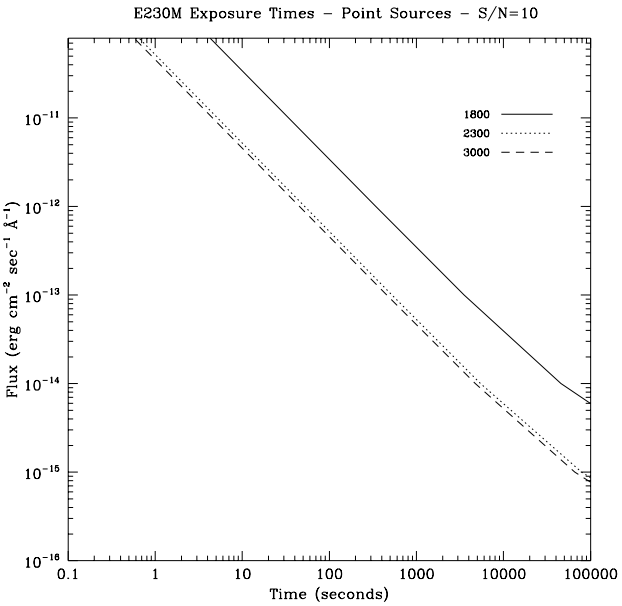

(b) Diffuse Sources

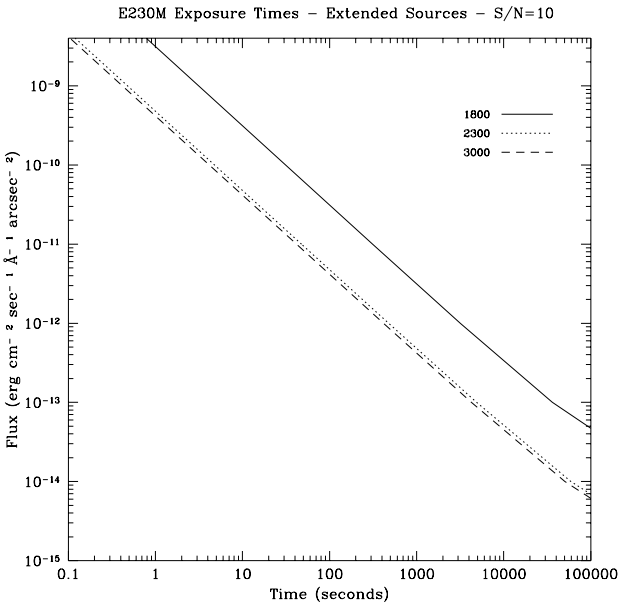

Figure 13.54: E230M Time to Saturate Peak Pixel as a Function of Source Flux, for observation taken through 0.2 arcsecond wide slit.

(a) Point Sources

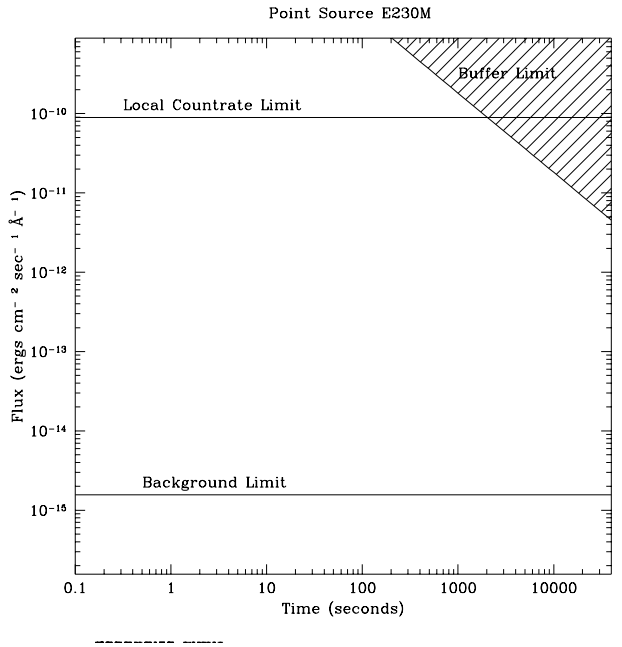

(b) Diffuse Sources

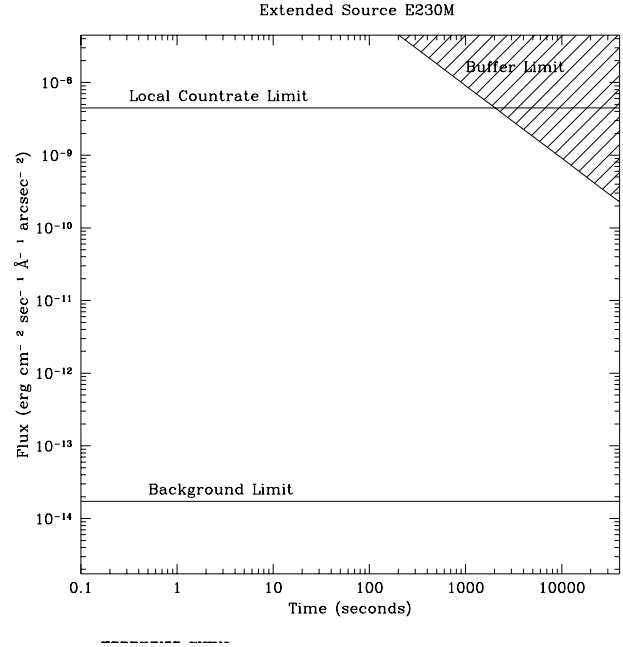

Echelle Grating E230H

The E230H grating is used with the NUV-MAMA and provides echelle spectra at a resolving power of ~100,000 from 1650-3100 Å. The table below summarizes this mode's properties.

Grating	Spectral Range		Dispersion		Central Wavelengths
	Complete	Per Tilt	Å per Pixel	Settings	
E230H	1625-3150	~267	λ/228,000	***Prime***	**1763, 2013, 2263, 2513, 2762, 3012**
				Secondary	1813, 1863, 1913, 1963, 2063, 2113, 2163, 2213, 2313, 2363, 2413, 2463, 2563, 2613, 2663, 2713, 2812, 2862, 2912, 2962

A single E230H echellogram covers ~267 Å, over ~20-70 orders. The orders are spaced by only ~ 12.7 pixels (0.37 arcseconds) at 1650 Å and 47.2 pixels (~1.38 arcseconds) at 3100 Å. The grating must be scanned, with a exposures taken at six distinct settings to cover the full spectral range of the grating. The full set of available scan settings (central wavelength and minimum and maximum wavelengths covered in a single exposures) are shown graphically in Figure 13.55.

Figure 13.55: Wavelength Ranges for the E230H Grating Settings

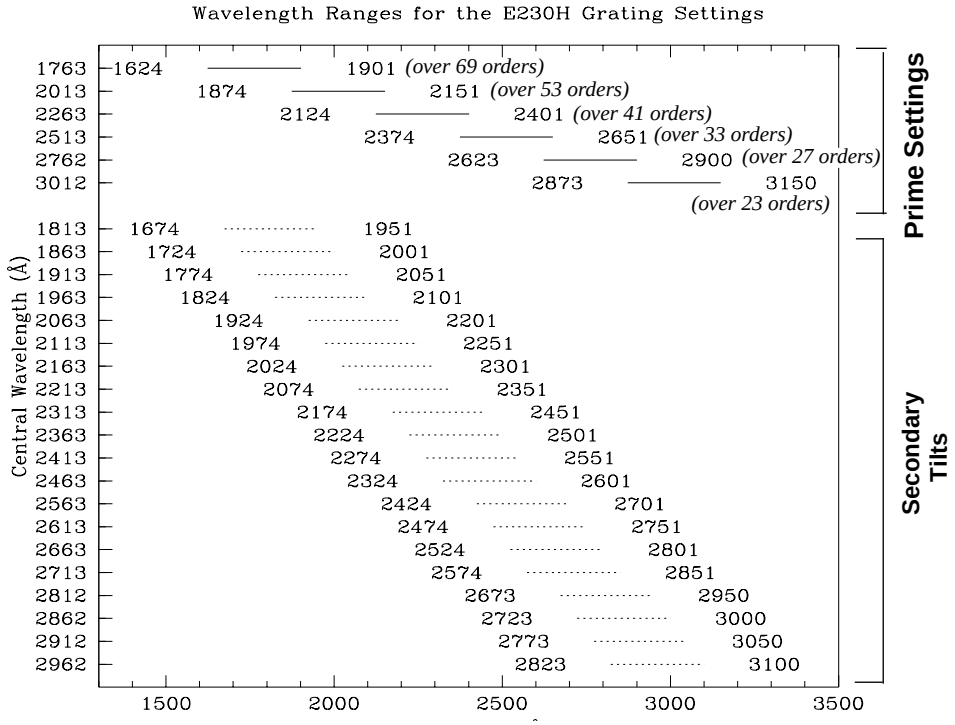

The sensitivity, exposure time signal-to-noise requirements, saturation exposure time limits, and bright object count limits for the E230M echelle grating mode are summarized below.

Figure 13.56: E230H Point Source (left axis), and Diffuse Source (right axis) Sensitivities. Point source sensitivity assumes full transmission (zero slit losses). Diffuse source sensitivity assumes a 0.1” wide slit.

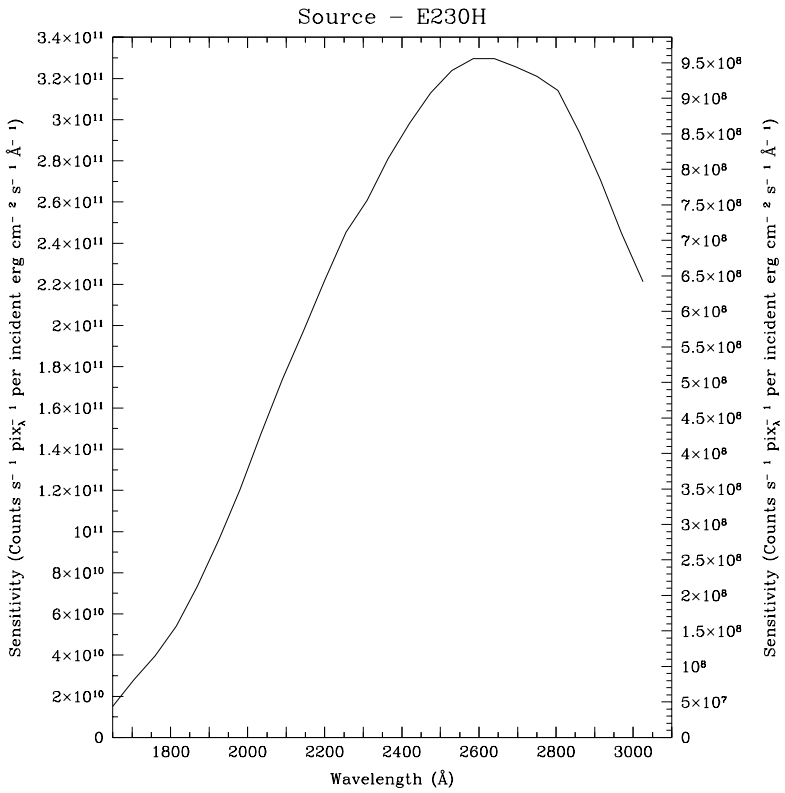

Table 13.12: E230H Point Source Sensitivities. Multiply sensitivity number by 0.029 times the slit width in arcseconds to obtain diffuse source sensitivity.

λ	**Sens.**	λ	**Sens.**	λ	**Sens.**	λ	**Sens.**
1700	2.7E10	2100	1.8E11	2500	3.2E11	2900	2.8E11
1800	5.0E10	2200	2.2E11	2600	3.4E11	3000	2.3E11
1900	8.6E10	2300	2.6E11	2700	3.3E11		
2000	1.3E11	2400	2.9E11	2800	3.2E11		

Figure 13.57: E230H Time to Achieve a Signal-to-Noise of 10 per Spectral Resolution Element for Stars of Different Spectral Types, observed through the 0.2 arcsecond wide slit.

(a) O5 star

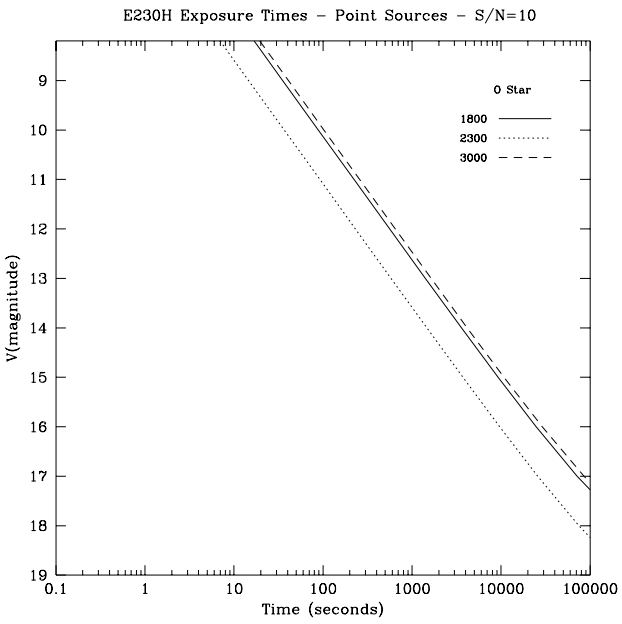

(b) AOV star

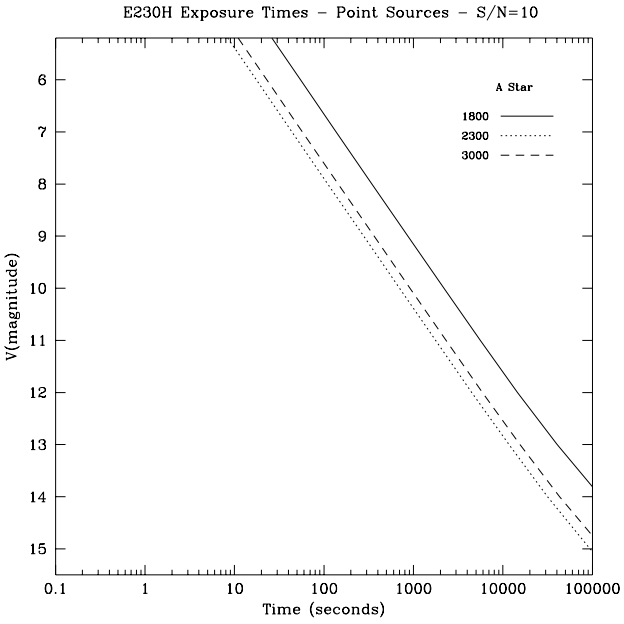

(c) G0V star

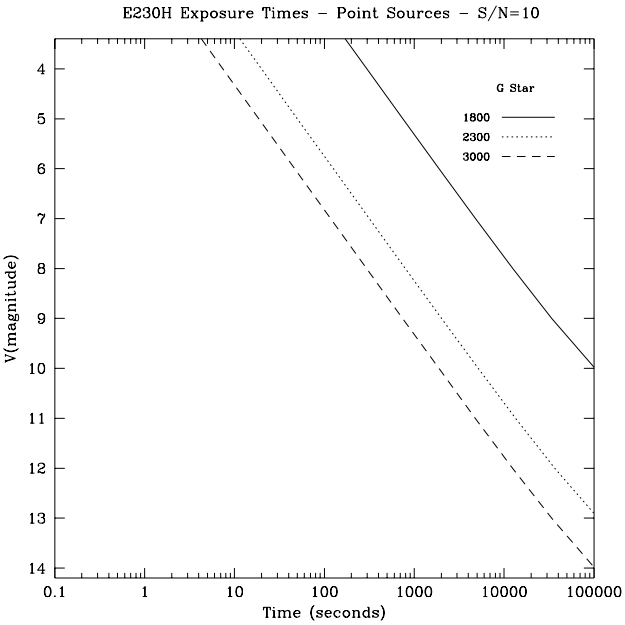

(d) M0V star

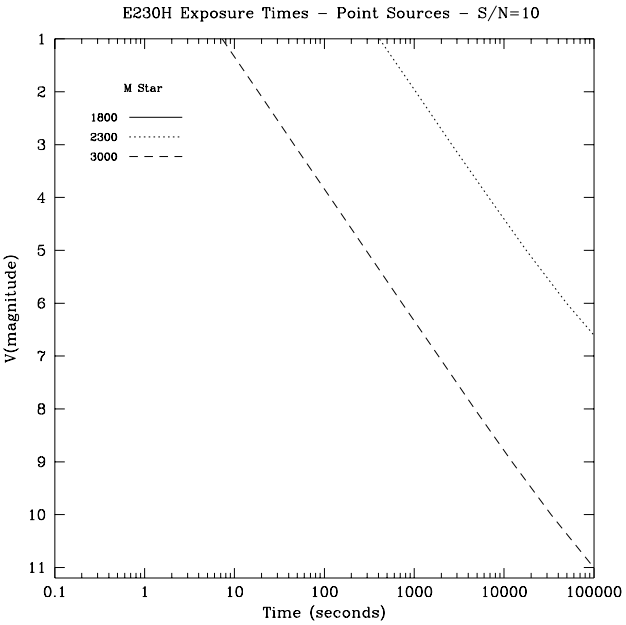

Figure 13.58: E230H Time to Achieve a Signal-to-Noise of 10 per Spectral Resolution Element for Point and Diffuse Source Observed with the 0.2” Wide Slit, cgs units. Point sources are integrated over the PSF, diffuse sources are per two spatial pixels.

(a) Point Sources

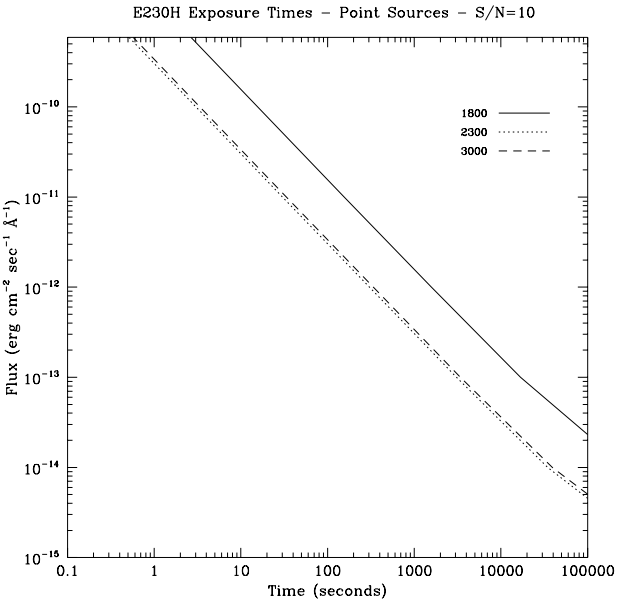

(b) Diffuse Sources

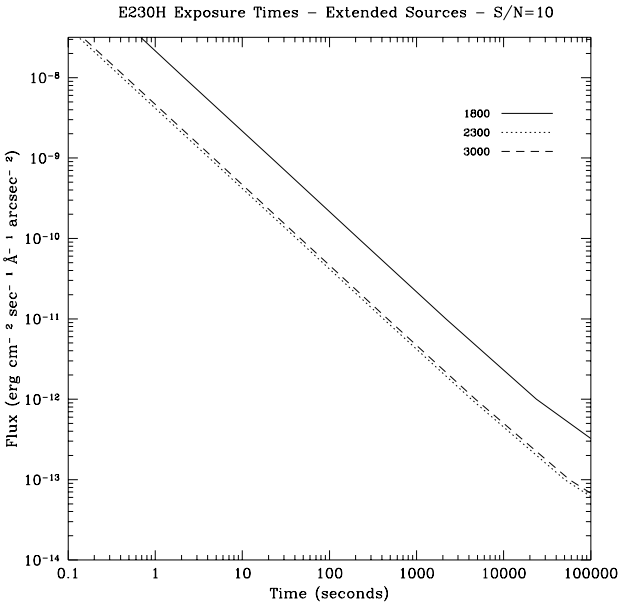

Figure 13.59: E230H Time to Saturate Peak Pixel as a Function of Source Flux, for observation taken through 0.2 arcsecond wide slit.

(a) Point Sources

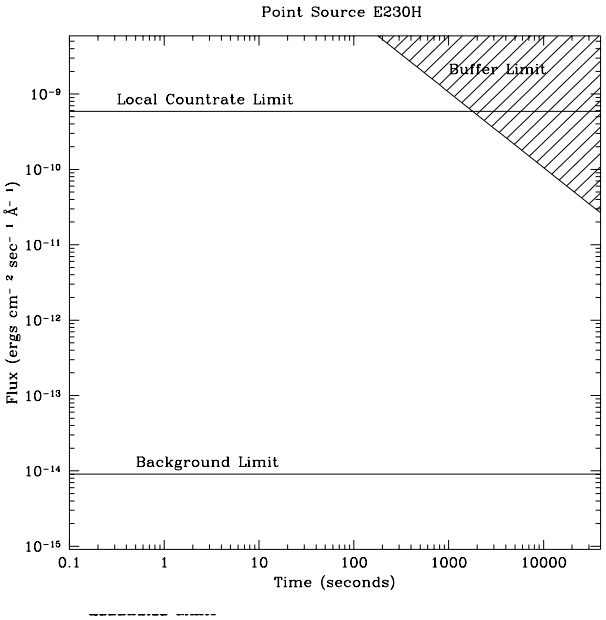

(b) Diffuse Sources

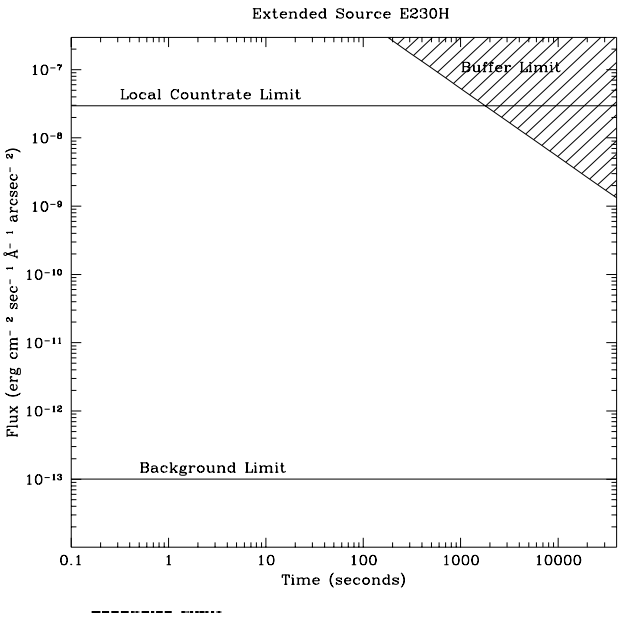

Echelle Grating E140M

The E140M grating is used with the FUV-MAMA and provides echelle spectra at a resolving power of 35000 from 1150-1700 Å. The table below summarizes this mode's properties.

Grating	Spectral Range		Dispersion		Central Wavelengths
	Complete	Per Tilt	Å per Pixel	Settings	
E140M	1150-1700	600	λ/91700	***Prime***	**1425 (see text below) - over ~45 orders**

A single E140M echellogram covers ~600 Å, however at wavelengths longward of 1649 Å, the echelle orders overrun the width of the detector in the dispersion direction, so there will be three small gaps in the wavelength coverage. One gap of ~0.2 Å, one of ~0.4 Å, and one of ~0.7 Å, are expected between 1649 and 1700 Å. Since grating alignment is not yet finalized, the precise locations of those gaps are not known at this time. Two prime central wavelengths will ultimately be defined for this grating; these central wavelengths will shift the echelle format along the dispersion axes, so that by taking two exposures, one at each central wavelength, complete spectral coverage between 1649 Å and 1700 Å can be achieved. When defining the central wavelength settings for this grating, care will be taken to assure, in as much as is possible, that important astronomical lines will not fall in the gap regions; however for the purposes of planning your Cycle 7 Proposal, if you require complete (or multiple line) wavelength coverage from 1649 to 1700 Å, you should assume you will need to take two separate exposures to cover this region. Note that complete wavelength coverage from 1150 Å to 1649 Å is provided in a single setting for this grating.

The separation between orders is ~15 pixels (or 0.44 arcseconds) at 1150 Å and ~33 (0.96 arcseconds) at 1700 Å.

The sensitivity, exposure time signal-to-noise requirements, saturation exposure time limits, and bright object count limits for the E140M echelle grating mode are summarized below.

Figure 13.60: E140M Point Source (left axis), and Diffuse Source (right axis) Sensitivities. Point source sensitivity assumes full transmission (zero slit losses). Diffuse source sensitivity assumes a 0.1” wide slit.

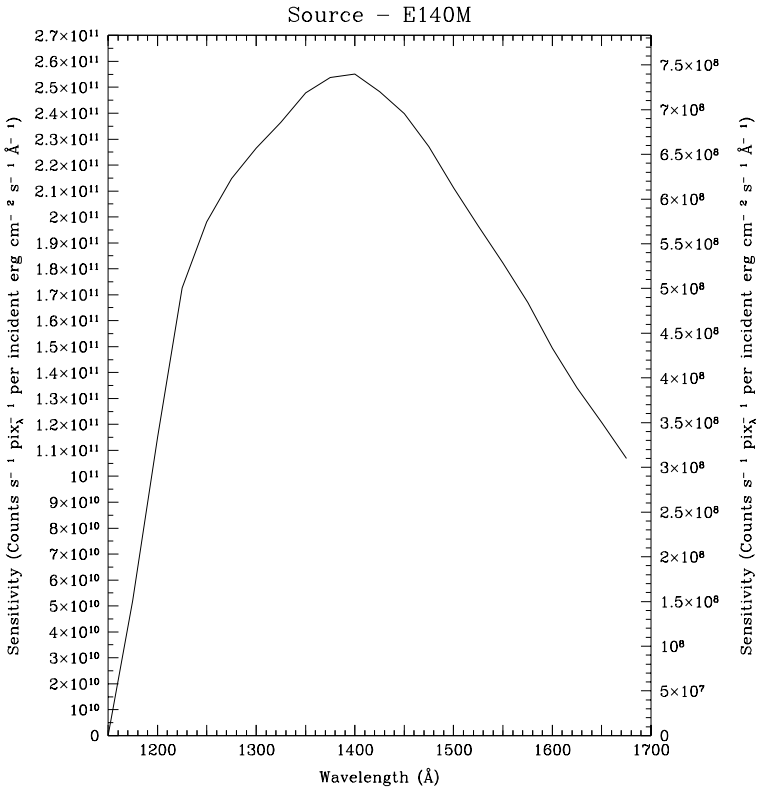

Table 13.13: E140M Point Source Sensitivities. Multiply sensitivity number by 0.029 times slit width in arcseconds to obtain diffuse source sensitivity.

λ	**Sens.**	λ	**Sens.**	λ	**Sens.**	λ	**Sens.**
1150	2.00E6	1250	2.0E11	1400	2.5E11	1550	1.8E11
1175	5.2E10	1300	2.3E11	1450	2.4E11	1600	1.5E11
1216	1.6E11	1350	2.5E11	1500	2.1E11	1650	1.2E11

Figure 13.61: E140M Time to Achieve a Signal-to-Noise of 10 per Spectral Resolution Element for Stars of Different Spectral Types, observed through the 0.2 arcsecond wide slit.

(a) O5 star

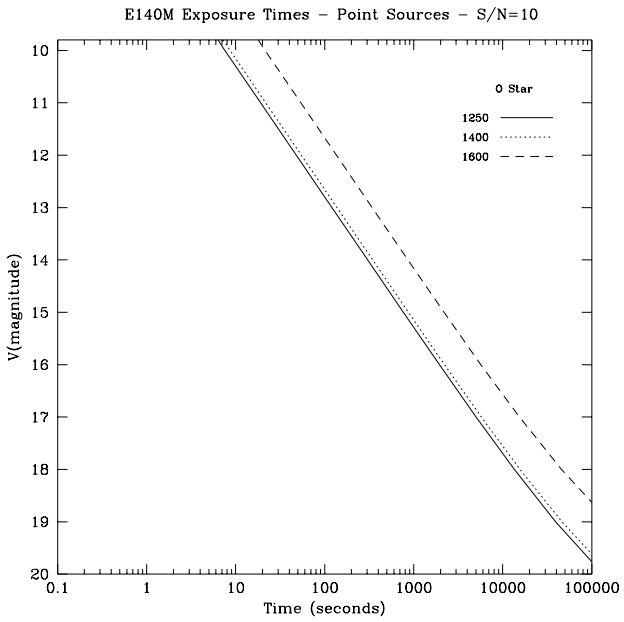

(b) AOV star

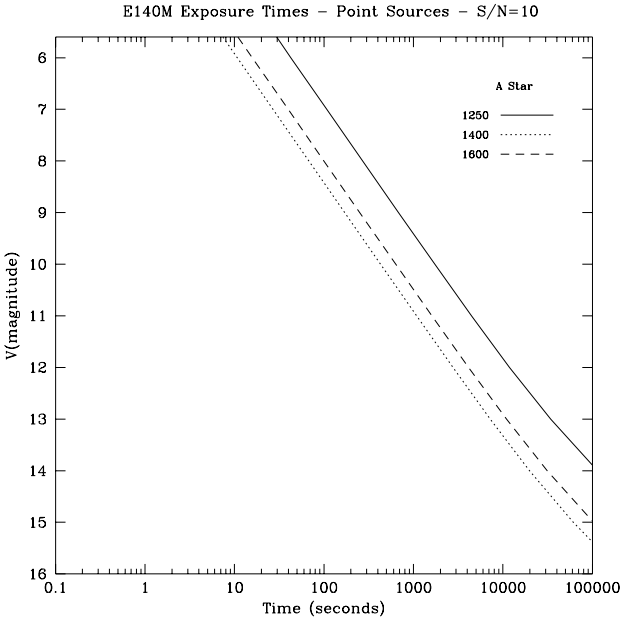

(c) G0V star

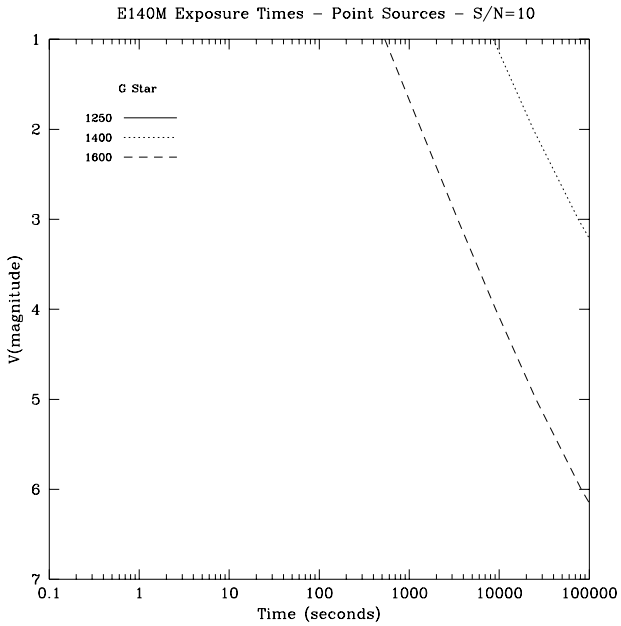

(d) M0V star

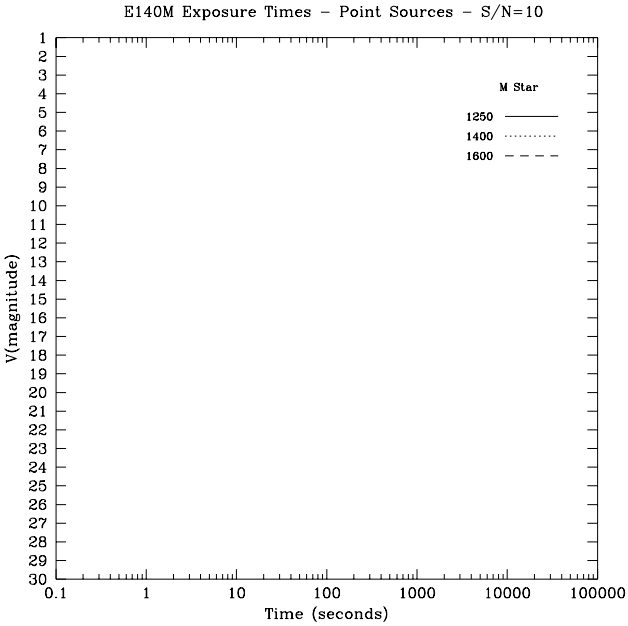

Figure 13.62: E140M Time to Achieve a Signal-to-Noise of 10 per Spectral Resolution Element for Point and Diffuse Source Observed with the 0.2” Wide Slit, cgs units. Point sources are integrated over the PSF, diffuse sources are per two spatial pixels.

(a) Point Sources

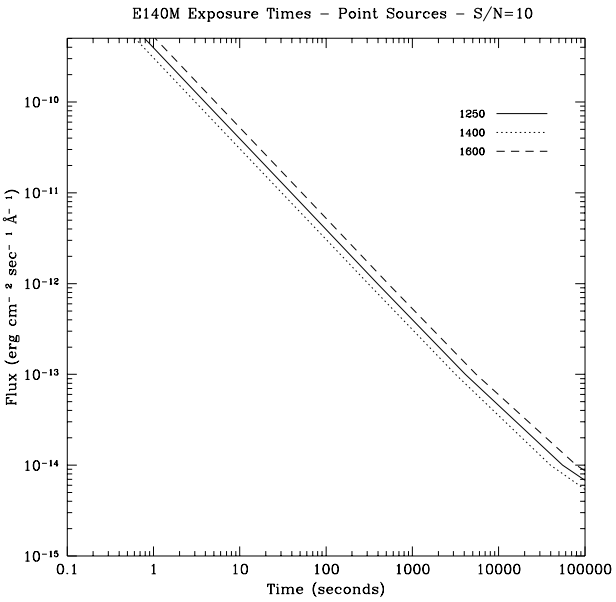

(b) Diffuse Sources

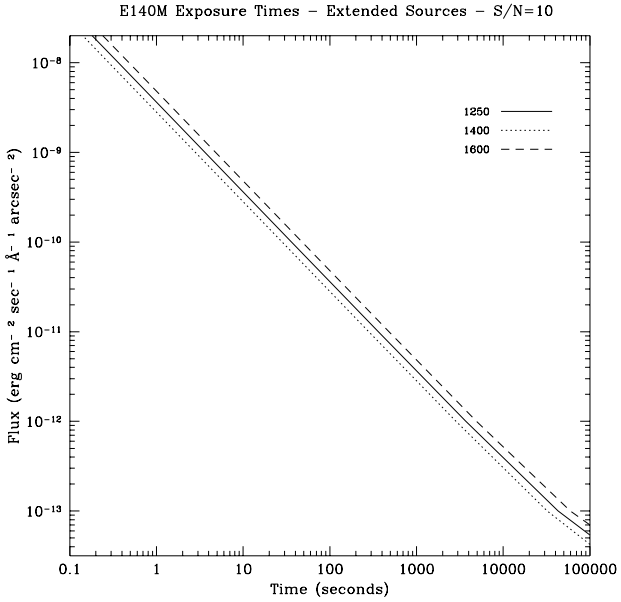

Figure 13.63: E140M Time to Saturate Peak Pixel as a Function of Source Flux, for observation taken through 0.2 arcsecond wide slit.

(a) Point Sources

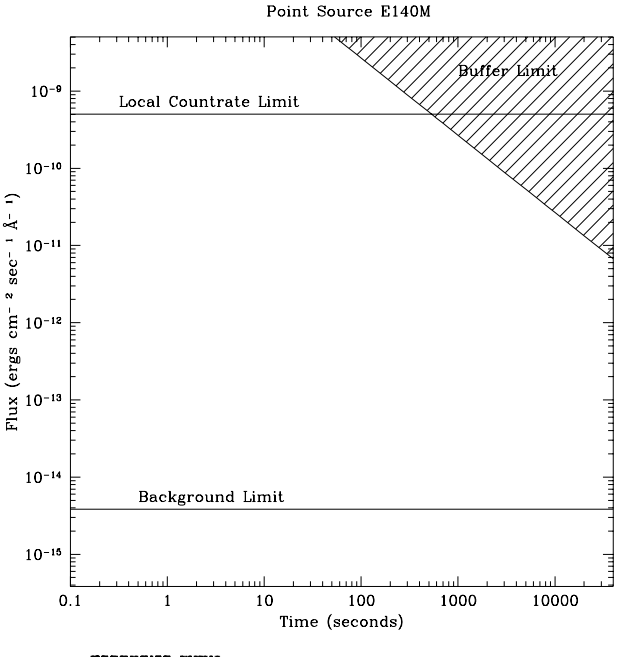

(b) Diffuse Sources

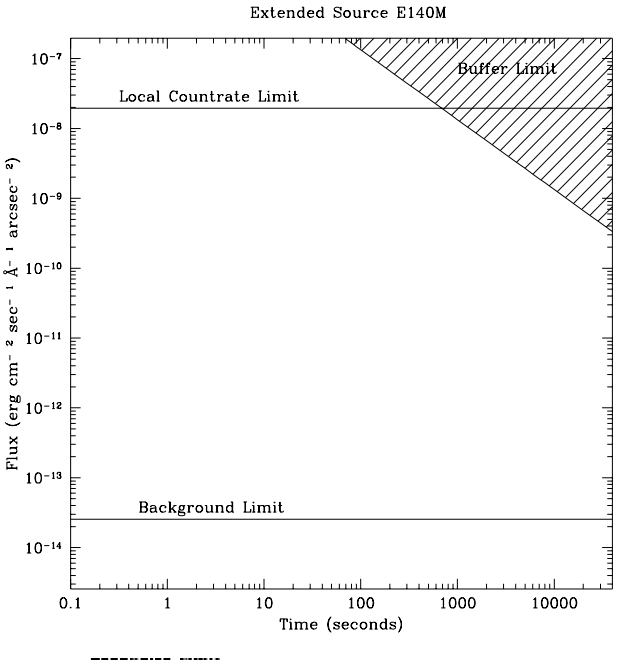

Echelle Grating E140H

The E140H grating is used with the FUV-MAMA and provides echelle spectra at a resolving power of ~100,000 from 1150–1700 Å. The table below summarizes this mode's properties.

Grating	Spectral Range		Dispersion		Central Wavelengths
	Complete	Per Tilt	Å per Pixel	Settings	
E140H	1150-1700	~210	λ/228,000	***Prime***	**1234, 1416, 1598**
				Secondary	1271, 1307, 1343, 1380, 1453, 1489, 1526, 1562

A single E140H echellogram covers 210 Å over ~50 orders. The order separation is ~16 pixels (0.47 arcseconds) at 1150 Å and ~36 pixels (1.05 arcseconds) at 1700 Å. The grating must be scanned, with exposures taken at three distinct settings to cover the full spectral range of the grating. The full set of available scan settings (central wavelength and minimum and maximum wavelengths covered in a single exposures) are shown graphically in Figure 13.64.

The sensitivity, exposure time signal-to-noise requirements, saturation exposure time limits, and bright object count limits for the E140H echelle grating mode are summarized below.

Figure 13.64: Wavelength Ranges for the E140H Grating Settings

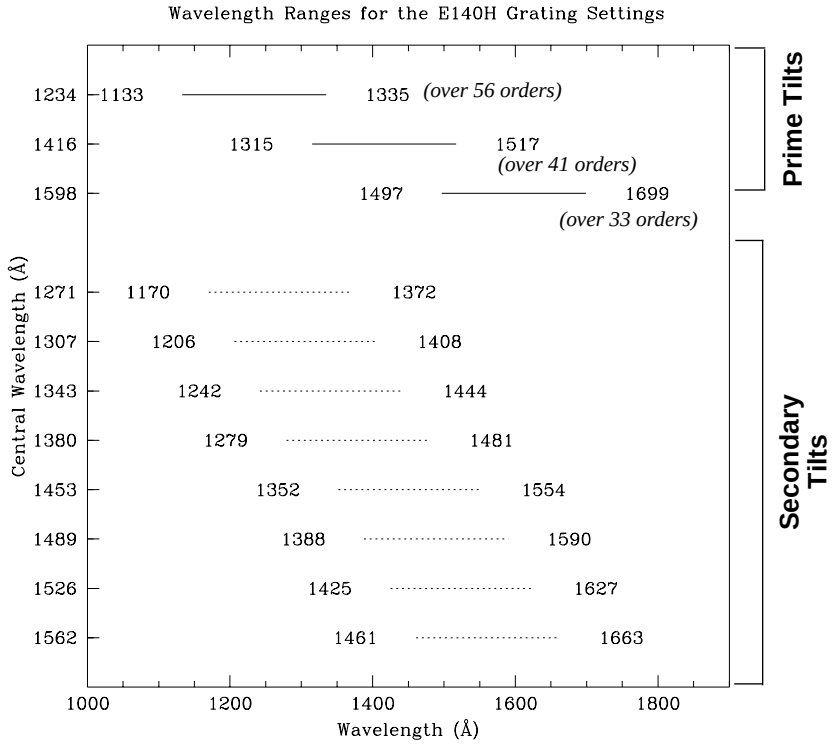

Figure 13.65: E140H Point Source (left axis), and Diffuse Source (right axis) Sensitivities. Point source sensitivity assumes full transmission (zero slit losses). Diffuse source sensitivity assumes a 0.1” wide slit.

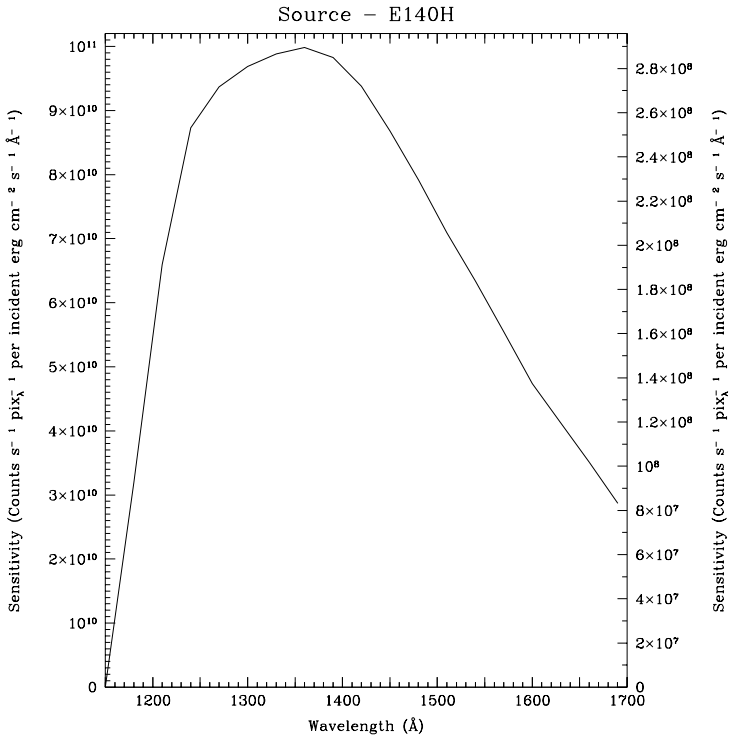

Table 13.14: E140H Point Source Sensitivities. Multiply sensitivity number by 0.029 times the slit width in arcseconds to obtain diffuse source sensitivity.

λ	**Sens.**	λ	**Sens.**	λ	**Sens.**	λ	**Sens.**
1150	1.15E6	1250	8.9E10	1400	9.7E10	1550	6.1E10
1175	2.6E10	1300	9.7E10	1450	8.7E10	1600	4.7E10
1216	7.4E10	1350	1.0E11	1500	7.4E10	1650	3.7E10

Figure 13.66: E140H Time to Achieve a Signal-to-Noise of 10 per Spectral Resolution Element for Stars of Different Spectral Types, observed through the 0.2 arcsecond wide slit.

(a) O5 star

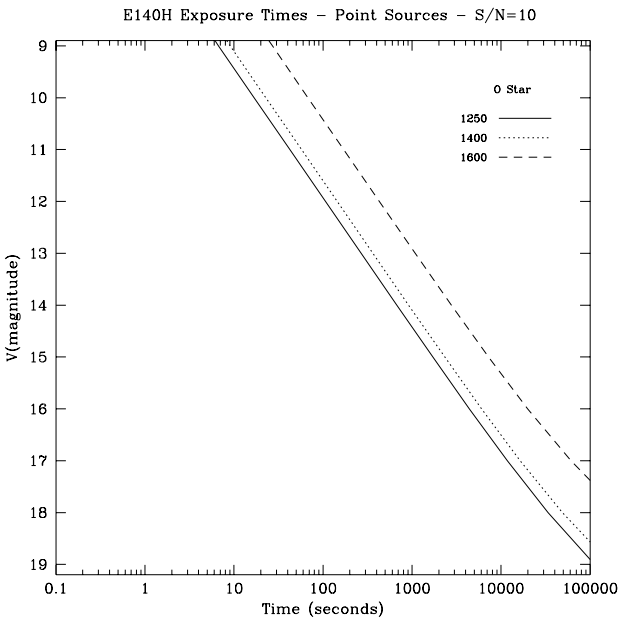

(b) AOV star

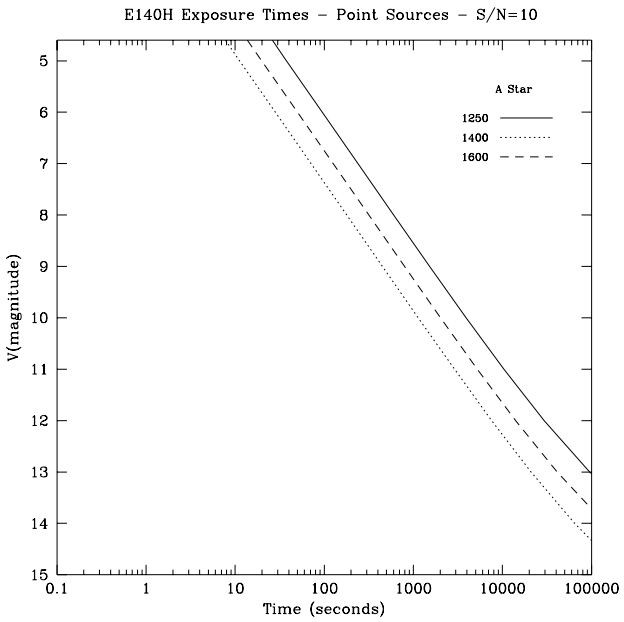

(c) G0V star

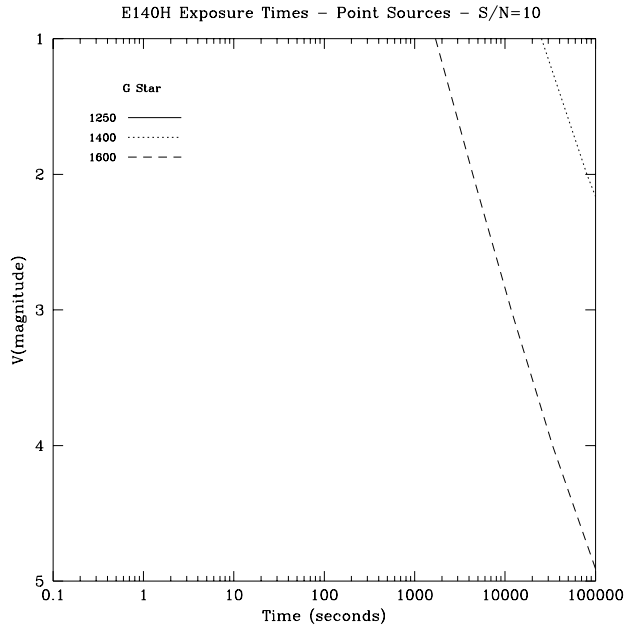

(d) M0V star

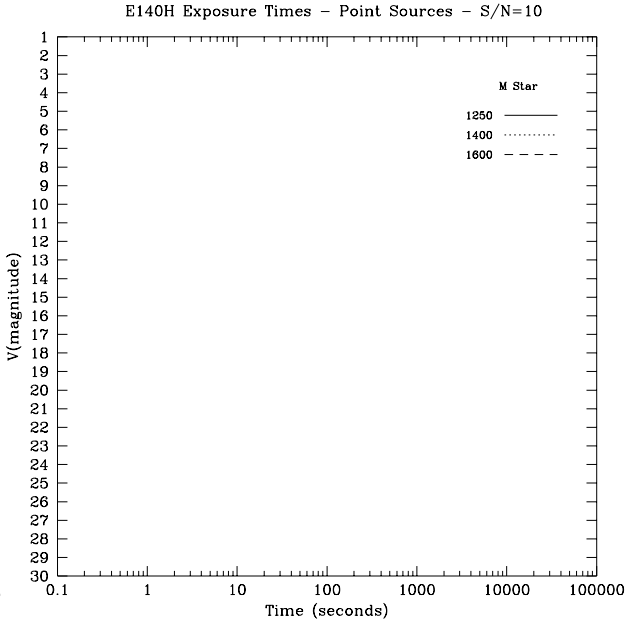

Figure 13.67: E140H Time to Achieve a Signal-to-Noise of 10 per Spectral Resolution Element for Point and Diffuse Source Observed with the 0.2” Wide Slit, cgs units. Point sources are integrated over the PSF, diffuse sources are per two spatial pixels.

(a) Point Sources

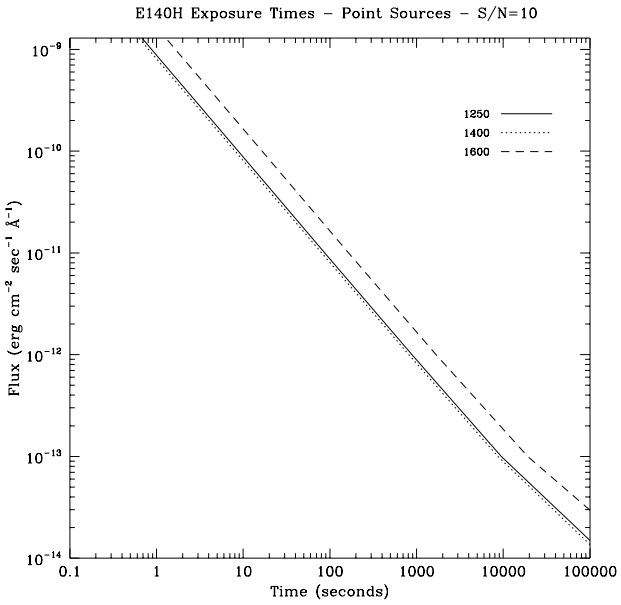

(b) Diffuse Sources

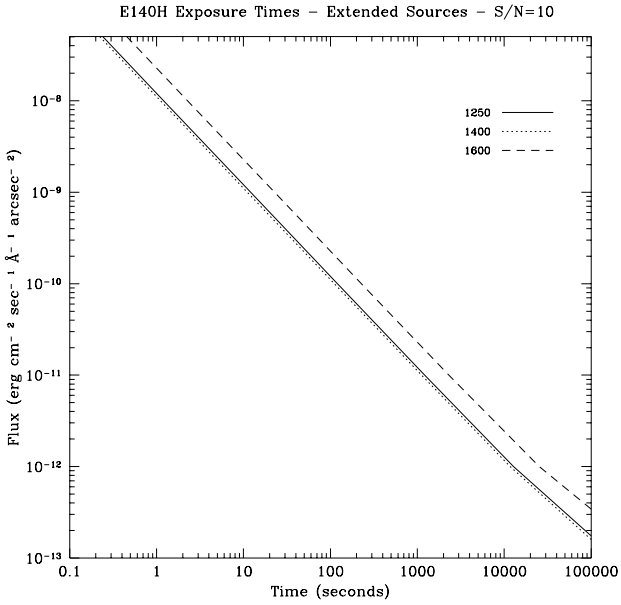

Figure 13.68: E140H Time to Saturate Peak Pixel as a Function of Source Flux, for observation taken through 0.2 arcsecond wide slit.

(a) Point Sources

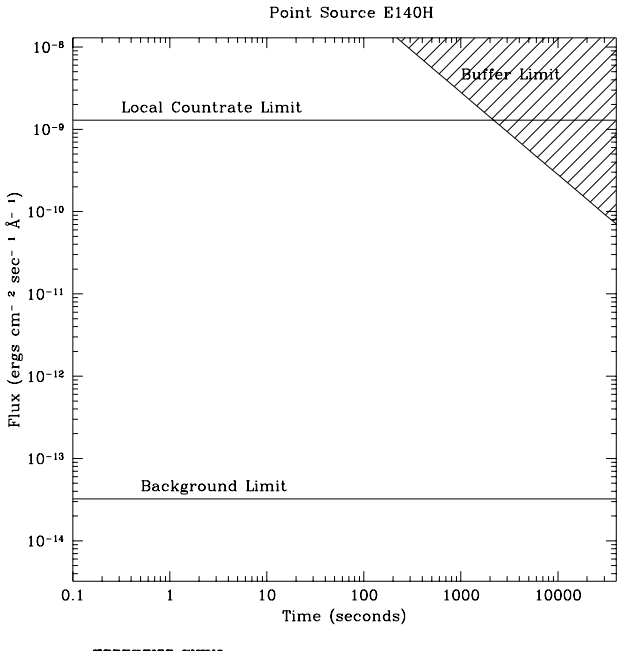

(b) Diffuse Sources

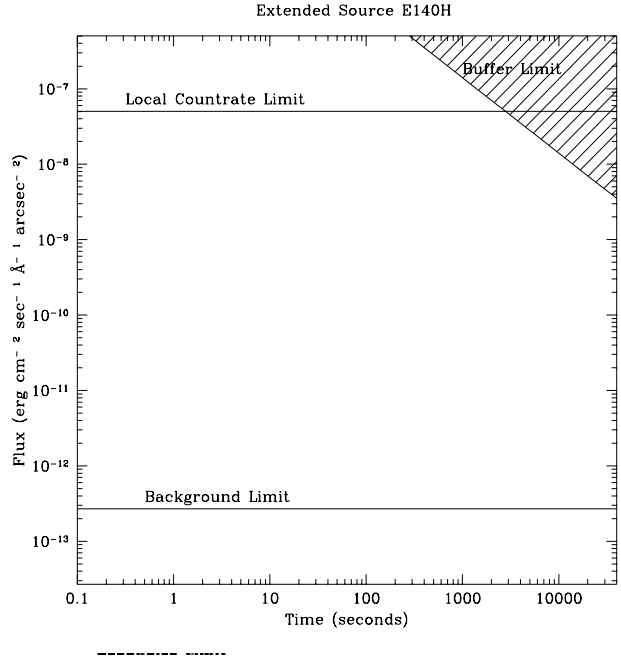

PRISM

The properties of the STIS prism mode are summarized in the table below. The PRISM is used with the NUV-MAMA.

The PRISM has two central wavelength settings—one optimized to cover the optical through the near-UV, and the second selected to provide coverage of the far-UV tail down to 1150 Å. The full dispersion spreads over ~450 pixels in dispersion as can be seen in Figure 13.70.; thus if you have sources covering the field of view in the dispersion direction, the blue tail will be lost off the field of view if you use the 2125 Å setting, and likewise the red tail will be lost if you use the 1200Å setting. We note that the dispersion of the PRISM at wavelengths longer than ~2600 Å is very poorly known at this time.

	Spectral Range		Dispersion		Central Wavelengths
Grating	**Complete**	**Per Tilt**	**Å per Pixel**	**Tilts**	
PRISM	1150-3100	1950	1.2–120	***Prime***	**1200, 2125**
				Secondary	1271, 1307, 1343, 1380, 1453, 1489, 1526, 1562

The available scan settings (central wavelength and minimum and maximum wavelengths covered in a single exposures) are shown graphically in Figure 13.69. The plate scale in the PRISM mode is 0.029 arcseconds per pixel in both dispersion and cross dispersion.

The sensitivity, exposure time signal-to-noise requirements, and saturation exposure time limits, are summarized in the figures below. Because the dispersion is so poorly known beyond 2600 Å and the sensitivities depend sensitively on the dispersion, we do not provide sensitivites longward of 2600 Å.

Figure 13.69: Wavelength Ranges for PRISM Central Wavelength Settings

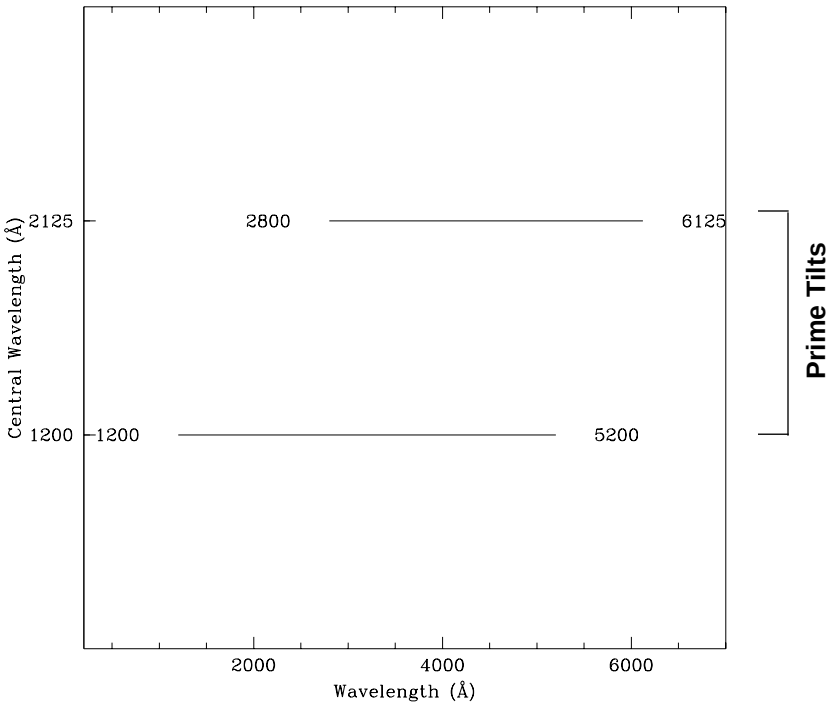

Figure 13.70: Wavelength as a Function of Number of Pixels, for the PRISM

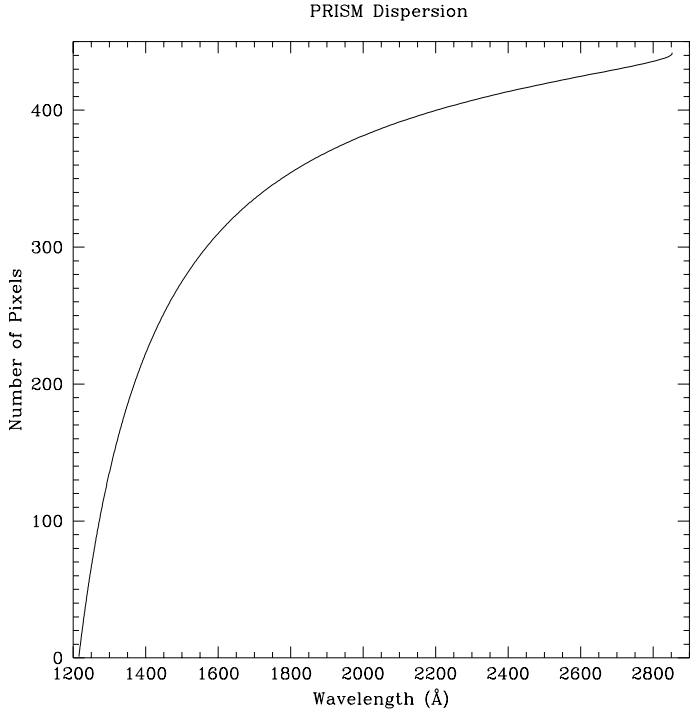

Figure 13.71: PRISM Point Source (left axis), and Diffuse Source (right axis) Sensitivities. Point source sensitivity assumes full transmission (zero slit losses). Diffuse source sensitivity assumes a 0.1” wide slit.

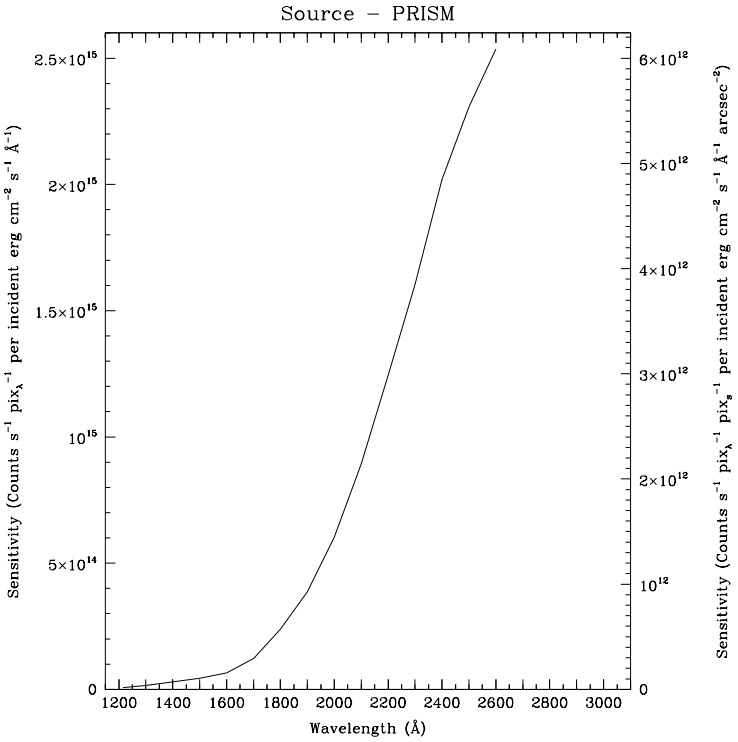

Table 13.15: Point Source Sensitivities for PRISM

Wavelength	Sensitivity	Dispersion Å/pix
1216	6.7E12	0.45
1300	1.6E13	0.87
1400	2.9E13	1.53
1500	4.5E13	2.39
1600	6.5E13	3.42
1700	1.2E14	4.62
1800	2.4E14	5.99
1900	3.9E14	7.52
2000	6.0E14	9.18
2100	8.9E14	10.96
2200	1.2E15	12.95
2300	1.6E15	14.76
2400	2.0E15	16.73
2500	2.3E15	18.33
2600	2.5E15	19.19

Figure 13.72: PRISM Time to Achieve a Signal-to-Noise of 10 per Spectral Resolution Element for Stars of Different Spectral Types, observed through the 0.2 arcsecond wide slit.

(a) O5 star

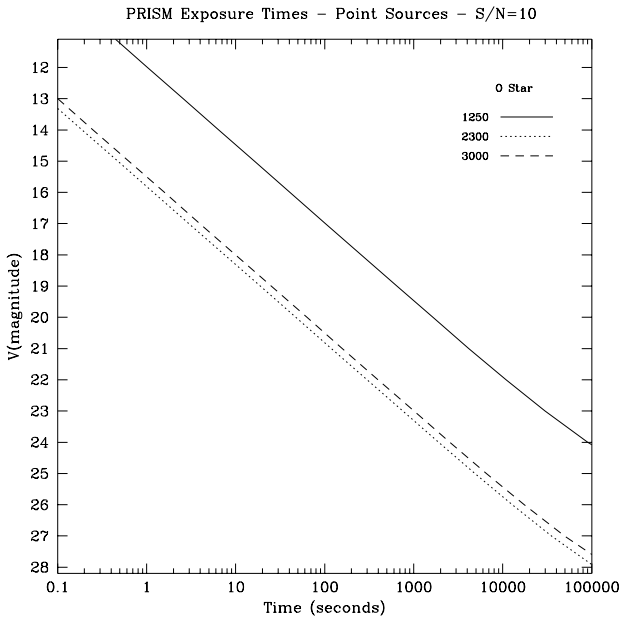

(b) AOV star

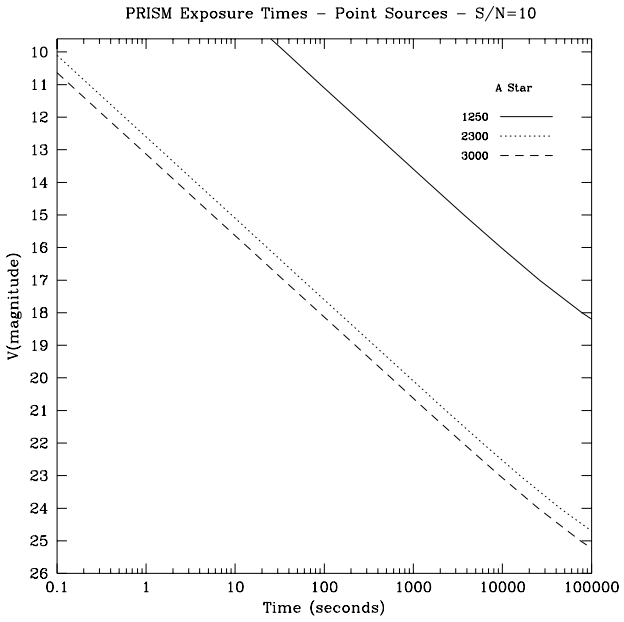

(c) G0V star

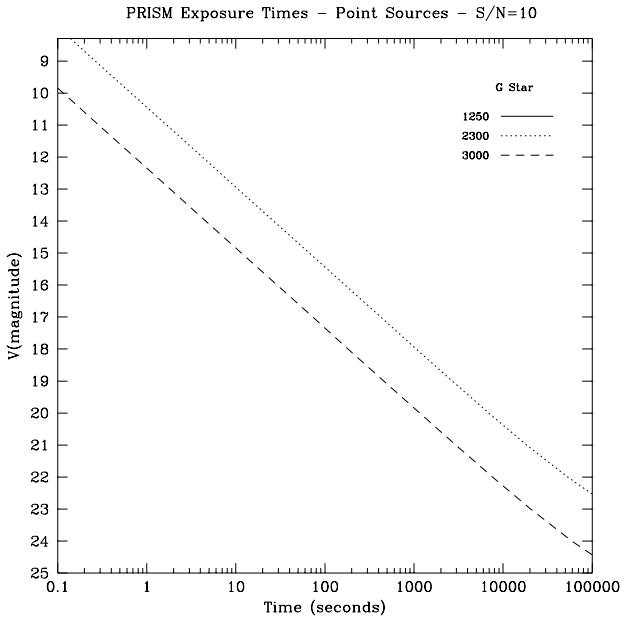

(d) M0V star

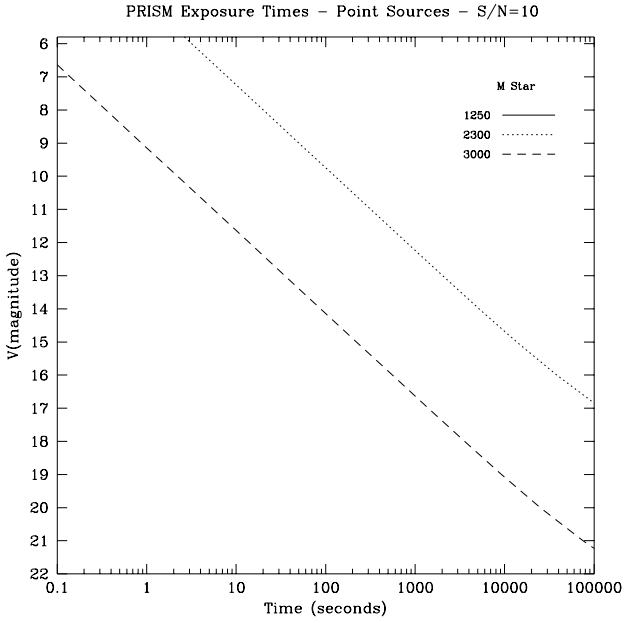

Figure 13.73: PRISM Time to Saturate as a Function of Source Flux

(a) Point Sources

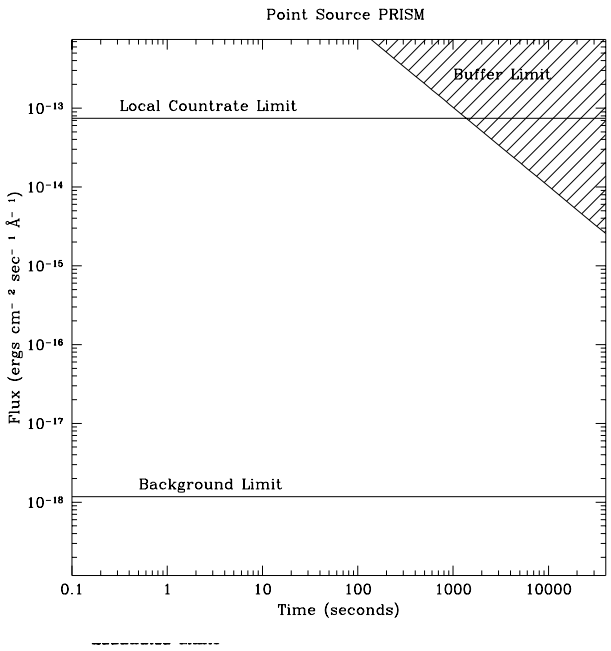

(b) Diffuse Sources

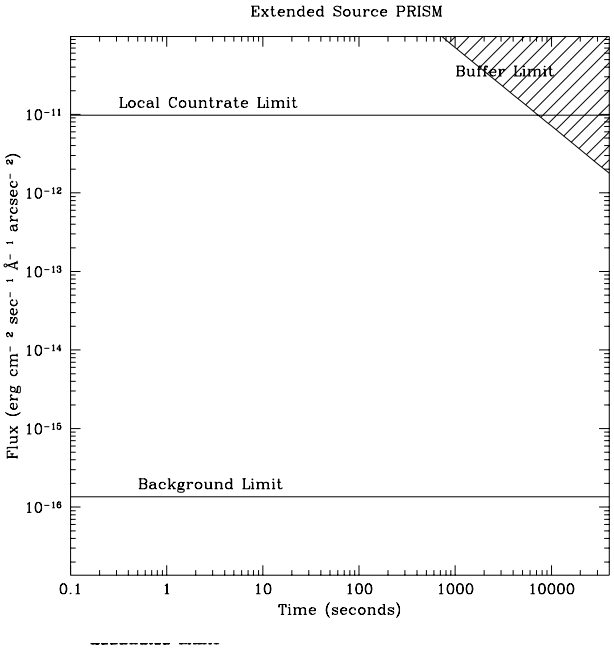

First Order Slits, LSFs, Scales and Encircled Energies

Slits for First Order Spectroscopy

In Table 13.16, we list the long slits to be used with the first order spectroscopic gratings, giving the name of the slit, length (in the spatial direction) and width (in the dispersion direction) of the slit, and a brief description of the purpose of the slit. “Fiducials on Bars” on page 244 below describes the physical structure of the STIS long slits.

In the companion Tables 13.17 (visible/CCD) and 13.15 (UV/MAMAs), we give best estimates of the expected throughput (fraction of light transmitted by the slit) and spectral resolution (in pixels per FWHM) for a point source at selected wavelengths, and the spectral resolution for an extended source which evenly fills the aperture. The principal effect of using a wider slit for point source observations is to increase the level of the wings of the line spread function (LSF), particularly at shorter wavelengths, as is most clearly illustrated in Figures 13.75 and 13.76. The information provided in the tables and the model LSFs, while sufficient for Cycle 7 Phase 1 proposal planning, are based on pre-instrument-integration predictions and are therefore only *illustrative*. The LSFs which are achieved in orbit will depend on the ultimate optical alignment and the grating and detector properties. We note that based on current predictions, the LSFs will be slightly undersampled in the first order modes (see also the special topic “Improving the Sampling of the Line Spread Function” on page 168)

Table 13.16: Long Slits for Use with First Order Gratings

Aperture	Length (arcsecs)		Width (arcsec)	Comment
	on CCD	projected on MAMA		
52X0.1	52.0	28.0 (G230M, G140M) 25.0 (G230L, G140L)	0.1	Best spatial and spectral resolution, requires peakup.
52X0.2	52.0	28.0 (G230M, G140M) 25.0 (G230L, G140L)	0.2	Utility slit—good compromise between spectral resolution and photometric throughput, target acq peakup required.
52X0.5	52.0	28.0 (G230M, G140M) 25.0 (G230L, G140L)	0.5	Photometric, no target acquisition peakup required.
52X2.0	52.0	28.0 (G230M, G140M) 25.0 (G230L, G140L)	2.0	Photometric—for diffuse sources, no target acq peakup needed.
52X0.2F1	52.0 fiducial 0.4”	28.0 (G230M, G140M) 25.0 (G230L, G140L) fiducial 0.5	0.2	Fiducial bar for spectroscopic coronography (see Figure 13.74 on page 244).

Table 13.17: Predicted CCD Long Slit Throughputs and Spectral Response.

Aperture	Point Source Photometric Throughput				Point Source Spectral Resolution (FWHM in pixels)				Extended Source Spectral Resolution
	3200 Å	5500 Å	7000 Å	10000 Å	3200 Å	5500 Å	7000 Å	10000 Å	
52X0.1	70%	65%	65%	60%	1.3	1.4	1.5	1.7	~2-3 pixels
52X0.2	75%	80%	80%	70%	1.3	1.5	1.6	2.0	~4 pixels
52X0.5	84%	86%	86%	85%	1.3	1.5	1.6	2.0	~10 pixels

Table 13.18: Predicted MAMA Long Slit Throughputs and Spectral Response

Aperture	Point Source Photometric Throughput					Point Source Spectral Resolution (FWHM in pixels)					Extended Source Spectral Resolution
λ=	1200	1500	1700	2000	2400	1200	1500	1700	2000	2400	
52X0.1	42%	50%	54%	60%	65%	1.6	1.5	1.4 with FUV-MAMA 2.2 with NUV-MAMA	2.2	2.1	~4 pixels
52X0.2	56%	62%	66%	69%	72%	1.7	1.5	1.4 with FUV-MAMA 2.2 with NUV-MAMA	2.2	2.1	~8 pixels
52X0.5	76%	78%	80%	81%	82%	1.7	1.5	1.4 with FUV-MAMA 2.2 with NUV-MAMA	2.2	2.1	~20 pixels
52X2	91%	92%	92%	92%	92%	1.7	1.5	1.4 with FUV-MAMA 2.2 with NUV-MAMA	2.2	2.1	~80 pixels

Fiducials on Bars

Each STIS long slit has two fiducial bars, located 11.2 arcseconds above and below the slit center (see Figure 13.74, below). They have several purposes. First, the bars provide structural integrity for the long slits. Second, the image of the bars obtained in wavecal (and target acquisition) images is used by the calibration software to locate the projection of the aperture on the detector in post-observation data processing. Lastly, the bars can be used to occult a source thereby providing a coronographic spectroscopic capability for STIS. For Cycle 7, we have enabled support of the 0.5 arcsecond long bar on the 52 x 0.2 arcsecond slit (the `52X0.2F1` aperture) for such observations. We refer you to “Coronagraphic Imaging and Spectroscopy” on page 170 for more information about performing coronographic spectroscopy.

Figure 13.74: 52” Long Slits and Location of Fiducial Bars

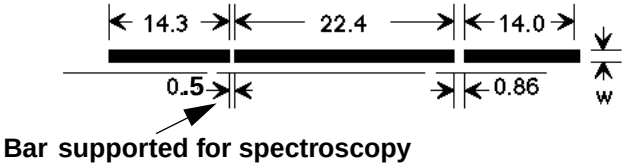

Line Spread Functions for First Order Spectroscopy

Below we show plots of derived line spread functions (LSFs) for CCD spectroscopic modes and MAMA first order modes, as a function of wavelength and slit width. These plots are predictive only; they are based on predicted PSFs at the aperture plane and detector PSFs from non-flight detectors. The ultimate LSFs achieved will depend sensitively on the alignment of the integrated optics and detectors and the properties of the flight detectors.

Figure 13.75: Predicted LSFs for CCD First Order Modes

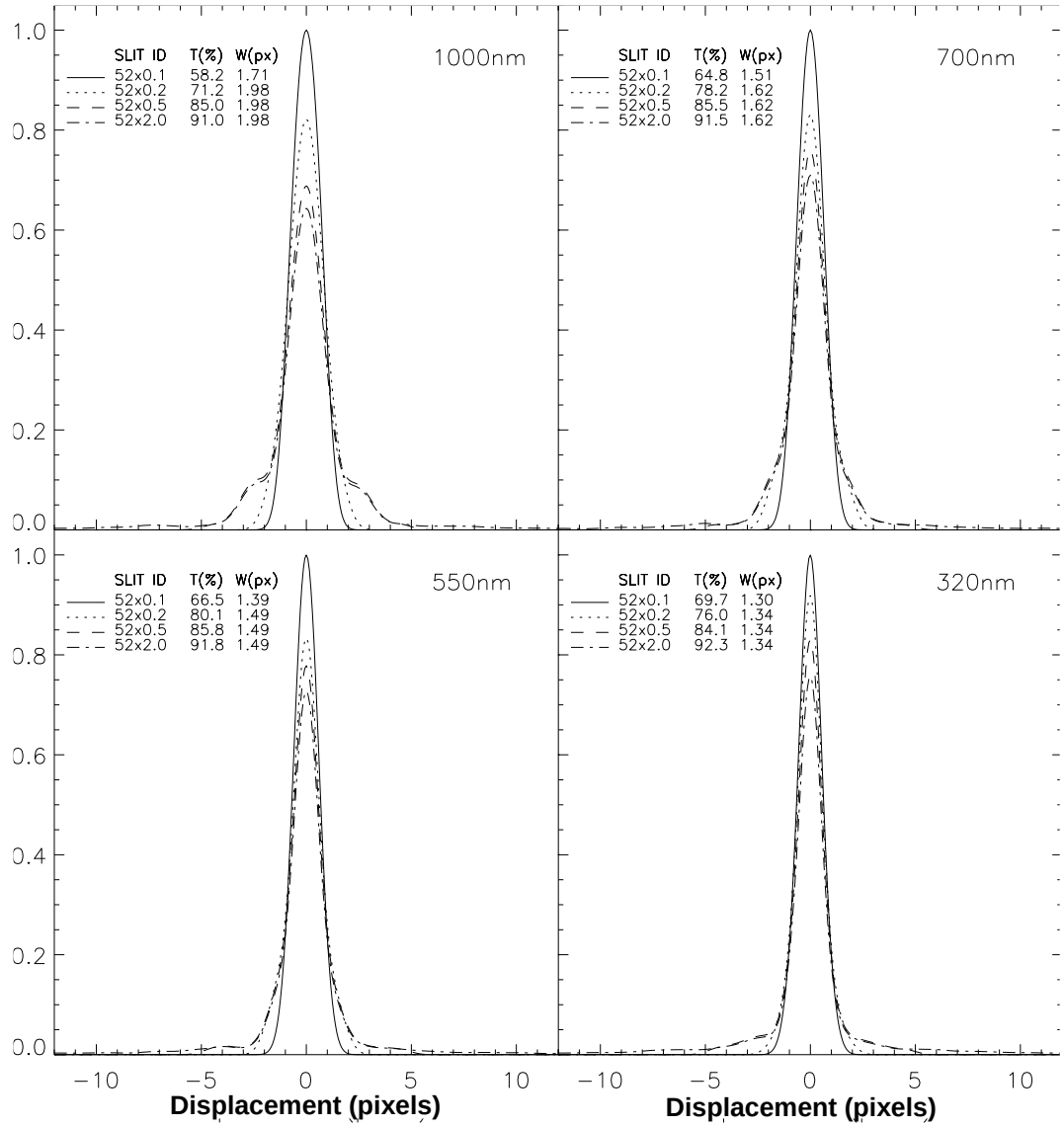

Figure 13.76: Predicted LSFs for MAMA First Order Modes

NUV-MAMA, G230M and G230L, First Order LSFs

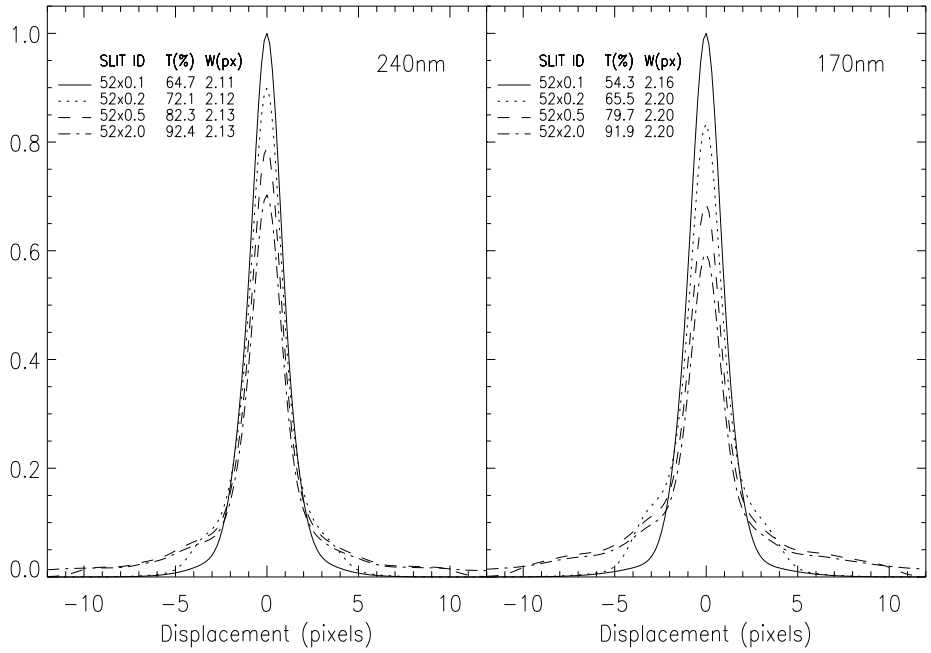

FUV-MAMA, G140M and G140L, First Order LSFs

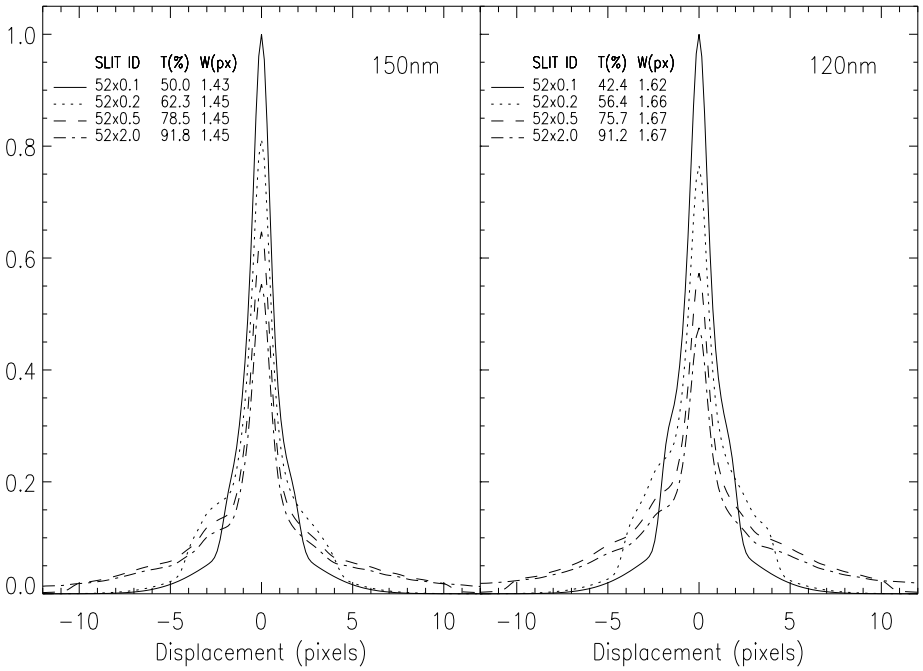

Plate Scales and Encircled Energies for First Order Long Slit Spectroscopy

CCD/Near-IR to Near-UV

For CCD spectroscopic observations, roughly 30% of the flux from a point source falls in the peak pixel, and 60% of the point source flux is contained within 2 spatial (cross-dispersion) pixels, where each pixel is 0.05 arcseconds on a side. The precise numbers are a function of observing wavelength, as can be seen in Table 13.19. Column two of the table gives the percentage of the total transmitted flux from a point source observed through the 0.2 arcsecond wide slit which is contained within the peak pixel. Columns three and four give the number of pixels in the cross-dispersion (spatial) direction you must integrate over to contain 60% and 80%, respectively, of the transmitted point source energy, where the LSF has been integrated over in the dispersion direction. While these numbers were derived for observations through a 0.2 arcsecond wide long slit, there is not too much variation with slit diameter.

Table 13.19: Plate Scales, Peak and Encircled Energies for CCD Spectroscopy

Wavelength (Å)	Percent of transmitted flux from a point source in peak pixel	Number of spatial pixels which contain 60% of transmitted point source flux	Number of spatial pixels which contain 80% of transmitted point source flux.
First Order CCD Modes G750L, G750M, G430L, G430M, G230LB, G230MB - Plate Scale = 0.05 arcsec/pixel			
10,000	20%	~ 2 (1.6)	~ 3 (2.9)
8,800	22%	~ 2 (1.6)	~ 3 (2.9)
7,000	25%	~ 2 (1.5)	~ 3 (2.5)
5,500	28%	~ 1 (1.3)	~ 2 (2.2)
4,400	32%	~ 1 (1.2)	~ 2 (2.0)
3,600	33%	~ 1 (1.1)	~ 2 (1.9)
2,800	35%	~ 1 (1.1)	~ 2 (1.9)
2,000	34%	~ 1 (1.2)	~ 2 (2.3)

UV/MAMA

In the ultraviolet for the first order modes, only roughly 15% of the transmitted point source flux is contained within a single spatial (cross-dispersion) pixel. Roughly 5 pixels in the NUV and 7 pixels in the FUV must be integrated over in the cross dispersion direction in order to contain 80% of the transmitted flux from a point source. These numbers vary with wavelength as can be seen in Table 13.20, below. Column two of the table gives the percentage of the total transmitted flux from a point source observed through the 0.2 arcsecond wide slit which is contained within the peak pixel. Columns three and four give the number of pixels in the cross-dispersion (spatial) direction you must integrate over to contain 60% and 80%, respectively, of the transmitted point source energy, where the LSF has

been integrated over in the dispersion direction. While these numbers were derived for observations through a 0.2 arcsecond wide long slit, there is not too much variation with slit diameter.

Table 13.20: Plate Scales and Peak and Encircled Point Source Energies for MAMA First Order Spectroscopy

Wavelength (Å)	Percent of transmitted flux from a point source in peak pixel	Number of spatial pixels to contain 60% of transmitted point source flux	Number of spatial pixels to contain 80% of transmitted point source flux
First Order NUV-MAMA Modes - Plate Scales = 0.024 arcsec/pixel (G230L), 0.029 arcsec/pixel (G230M)			
2,800	15%	~ 3 (2.5)	~ 4 (4.1)
2,400	14.5%	~ 2 (2.2)	~ 4 (4.2)
2,000	15%	~ 2 (2.2)	~ 5 (2.6)
1700	14%	~ 2 (2.1)	~ 5 (5.4)
First Order FUV-MAMA Modes - Plate Scales = 0.024 arcsec/pixel (G140L), 0.029 arcsec/pixel (G140M)			
1,700	17%	~ 3 (3.1)	6 (6.3)
1,500	15%	~ 4 (3.5)	7 (6.8)
1,200	11%	~ 4 (4.2)	8 (7.9)

Echelle Slits, LSFs, Scales, and Encircled Energies

Slits for Echelle Spectroscopy

Table 13.21 on page 249 lists the slits for use with the echelle gratings. The slits are explicitly matched to specific grating modes for the echelles (i.e., only specific slit-echelle grating combinations are supported). This is because the magnification (slit width which maps to two detector pixels) and the order separation (slit length which assures order separation) differ across the echelle modes. In this table we give the name of the slit, length (in the spatial direction) and width (in the dispersion direction) of the slit, and a brief description of the purpose of the slit.

In the companion Table 13.22, we give estimates of the expected throughput (fraction of light transmitted by the slit) and spectral resolution (in pixels per FWHM) for a point source at selected wavelengths, and the spectral resolution for an extended source which evenly fills the aperture. The principal affect of using a wider slit is to increase the level of the wings of the LSF, particularly at shorter wavelengths as is best illustrated in Figure 13.77 on page 251. The information provided in Table 13.22 and the sample LSFs, while sufficient for Cycle 7 Phase I proposal planning, are based on pre-instrument-integration predictions and are

therefore only *illustrative*. The LSFs which are achieved in orbit will depend on the ultimate optical alignment and the grating and detector properties. We note that based on current predictions, the LSFs will be slightly undersampled in the echelle modes (see also the special topic “Improving the Sampling of the Line Spread Function” on page 168).

Table 13.21: Slits for Use with the Echelle Gratings[a]

Aperture	Length (arcsec)	Width (arcsec)	Comment
		E230M	
0.2X0.06	0.2	0.06	Maximum spectral resolution
0.2X0.2	0.2	0.2	Utility slit —photometric
		E140M	
0.2X0.06	0.2	0.06	Maximum spectral resolution
0.2X0.2	0.2	0.2	Utility slit—photometric
		E230H	
0.1X0.09	0.1	0.09	Maximum spectral resolution
0.1X0.2	0.1	0.2	Utility slit—photometric
		E140H	
0.2X0.09	0.2	0.09	Maximum spectral resolution
0.2X0.2	0.2	0.2	Utility slit—photometric

a. The 6X0.2 long slit (6” long, 0.2” wide in dispersion) is also supported for use with these gratings, providing an extended source echelle capability, but producing order overlap (see “Long Slit Echelle Spectroscopy” on page 163).

Table 13.22: Predicted Echelle Slit Throughputs and Spectral Response

Aperture	Point Source Photometric Throughput					Point Source Spectral Resolution (FWHM in Pixels)					Extended Source Spectral Resolution (pixels)
λ=	1200	1500	1700	2000	2400	1200	1500	1700	2000	2400	
						E230M					
0.2X0.06	N/A	N/A	45%	50%	55%	N/A	N/A	1.7	1.8	1.7	~1.7
0.2X0.2	N/A	N/A	60%	60%	65%	N/A	N/A	1.9	2.0	1.9	~5.7
						E230H					
0.1X0.09	N/A	N/A	45%	50%	60%	N/A	N/A	1.7	1.7	1.7	~1.9
0.1X0.2	N/A	N/A	50%	60%	60%	N/A	N/A	1.8	1.8	1.7	~4.3
						E140M					
0.2X0.06	30%	40%	45%	N/A	N/A	1.13	1.1	1.1	N/A	N/A	~1.7
0.2X0.2	45%	55%	45%	N/A	N/A	1.25	1.1	1.1	N/A	N/A	~5.5
						E140H					
0.2X0.09	35%	45%	50%	N/A	N/A	1.10	1.0	1.0	N/A	N/A	~1.9
0.2X0.2	45%	55%	55%	N/A	N/A	1.16	1.0	1.0	N/A	N/A	~4.3

Line Spread Functions for Echelle Spectroscopy

Below we show plots of derived line spread functions (LSFs) for the echelle modes as a function of wavelength and slit width. These plots are predictive only; they are based on predicted PSFs at the aperture plane and detector PSFs from non-flight detectors. The ultimate LSFs achieved will depend sensitively on the alignment of the integrated optics and detectors and the properties of the flight detectors.

Figure 13.77: MAMA Echelle Mode Predicted LSFs

NUV-MAMA, E230M, Medium Resolution Echelle LSFs

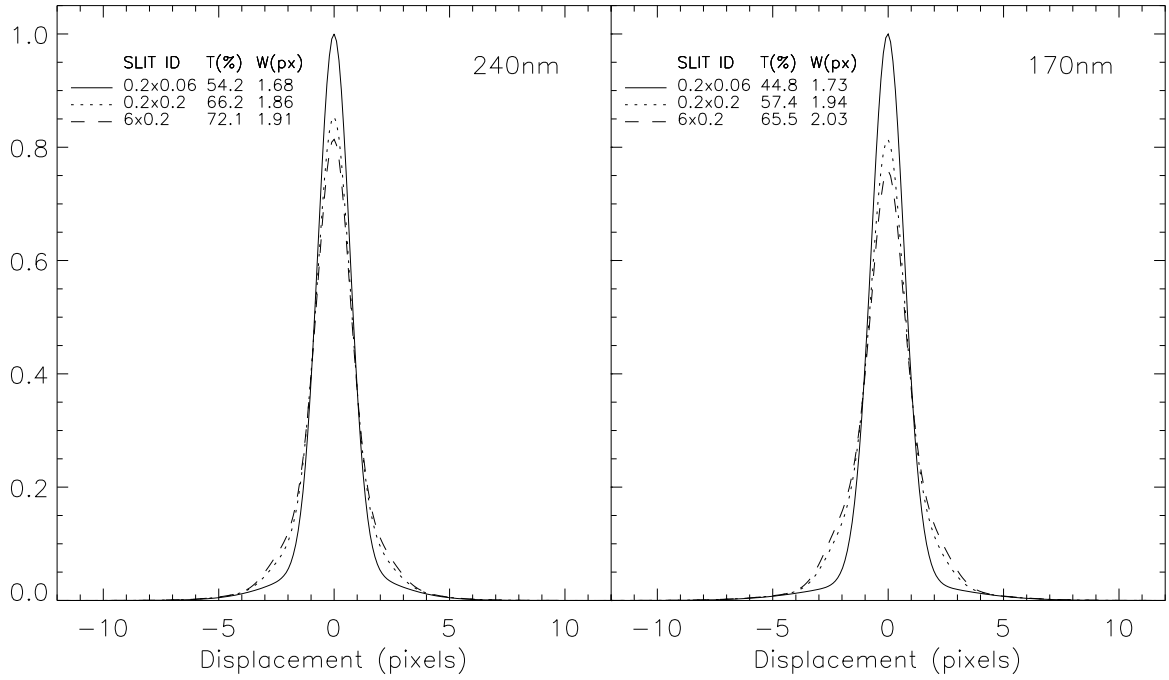

NUV-MAMA, E230H, High Resolution Echelle LSFs

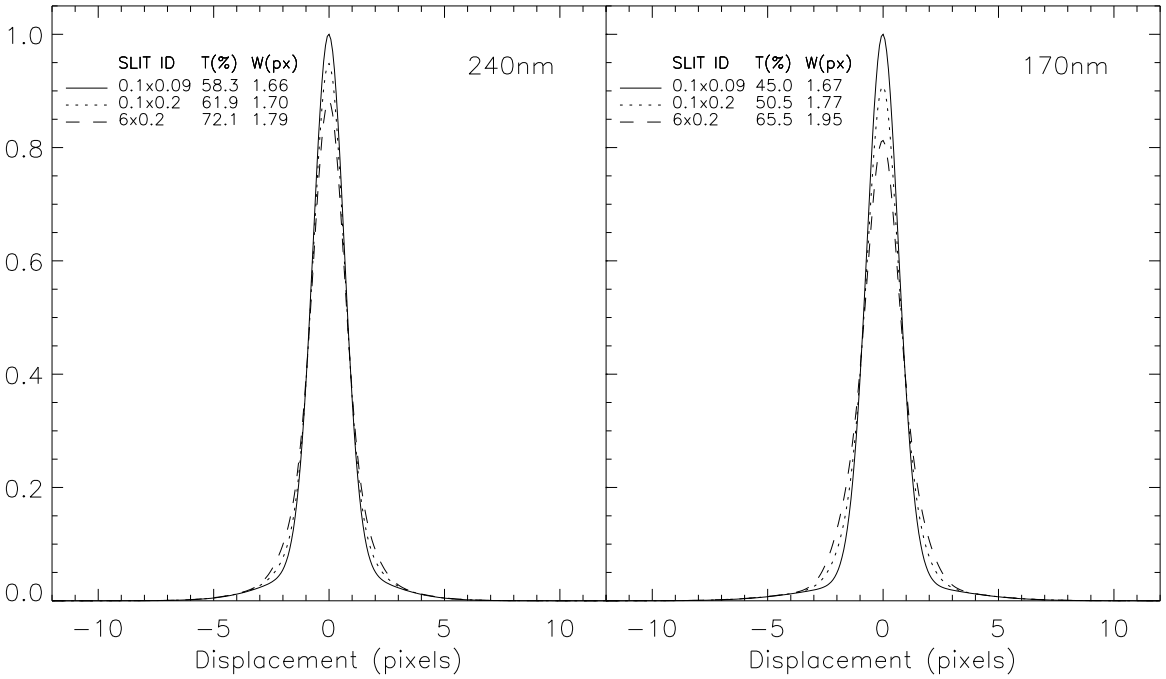

FUV-MAMA, E140M, Medium Resolution Echelle LSFs

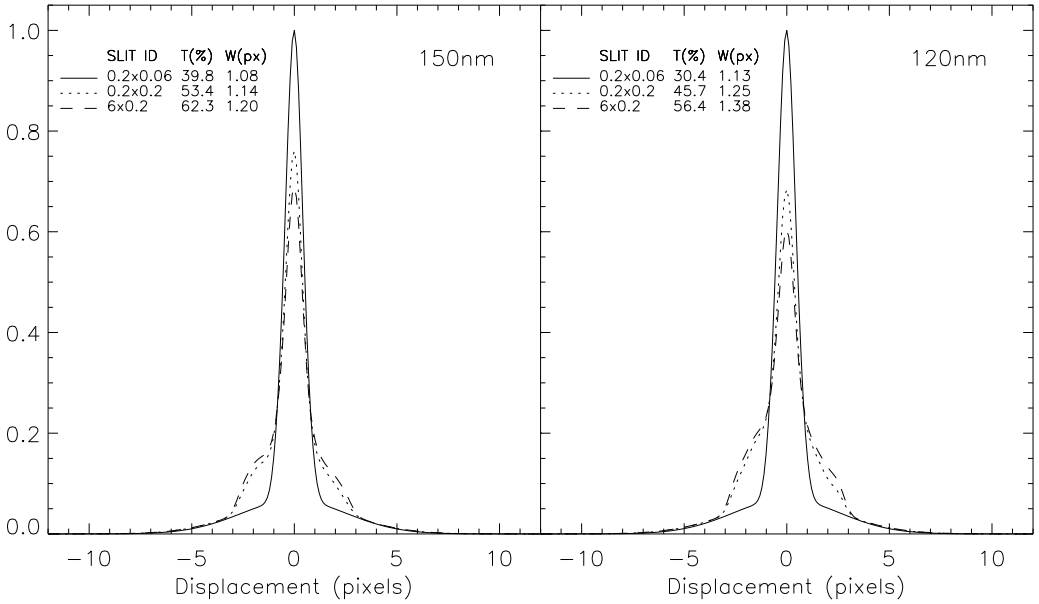

FUV-MAMA, E140H, High Resolution Echelle LSFs

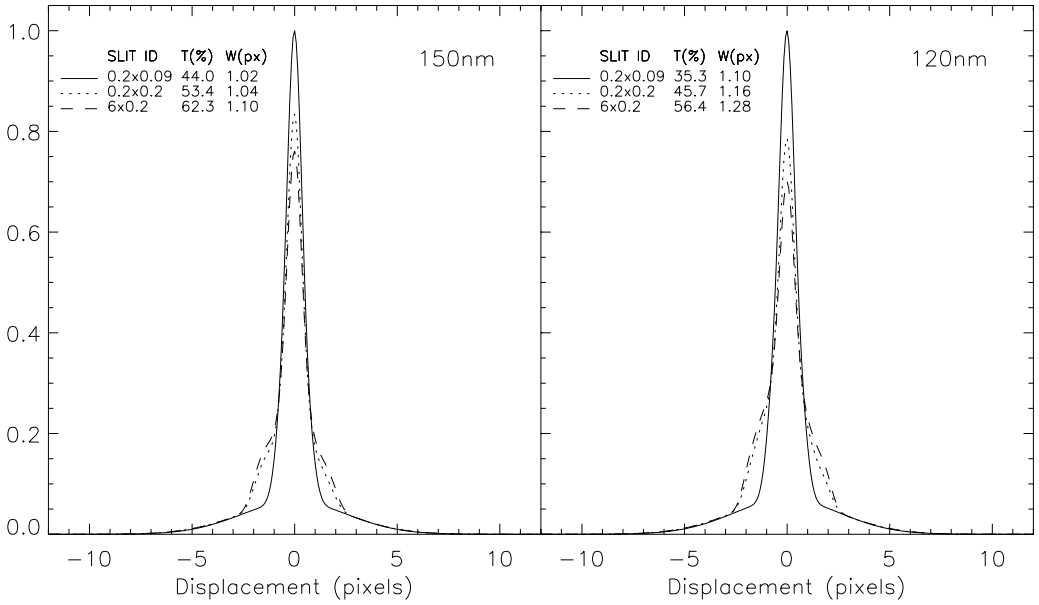

Echelle Plate Scales and Encircled Energies

In the ultraviolet echelle modes, roughly 20% of the energy from a point source falls in the peak pixel, and roughly 4 pixels in the spatial (cross dispersion) direction must be integrated over to contain 80% of the point source energy. The precise numbers are mode and wavelength dependent as illustrated in Table 13.23, below. Column two of the table gives the percentage of the total flux from a point source transmitted through the mode appropriate 0.2 arcsecond wide slit which is contained within the peak pixel. Columns three and four give the number of pixels in the cross-dispersion (spatial) direction you must integrate over to contain 60 and 80%, respectively, of the transmitted point source energy, where the LSF has been integrated over in the dispersion direction. While these numbers were derived for a 0.2 arcsecond wide slit, there is only a weak dependence on slit width. Note that the plate scale in the dispersion direction for the echelles vary from mode to mode. (see Table 13.23).

Table 13.23: Peak and Encircled Point Source Energies for MAMA Echelle Spectroscopy

Wavelength (Å)	Percent of transmitted flux from a point source in peak pixel	Number of spatial pixels to contain 60% of transmitted point source flux	Number of spatial pixels to contain 80% of transmitted point source flux
E230M *(plate scale 0.035” per pixel in dispersion, 0.029” per pixel along slit)*			
2,800	19%	~ 2 (1.8)	~ 3 (3.2)
2,400	19%	~ 2 (1.8)	~ 3 (3.2)
2,000	19%	~ 2 (1.8)	~ 3 (3.3)
1,700	18%	~ 2 (1.9)	~ 4 (3.5)
E230H *(plate scale 0.047” per pixel in dispersion, 0.029” per pixel along slit)*			
2,800	21%	~ 2 (1.7)	~ 3 (2.8)
2,400	22%	~ 2 (1.6	~ 3 (2.7)
2,000	22%	~ 2 (1.6)	~ 3 (2.6)
1,700	22%	~ 2 (1.7)	~ 3 (2.7)
E140M *(plate scale 0.036” per pixel in dispersion, 0.029” per pixel along slit)*			
1,700	22%	~ 2 (2.3)	~ 5 (4.6)
1,500	21%	~ 3 (2.5)	~ 5 (4.7)
1,200	17%	~ 3 (2.9)	~ 5 (5.0)
E140H *(plate scale 0.047” per pixel in dispersion, 0.029” per pixel along slit)*			
1,700	24%	~ 2 (2.3)	~ 5 (4.6)
1,500	23%	~ 3 (2.5)	~ 5 (4.7)
1,200	18%	~ 3 (2.9)	~ 5 (5.0)

MAMA Spectroscopic Bright Object Limits

As described in "MAMA Bright Object Limits" on page 97, within Chapter 7, the MAMA's are subject to absolute brightness limits, above which sources cannot be observed or they would potentially damage the detectors. In Table 13.24, below, we present the complete set of absolute bright object point source spectroscopic screening limits for the MAMA spectroscopic modes. Remember, sources cannot be observed in configurations where they exceed the absolute bright object limits. The information presented here should be used in conjunction with the material presented in Chapter 7. A few important points to note are:

- The limits are given either as V magnitude limits or in CGS units as indicated.
- The limits in this table have been calculated assuming zero slit losses. To determine if your source will violate the limits in this table, you must first correct the magnitude limit for the aperture throughput for your chosen slit. The maximum magnitude correction achieved without use of a neutral density filter using a supported slit is ~0.75 magnitudes.
- The limits in the tables assume zero extinction. To determine if your source will violate the limits in this table, correct the magnitude limit for the extinction of your source.
- The peak flux from an emission line or from the continuum from your source must be less than flux limit given in row two (for point sources—remember to correct for your aperture throughput) and row one for diffuse sources (remember to correct for the width of your source by scaling by your slit width in arcseconds divided by 0.2).
  - For first order gratings, the local (per pixel) count rate limit is hit prior to the global (over the detector) count rate limit—thus the peak point source flux and the bright object magnitude limits are equivalent for continuum sources.
  - For echelle observations, the global limit of 300,000 counts sec^{-1} over the detector sets the magnitude limits, and but you must also assure that your source does not violate the local limit, e.g., if it had a bright emission line.
  - If you are observing a source which has high equivalent width line emission (i.e., whose flux is dominated by line emission), you must assure that the *line emission* does not exceed the limits. This may be a concern for stars with strong emission lines, such as Wolf Rayet or T-Tauri stars.
- If you plan to place multiple bright stars in the long slit, or observe slitless, you must also assure that the sum from all targets imaged on the detector do not exceed the global limit of 300,000 counts sec^{-1}.
- The limits in this table are the worst case limits for the scanned gratings; use of a less sensitive central wavelength may have a brighter true limit, allowing you to observe your target.

Table 13.24: MAMA Spectroscopic Bright Object Limits - V Mags and cgs units.

Spectral Type	G140L	G140M	E140M	E140H	G230L	G230M	E230M	E230H	Prism
local limit surface brightness[a]	$9.7x10^{-11}$	$1.9x10^{-9}$	$1.7x10^{-8}$	$4.3x10^{-8}$	$4.5x10^{-11}$	$1.6x10^{-9}$	$3.8x10^{-9}$	$2.6x10^{-8}$	N/A
local limit point source flux[b]	$2.4x10^{-12}$	$5.6x10^{-11}$	$5.0x10^{-10}$	$1.3x10^{-9}$	$8.6x10^{-13}$	$3.8x10^{-11}$	$8.9x10^{-11}$	$5.9x10^{-10}$	N/A
O5V[c]	13.3	9.9	9.8	8.9	12.0	9.4	10.1	8.2	11.1
B1V	12.7	9.3	9.2	8.4	11.5	9.0	9.6	8.6	11.7
B3V	11.8	8.4	8.3	7.5	10.7	8.3	8.8	6.9	10.9
B6V	10.5	7.1	7.3	5.9	10.0	7.6	8.1	6.2	10.3
B9V	9.9	6.4	6.5	5.8	9.7	7.3	7.8	6.8	10.1
A1V	8.5	5.1	5.6	4.6	9.0	6.7	7.1	5.2	9.6
A3V	7.0	3.6	4.5	3.0	8.6	6.2	6.6	5.7	9.3
A5V	4.5	0.4	0.4	-0.3	8.2	5.7	6.0	5.1	9.1
A9IV	4.3	0.2	-0.2	-0.5	8.0	5.5	5.9	4.9	8.9
F2V	1.6				7.7	5.1	5.3	4.3	8.9
F4V	1.5				7.6	5.0	5.2	4.2	8.8
F6V	1.5				7.7	5.0	5.1	4.1	8.9
F8V	1.6				7.6	4.7	4.8	3.6	8.8
G2V	-0.9				7.7	4.5	4.5	3.4	8.3
G5IV	-1.5				7.0	3.8	3.9	2.7	7.7
G7IV					6.2	2.6	2.6	1.0	7.3
K0IV					5.9	2.2	2.2	0.6	6.9
K4V					5.6	1.7	1.8	0.3	6.7
K8V					5.6	1.5	1.6	0.0	6.5
M2V					5.6	1.5	1.5	0.3	5.8
M4V					5.4	1.3	1.3	0.1	5.6
M6V					4.9	0.8	0.8	-0.3	5.1
M8III					3.8	-0.3	-0.3	-1.5	4.0
T~50000^{o}K[d]	13.2	9.8	9.7	8.8	11.9	9.3	10.0	9.0	12.0
ν^{-1} [d]	9.6	7.7	6.7	6.6	10.46	8.6	8.2	7.7	14.4

[a] Peak surface brightness in ergs sec^{-1} cm^{-2} $Å^{-1}$ $arcsec^{-2}$ of the continuum or of an emission line from a diffuse source.
[b] Peak flux in ergs sec^{-1} cm^{-2} $Å^{-1}$ an emission line from a point source - for the first order slits this is also the peak flux from the continuum, but for the echelles the continuum flux limit is considerably lower, as the global limit and not the local limit dominates.
[c] Limits are V magnitudes, assuming zero reddening.
[c] Limits for a black body with a temperature of 50,000 degrees K.
[d] Limits for a source with a spectrum F_ν proportional to ν^{-1}.

CHAPTER 14

Imaging Reference Material

In This Chapter...

Introduction

In this section, we provide reference material in support of the material presented in Chapter 5 to help you select your imaging configuration and determinate your observing plan (e.g., total required exposure time, and number of exposures). This chapter is primarily organized by *imaging mode* (i.e., clear or filtered aperture). For each imaging mode the following are provided:

- Plots and tables of sensitivities as a function of wavelength.
- Plots of time as a function of source flux to achieve a signal-to-noise of 10.
- Plots of time versus source flux to saturate and time where source plus background counts dominate the background for CCD observations.

In addition,

- "Point Source Encircled Energies" on page 305 describes the optical performance of the imaging modes, and contain simulated encircled energy plots at a range of wavelengths.
- "MAMA Imaging Bright Object Limits" on page 307 presents screening tables of bright object magnitudes for sources of different spectral type.

The next section, "Using the Information in this Chapter" on page 258, explains the plots and tables found in the grating sections in this chapter.

Using the Information in this Chapter

Sensitivities

This chapter contains plots and tables of sensitivities for each imaging mode. "Determining Count Rates from Sensitivities" on page 66 in the Exposure Time Calculation chapter explains how to use sensitivities to calculate expected counts rates from your source.

The *imaging point source sensitivity,* $Sens^{p}_{\lambda}$, has the unit:

counts sec^{-1} $Å^{-1}$ per incident erg cm^{-2} s^{-1} $Å^{-1}$, where

- counts refer to the total counts from the point source integrated over the PSF.

The *imaging diffuse source sensitivity,* $Sens^{d}_{\lambda}$, has the unit:

counts sec^{-1} $Å^{-1}$ $pixel^{-1}$ per incident dimensional erg cm^{-2} s^{-1} $Å^{-1}$ $arcsec^{-2}$.

Thus $Sens^{p}_{\lambda}$ and $Sens^{d}_{\lambda}$ are related through the relation:

$$\mathrm{Sens}^{\mathrm{d}}_{\lambda} \cong (\mathrm{Sens}^{\mathrm{P}}_{\lambda} \times \mathrm{m}^{2})$$

where *m* is the plate-scale in arcsec per pixel.

Signal-To-Noise

For each imaging mode, plots of flux versus exposure time to achieve a signal-to-noise of 10 are presented in the individual sections for both point source and diffuse sources. The plots included are:

1. *Signal-To-Noise versus Exposure Time for stars of known spectral type and V magnitude.* The plots show V magnitude versus exposure time with a series of curves superposed showing the time to achieve a signal-to-noise of 10 integrated over the band pass for several different spectral types with unreddened main sequence stars with the flux distribution shown in Figure 1.1 on page 5. In making these plots we have integrated over the PSF

to contain 80% of the light and the bandpass. Plot (a) is for an O star, (b) is for a A star, (c) is for a G star, and (d) is for a M star. You can use these plots directly. If you know your source V magnitude, simply look up (or interpolate) the exposure time to achieve a signal-to-noise = 10.

2. *Signal-to-Noise ratio versus Exposure Time for Point and Diffuse Sources of known brightness, in CGS units.* Plot (a) is for point sources and plot (b) is for diffuse sources. In making these plots we have integrated over the PSF for point sources and show the signal-to-noise ratio per four pixels (2 in each dimension) for diffuse sources. We assume the spectrum of the source is flat (constant in F_λ) and integrate over the bandpass. If you know your source flux or brightness, you can directly look up (or interpolate) the time to achieve a signal-to-noise of 10 from these plots.

At high flux levels, where the detector and sky background is negligible (and for the CCD at high count levels, where the read noise is not important) the exposure time to achieve a given signal-to-noise scales directly as signal-to-noise^2 (see also “Calculating Exposure Times for a Given Signal-to-Noise” on page 70). However, at lower flux levels, the background, dark current and read noise (the latter for the CCD only) must be taken into account when estimating the time to achieve a given signal-to-noise. The following assumptions were made in producing the signal-to-noise plots presented in the grating sections below:

- For CCD observations, in order to assure that cosmic rays could be removed from the images in post-observation data processing, all observations have been ‘taken’ using the default value of `CRSPLIT=2`, i.e., have been split into at two exposures of equal duration.
- The sky background was taken from Figure 6.1 on page 74.
- The CCD read noise and background (dark current) and the MAMA backgrounds were taken from Table 6.2 on page 72.

Saturation

Both CCD imaging and MAMA imaging observations are subject to saturation at high total *accumulated* counts per pixel (see “CCD Saturation: the CCD Full Well” on page 90 and “MAMA Saturation—Overflowing the 16 Bit Buffer” on page 95. Plots of time to saturation as a function of source flux are presented for each imaging mode in the sections below. We assume F_λ=constant for these plots.

Superposed on the saturation plot, for the CCD, is a line indicating, for a given source flux, when the observation is no longer read noise dominated (taken to occur when the source plus background counts exceed two times the square of the read noise).

Encircled Energies

See page 305 for predicted imaging mode encircled energies.

50CCD - clear

Figure 14.1: 50CCD - clear Point Source (left axis), and Diffuse Source (right axis) Sensitivities. Bandpass integrated sensitivity for F_λ=1 is 1.5x10^{19}.

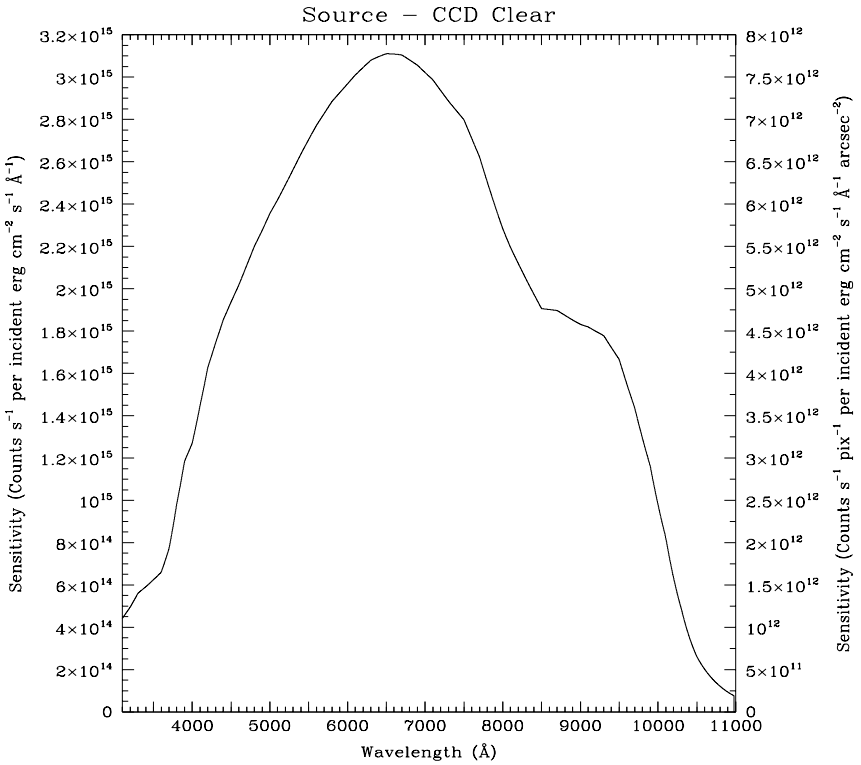

Table 14.1: Point Source Sensitivities for 50CCD Clear. Multiply sensitivity number by 0.0025 (the plate scale squared) to obtain diffuse source sensitivity.

λ	**Sens.**	λ	**Sens.**	λ	**Sens.**	λ	**Sens.**
2600	2.3E14	4800	2.2E15	7000	3.0E15	9200	1.8E15
2800	2.7E14	5000	2.4E15	7200	2.9E15	9400	1.7E15
3000	3.8E14	5200	2.5E15	7400	2.8E15	9600	1.5E15
3200	4.9E14	5400	2.6E15	7600	2.7E15	9800	1.3E15
3400	5.9E14	5600	2.8E15	7800	2.5E15	10000	9.8E14
3600	6.6E14	5800	2.9E15	8000	2.3E15	10200	6.3E14
3800	9.8E14	6000	3.0E15	8200	2.1E15	10400	3.6E14
4000	1.3E15	6200	3.0E15	8400	2.0E15	10600	2.0E14
4200	1.6E15	6400	3.1E15	8600	1.9E15	10800	1.2E14
4400	1.8E15	6600	3.1E15	8800	1.9E15		
4600	2.0E15	6800	3.1E15	9000	1.8E15		

Figure 14.2: 50CCD Time to Achieve a Signal-to-Noise of 10 integrated over the PSF and the bandpass for stars of different spectral types as a function of V band magnitude.

(a) O5 star

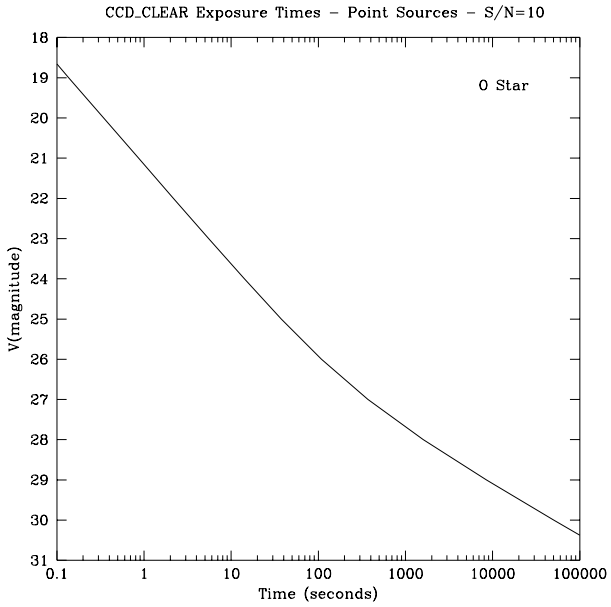

(b) AOV star

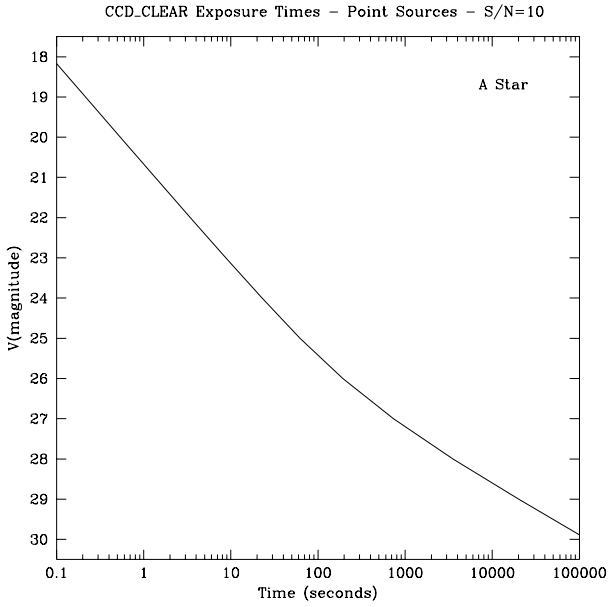

(c) G0V star

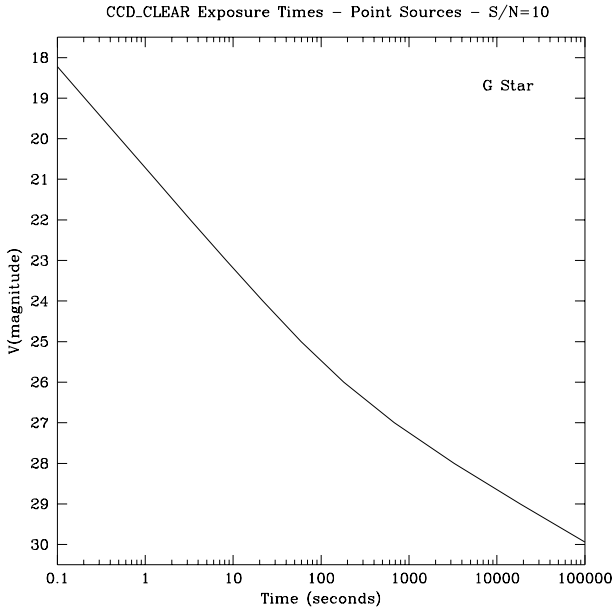

(d) M0V star

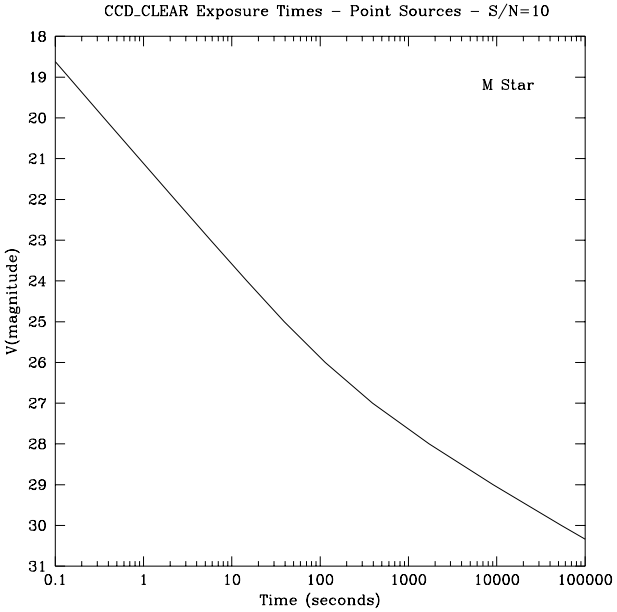

Figure 14.3: 50CCD Time to Achieve a Signal-to-Noise of 10 integrated over the bandpass, for point and diffuse sources, assuming a flat (in F_λ)spectrum, cgs units. Point source signal-to-noise is integrated over the PSF, diffuse sources are per 2x2 spatial pixels.

(a) Point Sources

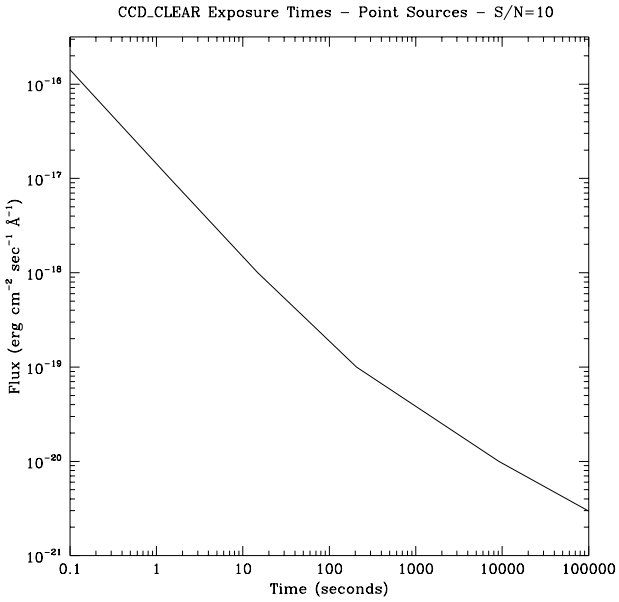

(b) Diffuse Sources

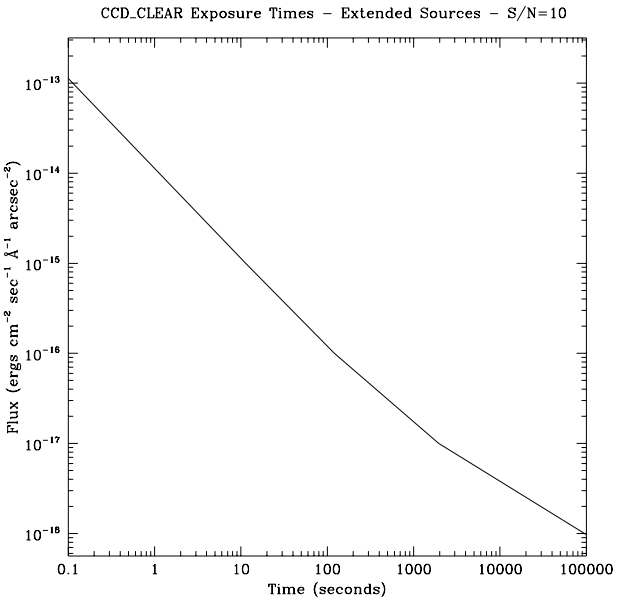

Figure 14.4: 50CCD Time to Saturate as a Function of Source Flux, assuming a flat (in F_λ) spectrum

(a) Point Sources

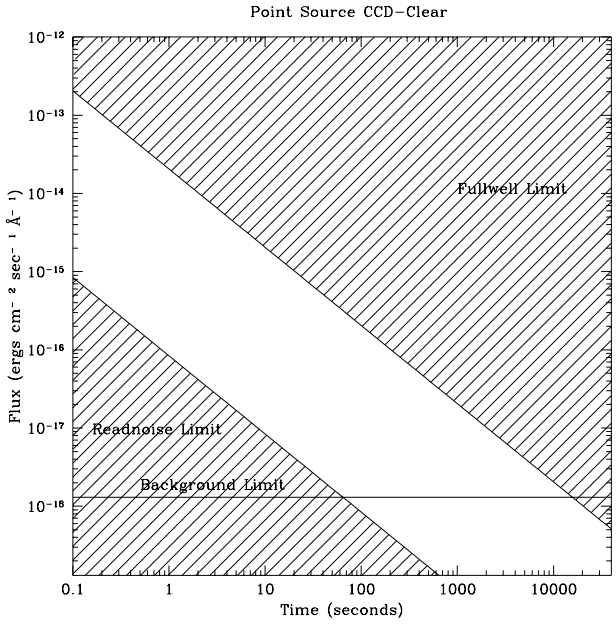

(b) Diffuse Sources

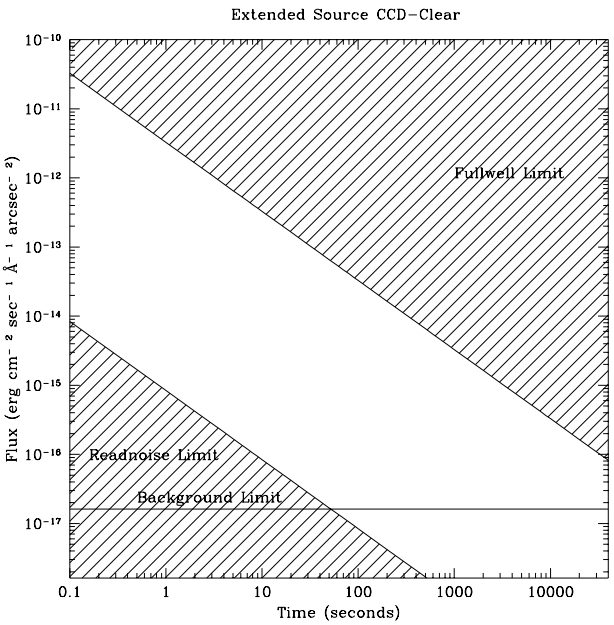

F28X50LP - CCD

Figure 14.5: F28X50LP-CCD Point Source (left axis), and Diffuse Source (right axis) Sensitivities. Bandpass integrated sensitivity for F_λ=1 is 1.1x10^{19}

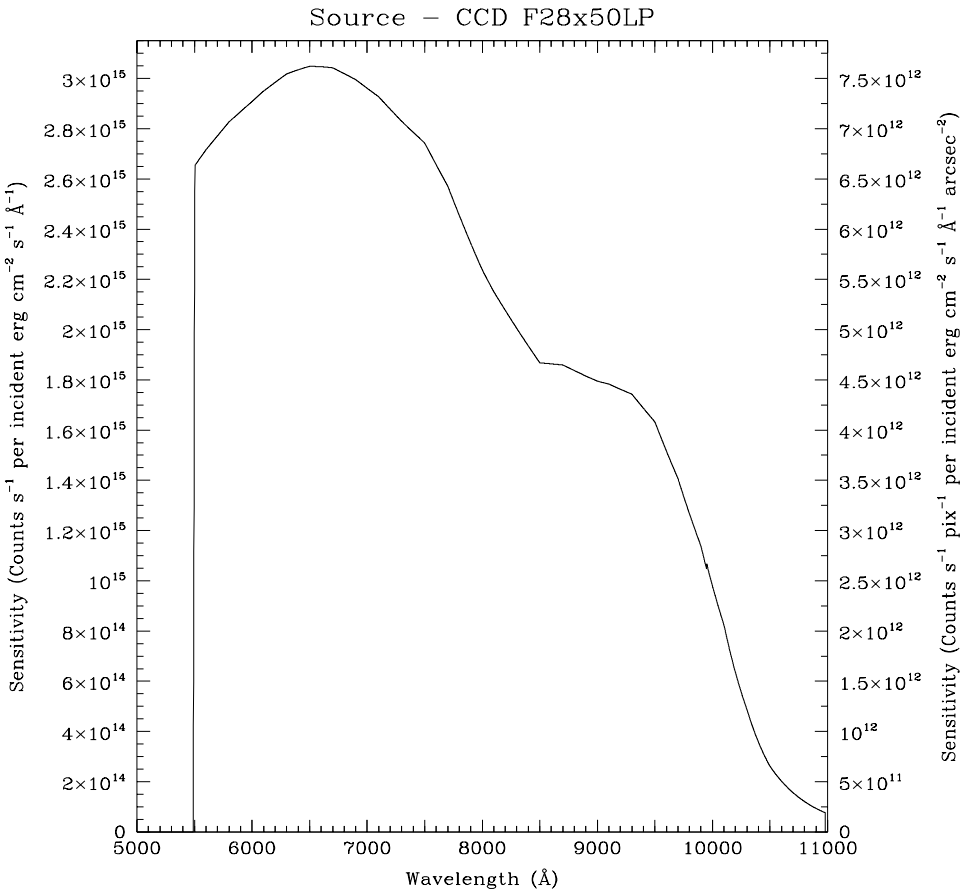

Table 14.2: Point Source Sensitivities for CCD F28x50LP. Multiply sensitivity number by 0.0025 (the plate scale squared) to obtain diffuse source sensitivity.

λ	**Sens**.	λ	**Sens**.	λ	**Sens**.	λ	**Sens**.
5600	2.7E15	7000	3.0E15	8400	1.9E15	9800	1.3E15
5800	2.8E15	7200	2.9E15	8600	1.9E15	10000	9.8E14
6000	2.9E15	7400	2.8E15	8800	1.8E15	10200	6.3E14
6200	3.0E15	7600	2.7E15	9000	1.8E15	10400	3.6E14
6400	3.0E15	7800	2.5E15	9200	1.8E15	10600	2.0E14
6600	3.0E15	8000	2.2E15	9400	1.7E15	10800	1.2E14
6800	3.0E15	8200	2.1E15	9600	1.5E15		

Figure 14.6: F28X50LP-CCD Time to Achieve a Signal-to-Noise of 10 integrated over the PSF and the bandpass for stars of different spectral types as a function of V band magnitude.

(a) O5 star

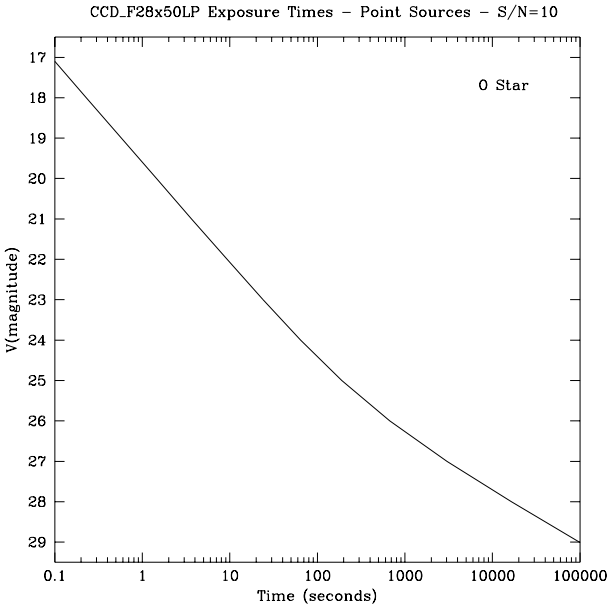

(b) AOV star

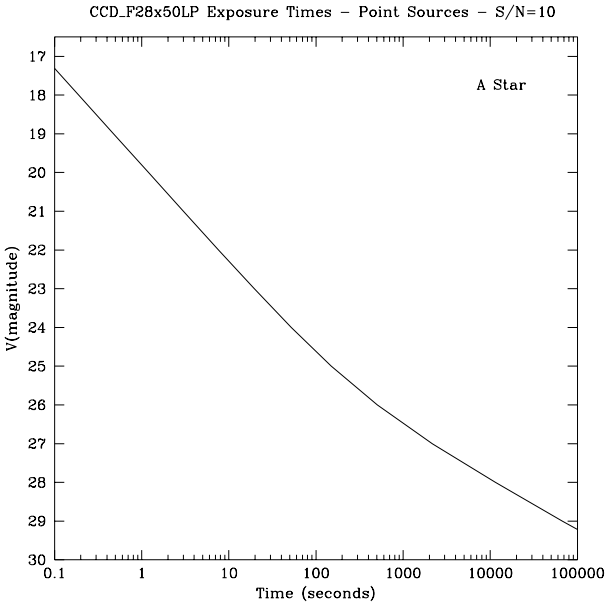

(c) G0V star

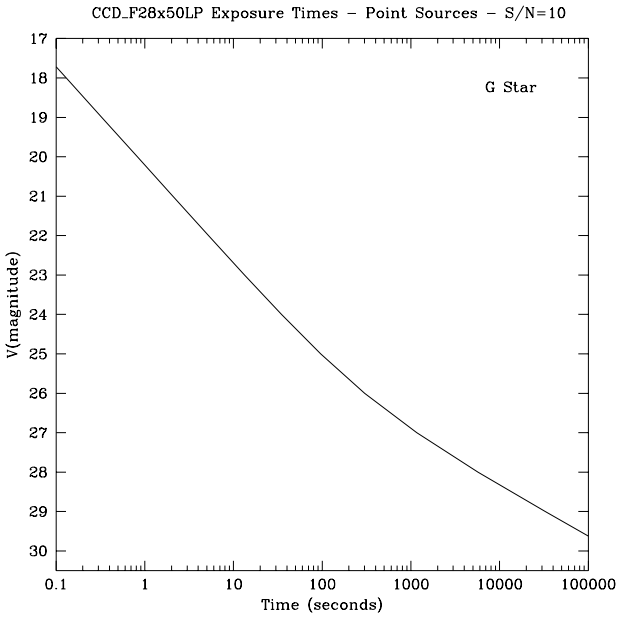

(d) M0V star

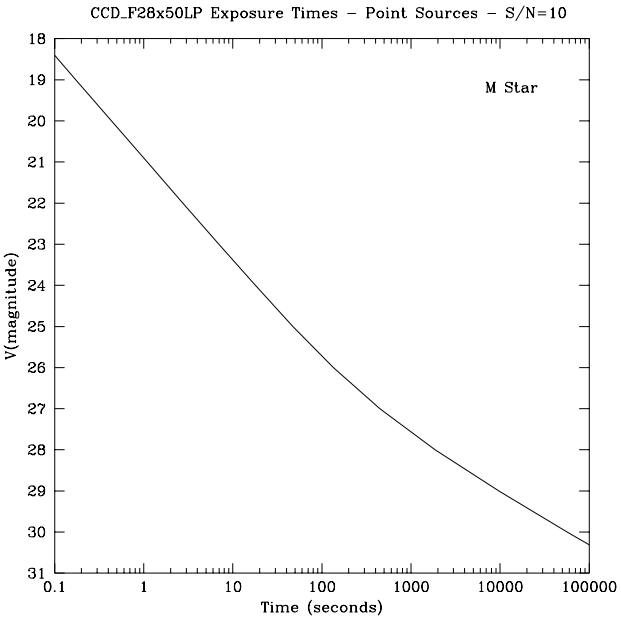

Figure 14.7: F28X50LP-CCD Time to Achieve a Signal-to-Noise of 10 integrated over the bandpass, for point and diffuse sources, assuming a flat (in F_λ) spectrum, cgs units. Point source signal-to-noise is integrated over the PSF, diffuse sources are per 2x2 spatial pixels.

(a) Point Sources

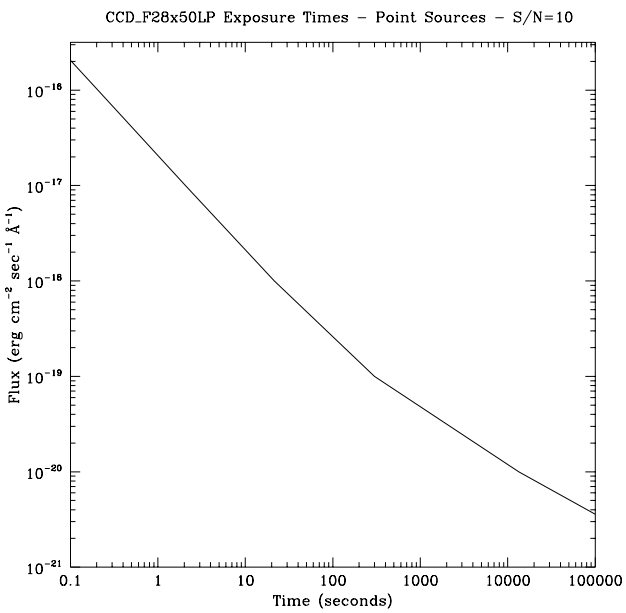

(b) Diffuse Sources

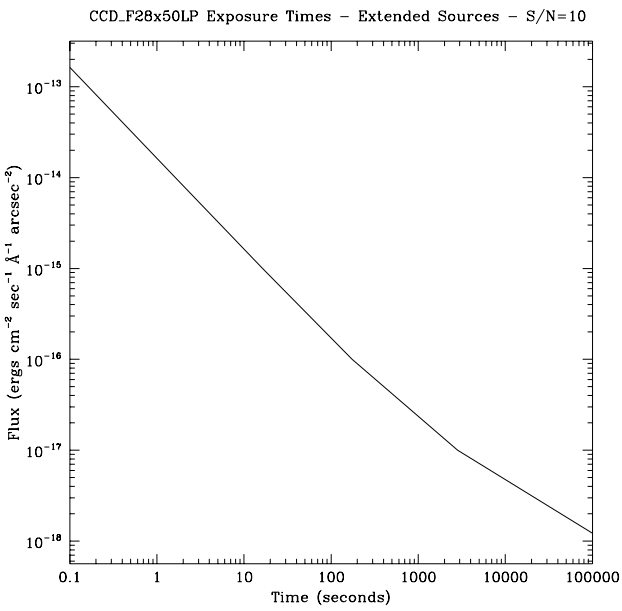

Figure 14.8: Time to Saturate as a Function of Source Flux, assuming a flat (in F_λ) spectrum

(a) Point Sources

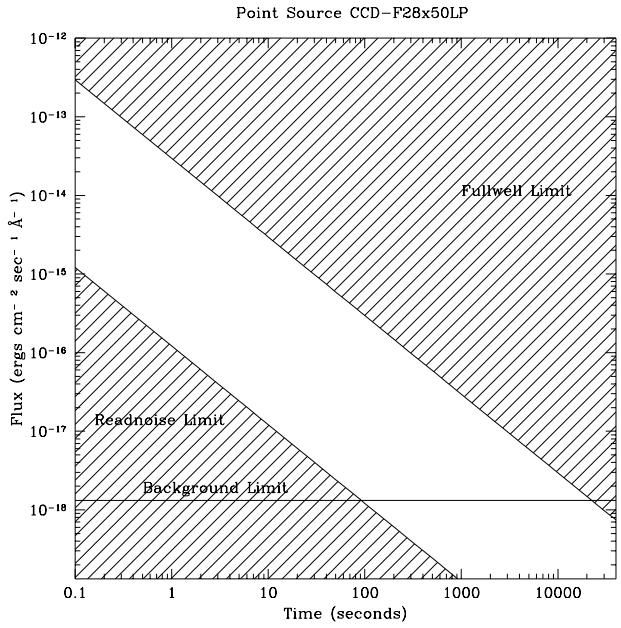

(b) Diffuse Sources

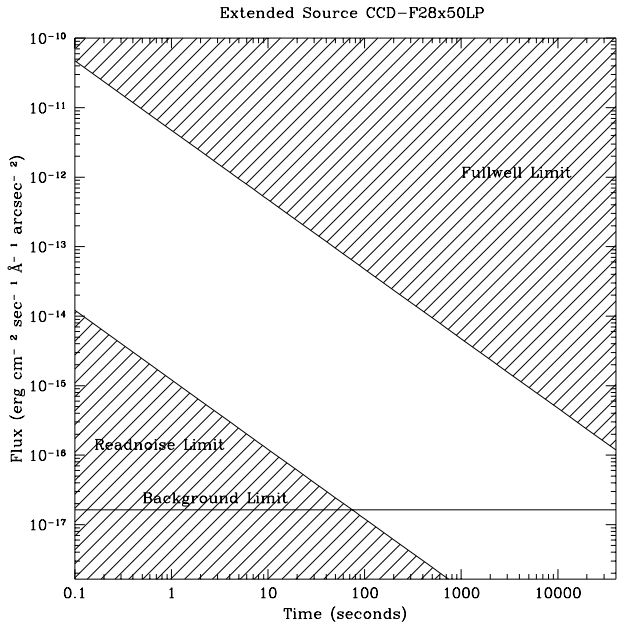

F28X50OIII - CCD

Figure 14.9: F28X50OIII-CCD Point Source (left axis), and Diffuse Source (right axis) Sensitivities. Bandpass integrated sensitivity for F_λ=1 is 1.1x10^{16}

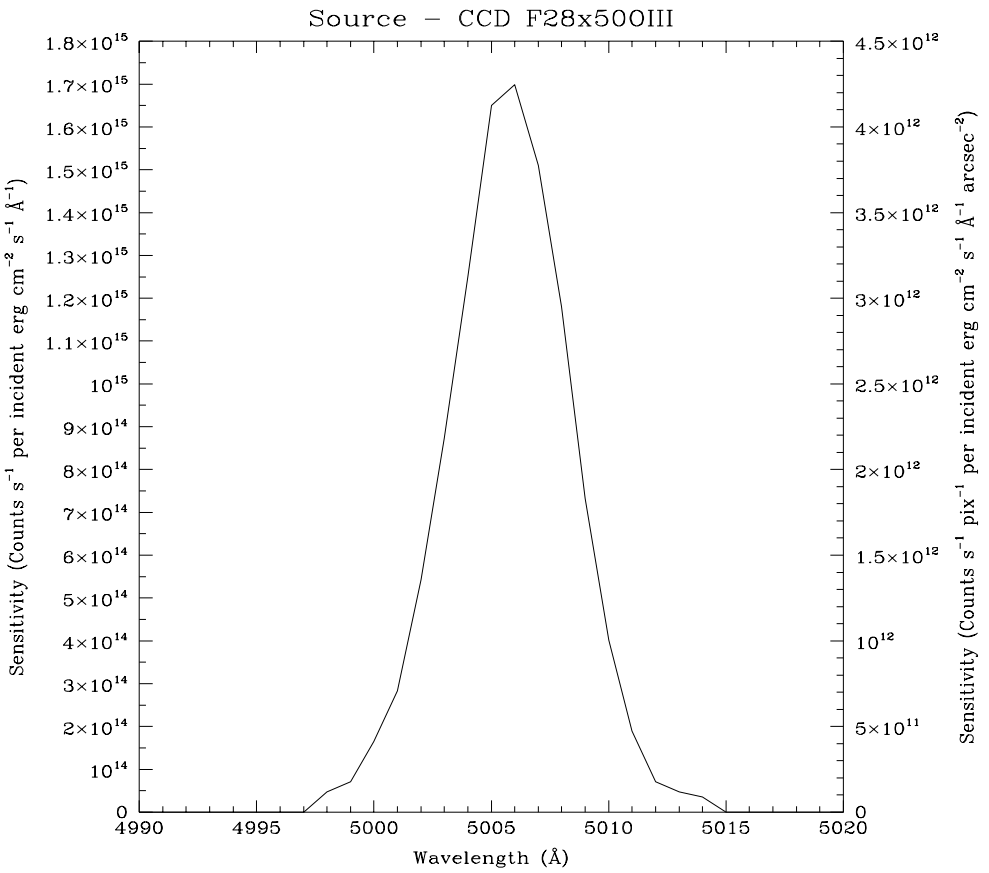

Table 14.3: Point Source Sensitivities for CCD 28x50OIII. Multiply sensitivity number by 0.0025 (the plate scale squared) to obtain diffuse source sensitivity.

λ	**Sens.**	λ	**Sens.**	λ	**Sens.**	λ	**Sens.**
4998	4.7E13	5003	8.7E14	5008	1.2E15	5013	4.7E13
4999	7.1E13	5004	1.3E15	5009	7.3E14	5014	3.5E13
5000	1.6E14	5005	1.7E15	5010	4.0E14		
5001	2.8E14	5006	1.7E15	5011	1.9E14		
5002	5.4E14	5007	1.5E15	5012	7.1E13		

Figure 14.10: F28X50OIII-CCD Time to Achieve a Signal-to-Noise of 10 integrated over the PSF and the bandpass for Stars of Different Spectral Types as a function of V band magnitude.

(a) O5 star

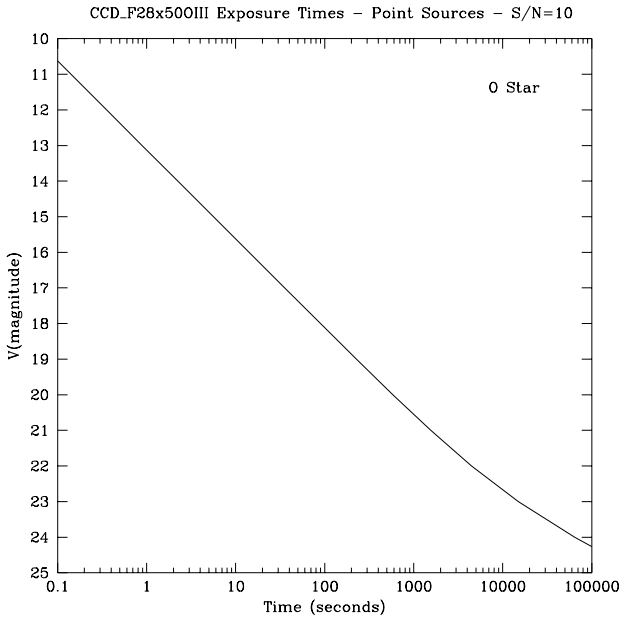

(b) AOV star

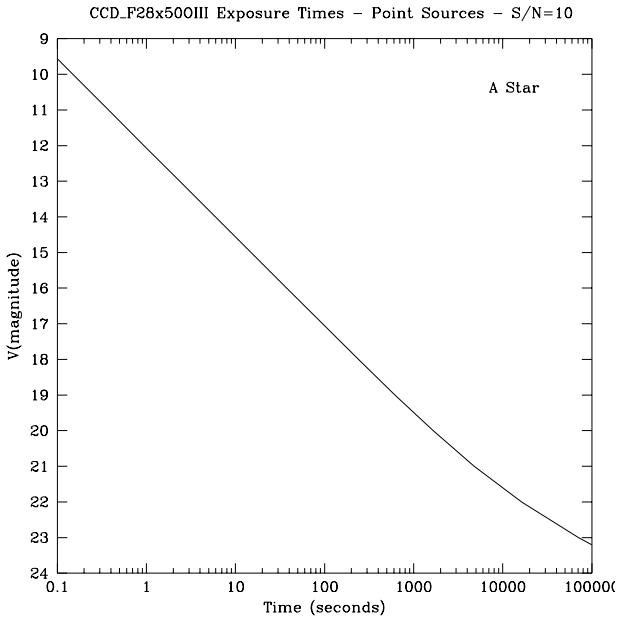

(c) G0V star

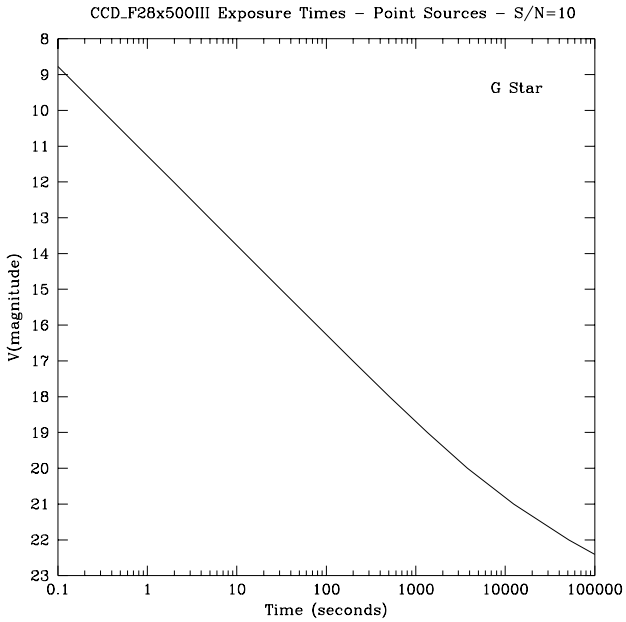

(d) M0V star

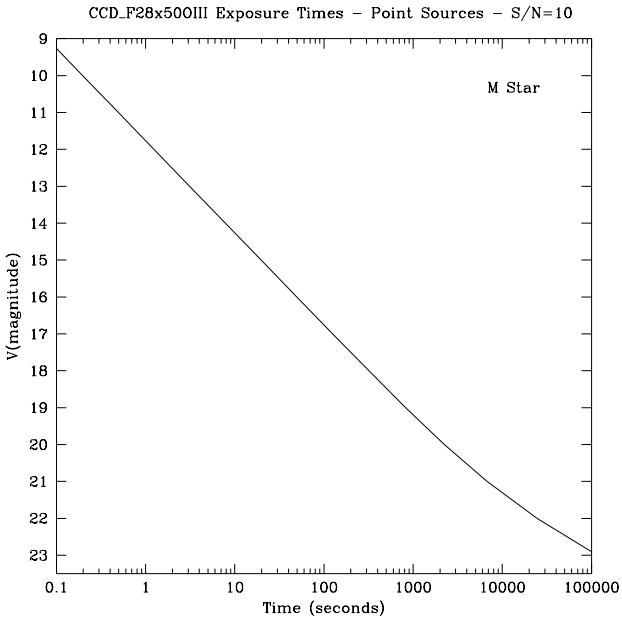

Figure 14.11: F28X50OIII-CCD Time to Achieve a Signal-to-Noise of 10 integrated over the bandpass, for Point and Diffuse Sources, assuming a flat (in F_λ) spectrum, cgs units. Point source signal-to-noise is integrated over the PSF, Diffuse sources are per 2x2 spatial pixels.

(a) Point Sources

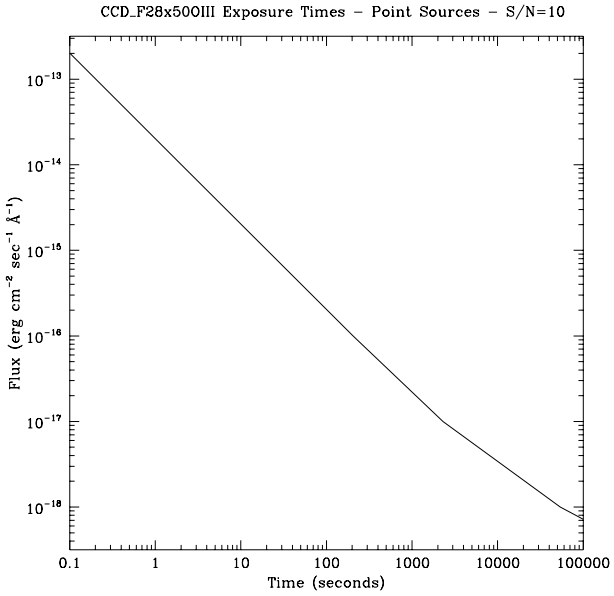

(b) Diffuse Sources

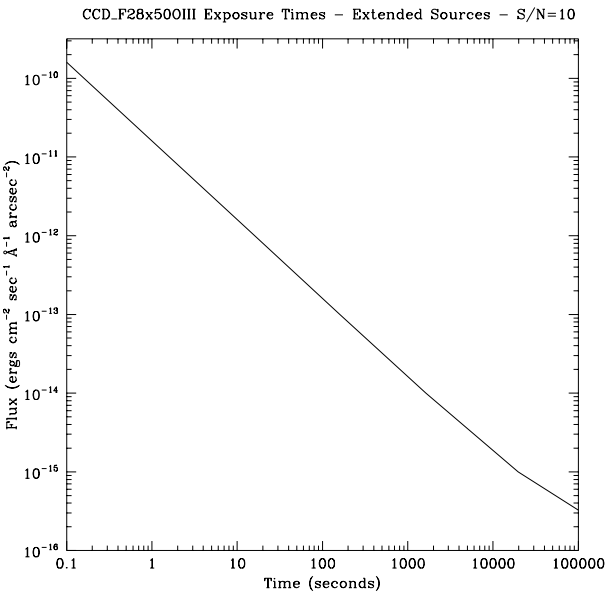

Figure 14.12: F28X50OIII-CCD Time to Saturate as a Function of Source Flux, assuming a flat (in F_λ) spectrum.

(a) Point Sources

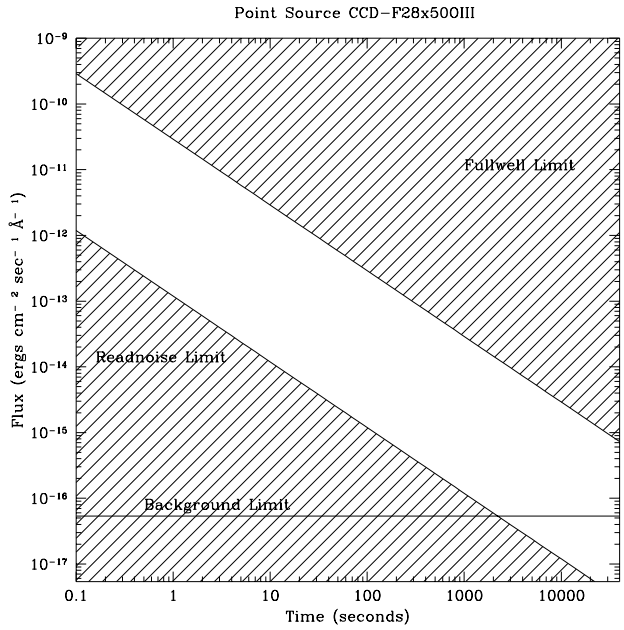

(b) Diffuse Sources

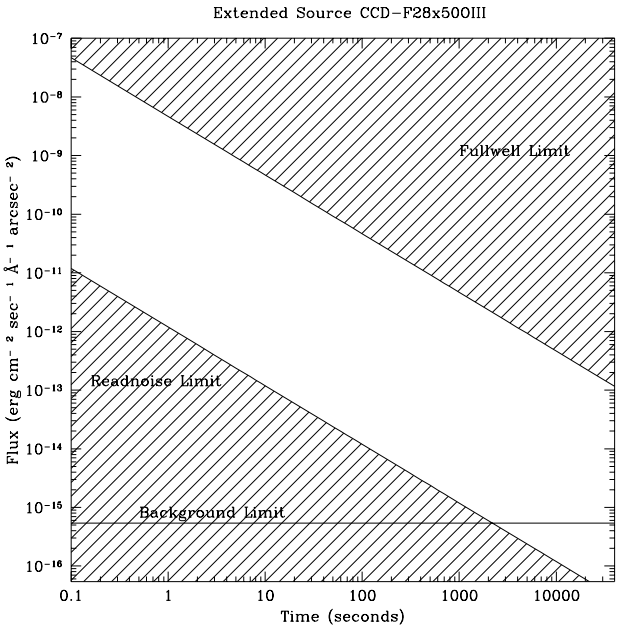

F28X50OII-CCD

Figure 14.13: F28X50OII-CCD Point Source (left axis), and Diffuse Source (right axis) Sensitivities. Bandpass integrated sensitivity for F_λ=1 is 2.8x10^{16}

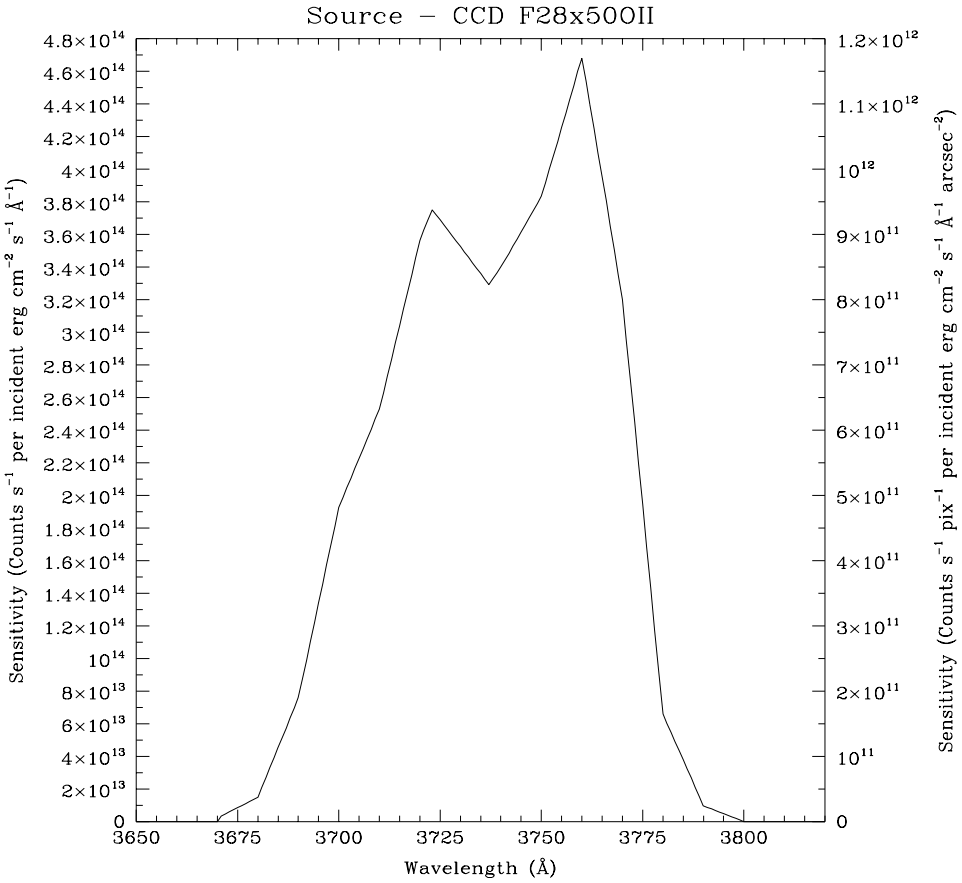

Table 14.4: Point Source Sensitivities for CCD 28x50OII. Multiply sensitivity number by 0.0025 (the plate scale squared) to obtain diffuse source sensitivity.

λ	**Sens**.	λ	**Sens**.	λ	**Sens**.	λ	**Sens**.
3670	5.36E9	3710	2.5E14	3750	3.8E14	3790	9.7E12
3680	1.5E13	3720	3.6E14	3760	4.7E14	3800	7.16E8
3690	7.6E13	3730	3.5E14	3770	3.2E14		
3700	1.9E14	3740	3.4E14	3780	6.6E13		

Figure 14.14: F28X50OII-CCD Time to Achieve a Signal-to-Noise of 10 integrated over the PSF and the bandpass for stars of different spectral types as a function of V band magnitude

(a) O5 star

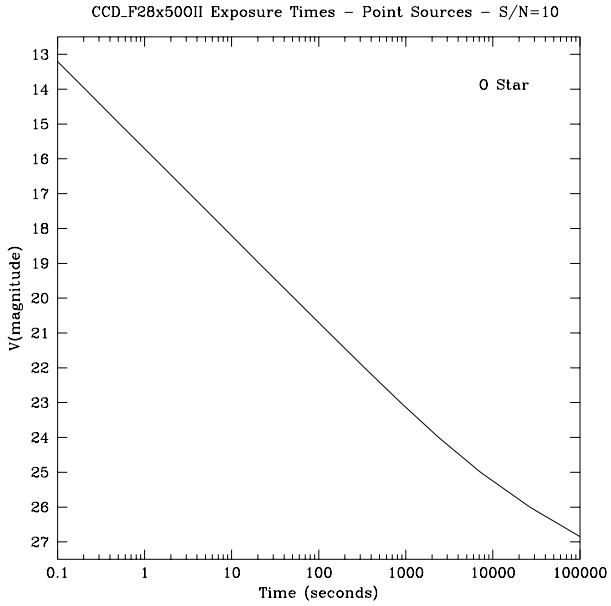

(b) AOV star

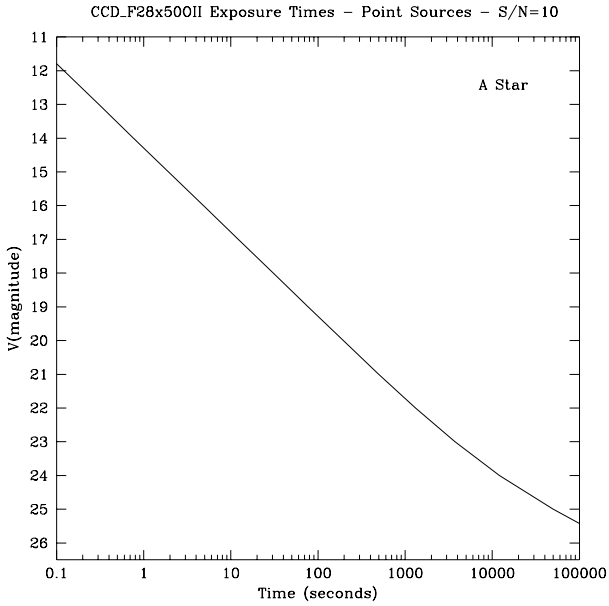

(c) G0V star

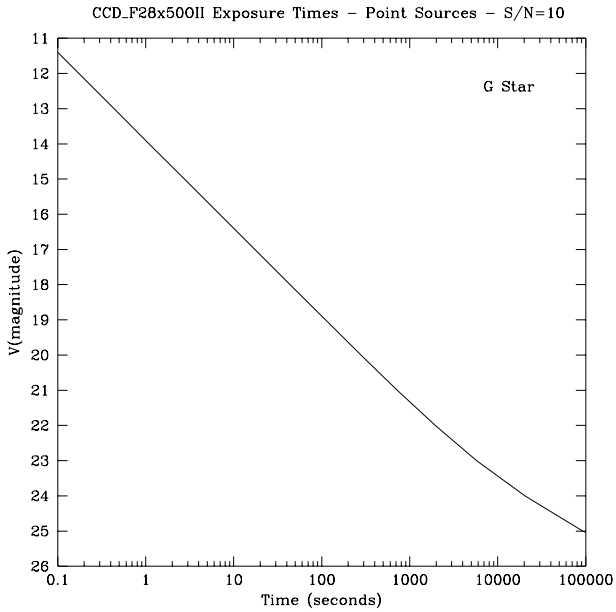

(d) M0V star

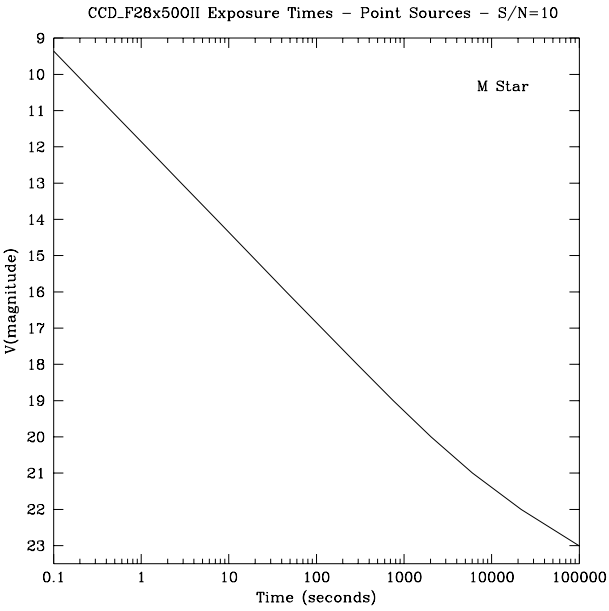

Figure 14.15: F28X50OII-CCD Time to Achieve a Signal-to-Noise of 10 integrated over the bandpass, for point and diffuse sources, assuming a flat (in F_λ) spectrum, cgs units. Point source signal-to-noise is integrated over the PSF, diffuse sources are per 2x2 spatial pixels.

(a) Point Sources

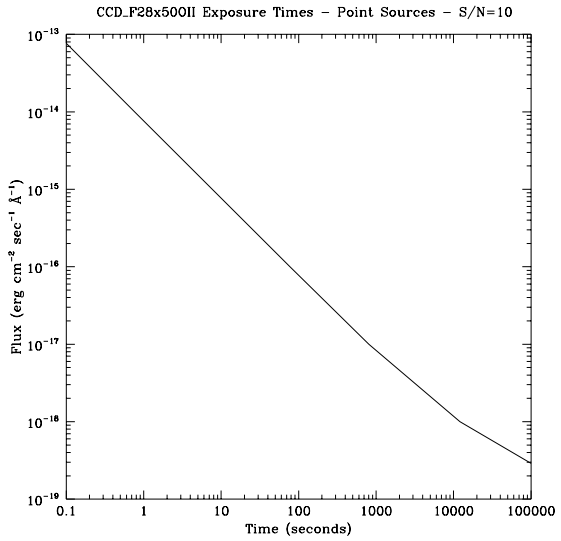

(b) Diffuse Sources

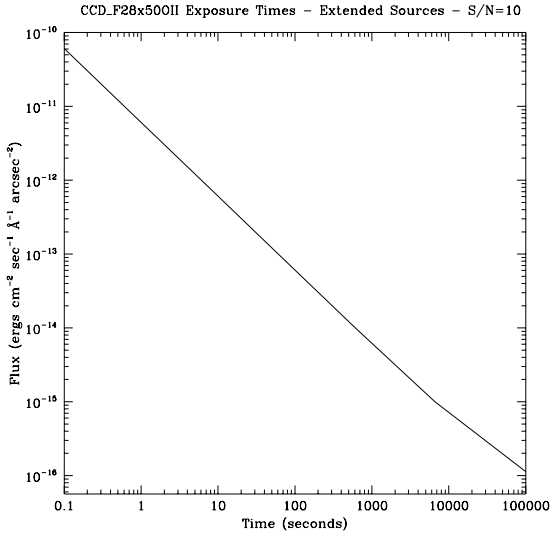

Figure 14.16: F28X50OII-CCD Time to Saturate as a Function of Source Flux, assuming a flat (in F_λ) spectrum,

(a) Point Sources

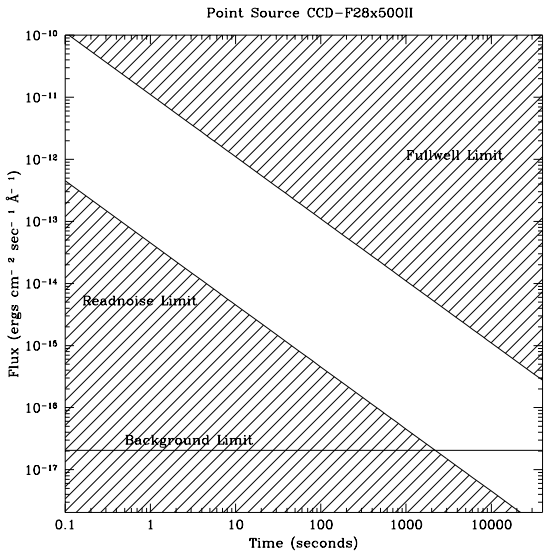

(b) Diffuse Sources

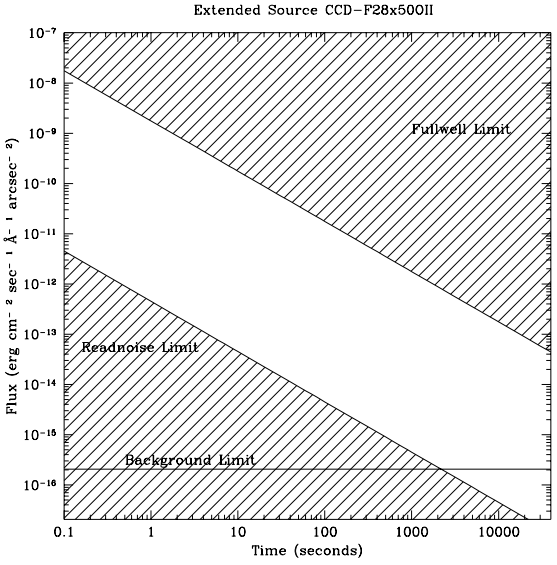

50CORON - CCD - clear

See “50CCD - clear” on page 260.

25MAMA - NUV-MAMA - clear

Figure 14.17: 25 NUVMAMA Point Source, and Diffuse Source Sensitivities. Bandpass integrated point source sensitivity for F_λ=1 is 2.4x10^{17}.

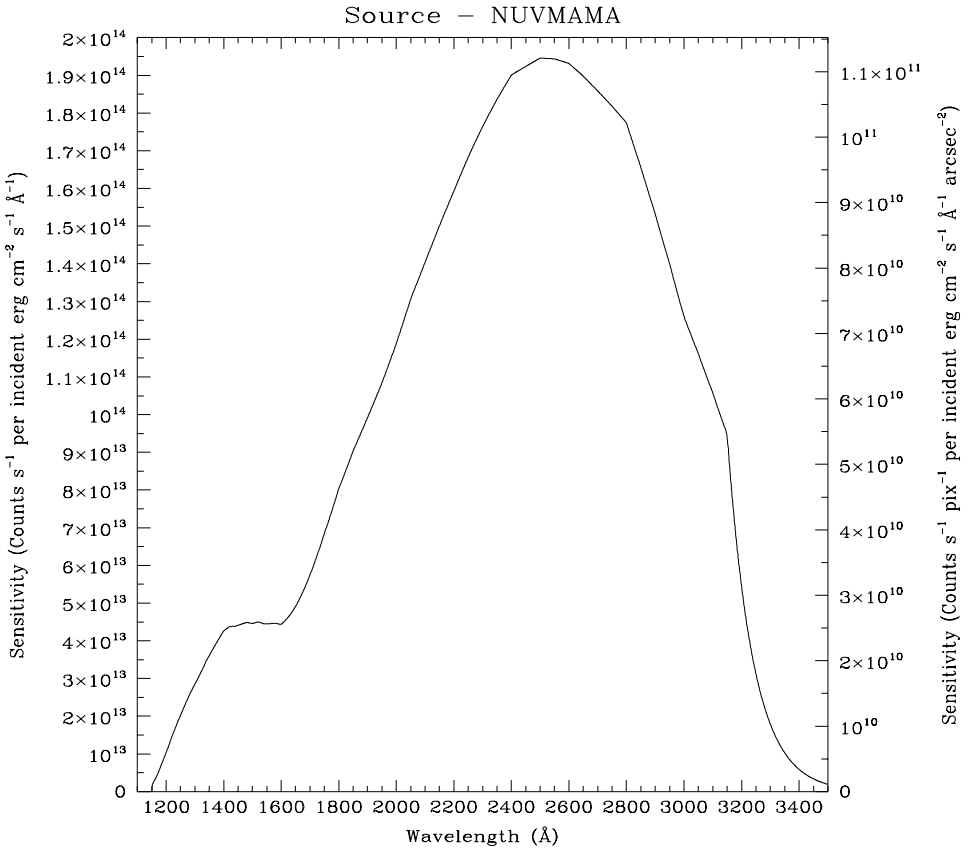

Table 14.5: Point Source Sensitivities for NUVMAMA. Multiply sensitivity number by 0.000576 (the plate scale squared) to obtain diffuse source sensitivity.

λ	**Sens.**	λ	**Sens.**	λ	**Sens.**	λ	**Sens.**
1200	1.0E13	2000	1.2E14	2800	1.8E14	3600	1.6E12
1300	2.8E13	2100	1.4E14	2900	1.5E14	3700	1.4E12
1400	4.3E13	2200	1.6E14	3000	1.3E14	3800	1.2E12
1500	4.5E13	2300	1.8E14	3100	1.1E14	3900	1.0E12
1600	4.4E13	2400	1.9E14	3200	5.4E13	4000	8.5E11
1700	5.7E13	2500	1.9E14	3300	1.8E13		
1800	8.0E13	2600	1.9E14	3400	5.9E12		
1900	9.9E13	2700	1.9E14	3500	2.0E12		

Figure 14.18: 25 NUVMAMA Time to Achieve a Signal-to-Noise of 10 integrated over the PSF and the bandpass for stars of different spectral types as a function of V band magnitude

(a) O5 star

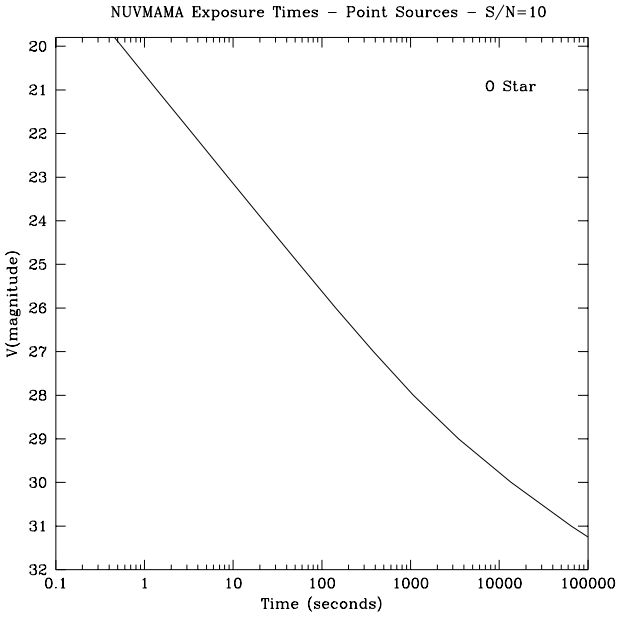

(b) AOV star

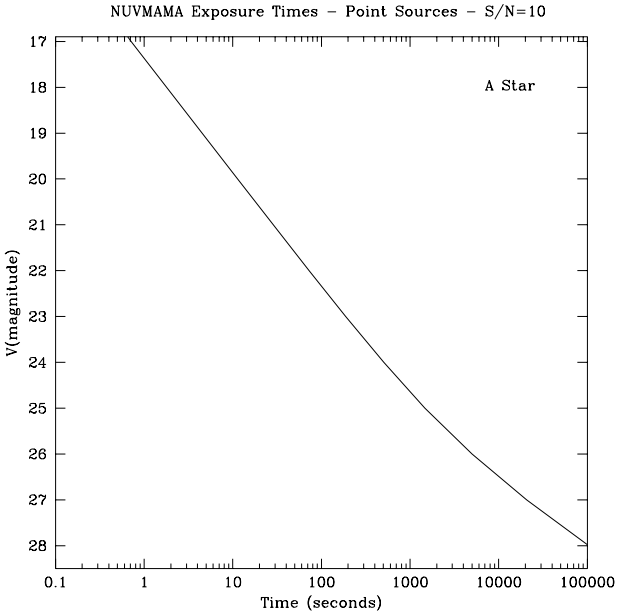

(c) G0V star

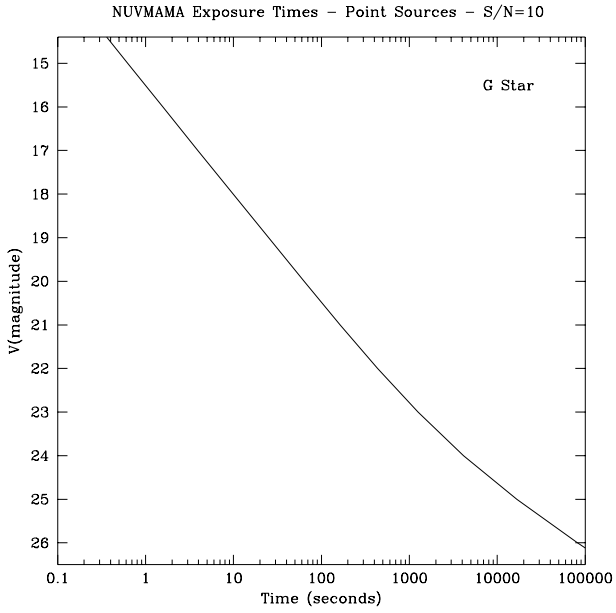

(d) M0V star

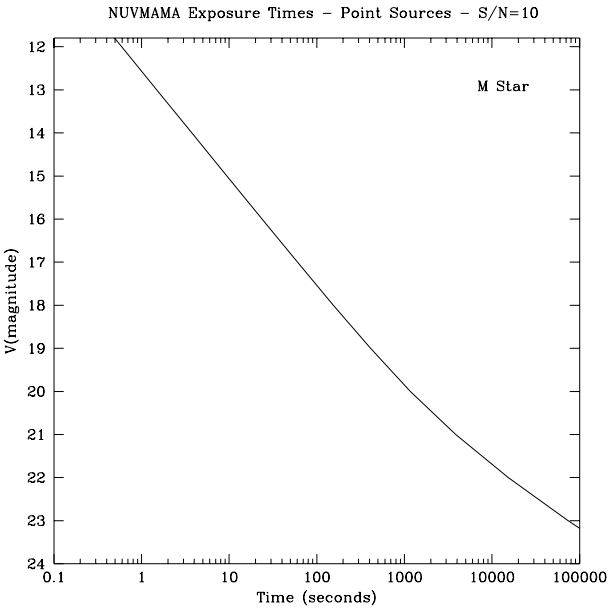

Figure 14.19: 25 NUVMAMA Time to Achieve a Signal-to-Noise of 10 integrated over the bandpass, for point and diffuse sources, assuming a flat (in F_λ) spectrum, cgs units. Point source signal-to-noise is integrated over the PSF, diffuse sources are per 2x2 spatial pixels.

(a) Point Sources

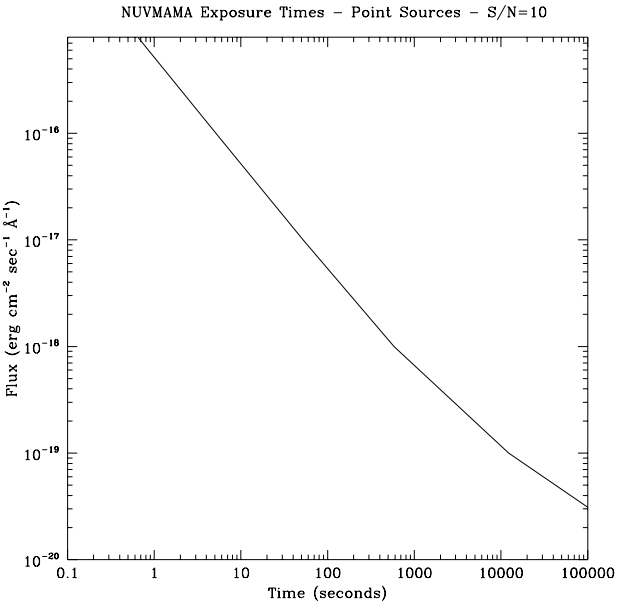

(b) Diffuse Sources

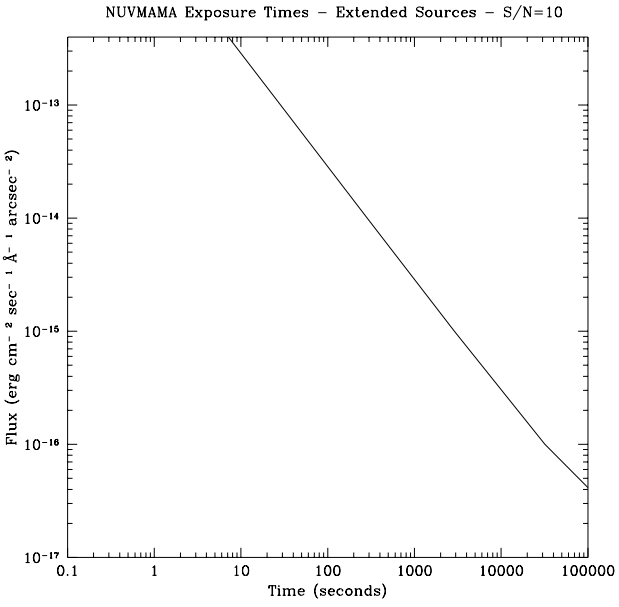

Figure 14.20: 25 NUVMAMA Time to Saturate as a Function of Source Flux, assuming a flat (in F_λ) spectrum

(a) Point Sources

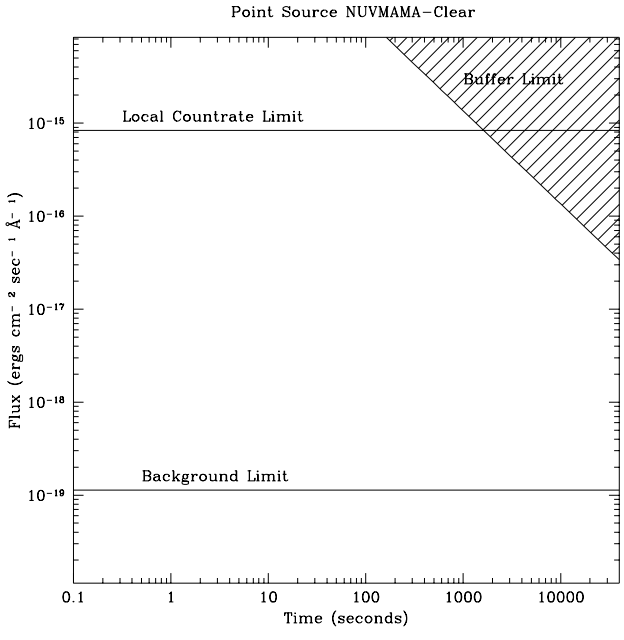

(b) Diffuse Sources

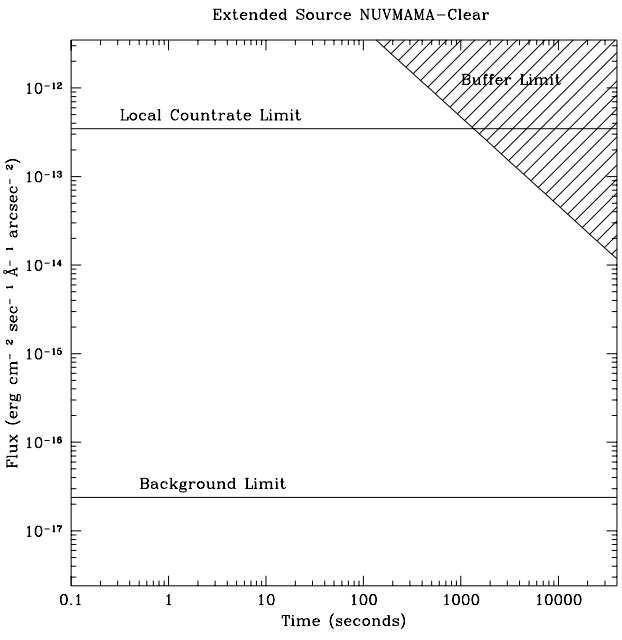

F25QTZ - NUV-MAMA - longpass

Figure 14.21: F25QTZ-NUVMAMA Point Source, and Diffuse Source Sensitivities. Bandpass integrated point source sensitivity for F_λ=1 is 2.1x10^{17}.

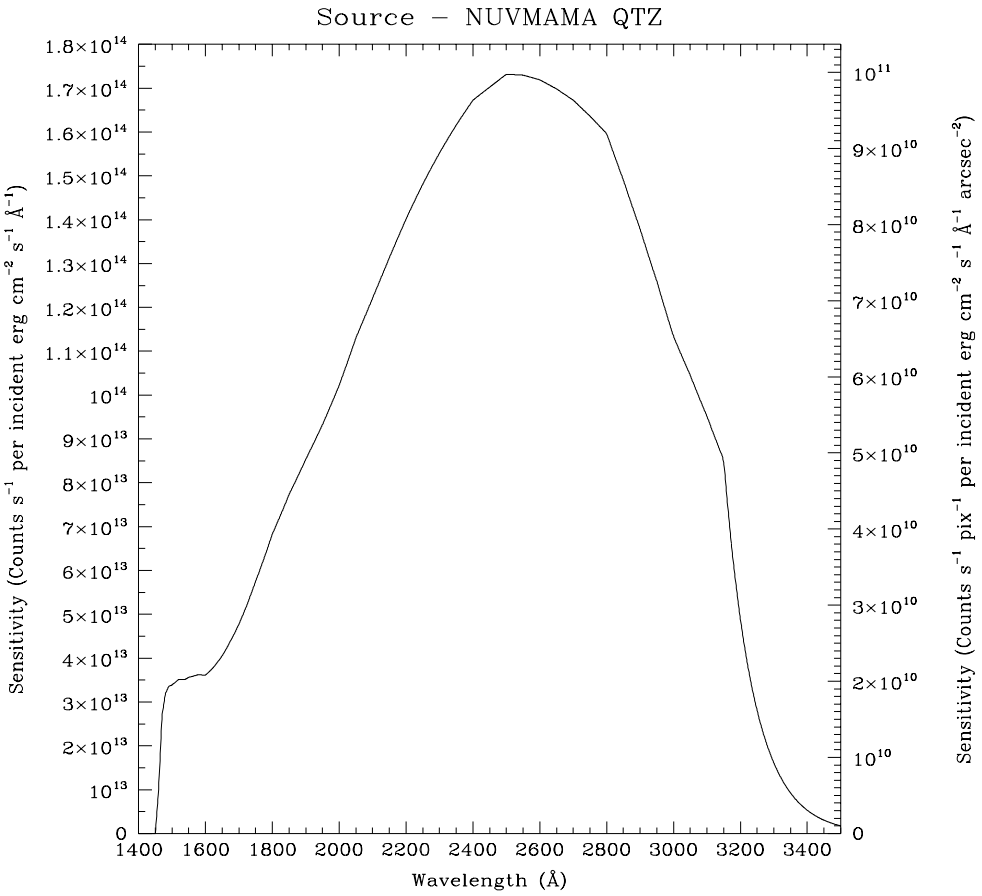

Table 14.6: F25QTZ-NUVMAMA Point Source Sensitivities for NUVMAMA QTZ. Multiply sensitivity number by 0.000576 (the plate scale squared) to obtain diffuse source sensitivity.

λ	**Sens.**	λ	**Sens.**	λ	**Sens.**	λ	**Sens.**
1500	3.4E13	2200	1.4E14	2900	1.4E14	3600	1.5E12
1600	3.6E13	2300	1.5E14	3000	1.1E14	3700	1.3E12
1700	4.8E13	2400	1.7E14	3100	9.5E13	3800	1.1E12
1800	6.8E13	2500	1.7E14	3200	4.9E13	3900	9.0E11
1900	8.5E13	2600	1.7E14	3300	1.6E13	4000	7.7E11
2000	1.0E14	2700	1.7E14	3400	5.3E12		
2100	1.2E14	2800	1.6E14	3500	1.8E12		

Figure 14.22: F25QTZ-NUVMAMA Time to Achieve a Signal-to-Noise of 10 integrated over the PSF and the bandpass for stars of different spectral types as a function of V band magnitude

(a) O5 star

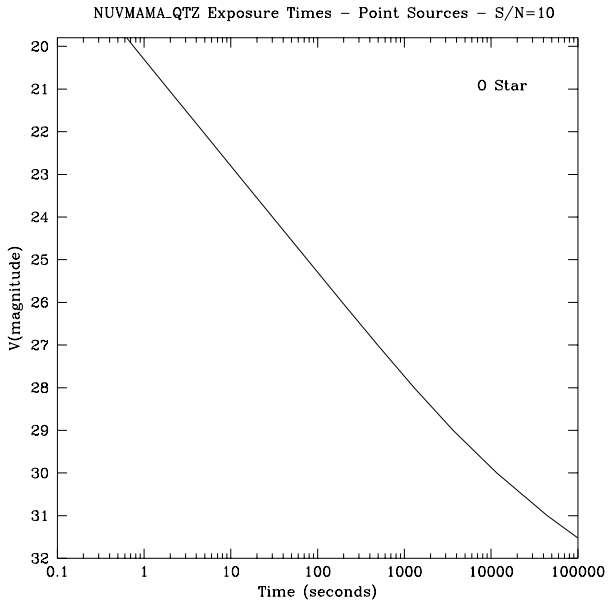

(b) AOV star

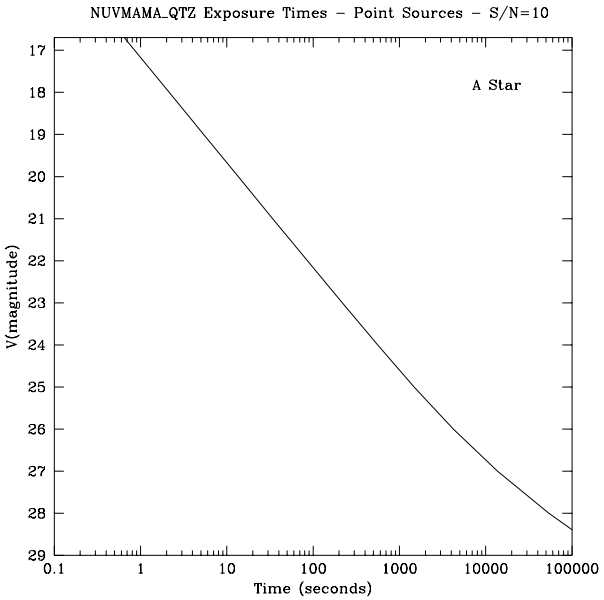

(c) G0V star

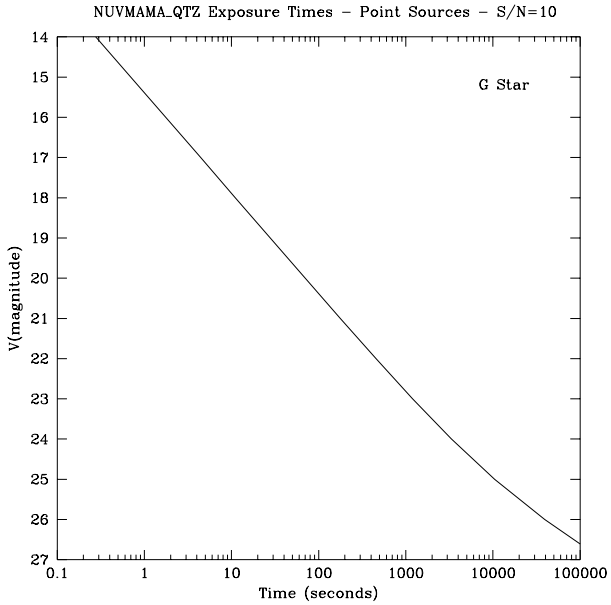

(d) M0V star

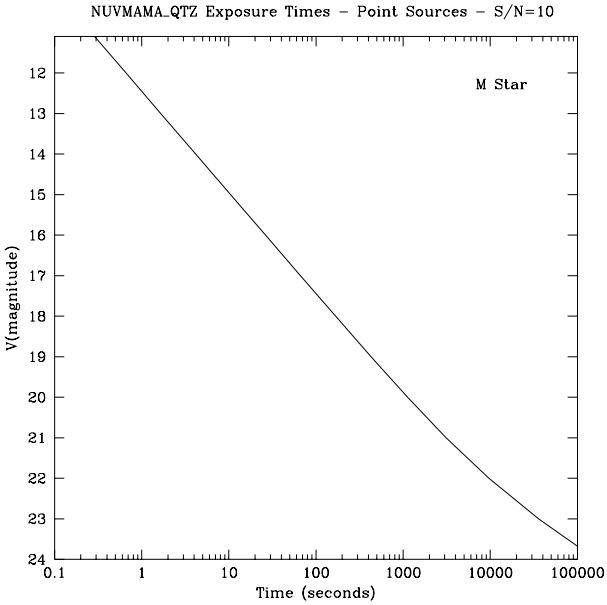

Figure 14.23: F25QTZ-NUVMAMA Time to Achieve a Signal-to-Noise of 10 integrated over the bandpass, for point and diffuse sources, assuming a flat (in F_λ) spectrum, cgs units. Point source signal-to-noise is integrated over the PSF, diffuse sources are per2x2 spatial pixels.

(a) Point Sources

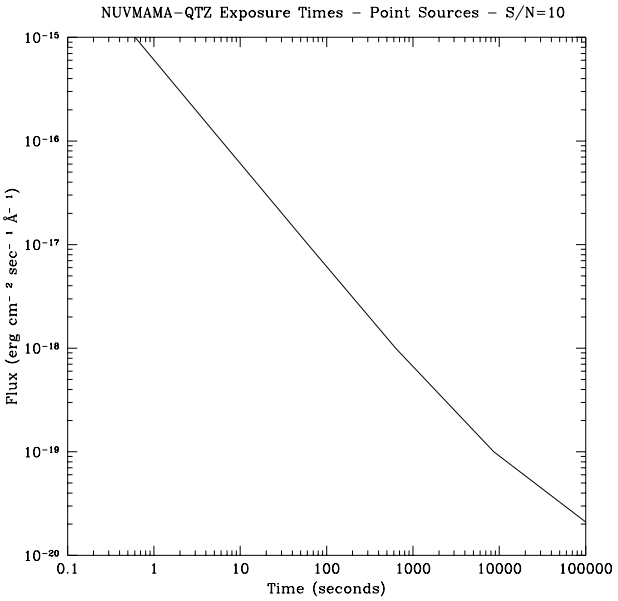

(b) Diffuse Sources

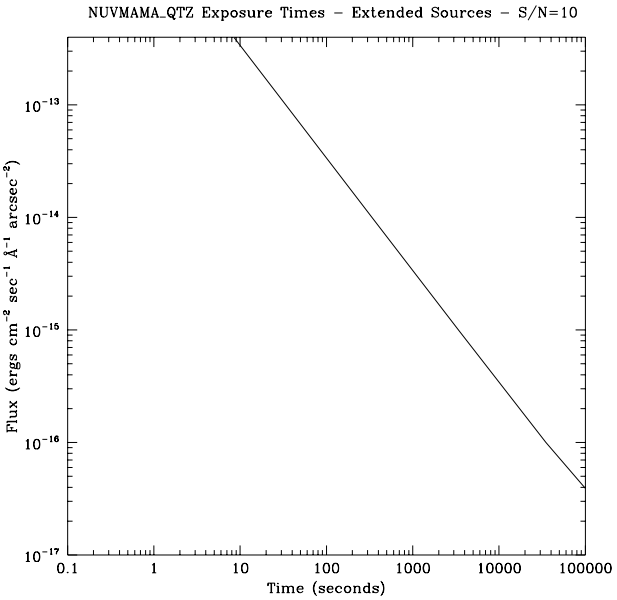

Figure 14.24: F25QTZ-NUVMAMA Time to Saturate as a Function of Source Flux, assuming a flat (in F_λ) spectrum

(a) Point Sources

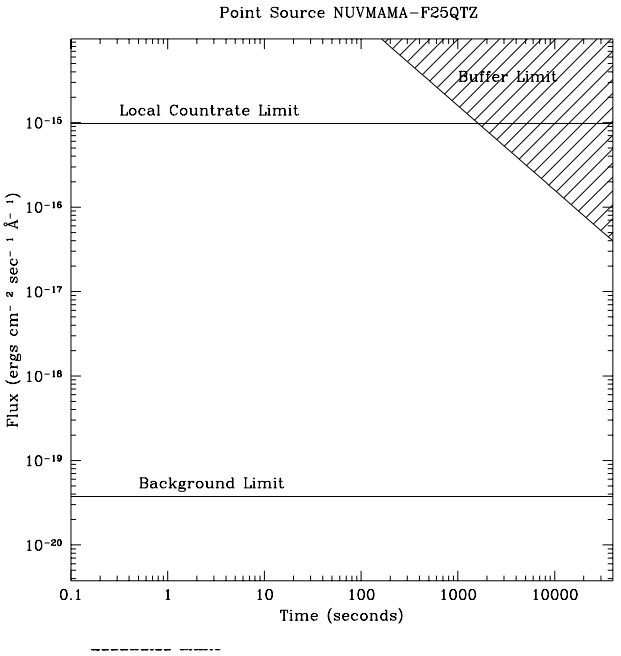

(b) Diffuse Sources

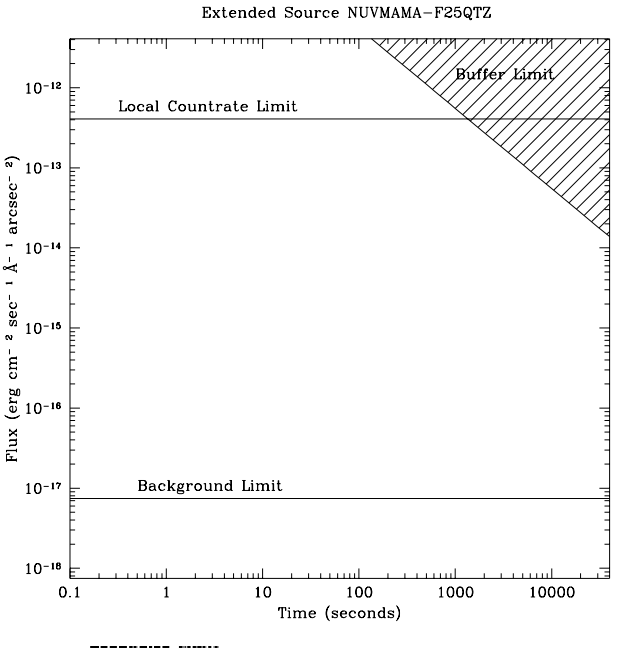

F25SRF2 - NUV-MAMA - longpass

Figure 14.25: F25SRF2-NUVMAMA Point Source (left axis), and Diffuse Source (right axis) Sensitivities. Bandpass integrated point source sensitivity for F_λ=1 is $2.0x10^{17}$.

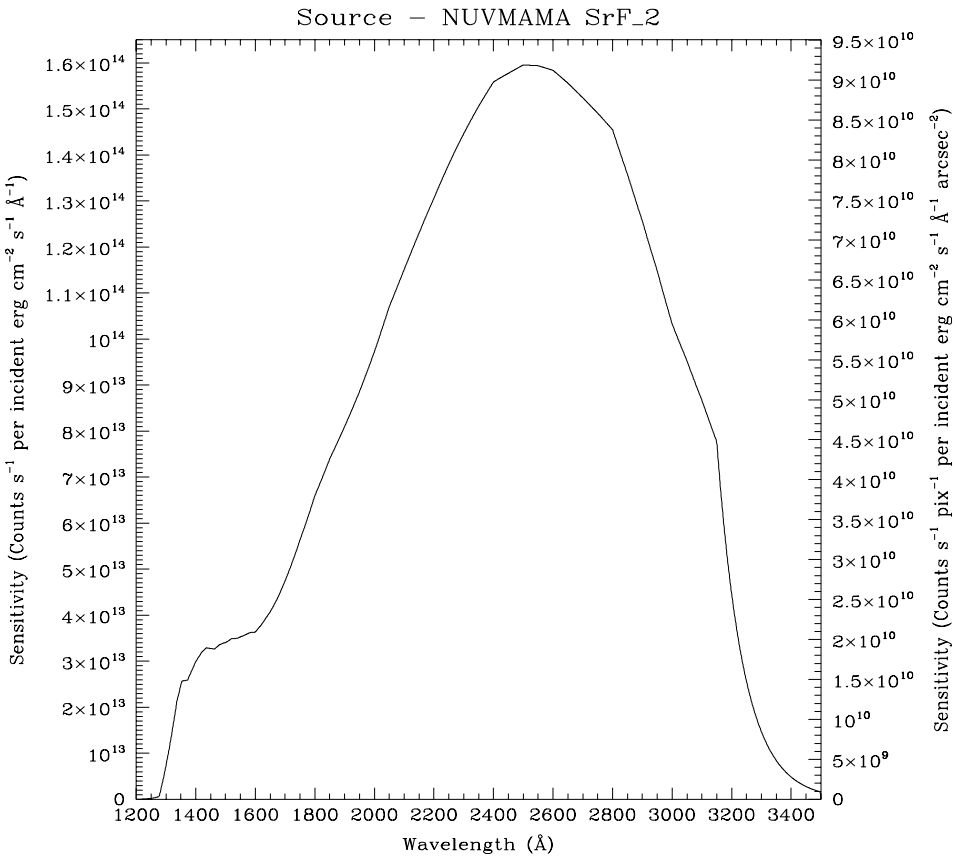

Table 14.7: F25SRF2-NUVMAMA Point Source Sensitivities for NUVMAMA SrF_2. Multiply sensitivity number by 0.000576 (the plate scale squared) to obtain diffuse source sensitivity.

λ	**Sens**.	λ	**Sens**.	λ	**Sens**.	λ	**Sens**.
1300	7.3E12	1900	8.1E13	2500	1.6E14	3100	8.7E13
1400	3.0E13	2000	9.7E13	2600	1.6E14	3200	4.5E13
1500	3.4E13	2100	1.1E14	2700	1.5E14	3300	1.5E13
1600	3.6E13	2200	1.3E14	2800	1.4E14	3400	4.8E12
1700	4.7E13	2300	1.4E14	2900	1.3E14	3500	2.61E8
1800	6.6E13	2400	1.6E14	3000	1.0E14		

Figure 14.26: F25SRF2-NUVMAMA Time to Achieve a Signal-to-Noise of 10 integrated over the PSF and the bandpass for stars of different spectral types as a function of V band magnitude

(a) O5 star

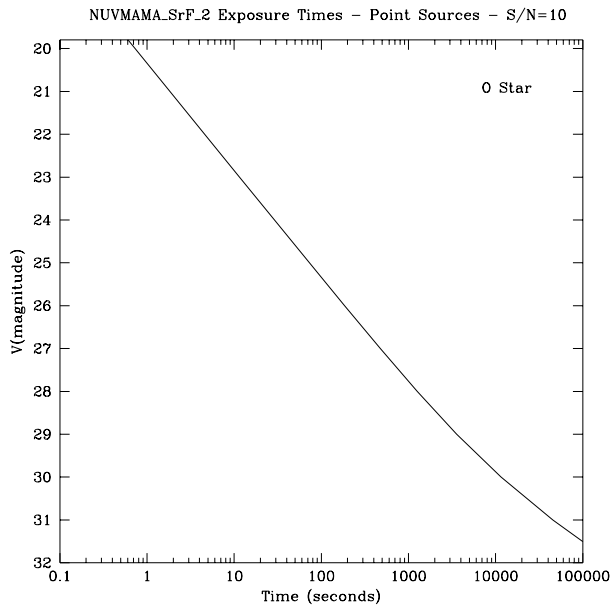

(b) AOV star

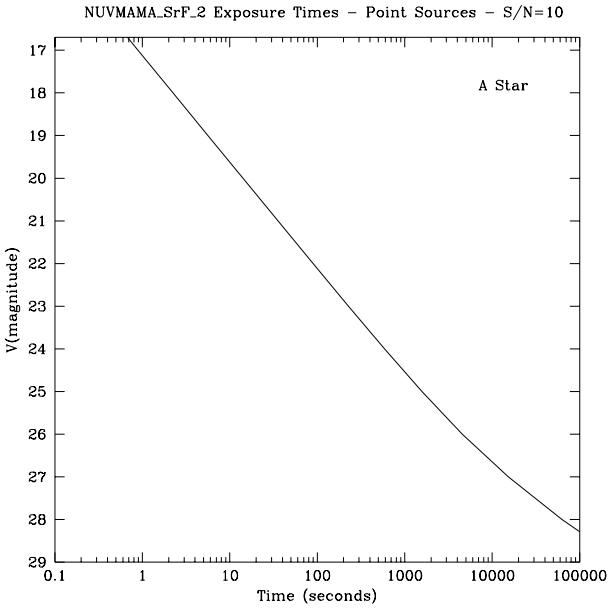

(c) G0V star

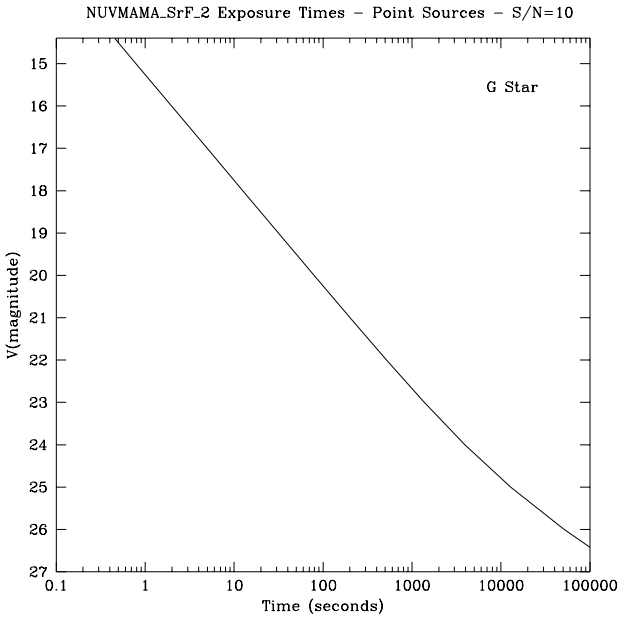

(d) M0V star

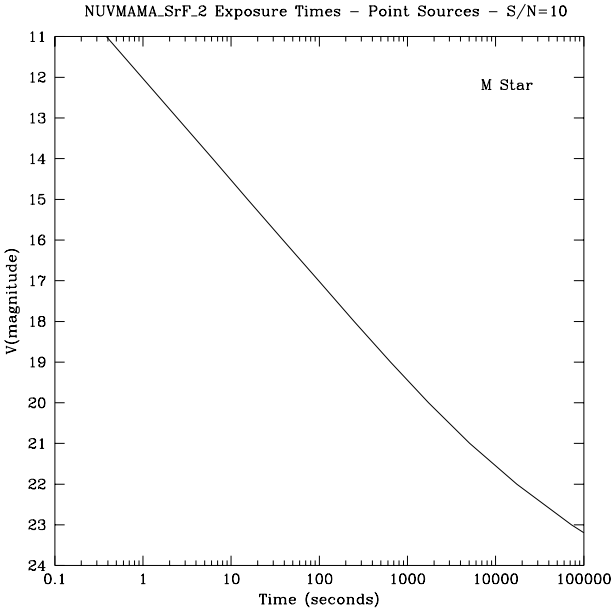

Figure 14.27: F25SRF2-NUVMAMA Time to Achieve a Signal-to-Noise of 10 integrated over the bandpass, for point and diffuse sources, assuming a flat (in F_λ) spectrum, cgs units. Point source signal-to-noise is integrated over the PSF, diffuse sources are per 2x2 spatial pixels.

(a) Point Sources

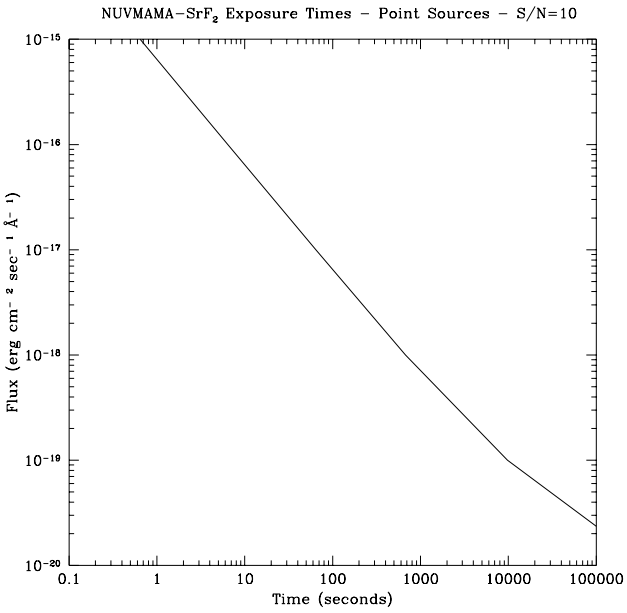

(b) Diffuse Sources

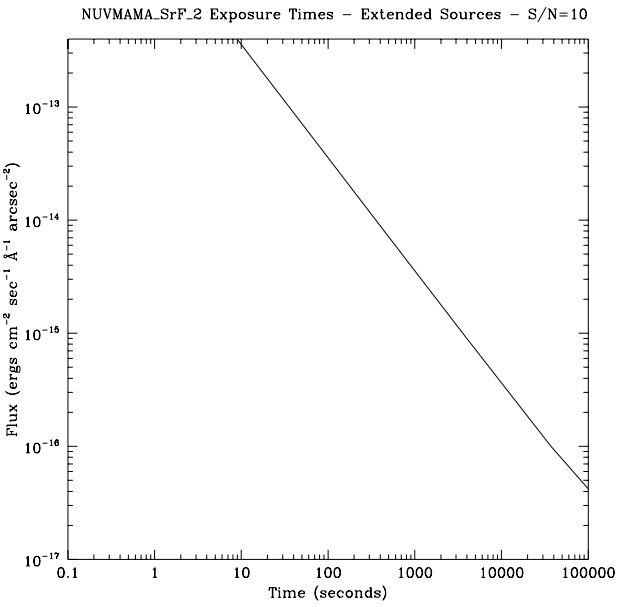

Figure 14.28: F25SRF2-NUVMAMA Time to Saturate as a Function of Source Flux, assuming a flat (in F_λ) spectrum

(a) Point Sources

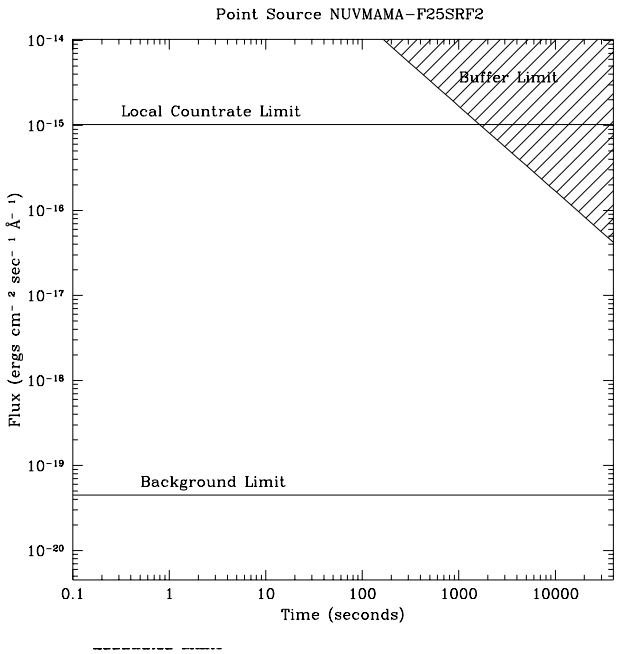

(b) Diffuse Sources

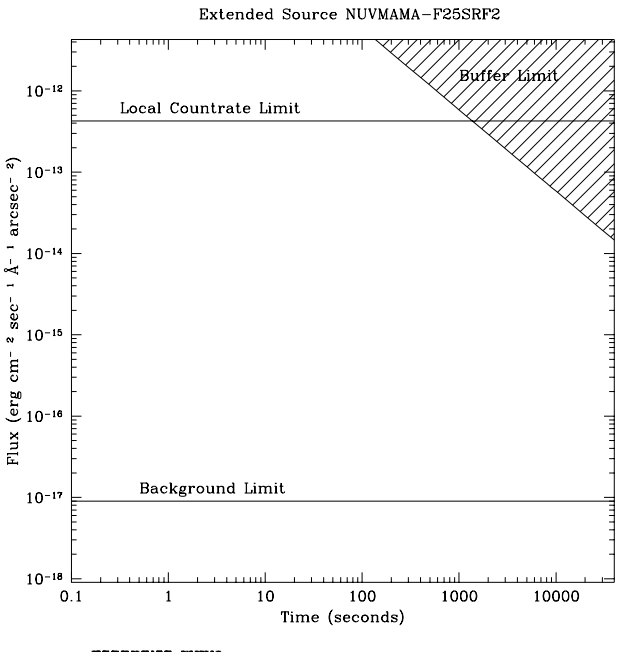

F25MGII - NUV-MAMA

Figure 14.29: F25MGII-NUVMAMA Point Source (left axis), and Diffuse Source (right axis) Sensitivities. Bandpass integrated point source sensitivity for F_λ=1 is 5.8x10^{15}.

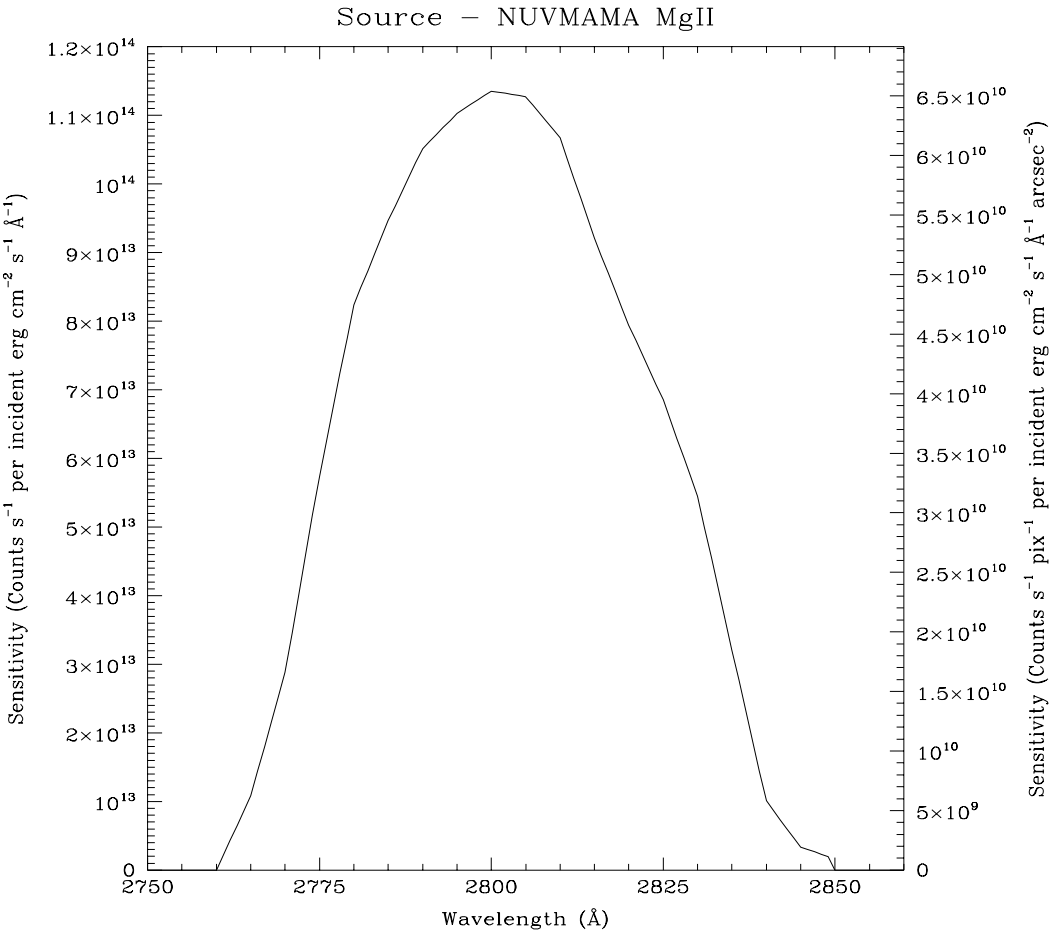

Table 14.8: F25MGII-NUVMAMA Point Source Sensitivities for NUVMAMA MgII. Multiply sensitivity number by 0.000576 (the plate scale squared) to obtain diffuse source sensitivity.

λ	**Sens.**	λ	**Sens.**	λ	**Sens.**	λ	**Sens.**
2765	1.1E13	2790	1.1E14	2815	9.2E13	2840	1.0E13
2770	2.9E13	2795	1.1E14	2820	7.9E13	2845	3.4E12
2775	5.7E13	2800	1.1E14	2825	6.9E13	2850	1.1E10
2780	8.2E13	2805	1.1E14	2830	5.4E13		
2785	9.5E13	2810	1.1E14	2835	3.2E13		

Figure 14.30: F25MGII-NUVMAMA Time to Achieve a Signal-to-Noise of 10 integrated over the PSF and the bandpass for stars of different spectral types as a function of V band magnitude

(a) O5 star

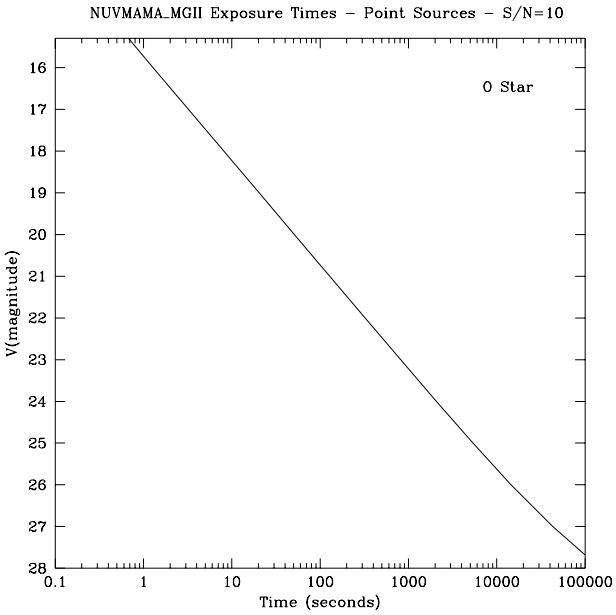

(b) AOV star

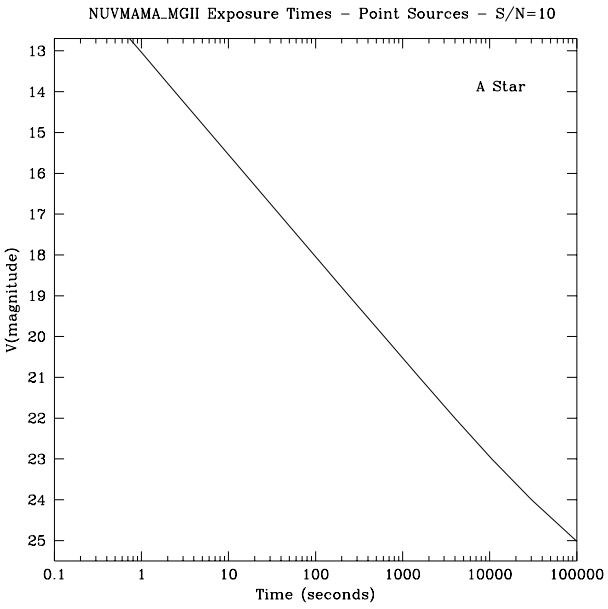

(c) G0V star

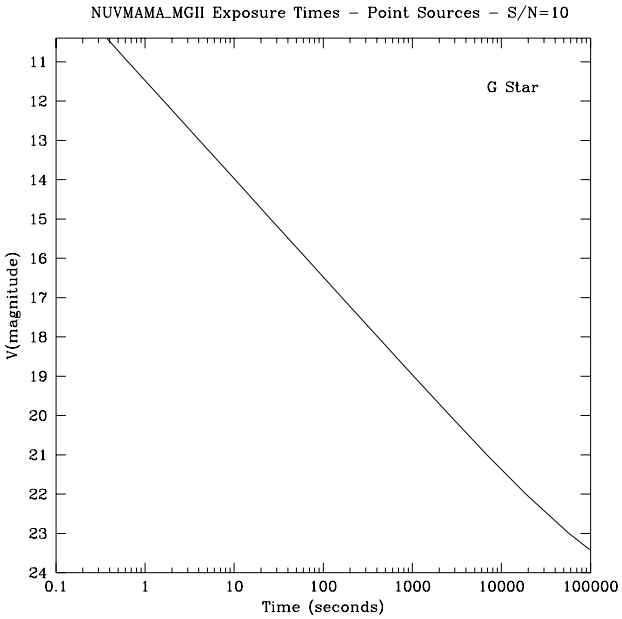

(d) M0V star

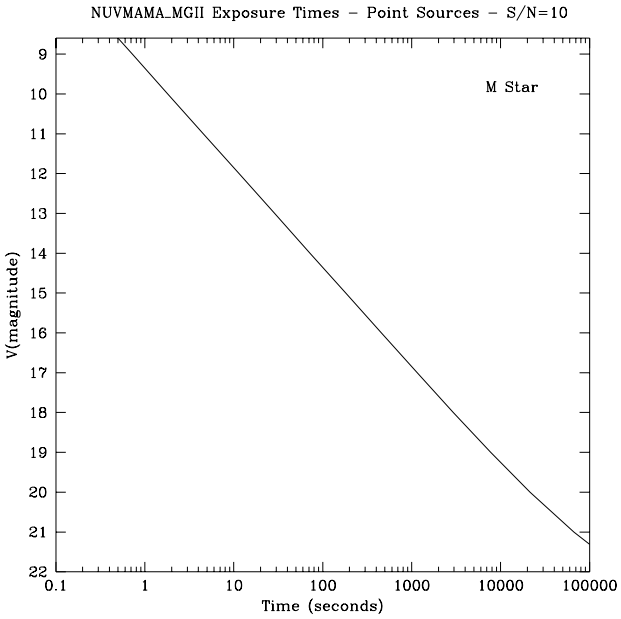

Figure 14.31: F25MGII-NUVMAMA Time to Achieve a Signal-to-Noise of 10 integrated over the bandpass, for point and diffuse sources, assuming a flat (in F_λ) spectrum, cgs units. Point source signal-to-noise is integrated over the PSF, diffuse sources are per 2x2 spatial pixels.

(a) Point Sources

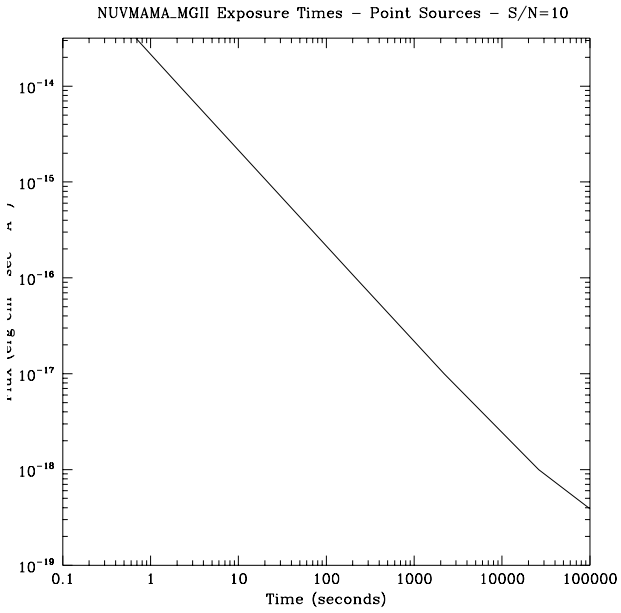

(b) Diffuse Sources

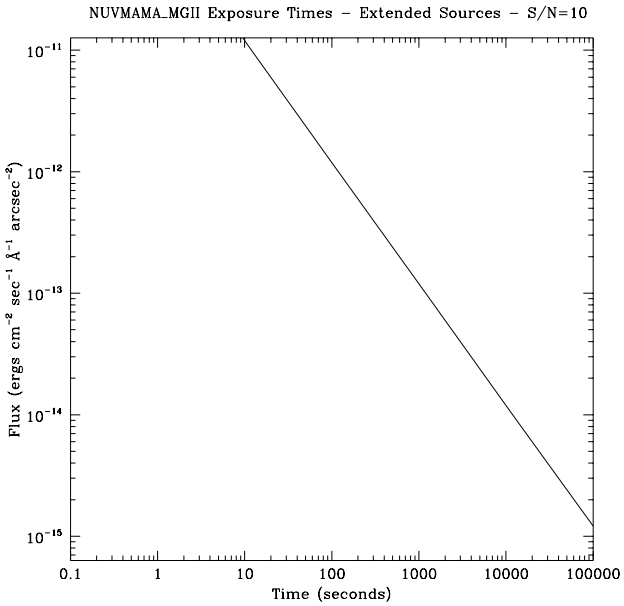

Figure 14.32: F25MGII-NUVMAMA Time to Saturate as a Function of Source Flux, assuming a flat (in F_λ) spectrum

(a) Point Sources

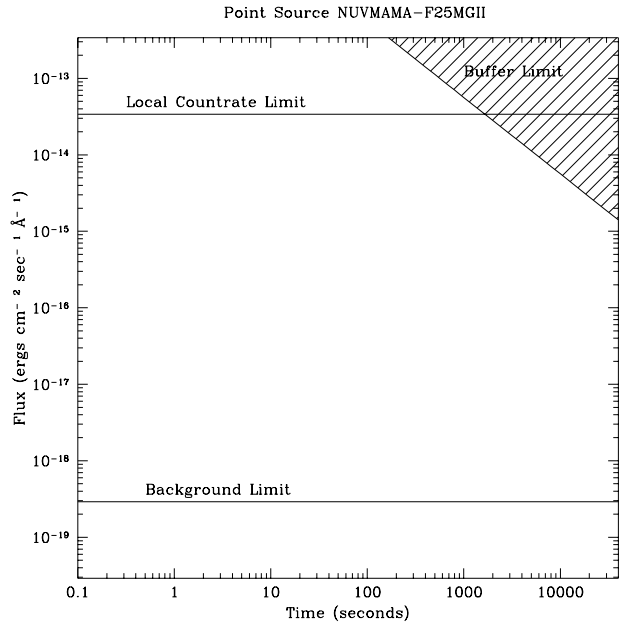

(b) Diffuse Sources

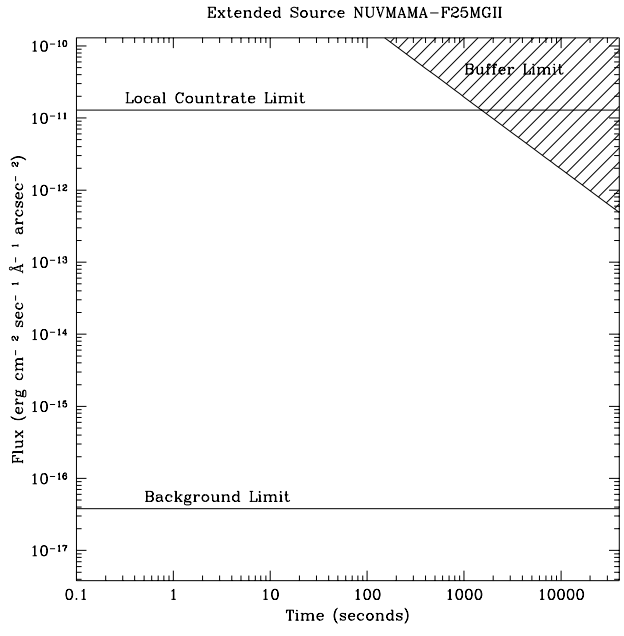

F25CN270 - NUV-MAMA

Figure 14.33: F25CN270-NUVMAMA Point Source (left axis), and Diffuse Source (right axis) Sensitivities. Bandpass integrated point source sensitivity for F_λ=1 is $2.6x10^{16}$.

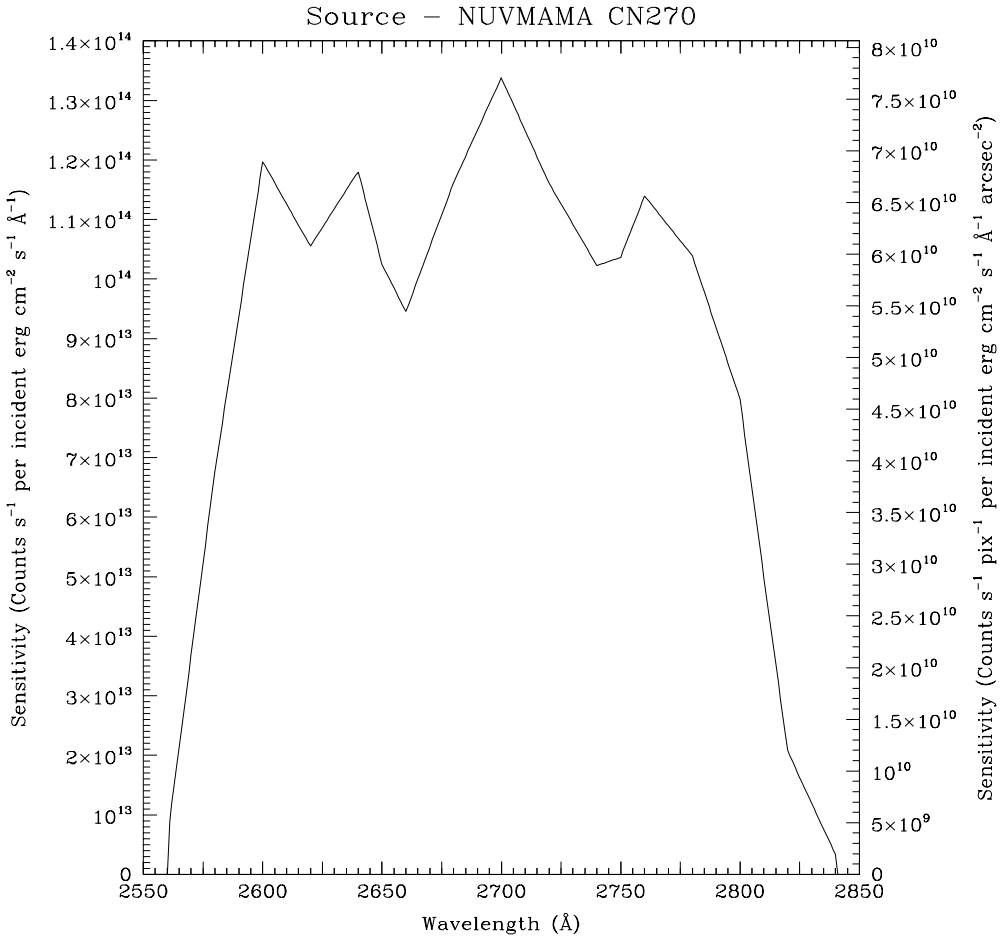

Table 14.9: F25CN270-NUVMAMA Point Source Sensitivities for NUVMAMA CN270. Multiply sensitivity number by 0.000576 (the plate scale squared) to obtain diffuse source sensitivity.

λ	**Sens.**	λ	**Sens.**	λ	**Sens.**	λ	**Sens.**
2575	5.2E13	2650	1.0E14	2725	1.1E14	2800	8.0E13
2600	1.2E14	2675	1.1E14	2750	1.0E14	2825	1.6E13
2625	1.1E14	2700	1.3E14	2775	1.1E14		

Figure 14.34: F25CN270-NUVMAMA Time to Achieve a Signal-to-Noise of 10 integrated over the PSF and the bandpass for stars of different spectral types as a function of V band magnitude

(a) O5 star

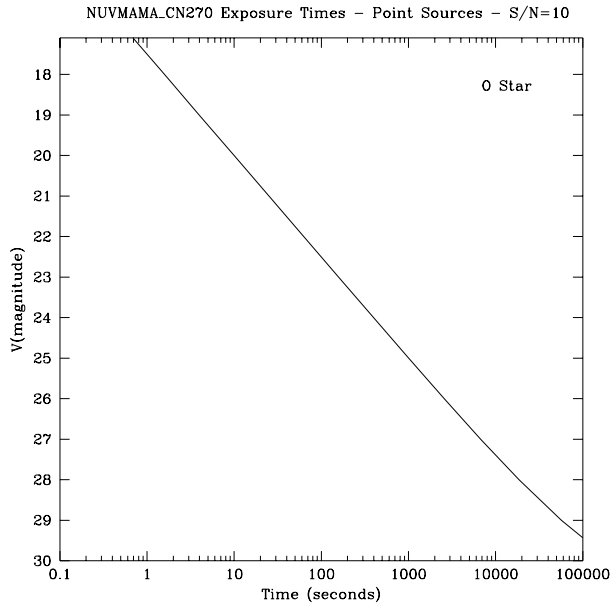

(b) AOV star

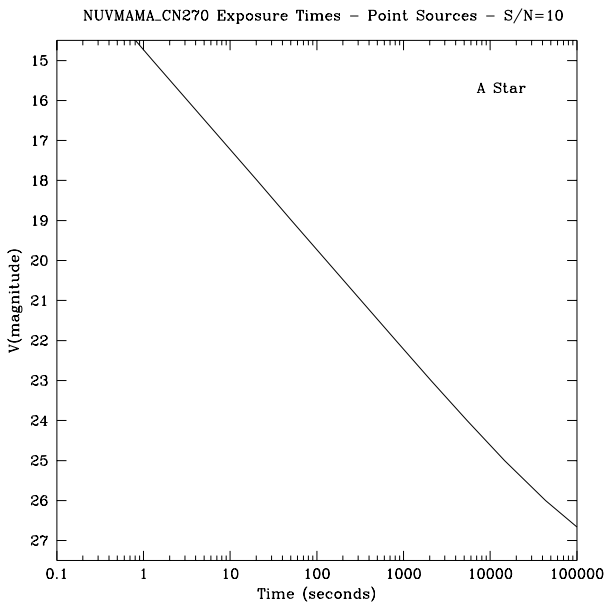

(c) G0V star

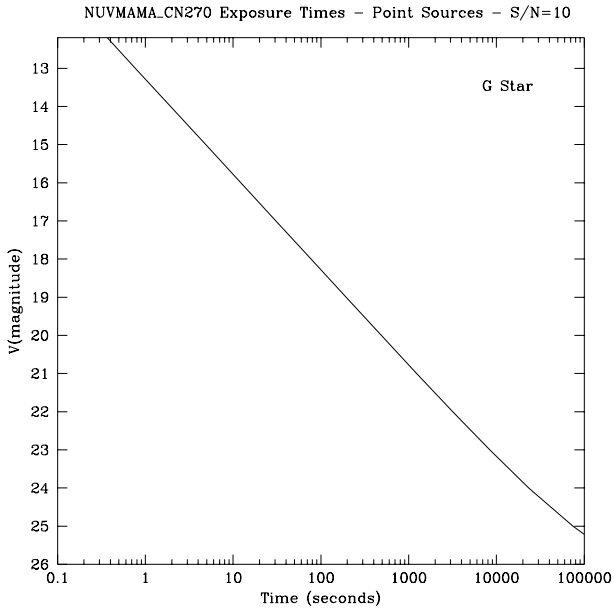

(d) M0V star

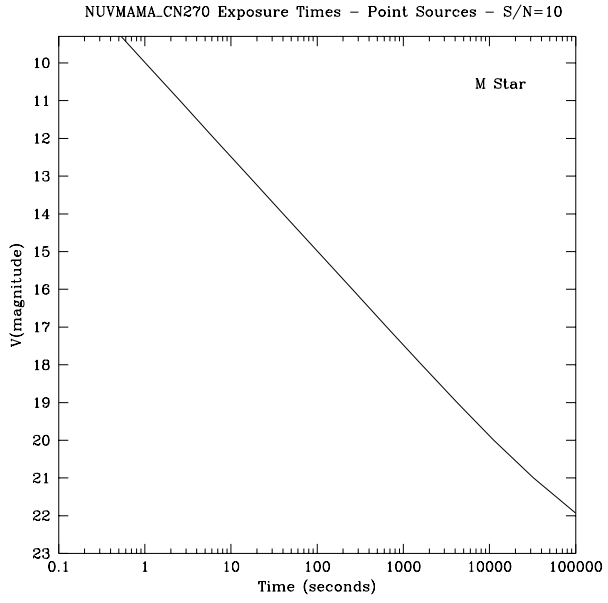

Figure 14.35: F25CN270-NUVMAMA Time to Achieve a Signal-to-Noise of 10 integrated over the bandpass, for point and diffuse sources, assuming a flat (in F_λ) spectrum, cgs units. Point source signal-to-noise is integrated over the PSF, diffuse sources are per 2x2 spatial pixels.

(a) Point Sources

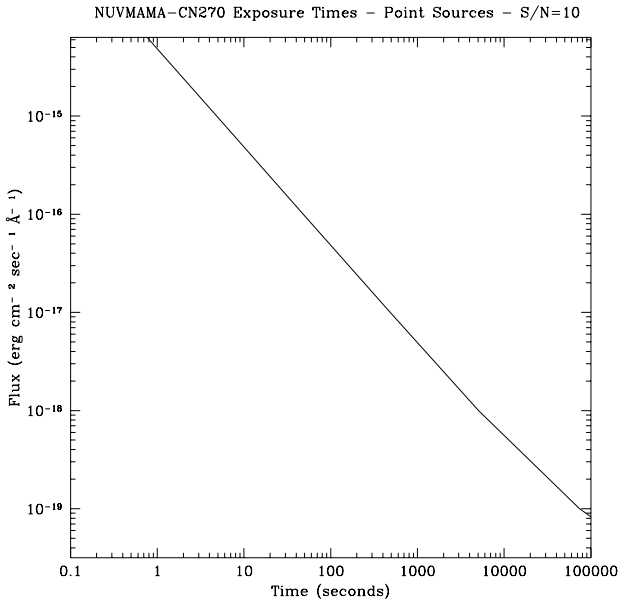

(b) Diffuse Sources

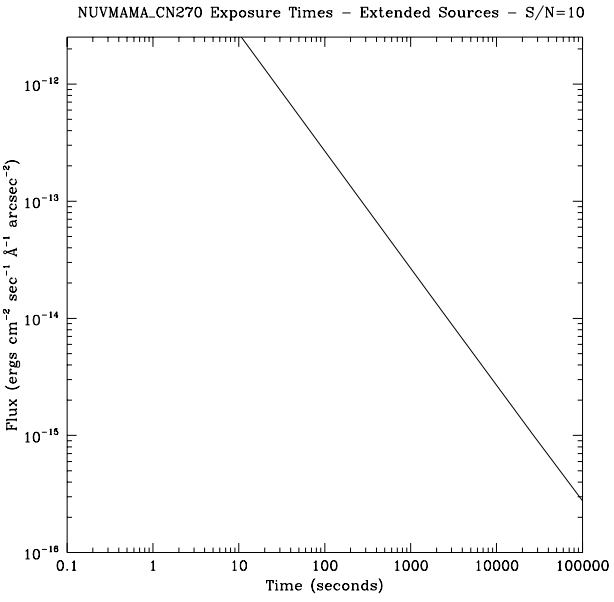

Figure 14.36: F25CN270-NUVMAMA Time to Saturate as a Function of Source Flux, assuming a flat (in F_λ) spectrum

(a) Point Sources

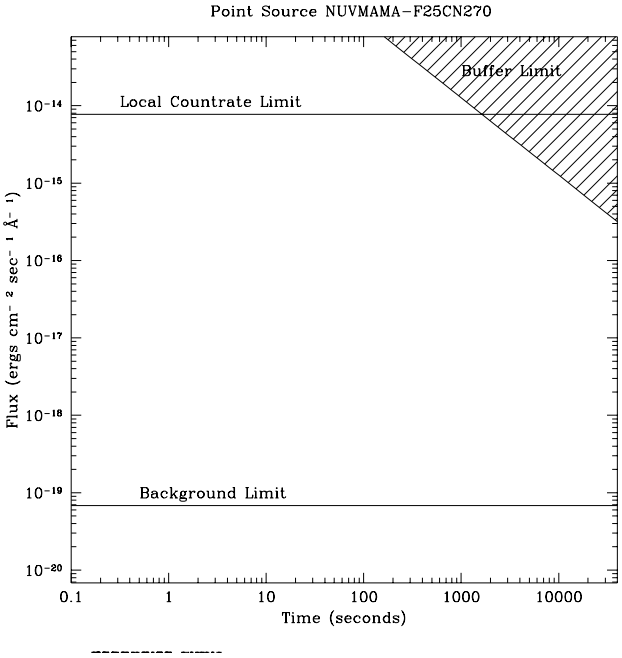

(b) Diffuse Sources

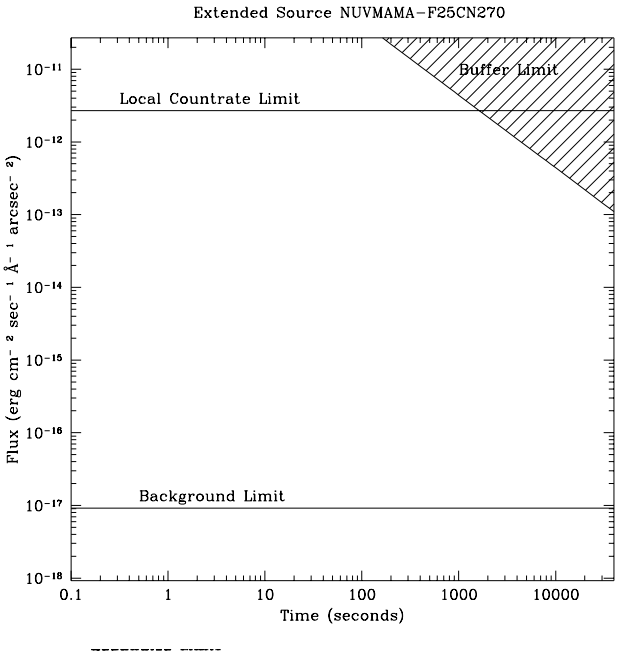

F25CIII - NUV-MAMA

Figure 14.37: F25CIII-NUVMAMA Point Source (left axis), and Diffuse Source (right axis) Sensitivities. Bandpass integrated point source sensitivity for F_λ=1 is $3.3x10^{15}$.

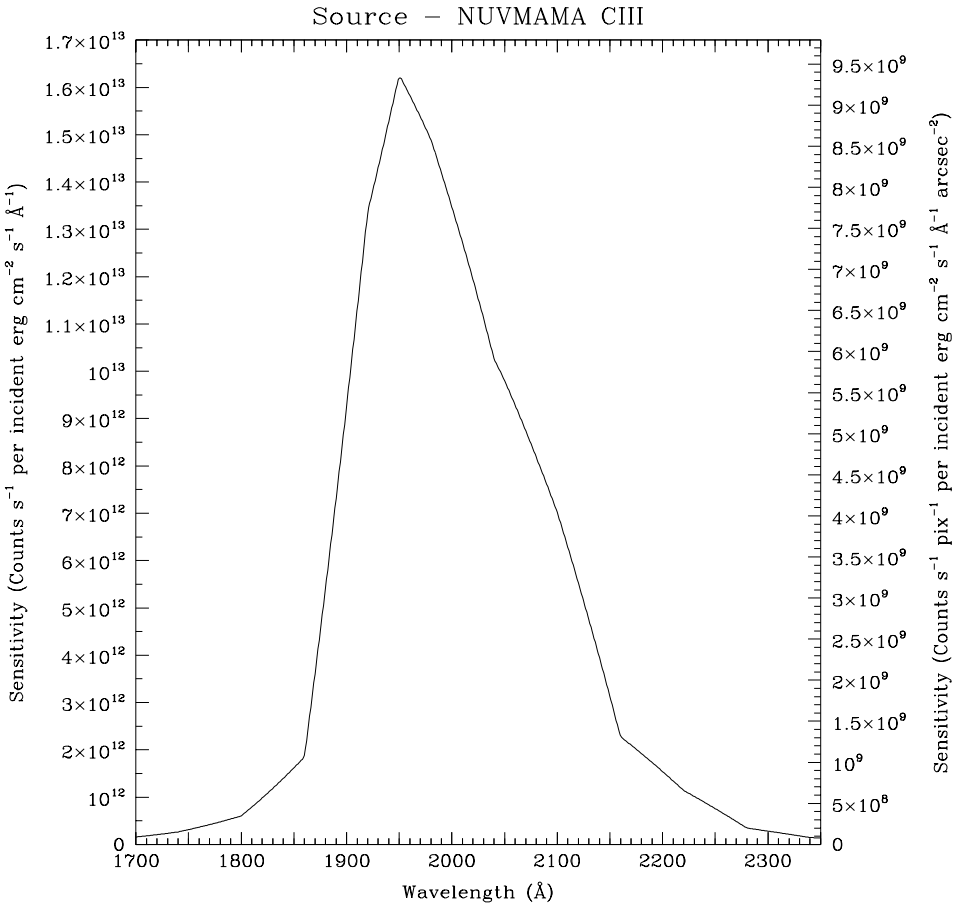

Table 14.10: F25CIII-NUVMAMA Point Source Sensitivities for NUV-MAMA CIII. Multiply sensitivity number by 0.000576 (the plate scale squared) to obtain diffuse source sensitivity.

λ	**Sens**.	λ	**Sens**.	λ	**Sens**.	λ	**Sens**.
1300	4.4E10	2000	1.3E13	2700	6.1E10	3400	7.85E9
1400	9.2E10	2100	7.0E12	2800	7.1E10	3500	7.48E9
1500	4.2E10	2200	1.5E12	2900	6.9E10	3600	2.2E10
1600	4.9E10	2300	2.8E11	3000	5.2E10	3700	1.1E11
1700	1.6E11	2400	8.6E10	3100	4.6E10	3800	1.1E11
1800	6.0E11	2500	5.9E10	3200	3.0E10	3900	7.0E10
1900	9.3E12	2600	5.7E10	3300	1.4E10	4000	3.0E10

Figure 14.38: F25CIII-NUVMAMA Time to Achieve a Signal-to-Noise of 10 integrated over the PSF and the bandpass for stars of different spectral types as a function of V band magnitude

(a) O5 star

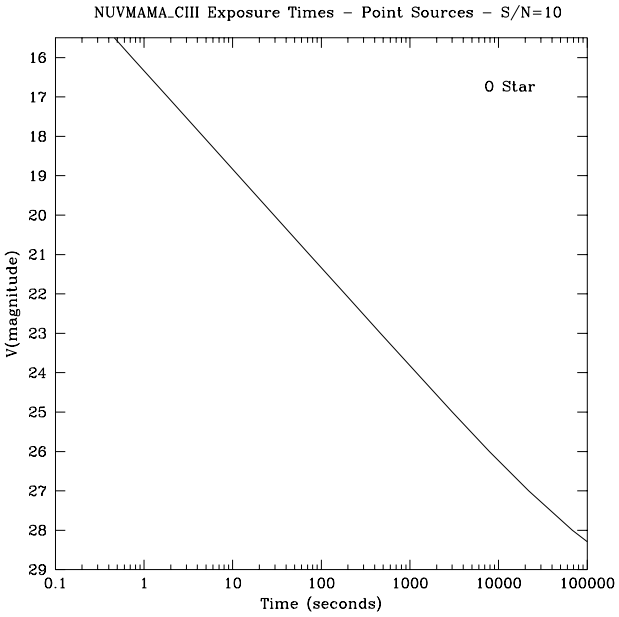

(b) AOV star

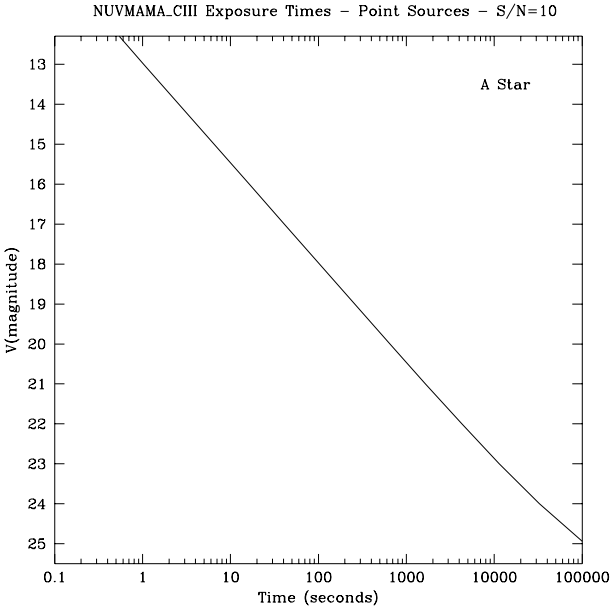

(c) G0V star

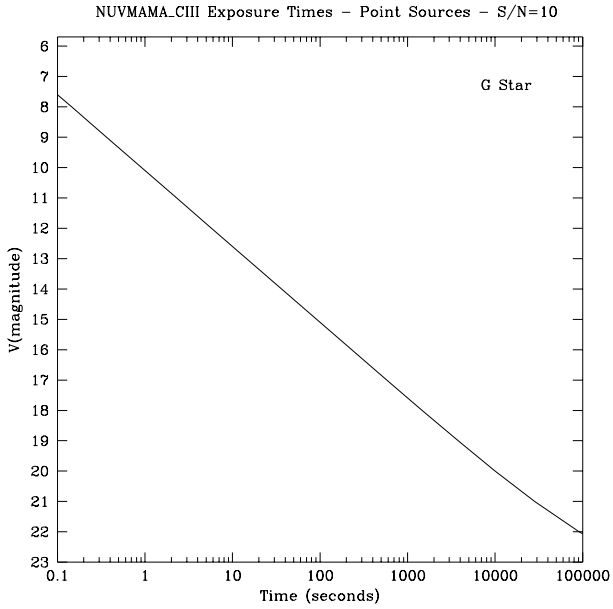

(d) M0V star

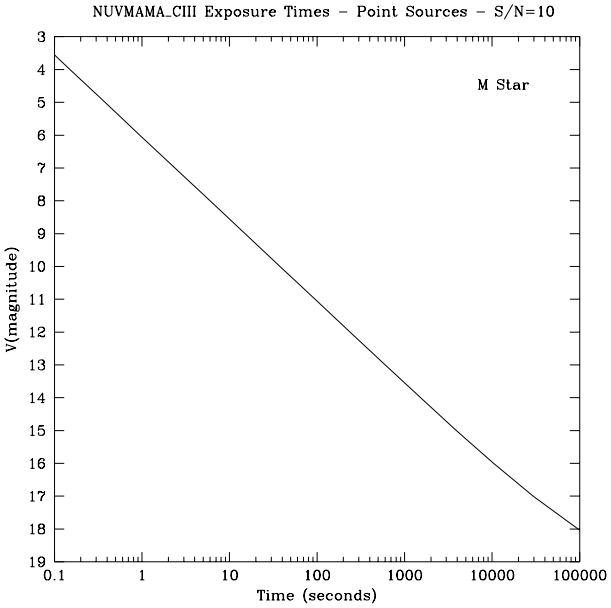

Figure 14.39: F25CIII-NUVMAMA Time to Achieve a Signal-to-Noise of 10 integrated over the bandpass, for point and diffuse sources, assuming a flat (in F_λ) spectrum, cgs units. Point source signal-to-noise is integrated over the PSF, diffuse sources are per 2x2 spatial pixels.

(a) Point Sources

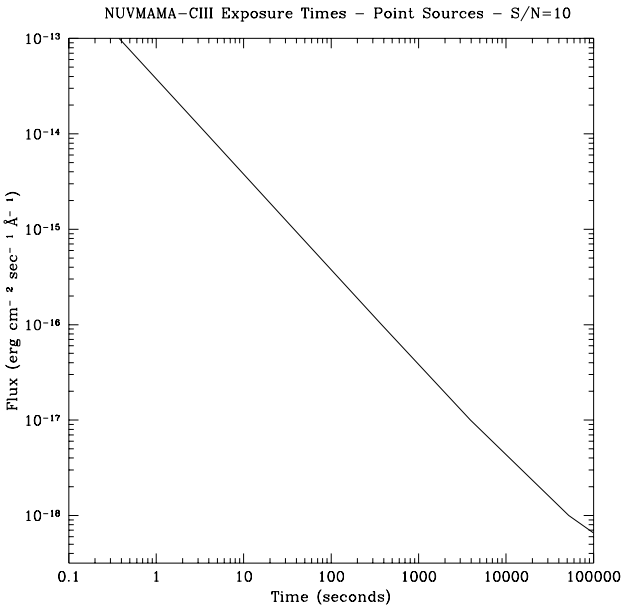

(b) Diffuse Sources

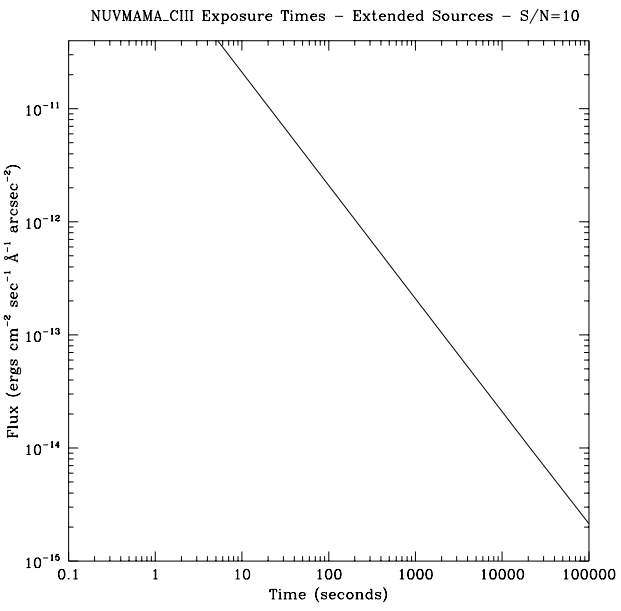

Figure 14.40: F25CIII-NUVMAMA Time to Saturate as a Function of Source Flux, assuming a flat (in F_λ) spectrum

(a) Point Sources

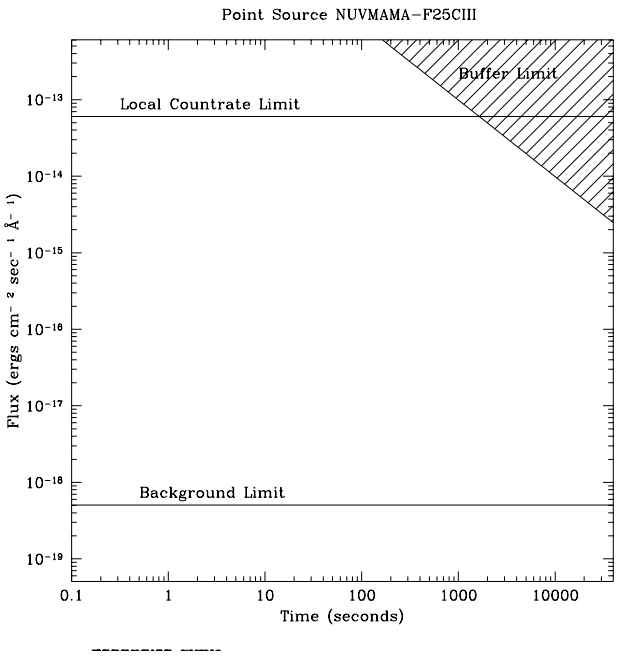

(b) Diffuse Sources

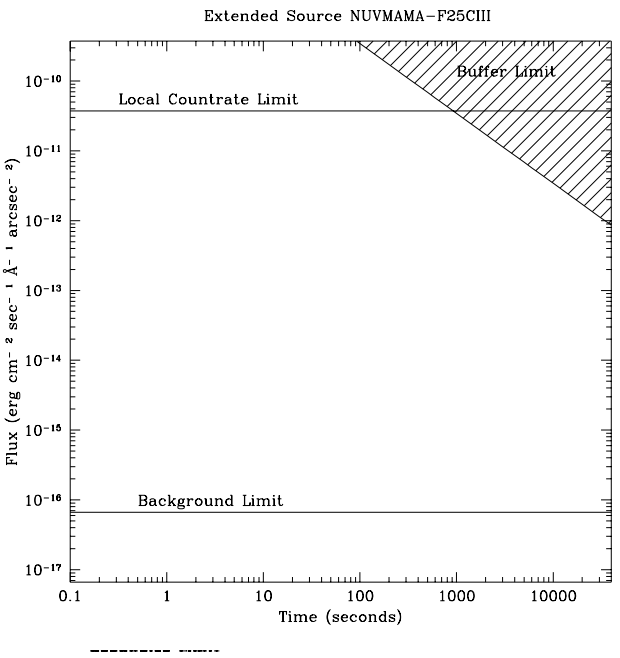

F25CN182 - NUV-MAMA

Figure 14.41: F25CN182-NUVMAMA Point Source (left axis), and Diffuse Source (right axis) Sensitivities. Bandpass integrated point source sensitivity for F_λ=1 is $2.3x10^{16}$.

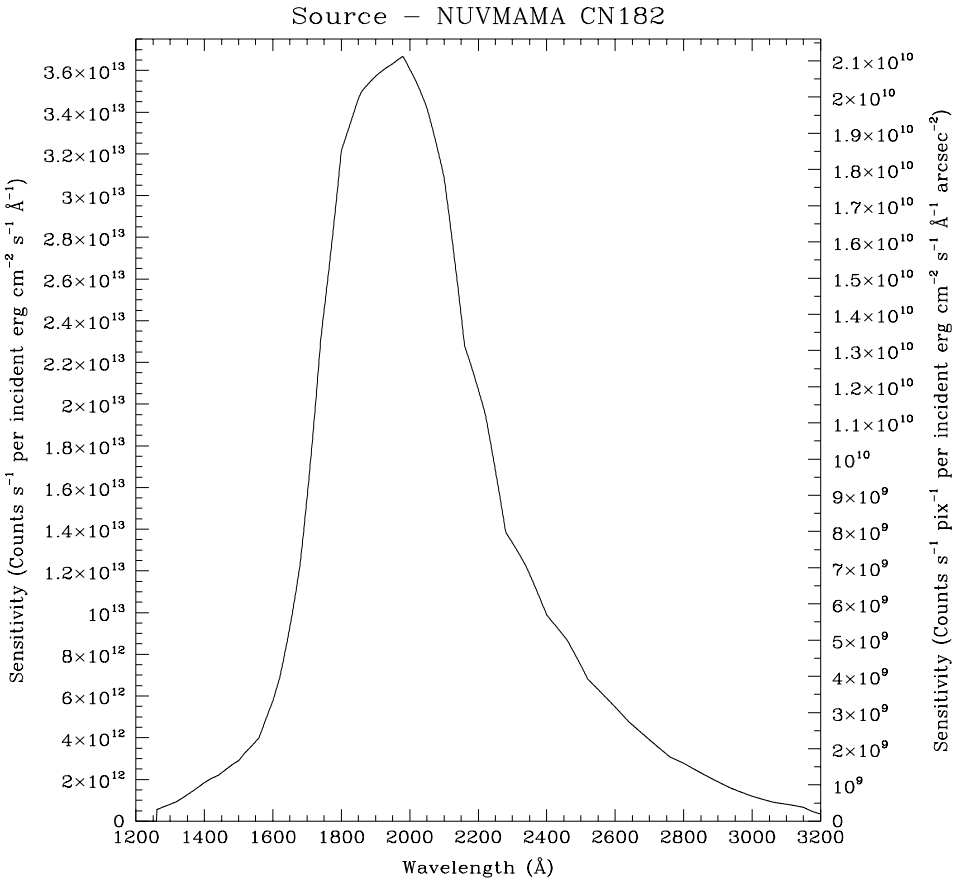

Table 14.11: F25CN182-NUVMAMA Point Source Sensitivities for NUVMAMA CN182. Multiply sensitivity number by 0.000576 (the plate scale squared) to obtain diffuse source sensitivity.

λ	**Sens.**	λ	**Sens.**	λ	**Sens.**	λ	**Sens.**
1300	8.1E11	2000	3.6E13	2700	3.9E12	3400	2.6E10
1400	1.8E12	2100	3.1E13	2800	2.8E12	3500	7.35E9
1500	2.9E12	2200	2.1E13	2900	1.9E12	3600	5.27E9
1600	5.8E12	2300	1.3E13	3000	1.2E12	3700	3.86E9
1700	1.5E13	2400	9.9E12	3100	8.1E11	3800	2.92E9
1800	3.2E13	2500	7.5E12	3200	3.4E11	3900	2.21E9
1900	3.6E13	2600	5.5E12	3300	9.3E10	4000	1.73E9

Figure 14.42: F25CN182-NUVMAMA Time to Achieve a Signal-to-Noise of 10 integrated over the PSF and the bandpass for stars of different spectral types as a function of V band magnitude

(a) O5 star

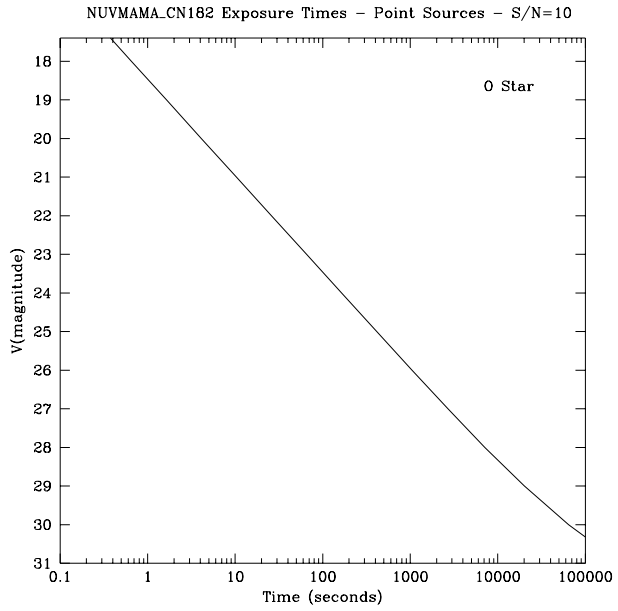

(b) AOV star

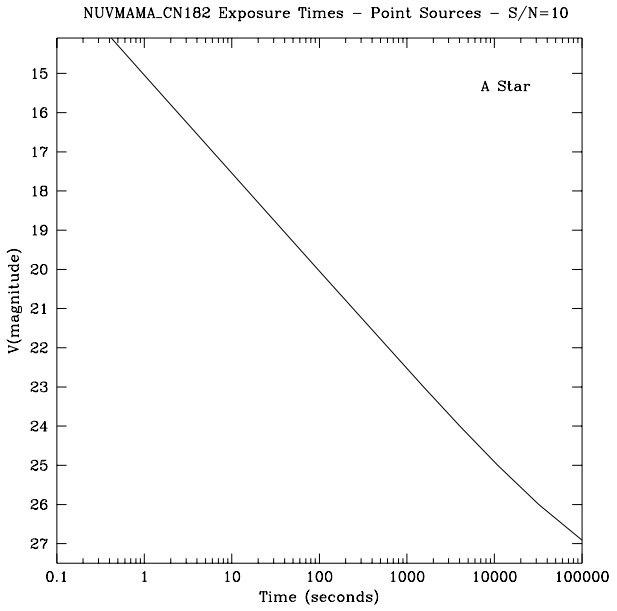

(c) G0V star

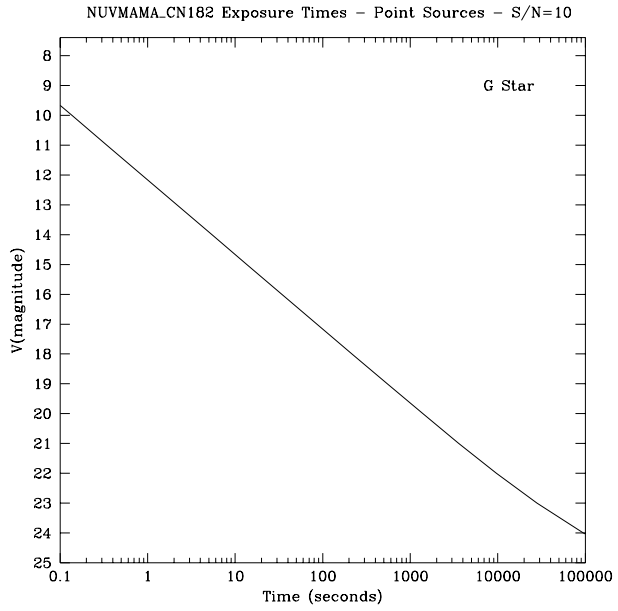

(d) M0V star

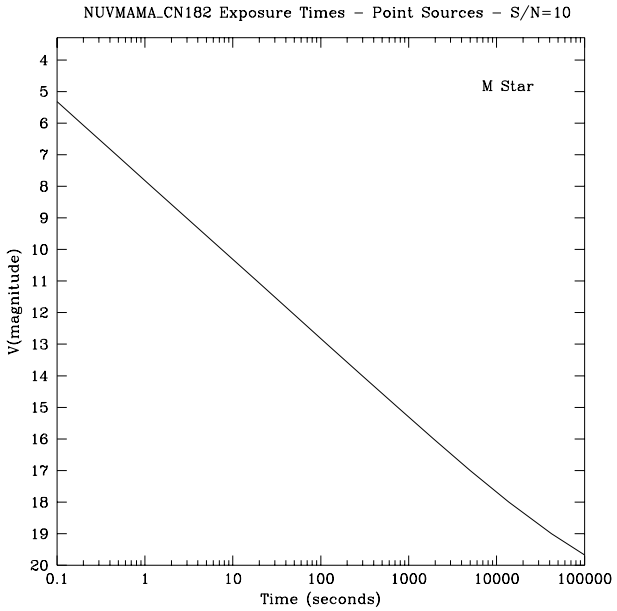

Figure 14.43: F25CN182-NUVMAMA Time to Achieve a Signal-to-Noise of 10 integrated over the bandpass, for point and diffuse sources, assuming a flat (in F_λ) spectrum, cgs units. Point source signal-to-noise is integrated over the PSF, diffuse sources are per pixel.

(a) Point Sources

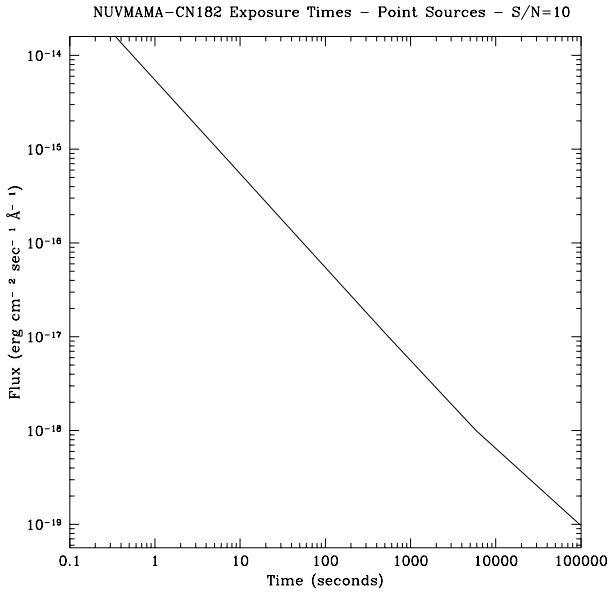

(b) Diffuse Sources

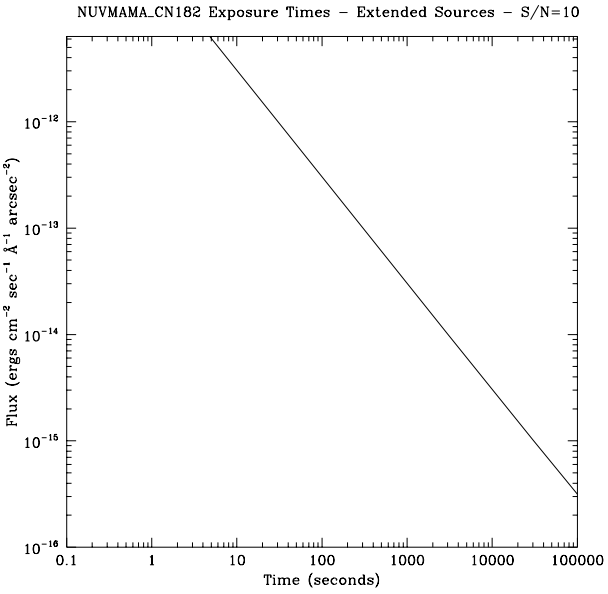

Figure 14.44: F25CN182-NUVMAMA Time to Saturate as a Function of Source Flux, assuming a flat (in F_λ) spectrum

(a) Point Sources

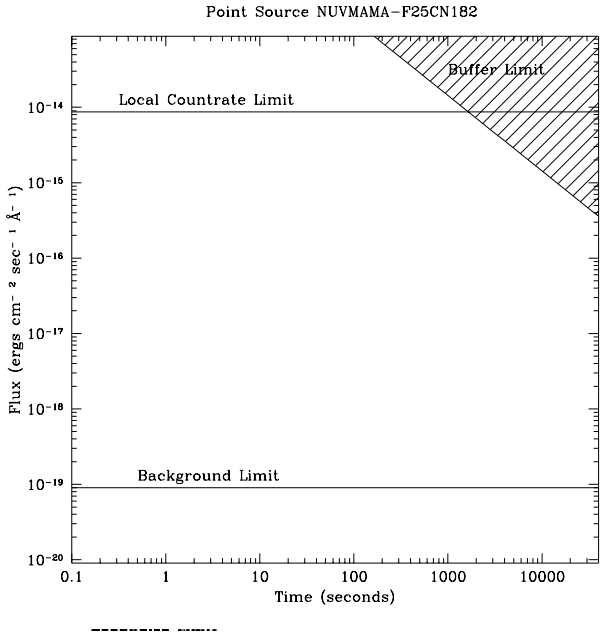

(b) Diffuse Sources

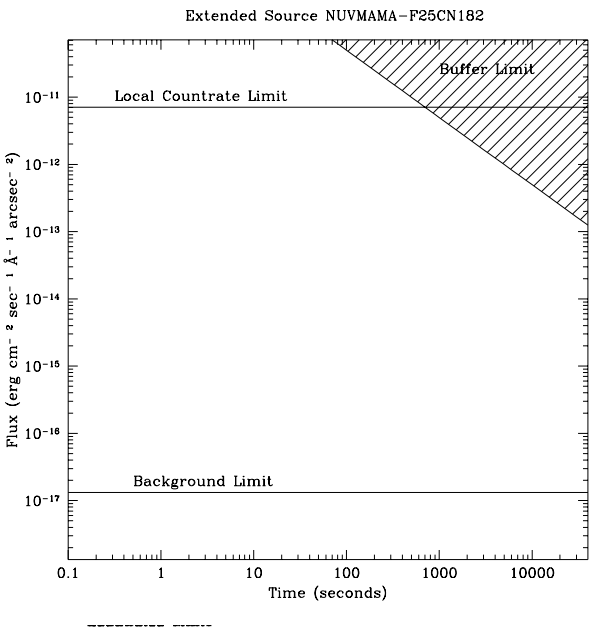

25MAMA - FUV-MAMA - clear

Figure 14.45: 25 FUVMAMA Point Source (left axis), and Diffuse Source (right axis) Sensitivities. Bandpass integrated point source sensitivity for F_λ=1 is $4.8x10^{16}$.

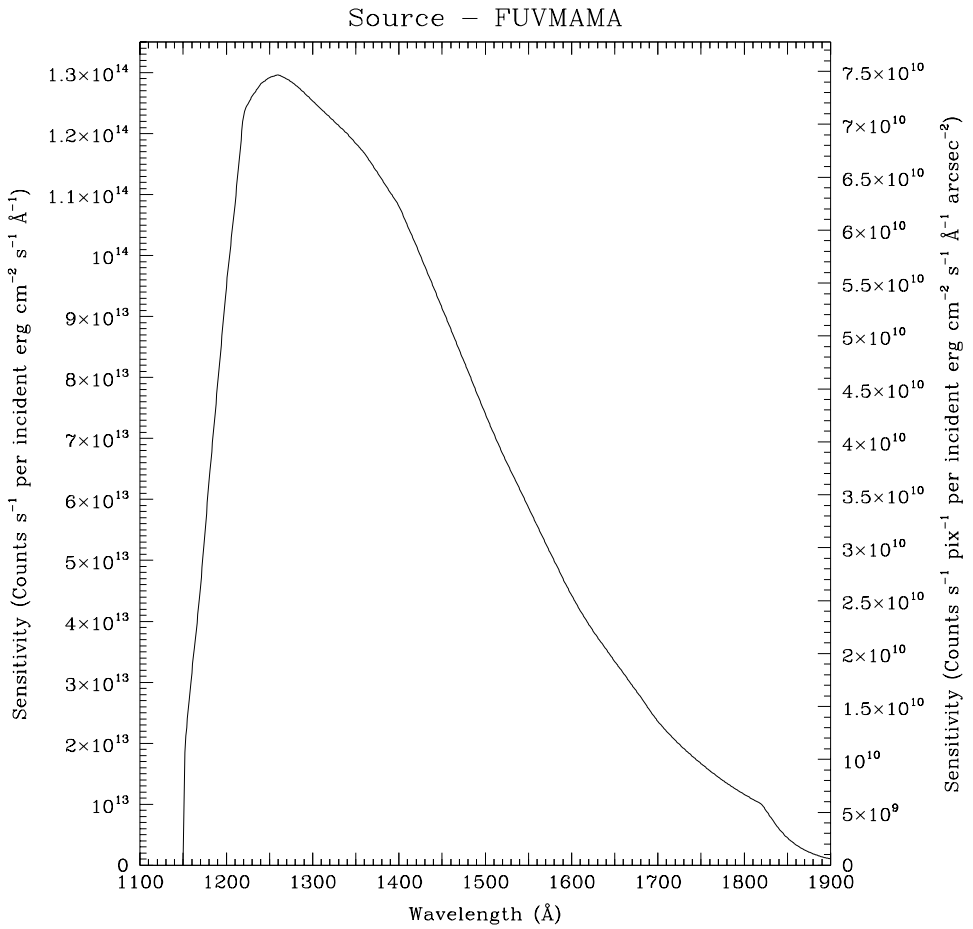

Table 14.12: 25 FUVMAMA Point Source Sensitivities for FUVMAMA. Multiply sensitivity number by 0.000576 (the plate scale squared) to obtain diffuse source sensitivity.

λ	**Sens.**	λ	**Sens.**	λ	**Sens.**	λ	**Sens.**
1150	1.13E9	1350	1.2E14	1600	4.4E13	1850	4.5E12
1175	5.4E13	1400	1.1E14	1650	3.3E13	1900	1.0E12
1200	9.5E13	1450	9.1E13	1700	2.4E13	1950	2.4E11
1250	1.3E14	1500	7.4E13	1750	1.7E13	2000	5.6E10
1300	1.2E14	1550	5.9E13	1800	1.2E13		

Figure 14.46: 25 FUVMAMA Time to Achieve a Signal-to-Noise of 10 integrated over the PSF and the bandpass for stars of different spectral types as a function of V band magnitude

(a) O5 star

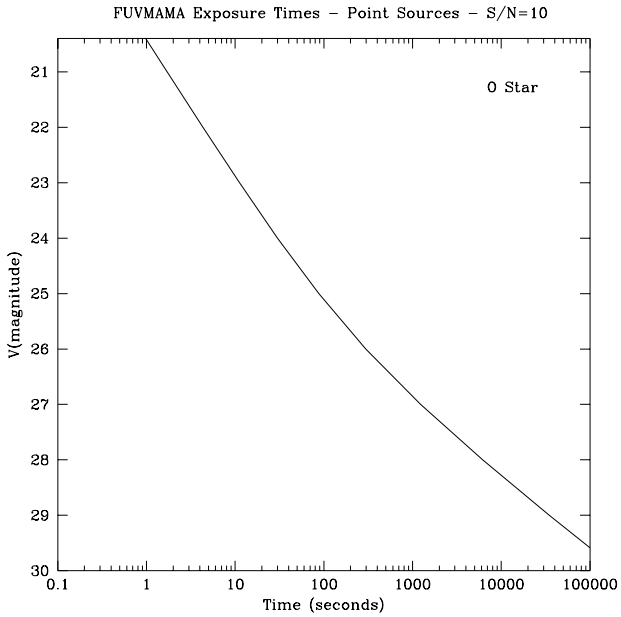

(b) AOV star

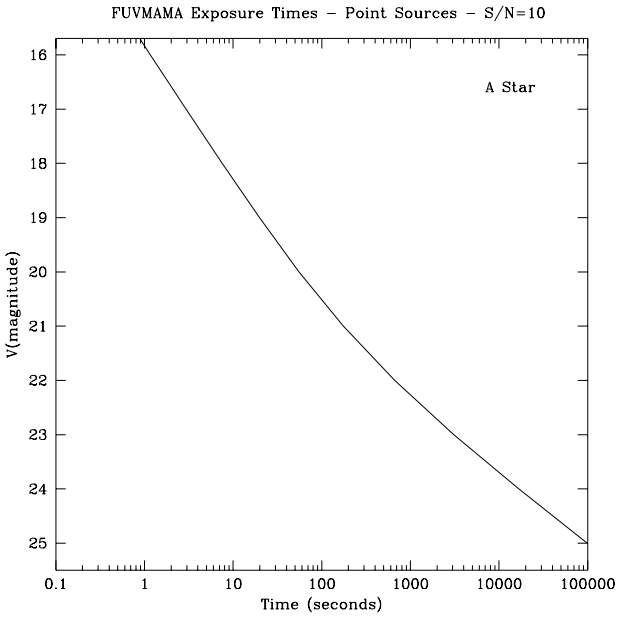

(c) G0V star

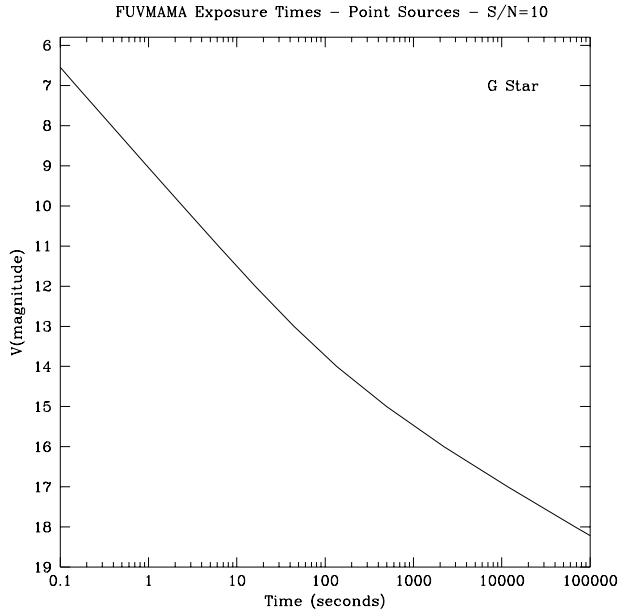

(d) M0V star

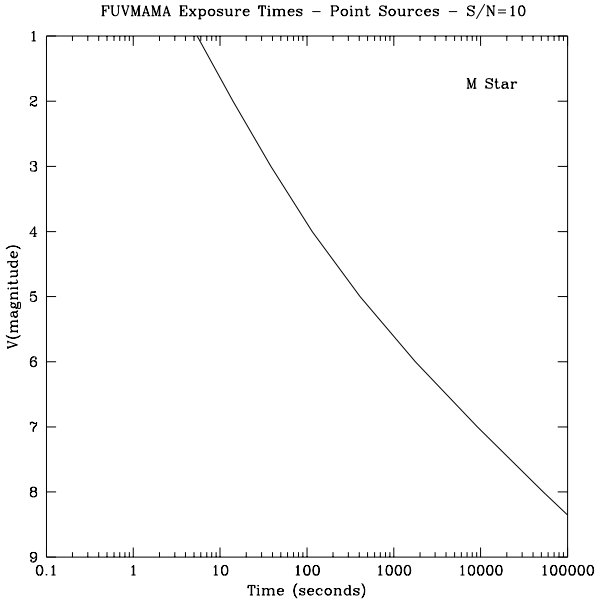

Figure 14.47: F25CN182-NUVMAMA Time to Achieve a Signal-to-Noise of 10 integrated over the bandpass, for point and diffuse sources, assuming a flat (in F_λ) spectrum, cgs units. Point source signal-to-noise is integrated over the PSF, diffuse sources are per 2x2 spatial pixels.

(a) Point Sources

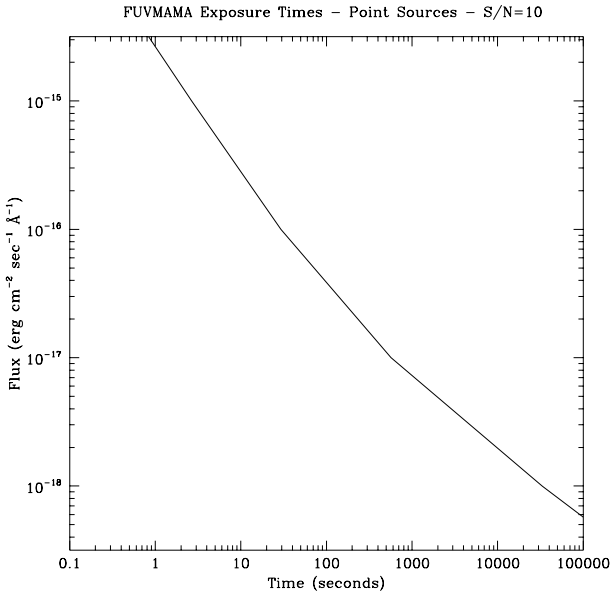

(b) Diffuse Sources

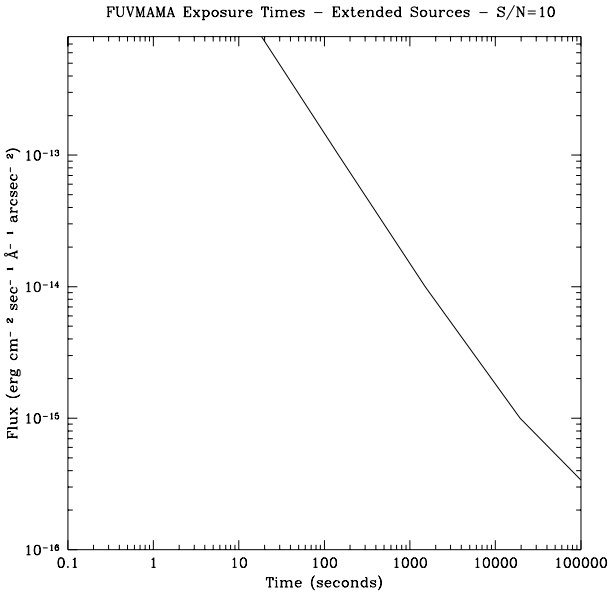

Figure 14.48: F25CN182-NUVMAMA Time to Saturate as a Function of Source Flux, assuming a flat (in F_λ) spectrum

(a) Point Sources

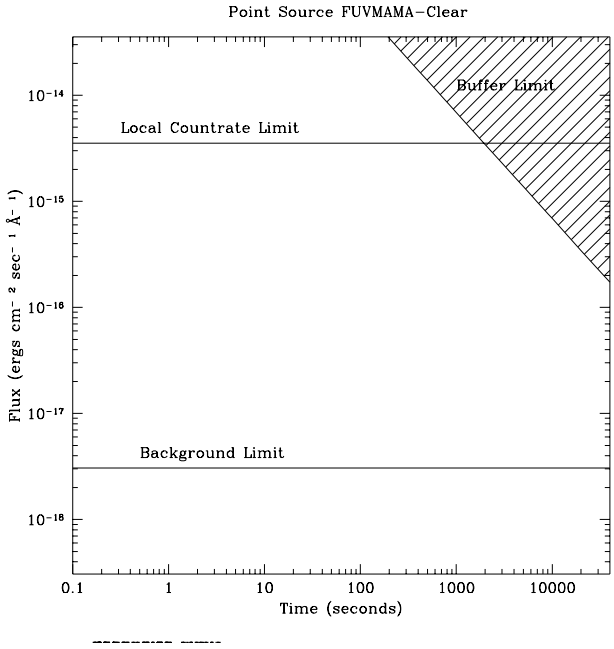

(b) Diffuse Sources

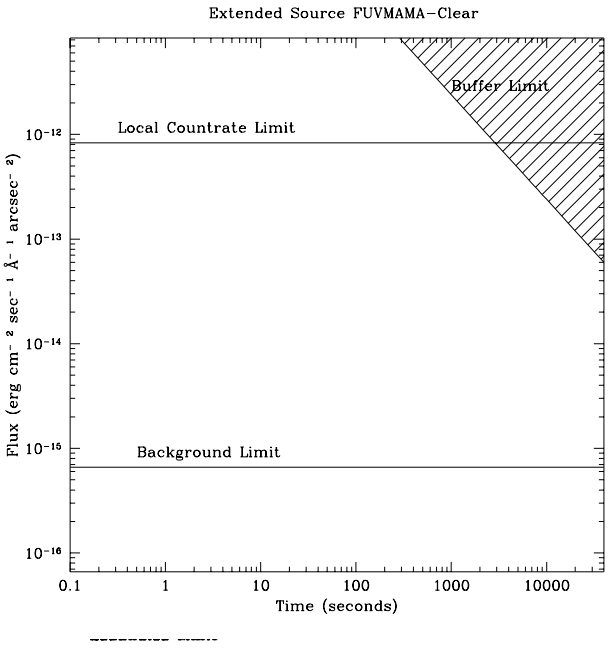

F25QTZ - FUV-MAMA - longpass

Figure 14.49: F25QTZ-FUVMAMA Point Source (left axis), and Diffuse Source (right axis) Sensitivities. Bandpass integrated point source sensitivity for F_λ=1 is $1.1x10^{16}$.

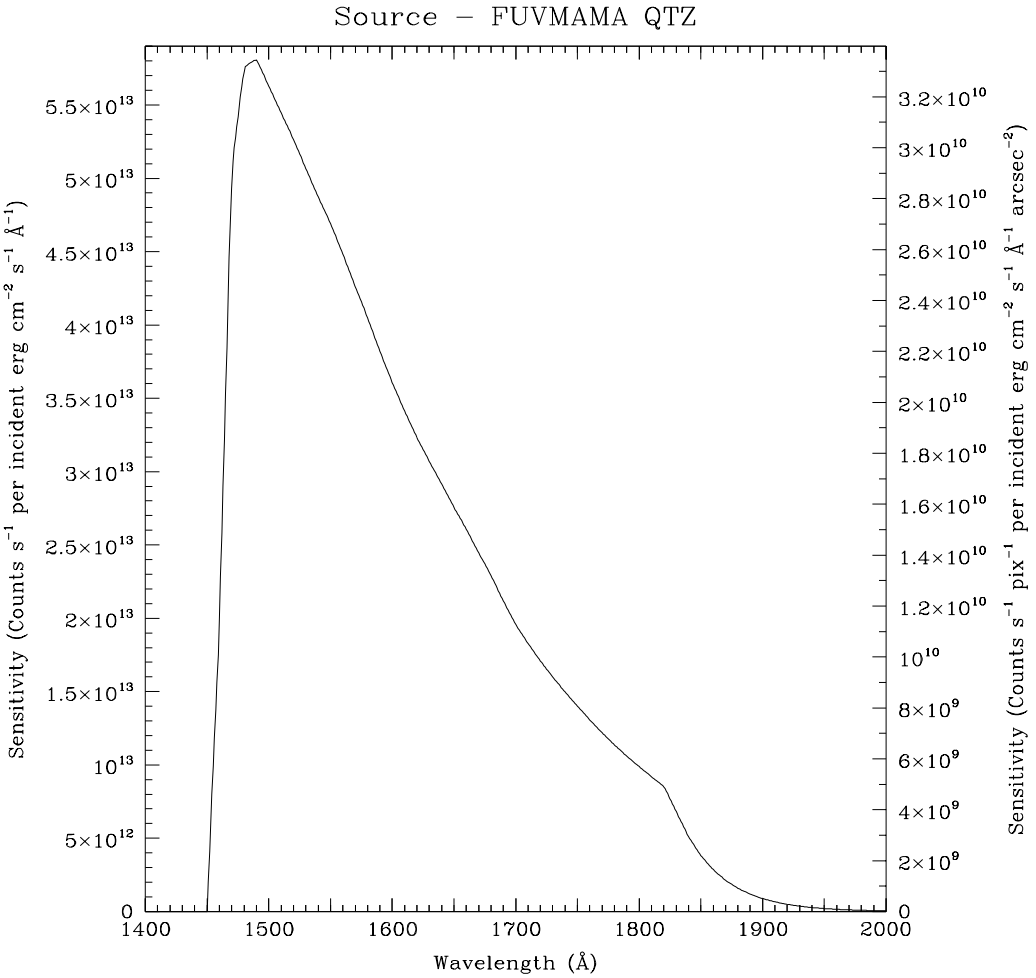

Table 14.13: F25QTZ-FUVMAMA Point Source Sensitivities for FUVMAMA QTZ. Multiply sensitivity number by 0.000576 (the plate scale squared) to obtain diffuse source sensitivity.

λ	**Sens.**	λ	**Sens.**	λ	**Sens.**	λ	**Sens.**
1450	7.50E8	1600	3.6E13	1750	1.4E13	1900	8.9E11
1500	5.6E13	1650	2.8E13	1800	9.9E12	1950	2.0E11
1550	4.7E13	1700	2.0E13	1850	3.8E12	2000	4.9E10

Figure 14.50: F25QTZ-FUVMAMA Time to Achieve a Signal-to-Noise of 10 integrated over the PSF and the bandpass for stars of different spectral types as a function of V band magnitude

(a) O5 star

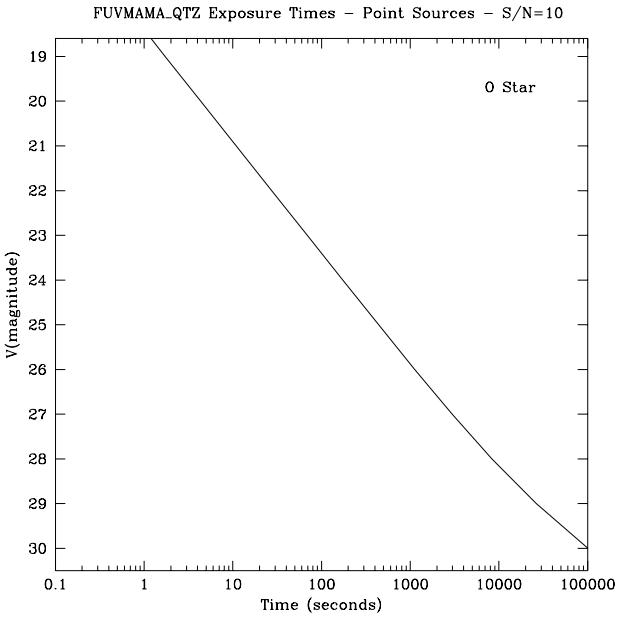

(b) AOV star

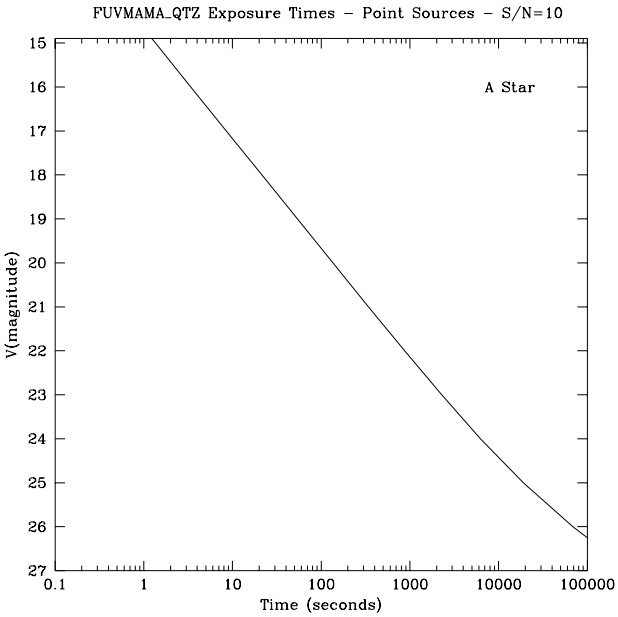

(c) G0V star

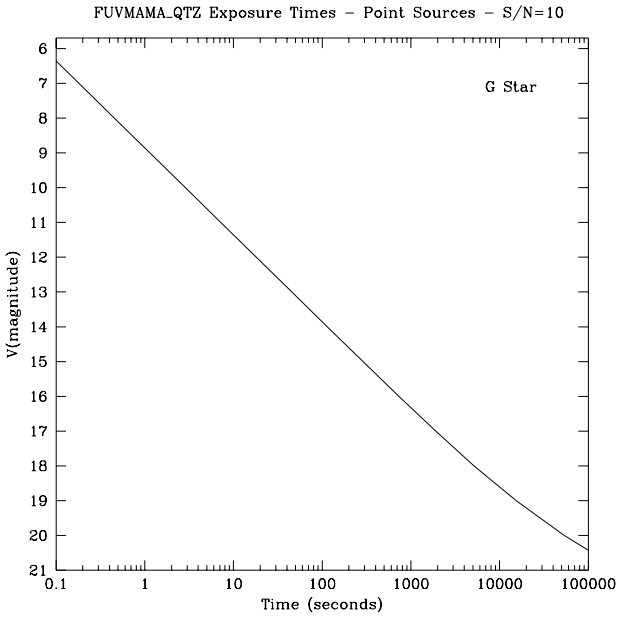

(d) M0V star

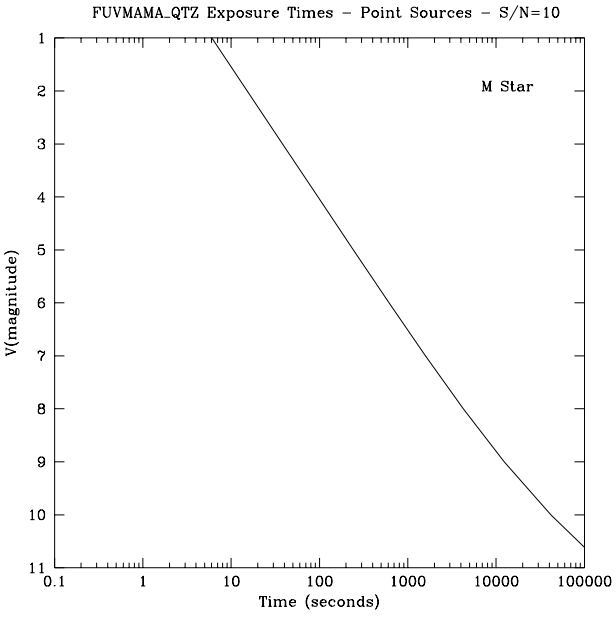

Figure 14.51: F25QTZ-FUVMAMA Time to Achieve a Signal-to-Noise of 10 integrated over the bandpass, for point and diffuse sources, assuming a flat (in F_λ) spectrum, cgs units. Point source signal-to-noise is integrated over the PSF, diffuse sources are per 2x2 spatial pixels.

(a) Point Sources

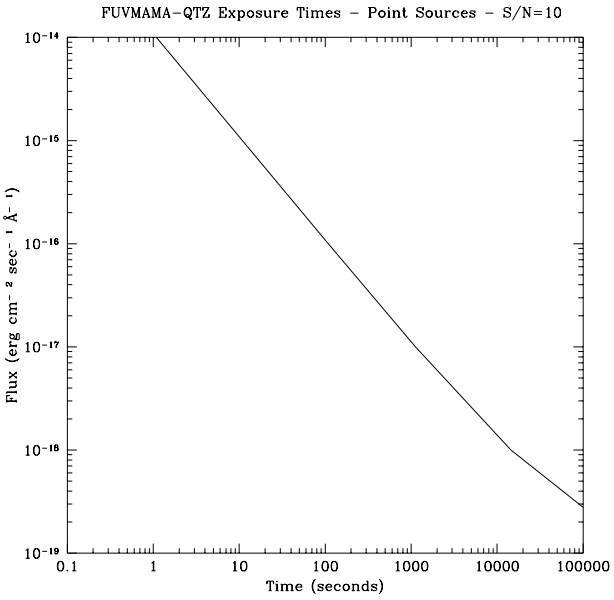

(b) Diffuse Sources

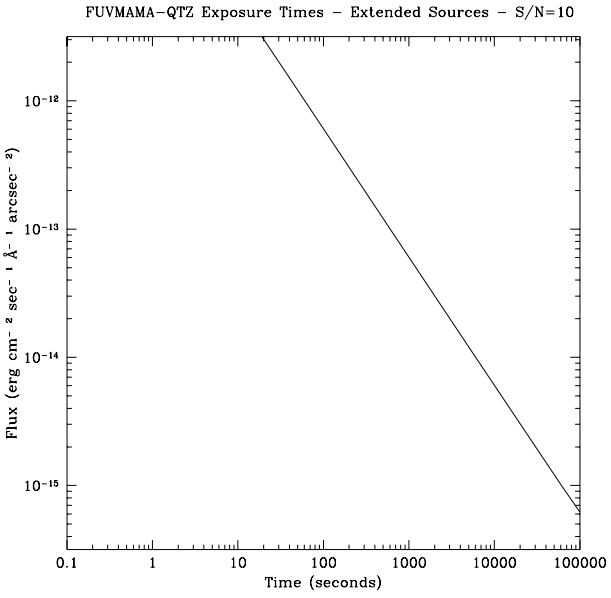

Figure 14.52: F25QTZ-FUVMAMA Time to Saturate as a Function of Source Flux, assuming a flat (in F_λ) spectrum

(a) Point Sources

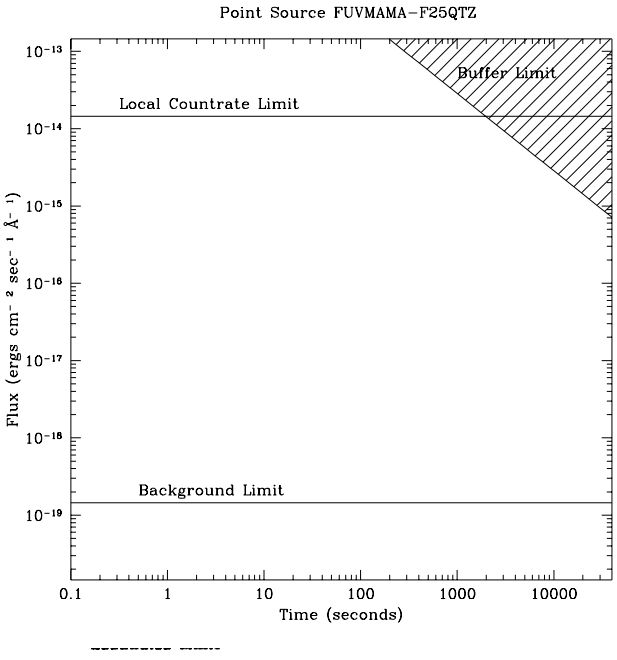

(b) Diffuse Sources

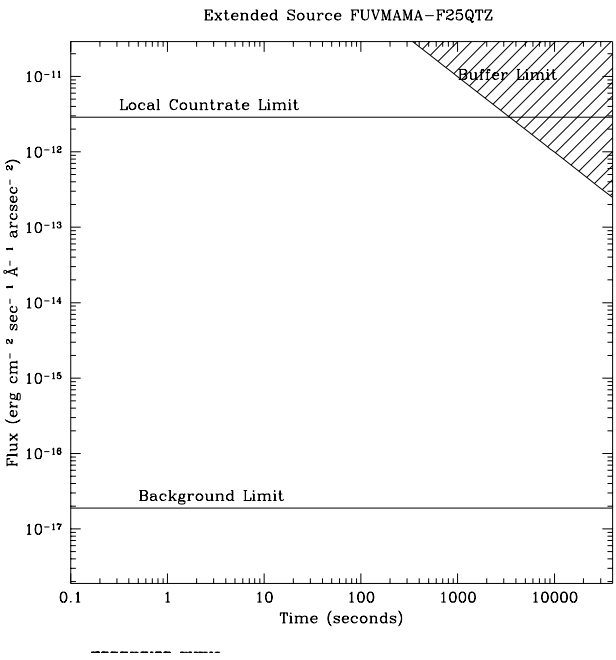

F25SRF2 - FUV-MAMA - longpass

Figure 14.53: F25SRF2-FUVMAMA Point Source (left axis), and Diffuse Source (right axis) Sensitivities. Bandpass integrated point source sensitivity for F_λ=1 is $2.3x10^{16}$.

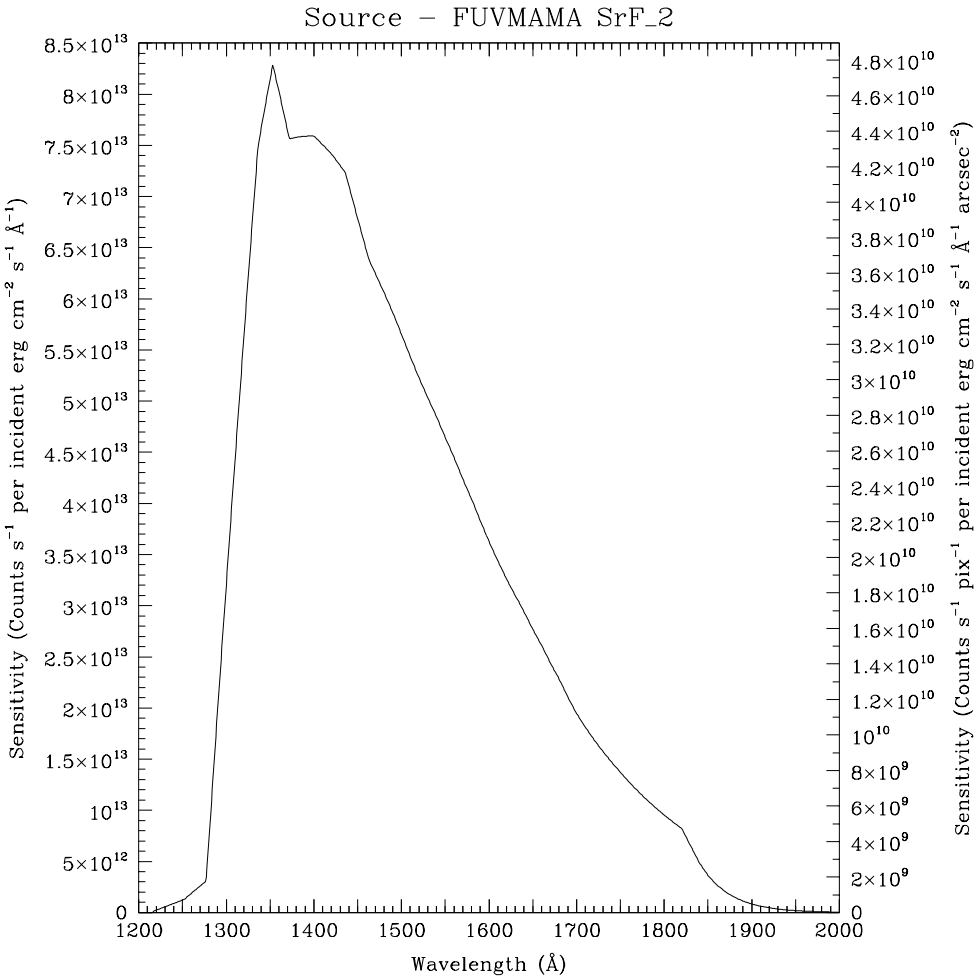

Table 14.14: F25SRF2-FUVMAMA Point Source Sensitivities for FUVMAMA SrF_2. Multiply sensitivity number by 0.000576 (the plate scale squared) to obtain diffuse source sensitivity.

λ	**Sens.**	λ	**Sens.**	λ	**Sens.**	λ	**Sens.**
1250	1.2E12	1450	6.8E13	1650	2.8E13	1850	3.6E12
1300	3.2E13	1500	5.6E13	1700	1.9E13	1900	8.4E11
1350	8.1E13	1550	4.6E13	1750	1.4E13	1950	1.9E11
1400	7.6E13	1600	3.6E13	1800	9.5E12	2000	4.6E10

Figure 14.54: F25SRF2-FUVMAMA Time to Achieve a Signal-to-Noise of 10 integrated over the PSF and the bandpass for stars of different spectral types as a function of V band magnitude

(a) O5 star

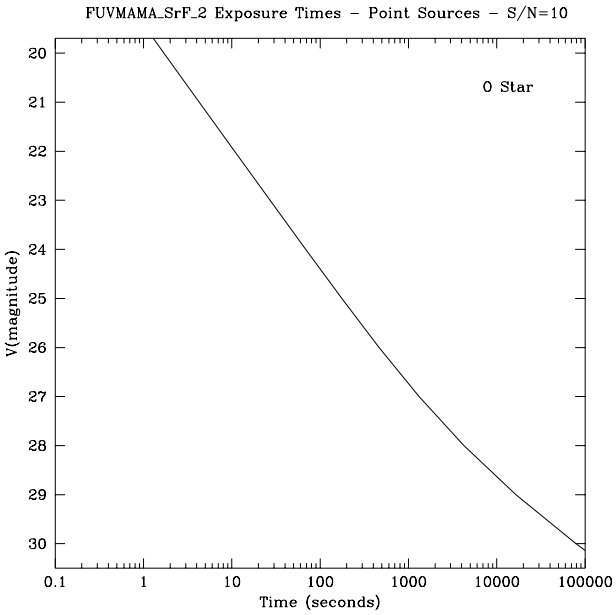

(b) AOV star

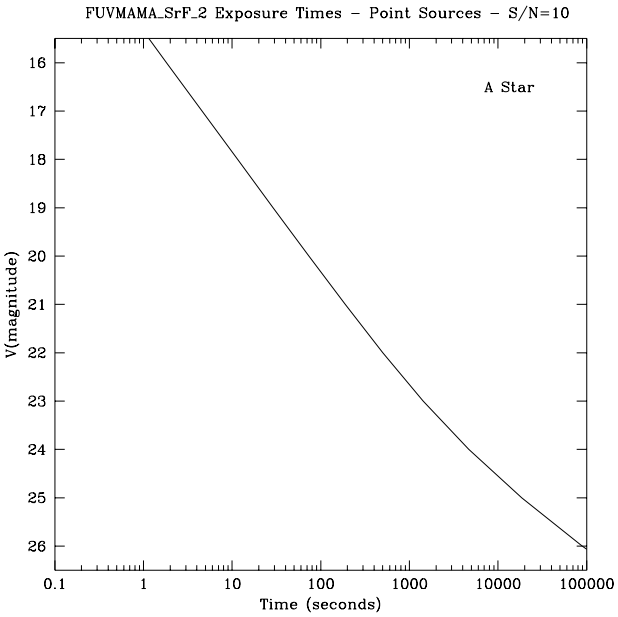

(c) G0V star

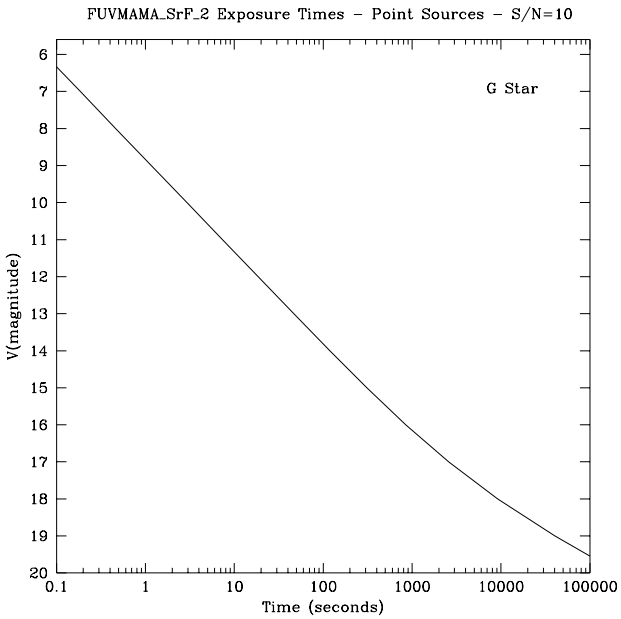

(d) M0V star

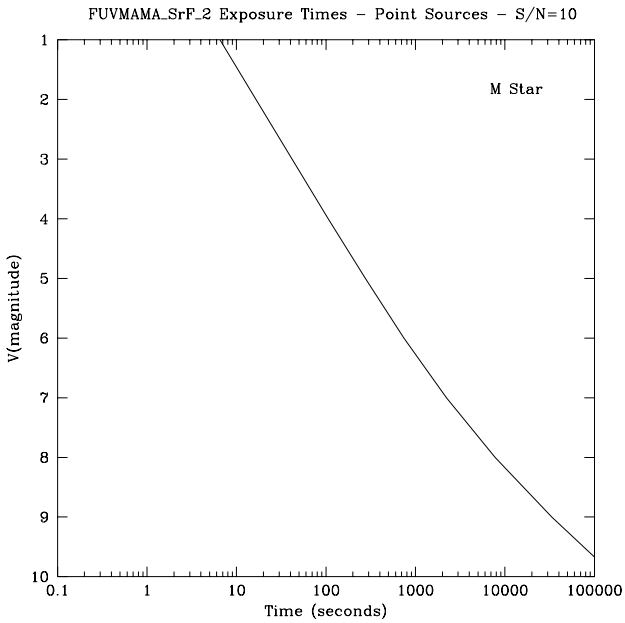

Figure 14.55: F25SRF2-FUVMAMA Time to Achieve a Signal-to-Noise of 10 integrated over the bandpass, for point and diffuse sources, assuming a flat (in F_λ) spectrum, cgs units. Point source signal-to-noise is integrated over the PSF, diffuse sources are per pixel.

(a) Point Sources

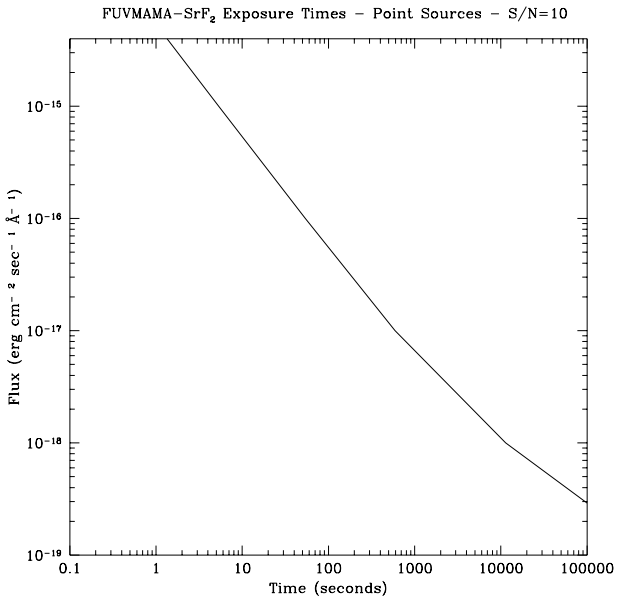

(b) Diffuse Sources

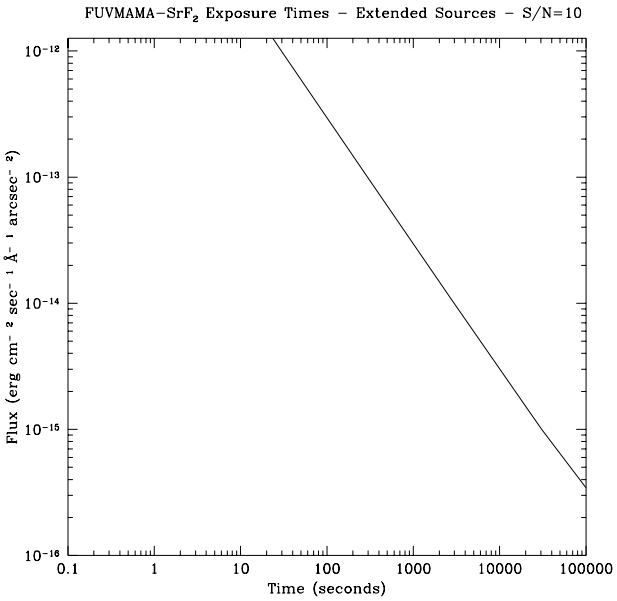

Figure 14.56: F25SRF2-FUVMAMA Time to Saturate as a Function of Source Flux, assuming a flat (in F_λ) spectrum

(a) Point Sources

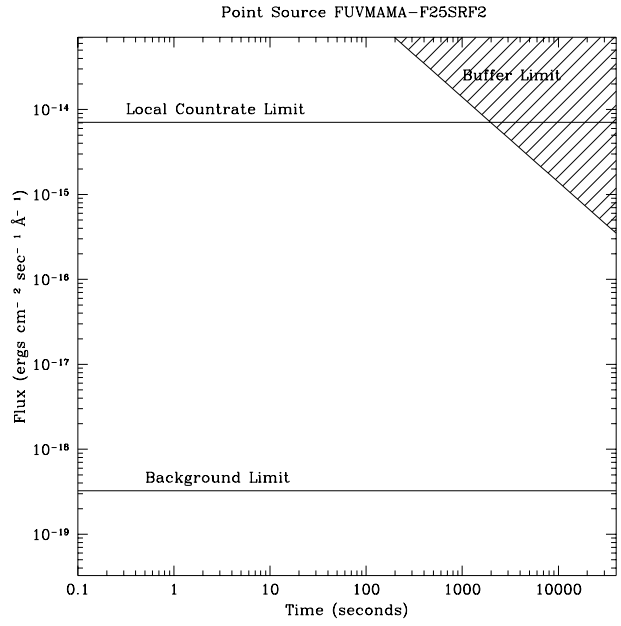

(b) Diffuse Sources

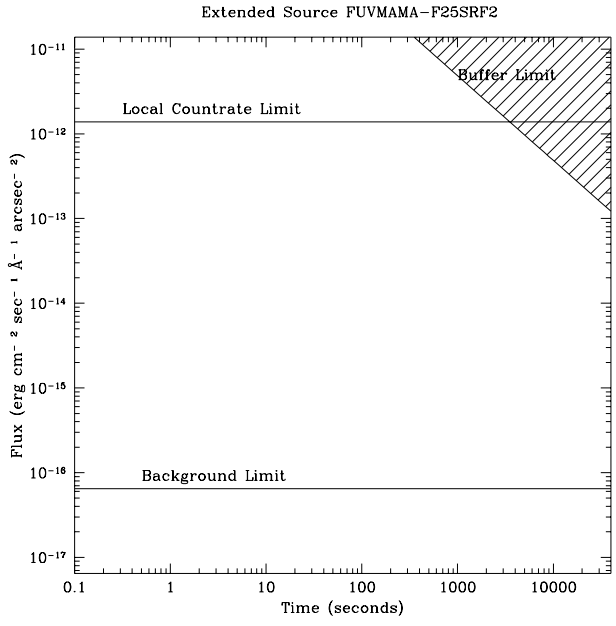

Lyman Alpha - FUV-MAMA

Figure 14.57: Lyman Alpha-FUVMAMA Point Source (left axis), and Diffuse Source (right axis) Sensitivities. Bandpass integrated point source sensitivity for F_λ=1 is 1.1x10^{15}.

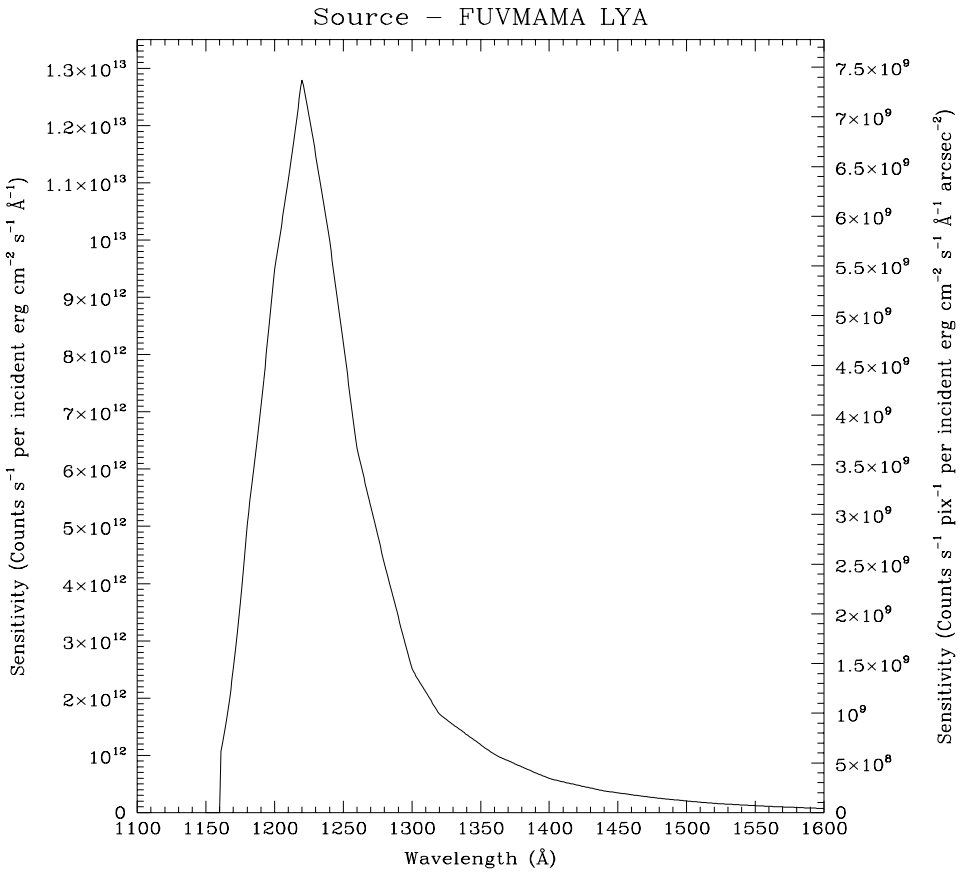

Table 14.15: Lyman Alpha-FUVMAMA Point Source Sensitivities for FUVMAMA LYA. Multiply sensitivity number by 0.000576 (the plate scale squared) to obtain diffuse source sensitivity.

λ	**Sens.**	λ	**Sens.**	λ	**Sens.**	λ	**Sens.**
1175	3.6E12	1400	5.9E11	1650	4.3E10	1900	5.15E8
1200	9.5E12	1450	3.4E11	1700	2.4E10	1950	1.00E8
1250	8.2E12	1500	2.0E11	1750	1.4E10	2000	2.08E7
1300	2.5E12	1550	1.2E11	1800	8.02E9		
1350	1.2E12	1600	7.2E10	1850	2.61E9		

Figure 14.58: Lyman Alpha-FUVMAMA Time to Achieve a Signal-to-Noise of 10 integrated over the PSF and the bandpass for stars of different spectral types as a function of V band magnitude

(a) O5 star

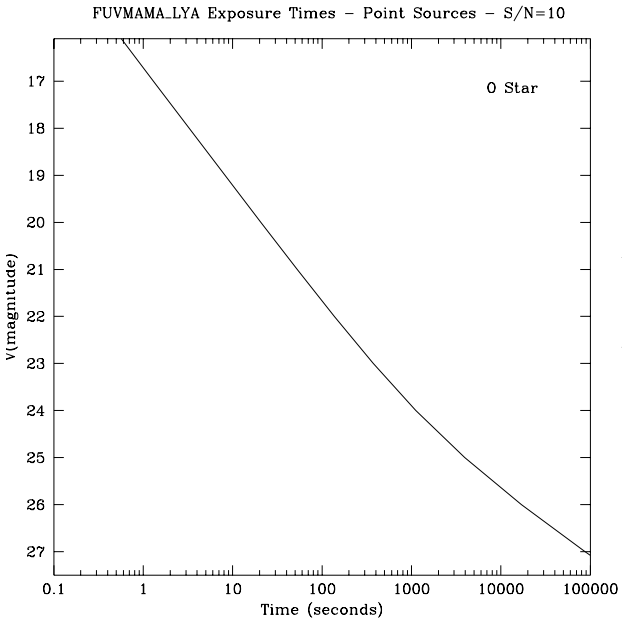

(b) AOV star

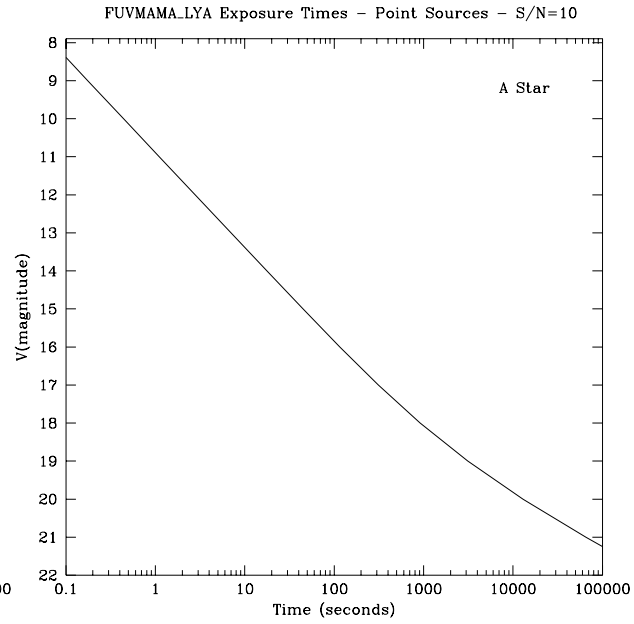

(c) G0V star

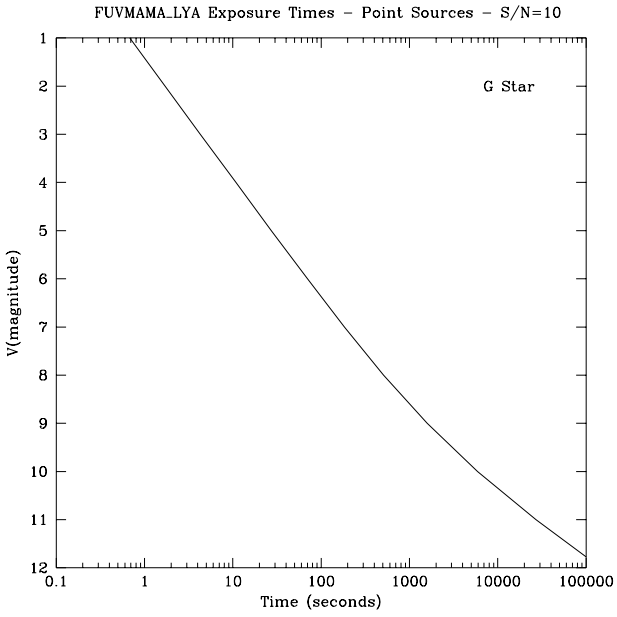

(d) M0V star

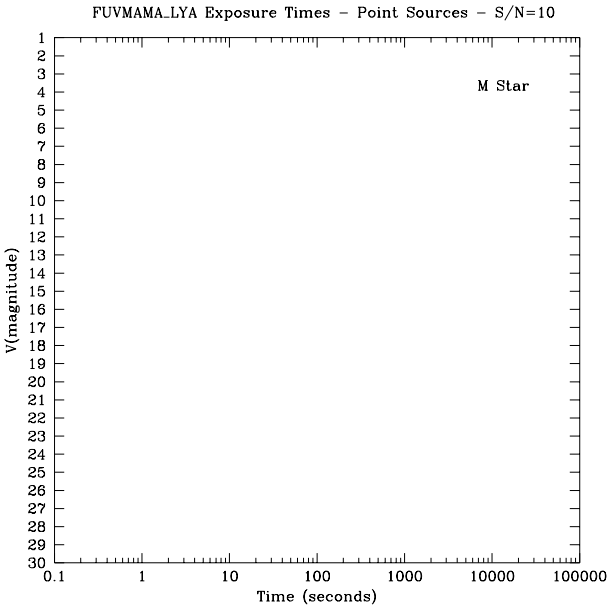

Figure 14.59: Lyman Alpha-FUVMAMA Time to Achieve a Signal-to-Noise of 10 integrated over the bandpass, for point and diffuse sources, assuming a flat (in F_λ) spectrum, cgs units. Point source signal-to-noise is integrated over the PSF, diffuse sources are per 2x2 spatial pixels.

(a) Point Sources

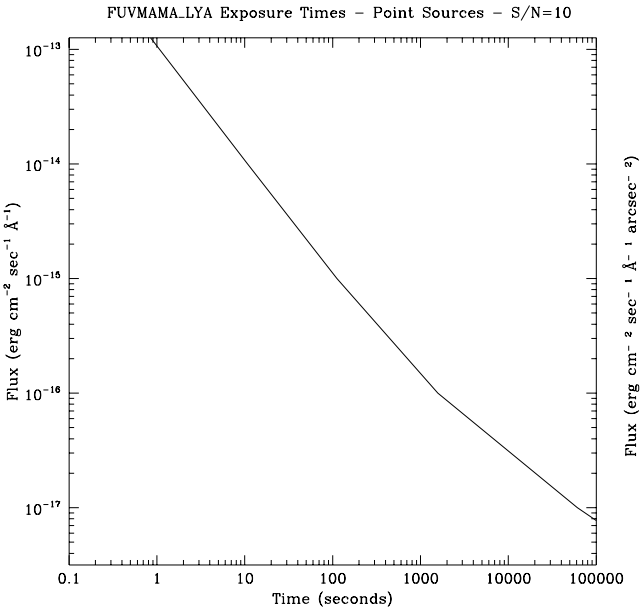

(b) Diffuse Sources

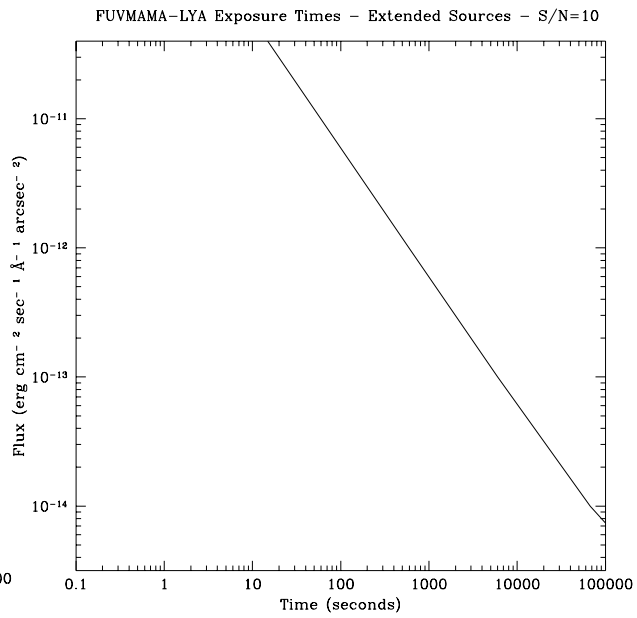

Figure 14.60: Lyman Alpha-FUVMAMA Time to Saturate as a Function of Source Flux, assuming a flat (in F_λ) spectrum

(a) Point Sources

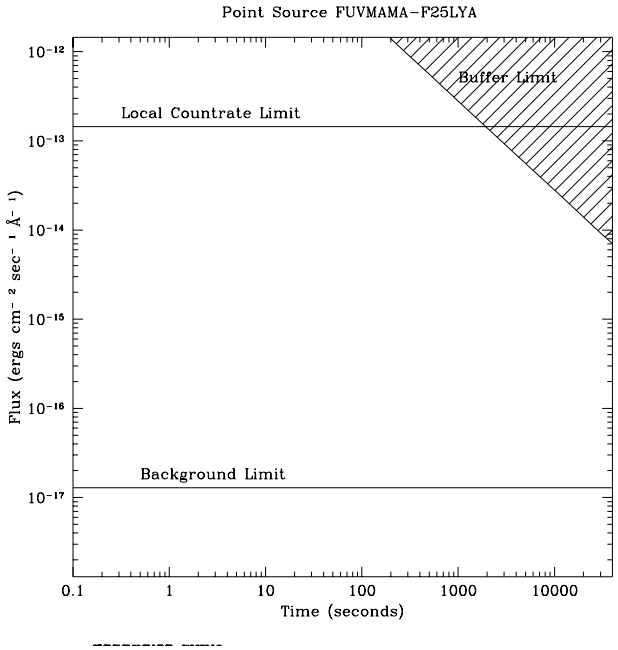

(b) Diffuse Sources

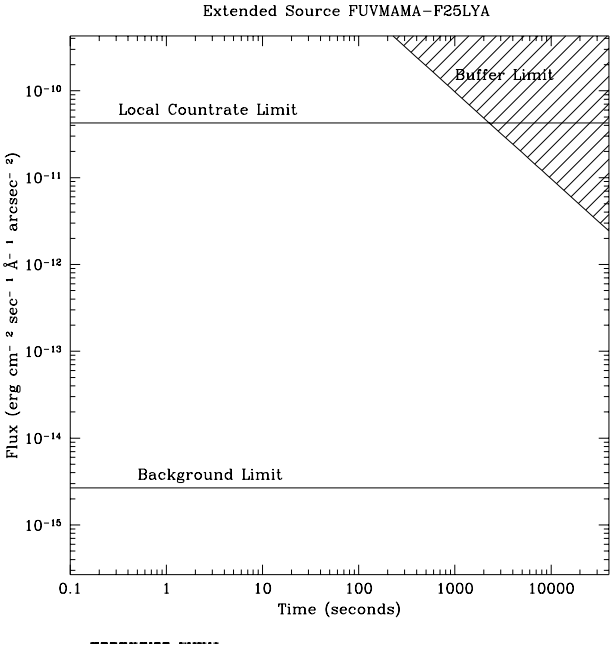

Point Source Encircled Energies

Below, in Figure 14.61 on page 306, we show plots of encircled energies for the CCD imaging modes (Figure 14.61 on page 306), the NUV-MAMA imaging modes and the FUV-MAMA imaging modes. These plots are predictive only; they are based on predicted PSFs at the aperture plane and detector PSFs from non-flight detectors. The ultimate encircled energy achieved will depend sensitively on the alignment of the integrated optics and detectors and the properties of the flight detectors.

The PSF in imaging mode is expected to be degraded by ~30% at the outer edge of the top and bottom of the field of view.

Figure 14.61: Predicted Image Mode Encircled Energies

(a) CCD
plate scale = 0.05 arcseconds per pixel

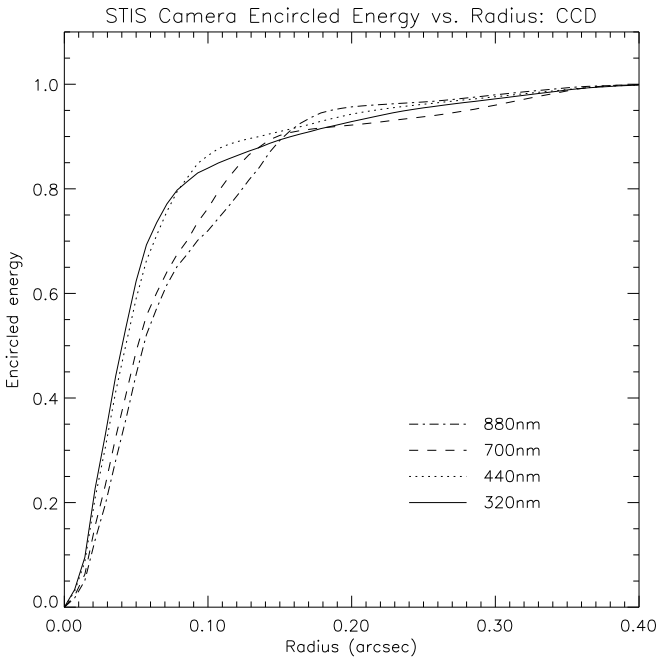

(b) NUV-MAMA
plate scale = 0.024 arcseconds per pixel

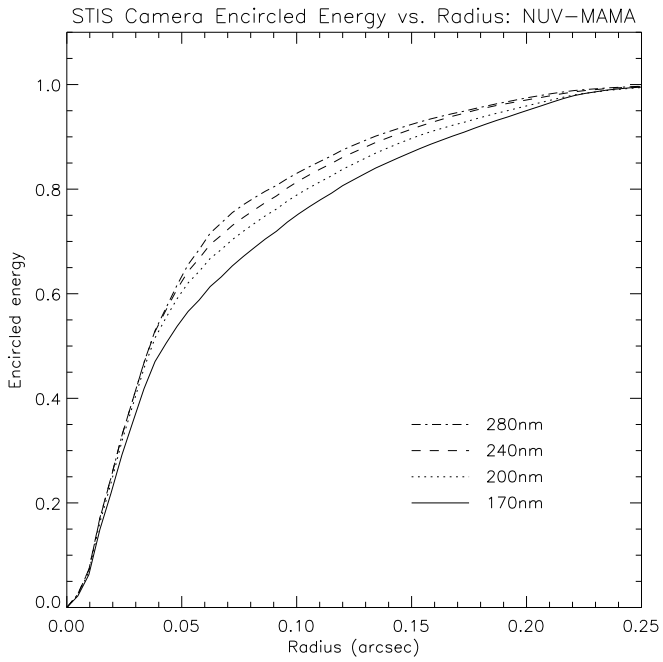

(b) FUV-MAMA
plate scale = 0.024 arcseconds per pixel

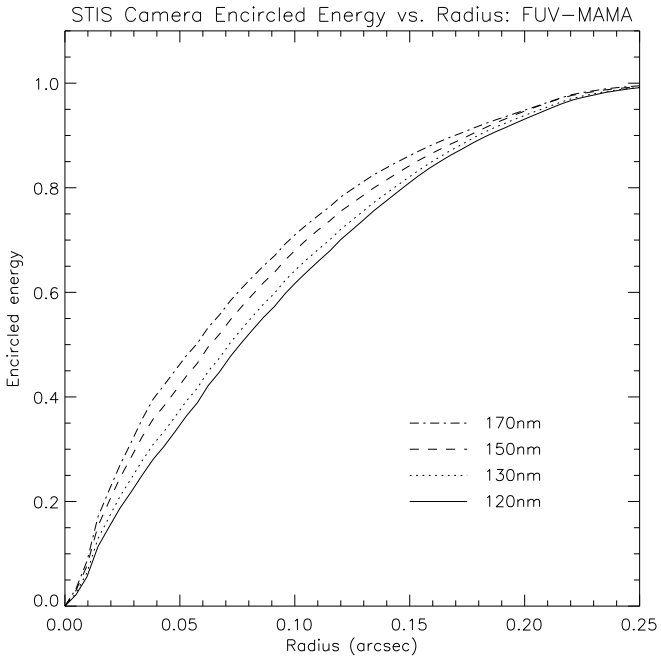

MAMA Imaging Bright Object Limits

As described in “MAMA Bright Object Limits” on page 97 in Chapter 7. the MAMA’s are subject to absolute brightness limits, above which sources cannot be observed or they would potentially damage the detectors. In Table 14.15, below, we present the complete set of absolute bright object point source and integrated magnitude screening limits for the MAMA imaging modes. Remember, sources cannot be observed in configurations where they exceed the absolute bright object limits. The information presented here should be used in conjunction with the material presented in Chapter 7.

A few important points to note.

- Limits are given as V magnitudes or in CGS units as indicated.
- The imaging table includes a single point source limit. No single source in the field of view can exceed this limit.
- The limits in the tables assume zero extinction. If your source, when corrected for Galactic extinction, does not exceed the absolute limits, then you will be allowed to observe your source.
- Because the MAMA imaging bright object limits are so faint, STScI cannot perform automatic screening for imaging and the observer must provide an image of the field and V and B-V magnitudes for each object in the field before they will be allowed to observe; see “MAMA Bright Object Limits” on page 97.
- The imaging table also includes an integrated magnitude limit. Remember that the global limit of 300,000 counts sec^{-1} applies to all sources imaged onto the MAMA detector. The integrated magnitude limit gives the total magnitude from all stars (or galaxies, or diffuse objects) of spectral type O which can appear in the MAMA field of view. Initial screening of all MAMA imaging observations will be done assuming all stars are O stars.

Table 14.16: MAMA Imaging Bright Object Limits, V Magnitudes and CGS as indicated.

Spectral Type	FUV-MAMA				NUV-MAMA						
	25MAMA (clear)	F25SRF2 (longpass)	F25QTZ (longpass)	F25LYA (Lyα)	25MAMA (clear)	F25SRF2 longpass	F25QTZ longpass	F25CIII (CIII)	F25CN182 (182 cont)	F25CN270 (270 cont)	F25MGII (MgII)
Surface Brightness[a]	$8.4x10^{-13}$	$1.4x10^{-12}$	$2.9x10^{-12}$	$4.2x10^{-11}$	$3.4x10^{-13}$	$4.3x10^{-13}$	$4.1x10^{-13}$	$3.7x10^{-11}$	$7.0x10^{-12}$	$2.7x10^{-12}$	$1.3x10^{-11}$
Point Source Flux[b]	$2.7x10^{-15}$	$4.4x10^{-15}$	$9.2x10^{-15}$	$1.4x10^{-13}$	$8.6x10^{-16}$	$1.1x10^{-15}$	$1.0x10^{-15}$	$9.1x10^{-14}$	$1.7x10^{-14}$	$6.8x10^{-15}$	$3.2x10^{-14}$
O5V[c]	20.4	19.7	18.6	16.1	20.1	19.8	19.8	15.5	17.4	17.1	15.3
B1V	19.8	19.2	18.2	15.2	19.6	19.4	19.3	15.1	17.0	16.7	14.9
B3V	18.9	18.3	17.3	14.1	18.8	18.5	18.5	14.1	16.1	16.1	14.3
B6V	17.8	17.3	16.4	12.7	18.0	17.7	17.7	13.2	15.2	15.4	13.6
B9V	17.1	16.7	15.9	11.5	17.6	17.4	17.4	13.0	14.8	15.1	13.3
A1V	15.7	15.5	14.9	7.9	16.9	16.7	16.7	12.3	14.1	14.5	12.7
A3V	14.4	14.2	13.8	6.5	16.4	16.1	16.2	11.7	13.5	14.1	12.4
A5V	11.4	11.2	11.3	0.5	15.7	15.5	15.5	10.7	12.3	13.5	11.8
A9IV	11.2	11.0	11.1	0.3	15.6	15.3	15.4	10.6	12.2	13.4	11.6
F2V	8.2	8.0	8.0		15.0	14.7	14.8	7.9	9.5	12.9	11.1
F4V	8.1	7.9	7.9		14.9	14.6	14.7	7.8	9.4	12.8	11.0
F6V	8.0	7.8	7.9		14.9	14.6	14.7	7.8	9.4	12.8	11.1
F8V	8.1	7.9	8.0		14.6	14.3	14.4	7.9	9.6	12.4	10.6
G2V	5.8	5.6	5.7		14.4	14.0	14.1	5.7	7.4	12.2	10.4
G5IV	5.1	4.9	5.0		13.8	13.4	13.5	5.0	6.8	11.6	9.8
G7IV	-1.7		-1.8		12.9	12.3	12.4		3.1	10.0	8.7
K0IV					12.6	11.9	12.0		2.8	9.6	8.3
K4V					12.4	11.6	11.7		3.3	9.3	8.3
K8V					12.2	11.4	11.5		3.0	9.4	8.7
M2V					11.8	11.0	11.1		3.3	9.3	8.6
M4V					11.7	10.9	10.9		3.2	9.1	8.4
M6V					11.3	10.4	10.4		2.7	8.7	7.9
M8III					10.8	9.2	9.3		1.5	7.5	6.8
T~50000°K[d]	20.3	19.6	18.6	15.9	20.0	19.7	19.7	15.5	17.4	17.1	15.2
ν^{-1}	16.8	16.0	15.1	12.5	17.5	17.3	17.3	13.0	15.1	15.0	13.3
Integrated Magnitude[f]	11.9	11.2	10.1	7.6	12.4	11.8	12.1	7.8	9.7	10.0	7.6

[a] Peak allowed diffuse source surface brightness in ergs sec^{-1} cm^{-2} $Å^{-1}$ $arcsec^{-2}$.
[b] Peak allowed point source flux in ergs sec^{-1} cm^{-2} $Å^{-1}$.
[c] Limits given are V magnitudes, for unreddened stars.
[d] Limits calculated for a black body at 50,000 degrees K.
[e] Limits calculated for a source with spectrum F_ν proportional to ν^{-1}.
[f] Maximum integrated magnitude of all stars in field, assuming all are O stars.

PART 4

Calibration

The chapters in this part describe the calibration of STIS. These chapters include an overview of the calibration pipeline process, expected accuracies for data taken in Cycle 7, and plans for calibrating and verifying the instrument's performance.

CHAPTER 15
Overview of Pipeline Products

In This Chapter...

In this chapter we summarize the basic reductions and calibration that will be performed in the STScI STIS pipeline and describe briefly the format of the data products the observer will receive. This information is intended to provide enough background to develop robust observing proposals. A STIS chapter in the *HST Data Handbook* will ultimately provide the detail needed for analyzing your data.

Pipeline Processing Overview

Science data taken by STIS will be received from the Space Telescope Data Capture Facility and sent to the STScI pipeline, where the data will be unpacked, keywords extracted from the telemetry stream, and the science data reformatted and repackaged into raw (uncalibrated) FITS[1] files by the generic conversion process. All STIS `ACCUM` mode data (i.e., images) will be stored in FITS using image extensions, as triplets of science, error, and data quality arrays. The structure of those files is discussed briefly below (see “STIS Data Products” on page 313).

The uncalibrated FITS files are passed through the **calstis** pipeline which calibrates the data, producing *calibrated* FITS files. The **calstis** program will propagate statistical errors and track data quality flags through the calibration process. The **calstis** code will be available to users in STSDAS, so they can recalibrate their data as needed.[2]

1. Flexible Image Transport System.

Calstis performs the following basic science data calibrations:

- Two-dimensional image reduction producing a flat fielded output image (*rootname*_flt.fits), which, depending on whether the data is from the MAMA or the CCD and whether it is imaging or spectroscopic data, includes the following: data quality initialization, dark subtraction, bias subtraction, non-linearity flagging, flat fielding, geometric correction, photometric calibration.
- Two-dimensional spectral extraction producing a flux calibrated, rectified spectroscopic image (*rootname*_x2d.fits) with distance along slit running linearly along the y axis and dispersion running linearly long the x axis.
- One-dimensional spectral extraction producing a one-dimensional spectrum of flux versus wavelength (*rootname*_x1d.fits), uninterpolated in wavelength space, but integrated across an extraction aperture in the spatial direction (this will be performed only for point sources in the case of long slit spectroscopy, but will be performed for all echelle short slit observations).

In addition, **calstis** will perform two types of *contemporaneous calibrations:*

- For CCD exposures which have been CRSPLIT, **calstis** will combine the exposures, producing a cosmic-ray rejected image (*rootname*_crj.fits) which is then passed through subsequent calibration (e.g., spectral extraction).
- For spectroscopic exposures, **calstis** will process the associated wavecal exposure (see “Routine Wavecals” on page 24) to determine the zero point offset of the wavelength and spatial scales in the science image, correcting thereby for the lack of repeatability of the mode select mechanism. Where the uncalibrated science data is stored in the *rootname*_raw.fits file, the accompanying wavecal observations will be stored in the *rootname*_wav.fits file.

The calibration steps that **calstis** performs on a given set of science observations depends on the nature of those observations. As noted earlier, slitless spectroscopic data and long slit echelle spectroscopic data and prism data will be processed only up to flatfielding. Data taken in TIMETAG mode will be corrected for the Doppler shift from the spacecraft motion and output as an uncalibrated event stream by the pipeline in a FITS binary table (*rootname*_tag.fits). Additionally the timetag data stream will be integrated in time to produce an uncalibrated ACCUM mode image (*rootname*_raw.fits) which is then passed through standard calibration. Figure 15.1 shows an example of spectroscopic ACCUM mode CRSPLIT CCD data passing through the **calstis** pipeline.

2. The **calstis** software is written in C and uses open IRAF in conjunction with a specially written I/O interface to the FITS data file.

Figure 15.1: STIS Calibration Process for CCD CRSPLIT Spectroscopic Data

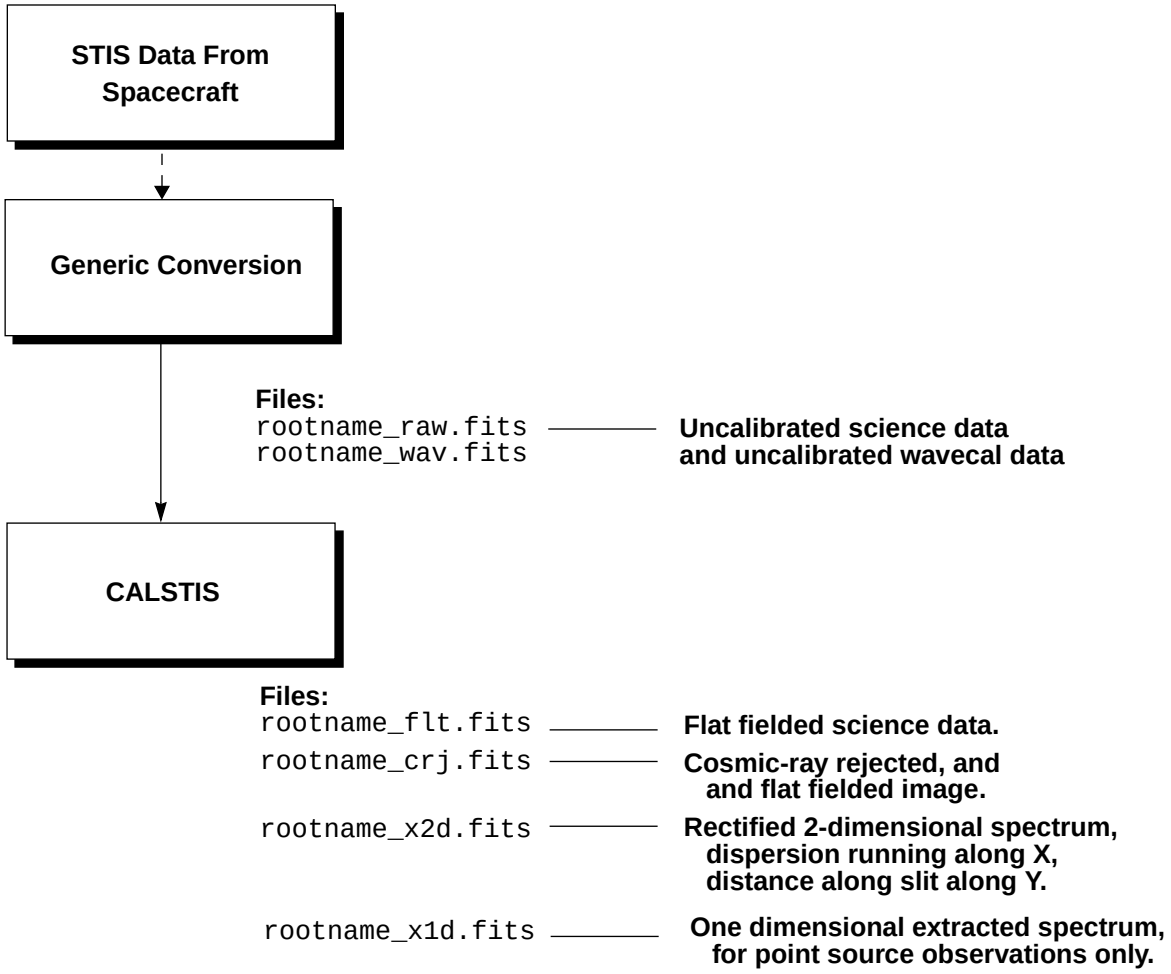

STIS Data Products

All STIS data products will be FITS files. The vast majority of the STIS data products are two-dimensional images which will be stored in FITS image extension files. Fits image extensions offer great flexibility in data storage and allow us to package related science data which is processed through calibration as a single unit together into one file. Tabular information, such as the `TIMETAG` mode event series or extracted one-dimensional spectra will be stored as FITS binary tables. Note that this format is compatible with the QPOE (Quick Position Oriented Event) format, so that the existing event software in the EUV and PROS packages can be used with the `TIMETAG` data.

The FITS files will be directly accessible in IRAF and STSDAS either through the newly created FITS image extension IRAF kernel for image extensions, or through the STSDAS **tables** package for binary tables—there will be no need to convert them to IRAF or STSDAS format.

Figure 15.2 illustrates the structure of a STIS FITS image extension file. It has:

- A primary header where keyword information describing all of the exposures in the file is stored (e.g., the target name, target RA and Dec, total exposure time of all exposures in the file, optical elements, detector, etc.).
- A series of image extensions, each containing a header with exposure level keyword information and a data array.

Figure 15.2: FITS Image Extension File for STIS

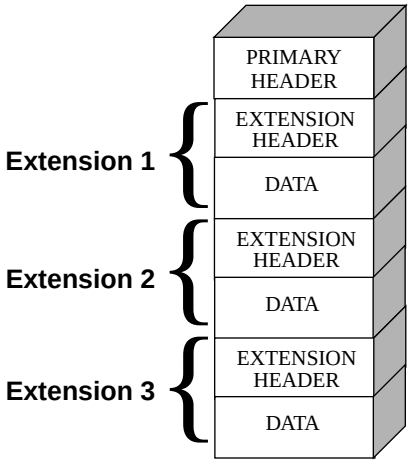

For each STIS exposure in a file, a triplet of FITS image extensions will be created:

- The first, of extension type SCI, stores the science values.
- The second, of extensions type ERR contains the statistical errors, which are propagated through the calibration process.
- The third, of extension type DQ, stores the data quality values which flag suspect pixels in the corresponding data.

A single FITS file will have multiple exposures in it whenever an associated set of science exposures are taken (see “Exposure Sequences: auto-wavecal, crsplits, repeats, and patterns” on page 151). For example, if exposures were taken with `CRSPLIT`=3, the *`rootname`*`_raw.fits` file will contain 3 science exposures, or 9 image extensions; one for each (SCI, ERR, DQ) triplet. After calibration, a single cosmic ray rejected image is produced along with its data quality and error file (Figure 15.4 on page 316). Similarly, for `REPEATOBS` observations, in which many identical exposures are taken to obtain a time series, all the science data will be stored in sequential triplet extensions of a single FITS file (Figure 15.5 on page 317). These will be processed through **calstis** as a unit, with each image

extension individually calibrated and the set of images also being combined to produce a total time-integrated calibrated image.

Accessing the images in the FITS image extension files through the IRAF FITS image extension kernel follows a simple convention. See the examples shown below.

Figure 15.3: Accessing FITS Images

To display the 3rd *science* extension of the file rootname_raw.fits, type:
```
>display rootname_raw.fits[SCI,3].
```

To use imexamine on the 2nd *data quality* extension, type:
```
>imexam rootname_raw.fits[DQ,2]
```

Figure 15.4: Data Format for CRSPLIT=3 Observations

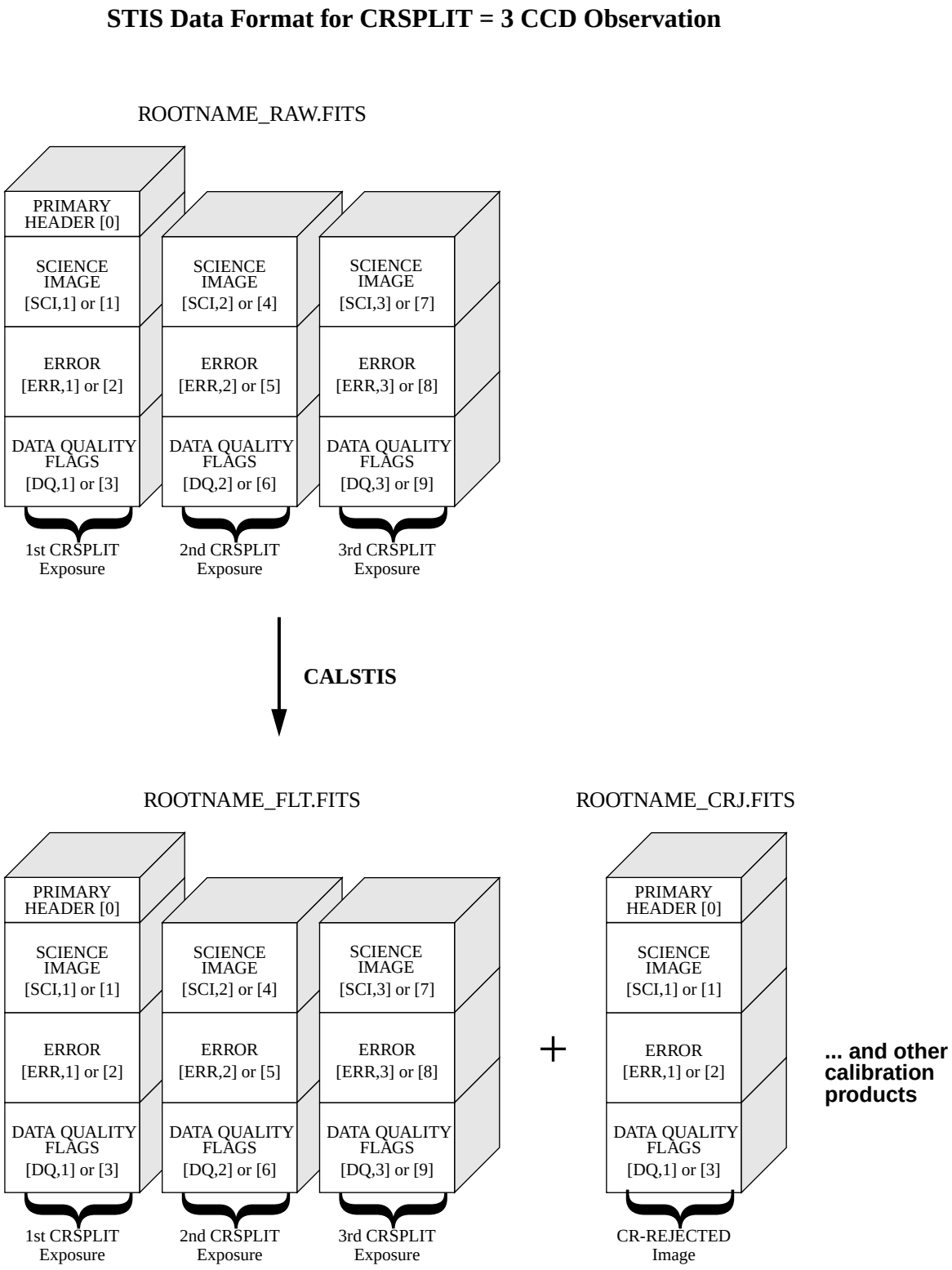

Figure 15.5: Data Format for REPEATOBS Observations

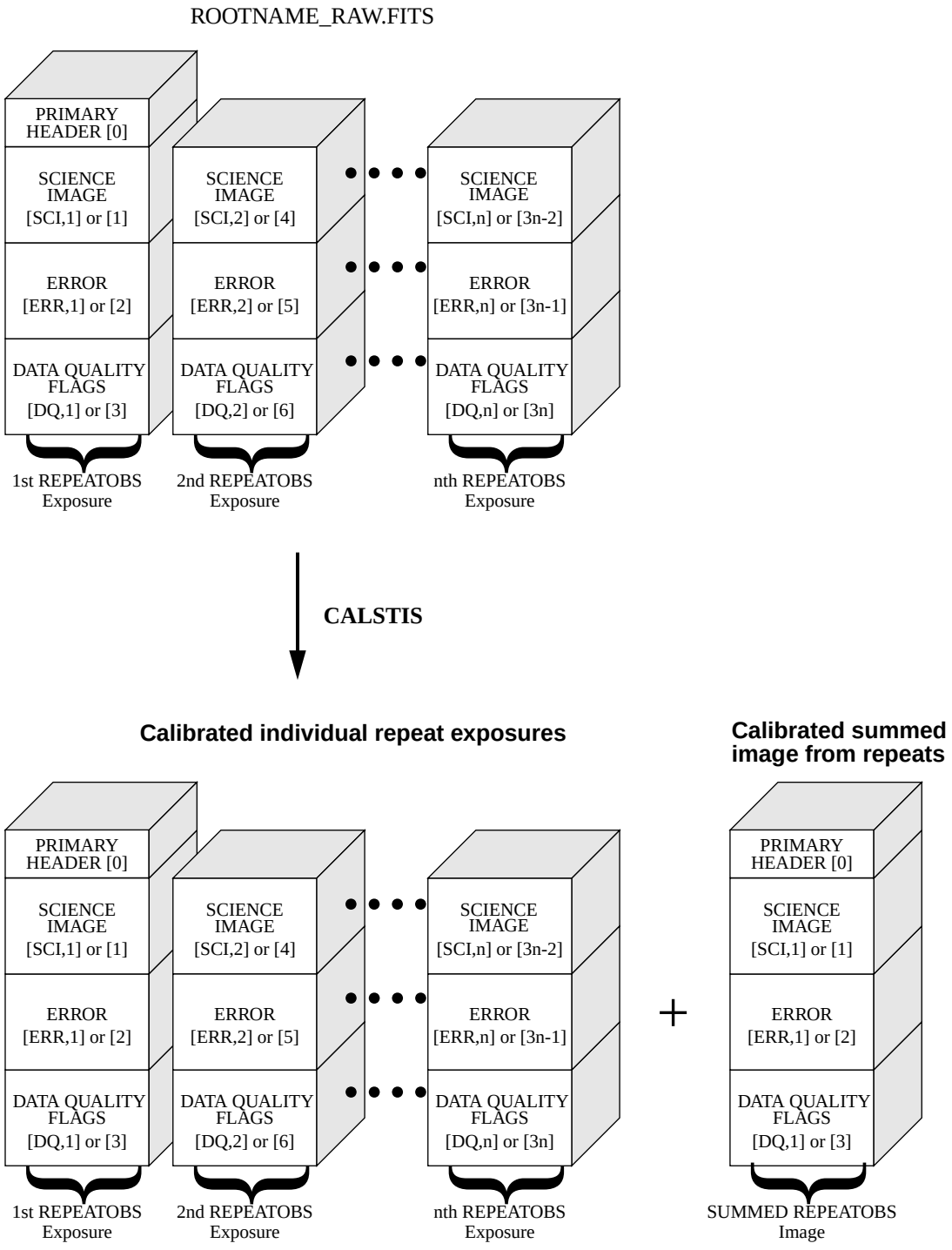

CHAPTER 16
Expected Accuracies

In This Chapter...

In this chapter we describe the accuracies we hope to achieve during Cycle 7 for the photometric, spectral, and astrometric calibration of STIS.

Summary of Expected Accuracies

We have begun the process of determining calibration accuracies for STIS. These accuracies will ultimately depend on the performance of the hardware, our ability to monitor the instrument performance in orbit, and the calibration software.

In Tables 16.1 through 16.5, we give the expected accuracies for each of STIS's basic observation modes: CCD spectroscopy, MAMA spectroscopy, CCD imaging, MAMA imaging and target acquisitions. We expect our understanding of the calibration of STIS to develop during Cycle 7, and early in the cycle accuracies will naturally be less well defined than later in the Cycle. The numbers given are the accuracy we plan to achieve by the end of Cycle 7, for any observation taken during Cycle 7. These projected accuracies are cautious estimates based on the CEI specifications for the instrument, our current *very limited* knowledge of the performance of the detectors (which is based exclusively on component testing), and our plans for on-orbit calibration during the Cycle.

Our expectation for the MAMAs are particularly uncertain, as there is little ground data on their performance at this time. MAMA calibration is a time consuming process, as the count rate over the detector must be kept below the global limits. Thus, for example, flat fields must be obtained at rates of ≤ 0.3 counts sec^{-1} $pixel^{-1}$ (to keep 1024 x 1024 x r < 300,000 counts sec^{-1}), and a single

100:1 signal-to-noise ratio per resolution element (2 x 2 pixel) flat field thus takes > 3 hours to obtain.

Table 16.1: CCD Spectroscopic Accuracies

Attribute	Accuracy	Limiting Factors
Relative wavelengths—within an exposure	0.1–0.25 pixels	Stability of optical distortion
Absolute wavelengths—across exposures	1.0 pixels	• Thermal stability • Internal versus external illumination • Derivation of wavecal zero point
Absolute photometry	10%	Instrument stability and photometric calibration
Relative photometry (within an exposure)	5%	Instrument stability and photometric calibration

Table 16.2: MAMA Spectroscopic Accuracies

Attribute	Accuracy	Limiting Factor
Relative wavelengths—within an exposure	0.25–0.5 pixels	Stability of small scale geometric detector + optical distortion
Absolute wavelengths—across exposures	1.0 pixels	• Thermal stability • Internal versus external stability • Derivation of wavecal zero point
Absolute photometry	15%	Instrument stability and calibration
Relative photometry (within an exposure)	5–10%	Instrument stability/flat fields

Table 16.3: CCD Imaging Accuracies

Attribute	Accuracy	Limiting Factor
Relative astrometry—within an image	0.1 pixels	Stability of optical distortion
Absolute photometry	5–10%	Instrument stability
Relative photometry within an image	5%	External illumination pattern

Table 16.4: MAMA Imaging Accuracies

Attribute	Accuracy	Limiting Factor
Relative astrometry—within an image	0.25 pixels	Small scale distortion stability
Absolute photometry	15%	Instrument stability and calibration
Relative photometry within an image	10%	Flat fields/external illumination

Table 16.5: Target Acquisition Accuracies

Attribute	Accuracy	Limiting Factor
Guide star acquisition	1–2”	Catalog uncertainties
Following target acquisition exposure	0.2”	Centering accuracy plus plate scale accuracy to convert pixels to arcsecond
Following peakup acquisition exposure	30% of the slit width	Number of steps in scan + PSF

CHAPTER 17
Calibration Plans

In This Chapter...

In this chapter we describe the current plans for the testing, verification and calibration of STIS on the ground, on orbit following launch, and during Cycle 7.

Introduction

At the time this Handbook is being written, the STIS instrument is still under construction and assembly. The CCD flight detector has been selected and is still being integrated into the instrument, and the MAMA detectors have yet to be finalized. Below we describe the very tentative plans for the ground (pre-launch) and Servicing Mission Orbital Verification (SMOV)—the time immediately following launch, which will be used for testing STIS. We also describe the philosophy that we expect to employ in the Cycle 7, on-orbit, calibration of STIS.

As these plans firm up, we will post more details about the plan on the STScI STIS World Wide Web page; ultimately a full report of the calibration program and results will be provided there.

Ground Testing and Calibration of STIS

The STIS Investigation Definition Team (Principal Investigator, Bruce Woodgate, GSFC) is responsible for the ground testing and calibration of STIS.

They are developing a plan to “ensure that the basic performance characteristics of this versatile instrument will be verified and documented before launch, and that the necessary operational and data reduction databases will be adequately populated” (Ebbets et al., 1995, from “Plans for the pre-launch calibration of the Space Telescope Imaging Spectrograph”). Opportunities for obtaining the necessary data on the ground occur at the component and subsystem level as well as during assembly and alignment. However, the major portion of the test results come once the instrument is integrated with its full complement of optics, detectors, mechanisms, electronics, and software and run through a series of functional, environmental, and thermal vacuum tests. The bulk of the calibration data is obtained during the thermal vacuum tests, currently scheduled for August, 1996. The thermal vacuum tests are currently planned to cover the following areas:

- Wavelength calibration.
- Mode radiometric sensitivity.
- Spectral resolution.
- Image quality.
- Mode sensitivity outside nominal range.
- Spectral flat field calibrations.
- Geometric distortions.
- Slit functions.
- Stray and scattered light.
- Count rate linearity.
- Calibration of backup modes.
- Routine internal mini-functional tests of stability, repeatability, and performance.

SMOV Testing and Calibration of STIS

The primary goals of the Second Servicing Mission’s Orbital Verification (SMOV) are the timely recommissioning of the HST observatory for normal Cycle 7 science operations and the performance of the Early Release (ERO) Program for STIS and NICMOS. Typical science instrument commissioning activities include activation, alignment, focusing, and preliminary calibration of the new science instruments to validate their nominal performance. *SMOV calibration* activities include only those calibrations which, when successfully complete, enable that science instrument to perform a significant fraction of potential Cycle 7 science. In addition to science instrument commissioning and recommissioning, SMOV re-verifies observatory level parameters, such as pointing control and stability, guide star acquisitions, and HST data recorder performance.

SMOV Commissioning Plans for STIS

The engineering and science activities which will be performed in order to commission STIS during SMOV are being finalized as of the writing of this Handbook. In Table 17.1 below, we itemize those activities. The activities in the table are grouped according to the requirement that they fulfill, and are *not* in the order in which they will be performed.

Table 17.1: STIS SMOV Activities

Requirements	Testing Steps
Engineering	
	• STIS Modes and Data Interfaces
	• Load and Dump On-board Memory
	• Science Data Buffer Check with Self-Test
	• Calibration Lamp Checkout
	• CCD Functional
	• CCD Temperature Set Point Determination
	• MAMA Functional
	• STIS SMOV Contamination Monitoring Plan
	• STIS Mechanisms Functional
	• On-board Doppler Processing Check-Out
Detector Operation	
	• Verification of Standard CCD Functions and Readout Modes
	• Verification of Standard MAMA Functions and Readout Modes
Optical Performance	
	• STIS Corrector Alignment, Coarse
	• STIS Corrector Alignment, Fine
	• Spectroscopic Mode Image Quality
	• Camera Mode Image Quality
	• Repeatability of Image Positions of STIS Modes
	• Verification of Optical Format of STIS Modes
	• STIS Slit to Detector Internal Stability
	• OTA-STIS Pointing and Throughput Stability
	• Measurement of Scattered Light When Occulting Bars are Used
	• PSF Measurement in Each Band[a]
Calibration	
	• CCD Dark Rate and Read Noise
	• Dark Measurements for the NUV-MAMA and FUV-MAMA
	• NUV-MAMA and FUV-MAMA Flat Field Uniformity
	• CCD Flat-Field Stability and Cosmetic Defect Fraction
	• STIS Pixel-to-Pixel Response Stability
	• STIS Sensitivity
	• Slit Transmissions
Target Acquisition	
	• STIS to FGS Alignment
	• STIS Acquisition Aperture and Slit Location
	• STIS CCD Point Source Acquisition
	• STIS CCD Diffuse Source Acquisition
	• STIS CCD Bright Target Acquisition
	• STIS CCD Coronographic Acquisition
	• STIS Target Centering
	• STIS Peakdowns for Coronographic Acquisitions

a. STIS's four bands are: Band I, covering the far-UV (1150–1700 Å), Band II, covering the near-UV (1700–3100Å), Band III, covering the blue (3000–5000 Å), and Band IV, covering the red (5000–11000 Å).

Cycle 7 Calibration Philosophy

The STIS Cycle 7 Calibration Plan will be developed to characterize the performance of the instrument in all *supported* configurations, as described in this handbook, and as needed to support Cycle 7 approved proposals, and within the constraints of the available time for such calibrations. Table 17.2 below summarizes the calibrations we hope to be able to obtain for supported configurations during Cycle 7. If STIS proves more time-consuming to calibrate than currently envisioned, then preference will be given to calibrating the most used of the supported configurations. The calibration accuracies we hope to achieve with this program are summarized in Chapter 15, page 319.

As explained in "Support of STIS Capabilities for Cycle 7," on page 12, no additional calibrations will be taken for *available-but-unsupported* configurations as part of the Cycle 7 Calibration Plan. Observers wishing to use non-standard configurations of STIS must take their own calibrations as part of their approved proposals or use calibration data for the supported modes, which will be available through the HST Data Archive, to calibrate their data.

Table 17.2: Cycle 7 Calibration Philosophy

Calibration Step	Performed for...	Calibration File
Wavelength calibration	Supported grating-aperture combinations	dispersion solution
Photometric calibration	Supported gratings	sensitivity
Photometric monitoring	Monthly or bi-monthly, at all four wavelength bands: 1150-1700 Å, 1700-3100 Å, 3000-5000 Å, 5000-11000 Å,	changes to sensitivity and contamination monitoring
Point source and lamp illuminated aperture transmission	For all supported slits. Point source at aperture center and at additional locations along long slits.	aperture throughput
Pixel-to-pixel sensitivity	Selected gratings and filters, as needed to construct pixel-to-pixel flats for all supported gratings and filters	pixel-to-pixel flat field
Pixel-to-pixel sens. monitoring	Monthly, per detector	delta flats
Large spatial scale sensitivity	Supported gratings and filters	low order flat field
Large spatial scale sensitivity monitoring	Monthly for selected gratings	modifications to low order flats
Plate scale distortions	CCD, NUV-MAMA, FUV-MAMA	geometric distortion
Darks (as function of geomagnetic position)	CCD, NUV-MAMA, FUV-MAMA	dark image
Dark monitoring	Weekly, per detector	revisions to darks

Table 17.2: Cycle 7 Calibration Philosophy

Calibration Step	Performed for...	Calibration File
Biases	CCD, per gain	bias image
Bias monitoring	Weekly, CCD	revisions to biases
Gain determination	CCD, per gain	gain factor
Focus and alignment monitoring	Done as part of photometric monitoring program	PSFs and LSFs

Glossary

The following terms and acronyms are used in this handbook.

A-D: Analog to digital.

CCD: Charge-coupled device. Solid-state, light detecting device.

CDBS: Calibration Data Base. System for maintaining reference files and tables used to calibrate HST observational datasets.

CEI: Contract End Item

CIM: Calibration insert mechanism.

COSTAR: Corrective Optics Space Telescope Axial Replacement.

CP: Call for Proposals.

CR: Cosmic ray.

CVZ: Continuous viewing zone.

DQ: Data quality.

DQE: Detector quantum efficiency.

DN: Data number.

FAQ: Frequently asked questions.

FGS: Fine Guidance Sensors.

FITS: Flexible Image Transport System. A generic IEEE- and NASA-defined standard used for storing image data.

FOC: Faint Object Camera.

FOS: Faint Object Spectrograph.

FOV: Field of view.

FSW: Flight software.

FTP: File Transfer Protocol. Basic tool used to retrieve files from a remote system. Ask your system manager for information about using FTP.

FUV: Far ultraviolet.

FWHM: Full width at half maximum.

GEIS: Generic Edited Information Set. The multigroup format used by STSDAS for storing some HST image data.

GHRS: Goddard High-Resolution Spectrograph.

GO: General Observer.

GTO: Guaranteed Time Observer.

HITM: Hole in the Mirror.

HSP: High-Speed Photometer.

HST: Hubble Space Telescope.

ICD: Interface control document. Defines data structures used between software or systems to ensure compatibility.

IDT: Investigation Development Team.

IM: Insert Mechanism.

IR: Infrared.

IRAF: Image Reduction and Analysis System. The system on which STSDAS is built.

IUE: International Ultraviolet Explorer.

K: Degree Kelvin.

LMC: Large Magellanic Cloud.

LSF: Line spread function.

MAMA: Multi-Anode Microchannel Array.

MCP: Microchannel Plate.

MSM: Mode Selection Mechanism.

ND: Neutral density.

NICMOS: Near-Infrared Camera and Multi-Object Spectrograph.

NUV: Near ultraviolet.

OPUS: OSS and PODPS Unified Systems.

OSS: Observation Support System.

PI: Principal investigator.

PODPS: Post-Observation Data Processing System.

PSF: Point spread function.

QE: Quantum efficiency.

QEH: Quantum efficiency hysteresis.

QPOE: Quick Position-Oriented Event (IRAF data format for x-ray data).

QSO: Quasi-stellar object.

RA: Right ascension.

rms: Root mean square.

SITe: Scientific Image Technologies.

SMOV: Servicing Mission Orbital Verification.

S/N: Signal-to-noise ratio.

ST-ECF: Space Telescope European Coordinating Facility.

STEIS: Space Telescope Electronic Information System. The World Wide Web host from which information, software, documentation, and other resources pertaining to the HST can be obtained.

STIS: Space Telescope Imaging Spectrograph.

STScI: Space Telescope Science Institute.

STSDAS: Space Telescope Science Data Analysis System. The complete suite of data analysis and calibration routines used to process HST data.

SV: Science verification. Process of taking observations that can be used for HST instrument calibration.

TAC: Telescope Allocation Committee.

URL: Uniform resource locator. Address for WWW.

UV: Ultraviolet.

WF/PC: Wide Field/Planetary Camera.

WFPC2: Wide Field Planetary Camera-2. Replacement for WF/PC installed during first servicing mission of December 1993.

WWW: World Wide Web. Hypertext-oriented method for finding and retrieving information over the Internet.

Index

D

E

F

G

H

I

L

T

U

W